VOL. 680 NO. 1 SEPTEMBER 30, 1994

6th Int. Symp. on High Performance Capillary Electrophoresis
San Diego, CA, January 31–February 3, 1994
Part I

JOURNAL OF CHROMATOGRAPHY A

INCLUDING ELECTROPHORESIS AND OTHER SEPARATION METHODS

SYMPOSIUM VOLUMES

ELSEVIER

JOURNAL OF CHROMATOGRAPHY A

INCLUDING ELECTROPHORESIS AND OTHER SEPARATION METHODS

Scope. The *Journal of Chromatography A* publishes papers on all aspects of **chromatography, electrophoresis** and related methods. Contributions consist mainly of research papers dealing with chromatographic theory, instrumental developments and their applications. In the *Symposium volumes*, which are under separate editorship, proceedings of symposia on chromatography, electrophoresis and related methods are published. *Journal of Chromatography B: Biomedical Applications* —This journal, which is under separate editorship, deals with the following aspects: developments in and applications of chromatographic and electrophoretic techniques related to clinical diagnosis or alterations during medical treatment; screening and profiling of body fluids or tissues related to the analysis of active substances and to metabolic disorders; drug level monitoring and pharmacokinetic studies; clinical toxicology; forensic medicine; veterinary medicine; occupational medicine; results from basic medical research with direct consequences in clinical practice.

Submission of Papers. The preferred medium of submission is on disk with accompanying manuscript (see *Electronic manuscripts* in the Instructions to Authors, which can be obtained from the publisher, Elsevier Science B.V., P.O. Box 330, 1000 AH Amsterdam, Netherlands). Manuscripts (in English; *four* copies are required) should be submitted to: Editorial Office of *Journal of Chromatography A*, P.O. Box 681, 1000 AR Amsterdam, Netherlands, Telefax (+31-20) 5862 304, or to: The Editor of *Journal of Chromatography B: Biomedical Applications*, P.O. Box 681, 1000 AR Amsterdam, Netherlands. Review articles are invited or proposed in writing to the Editors who welcome suggestions for subjects. An outline of the proposed review should first be forwarded to the Editors for preliminary discussion prior to preparation. Submission of an article is understood to imply that the article is original and unpublished and is not being considered for publication elsewhere. For copyright regulations, see below.

Publication information. *Journal of Chromatography A* (ISSN 0021-9673): for 1995 Vols. 683–714 are scheduled for publication. *Journal of Chromatography B: Biomedical Applications* (ISSN 0378-4347): for 1995 Vols. 663–674 are scheduled for publication. Subscription prices for *Journal of Chromatography A*, *Journal of Chromatography B: Biomedical Applications* or a combined subscription are available upon request from the publisher. Subscriptions are accepted on a prepaid basis only and are entered on a calendar year basis. Issues are sent by surface mail except to the following countries where air delivery via SAL is ensured: Argentina, Australia, Brazil, Canada, China, Hong Kong, India, Israel, Japan, Malaysia, Mexico, New Zealand, Pakistan, Singapore, South Africa, South Korea, Taiwan, Thailand, USA. For all other countries airmail rates are available upon request. Claims for missing issues must be made within six months of our publication (mailing) date. Please address all your requests regarding orders and subscription queries to: Elsevier Science B.V., Journal Department, P.O. Box 211, 1000 AE Amsterdam, Netherlands. Tel.: (+31-20) 5803 642; Fax: (+31-20) 5803 598. Customers in the USA and Canada wishing information on this and other Elsevier journals, please contact Journal Information Center, Elsevier Science Inc., 655 Avenue of the Americas, New York, NY 10010, USA, Tel. (+1-212) 633 3750, Telefax (+1-212) 633 3764.

Abstracts/Contents Lists published in Analytical Abstracts, Biochemical Abstracts, Biological Abstracts, Chemical Abstracts, Chemical Titles, Chromatography Abstracts, Current Awareness in Biological Sciences (CABS), Current Contents Life Sciences, Current Contents/Physical, Chemical & Earth Sciences, Deep-Sea Research/Part B: Oceanographic Literature Review, Excerpta Medica, Index Medicus, Mass Spectrometry Bulletin, PASCAL-CNRS, Referativnyi Zhurnal, Research Alert and Science Citation Index.

US Mailing Notice. *Journal of Chromatography A* (ISSN 0021-9673) is published weekly (total 52 issues) by Elsevier Science B.V., (Sara Burgerhartstraat 25, P.O. Box 211, 1000 AE Amsterdam, Netherlands). Annual subscription price in the USA US$ 5389.00 (US$ price valid in North, Central and South America only) including air speed delivery. Second class postage paid at Jamaica, NY 11431. **USA POSTMASTERS**: Send address changes to *Journal of Chromatography A*, Publications Expediting, Inc., 200 Meacham Avenue, Elmont, NY 11003. Airfreight and mailing in the USA by Publications Expediting.

See inside back cover for Publication Schedule, Information for Authors and information on Advertisements.

0021-9673/94/$07.00

Printed in the Netherlands

For Contents see p. VII.

JOURNAL OF CHROMATOGRAPHY A

VOL. 680 (1994)

JOURNAL OF CHROMATOGRAPHY A

INCLUDING ELECTROPHORESIS AND OTHER SEPARATION METHODS

SYMPOSIUM VOLUMES

ELSEVIER

Amsterdam – Lausanne – New York – Oxford – Shannon – Tokyo

0021-9673/94/$07.00

Printed in the Netherlands

SYMPOSIUM ISSUE

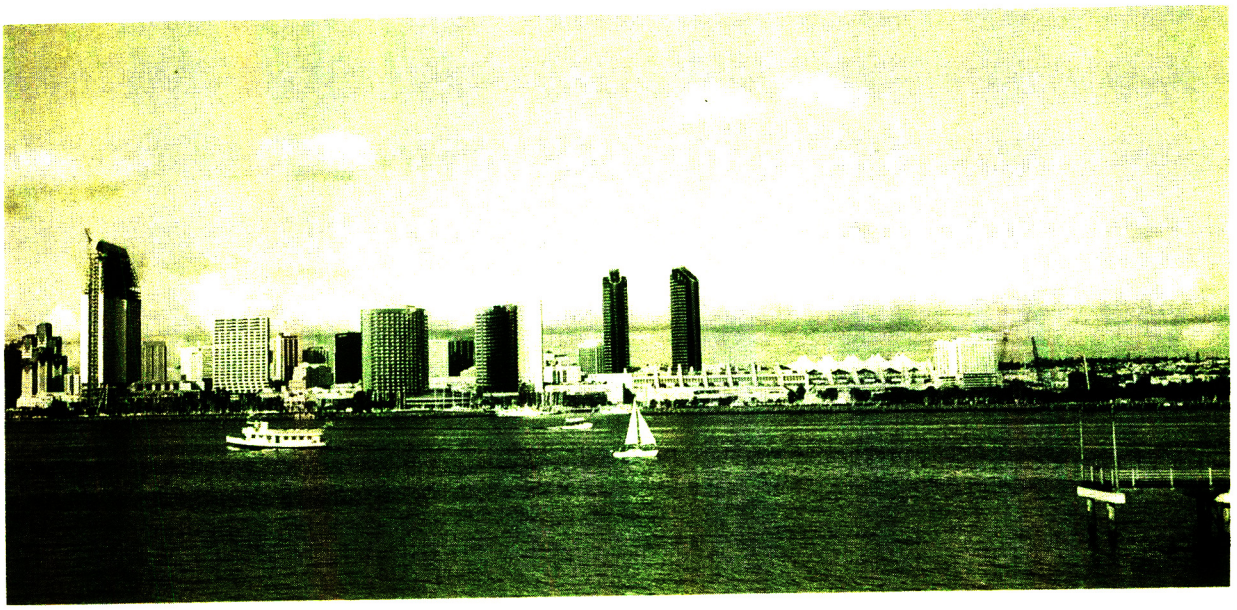

SIXTH INTERNATIONAL SYMPOSIUM ON HIGH PERFORMANCE CAPILLARY ELECTROPHORESIS

San Diego, CA (USA), January 31–February 3, 1994

Guest Editors

B.L. KARGER
(Boston, MA, USA)

S. TERABE
(Hyogo, Japan)

VOL. 680, NO. 1 JOURNAL OF CHROMATOGRAPHY A SEPTEMBER 30, 1994

CONTENTS

6TH INTERNATIONAL SYMPOSIUM ON HIGH PERFORMANCE CAPILLARY ELECTROPHORESIS, SAN DIEGO, CA, JANUARY 31–FEBRUARY 3, 1994

PART I: VOLUME 680, NO. 1

PHENOLIC COMPOUNDS AND O-HETEROCYCLES

CARBOHYDRATES AND GLYCOPROTEINS

ORGANIC ACIDS

AMINES, AMINO ACIDS AND PEPTIDES

PART II: VOLUME 680, NO. 2

PROTEINS

NUCLEIC ACIDS CONSTITUENTS AND PCR PRODUCTS

DYES AND HETEROCYCLIC COMPOUNDS

DRUGS

ENVIRONMENTAL ANALYSIS AND IONS

ELSEVIER

Journal of Chromatography A, 680 (1994) 1

JOURNAL OF CHROMATOGRAPHY A

Foreword

The *6th International Symposium on High Performance Capillary Electrophoresis, HPCE'94*, was held in San Diego, CA, January 31–February 3, 1994. The meeting was the largest and most successful of the series in all respects, with over 700 participants from all over the world in spite of the serious economic recession; 353 papers were presented and the newest instruments and supplies were shown by 19 companies.

Although many new developments in CE stimulated the participants, a clear trend seen in the previous meetings was extended further in this symposium: CE has become an indispensable tool for solving real analytical problems. Great interest was shown in method validation in CE, which is essential for CE to be used as a routine analytical tool. The advantages of the micro- and nanoscale analyses by CE will be accelerated by miniaturization of the CE system on a glass chip or by applying CE to single-cell analysis.

The success of the meeting was mainly due to the many individuals who contributed to the symposium. I would like to express my sincere thanks to Tom Gilbert and Shirley Schlessinger for their expert work in organizing and running the symposium. Takashi Manabe and Nobuo Tanaka also were most helpful in running the symposium. The scientific programme was carefully arranged with the advice and assistance of the Science Advisory Committee: Heinz Engelhardt, Frans Everaerts, William Hancock, Stellan Hjertén, James Jorgenson, Barry Karger (also as a co-organizer) and Edward Yeung. I would also like to thank Dr. Zdenek Deyl for his fine editorial work on this symposium issue.

HPCE'95 is to be held in Würzburg, Germany, January 29–February 2, 1995, under the chairmanship of Professor Heinz Engelhardt, Universität des Saarlandes. We look forward to another exciting and successful meeting.

Kamigori, Hyogo, Japan Shigeru Terabe

SSDI 0021-9673(94)00530-M

ELSEVIER

Journal of Chromatography A, 680 (1994) 3–13

JOURNAL OF CHROMATOGRAPHY A

Terminology and nomenclature in capillary electroseparation systems

John H. Knox

Department of Chemistry, University of Edinburgh, West Mains Road, Edinburgh EH9 3JJ, UK

Abstract

An outline of the basic theory of capillary electroseparations (CES) is given. This forms the basis for recommended naming of the various techniques and recommended methods for reporting migration and elution data. For those techniques where the separation process is primarily based upon electrophoresis [capillary electrophoresis (CE) and capillary gel electrophoresis (CGE)], the electroosmotic mobility of the electrolyte (if not zero) and the electrophoretic mobilities of the analytes should be reported. For those techniques where separation is primarily based upon partitioning between phases that move at different rates [capillary electrochromatography (CEC) and capillary micellar electrochromatography (CMEC)], the electroosmotic mobility of the electrolyte and the electromigration mobility of any moving secondary phase should be reported, along with the capacity factors (k') or effective capacity factors of the analytes. The band dispersion of CES systems should be measured in terms of the HETP, as in chromatography.

1. Introduction

Capillary electroseparation (CES) methods are characterized by the fact that they are all carried out in essentially the same equipment which consists of the following main components:

(a) a fine capillary, usually of quartz, within which separation occurs (bore 50–200 μm, length 200–1000 mm);

(b) a high-voltage power supply capable of delivering 50 kV at 100 μA;

(c) two electrolyte reservoirs into which the ends of the capillary dip, one connected to the high-voltage supply and the other earthed;

(c) an on-column injection system, usually at the high-voltage end of the capillary;

(d) an on-column detector quantitating analyte within a short segment of the capillary (<1 mm), UV and fluorescence detectors being the commonest;

(e) optionally, a means of pressurizing either or both of the inlet and outlet ends of the capillary;

(f) suitable electronics for managing the above, including means of measuring the current flowing through the capillary;

(g) a suitable Faraday cage to ensure safe operation of the high-voltage section of the equipment;

0021-9673/94/$07.00
SSDI 0021-9673(94)00483-P

(h) preferably, thermostating of the capillary by either forced air or liquid.

2. Capillary electroseparation techniques – names

Currently four distinct CES techniques have been described, as shown in Table 1. They are variously carried out in open or packed tubes, and they can separate both charged and uncharged species through differences in either their electrophoretic mobilities or their partition coefficients between phases that move at different rates.

Capillary electrophoresis was originally called capillary zone electrophoresis [1], which indicated that separated analytes migrated as separate independent non-contiguous zones, and distinguished it from isotachophoresis, but the word "zone" has now fallen out of use and it is recommended that the simpler term capillary electrophoresis (CE) should be universally adopted. The term capillary gel electrophoresis concisely describes the process whereby ionic analytes are separated in a capillary filled with gel (often polyacrylamide). Although molecules such as DNA fragments have very similar electrophoretic mobilities in open solution, they migrate at different rates when their electrophoresis is obstructed by the presence of a gel. The larger species are more seriously obstructed than the smaller species and so move more slowly. There seems every reason to retain the term capillary gel electrophoresis (CGE).

Capillary liquid chromatography in which the liquid is driven along the tube by an electric field rather than pressure [2,3] is basically similar to ordinary liquid chromatography and uses a tube packed with a conventional HPLC stationary phase (although the particles may be much smaller). Analytes are separated primarily because of their different partition ratios between a mobile phase, the electrolyte, and a stationary phase borne by the packing material. As the flow of electrolyte is achieved by electroosmosis (formerly called electroendosmosis), rather than by application of pressure, the technique was originally termed capillary electroendosmotic chromatography. However, this name is unnecessarily complicated and it is recommended that the technique now be called capillary electrochromatography (CEC). The term electrochromatography has also been used by Tsuda [4] to describe an HPLC technique in which pressure is the primary driving force but an electric field is used to achieve additional selectivity; it is proposed that this technique should now be called pressurized electrochromatography.

The elegant technique invented by Terabe and co-workers [5,6], whereby analytes are partitioned between background electrolyte and micelles in a micellar solution, was originally called micellar electrokinetic chromatography. Again, this is unnecessarily lengthy and the

Table 1
Electroseparation techniques

Technique	Open tube	Packed tube
Electrophoresis	CE	CGE
Chromatography	CMEC	CEC

Electrophoresis methods
CE = capillary electrophoresis (ions only)
CGE = capillary gel electrophoresis (ions only)

Chromatographic methods
CMEC = capillary micellar electrochromatography (neutrals, ion pairs, ions)
CEC = capillary electrochromatography (neutrals, ion pairs, ions)

method is now commonly known either as micellar electrochromatography or micellar electrophoresis. As the separation is primarily based on partitioning between two phases, the electrolyte and the micelles, the process is strictly chromatographic and not electrophoretic. Accordingly, it is recommended that the name capillary micellar electrochromatography (CMEC) should be adopted.

In summary, the names of the techniques should include the word "electrophoresis" when the basis for separation is primarily differences in electrophoretic mobility, and should include the word "chromatography" when the basis for separation is primarily differences in the partition ratios of analytes between phases which move at different rates (the rate of movement of one of the phases can of course be zero, as in simple packed column electrochromatography).

3. Basic electrochemical phenomena relevant to CES

All CES methods by definition must involve one or both of the primary electrochemical phenomena, electroosmosis and electrophoresis. Some of them also involve chromatographic partitioning between phases.

3.1. The electrical double layer

Both of the primary electrochemical phenomena result from the presence of the electrical double layer which is present at virtually all interfaces, and particularly at interfaces between a solid and an electrolyte. Fig. 1 illustrates, in a highly diagramatic way, the surface of silica in contact with an electrolyte. The surface contains chemically bound $Si-O^-$ groups at its surface, and is therefore permanently electrically charged. When in contact with an electrolyte, these surface ions are balanced by an excess of positive ions within the electrolyte. Owing to the strong electrostatic interactions between the negative ions in the surface and the positive ions in the solution, the layer of excess positive ions

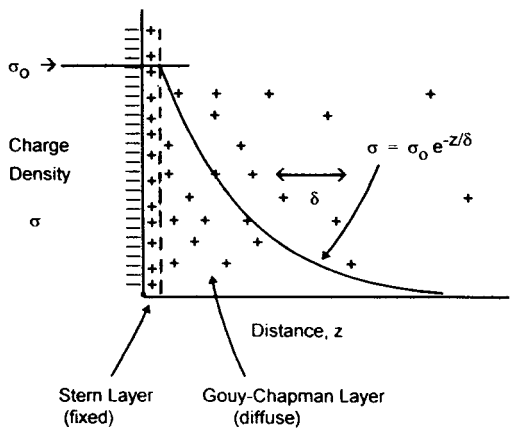

Fig. 1. Diagramatic representation of the electrical double layer showing the negatively charged surface, fixed excess positive ions in the Stern layer and mobile excess positive ions in the diffuse Gouy–Chapman layer. The so-called "thickness of the double layer" is shown as δ.

in the solution is very thin. It is generally agreed (see, for example, Bockris and Reddy [7]) that this layer of excess positive ions can be separated into two parts. Close to the surface is a layer of ions which are adsorbed on the surface and are essentially fixed. They do not enter into the electrokinetic phenomena. This is called the Stern or Helmholz layer. The remaining ions form a diffuse layer called the Gouy–Chapman layer. The ions in this diffuse layer exchange continuously with those in the rest of the solution, and are indeed indistinguishable from them. The charge density of the excess ions, σ, falls exponentially with distance, z, from the surface according to Eq. 1, as shown in Fig. 1.

$$\sigma = \sigma_0 \exp(-z/\delta) \quad (1)$$

where δ is the so-called "thickness" of the double layer (often denoted by $1/\kappa$), and is given by

$$\delta = [(\varepsilon_0 \varepsilon_r RT)/(2cF^2)]^{1/2} \quad (2)$$

Typical values of δ are given in Table 2. The electrical potential at the boundary between the Helmholtz layer and the diffuse part of the

Table 2
Thickness of the electrical double layer, δ

c (mol l^{-1})	δ (nm)
0.1	1.0
0.01	3.1
0.001	10.0

double layer is called the "zeta potential", ζ, and is of the order of 10–100 mV.

3.2. Electroosmosis

When a potential difference is applied to a surface, as is the case when a field is applied along the length of a quartz capillary, the ions in the diffuse layer experience a force parallel to the surface. Because there is a slight excess of positive ions in this layer, the solvent immediately in contact with the surface experiences a net force towards the negative electrode; this is resisted by the viscosity of the liquid, resulting in shear developing within the double layer which is proportional to the excess charge density at any point in the layer. The result, as shown in Fig. 2, is that the liquid at the solution-side boundary of the double layer moves at a constant velocity, u_{eo}, given by Eq. 3. The process is called electroosmosis, with electroosmotic velocity,

$$u_{eo} = (\varepsilon_0 \varepsilon_r \zeta/\eta)E \quad (3)$$

As the field E is an experimental variable, it is generally more convenient to characterize electroosmotic movement by the electroosmotic mobility, μ_0(m^2 s^{-1} V^{-1}):

$$\mu_{eo} = (\varepsilon_0 \varepsilon_r \zeta/\eta) \quad (4)$$

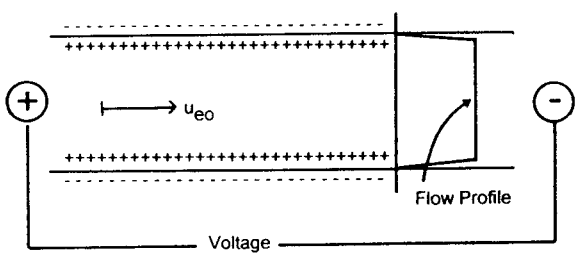

Fig. 2. The phenomenon of electroosmosis in a narrow tube, showing the plug-like flow profile with the very thin shear layer close to the wall of the tube.

In the case of a narrow open tube, the liquid within the tube moves as a plug, so that the velocity of the liquid is constant over more or less the entire tube section except for a very thin layer at the wall which is a few δ's thick. A very important feature of the electroosmotic flow is that its velocity is independent of the bore of the tube in which it occurs, provided that the bore is significantly greater than the thickness of the double layer. In previous papers [2,3] we have shown, using the results of Rice and Whitehead [8], how the mean flow velocity depends on the ratio of the tube diameter, d, to the double layer thickness, δ. Table 3 gives some typical values. With typical values of δ, and an electrolyte concentration of 0.01 M, the minimum bore required to maintain good electroosmotic flow will be around 100 nm. Typical bores used in CES are 500–1000 times larger.

3.3. Electrophoresis

A spherical particles of radius, a, will move in its surrounding electrolyte according to Eqs. 5 and 6. This process is called electrophoresis, and is illustrated in Fig. 3.

$$\text{electrophoretic velocity}, \quad u_{ep} = (\varepsilon_0 \varepsilon_r \zeta/\eta) f(a/\delta) E \quad (5)$$

$$\text{electrophoretic mobility}, \quad \mu_{ep} = (\varepsilon_0 \varepsilon_r \zeta/\eta) f(a/\delta) \quad (6)$$

Table 3
Dependence of mean flow velocity on ratio of tube diameter, d, to double layer thickness, δ

d/δ	u_{av}/u_0
2	0.10
5	0.39
10	0.64
20	0.81
50	0.92
100	0.98

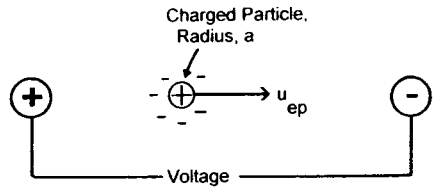

Fig. 3. The phenomenon of electrophoresis showing a positively charged particle of radius a surrounded by its negatively charged ionic atmosphere.

$f(a/\delta) = 1$ for $a/\delta \gg 1$ and 2/3 for $a/\delta \ll 1$. Thus, when the radius of the particle is large compared with δ, the particle moves at the same velocity as if it were subject to electroosmosis, but when the radius is small compared with δ, as for an ion, the velocity is 2/3 that for electroosmosis with the same zeta potential.

3.4. Flow in packed beds

In a bed packed with particles, e.g., dense silica monospheres, the electrolyte will try to flow over these particles at the rate given by Eq. 3 or 5 provided that the particles are large enough. This is shown diagramatically in Fig. 4, where the surfaces of the particles are shown bearing negative charge and the liquid in contact with them bearing excess positive charge. As the particles are fixed in the bed the liquid moves through the bed much in the same way as it moves along a narrow open capillary. Generally, the channels between particles of a packed bed have a mean diameter of about one third that of the particles. Hence, on the basis of Table 3, the flow rate through a packed bed will begin to decrease noticeably only when the particle diameter is less than about 100δ. Reference to Table 2 indicates that with a 0.01 M electrolyte this will occur when the particle diameter is about 0.3 μm.

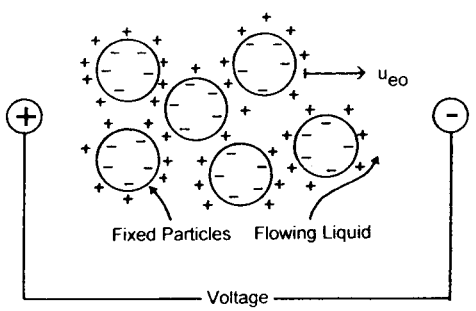

Fig. 4. The phenomenon of electroosmosis in a packed bed showing particles with a negatively charged surface and surrounding liquid containing excess positive charge.

However, when the diameter of the channels in a packed bed is reduced to 2δ, corresponding to spherical particles 6δ in diameter, or 20 nm for a 0.01 M electrolyte, there will be virtually no electroosmotic flow. This would be the case for a column packed, for example, with a gelled silica sol (typical particle diameter 13 nm), and of course for a column packed with a polymer gel as in GCE. In such cases migration can occur only by electrophoresis.

When the particles of a packed bed are porous, the extra-particle flow-rate will be the same as in a bed of impermeable particles but, unless the pore diameter within the particles is very large, there will be virtually no flow within the particles. Accordingly, the mean flow-rate averaged over the entire cross-section of the bed will be reduced below the interparticle flow-rate in the same way as when the flow is pressure driven.

3.5. Molar conductivity, ionic mobility, diffusion coefficient

The molar conductivity, Λ, of a dissolved salt A_nB_m is the conductivity measured between two plates unit distance apart which have between them a perpendicular cylinder containing 1 mol of A_nB_m. This definition is illustrated in Fig. 5.

The individual ionic molar conductivities, λ, of the separate ions of an electrolyte are the contributions to the total molar conductivity from 1 mol of ion (A or B). The molar conductivities are related to the ionic mobilities by the equations

$$\text{ionic molar conductivity, } \lambda = zF\mu \tag{7}$$

$$\text{molar conductivity, } \Lambda = z_{tot}F(\mu_A + \mu_B) \tag{8}$$

where z is the charge on an individual ion and

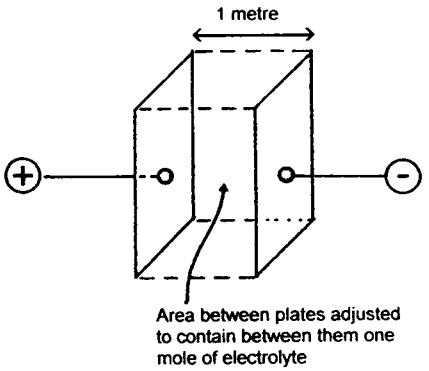

Fig. 5. Illustration of definition of molar conductivity.

z_{tot} is the total charge on the anions (or cations) of the salt A_nB_m.

The molar conductivity of the background electrolyte in a CE system is readily obtained from the resistance per unit length of the capillary, $R(=E/i)$, the molar concentration of the electrolyte, c (mol m^{-3}), and the cross-sectional area of the capillary, A (m^2):

$$\lambda = 1/(RcA) = i/(EcA) \tag{9}$$

The mobility of an ion is also related to its diffusion coefficient. According to Einstein, the diffusion coefficient of a species can be related to its drift velocity in a field (see [7]). For an ion in an electric field the appropriate relation is given by

$$D_m = \mu RT/(zF) \tag{10}$$

If typical values are inserted, e.g., $\mu = 1.0 \times 10^{-7}$ m^2 s^{-1} V^{-1}, $z = 1$, $T = 300$ K, we obtain

$$D_m = 1.0 \times 10^{-7} \times 8.3 \times 300/96\,500$$
$$= 2.5 \times 10^{-9}\ m^2\ s^{-1}$$

4. Partitioning in CES systems

Whereas ionized species can be separated purely on the basis of their different electrophoretic mobilities, uncharged species can be separated only by differential partitioning between two phases which moves at different velocities. With a background electrolyte necessarily being one of the phases, there are two second phases which have been used: (a) particles fixed in a packed bed as in HPLC and (b) charged micelles which move by electrophoresis within the background electrolyte. Micro-emulsion particles have also been used in place of micelles, and most of the discussion given below also applies equally to CES with microemulsions.

In each instance the extent of partitioning is best represented by the chromatographic capacity factor k', which is defined as

$$k' = \frac{\text{amount of analyte in disperse phase}}{\text{amount of analyte in dispersion medium}} \tag{11}$$

The use of the term "disperse phase" in place of "stationary phase" may not be familiar to chromatographers. However, the former term is more in keeping with the theory of micelles and emulsions. The difference between CEC on the one hand and CMEC on the other is chiefly that in CEC the disperse phase is truly stationary, being in the form of particles packed into a bed, whereas in the CMEC the disperse phase moves with the background electrolyte but at a different speed. The concept of k' nevertheless applies equally to both systems; k' is related to the concentration distribution coefficient, D, through the phase ratio, ϕ:

$$k' = \frac{\text{concentration in disperse phase}}{\text{concentration in dispersion medium}} \cdot \frac{\text{volume of disperse phase}}{\text{volume of dispersion medium}}$$
$$= D\phi \tag{12}$$

It is reasonable to assume that the phase ratio, ϕ, is very nearly independent of temperature and therefore that the temperature dependence of k' is essentially the same as that of D. Accordingly, it provides the enthalpy of exchange between the two phases, ΔH, via the Van't Hoff relationship:

$$\mathrm{d} \ln k'/\mathrm{d}T = \mathrm{d} \ln D/\mathrm{d}T = \Delta H/RT^2 \tag{13}$$

5. Plate efficiency in CES systems

Band dispersion is characterized in CES systems in the same way as in chromatography, and the dispersive processes which can in principle occur are exactly the same. Thus the plate efficiency, N, and the plate height, H, for any analyte are obtained from the standard deviation of its peak profile, σ, and its migration time, t, using the equations

$$N = (t/\sigma)^2 \tag{14}$$

$$H = L/N = L(\sigma/t)^2 \tag{15}$$

Jorgenson and Lukacs [1] were the first to point out that because of the plug flow profile in CE the only contribution to the plate height was that given by the B term of the Van Deemter equation, i.e., the term which provided for axial diffusion. With no packing there was no contribution from the A term (eddy diffusion), and with no retention at the walls of the tube and no variation in flow velocity across the tube there were no contributions from C terms (resistance to mass transfer). The same argument applies to CMEC and CGE because the small size of the micellar particles in the former and the fine reticulation of the gel in the latter make mass transfer between and within the phases so fast as to produce no dispersion.

Accordingly, we can write for the plate height H

$$H = 2D_m/u \tag{16}$$

where u is the overall migration rate of the analyte. With values of D_m around 10^{-9} m^2 s^{-1} for small analytes in water and u values of around 2 mm^{-1} s we can expect plate heights of the order of 1 μm and plate efficiencies of 500 000 for 0.5-m columns. In the case of CGE the diffusion of the analytes (usually DNA fragments) is severely restricted by the presence of the gel, but being multi-charged they still experience a large enough force to provide adequate migration rates. The result is migration rates similar to those in CE, but diffusion coefficients that are 10 or possibly 100 times lower. The plate efficiencies then achieved, as shown in numerous examples, may be as high as 10^7.

The situation with CEC at first sight looks less encouraging, as we now have to contend with the flow and mass transfer problems which we normally encounter in HPLC. If indeed we were restricted to particles of 3 or 5 μm this conclusion would be justified. However, in CEC, it should be possible to work with particle no larger than 0.5 μm [2,3]. The reduced velocity at 1 mm s^{-1} then falls from a typical HPLC value of around unity to around 0.1. Both the A and C term contributions then fall to low values, and it again becomes possible to approach the ideal value of H given by Eq. 12. Current progress on using small particles [9] in electrochromatography shows that with 1.5-μm porous particles it is possible to achieve at least 250 000 plates per metre. Higher efficiencies are achievable, but without retention, using non-porous silica monospheres.

6. Characterization of migration parameters in CE and CGE

Electropherograms are sufficiently similar to chromatograms that it is tempting to think that they can be characterized by quoting effective k' values for the different analytes using a neutral marker as the analogue of an unretained solute. Such a species would migrate at the electroosmotic velocity u_{eo}. Regrettably, this is not an acceptable procedure.

As shown in Figure 6 (top), any ionized species will migrate with an overall velocity, u, given by

$$u = u_{eo} + u_{ep} \tag{17}$$

where u_{eo} and u_{ep} are taken as positive when the movement is towards the cathode (the negative electrode) and negative when in the opposite direction. It is readily shown that the effective k' for any analyte would then be a function of the ratio u_{eo}/u_{ep}. However, u_{eo} and u_{ep} are totally

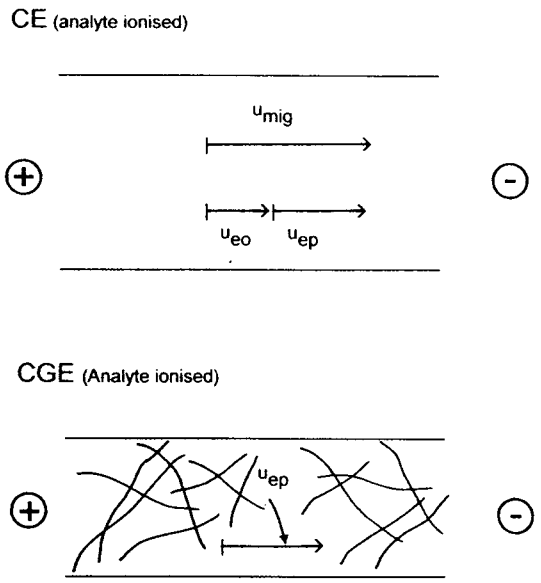

Fig. 6. Key parameters that characterize capillary electrophoresis (CE) (top) and capillary gel electrophoresis (CGE) (bottom).

independent: u_{eo} is a property of the electrolyte/silica surface and u_{ep} is a property of the analyte. Their ratio has no fundamental significance, and is not therefore a valid parameter for characterizing the system. Accordingly, a CE system can only be characterized by quoting both u_{eo} and u_{ep} separately. As both of these are proportional to the field, it is recommended that CE systems should be characterized by quoting the electroosmotic mobility, μ_{eo}, for the electrolyte/capillary, and the electrophoretic mobility, μ_{ep}, of each analyte. μ_{eo} should be established by including a neutral marker in the analyte sample. The two mobilities are obtained from the migration/elution times of neutral and ionized species, t_n and t_{ion}, by the equations

$$\mu_{eo} = (L/E)(1/t_n) \quad (18)$$

$$\mu_{ep} = (L/E)[(1/t_{ion}) - (1/t_n)] \quad (19)$$

For CGE systems there is no electroosmosis (see Fig. 6, bottom), and it is therefore recommended that CGE systems should be characterized by quoting the electrophoretic mobility, μ_{ep}, of each analyte.

7. Characterization of elution parameters in CEC

7.1. Neutral analytes

Fig. 7 illustrates the essential features of the CEC process. The flow in CEC is primarily by electroosmosis, and its velocity is characterized by stating the electroosmotic mobility, μ_{eo} of the electrolyte (eluent) in the packed column. This may be found using an unretained neutral marker by Eq. 18. The degree of retention or capacity factor, k', of the other analytes is obtained directly from the electrochromatogram as in HPLC by measuring retention times of the unretained neutral marker, t_n, and of each analyte, t_R:

$$k' = (t_R - t_n)/t_n \quad (20)$$

7.2. Neutral and ionized analytes

When both neutral and ionized analytes are present there is the added complication that the ions when in the mobile phase will migrate at a

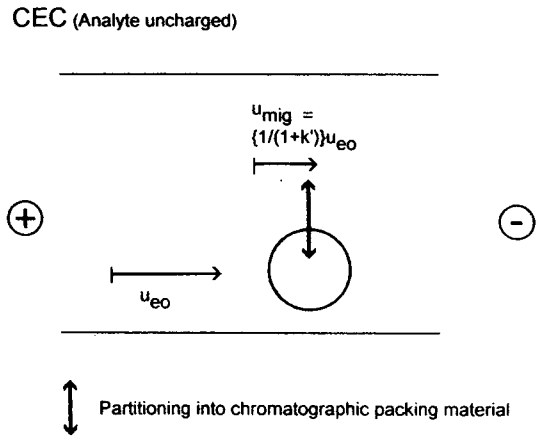

Fig. 7. Key parameters that characterize capillary electrochromatography (CEC).

velocity u_{ion} ($=u_{eo}+u_{ep}$). It is not possible in a single experiment to distinguish between the contributions to the elution time from electrophoresis and partitioning. The two factors can be distinguished only by carrying out a further independent experiment. For example, a pressure-driven chromatogram will provide k' values, whereas a CE experiment will provide electrophoretic mobilities.

In practice, it is likely that electrochromatographic separations will stand on their own, and it will not generally be necessary to separate electrophoretic and partitioning contributions to the elution velocity, so that "effective k' values" will most likely be quoted. It must be noted, however, that irreproducibility from column to column could result from assuming that there will always be a constant relationship between electroosmotic and electrophoretic mobilities for a given type of column packing.

Accordingly, it is recommended that CEC separations should be characterized by quoting the electroosmotic mobility of the electrolyte/packing, μ_{eo}, and the effective k' values for each analyte, having included an unretained neutral marker in the analyte sample to establish t_n. The effective k' values should be obtained from Eq. 20 even when there are ionized analytes present.

8. Characterization of elution parameters in CMEC

8.1. Neutral analytes

Fig. 8 illustrates the essential features of the CMEC process. In CMEC the analytes are partitioned between the background electrolyte and the micelles. The electrolyte moves at a velocity u_{eo}, while the micelles migrate within the electrolyte at a their electrophoretic velocity $u_{ep(mic)}$. The net migration velocity of the micelles in the capillary, u_{mic}, is thus

$$u_{mic} = u_{eo} + u_{ep(mic)} \tag{21}$$

An analyte that is not partitioned into the micelles ($k' = 0$) moves at a velocity u_{eo}, whereas an analyte this is completely partitioned into the micelles ($k' = \infty$) moves at a velocity u_{mic}. There is therefore a window of elution velocity and elution time within which all neutral analytes will emerge from the column. In more detail, the k' value of an analyte, which characterizes its partitioning, is defined as

$$k' = \frac{\text{amount of analyte in micelles}}{\text{amount of analyte in electrolyte}} \tag{22}$$

The proportions of analyte present at any instant within the electrolyte and within the micelles are $1/(1+k')$ and $k'/(1+k')$, respectively. When an analyte molecule is within the electrolyte it moves at a velocity u_{eo}, and when it is within the micelle it moves at a velocity u_{mic}. The mean rate of movement of a band of analyte is therefore

$$\begin{aligned} u &= [k'/(1+k')]u_{mic} + [1/(1+k')]u_{eo} \\ &= [k'/(1+k')]u_{ep(mic)} + u_{eo} \end{aligned} \tag{23}$$

The k' value for any analyte is readily found from Eq. 23 as

$$k' = (u_{eo} - u)/(u - u_{mic}) \tag{24}$$

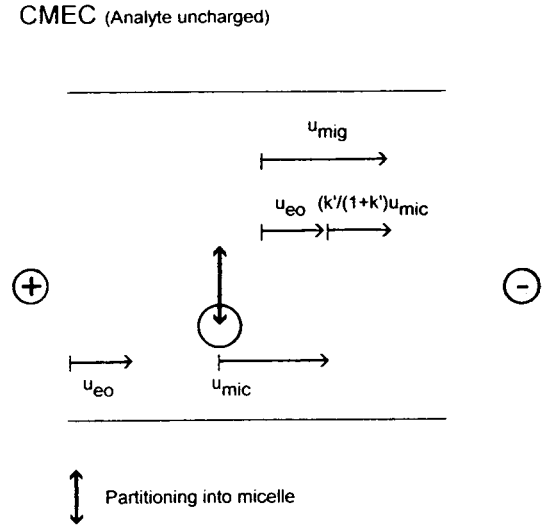

Fig. 8. Key parameters that characterize capillary micellar electrochromatography (CMEC).

In terms of elution times:

$$k' = [(1/t_n) - (1/t_R)]/[(1/t_R) - (1/t_{mic})]$$
$$= [1 - (t_R/t_n)]/[(t_R/t_{mic}) - 1] \quad (25)$$

where t_n is the time of elution of an analyte confined to the electrolyte and t_{mic} is the time of elution of an analyte confined to the micelles; k' varies in a non-linear, but well defined, manner with the retention time t_R, ranging from $k' = 0$ when $t_R = t_n$ to $k' = \infty$ when $t_R = t_{mic}$.

8.2. Neutral and ionized analytes

The situation is again complex, as in CEC. Ionized solutions will migrate while in the electrolyte at their own velocity $u_{ion} = u_{eo} + u_{ep}$. The contributions to the overall elution time arising from electrophoresis and partitioning cannot be separated in a single experiment. It is not possible, as in CEC, to carry out a pressure-driven experiment to establish the k' values of all solutes, so the only possible way to separate the electrophoretic and partitioning components is to vary the degree of partitioning relative to electrophoresis. This can be achieved by carrying out experiments with differing contents of the micellar agent because, as shown by Terabe et al. [6], k' is proportional to the concentration of micellar agent in excess of the critical micelle concentration (cmc).

Following Eq. (23) we can write

$$u = [k'/(1 + k')]u_{mic} + [1/(1 + k')]u_{ion} \quad (26)$$

where u_{ion} now replaces u_{eo}. As k' is proportional to the excess concentration, c, of micellar agent we can replace k' by αc, resulting in

$$u = [\alpha c/(1 + \alpha c)]u_{mic} + [1/(1 + \alpha c)]u_{ion} \quad (27)$$

where u, u_{mic} and c are known but α and u_{ion} are unknown. Rearrangement gives

$$c(u - u_{mic}) = (u_{ion}/\alpha) - (u/\alpha) \quad (28)$$

A plot of $c(u - u_{mic})$ against u will then give a straight line of gradient $1/\alpha$ and intercept u_{ion}/α. This analysis assumes that u_{ion} and u_{mic} do not change with c, the micellar concentration. The assumption seems likely to hold. However, the simplest way to isolate u_{ion} is undoubtedly to carry out the experiment with the micellar agent present at a concentration just below the cmc when $u = u_{ion}$. Under these conditions the zeta potential should be unchanged.

As with CEC, it is probably unnecessary in most practical cases to determine the electrophoretic mobility and capacity factor of an ionized solute separately. Accordingly, it seems best to characterize all capillary micellar electrochromatograms by stating "effective k' values" defined according to Eq. 25 whether the analytes are neutral or ionized. However, it must be noted that analytes with extreme values of u_{ep} may elute outside the window formed by the micellar peak and the unretained peak. In such cases the effective k' values will be negative. Eq. 25 indicates that when an analyte elutes outside the window beyond the micelle (for which $k' = \infty$), it will have an effective k' between $-\infty$ and -1; when it elutes beyond the unretained neutral marker (for which $k' = 0$), it will have an effective k' between 0 and -1.

It is recommended that capillary micellar electrochromatograms should be characterized by stating the electroosmotic mobility of the electrolyte/capillary, μ_{eo}, and the overall electromigration mobility of the micelles, μ_{mic} $[=\mu_{ep(mic)} + \mu_{eo}]$, and by stating the effective k' values for each analyte. Where some of the analytes are ionized, their effective k' values may be negative.

9. Summary of recommendations

It is recommended:

(1) that the four distinct capillary electroseparation methods should be named capillary electrophoresis (CE), capillary gel electrophoresis (CGE), capillary electrochromatography (CEC) and capillary micellar electrochromatography (CMEC);

(2) that, where the primary separation process is electrophoresis (CE, CGE), the separation should be characterized by stating the electroosmotic mobility of the electrolyte and the electrophoretic mobilities of the analytes;

(3) that, where the primary separation processes is partitioning (CMEC, CEC), the system as a whole should be characterized by stating the electroosmotic mobility of the electrolyte and the overall migrational mobility of the micelles (where relevant); the separation itself should be characterized by stating the k' or effective k' values of the analytes;

(4) that band dispersion should be characterized by stating the HETP or plate number, these being measured in the same way as in liquid chromatography.

Symbols

a	Radius of particle or ion
A	Cross-section of capillary
c	Concentration of electrolyte or micellar material
D	Distribution coefficient between phases
D_m	Diffusion coefficient
E	Electric field strength
F	Faraday constant = 96 500 C mol^{-1}
H	HETP
ΔH	Enthalpy of transfer between phases
i	Electric current along capillary
k'	Capacity factor
L	Length of capillary from injector to detector
N	Number of theoretical plates
R	Resistance per unit length of electrolyte in capillary
	Universal gas constant = 8.314 J K^{-1} mol^{-1}
T	Absolute temperature
t	Migration time
$t_{ion}, t_{mic}, t_n, t_R$	Migration time of ion, micelle, neutral solute, analyte
u	Migration velocity
u_{ion}, u_{mic}	Migration velocity of ion, micelle
u_{eo}, u_{ep}	Electroosmotic velocity, electrophoretic velocity
z	Distance from surface,
z, z_{tot}	Charge on ion (in units of electronic charge), or salt
α	Constant
δ	Double-layer thickness
ε_0	Permittivity of vacuum = $8.85 \cdot 10^{-12}$ C^2 N^{-1} m^{-2}
ε_r	Dielectric constant
ϕ	Phase volume ratio
η	Viscosity
κ	Reciprocal of double-layer thickness
λ	Ionic molar conductivity
Λ	Molar conductivity of salt
μ	Mobility (subscripts as for u)
σ	Standard deviation of peak (in time units)
σ, σ_0	Charge density, standard charge density
ζ	Zeta potential

References

[1] J.W. Jorgenson and K.D. Lukacs, *J. Chromatogr.*, 218 (1981) 209–216.

[2] J.H. Knox and I.H. Grant, *Chromatographia*, 24 (1987) 135–143.

[3] J.H. Knox and I.H. Grant, *Chromatographia*, 32 (1991) 317–328.

[4] T. Tsuda, *Anal. Chem.*, 59 (1987) 521.

[5] S. Terabe, K. Otsuka, K. Ichikawa, A. Tsuchiya and T. Ando, *Anal. Chem.*, 56 (1984) 111–113.

[6] S. Terabe, K. Otsuka and T. Ando, *Anal. Chem.*, 57 (1985) 834–841.

[7] J. O'M. Bockris and A.K.N. Reddy, *Modern Electrochemistry* Plenum Press, New York, 6th ed., 1977.

[8] C.L. Rice and R. Whitehead, *J. Phys. Chem.*, 69 (1965) 4017–4024.

[9] I.H. Grant, personal communication.

ELSEVIER

Journal of Chromatography A, 680 (1994) 15–24

JOURNAL OF CHROMATOGRAPHY A

Use of zwitterionic detergents for the separation of closely related peptides by capillary electrophoresis

Kimberly F. Greve, Wassim Nashabeh, Barry L. Karger*

Barnett Institute, Northeastern University, 341 Mugar Hall, 360 Huntington Avenue, Boston, MA 02115, USA

Abstract

Capillary electrophoresis incorporating hydrophobic selectivity is shown to be a powerful technique for separating closely related peptide species. In this work, hydrophobic interaction was induced through the addition of suitable amounts of a zwitterionic detergent (N-dodecyl-N,N-dimethyl-3-ammonio-1-propanesulfonate) and further modified with organic solvents. A neutral, hydrophilic-coated capillary was used to minimize electroosmotic flow. Two test solutes, Met^{15}- and Leu^{15}-gastrin, were employed to probe hydrophobic selectivity with various electrophoretic conditions. The nature and concentration of the detergent and the organic modifier were varied to adjust the selectivity. Operation near the critical micelle concentration of the zwitterionic detergent in the presence of acetonitrile or various alcohols produced the highest hydrophobic selectivity among the conditions studied. The zwitterionic detergent approach was also briefly compared to the use of non-ionic detergents for hydrophobic selectivity.

1. Introduction

Hydrophobic selectivity is widely used to separate peptides and proteins, e.g. reversed-phase liquid chromatography. Capillary electrophoresis (CE) is a separation technique based on electrophoretic mobility differences among analytes, i.e. charge and mass. The incorporation of hydrophobic selectivity in CE is thus important to broaden the scope of the method for the analysis of peptides and proteins.

Previously, we utilized hydrophobic selectivity in CE for the separation of insulin-like growth factor I (IGF-I) variants through the use of mixed aqueous–organic buffers with various amounts of a zwitterionic detergent [1]. IGF-I is a basic polypeptide composed of 70 amino acid residues with three disulfide bonds. Our work examined five different variants that can be produced in the production of the molecule by recombinant DNA technology. With the modified buffer system, separation of methionine sulfoxide IGF-1 from IGF-1 and IGF-1 from the variant missing the first N-terminal amino acid in its sequence, Gly, was possible. Also, complete identification of all variants was achieved with on-line CE–electrospray mass spectrometry (MS). Since a coated capillary was employed, the neutral zwitterionic buffer modifiers did not enter the mass spectrometer and thus did not provide interference in peak detection or identification.

Traditionally, micellar electrokinetic chromatography (MEKC) [2] has been used for separating neutral, low-molecular-mass compounds by differential partitioning between a micellar phase

* Corresponding author.

0021-9673/94/$07.00
SSDI 0021-9673(94)00629-6

and an aqueous buffer phase in CE. The surfactants aggregate to create a pseudo-stationary phase for solute–surfactant interactions *via* hydrophobic, electrostatic, hydrogen bonding, or a combination of these forces. Neutral solutes migrate in order of increasing hydrophobic character, whereas ionic species separate on the basis of a combination of mass-to-charge ratio, hydrophobic character and, in some cases, ion pairing with a charged detergent [3]. Separation of peptides and small proteins that differ in hydrophobicity by MEKC has met with some limited success [4–8].

Most of the above studies used charged surfactants. On the other hand, we have focused on zwitterionic detergents to create hydrophobic selectivity. As with non-ionic detergents, zwitterionic detergents allow pH or ionic strength variation of the running buffer over a wide range of conditions without drastic effects on the properties of the detergent. Secondly, such detergents do not contribute to the solution conductivity, permitting the use of high electric fields without excessive heating of the capillary. Thirdly, these detergents should not, in principle, alter the net charge of the analytes to which they are bound. Finally, these detergents do not, in general, induce biopolymer denaturation.

The purpose of this article is to explore further the zwitterionic detergent approach utilized for the IGF-I variants. Closely related peptides, namely Met^{15}- and Leu^{15}-gastrin; Ala^{1}- and Tyr^{1}-somatostatin; and Met^{13}- and Leu^{13}-motilin were used as test solutes (see Fig. 1 for sequences). The effect of a wide range of operating conditions including the nature and concentration of the organic modifiers as well as the zwitterionic detergent on separation was studied. As previously described, coated capillaries were utilized to minimize electroosmotic flow and thus to be able to determine directly the influence of buffer additives on the electrophoretic mobility of the analytes. It was found that operation near the critical micelle concentration (CMC) of the

Met^{15}-Gastrin I (human) 17 amino acids
pGlu-Gly-Pro-Trp-Leu-Glu-Glu-Glu-Glu-Glu-Ala-Tyr-Gly-Trp-**Met**-Asp-PheCOONH$_2$
Leu^{15}-Gastrin I (human) 17 amino acids
pGlu-Gly-Pro-Trp-Leu-Glu-Glu-Glu-Glu-Glu-Ala-Tyr-Gly-Trp-**Leu**-Asp-PheCOONH$_2$

Ala^{1}-Somatostatin 14 amino acids
Ala-Gly-Cys-Lys-Asn-Phe-Phe-Trp-Lys-Thr-Phe-Thr-Ser-Cys

Tyr^{1}-Somatostatin 14 amino acids
Tyr-Gly-Cys-Lys-Asn-Phe-Phe-Trp-Lys-Thr-Phe-Thr-Ser-Cys

Met^{13}-Motilin (porcine) 22 amino acids
Phe-Val-Pro-Ile-Phe-Thr-Tyr-Gly-Glu-Leu-Gln-Arg-**Met**-Gln-Glu-Lys-Glu-Arg-Asn-Lys-Gly-Gln
Leu^{13}-Motilin (porcine) 22 amino acids
Phe-Val-Pro-Ile-Phe-Thr-Tyr-Gly-Glu-Leu-Gln-Arg-**Leu**-Gln-Glu-Lys-Glu-Arg-Asn-Lys-Gly-Gln

Ile^{5}-Angiotensin II (human) 8 amino acids
Asp-Arg-Val-Tyr-**Ile**-His-Pro-Phe
Val^{5}-Angiotensin II (human) 8 amino acids
Asp-Arg-Val-Tyr-**Val**-His-Pro-Phe

Fig. 1. Peptide sequences.

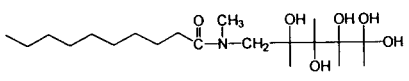

A. MEGA 10

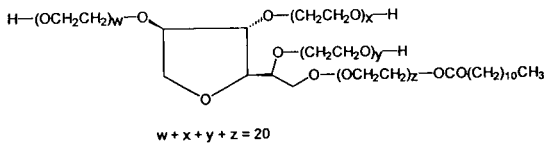

B. TWEEN 20

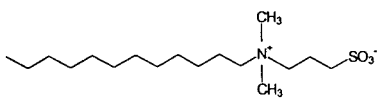

C. DAPS

Fig. 2. Structures of detergents used for this work: (A) MEGA 10 (decanoyl-N-methylglucamide); (B) Tween 20; (C) DAPS (N-dodecyl-N,N-dimethyl-3-ammonio-1-propanesulfonate).

zwitterionic detergent with addition of small amounts of organic modifier provided a highly selective separation of the acidic and basic peptides differing by a single neutral amino acid residue. The use of non-ionic detergents at relatively moderate concentrations will also be briefly discussed. Fig. 2 provides the structures of the detergents studied in this work.

2. Experimental

2.1. CE instrumentation and methods

A Beckman P/ACE instrument, version 2100 (Beckman, Palo Alto, CA, USA) was used. System Gold version 7.11 controlled the instrument. The electropherograms were monitored at 214 nm with a data collection rate of 10 Hz. A 75 μm I.D. $\times$ 375 μm O.D. fused-silica capillary (Polymicro Technologies, Phoenix, AZ, USA) was coated with a polyvinylmethylsiloxane sublayer and then a layer of polyacrylamide [9]. The capillary, with an effective length of 40 cm and a total length of 47 cm, was kept at a constant temperature of 25°C, and stored in water overnight. A chromatographic software package, Chrom Perfect, was employed to compare and reanalyze electropherograms (Justice Innovations, Palo Alto, CA, USA).

To ensure reproducible separations, the capillary column was purged with fresh buffer for 3 min before each injection. Stock solutions of buffer, detergent, and organic solvent were combined to form the running buffer daily. The pH of the buffer was only adjusted if the organic content was over 20% (v/v).

2.2. Reagents and materials

Samples were obtained from Sigma (St. Louis, MO, USA): Met^{15}- and Leu^{15}-gastrin, Met^{13}- and Leu^{13}-motilin and Ala^{1}- and Tyr^{1}-somatostatin. The detergents, N-dodecyl-N,N-dimethyl-3-ammonio-1-propanesulfonate (DAPS), decanoyl-N-methylglucamide (MEGA 10), and Tween 20 were purchased from Calbiochem (San Diego, CA, USA). Analytical-grade buffer materials [N-tris(hydroxymethyl)methyl-3-aminopropanesulfonic acid (Taps), 2-amino-2-(hydroxymethyl)-1,3-propanediol (Tris), ϵ-amino-*n*-caproic acid (ϵACA) and acetic acid] as well as bromophenol blue were purchased from Sigma. HPLC-grade acetonitrile (ACN) and ethanol were obtained from J.T. Baker (Phillipsburg, NJ, USA); methanol, isobutanol and 1-butanol were purchased from Fisher Scientific (Fairlawn, NJ, USA); propanol was obtained from EM Science (Cherry Hill, NJ, USA) and isopropanol from Fluka (Ronkonkoma, NY, USA). Milli-Q water (18.2 MΩ water; Millipore, Bedford, MA, USA) was employed to prepare all buffer and sample solutions. All buffers were filtered with a 0.2-μm pore-size filter (Schleicher and Schuell, Keene, NH, USA) before use.

2.3. CMC determination

CMC measurements were made by determining the absorption of a dye, bromophenol blue (8.3 m*M*), that interacts with the micelle as a function of the concentration of the surfactant [10–12]. The spectra of the solutions were taken

with a Beckman DU-60 spectrophotometer using a wavelength range of 560 to 620 nm and a scan speed of 500 nm/min. The maximum wavelength values were recorded and plotted versus the detergent concentration. The concentration at which a sharp transition occurred in the λ_{max} of bromophenol blue (dye interacting with the detergent) was taken as the CMC.

3. Results and discussion

3.1. Zwitterionic detergent

In order to examine hydrophobic differences between peptides, two test solutes, Met^{15}- and Leu^{15}-gastrin (Fig. 1), were chosen because of their identical peptide sequence except for the one neutral amino acid substitution. An unsuccessful attempt to separate the peptides using a polyvinylmethylsiloxane–polyacrylamide-coated capillary with a buffer of 20 m*M* Taps–Tris pH 8.0 was made. Since the gastrins did not separate, a system which incorporated an added hydrophobic selectivity was deemed necessary.

The zwitterionic detergent, DAPS (Fig. 2), at concentrations at and above the CMC was chosen for this additional selectivity. At 5 m*M*, Fig. 3A (the CMC is 3.7 m*M* in aqueous solution, see Table 1), some shouldering in the peak as well as broadening and peak tailing was observed. Further increases in the detergent concentration resulted in a single peak being obtained, e.g. 20 m*M* (Fig. 3B). Concentrations up to 50 m*M* DAPS were investigated, and still no separation was observed. Since detergent alone was unsuccessful in separating the species, addition of small amounts of organic modifiers

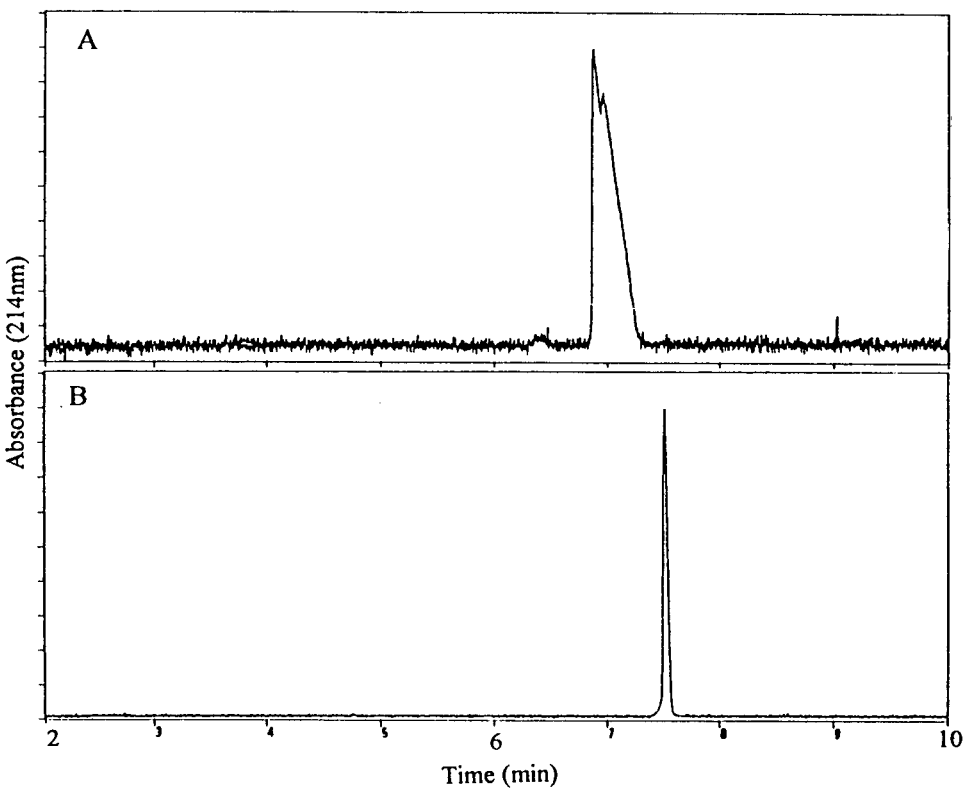

Fig. 3. Separation of Met^{15}- and Leu^{15}-gastrin with several concentrations of DAPS: (A) 5 m*M*, 9 μA, (B) 20 m*M*, 8 μA; running voltage, 30 kV; 20 m*M* Tris–Taps, pH 8.0. Other conditions are as in the Experimental section.

Table 1
CMC Values for DAPS

Buffer	pH	Organic (%, v/v)	Organic type	CMC (m*M*)
20 m*M* Taps–Tris	8.0	0		3.7
20 m*M* Taps–Tris	8.0	10	ACN	5.0
20 m*M* Taps–Tris	8.0	20	ACN	26.3
20 m*M* Taps–Tris	8.0	30	ACN	60.5
20 m*M* Taps–Tris	8.0	10	Isopropanol	3.5
20 m*M* Taps–Tris	8.0	10	Propanol	3.1
20 m*M* Taps–Tris	8.0	20	Propanol	14.7
20 m*M* β-alanine–citric acid	3.8	2.5	Butanol	2.6

Note: at different pH values the change in CMC was negligible. The CMC in water is 2–4 m*M*.

was tested, based on the results of our previous work [1]. As shown in Fig. 4, the inclusion of 10% (v/v) ACN in the background electrolyte, under otherwise identical conditions to that in Fig. 3A, resulted in baseline separation of the two test solutes. The migration order of the analytes is based on the hydrophobic differences, i.e. the more hydrophobic Leu^{15}-gastrin migrates slower. The analytes presumably interacted differentially with the zwitterionic detergent, and the addition of the small amount of acetonitrile likely affected the extent of that interaction. It is worthwhile to note that the conditions in Fig. 4 are similar as those used to resolve the IGF-I variants [1].

Control experiments were performed to determine if the organic modifier could independently (in the absence of detergent) affect the selectivity of the system. Up to 20% (v/v) ACN was added to the aqueous buffer and still no separation was obtained with the gastrins, although a slight increase in migration time was observed. *n*-Alcohols (methanol through 1-butanol) were also investigated, with no separation observed. Therefore, since the results in Fig. 4 must include the combination of the zwitterionic detergent and organic modifier, the concentration of the detergent as well as the type and amount of the organic modifier were explored further.

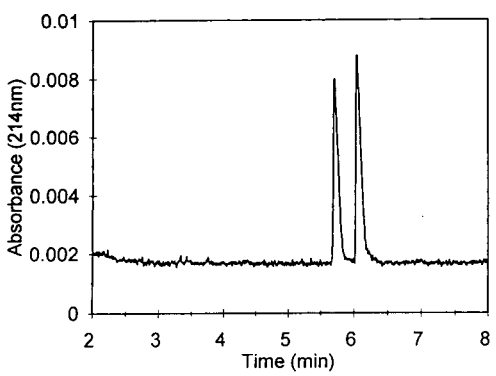

Fig. 4. Complete separation of Met^{15}- and Leu^{15}-gastrin using 10% ACN and 5 m*M* DAPS. All other conditions as in Fig. 3.

With 10% (v/v) ACN, the concentration of hydrophobic selector was varied from 0 to 70 m*M* (Fig. 5). Little or no separation was observed at low and very high DAPS concentrations, but an optimum separation was achieved at moderate concentrations. Relative mobilities, or selectivity, of the two gastrins as a function of DAPS are shown in Fig. 6. A bell-shaped curve is obtained at 10% ACN with an abrupt maximum around the CMC value of DAPS (5 m*M*, see Table 1). Optimum selectivity at 20% ACN was also observed around the CMC (26 m*M*) with a slow reduction in selectivity at higher organic modifier concentrations, ultimately leading to no separation. These plots suggest that the interaction of the analytes with the micelles may be non-selective, because increases in the micelle concentration reduced selectivity. It should be

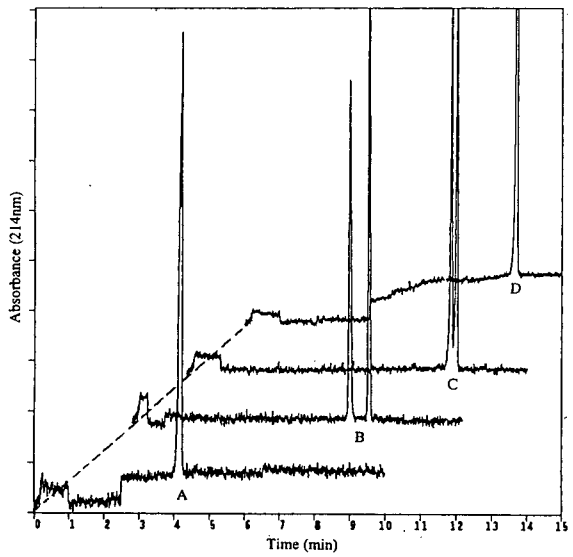

Fig. 5. Electropherograms of the gastrins at constant organic percentage and various DAPS concentrations: (A) 3.5 m*M*, (B) 7.5 m*M*, (C) 20 m*M*, (D) 70 m*M*. All other conditions as in Fig. 3.

noted that at concentrations beyond the CMC, the amount of free detergent remained fixed while the concentration of micelles increased. As discussed previously, it would appear that solute-free zwitterionic detergent interactions are hydrophobically selective. Addition of higher concentrations of DAPS beyond the CMC may simply have increased the relative extent of the non-selective micelle interaction at the expense of the free detergent selective interaction. The lower maximum in the selectivity at 20% (v/v) ACN in comparison to 10% (v/v) ACN and the broad peak may simply reflect weaker hydrophobic interactions with the higher organic composition.

Fig. 7 displays peptide mobility as a function of the detergent concentration at 10 and 20% ACN. With 10% ACN, a sharp change in the mobility is again observed in contrast to 20% ACN. Since the CMC increased upon the addition of organic, more free detergent molecules may be present to interact with the analytes (Table 1: CMC is 5 m*M* with 10% ACN vs. 3.7 m*M* in buffer alone). Furthermore, it appears that the ACN modulates the extent of interaction of DAPS with the peptide to yield optimum selectivity in Fig. 6. At 20% ACN, a gradual decrease in the electrophoretic mobility was obtained with increasing DAPS concentration, eventually approaching the maximum mobility found with 10% ACN. Fig. 7 suggests that the interaction of the analytes with the

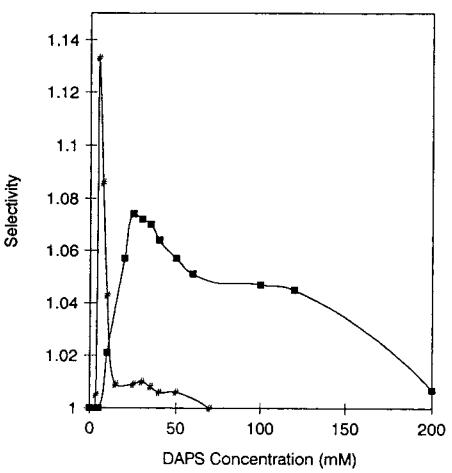

Fig. 6. Effect of detergent concentration at 10% ACN (#) and 20% ACN (□) on selectivity (migration time ratio of Leu^{15}-gastrin/Met^{15}-gastrin). All other conditions as in Fig. 3.

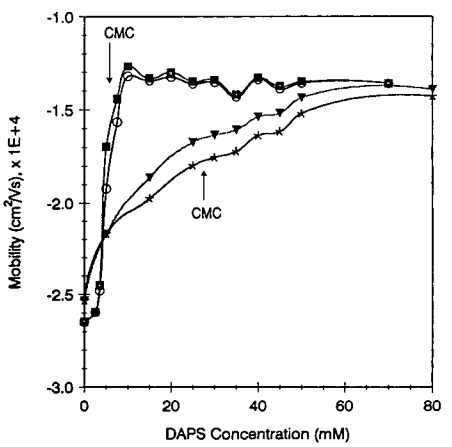

Fig. 7. Effect of detergent concentration at constant organic percentage on the electrophoretic mobility of gastrins. All other conditions as in Fig. 3. ○ = 10% ACN, Met^{15}-gastrin; □ = 10% ACN, Leu^{15}-gastrin; * = 20% ACN, Met^{15}-gastrin; ▼ = 20% ACN, Leu^{15}-gastrin.

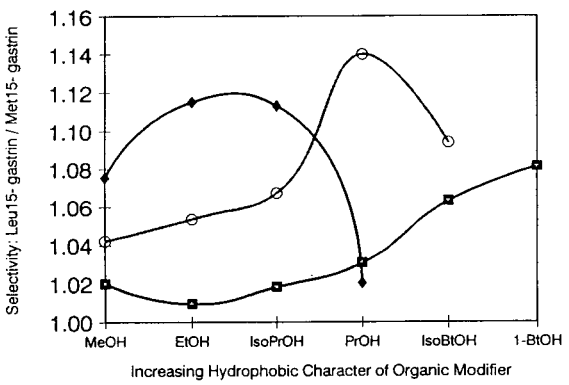

Fig. 8. Effect of organic modifier at constant detergent concentration (□ = 5%; ○ = 10%; ◆ = 20%). Plot of selectivity vs. nature of organic modifier. All other conditions are as in Fig. 3.

micelles is weaker than the free detergent (monomer form).

In our previous report [1], the type of organic modifier was shown to have an effect on the selectivity of the small, closely related IGF-I variants. For example, improved resolution was obtained when the separation of des(Gly)-IGF-I from IGF-I was performed using 1-butanol, relative to ACN. To explore further the role of the organic modifier in manipulating selectivity, CMC measurements of DAPS in the presence of various organic modifiers were first performed. Table 1 shows that ACN disrupts micelle formation regardless of the ACN percentage, as the CMC rapidly increases with concentration of ACN, e.g. 26.3 m*M* for 20% and 60.5 for 30% ACN. Also, low percentages of *n*-alcohols (e.g. propanol and 1-butanol) facilitate micelle formation (i.e. decrease CMC to 3.1 or 2.6 m*M*, respectively) and high percentages (e.g. propanol) reduce micelle formation (i.e. CMC increases to 14.7 m*M*). These results for short-chain alcohols agree with literature findings [13].

We next examined the separation of the gastrins using alcohol modifiers of increasing carbon chain length (i.e. increasing hydrophobic character, methanol through 1-butanol) at a fixed concentration of DAPS, 5 m*M*. In all cases complete separation was achieved near the CMC for each system. Fig. 8 displays a plot of selectivity vs. organic modifier, and Table 2 shows the selectivity vs. the percent of organic modifier at a fixed concentration of DAPS, again 5 m*M*. Increased hydrophobic character (increasing carbon number) of the alcohol shifted the maximum selectivity to lower organic percentages [i.e. 20% (v/v) for ethanol, 12% (v/v) for propanol and 7% (v/v) for isobutanol]. This trend may be related to the reduction of the CMC with increasing chain length of the alcohol (Table 1). At high percentages [greater than 15% (v/v) organic], short-carbon-chain alcohols display bet-

Table 2
Effect of organic modifier at 5 m*M* DAPS

	Selectivity values for Leu[15]-/Met[15]-gastrin								
	Organic (%)								
	2	5	7	10	12	15	20	25	30
ACN	1.01	1.03	1.035	**1.13**	1.037	1.035	1		
MeOH	1.02	1.02	1.05	1.04	1.05	**1.09**	1.08	1.04	1.00
EtOH	1.03	1.01	1.05	1.05	1.06	1.09	**1.12**	1.07	1.02
IsoPrOH	1.02	1.02	1.04	1.07	1.09	**1.12**	**1.11**	1.02	1.01
PrOH	1.02	1.03	1.06	1.14	**1.18**	1.13	1.02		
IsoBtOH	1.03	1.06	**1.13**	1.09					
1-BtOH[a]	1.03	1.08	**1.14**						

Values in bold are maximum values. Bt = Butyl.
[a]1-Butanol will not dissolve at 10%.

ter selectivity than longer-chain alcohols, and at low percentages (less than 7%, v/v) of organic solvent, the opposite is true. As for ACN, the maxima in selectivity occur close to the CMC.

Since the chosen zwitterionic detergents are insensitive to changes in pH, successful hydrophobic-based separation can also be observed at low pH. A pH 4.4 buffer using DAPS was used to separate a mixture of four acidic peptides, Ala^{1}- and Tyr^{1}-somatostatin and Met^{13}- and Leu^{13}-motilin (Fig. 1). The somatostatin peptides contain 14 amino acids with a disulfide bond between the third and the last cysteine amino acids, whereas the motilins are 22 amino acids long. Each pair of peptides have similar mass-to-charge ratios and only differ by one neutral, amino acid in their sequence. Separation of the four acidic peptides (Fig. 9) was made possible through the use of 20 m*M* ϵACA–acetic acid, pH 4.4, modified with 5 m*M* DAPS with either 15% ACN or 5% 1-butanol. The peptides could not be separated without the zwitterionic detergent. Furthermore, the selectivity of the motilins was higher when using 1-butanol as the organic modifier. Fig. 9 demonstrates again that the zwitterionic detergent system with small amounts of organic modifier can be used to resolve peptides that differ in hydrophobicity.

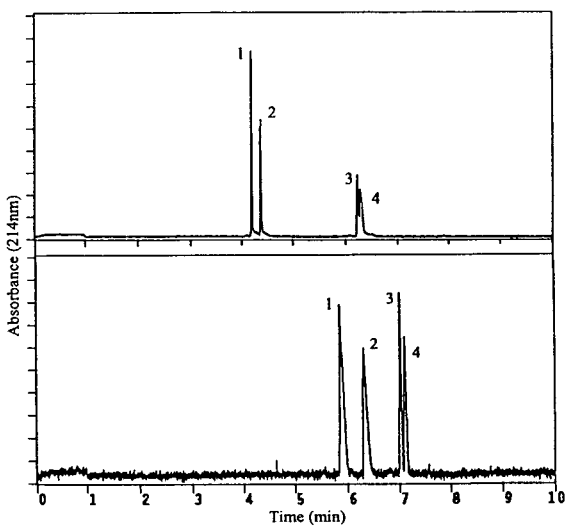

Fig. 9. Separation of Met^{13}- and Leu^{13}-motilin and Ala^{1}- and Tyr^{1}-somatostatin. Coated capillary: 37 cm (30 cm effective length) × 75 μm I.D.; running voltage 30 kV; detection at 214 nm; 25°C; buffer, 20 m*M* ϵACA–acetic acid, pH 4.4 with (top) 15% ACN and 5 m*M* DAPS and (bottom) 5% 1-butanol and 5 m*M* DAPS. Peaks: 1 = Ala^{1}-somatostatin; 2 = Tyr^{1}-somatostatin; 3 = Met^{13}-motilin; 4 = Leu^{13}-motilin. See Fig. 1 for amino acid sequence.

3.2. Neutral detergents

Neutral detergents can be used as an alternative to the zwitterionic detergents for hydrophobic selectivity. MEGA 10 (Fig. 1) was previ-

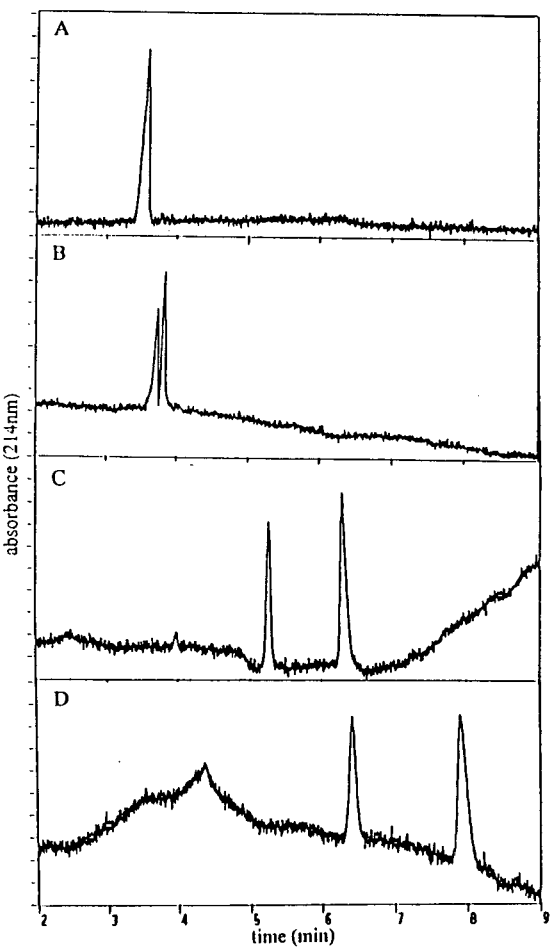

Fig. 10. Separation of Met^{15}- and Leu^{15}-gastrin using MEGA 10. Coated capillary: 47 cm (40 cm effective length) × 75 μm I.D.; running voltage 30 kV; detection at 214 nm; 25°C; buffer, 20 m*M* Taps–Tris pH 8.0 containing various amounts of MEGA 10: (A) 5 m*M*, (B) 10 m*M*, (C) 30 m*M*, (D) 50 m*M*.

ously used in MEKC as an anionic-borate complex for the separation of neutral and charged herbicides [14]. For our purposes, a coated capillary that eliminated electroosmotic flow and reduced analyte adsorption was again utilized in conjunction with MEGA 10 to separate closely related peptides (Fig. 10). The hydrophobic interaction imparted by this neutral detergent allows complete separation of the closely related peptides, Met^{15}- and Leu^{15}-gastrin above the CMC. (The CMC of MEGA 10 is 16.9 m*M* at pH 8.) In contrast to DAPS, increasing the concentration of MEGA 10 above the CMC improves separation, suggesting that the micelle partitioning may be selective. The problem with using MEGA 10 as the surfactant, however, is the unstable baseline at 214 nm due to the UV absorbance of the amide bond in the detergent. In an attempt to lower the amount of detergent needed for the separation, organic modifiers were investigated. This approach was not successful, in that addition of 10% ACN to 30 m*M* MEGA 10 decreased the selectivity of the two analytes, and 10% ACN with 10 m*M* MEGA 10 resulted in no separation.

Another neutral detergent that has been previously used is Tween 20 (Fig. 2), which allowed separation of closely related angiotensin II and motilin peptides using a bare silica capillary [5]. It was found that Tween 20 required quite high concentrations (80–250 m*M*, well above the CMC of 100 μM) to obtain the proper selectivity of peptides. This can be contrasted with the zwitterionic detergent used in this work where ca. 5 m*M* was sufficient for separation.

4. Conclusions

Hydrophobic selectivity is an important separation factor for peptide and protein species. In general, CZE with simple buffer systems is inadequate for the separation of closely related peptides having similar mass-to-charge ratios. Therefore, incorporating a hydrophobic mechanism into CE is important for its application to protein chemistry. Separation of closely related peptides that differ in hydrophobicity can be achieved under mild conditions using low concentrations of organic modifier and zwitterionic detergent, such as DAPS. Optimum selectivity is generally observed in the region of the CMC of DAPS in the presence of organic modifiers. Comparisons of relative mobilities of the gastrins suggest that the interaction of the micelles with the analytes may be non-selective, because increases in the micelle concentration did not improve the selectivity of the analytes. To enable the separation of a wide variety of species, the selectivity can be adjusted by varying the nature and concentration of the organic modifier as well as the concentration of the zwitterionic detergent. Using a coated capillary with no electroosmotic flow enhances reproducibility and makes the system simple to manipulate since additives to the buffer will only affect electrophoretic mobility and not simultaneously influence electroosmotic flow, as found, with bare silica [15]. An alternative approach to the use of zwitterionic detergents with organic modifiers is nonionic detergents depending on the sample and the overall separation desired of the closely related peptide species. Also, organic modifiers and zwitterionic detergents in conjunction with coated capillaries are compatible with on-line electrospray MS, since the detergent does not migrate into the mass spectrometer [1]. A more detailed report of the use of detergents with MS will be published separately [16].

Acknowledgement

The authors gratefully acknowledge support of the NIH under GM15847. Contribution No. 605 from the Barnett Institute.

References

[1] W. Nashabeh, K.F. Greve, D. Kirby, D.H. Reifsnyder, S. Builder, F. Foret and B.L. Karger, *Anal. Chem.*, 66 (1994) 2148.

[2] S. Terabe, K. Otsuda, K. Ichikawa, A. Tsuchiya and T. Ando, *Anal. Chem.*, 56 (1984) 111.

[3] M.G. Khaledi, in J.P. Landers (Editor), *Handbook of Capillary Electrophoresis*, CRC Press, Boca Raton, FL, 1993, pp. 43–93.
[4] H.K. Kristensen and H. Hansen, *J. Liq. Chromatogr.*, 16 (1993) 2961.
[5] N. Matsubara and S. Terabe, *Chromatographia*, 34 (1992) 493.
[6] M.A. Strege and A.L. Lagu, *Anal. Biochem.*, 210 (1993) 402.
[7] H. Gaus, A.G. Beck-Sichinger and E. Bayer, *Anal. Chem.*, 65 (1993) 1399.
[8] T. Yashima, A. Tsuchiya, O. Morita and S. Terabe, *Anal. Chem.*, 64 (1992) 2981.
[9] D.K. Schmalzing, C.A. Piggee, F. Foret, E. Carrilho and B.L. Karger, *J. Chromatogr A*, 652 (1993) 149.
[10] S. Hjertén, L. Valtcheva, K. Elenbring and D. Eaker, *J. Liq. Chromatogr.*, 12 (1989) 2471.
[11] P. Mukerjee and K.J. Mysels, in *Critical Micelle Concentrations of Aqueous Surfactant Systems; NSRDS-NBS 36*, US Goverment Printing Office, Washington, DC, 1971, pp. 1–21.
[12] B.V. Normand and J. Eiselé, *Anal. Biochem.*, 208 (1993) 241.
[13] W.L. Hinze, in W.L. Hinze and D.L. Armstrong (Editors), *Ordered Media in Chemical Separations*, American Chemical Society, Washington, DC, 1987, pp. 6–9.
[14] J.T. Smith, W. Nashabeh and Z. El Rassi, *Anal. Chem.*, 66 (1994) 1119.
[15] G. Frosberg, G. Palm, A. Ekebacke, S. Josephson and M. Hartmanis, *Biochem. J.*, 271 (1990) 375.
[16] D. Kirby, K.F. Greve, W. Nashabeh, F. Foret, P. Vouros and B.L. Karger, presented at the *42nd ASMS Conference on Mass Spectrometry, Chicago, IL, 29 May–3 June 1994*, poster No. 124.

ELSEVIER

Journal of Chromatography A, 680 (1994) 25–31

JOURNAL OF CHROMATOGRAPHY A

Wall adsorption of small anions in capillary zone electrophoresis induced by cationic trace constituents of the buffer

B. Gassner, W. Friedl, E. Kenndler*

Institute for Analytical Chemistry, University of Vienna, Währingerstr. 38, A-1090 Vienna, Austria

Abstract

Fe(III), present as a trace constituent in the buffer, induces wall adsorption of small anions in coated and uncoated fused-silica capillaries even in the ppb concentration range. For di- and tribasic benzoates, drastic adsorption effects were found when the carboxylate groups were in an *ortho* position, leading to severely tailing peaks and a lower reproducibility of migration times. Benzoates with carboxylate groups in 1,3- or 1,4-positions were less affected than the *ortho* derivatives. The adsorption of the anions is related to Fe(III) attached to the capillary wall.

1. Introduction

In capillary zone electrophoresis (CZE), highly reproducible migration times and peak shapes can be obtained with the presumption that the measurements are carried out under controlled conditions. Many effects may influence the electrophoretic behaviour of the separands, but the reproducibility can be affected most unpredictably by adsorption effects at the capillary wall. This is caused by the fact that the inner surface often changes its state not only from run to run, but even during one run. Although advanced theories on adsorption phenomena in CZE have already been formulated [1–5], the behaviour of the system is difficult to predict, because the values of the adsorption–desorption isotherms or rate constants, parameters which are necessary for accurate calculation, are unknown in nearly all instances.

Although adsorption is the usual principle for HPLC separations, it is not desirable in CZE. However, it is often observed with biopolymers such as proteins, which can exhibit different interactions, both hydrophobic and Coulombic attraction. The latter takes place between positively charged analytes and the negatively charged sites on the fused-silica surface (see, *e.g.*, ref. 6). In contrast, such behaviour is uncommon for small and negatively charged ions such as aromatic carboxylates, the separands on which this paper is focused. These anions are normally not adsorbed under the pH conditions where they are formed, because the silanol groups of the fused-silica surface (also weak acids) are in that case also negatively charged. Hence, a high reproducibility of the migration times can be obtained for these solutes, especially when the electroosmotic flow is suppressed. In

* Corresponding author.

0021-9673/94/$07.00
SSDI 0021-9673(94)00181-8

this instance the precision of the migration times, expressed by the resulting relative standard deviation, is in the range of a few tenths of a percent.

This was in fact the case during our investigations concerning the prediction of the optimum pH of the buffer as described in previous papers [7,8]. Strong deviations occurred, however, in some instances, which were unexpected and unusual for such systems. They could be related to adsorption of the separands induced by higher charged cationic constituents present at trace concentrations in the buffer.

This paper reports on a systematic investigation of the source and the magnitude of these adsorption effects in CZE. Such effects limit the applicability of particular ions to adjust the electrophoretic selectivity by secondary equilibria in the solution, *e.g.*, due to complexation reactions.

2. Experimental

2.1. Reagents

Chemicals used for the preparation of the buffer (sodium acetate, 0.01 mol/l) were acetic acid and sodium hydroxide; $FeCl_3$ and $CaCl_2$ were added to the buffer (all of analytical-reagent grade from Merck, Darmstadt, Germany). The following compounds were used as test substances, each at a concentration of 0.02 mg/ml in water: 1,2-benzenedicarboxylic acid, 1,3-benzenedicarboxylic acid and 1,2,4-benzenetricarboxylic acid (all 99%; Aldrich, Steinheim, Germany), 1,4-benzenedicarboxylic acid and 1,3,5-benzenetricarboxylic acid (both 98%; Aldrich), 1,2,3-benzenetricarboxylic acid dihydrate (98%; Fluka, Buchs, Switzerland).

For the coating procedure, methylcellulose (Methocel MC, 3000–5000 mPa s; Fluka) was cross-linked using formic acid and formaldehyde (both of analytical-reagent grade; Merck). Water was distilled twice from a quartz apparatus.

2.2. Apparatus

The instrument used for the measurements was a P/ACE System 2100 (using System Gold 6.01 software) (Beckman, Palo Alto, CA, USA) equipped with a UV absorbance detector. The absorbance was measured at 214 nm at the anode side of the capillary. The separation capillary was made from 75 μm I.D. fused silica (Scientific Glass Engineering, Ringwood, Australia). The total length was 0.269 m and the effective length (the distance from the injector to the detector) was 0.202 m. The capillary was thermostated at 25.0°C. Electrophoresis was carried out either with or without electroosmotic flow at a total voltage of 5000 V (field strength 18 600 V/m), leading to an effective potential drop of 3750 V along the migration distance from the injector to the detector.

Injection of the sample was carried out by pressure for 1 s from pure aqueous solution. Between the runs the capillary was rinsed with buffer for 5 min. The coating procedure described by Hjertén [9] was applied.

3. Results and discussion

Electropherograms, which were measured for the experimental evaluation of the theoretical prediction of the resolution as a function of the pH of the buffer, described in a previous paper [8], are presented in Fig. 1 for the solutes given in Table 1. It was found that they were highly reproducible under controlled conditions also in the long term, namely over several months, even with different capillaries (see Fig. 1a). Migration times were obtained within a deviation of less than 1%, and the peak shapes remained nearly identical.

During this investigation the reproducibility was, however, found to be drastically reduced in one series, leading to large variations in migration times and changes of peak shapes. One example of this effect is shown in Fig. 1b. The substantial peak tailing indicated the presence of adsorption effects.

Based on the large number of deviating electropherograms, a certain tendency could be derived with respect to the extent of peak tailing and shift of migration times: those components with carboxylic functions in an *ortho* position seemed to exhibit the strongest effects (see, *e.g.*,

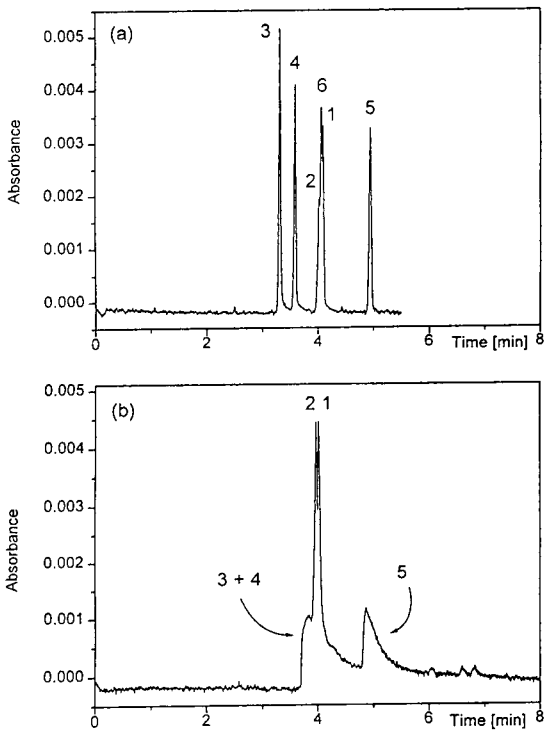

Fig. 1. Typical electropherograms of the test benzenecarboxylates in coated capillaries at pH 5.03: (a) representative of the long-term reproducibility; (b) with deviations of migration times and peak shapes obtained with a buffer having enhanced Fe^{3+} and Ca^{2+} contents. Numbering of the separands according to Table 1. Conditions: sodium acetate buffer, 0.01 mol/l; coated fused-silica capillary (75 μm I.D., total length 0.269 m, effective length 0.202 m); total voltage, 5000 V; effective potential drop, 3750 V; detector located on the anode side of the capillary.

Table 1
Separands investigated

No.	Separand (benzenecarboxylic acid)	No. of *ortho* positions
1	1,3-Dicarboxylic	0
2	1,4-Dicarboxylic	0
3	1,3,5-Tricarboxylic	0
4	1,2,4-Tricarboxylic	1
5	1,2-Dicarboxylic	1
6	1,2,3-Tricarboxylic	2

Fig. 1b). This led us to the presumption that the interaction with some cationic species attached to the wall is possibly operative, probably favoured by the formation of a ring that stabilizes the adduct. In the following investigations, the test solutes were therefore subdivided into two groups: (i) with substituted carboxylic groups in non-*ortho* positions and (ii) with one or two *ortho*-substituted carboxylic functions (see Table 1).

To clarify the origin of these effects, a number of instrumental and chemical parameters were varied. As a result of the systematic investigation of all the sources possibly involved, it was found that the replacement of the sodium hydroxide stock solution used hitherto with a freshly prepared solution led again to the highly reproducible electropherograms that we were used to obtaining.

Based on this result, an analysis of a number of inorganic components in the sodium hydroxide solution used so far was carried out by atomic emission spectrometry with an inductively coupled plasma (ICP), which gave an enhanced content of iron and calcium, namely about 800 ppb of Fe and 1 ppm of Ca, which is at least three orders of magnitude higher than that specified by the manufacturer. The origin of those traces is unknown to us. Possibly the solution was contaminated from the glassware used during the long-term manipulations.

The effect of these two cations as buffer trace constituents on the electrophoretic behaviour of the analytes was therefore investigated in more detail. All these effects were originally observed in coated capillaries, but both types of capillary surfaces, coated and uncoated, were subjected to the following investigations.

3.1. Coated capillaries

Electropherograms obtained in coated capillaries with suppressed electroosmotic flow are shown in Figs. 2 and 3 for different concentration levels of Fe^{3+} and Ca^{2+}. In pure buffer (indicated by zero iron and calcium, respectively) all separands show fairly symmetrical peaks. Whereas the peak shapes remain almost symmetrical on addition of Ca^{2+} to the buffer

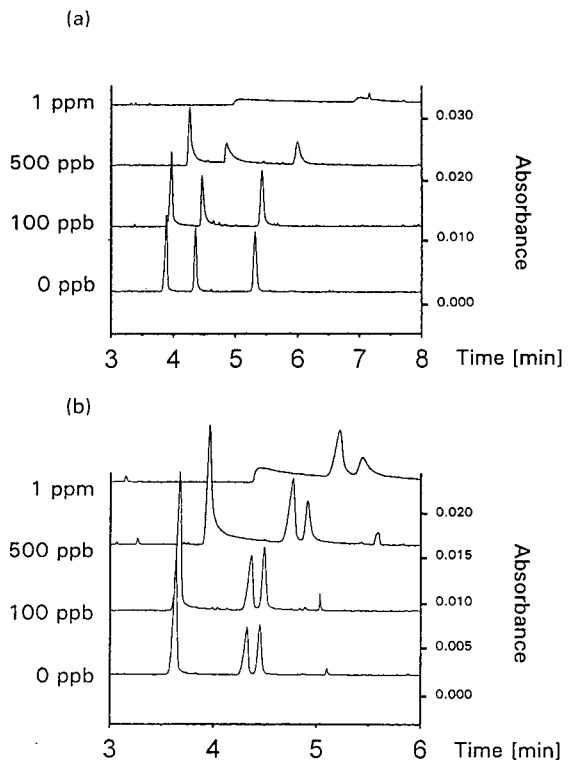

Fig. 2. Electropherogram of (a) *ortho*-substituted and (b) non-*ortho*-substituted benzenecarboxylic acids in a coated fused-silica capillary at different concentrations of Fe^{3+} in the buffer electrolyte solution at pH 4.50. Migration sequence of separands: (a) **4**, **6**, **5**; (b) **3**, **2**, **1** (numbering according to Table 1). Conditions as in Fig. 1.

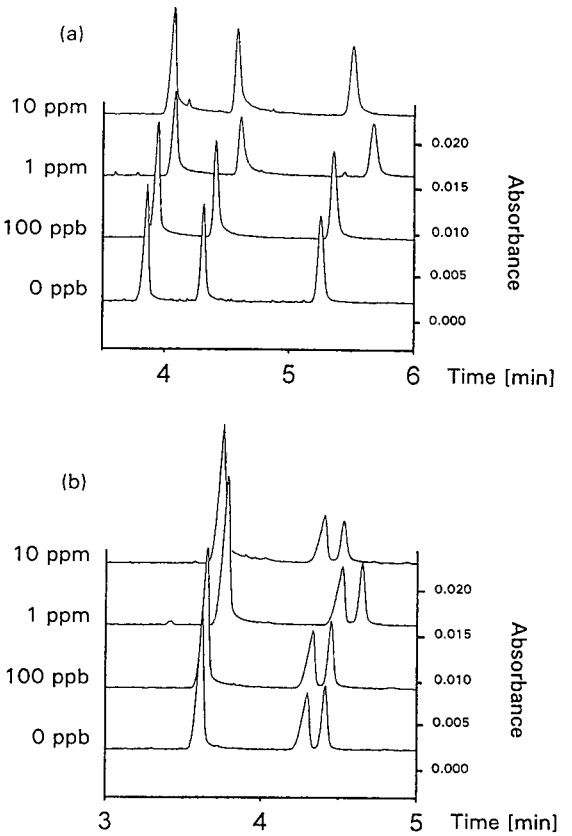

Fig. 3. Electropherogram of (a) *ortho*-substituted and (b) non-*ortho*-substituted benzenecarboxylic acids in a coated fused-silica capillary at different concentrations of Ca^{2+} in the buffer electrolyte solution at pH 4.50. Migration sequence of separands as in Fig. 2. Conditions as in Fig. 1.

even up to 10 ppm (w/w) (with the occurrence of only a slight tailing for components **4** and **6**), a very different situation arises when Fe^{3+} is added: even at 100 ppb (w/w) the peaks of the two first migrating ortho-substituted separands (**4** and **6**, Fig. 2a) tail significantly, and at 1 ppm of Fe^{3+} the peaks are so distorted that only two of them can be recognized in the electropherogram. The increase in tailing is accompanied by the retardation of the separands, leading to an increase in retention times.

It follows from Fig. 2b that the non-*ortho* derivatives undergo this adsorptive effect to a much smaller extent. At least the peaks of components **2** and **1** remain nearly symmetrical even up to 1 ppm of Fe^{3+}. As Ca^{2+} seems to have only a minute effect on solute adsorption, the further discussion is focussed on Fe^{3+}.

In Fig. 4 the electropherograms of three subsequent injections of the *ortho*-substituted solutes is shown for two different Fe^{3+} concentrations. From the similar shape of the electropherograms it can be assumed that steady conditions concerning the attachment of the Fe species on the solid capillary surface are established for a given concentration of Fe in the buffer.

It is known from the literature that doping of (bare) silica particles with ions in HPLC [10–19], applied to change the selectivity of the chromatographic system, can influence the retention of certain solutes. For the doping with Fe^{3+} [17]

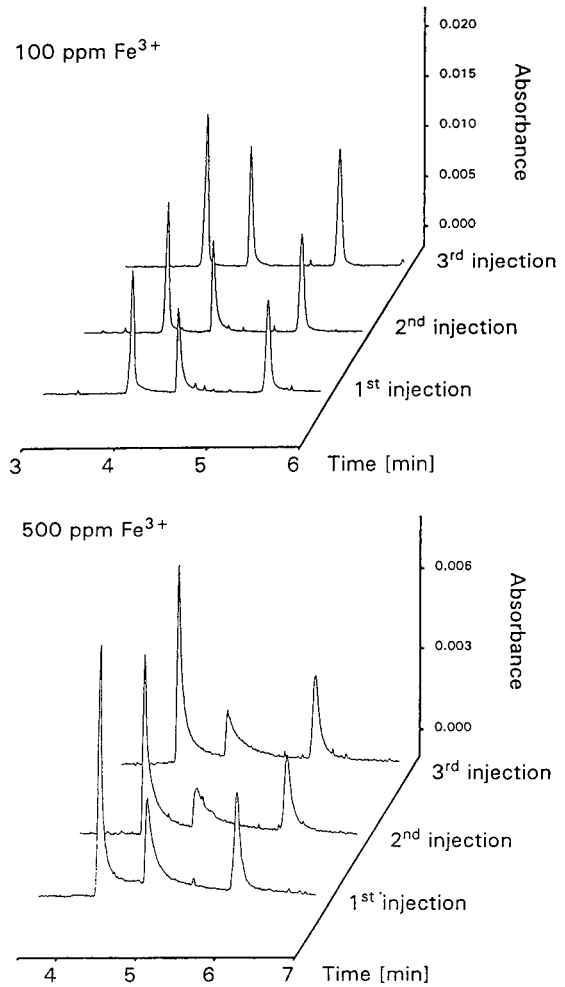

Fig. 4. Effect of three repetitive injections obtained at two different concentration levels of Fe^{3+}, 100 and 500 ppb, of the buffer solution at pH 4.50 for *ortho*-substituted benzenecarboxylic acids. Migration sequence of separands as in Fig. 2a. Conditions as in Fig. 1.

it was found that for compounds possessing hydroxyl functions (phenols), adsorptive retardation leads to an increase in the capacity factors by up to a factor of two, whereas components without such functional groups were not found to be retarded. An analogous mechanism seems to be operative in our system, although not a bare, but a coated silica surface is under consideration. This assumption is supported, however, by experimental findings of peak broadening in CZE in the presence of triply charged lanthanoids due to wall adsorption for C-1 modified fused-silica capillaries [20].

3.2. Uncoated capillaries

The electropherograms obtained with uncoated capillaries, presented in Fig. 5, show symmetrical peaks in the absence of Fe^{3+}. In contrast to coated capillaries, the migration times are longer, because the (relatively low) electroosmotic flow occurring in bare fused silica at pH 4.50 is directed against the electrophoretic migration of the anionic solutes. Those anions with low ionic mobilities are stronger influenced by this counterflow. In that event, a higher separation selectivity can be obtained. This ef-

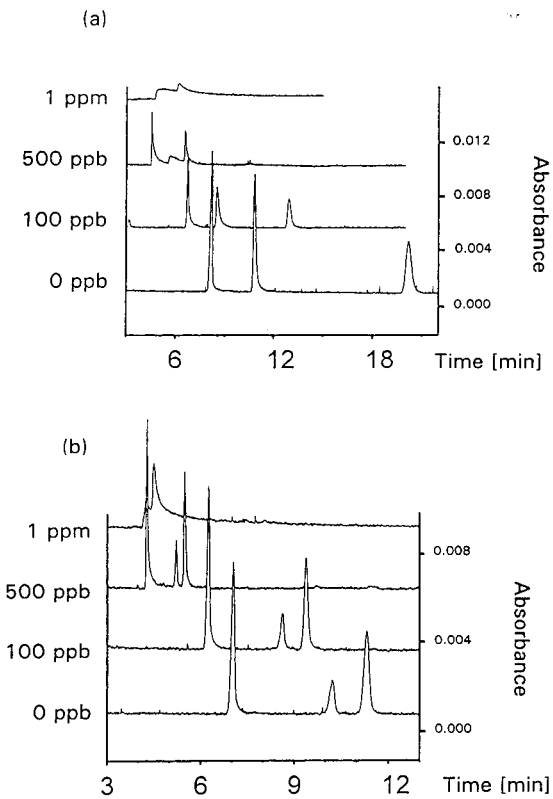

Fig. 5. Effect of the Fe^{3+} concentration of the buffer electrolyte solution at pH 4.50 on peak shapes and migration times of (a) *ortho*-substituted and (b) non-*ortho*-substituted benzenecarboxylic acids in uncoated fused-silica capillaries. Migration sequence of separands as in Fig. 2. Conditions as in Fig. 1.

fect can be observed, *e.g.*, for the pair of separands **1** and **2**. This pair is baseline separated in the coated capillary, but exhibits a much higher resolution in the uncoated capillary.

When Fe^{3+} ions are added to the buffer, two effects can be observed: first, the migration times decrease, and second, the peaks show increasing tailing. The former effect is caused by the decrease in the charge density and thus the zeta potential due to the adsorption of the Fe species on the silica wall. This effect is well known. It is used to modify the electroosmotic flow by addition of, *e.g.*, alkylamines to the buffer (see, *e.g.*, refs. 6 and 21). It is also in agreement with results observed in the presence of other higher charged cations in the buffer [22,23].

In the case under consideration, the decrease in the electroosmotic flow leads, *e.g.*, at about 500 ppb of Fe^{3+} to electroosmotic conditions as for the coated capillaries shown above. Owing to the attachment of the Fe species on the wall, adsorptive sites for the separands seem to be formed, reflected by severe peak tailing, yet again, especially of the *ortho*-substituted anions. From the comparison with Fig. 2, it can be concluded that this extent of adsorption is of the same order for coated as for uncoated capillaries. The coating does not prevent or even reduce the adsorption effect.

With respect to the nature of the Fe species attached on the wall only speculations are possible. Given the value of $2.64 \cdot 10^{-39}$ (at 25°C) for the solubility product of iron(III) hydroxide [24], at pH 4.5 the solubility of $Fe(OH)_3$ is considerably exceeded for the concentration range under investigation. On the other hand, it is well known that such hydroxides form colloids before precipitation. These colloidal particles can be attached on the wall in addition to the free Fe^{3+} ions. If the colloid is formed in fact [and it is not a metastable condition which is established, namely a supersaturated solution of $Fe(OH)_3$], it must consist of particles of very small size, because these particles were not visible, *e.g.*, as spikes, in the detector.

The assumption that the resulting phenomena are in fact caused by adsorption on the capillary surface rather than by secondary equilibria in the bulk liquid phase is supported by the observed "memory effect" when the buffer containing Fe^{3+} is replaced with an Fe^{3+}-free electrolyte, as shown in Fig. 6: the tailing of the peaks still remains.

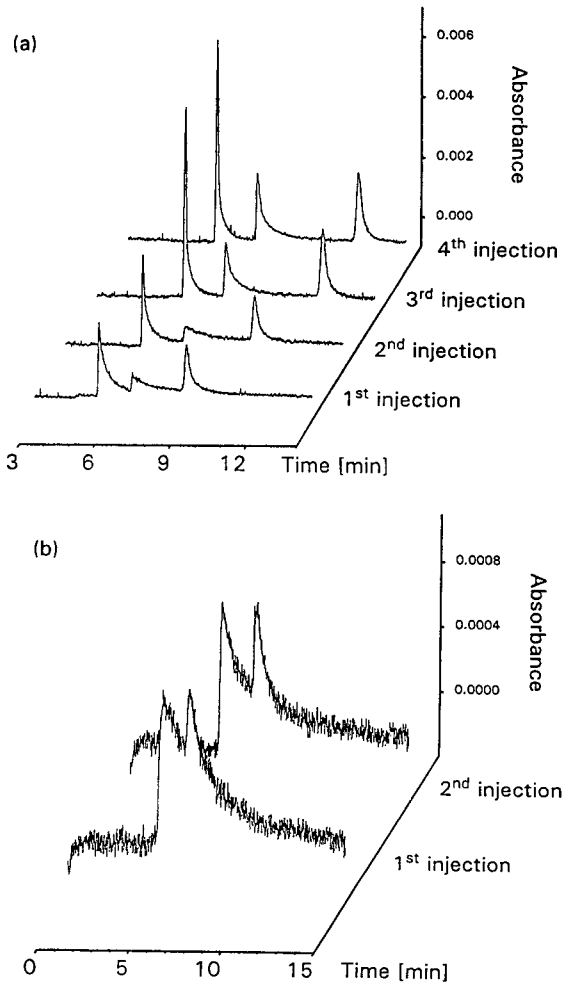

Fig. 6. "Memory effect" on the peak shapes of *ortho*-substituted benzenecarboxylic acids due to attachment of Fe(III) on the wall of the uncoated fused-silica capillary after replacing the buffer containing (a) 500 ppb and (b) 1 ppm of Fe^{3+} by an Fe^{3+}-free running buffer at pH 4.50. Prior to each run the capillary was rinsed with 20 column volumes of Fe-free buffer. Migration sequence of separands as in Fig. 2a. Conditions as in Fig. 1.

Acknowledgements

The authors thank I. Steffan and H. Hinterhofer for carrying out the ICP measurements.

References

[1] J.C. Giddings, *Dynamics of Chromatography*, Marcel Dekker, New York, 1965.
[2] H.H. Lauer and D. McManigill, *Anal. Chem.*, 58 (1986) 166.
[3] S.A. Swedberg and D. McManigill, in T. Hugli (Editor), *Techniques in Protein Chemistry*, Academic Press, San Diego, 1989, p. 468.
[4] M.R. Schure and A.M. Lenhoff, *Anal. Chem.*, 65 (1993) 3024.
[5] B. Gas, M. Stedry, A. Rizzi and E. Kenndler, *J. Chromatogr. A*, in press.
[6] N.A. Guzman (Editor), *Capillary Electrophoresis Technology* (*Chromatographic Science Series*, Vol. 64), Marcel Dekker, New York, 1993.
[7] E. Kenndler and W. Friedl, *J. Chromatogr.*, 608 (1992) 161.
[8] W. Friedl and E. Kenndler, *Anal. Chem.*, 65 (1993) 2003.
[9] S. Hjertén, *Chem. Rev.*, 9 (1967) 122.
[10] D. Kunzru and R.W. Frei, *J. Chromatogr. Sci.*, 12 (1974) 191.
[11] R. Aigner, H. Spitzy and R.W. Frei, *Anal. Chem.*, 48 (1976) 2.
[12] N.H.C. Cooke, R.L. Viavattene, R. Ecksteen, W.S. Wong, G. Davies and B.L. Karger, *J. Chromatogr.*, 149 (1978) 391.
[13] R. Aigner-Held, W.A. Aue and E.E. Pickett, *J. Chromatogr.*, 189 (1980) 139.
[14] G.J. Shahwan and J.R. Jezorek, *J. Chromatogr.*, 256 (1983) 39.
[15] G.A. Eiceman and F.A. Janecka, *J. Chromatogr. Sci.*, 21 (1983) 555.
[16] R.A. Djerki, R.W. Laub and S.K. Milonjir, *J. Liq. Chromatogr.*, 8 (1985) 281.
[17] Z. Deng, J.Z. Zhang, A.B. Ellis and S.H. Langer, *J. Chromatogr.*, 626 (1992) 159.
[18] B. Pfleiderer and E. Bayer, *J. Chromatogr.*, 468 (1989) 67.
[19] J. Wawrocki, *Chromatographia*, 31 (1991) 177.
[20] M. Chen and R.M. Cassidy, *J. Chromatogr.*, 640 (1993) 425.
[21] S.F.Y. Li, *Capillary Electrophoresis* (*Journal of Chromatography Library*, Vol. 52), Elsevier, Amsterdam, 1992.
[22] S. Chen, D.J. Pietrzyk, *Anal. Chem.*, 65 (1993) 2770.
[23] T.-L. Huang, P. Tsai, C.-T. Wu and C.S. Lee, *Anal. Chem.*, 65 (1993) 2887.
[24] R.C. Weast (Editor), *Handbook of Chemistry and Physics*, CRC Press, Boca Raton, FL, 70th ed., 1989–90, p. B207.

ELSEVIER

Journal of Chromatography A, 680 (1994) 33–42

JOURNAL OF CHROMATOGRAPHY A

The use of a microconcentric column in capillary electrophoresis

Chuzo Fujimoto*, Hirofumi Matsui, Hirokazu Sawada, Kiyokatsu Jinno

Department of Materials Science, Toyohashi University of Technology, Toyohashi 441, Japan

Abstract

The results from preliminary investigations into the use of a concentric column having a thin (*ca.* 95 μm) separation chamber for capillary electrophoresis (CE) are presented. The concentric column is constructed by winding a plastic line helically on a fused-silica capillary and then by inserting it into a larger diameter fused-silica capillary. Characteristics of the concentric column are determined and compared with conventional CE columns. The microconcentric column allows increased sample loading over the conventional columns while maintaining peak integrity. The feasibility of using the concentric column for micropreparative CE is demonstrated by the collection of fractions and subsequent analysis by analytical CE.

1. Introduction

The need for the isolation of small amounts (less than 1 μg) of purified components for use as standards or for characterization, especially in the fields related to biology and medicine, is increasing. There is no doubt that the materials to be examined in the future are present at even smaller levels in extraordinarily complex mixtures or are too labile to be amenable to conventional methods. In response to this challenge, much research has been directed toward the development of preparative techniques based upon capillary electrophoresis (CE).

In CE, the inner diameter (I.D.) of the column is the key to achieve highly efficient separations. Since the emergence of CE in 1981 [1,2], separations in narrow-bore columns (100 μm or less) have been recommended to minimize the effect of Joule heating generated by the passage of electrical current through the separation buffer. With wide-bore capillaries, a significant radial temperature gradient can be formed within the column bore, which in turn results in density gradient and convection. Such convection means sample zone broadening. Because of the high inner surface-area-to-internal volume ratio (the S/V ratio, typically more than several tens mm^{-1}), broadening of sample zones is minimized by effective dissipation of heat through the surrounding walls.

Assuming that sample volumes occupy 1% of the total column volume, the injection volume for a 100 μm I.D. capillary with a 50 cm length will be approximately 40 nl. When the initial concentration of the desired constituent is in the order of mg/ml, the injected amount is 40 ng: this represents 40 pmol to a constituent having a relative molecular mass of 1000. The loading capacity of CE is well above the detection limits

* Corresponding author. Present address: Department of Chemistry, Hamamatsu University School of Medicine, Hamamatsu 431-31, Japan.

0021-9673/94/$07.00
SSDI 0021-9673(94)00282-E

of mass spectrometry (MS) even if the whole mass range is scanned, or even if MS–MS experiments are to be performed [3,4]. Also, automated high-sensitivity methods are capable of the sequence determination of peptide samples at levels of less than 20 pmol [5]. However, as is often the case, further material is necessary to make the identification or sequence of the isolated components more reliable and to enable the purified material to be used as standards.

Provided that the generated heat is rapidly removed from the column, the sample loading capacity of CE should be proportional to the cross-sectional area of the separation column. Smith and co-workers [6,7] investigated the use of larger bore capillaries (150 or 200 μm I.D.). They showed that the larger I.D. capillaries provide a resolution of peptides comparable to that obtained with common analytical capillaries (50 μm I.D. or 75 μm I.D.). Although the starting peptide concentrations were in the mg/ml range, this approach demonstrated sequence analysis at low-pmol levels of peptides.

Tsuda *et al.* [8] demonstrated that increasing the sample load capacity can be achieved by the use of a rectangular cross-section capillary column in stead of a circular cross-section capillary column. Rectangular borosilicate-glass capillaries with dimensions ranging from 195 μm × 16 μm to 1000 μm × 50 μm were employed. Because of the large S/V ratio, and hence the excellent heat dissipation ability, large cross-sectional rectangular capillaries can be used without loss in separation efficiencies.

Other approaches that permit larger sample loading included a multicapillary system [7,9–12], field amplified sample loading [13–15], isotachophoretic sample loading [16–18], and a concentrator capillary system [12,19]. Each method has its own advantages and disadvantages, which have been reviewed previously [20–22].

In this paper, we explore the use of a microconcentric column for micropreparative CE separations. Electrophoresis is carried out in a separation chamber which is formed between coaxially disposed, double fused-silica capillaries. The double capillary column allows much higher sample loading than a single capillary column without degrading peak integrity.

2. Experimental

2.1. Construction of the microconcentric column

The procedure for preparing a microconcentric column is illustrated in Fig. 1. We use commercially available fused-silica tubings (GL Sciences, Tokyo, Japan) to construct the microconcentric column. The inner capillary is a 5-μm I.D. (or 10 μm I.D.) × 375 μm O.D. fused-silica tubing with an external coating. In order to remove the coating, the capillary is immersed in concentrated sulphuric acid at ambient temperature overnight. After this treatment the coating can be readily peeled off. The capillary is thoroughly washed with tap water and deionized water, and is then dried at ambient temperature. The naked capillary has now an O.D. of approximately 340 μm. Next, a line having a nominal diameter of 90 μm is wound around the bare fused-silica

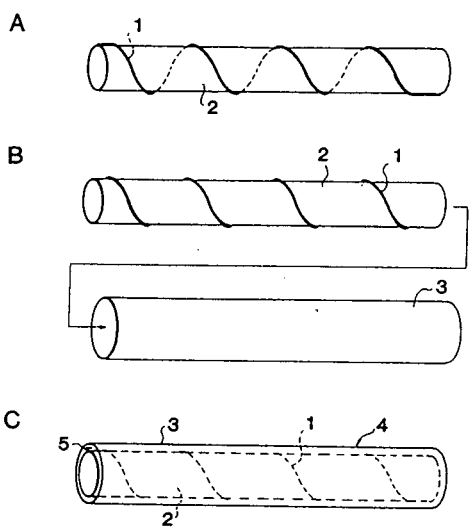

Fig. 1. Steps illustrating the construction of the concentric column. (A) Prepare a clad-removed fused-silica tube, used as the inner tube of the column, and wind a line helically around it; (B) insert the inner tube into a wider I.D. fused-silica tube; (C) completed. 1 = line; 2 = inner tube; 3 = outer tube; 4 = polyimide clad of outer tube; 5 = separation chamber.

capillary (Fig. 1A). A glue is placed on each end of the capillary to fix the line on the capillary. The line is made of synthetic resin and available from several sources (*e.g.*, Toray, Tokyo, Japan). Column construction is easy when the number of turns is 40 to 100 per meter along the column axis. At smaller numbers of turns, the inner capillary is not fixed well in the outer capillary. On the other hand, at larger numbers of turns, it is hard to insert the line-wound, inner capillary into the outer capillary. The line-wound capillary is inserted into a 530 μm I.D. × 630 μm O.D. fused-silica capillary tubing (GL Sciences) with polyimide clad (Figs. 1B and 1C). A detection window is made on the outer capillary by burning off the polyimide with an electrically heated filament before the column is assembled.

2.2. Apparatus

The apparatus used is pictured in Fig. 2. Surprisingly, the microconcentric column is fairly robust once it is assembled. The columns are flexible and can be looped into relatively small diameters (smaller than 18 cm). This permits a U-shape column configuration (Fig. 2B) besides the straight column configuration (Fig. 2A). The former configuration can be advantageous when designing a compact apparatus.

For preparative work, an electrical connector was made on the microconcentric column as described previously [23]. Briefly, a small portion of the polyimide coating is removed from the outer capillary at a distance of 2 cm from the outlet end. After the exposed section is cemented onto a plastic mount, the bared area of the capillary is scratched. A fracture is produced by bending the column carefully at the scratch until it breaks. The fracture is then surrounded by a certain thickness of polyacrylamide gel (10%T–3.6%C). The polyacrylamide joint is placed in a buffer reservoir that is connected to a high voltage. By this means, an extremely higher flow resistance exists in the direction of the fracture so that the bulk flow is directed toward the column outlet [11,23]. The quantity of the sample which may be lost through the fracture should depend on the ratio of the flow resistances in the two directions [11], which will be negligible in this case.

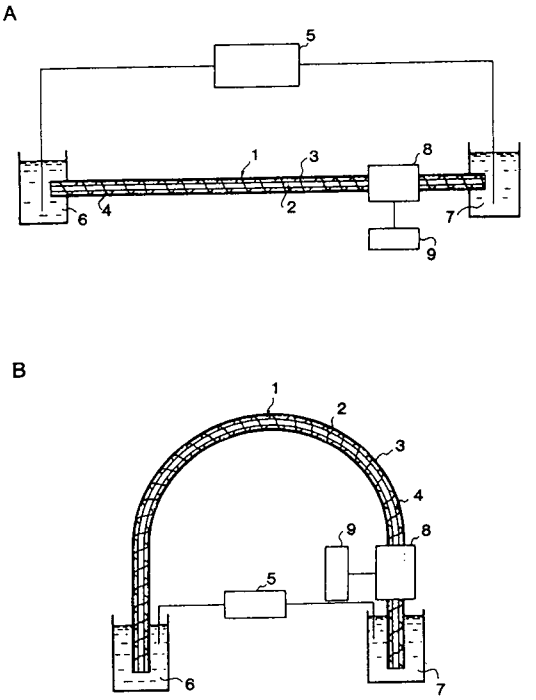

Fig. 2. CE setups with the microconcentric column. (A) Straight column configuration; (B) U-shape column configuration. 1 = Line; 2 = inner tube; 3 = outer tube; 4 = polyimide clad of outer tube; 5 = high-voltage power supply; 6 = inlet-end buffer reservoir; 7 = outlet-end buffer reservoir; 8 = UV detector; 9 = integration system.

On-column detection was accomplished using a modified UV detector (Model 870-CE, Jasco, Tokyo, Japan). The wavelength was set at 220 nm. The microconcentric, double capillary column was attached to a capillary mount which was made in-house for detection. Care was taken to ensure that the coiled line did not intercept the light from the UV source. For experiments using a single capillary column, the commercial capillary amount (Part No. 6627-425A, Jasco) was employed as received. A 50 μm × 500 μm slit (Part No. 6680-4117A, Jasco) was affixed on the backside of these capillary mounts. The signal from the detector was fed to a Labchart 180 (System Instruments, Tokyo, Japan) integration system.

A Matsusada Precision Devices (Kusatsu, Japan) Model HSR-30N-TU negative power supply was used to provide the electrical field for electrophoresis. The current in the system was measured over a 10-kΩ resistance in the return circuit of the power supply by means of a digital multimeter (Model VOAC 81, Iwatsu Electric, Tokyo, Japan). No column temperature control was available.

2.3. Chemicals

Tris(hydroxymethyl)aminomethane (Tris) and 2-[4-(2-hydroxyethyl)-1-piperazinyl]ethanesulfonic acid (HEPES) were obtained from Nacalai Tesque (Kyoto, Japan). All buffers were prepared daily using water from a Milli-Q unit (Millipore, Bedford, MA, USA). The other chemicals were of analytical grade and purchased from various distributors.

2.4. Estimation of sample plug length

The Fanning (or Darcy) equation can be used to estimate the sample plug length introduced into a column due to a pressure difference across the length of the column [24]:

$$\Delta p = 4f(\rho v^2/2g_c)(L/D_h) \quad (1)$$

where Δp is the pressure difference across the column (kgf m^{-2}; kgf = kilogram-force), f is the Fanning friction factor (dimensionless), ρ is the density of the fluid (kg m^{-3}), v is the average velocity of the fluid (m s^{-1}), g_c is dimensional constant (kg m $kgf^{-1}s^{-2}$), L is the length of the column (m), and D_h is the hydraulic (or equivalent) diameter (m). For hydrodynamic (gravity) flows, Δp is given by

$$\Delta p = \rho g \, \Delta h / g_c \quad (2)$$

where g is the constant for gravitation acceleration (m s^{-2}) and Δh is the height difference between the fluid levels at both ends of the column (m). The hydraulic diameter for circular cross-section columns equals to the geometric diameter, D (m), whereas that for concentric annular columns is given by

$$D_h = D_o - D_i \quad (3)$$

where D_o and D_i are the O.D. and I.D. of the annulus, respectively. The Fanning restriction factors are

$$f = 16/Re \text{ (for circular cross section columns)} \quad (4)$$

$$f = 16\{(D_o - D_i)^2/[(D_o^2 + D_i^2) - (D_o^2 - D_i^2)/\ln(D_o/D_i)]\}/Re$$

(for concentric annular columns) (5)

where Re is the Reinolds number (dimensionless) and is defined as

$$Re = \rho v D_h/\eta \quad (6)$$

where η is the Newtonian viscosity of the fluid (kg $m^{-1}s^{-1}$).

Substituting Eqs. 4 and 6 into Eq. 1 gives

$$\Delta p = 32 v \eta L/g_c D^2 \quad (7)$$

which is known as the Hagen–Poiseuille equation. The pressure difference for the concentric annular columns is

$$\Delta p = 32 v \eta L/\{g_c[(D_o^2 + D_i^2) - (D_o^2 - D_i^2)/\ln(D_o/D_i)]\} \quad (8)$$

The average velocity of the sample introduced by gravity flow at a given height difference for circular cross-section columns and concentric annular columns can be obtained from Eqs. 7 and 8, respectively. Multiplication of the average fluid velocity by the introduction time gives the length of sample introduced during hydrodynamic flow introduction:

$$l = \rho g \, \Delta h \, D^2 t_i/32\eta L \text{ (for circular cross section columns)} \quad (9)$$

$$l = \rho g \, \Delta h \, t_i[(D_o^2 + D_i^2) - (D_o^2 - D_i^2)/\ln(D_o/D_i)]/32\eta L$$

(for concentric annular columns) (10)

where t_i is the introduction time (s).

3. Results and discussion

3.1. Characterization of the microconcentric column

The heat dissipation ability of a CE column should depend upon the S/V ratio while the sample loading ability should depend upon the cross-sectional area of the column. Table 1 summarizes several characteristics of the three types of columns having different dimensions. From the table we can see that the concentric column allows the sample load that is enhanced by a factor of 16.6, although the S/V ratio for the concentric column is about one-half of that for a 100-μm I.D. capillary column. In general, the use of wider bore columns (*e.g.*, 150 μm I.D. columns) is somewhat limited in that a dramatic increase in separation efficiency is observed [8,25]. The sample loading ability of the concentric column is higher by a factor of 2.6 than a 1000 μm $\times$ 50 μm rectangular column, although the heat dissipation is expected to be less effective with the former column than with the latter column.

There are further advantages of the concentric column over the rectangular column. Because the concentric column is made of fused-silica, it shows good transparency at short wavelengths ($<$210 nm) of UV detection, which is perhaps the most widely used CE detection method, unlike the rectangular column which is made of borosilicate glass. This advantage is manifested when short wavelength UV detection is used for detecting proteins and peptides [26–29]. According to Mayer and Miller [30], the absorbance at 193 nm is directly proportional to the number of peptide bonds in the molecule. More importantly, detection at 193 nm yields higher absorbance for peptide bonds [30]. The line of mercury at 185 nm can be also used for detection of peptides and oligosaccharides which are separated by CE with certain buffers [31].

The concentric column also alleviates the problem of the capillary fragility which has been encountered with the borosilicate-glass rectangular columns. Because the concentric column is flexible like a single fused-silica capillary column, it is not necessary to cut a channel in the optical compartment of the UV detector when installing the column to the detection unit (see Ref. [8]). In addition, the flexibility of the concentric column allows the design of a compact apparatus, as mentioned in the Experimental section.

With the use of the concentric column for CE, a question needs to be addressed before the column performance is examined: does the solute go through the helical channel that is formed by partitioning the space between the double capillaries with the line? Note that the calculated space (*ca.* 95 μm) is larger than the nominal diameter of the line. To answer this question, methyl orange was dissolved in water at a high concentration. A 5-mm wide section of the polyimide coating was removed from the outer

Table 1
Characteristics of columns having different separation chamber shapes

Shape of cross section	Circle	Rectangle	Rectangle	Annulus
Materials	Fused-silica	Borosilicate	Borosilicate	Fused-silica
Size, μm	100 I.D.	16 $\times$ 195[a]	50 $\times$ 1000[a]	340 I.D. $\times$ 530 O.D.
Circumference, mm	$3.14 \cdot 10^{-1}$	$4.22 \cdot 10^{-1}$	2.10	2.73
Cross-sectional area, mm^2	$7.85 \cdot 10^{-3}$	$3.12 \cdot 10^{-3}$	$5.00 \cdot 10^{-2}$	$1.30 \cdot 10^{-1}$
Rel. cross-sectional area	1.00	$3.97 \cdot 10^{-1}$	6.37	16.6
S/V, mm^{-1}	40	135	42	21

[a]Values taken from Ref. [8].

capillary (44 cm in length) at a distance of 2 cm from the inlet, and placed on the sample stage of a microscope. The column and the outlet reservoir were filled with 100 m*M* HEPES, pH 5.2, while the inlet reservoir was filled with the dye solution. Each end of the column was placed into the reservoirs and then a high voltage (− 10 kV) was applied over the column. We were able to observe the dye traveling through the helical separation channel under the microscope.

It is worth noting that the separation channel is not very extended by winding the line. For example, the increment in the separation length is estimated to be only *ca.* 0.6% for a 50-cm long column having 50 turns of the line. It follows that the change in the field strength at a given voltage is negligible. The effect of a helical separation channel on the separation efficiency was not examined because of the difficulties in performing such an experiment, although some previous work [32,33] showed that in open tubular columns, no significant effect of column coiling occurred while the influence of coiling on efficiency was significant with gel-filled columns. Alternatively, the influence of using the U-shaped column configuration (Fig. 2B) was investigated, and as a result, it was found that this column configuration did not influence the column performance.

The effects of Joule heating on the separation have been generally a great concern when working with large cross-sectional columns, since increasing the cross-sectional area causes an increase in the electric current passing through the column, which can seriously reduce the efficiency of the system. Because the amount of heat that must be removed is proportional to the square of the field strength, the equivalent conductance and the buffer concentration [34], the choice of these parameters becomes critical when using large bore columns. Low conductivity and low concentration buffers have been used to circumvent the heating problems [6–8], despite the problems of limited sample loading and possible adsorption effects [25]. It was expected that this would be the case for the authors' column system. To investigate the influence of excessive heat generation, the applied field

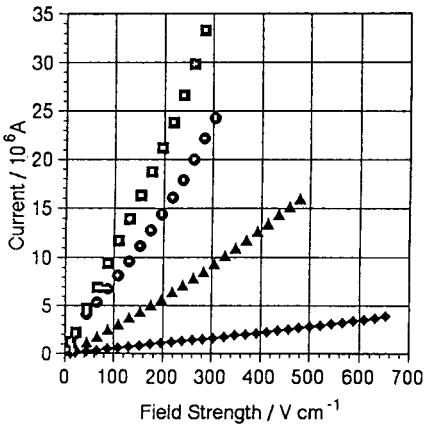

Fig. 3. Plots of applied field strength *vs.* resulting current for different running solutions. □ = 5 m*M* HEPES, pH 7.0; ○ = 100 m*M* HEPES, pH 5.2; ▲ = 3 m*M* Tris, pH 9.2; ◆ = 5 m*M* HEPES, pH 5.2. Column length, 46 cm.

strength *vs.* the resulting current was plotted. The results are shown in Fig. 3 for the four running solutions, which were chosen for having low conductivities. The field strength at which the curve begins to deviate from the linearity can be considered as the maximum voltage, beyond which the generated heat is excessive for the column system [35,36]. In the present work, the maximum field strength for each running solution was tentatively defined as the value beyond that the correlation coefficient begins to drop below 0.998 on the linear regression analysis. The results are shown in Table 2, together with the values of the heat generation rate. It can be seen that the maximum field strength and the heat generation rate per meter for the concentric column are in the same order of magnitude as is common for CE separations using circular cross-section capillaries without any cooling system (see, Ref. [37]). On the other hand, because of the increased volume of the concentric column, the heat generation rate per unit volume is two orders of magnitude smaller than that for circular cross-section capillaries operated under typical conditions (see, Ref. [34]). Undoubtedly, Good's buffers are the most promising candidates for such a large cross-sectional column, since they can cover a wide range of pH while

Table 2
The heat generation rate at the maximum field strength

Buffer medium	Maximum field strength ($V\ cm^{-1}$)	Heat generation rate ($W\ m^{-1}$)	($W\ cm^{-3}$)
3 m*M* Tris, pH 9.2	413	0.558	4.29
5 m*M* HEPES, pH 7.0	260	0.777	5.98
5 m*M* HEPES, pH 5.2	630	0.213	1.79
100 m*M* HEPES, pH 5.2	260	0.467	3.59

having low conductivities even at high concentrations.

To evaluate whether or not concentric annular columns maintain CE performance, a mixture containing dansyl acid (0.05 mg/ml) and benzyl alcohol (1.0 mg/ml) was electrophoresed with a concentric annular column and circular cross-section capillary columns (100 and 250 μm I.D.). The sample was introduced by the gravity flow for 6 s at 5 cm and then a voltage of −10 kV was applied. Note that the lengths of the sample introduced into individual columns are not equal (see Experimental section for the estimation of the sample plug length). A comparison of the electropherograms obtained with those columns is shown in Fig. 4. A summary of the migration time, peak width, peak asymmetry and plate count for the benzyl alcohol peak is given in Table 3. With either the concentric column or the 100-μm I.D. capillary column, the components eluted with base line resolution; the peaks are only partially resolved with the 250-μm I.D. capillary column. It is worthy to note that *the volumes* introduced into the 250-μm I.D. column and the concentric column are almost the same, being 40 times that of the 100-μm I.D. column: the volumes of sample applied to the former columns are approximately 0.73 μl and the amounts of dansyl acid and benzyl alcohol are 36 ng and 730 ng, respectively. The migration times of the components are longer with the concentric column than with the 100-μm I.D. capillary column, indicating that the rate of electroosmotic flow is smaller with the concentric column compared with the 100-μm I.D. circular cross-section capillary. This would be responsible for the difference in the state of the inner surface between those columns. We can also see that the concentric column and the 100-μm I.D. column are different in the values of plate count and resolution. There are several probable explanations for this. First, in this case, the decrease in the velocity of electroosmotic flow can yield improved resolution and a decrease in plate count. Second, the concentric column was operated near the maximum field strength for the buffer, which makes the heat dissipation less effective. Third, the injection length of the

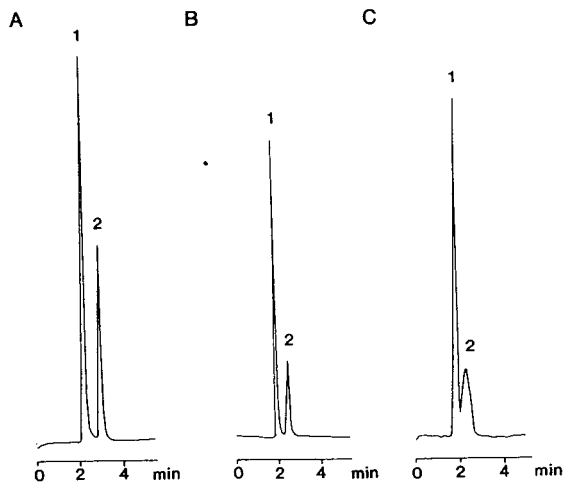

Fig. 4. Electropherograms of benzyl alcohol and dansyl acid for microconcentric column (A) and round cross-section columns of 100 μm I.D. (B) and 250 μm I.D. (C). Peaks: 1 = benzyl alcohol; 2 = dansyl alcohol. Conditions: 46 cm column length (27 cm effective column length) each; −10 kV applied voltage; 220 nm detection wavelength; 3 m*M* Tris buffer, adjusted to pH 9.2 with glycine.

Table 3
Summary of column performance determination experiments

Column	100 μm I.D.	250 μm I.D.	Concentric
Migration time, min	1.87	1.84	2.18
Peak width[a], s	5.2	10.6	8.6
Peak asymmetry[b]	2.82	1.07	1.66
Plate count[c], m^{-1}	5606	1306	2786
Resolution[d]	1.29	N.D.[e]	2.79

Conditions as in Fig. 4. Average values are given for benzyl alcohol ($n = 5$).
[a] Based on half height peak width measurement.
[b] Based on 15% peak height.
[c] Calculated using the equation: $N = 5.54(t/w_h)^2$; where t is the migration time of the peak and w_h is the half-height peak width.
[d] Resolution between benzyl alcohol (peak 1) and dansyl acid (peak 2) was determined by the equation: $R = (t_2 - t_1)/(w_{1R} + w_{2L})$; where t_1 and t_2 are the migration times of peaks 1 and 2 ($t_2 > t_1$), w_{1R} is the portion of the width of peak 1 which is to the right of t_1, and w_{2L} is the portion of the width of peak 2 which is to the left of t_2.
[e] Not determined.

sample for the concentric column is longer by a factor of 2.4 than that for the 100-μm I.D. capillary. The two latter matters tend to decrease the efficiency of separation. It follows that direct comparison of the column performance between those columns is inappropriate. However, it seems to us that the separation power is adequate for many applications and can be improved by optimizing the operating conditions.

Table 4 shows the relative standard deviation (R.S.D.) in the migration time and peak area for the concentric column, together with those for the 100-μm I.D. capillary column. From the table we can see that the values obtained with the concentric column are comparable to those for the 100-μm I.D. column.

3.2. Eluate collection

The concentric column enabled us to collect enough material from a single run. To collect eluate continuously, the electrical circuit in the column was completed prior to its outlet by the use of the polyacrylamide joint. This design allows the collection of fractions at an electrically isolated outlet [11,23]. Thymine was dissolved at a concentration of 1.0 m*M* in a 100-m*M* HEPES (pH 5.2) buffer and injected into the concentric column having a polyacrylamide joint with gravity flow for 6 s at 5 cm. The resulting electropherogram is shown in Fig. 5A. The amount of sample applied is approximately 92 ng. We can see a thymine peak eluting at 5.95 min from the electropherogram. Eluate was collected into a

Table 4
Comparison of R.S.D. values of the concentric column system and the circular column system ($n = 5$)

Component	Concentric		100 μm I.D.	
	Migration time	Peak area	Migration time	Peak area
Benzyl alcohol	0.461	5.83	1.56	5.51
Dansyl acid	1.87	6.95	1.65	4.67

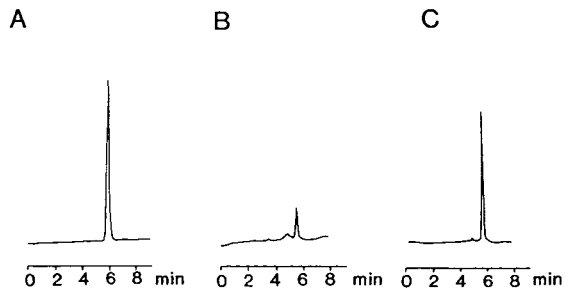

Fig. 5. (A) Electropherogram of thymine on microconcentric column; (B) electropherogram of fraction collected from preparative run, obtained on 100 μm I.D. analytical column; (C) electropherogram of thymine on 100 μm I.D. analytical column. Conditions: 46 cm column length (27 cm effective column length) each; −10 kV applied voltage; 220 nm detection wavelength; 100 m*M* HEPES buffer, pH 5.2. The polyacrylamide joint (on-column fracture) is positioned 2 cm from the exit of the concentric column. The lengths of the columns over which the high voltage is applied are 44 cm and 46 cm in (A) and (B), respectively.

small vial during the period 1.5–3.5 min after the emergence of the thymine peak on the UV electropherogram. The UV detector was located 10 cm prior to the column outlet and the time required for the analyte to travel from the detection point to the column outlet was approximately 98 s. Electrophoresis of the collected fraction (*ca.* 16 μl in volume) was carried out using a second CE system with a 100-μm I.D. circular capillary column. A small portion (*ca.* 8.3 nl) of the fraction was syphoned for 12 s at 5 cm. The resulting electropherogram is shown in Fig. 5B, where the thymine peak appears at 5.47 min and an artificial peak appears at 4.85 min. Because the migration times of thymine were different for the two columns, we injected the original sample solution into the 100-μm I.D. column. As expected, the peak of thymine was observed to elute at the same migration time as that of the collected fraction (see Fig. 5C). This indicates that the concentric column can be employed for micropreparative purposes. A comparison between the electropherograms in Figs. 5A and C reveals that the peak width is broader with the concentric column than with the 100-μm I.D. column: the calculated plate counts were 7320 m^{-1} and 22 790 m^{-1} for the concentric column and the 100-μm I.D. column, respectively. Further work is required for the explanation for the lower plate count with the concentric column, but it seems to us that the decreased velocity of electroosmotic flow and the lengthened sample plug are in part responsible for the difference in plate count.

4. Conclusions

We have demonstrated that large quantities of separated components could be continuously collected from a single separation using a concentric column. The column provides many favorable features, involving ease of construction, robustness and UV transparency at short wavelengths. Obviously, more work is required to fully evaluate microconcentric columns for use as preparative columns. These include the optimization of the O.D. of the inner tube and the I.D. of the outer tube, the proper selection of the buffer for the particular separation, the use of a cooling system and the development of an injection system that is suited for the concentric column. We expect further improvement in the column performance when these conditions are realized.

Acknowledgements

This work was supported partly by the Asahi Glass Foundation, the Nakano Foundation and the Research Foundation of Toyohashi University of Technology.

References

[1] J.W. Jorgenson and K.D. Lukas, *Anal. Chem.*, 53 (1981) 1298.
[2] J.W. Jorgenson and K.D. Lukas, *J. Chromatogr.*, 218 (1981) 209.
[3] C. Schwer and F. Lottspeich, *J. Chromatogr.*, 623 (1992) 345.
[4] R. Takagiku, T. Kough, M.P. Lacey and R.E. Schneider, *Rapid Commun. Mass Spectrosc.*, 4 (1990) 24.

[5] B.L. Karger, A.S. Cohen and A. Guttman, *J. Chromatogr.*, 492 (1989) 585.
[6] A. Smith and J.W. Kenny, *Tech. Protein Chem.*, 3 (1991) 113.
[7] J.W. Kenny, J.I. Ohms and A. Smith, *Tech. Protein Chem.*, 4 (1992) 363.
[8] T. Tsuda, J.V. Sweedler and R.N. Zare, *Anal. Chem.*, 62 (1990) 2149.
[9] N.A. Guzman, L. Hernandez and B.G. Hoebel, *BioPharm.*, 2 (1989) 22.
[10] T. Hanai, H. Hatano, N. Nimura and T. Kinoshita, *J. High Resolut. Chromatogr.*, 13 (1990) 573.
[11] C. Fujimoto, Y. Muramatsu, M. Suzuki and K. Jinno, *J. High Resolut. Chromatogr.*, 14 (1991) 178.
[12] N.A. Guzman, M.A. Trebilcock and J.P. Advis, *J. Liquid Chromatogr.*, 14 (1991) 997.
[13] D.S. Burgi and R.L. Chien, *Anal. Chem.*, 63 (1991) 2042.
[14] R.L. Chien and D.S. Burgi, *J. Chromatogr.*, 559 (1991) 141.
[15] R.L. Chien and D.S. Burgi, *J. Chromatogr.*, 559 (1991) 153.
[16] F.E.P. Mikkers, F.M. Everaerts and Th.P.E.M. Verheggen, *J. Chromatogr.*, 169 (1979) 1.
[17] P. Jandik and W.R. Jones, *J. Chromatogr.*, 546 (1991) 431.
[18] S. Hjerten, K. Elenbring, F. Kilar, J.-L. Liao, A.J.C. Chen, C.J. Siebert and M.-D. Zhu, *J. Chromatogr.*, 403 (1987) 47.
[19] M.E. Swartz and M. Merion, *J. Chromatogr.*, 632 (1993) 209.
[20] T. Tsuda, in N.A. Guzman (Editor), *Capillary Electrophoresis Technology*, Marcel Dekker, New York, 1993, Ch. 14, p. 489.
[21] C. Fujimoto and K. Jinno, in N.A. Guzman (Editor), *Capillary Electrophoresis Technology*, Marcel Dekker, New York, 1993, Ch. 15, p. 509.
[22] F. Foret, L. Krivankova and P. Bocek, *Capillary Zone Electrophoresis*, VCH, Weinheim, 1993, Ch. 8, p. 187.
[23] C. Fujimoto, T. Fujikawa and K. Jinno, *J. High Resolut. Chromatogr.*, 15 (1992) 201.
[24] R.H. Perry (Editor), *Chemical Engineer's Handbook*, McGraw-Hill Kogakusha, Tokyo, 5th ed., 1976, Section 5.
[25] R.J. Nelson, A. Paulus, A.S. Cohen, A. Guttman and B.L. Karger, *J. Chromatogr.*, 480 (1989) 111.
[26] J. Tehrani, R. Macomber and L. Day, *J. High Resolut. Chromatogr.*, 14 (1991) 10.
[27] R.M. McCormic, *Anal. Chem.*, 60 (1988) 2322.
[28] J.J. Kirkland and R.M. McCormic, *Chromatographia*, 24 (187) 58.
[29] J.S. Green and J.W. Jorgenson, *J. Chromatogr.*, 478 (1989) 63.
[30] M.M. Mayer and J.A. Miller, *Anal. Biochem.*, 36 (1970) 91.
[31] M. Fuchs, P. Timmoney and M. Merion, presented at *HPCE'91, San Diego, CA, 1991*, Poster No. PM/24.
[32] S. Wicar, M. Vilenchik, A. Belenkii, A.S. Cohen and B.L. Karger, *J. Microcol. Sep.*, 4 (1992) 339.
[33] T. Srichaiyo and S. Hjerten, *J. Chromatogr.*, 604 (1992) 85.
[34] J. Knox, *Chromatographia*, 26 (1988) 329.
[35] R. Kuhn and S. Hoffstetter-Kuhn, *Capillary Electrophoresis: Principles and Practice*, Springer-Verlag, Berlin, 1993, Ch. 3, p. 37.
[36] F. Foret, L. Krivankova and P. Bocek, *Capillary Zone Electrophoresis*, VCH, Weinheim, 1993, Ch. 4, p. 37.
[37] M.J. Sepanik and R.O. Cole, *Anal. Chem.*, 59 (1987) 472.

ELSEVIER

Journal of Chromatography A, 680 (1994) 43–48

JOURNAL OF CHROMATOGRAPHY A

Capillary zone electrophoresis for the determination of dissociation constants

S.J. Gluck*[,a], J.A. Cleveland, Jr.[b]

[a]*Analytical Sciences, 1897B Bldg, Dow Chemical Co., Midland MI 48667, USA*

[b]*Discovery Research, DowElanco, 9410 Zionsville Rd, Indianapolis IN 46268-1053, USA*

Abstract

Automated capillary electrophoresis is an effective method for the determination of pK_a values. Advantages include having high sensitivity for poorly soluble solutes, not having to know the concentration of the solutes, and the simplicity of the method. The procedure, further investigated in this work, yielded determined pK_a values to within 0.07 units of literature values from the IUPAC database for 18 solutes having pK_a values of less than 9. The range evaluated was 2.43 to 9.99. Bases with pK_a values above 9 had significant differences with the literature values. Wall adsorption and concentration effects were not potential contributors to these differences. Spectroscopic pK_a determinations for three solutes showing large differences with the literature values agree with the capillary electrophoresis determinations.

1. Introduction

Dissociation constants (i.e., pK_a values) can be a key parameter for understanding and quantifying chemical phenomenon such as reaction rates, biological activity, biological uptake, biological transport and environmental fate [1–3]. The determination of dissociation constants of weakly acidic or basic compounds is routine using established techniques if the compound has amenable physical properties [4–7]. However, the low solubility of many pharmaceutical and agricultural compounds in water precludes convenient pK_a determinations. Indeed, many new herbicides and pesticides have poor water solubility specifically designed into the molecules for environmental concerns. Previous papers [8–10] have introduced the use of capillary electrophoresis (CE) for pK_a determination. We have used this approach because of its high sensitivity and selectivity relative to potentiometry. In this paper we continue to explore the benefits of CE for pK_a measurements and build upon the previous work in this area. In particular, this work includes more compounds of known literature pK_a values thus extending the demonstrated range.

Equations which relate electrophoretic mobility to pK_a have been adequately derived previously [10]. In brief, the thermodynamic pK_a is related in an expression similar to the Henderson–Hasselbach equation with electrophoretic

* Corresponding author.

SSDI 0021-9673(94)00369-K

mobility used to describe the state of solute ionization

$$pK_a = pH + \log\left[\frac{\mu_e}{\mu_{BH^+} - \mu_e}\right] - \frac{0.5085z^2\sqrt{I}}{1 + 0.3281a\sqrt{I}} \text{ (bases)} \quad (1)$$

$$pK_a = pH - \log\left[\frac{\mu_e}{\mu_{A^-} - \mu_e}\right] + \frac{0.5085z^2\sqrt{I}}{1 + 0.3281a\sqrt{I}} \text{ (acids)} \quad (2)$$

where μ_{BH^+} is the electrophoretic mobility of the fully protonated base, μ_{A^-} is the electrophoretic mobility of the fully deprotonated acid and μ_e is the electrophoretic mobility observed at the experimental pH. The third term in Eqs. 1 and 2 is the activity correction for buffer ionic strength, I. The variable z is the valency of the buffer and a is the ionic size parameter, 5 Å.

An alternative approach is to use linear forms of Eqs. 1 and 2 [9,11]. In theory, either approach is acceptable, but in practice, the non-linear equations shown here will give better results [11]. The K_a is linear with $1/\{H^+\}$. To cover a wide range of pH, buffers are generally chosen with equally spaced pH values. When linear regression is performed to determine the K_a, there will be highly leveraged, influential data introducing a significant error in the result. A weighted linear regression requires too many runs to determine the weights and is thus impractical. Non-linear regression of Eqs. 1 or 2 using equally spaced pH buffers about the pK_a minimizes the potential for highly leveraged, influential data.

2. Experimental

2.1. Apparatus and method

A SpectraPHORESIS 1000 CE (Thermal Separation Systems, Fremont, CA, USA) was used for all experiments. Typically, a 2-s hydrodynamic injection was performed. Since the hydrodynamic injection rate is ca. 6 nl/s for a 67 cm × 75 μm untreated fused-silica capillary (Polymicro Technology, Phoenix, AZ, USA), ca. 12 nl was loaded onto the column. The separation distance, L_d, was 59.5 cm. The temperature was set at 25°C. Absorbance was monitored at a wavelength appropriate for the solute and, usually, at 240 nm for the neutral marker, mesityl oxide. This instrument has a high speed slewing monochromator allowing multiple wavelength detection. With the instrument operating at 25 kV, typical currents were less than 20 μA.

In order to equilibrate the column and thereby minimize hysteresis effects [10,12], the following wash cycle was performed prior to each run in a sequence: (1) 5 min with 1 *M* NaOH, (2) 5 min with H_2O, and (3) 3.0 min with running buffer.

Because the SpectraPHORESIS 1000 is equipped with a single reservoir for the buffer near the detector, it is not possible to match buffers at each end of the column in a sequence. Tricine (0.02 *M*, pH 7.6 to 8.1) was used as the buffer at the detector end of the column.

Buffer pH was measured with an Orion Ross pH electrode and an Orion Model 601A pH meter and in later work a Fisher Accuphast pH electrode or an Orion Model EA940 meter. Meter calibrations were made with Fisher NIST traceable buffer solutions.

Method

All solutions were prepared using distilled, deionized, and filtered water (ASTM type I specification). A 100-μl aliquot of 10 m*M* mesityl oxide in water (neutral marker) and 900 μl analyte solution typically were combined into a 2-ml sample vial to give a final concentration of between 10 and 900 μ*M* analyte and 1 m*M* mesityl oxide.

Data pairs of the activity corrected pH and μ_e were imported into Mathcad 4.0 (MathSoft, Cambridge, MA, USA) where μ_{BH^+} or μ_{Z^-} and pK_a were determined by performing a non-linear fit to Eqs. 1 or 2.

3. Spectroscopic pK_a determination

Spectroscopic pK_a values of several bases were determined by taking UV spectra with an Hitachi Model 3101 spectrophotometer using 1-cm

cuvets at 23°C. Samples were prepared in the same buffer series as used in the CE experiments. Absorbance measurements were taken at a wavelength which showed a significant difference as a function of pH for each solute, 220 nm for 2- and 3-methylbenzylamine, 230 nm for 2-methoxybenzylamine. The pK_a values were determined using a non-linear fit of the absorbance, A, versus the pH [13]

$$pK_a = pH + \log\left[\frac{A - A_{BH^+}}{A_{BH^+} - A_B}\right] - \frac{0.5085z^2\sqrt{I}}{1 + 0.3281a\sqrt{I}} \quad (3)$$

Where A_{BH^+} and A_B are parameters also determined by the regression.

3.1. Buffer series

Different buffer series were used throughout this investigation. Most of the work was done at a constant ionic strength to enable a more consistent electroosmotic flow (EOF) between different buffers [14]. At an ionic strength of 0.01 M, the activity correction for the ionic strength of the solution is 0.05 making calculations somewhat simpler. The concentrations and the pH values of this buffer series are listed in Table 1. Buffer components were obtained from different producers and were of the highest available purity.

4. Results

4.1. Buffer capacities

A consideration in creating the buffer series in Table 1 was the buffer capacity, β, of each buffer. The β is defined as [15]

$$\beta = \frac{dC_a}{dpH} = 2.3\left(\frac{K_w}{[H^+]} + [H^+] + \frac{K_a C_t [H^+]}{(K_a + [H^+])^2}\right) \quad (4)$$

Table 1
Buffer series, pH, pK_a values, concentrations, buffer capacities and estimated pH change upon the addition of a 1-s injection of a 100 μM strong acid or base

Buffer[a]	pH	pK_a	Concentration of buffer (M)	Buffer capacity β (M/pH)	Estimated pH change
CAPS	10.96	10.4	$1.22 \cdot 10^{-2}$	$6.85 \cdot 10^{-3}$	$4.82 \cdot 10^{-3}$
CAPS	10.65	10.4	$1.71 \cdot 10^{-2}$	$1.01 \cdot 10^{-2}$	$3.27 \cdot 10^{-3}$
CAPS	10.12	10.4	$3.24 \cdot 10^{-2}$	$1.71 \cdot 10^{-2}$	$1.93 \cdot 10^{-3}$
CAPSO	9.76	9.6	$2.12 \cdot 10^{-2}$	$1.19 \cdot 10^{-2}$	$2.77 \cdot 10^{-3}$
AMPSO	9.16	9	$1.89 \cdot 10^{-2}$	$1.05 \cdot 10^{-2}$	$3.13 \cdot 10^{-3}$
TAPS	8.61	8.4	$1.71 \cdot 10^{-2}$	$9.29 \cdot 10^{-3}$	$3.55 \cdot 10^{-3}$
Tricine	7.94	8.1	$2.12 \cdot 10^{-2}$	$1.18 \cdot 10^{-2}$	$2.80 \cdot 10^{-3}$
HEPES	7.43	7.5	$1.89 \cdot 10^{-2}$	$1.08 \cdot 10^{-2}$	$3.06 \cdot 10^{-3}$
MOPS	6.94	7.2	$2.41 \cdot 10^{-2}$	$1.27 \cdot 10^{-2}$	$2.60 \cdot 10^{-3}$
ACES	6.53	6.8	$2.78 \cdot 10^{-2}$	$1.45 \cdot 10^{-2}$	$2.27 \cdot 10^{-3}$
MES	6.09	6.1	$2.12 \cdot 10^{-2}$	$1.22 \cdot 10^{-2}$	$2.71 \cdot 10^{-3}$
Acetic	5.46	4.75	$1.16 \cdot 10^{-2}$	$3.65 \cdot 10^{-3}$	$9.04 \cdot 10^{-3}$
Acetic	5.04	4.75	$1.50 \cdot 10^{-2}$	$7.75 \cdot 10^{-3}$	$4.26 \cdot 10^{-3}$
Acetic	4.45	4.75	$2.58 \cdot 10^{-2}$	$1.33 \cdot 10^{-2}$	$2.49 \cdot 10^{-3}$
Formic	4.16	3.75	$1.50 \cdot 10^{-2}$	$7.12 \cdot 10^{-3}$	$4.64 \cdot 10^{-3}$
Formic	3.54	3.75	$2.58 \cdot 10^{-2}$	$1.47 \cdot 10^{-2}$	$2.25 \cdot 10^{-3}$
Formic	3.05	3.75	$6.01 \cdot 10^{-2}$	$2.12 \cdot 10^{-2}$	$1.56 \cdot 10^{-3}$

[a] Buffer abbreviations: CAPSO = 3-[cyclohexylamino]-2-hydroxy-1-propanesulfonic acid; CAPS = 3-[cyclohexylamino]-1-propanesulfonic acid; AMPSO = 3-[(1,1-dimethyl-2-hydroxyethyl)amino]-2-hydroxypropane sulfonic acid; TAPS = N-tris[hydroxymethyl]methyl-3-amino-propanesulfonic acid; Tricine = N-tris[hydroxymethyl]methylglycine; HEPES = N-[2-hydroxyethyl]piperazine-N′-[2-ethanesulfonic acid]; MOPS = 3-[N-morpholino]propanesulfonic acid; ACES = (N-[2-acetamido]-2-aminoethanesulfonic acid; MES = 2-[N-morpholino]ethanesulfonic acid.

Where C_a is the concentration of the buffer acid, K_w is the equilibrium constant for the dissociation of water, K_a is the equilibrium constant for the dissociation of the buffer acid, and C_t is the total concentration of the buffer. Too low of a buffer capacity would result in the inability of the buffer to maintain pH control in the analyte zone. At the pH of the buffers, the actual buffer capacities are listed in Table 1 as well as the expected change in pH for the 1-s injection of a 100 μM strong acid or base. The maximum impact on the pH for a 6-nl (1-s) injection, with a typical 18-nl peak width at the detector, of a 100 μM strong acid or base is estimated to be insignificant ($\Delta pH < 0.01$) for every buffer in the series. Indeed, if the pH of the analyte zone were different than that of the run buffer, then there would be a bias in the final pK_a determination.

4.2. pK_a determinations

The pK_a values for a series of 23 acids and bases were determined (7 of these values were reported by us previously [10]). The results of those determinations are shown in Table 2. Less than a 0.07 difference of pK_a with the literature values [16,17] were obtained for pK_a values less than 9. These differences are probably reflective of the random error of the procedure. As an example, for a single compound, the random error was ± 0.071 at 95% confidence, from 10 separate determinations of 2-aminopyridine.

There were significant differences between the CE-determined pK_a values of bases with literature pK_a values greater than 9. A series of simple experiments were run to elucidate this inconsistency. In the first experiment, a weak acid with a high pK_a value, phenol, was shown to be in agreement with the literature value. This determination suggests that there is no inherent problem with the high pH buffers which could bias the result. Ionic interactions of amines with silica surfaces are a well established phenomenon in separations. At pH values greater than 8, the silica surface is fully charged. Indeed, the EOF is nearly consistent above pH 7, whereas below 7 it decreases. Thus, ion exchange with the column surface for the simple molecules in this study would be expected to correlate with α, the fractional degree of ionization. The ion-exchange wall effects would result in a proportionately decreased mobility relative to no ion exchange with the wall, and hence, would not impact the pK_a determination. Any other adsorptive effect could be measured by a non-zero mobility at a pH 2 or more units below the pK_a. There was no adsorptive effect which was measurable in our experiments. Indeed, if the electrophoretic mobility were slower due to adsorption, then the determined pK_a would be less than the actual pK_a. In the questioned data here, all of the pK_a values were higher. Also, there was excellent agreement of the literature values for nicotine, 8.08 by CE versus 8.02 literature and quinine, 8.52 by both CE and literature. The wall would be expected to have a similar effect in all the pH buffers above 7.

If there was an effect from adsorption or ion exchange, then the effect could be masked with an amine with a higher pK_a value than the solute at a higher concentration in the buffer. Indeed,

Table 2
CE pK_a determinations versus literature values

Molecule	pK_a (lit.)	pK_a (CE)	Difference
o-Bromoaniline	2.53	2.55	−0.02
Salicylic acid	2.98	2.96	0.02
p-Bromoaniline	3.88	3.85	0.03
Benzoic acid	4.2	4.18	0.02
2-Ethylaniline	4.37	4.32	0.05
Cinnamic acid	4.4	4.4	0
Aniline	4.6	4.66	−0.06
2-Ethylaniline	4.7	4.69	0.01
3-Ethylaniline	5.07	5.09	−0.02
Pyridine	5.19	5.26	−0.07
N,N'-dimethylaniline	5.99	5.96	0.03
4-Nitrophenol	7.15	7.15	0
2-Aminopyridine	6.71	6.76	−0.05
Nicotine	8.02	8.08	−0.06
Quinine	8.52	8.52	0
4-*tert.*-Butylpyridine	9.08	9.52	−0.44
4-Aminopyridine	9.11	9.25	−0.14
2-Methybenzylamine	9.19	9.4	−0.21
3-Methylbenzylamine	9.33	9.57	−0.24
2-Methoxybenzylamine	9.71	0.05	−0.35
α-Methylbenzylamine	9.83	9.94	−0.11
Phenethylamine	9.83	10.03	−0.2
Phenol	9.99	9.9	10.08

Table 3
Spectroscopic determination of pK_a values compared to literature and CE

Solute	pK_a literature	pK_a spectroscopic	pK_a CE
2-Methylbenzylamine	9.19	9.48	9.40
3-Methylbenzylamine	9.70	9.54	9.57
2-Methoxybenzylamine	9.33	9.92	10.05

the buffer series was prepared using pyrollidine ($pK_a = 11.27$) as the neutralizing base instead of sodium hydroxide. With the pyrollidine buffer series, the pK_a was determined for 2-methoxybenzylamine to be 9.96, more consistent with the previously determined CE value of 10.05 and inconsistent with the literature value of 9.70.

As calculated above, the buffers had enough capacity to prevent a significant change in the pH of the zone impacting the measurement. To prove this effect, the concentration of 4-aminopyridine was varied from 10 to 900 μM and there was no correlation with the pK_a determined.

To referee this inconsistency with the literature, the pK_a values of three bases with large errors were determined spectroscopically. (Solubility was too low for an accurate potentiometric determination.) Spectroscopic pK_a determination relies on the change in solute absorbance at a specific wavelength versus pH. As shown in Table 3, the spectroscopic determined pK_a values agree much more closely with the CE determined values.

All of the experiments to elucidate the inconsistency of the CE data with the literature data together suggest problems with the literature values for these particular bases. The method cited in the IUPAC database for these compounds was to prepare a sample at 0.02 M containing an equal concentration of salt and base and to measure the pH of that solution with a hydrogen electrode [18].

5. Conclusions

CE is an effective method for determining pK_a values. The method is particularly useful for determining the pK_a values of compounds with low water solubility. For example, compounds of limited water solubility need not be prepared in a co-solvent as is required by potentiometry, and it is not necessary to accurately know the concentration of a titrant or solute. There is no time consuming preparation of carbonate-free buffers. The detection limit for a 12-nl injection, reported previously [10] was $\epsilon^{220}bc = 1 \cdot 10^{-4}$ which, for benzoic acid, was 2 μM, 50 times lower than a typical determination limit via potentiometric titration. The procedure gave determined pK_a values to within 0.07 units of literature values from the IUPAC database for analytes below a pK_a value of 9. The range evaluated was 2.43 to 9.99. The analysis time was between 2 and 3.5 h per solute and no attempts were made to minimize this time.

Differences between CE-determined values and literature values for high pK_a bases were investigated by taking a series of 9 bases with literature pK_a values ranging between 8.02 and 9.83 and comparing the CE determined values with the literature values. Literature values above 9 were significantly lower than the CE-determined values. This difference was not due to an inherent limitation in the procedure for high pK_a determinations; a weak acid with a pK_a above 9 was accurately determined. Concentration effects and ionic interactions with the capillary wall were systematically eliminated as potential reasons for the differences also. To referee the differences between the historical data and the CE data, the pK_a values were determined spectroscopically for three compounds with large errors. The spectroscopic results agreed more closely with the CE results suggesting that the literature values of the solutes chosen may be unreliable.

Acknowledgements

The inspiration and support of Yvonne Walbroehl of the Dow Chemical Analytical Sciences Laboratory and Marguerite Benko of the DowElanco Discovery Department are gratefully acknowledged.

References

[1] L.Z. Benet and J.E. Goyan, *J. Pharm. Sci.*, 56 (1967) 665.
[2] A. Roda, A. Minutello and A. Fini, *J. Lipid Res.*, 31 (1990) 1433.
[3] R.A. Scherrer, in P.S. Magee, G.K. Kohn and J.J. Menn (Editors), *Pesticide Synthesis through Rational Approaches* (*ACS Symposium Series*, No. 255), American Chemical Society, Washington, DC, 1984, p. 225.
[4] R.F. Cookson, *Chem. Rev.*, 74 (1974)1.
[5] A. Albert and E.P. Serjeant, *The Determination of Ionization Constants: A Laboratory Manual*, Chapman and Hall, New York, 3rd ed., 1984.
[6] E.J. King, *Acid-Base Equilibria*, Pergamon, Oxford, 1965.
[7] J.B. Hansen and O. Hafliger, *J. Pharm. Sci.*, 72 (1983) 429.
[8] J.L. Beckers, F.M. Everaerts and M.T. Ackermans, *J. Chromatogr.*, 537 (1991) 407.
[9] J. Cai, J.T. Smith and Z. El Rassi, *J. High Resolut. Chromatogr.*, 15 (1992) 30.
[10] J.A. Cleveland, M.H. Benko, S.J. Gluck and Y.M. Walbroehl, *J. Chromatogr. A*, 652 (1993) 301.
[11] S.J. Gluck and J.A. Cleveland, *J. Chromatogr. A*, 680 (1994) 49.
[12] W.J. Lambert and D.L. Middleton, *Anal. Chem.*, 62 (1990) 1585.
[13] J.A. Cleveland, C.L. Martin and S.J. Gluck, *J. Chromatogr. A*, 679 (1994) 167.
[14] J. Vindevogel and P. Sandra, *J. Chromatogr.*, 541 (1991) 483.
[15] C.J. Nyman and R.E. Hamm, *Chemical Equilibrium*, Raytheon Education Company, 1968.
[16] Z. Rappoport (Editor), *CRC Handbook of Tables for Organic Compound Identification*, CRC Press, Cleveland., 3rd ed., 1967, pp. 428–439.
[17] D.D. Perrin (Editor), *Dissociation Constants of Organic Bases in Aqueous Solution*, Butterworths, London, 1965.
[18] W.H. Carothers, C.F. Bickford and G.J. Hurwitz, *J. Am. Chem. Soc.*, 49 (1927) 2908.

ELSEVIER

Journal of Chromatography A, 680 (1994) 49–56

JOURNAL OF CHROMATOGRAPHY A

Investigation of experimental approaches to the determination of pK_a values by capillary electrophoresis

S.J. Gluck*[,a], J.A. Cleveland, Jr.[b]

[a]*Analytical Sciences, 1897B Bldg, Dow Chemical Co., Midland MI 48667, USA*

[b]*Discovery Research, DowElanco, 9410 Zionsville Rd, Indianapolis IN 46268-1053, USA*

Abstract

The calculation of pK_a values from capillary electrophoresis data may be accomplished in several ways. Electrophoretic mobilities are fitted to a model which describes the dissociation versus the pH. For a linear model, a linear regression approach yields biased results. Weighted linear regression requires many replicates to determine weighting factors and is thus a time-consuming experiment. For an exponential model, non-linear regression of the electrophoretic mobilities in different, equally pH spaced buffers of the analyte gives the least biased determination. Another experimental approach to this determination is to use a permanently charged solute to correct for potential biases in the expected electrophoretic mobilities obtained between different buffers. In the buffer series chosen, there was no significant bias observed. Buffer pH may be determined by an in situ approach using an internal standard of known pK_a. However, the precision obtained is much less than using a pH meter.

1. Introduction

The measurement of electrophoretic mobility versus pH has been developed for pK_a value determination in several laboratories [1–4]. This procedure was developed for poorly soluble compounds with typical working concentrations of 10 to 1000 μM. As an example of the sensitivity of the procedure, the detection limit was 2 μM for benzoic acid [3]. Several reasonable methods are feasible for calculating the pK_a values from electrophoretic mobilities and buffer pH. In addition, we previously suggested two possible alternative calculation and experimental approaches. Corrections for potential discontinuities in electrophoretic mobilities between buffers were proposed by adding a fixed charge solute to the analysis mixture. In the other approach, an internal standard of known pK_a was added as an in situ approach to determine the pH of each buffer. These issues regarding the experimental and calculational approaches are examined in this investigation.

2. Theory

The determination is based on the principle that a solute has its maximum electrophoretic mobility when it is fully ionized, has no mobility in its neutral form, and has an intermediate, well modeled, mobility in the pH region surrounding

* Corresponding author.

SSDI 0021-9673(94)00270-O

its pK_a [1–3]. Electrophoretic mobility is calculated from the migration time of a neutral marker, t_{eof}, the migration time of the solute, t, the length of the column, L_c, the length of the column between the injection end and the detector, L_d, and the applied voltage, V, according to the relation

$$\mu = \left(\frac{L_c L_d}{V}\right)\left(\frac{1}{t} - \frac{1}{t_{oef}}\right) \quad (1)$$

There are several experimental approaches and models which apply. Derivations of these expressions were developed elsewhere [1–4].

2.1. Non-linear model

The non-linear model at 25°C is

$$pK_a = pH - \log\left(\frac{\mu}{\mu_{z^-} - \mu}\right) + \frac{0.5085 z^2 \sqrt{I}}{1 + 0.3281 a \sqrt{I}} \quad (2)$$

where pK_a is the thermodynamic pK_a, μ, the electrophoretic mobility at the pH of the buffer in the CE column, μ_{z^-} the electrophoretic mobility of the fully ionized acid, z the valency of the ion, I the ionic strength of the buffer solution, and a is the ion size parameter, generally unknown but assumed to be 5 Å [5]. The third term in the equation is equal to $-\log \gamma$, where γ is the activity coefficient of the ions in solution.

The analogous expression for a base, B is

$$pK_a = pH + \log\left(\frac{\mu}{\mu_{BH^+} - \mu}\right) - \frac{0.5085 z^2 \sqrt{I}}{1 + 0.3281 a \sqrt{I}} \quad (3)$$

The compounds used in this study were all bases and hence, only equations for bases will be shown for simplicity. Eq. 3 is rearranged for non-linear regression to

$$\mu = \frac{\mu_{BH^+} 10^{(pK_a - pH_c)}}{1 + 10^{(pK_a - pH_c)}} \quad (4)$$

The pH_c is the activity corrected pH:

$$pH_c = pH - \frac{0.5085 z^2 \sqrt{I}}{1 + 0.3281 a \sqrt{I}} \quad (5)$$

2.2. Linear model

The linear model, derived from the same equilibrium expressions as Eq. 3 is

$$\frac{1}{\mu} = \frac{1}{K \cdot \mu_{BH^+}} \cdot \frac{\gamma}{\{H^+\}} + \frac{1}{\mu_{BH^+}} \quad (6)$$

where $\{H^+\}$ is the hydrogen ion activity. The inverse of the intercept times the slope of the line gives K. The same equation is used for weighted linear regression. The standard deviations of the inverse mobilities are used for the weighting factors.

2.3. Use of ionic mobility reference

The electrophoretic mobility of a solute, modeled as a solid sphere, is usually expressed as

$$\mu = \frac{q}{6\pi\eta R} \quad (7)$$

where q is the net charge, η is the solution viscosity and R is the apparent hydrodynamic radius of the sphere. This equation is only valid in an infinitely dilute solution but we use it here to show the potential for experimental bias in pK_a determinations. In a plot of μ versus pH from experimental data, there may be individual values of μ which appear to either have random error or a bias. We refer to a bias in the mobility between separate run buffers as a discontinuous effect. Discontinuity in μ as measured from Eq. 7 would result from assumptions that q, η, and R are the same in all the buffers. For weak acids and bases, q is expected to change predictably as a function of pH. The R may be expected to change as a function of pH, a continuous effect, or buffer ion species, a discontinuous effect, although the direction of the change would be opposite for cations relative to anions. If η changes, then the effect can be quantitated and corrected by an external measurement. An approach was proposed to use an internal mobility

marker which is fully charged throughout the pH range of the experiment [3]. The anion, 4-toluenesulfonate (TSA), has a pK_a of approximately −7 and is thus fully charged throughout the experiment. The mobility of a weak base can be referenced to the mobility of the TSA and Eq. 3 becomes:

$$pK_a = pH + \log\left(\frac{\mu}{\mu_{BH^+} \cdot \frac{\mu_{TSA}'}{\mu_{TSA}} - \mu}\right) - \frac{0.5085z^2\sqrt{I}}{1 + 0.3281a\sqrt{I}} \quad (8)$$

The ratio, μ_{TSA}'/μ_{TSA} is referred to as the buffer discontinuity factor. The μ_{TSA} is the electrophoretic mobility of the TSA in the pH buffer. The μ_{TSA}' is the minimum electrophoretic mobility of the TSA in the whole buffer series. Since anions move in the opposite direction of the electroosmotic flow, their mobilities are negative and thus, the minimum electrophoretic mobility has the largest absolute value of the series. A buffer series consists of all the buffers used in a pK_a determination experiment. Thus, as an example, if the measured μ_{TSA} in a pH 6 buffer is lower than the μ_{TSA} values measured in the other pH buffers in the series, then the μ_{TSA} for the pH 6 buffer becomes μ_{TSA}'. If the only difference between all the μ_{TSA} values in the whole buffer series is the experimental error, then the inclusion of the buffer discontinuity factor in Eq. 8 will not have a significant impact on the pK_a determination.

2.4. Use of an internal electrophoretic mobility standard

The pH can be defined from the mobility of a second solute, a base, with a dissociation constant having the value pK_a'

$$pH = pK_a' - \log\left(\frac{\mu'}{\mu_{BH^+}' - \mu'}\right) + \frac{0.5085z^2\sqrt{I}}{1 + 0.3281a\sqrt{I}} \quad (9)$$

Substituting into Eq. 3 gives

$$pK = pK_a' - \log\left(\frac{\mu'}{\mu_{BH^+}' - \mu'}\right) + \log\left(\frac{\mu}{\mu_{BH^+} - \mu}\right) \quad (10)$$

In Eq. 10, it is interesting to note that the activity correction drops out.

3. Experimental

3.1. Instrument parameters

A SpectraPHORESIS 1000 (Thermo Separation Products, Fremont, CA, USA) was used for all experiments. Typically, a 2-s hydrodynamic injection was performed. Since the hydrodynamic injection rate is 6 nl/s for a 67 cm × 75 μm untreated fused-silica capillary (Polymicro Technology, Phoenix, AZ, USA), 12 nl was loaded onto the column. The separation distance, L_d, was 59.5 cm. The temperature was set at 25°C. UV absorption was monitored at 220 and 240 nm. With the instrument operating at 25 kV, typical currents were less than 20 μA.

In order to equilibrate the column and thereby minimize hysteresis effects, the following wash cycle was performed prior to each run in a sequence: (1) 2.5 min with 0.1 *M* NaOH, (2) 2.5 min with water, and (3) 3.0 min with running buffer.

Because the SpectraPHORESIS 1000 is equipped with a single reservoir for the buffer near the detector, it is not possible to match buffers at each end of the column in a sequence. Tricine (0.02 *M*, pH 7.6 to 8.1) was used as the buffer at the detector end of the column.

Buffer pH was measured using a Fisher Accuphast pH electrode with an Orion Model EA940 meter. Meter calibrations were made with Fisher NIST traceable buffer solutions.

3.2. Methods

All sample and buffer solutions were prepared using distilled, deionized, and filtered water (ASTM type I specification). The buffers used

were similar to those described in Refs. [3,4]. In the regression model evaluations, the sample consisted of 200 μM 2-aminopyridine and 1 mM mesityl oxide. In the experiments to investigate buffer discontinuity, the sample was 1 mM mesityl oxide, 100 μM α-methylbenzene and 75 μM toluenesulfonate. In the experiments with the internal standards to determine pH in situ, the sample was 1 mM mesityl oxide and 50 μM each of 2- and 3-ethylaniline.

Several routines were written in the Mathcad 4.0 (MathSoft, Cambridge, MA, USA) program to do the non-linear regressions, the linear regression and the weighted linear regression required as in Eqs. 4, 6, 8, 9 and 10. The weights for the weighted regression were the standard deviations of the inverse mobilities.

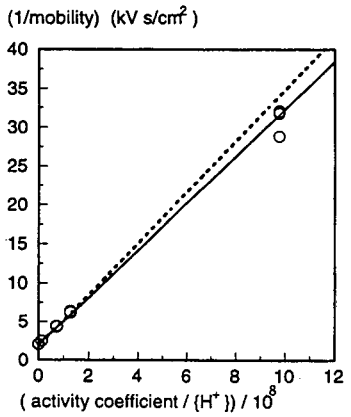

Fig. 1. Comparison of linear regression (solid line), weighted linear regression (dashed line) and the raw data (○).

4. Results

4.1. Evaluation of the different regression models

Repeatability of mobilities and migration times

At each of 6 pH values, 10 replicate determinations were performed for 2-aminopyridine. The mean electrophoretic mobilities, analyte migration times, and neutral marker migration times are listed in Table 1 along with their respective standard deviations. As the migration times of the neutral marker increased, the standard deviation also increased, indicating a potential problem with the precision of the parameters calculated from linear regression; linear regression assumes that the standard deviations of the y-values are constant.

Linear and weighted linear regression

Linear regression gave a pK_a value of 6.84 and weighted linear regression gave a pK_a value of 6.77 with $n = 60$. For comparison, the literature value is 6.71 [6]. The data are plotted in Fig. 1. The precision of the pK_a value at the 95%

Table 1
Mean and standard deviations of the electrophoretic mobilities and migration times of 2-aminopyridine and mesityl oxide

pH	Mean mobility (cm^2/Vs)	Standard deviation of mobility (cm^2/Vs)	Migration time (min)	Standard deviation of migration time (min)	Migration time of neutral marker (min)	Standard deviation of neutral marker migration time (min)
8.03	$-3.17 \cdot 10^{-5}$	$1.06 \cdot 10^{-6}$	3.46	$1.07 \cdot 10^{-2}$	3.57	$8.23 \cdot 10^{-3}$
7.15	$-1.60 \cdot 10^{-4}$	$1.93 \cdot 10^{-6}$	3.35	$1.75 \cdot 10^{-2}$	3.95	$1.66 \cdot 10^{-2}$
6.91	$-2.29 \cdot 10^{-4}$	$3.27 \cdot 10^{-6}$	3.11	$2.21 \cdot 10^{-2}$	3.89	$2.36 \cdot 10^{-2}$
6.16	$-4.10 \cdot 10^{-4}$	$3.07 \cdot 10^{-6}$	2.77	$4.22 \cdot 10^{-3}$	4.08	$1.25 \cdot 10^{-2}$
5.45	$-4.91 \cdot 10^{-4}$	$3.47 \cdot 10^{-6}$	2.80	$2.72 \cdot 10^{-2}$	4.62	$8.75 \cdot 10^{-2}$
4.88	$-5.10 \cdot 10^{-4}$	$1.38 \cdot 10^{-6}$	2.97	$3.60 \cdot 10^{-2}$	5.20	$1.12 \cdot 10^{-1}$

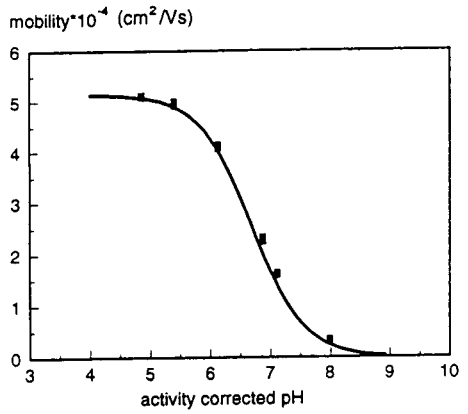

Fig. 2. Raw data and the calculated line based on the non-linear regression.

confidence level for linear regression was ±0.071, and for weighted regression the value was ±0.025. The linear regression was significantly influenced by the wider variance in mobilities in the lower pH buffers. The experiment was designed with buffer pH values equally spaced about the pK_a of the solute. In the inverse linear format of Eq. 6 required for the linear regression, this experimental design is unbalanced; hence, the lowest pH data has significant leverage over the rest of the data. Weighted regression removed this leverage by minimizing the significance of the data relative to its variance.

Non-linear regression

Non-linear regression using Eq. 4 takes advantage of the experimental design of equally spaced pH buffers about the pK_a of the solute and gives a pK_a of 6.76, in close agreement with the weighted linear regression. Fig. 2 shows the raw data and the calculated line for the non-linear regression.

4.2. Use of ionic mobility reference

Table 2 gives the pH values, the electrophoretic mobilities of α-methylbenzylamine and TSA, and the buffer discontinuity correction factors based on the TSA mobilities. With the exception of the pH 10.03 buffer, the correction factors appear to be very small relative to amounts which would make a significant difference in the final pK_a determination. Using all of the data, the pK_a value determined using the uncorrected mobilities was 9.43, and using the factored mobilities was 9.42. The discontinuity between buffers was not significant enough to impact pK_a determinations. Under the conditions of this experiment, there was not a measurable difference in electrophoretic mobility discontinuity between buffers with the exception of

Table 2
Activity corrected pH values and mobility data

Activity corrected pH	α-Methylbenzylamine mobility (cm^2/Vs)	TSA mobility (cm^2/Vs)	Discontinuity factor (μ_{TSA}'/μ_{TSA})
6.11	$-3.71 \cdot 10^{-4}$	$3.93 \cdot 10^{-4}$	1.06
6.86	$-3.66 \cdot 10^{-4}$	$3.94 \cdot 10^{-4}$	1.05
7.10	$-3.71 \cdot 10^{-4}$	$4.00 \cdot 10^{-4}$	1.04
7.49	$-3.57 \cdot 10^{-4}$	$3.86 \cdot 10^{-4}$	1.07
8.29	$-3.43 \cdot 10^{-4}$	$3.91 \cdot 10^{-4}$	1.06
8.60	$-3.16 \cdot 10^{-4}$	$3.97 \cdot 10^{-4}$	1.05
9.19	$-2.38 \cdot 10^{-4}$	$3.91 \cdot 10^{-4}$	1.06
9.55	$-1.50 \cdot 10^{-4}$	$3.95 \cdot 10^{-4}$	1.05
10.03	$-7.98 \cdot 10^{-5}$	$4.15 \cdot 10^{-4}$	1.00

The discontinuity factor is the ratio of the minumum mobility of the toluene sulfonic acid in the whole buffer series divided by the toluene sulfonic acid mobility at the pH of the run buffer

one buffer, pH 10.03 CAPS. The reason for the discontinuity for the one buffer is not understood and is likely to be an experimental error. The magnitude of the discontinuity does not impact the pK_a value determination.

4.3. Use of an internal electrophoretic mobility standard

Determination of pH via electrophoretic mobility

The electrophoretic mobility of a solute of known pK_a can, in theory, be used to determine pH. Table 3 shows the results of calculating pH from Eq. 9 using the mobilities obtained within the different buffers. The μ_{BH^+} was estimated as having a slightly greater mobility than the mobility at pH 3.05 where the solutes, 3- and 2-ethylaniline, should be fully ionized. The pK_a values of the solutes were already known. The errors in the calculated pH values along with the actual measured pH values corrected for their activities (see Eq. 5) are presented in Fig. 3. A more complete understanding of these errors can be obtained from propagation of errors analysis.

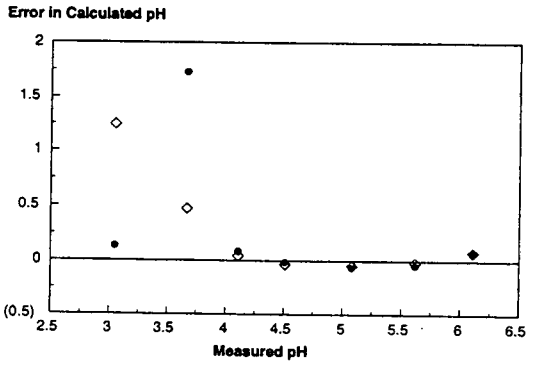

Fig. 3. Error in calculated pH from the mobilities of (●) 3- and (◇) 2-ethylaniline at different pH values.

Propagation of errors in pH determination via electrophoretic mobility

Assuming the μ_{BH^+} and the pK_a to be constants in the determination of pH, the only variables are t and t_{eof}. From Eqs. 1, 3 and 5, pH may be expressed as

$$\mathrm{pH} = pK_a - \log\left[\frac{\left(\frac{1}{t}-\frac{1}{t_{eof}}\right)}{\left(\frac{1}{t_{BH^+}}-\frac{1}{t}\right)-\left(\frac{1}{t}-\frac{1}{t_{eof}}\right)}\right] + \frac{0.5085z^2\sqrt{I}}{1+0.3281a\sqrt{I}} \quad (11)$$

The variance in pH determination is the sum of the variances due to each variable obtained from the experiment

$$\frac{\partial \mathrm{pH}}{\partial t} = \left(\frac{\partial \mathrm{pH}}{\partial t_{eof}}\right)^2 \sigma^2_{t_{eof}} + \left(\frac{\partial \mathrm{pH}}{\partial t}\right)^2 \sigma^2_t \quad (12)$$

where σ is the standard deviation. For the purposes of this error propagation, t_{eof} is assumed to be a constant.

Table 3
Calculated pH values from electrophoretic mobilities

pH Measured less	pH calculated from	
The activity correction	3-Ethylaniline mobility	2-Ethylaniline mobility
3.05	2.92	1.81
3.67	1.94	3.20
4.11	4.03	4.07
4.51	4.53	4.54
5.08	5.14	5.13
5.62	5.66	5.64
6.11	6.03	6.03

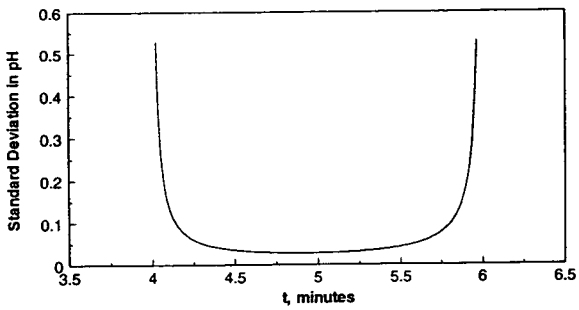

Fig. 4. Estimated standard deviation in the determination of pH by CE versus migration time where $t_{eof} = 6$ min, $\sigma_{t_{eof}} = 0.03$, $\sigma_t = 0.03$ and $t_{BH^+} = 4$ min.

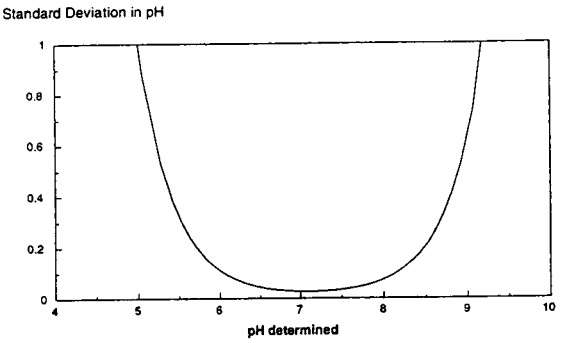

Fig. 5. Estimated standard deviation in pH versus pH measured for a solute with a pK_a equal to 7.

From Eq. 12, the partial derivatives of pH with respect to t and t_{eof} are

$$\frac{\partial \mathrm{pH}}{\partial t} = \frac{(t_{BH^+} - t_{eof})}{2.303(t - t_{BH^+})(t - t_{eof})} \tag{13}$$

$$\frac{\partial \mathrm{pH}}{\partial t_{eof}} = \frac{-1}{t_{eof}^2\left(\frac{1}{t} - \frac{t}{t_{eof}}\right)\ln(10)} \tag{14}$$

Substituting Eqs. 13 and 14 into Eq. 12, the variance in pH can be expressed as in Eq. 15. Using typical values ($pK = 7$, $t_{eof} = 6$ min, $\sigma_{t_{eof}} = 0.03$, $\sigma_t = 0.03$, $t_{BH^+} = 4$ min), the standard deviation of the error in pH determination is plotted in Fig. 4.

A more general way of expressing the error in the determined pH is to use actual pH values for the x-axis (Fig. 5).

As can be seen from Figs. 4 and 5, the estimated standard deviation in the calculated pH is high in the extremes where t is near t_{eof} and t_{BH^+}. This corresponds to ± 1 pH unit from the pK_a. Hence, when a solute of known pK_a is used to determine the pH, the most reliable determination will result from using mobilities taken in buffers which are within ± 1 pH unit of the pK_a values of the solutes.

pK_a determination using a second solute of known pK_a

The pK_a of 3-ethylaniline was determined with Eq. 10 using the mobilities of 2-ethylaniline at different pH values. These mobilities are listed in Table 4. The pK_a as determined by non-linear regression was 4.35, compared to a literature value of 4.37, was very sensitive to reasonable initial estimates of the μ_{BH^+}, the μ_{BH^+}' and the pK_a. The dependence on the initial estimates was so sensitive that pK_a values at least as wide as 4.1 to 4.6 could be determined with a minimized sum of squares. Using known pH values determined by a pH electrode, the procedure is insensitive to reasonable initial values of the parameters required for the non-linear regression analysis. Indeed, the variables μ and μ' are statistically highly correlated with each other, thus the regression analysis becomes mathematically unstable yielding large uncertainties in the parameter estimates.

5. Conclusions

Non-linear regression is the simplest and most precise regression procedure for determining the pK_a value of a solute by CE. Weighted regres-

$$\sigma_{\mathrm{pH}}^2 = \frac{t^4\sigma_{t_{eof}}^2 - 2t^3\sigma_{t_{eof}}^2 t_{BH^+} + t^2\sigma_{t_{eof}}^2 t_{BH^+} + t_{eof}^4\sigma_t^2 - 2t_{eof}^3\sigma_t^2 t_{BH^+} + t_{eof}^2\sigma_t^2 t_{BH^+}}{t_{eof}^2(t - t_{eof})^2\ln(10)^2(t - t_{BH^+})^2} \tag{15}$$

Table 4
Activity correction factor for solution ionic strength, mobilities (cm^2/Vs), calculated pH based on the mobility of 2-ethylaniline and its known pK_a, and actual pH as measured from a pH meter

$-\log(\gamma_{BH^+})$	3-Ethylaniline mobility (cm^2/Vs)	2-Ethylaniline mobility (cm^2/Vs)	pH calculated from 2-ethylaniline mobility	pH measured
0.03	$3.74 \cdot 10^{-4}$	$3.50 \cdot 10^{-4}$	1.81	3.08
0.02	$3.79 \cdot 10^{-4}$	$3.30 \cdot 10^{-4}$	3.20	3.69
0.02	$3.16 \cdot 10^{-4}$	$2.38 \cdot 10^{-4}$	4.07	4.13
0.02	$2.32 \cdot 10^{-4}$	$1.45 \cdot 10^{-4}$	4.54	4.53
0.04	$1.08 \cdot 10^{-4}$	$5.64 \cdot 10^{-5}$	5.13	5.12
0.06	$4.21 \cdot 10^{-5}$	$2.04 \cdot 10^{-5}$	5.64	5.68
0.04	$1.85 \cdot 10^{-5}$	$8.14 \cdot 10^{-6}$	6.03	6.15

sion gives precise values; however, it requires many replicates to determine the standard deviations of the electrophoretic mobilities at different pH values. Linear regression is the least precise procedure because of its sensitivity to influential outliers. An experimental design appropriate for non-linear regression is to space the buffer pH values equal distances around the pK_a of the solute. Linear regression would require an experimental design using equally spaced ionic activity coefficients divided by the proton activity around the K of the solute. This design would not be linear with respect to the fraction of ionization. In the investigation of solutes of unknown pK_a, it is important to cover a wide pH range. This is most easily accomplished with a series of equally spaced pH buffers which are linear with respect to the fraction of ionization. Hence, non-linear regression is the recommended statistical procedure.

Correcting for a potential experimental bias or discontinuity in electrophoretic mobilities between different buffers in a series of buffers was investigated by using a solute with a constant mobility in all pH buffers. If a chemical or physical effect of the buffer were to cause a change in hydrodynamic radius of the solute, or if the buffers varied in viscosity, then this effect could be quantitatively corrected. In a test of this hypothesis, there was not a significant change in the mobilities of the totally ionized solute versus pH. Hence, the same pK_a, within statistical significance, was determined with both corrected and raw mobilities. For simplicity, it is recommended that future pK_a determinations do not include a constant mobility marker when using experimental conditions similar to those in this report.

The internal standard procedure of using a solute with a known pK_a for determining an unknown solute's pK_a value by CE is not recommended because it yields less precise pK_a determinations than the normal means of using buffers with their pH measured with a pH meter. The source of the imprecision is the narrow range of accurate pH prediction from the internal standard as demonstrated through experimentation and a propagation of error study. Indeed, the best pH prediction by this procedure would inherently rely on the accuracy of the literature pK_a value of the internal standard. A second reason for the technique's imprecision is the high correlation between the electrophoretic mobilities of the reference solute and the unknown solute. The recommended procedure remains to measure the pH of the running buffers with a pH meter.

References

[1] J.M. Beckers F.M. Everaerts and M.T. Ackermans, *J. Chromatogr.*, 537 (1991) 407.
[2] J. Cai, J.T. Smith and Z. El Rassi, *J. High Resolut. Chromatogr.*, 15 (1992) 30.
[3] J.A. Cleveland, M.H. Benko, S.J. Gluck and Y.M. Walbroehl, *J. Chromatogr. A*, 652 (1993) 301.
[4] S.J. Gluck and J.A. Cleveland, *J. Chromatogr. A*, 680 (1994) 43.
[5] J. Kielland, *J. Am. Chem. Soc.*, 59 (1937) 1675.
[6] D.D. Perrin, *Dissociation Constants of Organic Bases in Aqueous Solution*, Butterworths, London, 1965.

ELSEVIER

Journal of Chromatography A, 680 (1994) 57–61

JOURNAL OF CHROMATOGRAPHY A

Imprinted polymers as antibody mimetics and new affinity gels for selective separations in capillary electrophoresis

Kurt Nilsson[a,*], Johan Lindell[a], Olof Norrlöw[b], Börje Sellergren[c]

[a]*Department of Biotechnology, Chemical Centre, University of Lund, P.O. Box 124, S-22100 Lund, Sweden*
[b]*Department of Technical Analytical Chemistry, Chemical Centre, University of Lund, P.O. Box 124, S-22100 Lund, Sweden*
[c]*Department of Analytical Chemistry, Chemical Centre, University of Lund, P.O. Box 124, S-22100 Lund, Sweden*

Abstract

Methacrylate-based imprinted dispersion polymers could be prepared in situ in a fused-silica capillary as agglomerates (*ca.* 10 μm) of micrometer-sized globular particles, exhibiting antibody mimetic, molecular recognition properties. Thus, in one example, imprinted polymer particles selective for pentamidine (PAM), a drug used for the treatment of AIDS-related pneumonia, could be prepared in situ in the capillary. The retention could be varied predictably by changing the electrolyte pH. Thus, whereas no observable elution of PAM was achieved at near neutral pH, the PAM-selective capillary gave a retention time of 18 min for PAM and 7.8 min for benzamidine at pH 3.5, whereas the retention times were 6.6 and 6.1 min, respectively, with a reference capillary. Importantly, the electrolyte could by pumped hydrodynamically through the capillaries, allowing rapid phase changes and micro-chromatographic possibilities with high plate numbers.

1. Introduction

In capillary affinity gel electrophoresis a receptor molecule [1], e.g. a specific oligonucleotide sequence [2], or a protein [3] is bound to the gel or is dissolved in the electrolyte. The efficiency of this method together with the small sample amounts required are attractive for chiral drug bioanalysis. However, the acrylamide gels often suffer from poor stability, air bubble formation and limitations with respect to solvents. Moreover, gels or methods based on antibodies and other proteins suffer from poor stability and a complicated preparation scheme. Even if one can expect that some of these problems can be solved [4], the development of alternative polymeric phases for affinity capillary electrophoresis (CE) is worthwhile.

Previously, methacrylate-based polymers prepared by molecular imprinting around a template molecule [5] have been used as affinity stationary phases in HPLC for the successful and selective separation of several types of organic compounds, such as enantiomeric amino acid derivatives [6] and commercial drugs [7]. In general, this type of solid phase has shown high selectivity and good stability. We thought this type of technology would be useful in CE applications where high selectivity is required [8].

We now introduce imprinted polymer capillary electrophoresis (IMPCE) for analysis. In general, the gel material is prepared by template polymerization, which we found can be done directly in the capillary, whereby functional

* Corresponding author.

0021-9673/94/$07.00
SSDI 0021-9673(94)00497-W

monomers, preorganized around a template molecule, are copolymerized with a cross-linking monomer. After washing, the gel capillary can be used for the separation of the template molecule and analogues thereof.

We tested the selectivity of different methacrylate-based polymers prepared by template-dispersion polymerization in various CE applications, the results of which are described below.

2. Experimental

2.1. Chemicals and equipment

The monomers ethylene glycol dimethacrylate (EDMA) and methacrylic acid (MAA) and the initiator azobisisobutyronitrile (AIBN) were obtained from Aldrich and purified before polymerization experiments according to standard procedures and D- and L-phenylalanine anilide (D- and L-PA) were synthesized as described previously [6]. Benzamidine (BAM) (Aldrich) and pentamidine (PAM) (Rhone-Poulenc Pharma, Helsingborg, Sweden) were used in their free-base form. The electrophoretic separations were carried out using a Beckman P/ACE System 2100 electrophoresis unit equipped with System Gold software. Capillaries (polyimido-coated fused silica; 25 cm × 100 μm I.D.) were obtained from Skandinaviska Genetech (Gothenburg, Sweden).

2.2. Preparation of imprinted polymer capillaries

Capillaries pretreated with trimethoxysilylpropyl methacrylate and blocked with hexamethyldisilazane were used in the polymerization procedure with L-PA as the template molecule [9]. AIBN (0.1 ml) was added to a mixture of monomers, EDMA (0.38 ml) and MAA (0.034 ml), and L-PA (18 mg) in 2.9 ml of cyclohexanol–dodecanol (4:1, v/v). The mixture was gently heated, purged with nitrogen and sonicated. One end of the silica capillary was allowed to dip into the solution and the other end was connected to an aspirator vacuum flask. After passage through the capillary of an appropriate amount (five drops) of the template polymerization mixture, both ends of the capillary were fixed in contact with the mixture and polymerization was carried out for 24 h at 60°C. The polymer remaining in the vials was washed with ethanol, dried and characterized.

The preparation of the capillary selective for PAM followed basically the same procedure, but was carried out in 2-propanol and employing capillaries that were used as supplied (see Section 2.1). Addition of MAA (0.05 mmol) to a solution of the free-base form of PAM (12.5 μmol) in a vial containing 2-propanol (0.28 ml) and EDMA (1.2 mmol) caused the formation of a precipitate that dissolved on addition of water (0.13 ml). The template polymerization was initiated by addition of AIBN (1.2 mg in 0.05 ml of 2-propanol), with polymerization in the capillary as above. The polymerization with BAM was carried out similarly.

2.3. Capillary electrophoresis

The polymer-containing capillaries were loaded into cassettes and acetonitrile–0.05 *M* potassium phosphate buffer (pH 2) (7:3, v/v) was pumped hydrodynamically through the capillary in order to wash out the template molecule and replace the 2-propanol used as solvent during the polymerization at a pressure of 1300 p.s.i. (1 p.s.i. = 6894.76 Pa). Both the current and UV baseline stabilized within a few hours. Injection of samples was carried out at 6 kV for 2 s (D- or L-PA, 0.33 mg/ml) or at 5 kV for 3 s (PAM, 1 m*M*, BAM, 5 m*M*). BAM was injected at a higher concentration owing to its low absorbance. Separations were carried out at ambient temperature with a separation voltage of 5 kV (unless stated otherwise). UV detection was used to record the electropherograms (254 nm; 280 nm for PAM).

3. Results and discussion

A facile strategy was used to prepare the new type of gel-filled capillaries: a mixture of meth-

acrylate monomers, initiator and template molecule was sucked into the capillary and after polymerization the template molecule was washed out of the column by hydrodynamic solvent replacement. No leakage of polymer was observed and only a relatively low pressure (1300 p.s.i. or lower) had to be applied. This constitutes an important advantage of the polymers, allowing facile removal of any air bubbles by hydrodynamic pumping of electrolyte, and also allows the use of the imprinted polymer capillaries for separations in the chromatographic mode.

Characterization, as described elsewhere [10], of the polymer formed outside the capillaries indicated the formation of agglomerates, *ca.* 10 μm in size, consisting of globular particles, which were in the size range 0.5–2 μm when L-PA was used as the template and 2–4 μm when BAM or PAM was used as the template.

In the first type of imprinted polymer capillary, L-PA was used as the template molecule. Here, the polymerization was carried out in cyclohexanol–dodecanol as the solvent and the ratios of cross-linker to methacrylate and of monomer to solvent (w/w) were relatively low (80% and 14%, respectively), compared with previous preparations of imprinted polymers used in HPLC applications [6,7]. This facilitated pumping of the electrolyte through the capillary and exchange of solvent. However, owing to the low concentration of monomers during polymerization, no enantiomeric selectivity towards L-PA amide over D-PA was observed (see Fig. 1). Higher selectivity might be expected using other polymerization conditions.

The runs could be repeated reproducibly with a stable current. The presence of polymer was indicated by the ca. four times higher current in the gel-filled capillary, whereas the migration times of the eluted compounds were *ca.* half those with an open pretreated capillary. No selectivity compared with blank polymer capillaries was observed in the above L-PA capillary. Photoinitiation of the polymerization may produce selective capillaries in analogy with previous studies [11].

The use of the drug PAM and of BAM as

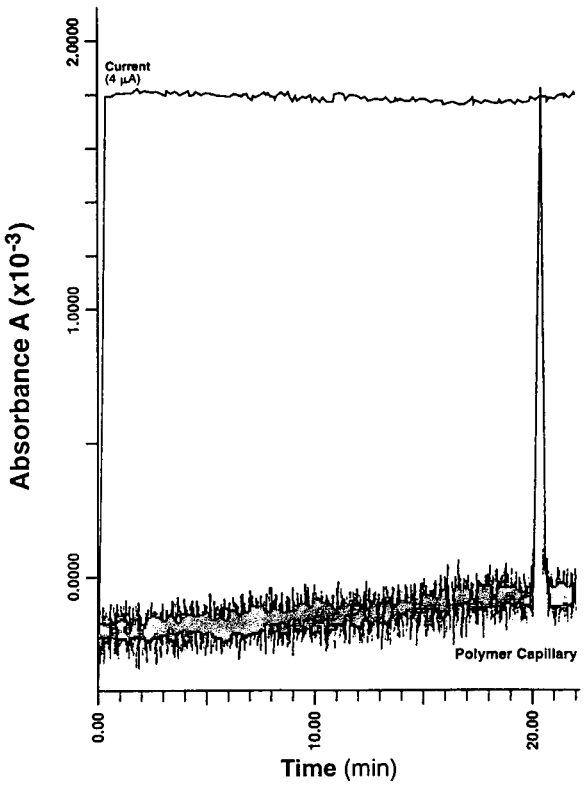

Fig. 1. Electropherogram of D,L-phenylalanine anilide (D,L-PA) injected on a polymer capillary prepared with L-PA as template.

template molecules was also investigated. Here, 2-propanol was used as the solvent during template polymerization, instead of cyclohexanol–dodecanol. Also, a higher concentration of monomers (52%, w/w solvent) and a higher ratio of cross-linker to methacrylate (96%, w/w) than in the L-PA polymerization were used.

In the CE application, the PAM-imprinted polymer capillary showed a very high selectivity towards PAM compared with BAM, which became much more pronounced at increased pH, whereas no such selectivity was observed with the BAM-imprinted or blank capillaries (see Table 1 and Fig. 2). Thus, whereas the BAM and blank capillaries showed similar retentions of PAM and BAM in the pH range 2–4, the PAM-imprinted capillary gave retention times of 6.8 and 6.1 min at pH 2 and 18 and 7.8 min at

Table 1
Retention times for benzamidine (BAM) and pentamidine (PAM) employing a PAM-imprinted polymer capillary or a BAM-imprinted capillary and different electrolyte pH

Capillary	Injected compound	Retention time (min)		
		pH 2	pH 3	pH 4
BAM-imprinted	PAM	5.8	6.1	6.5
	BAM	6.1	6.6	6.5
PAM-imprinted	BAM	6.1	7.5	7.1
	PAM	6.8	10.8	>20

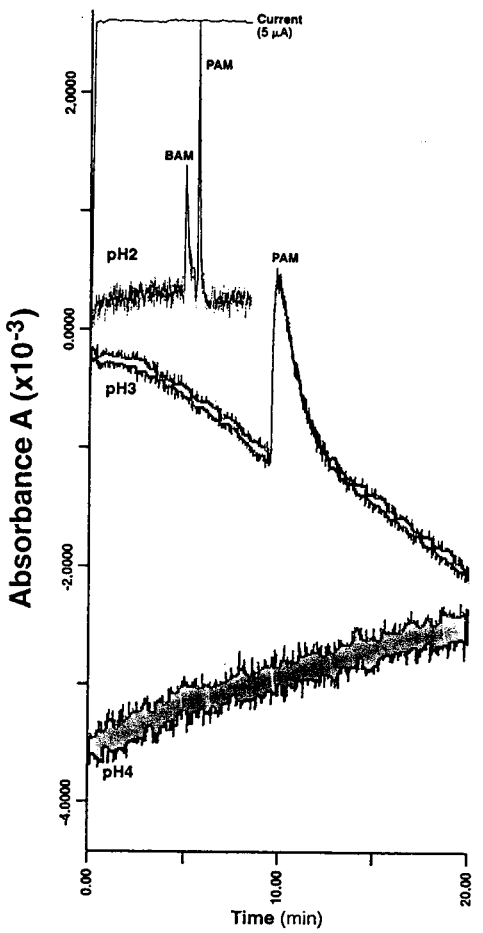

Fig. 2. Electropherograms of PAM and BAM injected onto a polymer capillary prepared with PAM as template and employing an electrolyte pH of 2, with superimposed electropherograms of PAM injected on to the same polymer capillary under the same conditions, but employing an electrolyte pH of 3 and 4, respectively.

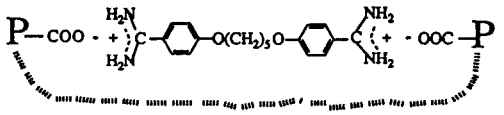

Fig. 3. Proposed interaction between PAM and the PAM-imprinted polymer.

pH 3.5 for PAM and BAM, respectively. At pH 4, PAM was apparently totally retained on the PAM-imprinted capillary. Also, considerable band broadening was observed for PAM on the PAM-imprinted capillary with increasing pH, whereas at low pH a fairly high plate number was observed ($N = 115\,000$/m at pH 2).

The results indicate that specific cavities for pentamidine might have been formed during the polymerization process and that the polymer might contain complementary carboxyl-groups containing binding sites to the two positively charged groups of PAM, as suggested in Fig. 3. BAM, which contains only one such group, does not interact specifically with the polymer.

In fact, the imprinted polymer capillaries behave similarly to antibody affinity columns, which show strong specific binding of antigen at near neutral pH and a dramatically decreased binding efficiency at lower pH, which, however, still allows specific elution of the bound material.

In conclusion, we have demonstrated the use of imprinted methacrylate polymers in CE. The polymer capillaries were prepared with straightforward methods and could be used repeatedly for several weeks. Moreover, solvents could easily be exchanged by hydrodynamic pumping. By using the proper conditions we could obtain capillaries with very high induced selectivity, which could be gradually modified from almost no selectivity to complete selective retention of the template molecule, by changing the electrolyte pH. We are further investigating the IMPCE technique for other template molecules and for chiral separation.

Acknowledgements

This research was supported by grants to K.N. from the Swedish Board of Technical Develop-

ment and to B.S. from the Swedish Board of Natural Sciences. Support from Glycorex (Lund, Sweden) is gratefully acknowledged.

References

[1] Y.H. Chu and G.M. Whitesides, *J. Org. Chem.*, 57 (1992) 3524.
[2] Y. Baba, M. Tsuhako, T. Sawa, M. Akashi and E. Yashima, *Anal. Chem.*, 64 (1992) 1920.
[3] S. Birnbaum and S. Nilsson, *Anal. Chem.*, 64 (1992) 2872.
[4] S. Hjertén, *J. Chromatogr.*, 646 (1993) 121.
[5] G. Wulff, in W.T. Ford (Editor), *Polymeric Reagents and Catalysts* (*ACS Symposium Series No.*, 308), American Chemical Society, Washington, DC, 1986, pp. 186–230.
[6] B. Sellergren, M. Lepisto and K. Mosbach, *J. Am. Chem. Soc.*, 110 (1988) 5853.
[7] G. Vlatakis, L. Anderson, R. Muller and K. Mosbach, *Nature*, 361 (1993) 645.
[8] K.G.I. Nilsson and B. Sellergren, *PCT Application No. SE/94/00025.*
[9] J. Lindell and K. Nilsson, unpublished results.
[10] B. Sellergren, J. Lindell, O. Norrlöw and K. Nilsson, *Anal. Chem.*, submitted for publication.
[11] B. Sellergren, and K. J. Shea, *J. Chromatogr.*, 635 (1993) 31.

ELSEVIER

Journal of Chromatography A, 680 (1994) 63–71

JOURNAL OF CHROMATOGRAPHY A

Preparation of highly condensed polyacrylamide gel-filled capillaries

Yi Chen*, Joachim-Volker Höltje, Uli Schwarz

Abteilung Biochemie, Max-Planck-Institut für Entwicklungsbiologie, Spemannstrasse 35/II, D-72076 Tübingen, Germany

Abstract

A fairly quick method has been established for the production of highly condensed polyacrylamide gel-filled capillaries. Void-free capillaries with inner diameters as small as 25 μm and monomer concentrations of up to over 30% T + 5% C can successfully be prepared within 5 h. These capillaries can be used for over 20 injections of poly-(α,β)-D,L-aspartate at 200 V/cm and 25°C, with gels immobilized at the capillary tips after polymerization, and for more than 70 injections with gels immobilized, during polymerization, over a longer section of at least 0.5 cm. The important polymerization conditions in this method are the application of a slight pressure, controlled polymerization directions and the selections of buffer components and/or the concentrations of radicals and catalyst.

1. Introduction

Highly condensed polyacrylamide gel-filled capillaries ($\geq$15% T + x% C*, $x > 0$) have been shown to be one of the basic conditions in capillary gel electrophoresis (CGE) of polyamino acids and oligosaccharides [1–4]. However, the preparation of these capillaries, which are not commercially available, is much more difficult than that of low-concentration gel-filled capillaries. Voids [5] or vacuum bubbles [6,7], formed inside the gels because of the volumetric losses of the resulting gels [5], increase dramatically with monomer concentration. The reason is not clear. A possible explanation might be the increase in gelatinization speed or more fragile gels formed.

To overcome the void problem, we tried several existing methods, such as pressurized (20 atm; 1 atm = 101 325 Pa) polymerizations [8,9] and programmed temperature polymerization [5]. Unfortunately, the success rate was less than 30%. We then turned to isotachophoretic polymerization [4,5]. In preparing 20 tubes of 50 cm × 50 μm I.D. with gel of 20% T + 5% C, there were 12 usable capillaries, having at least a 27 cm void-free length after equilibration. This is an excellent method, with a success rate of > 60%. However, the preparation time is fairly long. In a routine procedure, the time for producing a 50-cm capillary with a 20% T + 5% C gel is about 80 h, including 50 h of polymerization and 30 h of equilibration [4]. It seemed desirable to establish a faster polymerization procedure.

In this paper, we present a 5-h method developed from the pressurized polymerizations [8,9] and programmed-temperature polymeriza-

* Corresponding author.

* %T = g acrylamide + g bisacrylamide per 100 ml of solution, %C = % bisacrylamide in T.

0021-9673/94/$07.00
SSDI 0021-9673(94)00301-O

tion [5]. The gels are chemically immobilized at the capillary tips by co-polymerization [10,11] and/or after polymerization. The stability of the prepared capillaries was examined with poly-aspartate as a testing sample and the important polymerization conditions were studied and are discussed.

2. Experimental

2.1. Materials

N-Tris(hydroxymethyl)methylglycine (Tricine), boric acid and urea (electrophoretically pure); γ-methacryloxypropyltrimethoxysilane; nuclease P1, polyadenylic acid [poly(A)], hydroxypropylmethylcellulose (HPMC), poly-(α,β)-D,L-aspartate Na^+, M_r (the average molecular mass detected by viscosity) = 5400 [$poly(Asp)_{5400}$] were purchased from Sigma (St. Louis, MO, USA). Oligoadenylic acid of 12- to 18mers [$poly(A)_{12-18}$] was supplied by Pharmacia LKB (Uppsala, Sweden). Acrylamide and N,N'-methylenebis(acrylamide) (bis), electrophoretically pure, were from Bio-Rad Labs. (Richmond, CA, USA). Tris(hydroxymethyl)aminomethane (Tris), N,N,N',N'-tetramethylethylenediamine (TEMED), ammonium persulfate (APS) and other chemicals were all reagent grade from E. Merck (Darmstadt, Germany). Fused-silica capillaries with an outer diameter of 375 μm were from Composite Metal Services (Worcestershire, UK). The water used was purified with the Millipore Super Q system.

2.2. Preparation of samples

$Poly(Asp)_{5400}$ (50 mg/ml) and $poly(A)_{12-18}$ (1.7 units/μl) were dissolved in water. A partial hydrolysate of poly(A) was prepared by hydrolyzing poly(A) with nuclease P1: a 50-μl solution of 1.25% (w/v) poly(A) in water–0.3 *M* acetate, pH 6 (1:1) was digested with 1 μl Nuclease P1 (1 μg/1 μl water) at 40°C for 8 min and then stored at −20°C before use.

2.3. Preparation of gel-filled capillaries

Filling device

Sealed glass vials are used as "micro-pumps". A 4.7-ml (measured volume) threaded sample vial from Beckman (part No. 358807) is sealed by a modified screw-cap (Beckman, 360004), a rubber septum (3 mm thickness, cut from a rubber stopper) and a PTFE septum from Millipore (73005) as shown in Fig. 1A. The vial is evacuated or pressurized with a plastic syringe after plugging in the capillaries (Fig. 1B and C).

Preparation of one-end-modified capillaries [10,11,14]

One end of a new capillary is dipped into a 0.5% (v/v) modification solution (MS) of γ-methacryloxypropyltrimethoxysilane in water–acetic acid (1:1) until the solution reaches a height of 5–10 cm from the dipped end (checked against a light). This part is considered to be completely

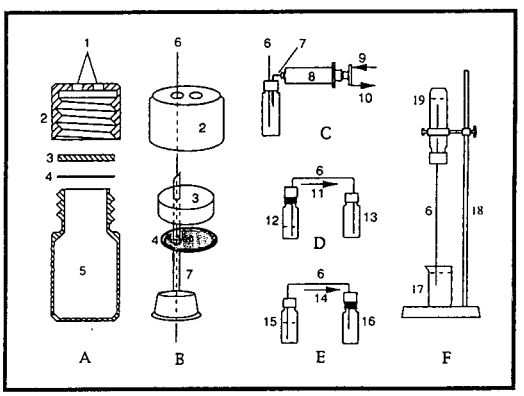

Fig. 1. Sealed vial and its use. (A) Construction of the sealed vial: 1 = 1.5-mm-diameter holes (one for plugging capillary and the other for syringe needle); 2 = plastic screw-cap; 3 = rubber pad; 4 = PTFE septum; 5 = 4.7-ml glass vial. (B) Plugging a capillary (6) through the rubber pad with the help of a syringe needle (7). (C) The sealed vial is being pressurized (9) or evacuated (10) with a 60-ml plastic syringe (8). (D) Evacuation filling: 11 = flow direction; 12 = unsealed vial with solution; 13 = evacuated vial. (E) Pressurization filling: 14 = flow direction; 15 = pressurized vial with solution; 16 = unsealed vial. (F) Polymerization position: 6 = capillary filled with acrylamide solution; 17 = beaker with 25–35°C water; 18 = hanging shelf; 19 = vial pressurized by injection of *ca.* 4 ml ice-cooled water.

modified. The capillary is kept at room temperature for 20 min, neglecting the natural evaporation of MS, and then washed for 5 min by pumping water into the non-modified end.

Preparation of full-length-modified capillaries

A new capillary is completely filled with MS, kept at room temperature for 20 min and then washed with water for 5 min.

Polymerization process

A 30–60-cm capillary, with or without modification, is rinsed for 2–5 min with a 0.5% solution of HPMC or a radical-free monomer solution and then filled with a polymerizing solution by an evacuated vial (Fig. 1D). Once the polymerizing solution reaches the outlet, the filling is stopped, and one tip of the tube, or the modified end in the case of filling a one-end-modified capillary, is immediately dipped into 50–70°C water for 1 min to start the polymerization from this end. The other end is then mounted tightly to a vial and about 4 ml of ice-cooled water are injected into the vial to cool this end and to build up pressure (the pressure calculated according to the law of the ideal gas is *ca.* 6 atm at 0°C). To finish polymerization, the capillary is hung vertically for 4 h in a shockless and windless place (20–30°C), with the pressurized end up and the polymerized end in 25–35°C water (Fig. 1F). After polymerization, the pressurized end (*ca.* 2–4 cm) is cut off to remove empty and/or liquid parts. The other end is checked under a microscope for possible voids.

The polymerizing solution mentioned above is a degassed monomer solution, containing 0.05% (v/v) TEMED and 0.03–0.05% (w/v) APS. It is prepared from a stock solution of 40% T + 5% C with buffer and water, ignoring the changes of final volumes [12,13]. For example, a polymerizing solution of 15% T + 5% C/TT15 (0.1 *M* Tricine + 0.05 *M* Tris) is a 3:4:1 (v/v/v) mixture of the stock solution–0.2 *M* Tricine + 0.1 *M* Tris–water, degassed in an evacuated vial by ultrasonic shocking for 1 min.

Partial gel immobilization

Procedure A: a one-end-modified capillary is filled with a gel as described above. The gel will be immobilized at the modified part of the capillary during polymerization [10,11]. *Procedure B*: a capillary without any modification is filled with a gel according to the polymerization process. After 4 h, its ends are dipped into MS for 10 min. The bifunctional silane will diffuse into the capillary tips and forms chemical bonds between the gel and the capillary tips. The capillary ends are then dipped for 10–15 min into a solution of 2% T + 3% C/TT15 + 1% TEMED + 1% APS to enhance the immobilization. This method immobilizes the gels at the capillary tips.

By combining procedures A and B, four types of capillaries can be prepared: CapA, with gel immobilized by A; CapAB, with gels immobilized first at one end by A then at the other end by B; CapB, with gels immobilized at one end by B; CapBB, with gels immobilized at both ends by B.

Full-length gel immobilization

For low-concentration gels (below 8% T), the full-length-modified capillaries are filled with the gels by the same polymerization process and the gels are immobilized along the entire capillary wall during polymerization.

The prepared capillaries are generally equilibrated with running buffer at 200 V/cm for 1 h and then stored at room temperature with both ends dipped into the running buffer. The capillary tips are re-immobilized by procedure B every month for long term storage (up to 6 months). The detection window is made just before separation of samples. About 2 mm of the polyimide over-coating are removed manually with a scalper and cleaned with methanol.

2.4. Electrophoresis

Electrophoresis was performed using the Beckman P/ACE system 2100, controlled by an IBM computer of Model SP/2 with the System Gold software (version 7.0). The running buffer was

the same as that used for preparing monomer solutions, degassed just before use and renewed every five runs. The temperature was set at 25 ± 0.1°C. The detection wavelengths were 220 nm for poly(Asp)$_{5400}$ [4] and 254 nm for poly(A). The data rate was 1 Hz and the rise time 1 s. The sample was introduced into the negative end by applying voltage for a few seconds.

3. Results and discussion

3.1. Gel immobilization and stability

To produce stable capillaries, gels are generally immobilized along the entire capillary wall by a co-polymerization method, that is, by polymerization of acrylamide in the capillaries pre-coated with bifunctional silanes [14–20]. Without immobilization, gels migrate from the capillary ends due to electroosmosis and/or electrostriction [11], resulting in irreproducible separation and a short life time (running stability) of the capillaries. However, this immobilization technique dramatically enhances the formation of voids because the gel shrinkage, which is caused by the volumetric losses of the resulting gels compared to the initial solution [5], is inhibited. If the gels are unable to shrink or can only shrink locally because of forming chemical bonds or strongly adsorbing to the capillary wall, the formation of voids becomes a natural way to compensate the volumetric losses which leads to current drop, serious disruption of the applied electric field and irreproducible or no separation. Void-free and stable capillaries are thus the prerequisite in CGE. A simple method to overcome the problem is to confine the immobilization to within a short section [10,11] so that most parts of the gels can shrink more freely. An even better idea is to immobilize the gel after polymerization which requires an immobilization agent able to form bonds with the gels by a different mechanism. At present, when using the

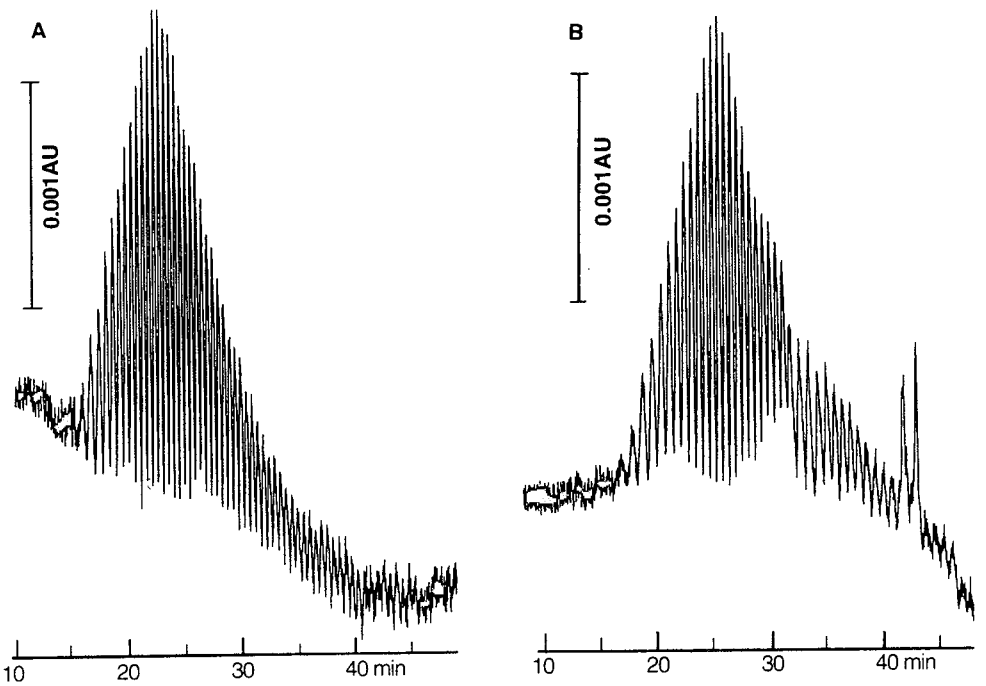

Fig. 2. Electrophoresis of poly(Asp)$_{5400}$ with CapB, obtained from the 20th injection (A) and 27th injection (B). Capillary: 27 cm (effective length 20 cm) × 75 μm I.D.; gel: 20% T + 5% C; buffer: 0.2 *M* Tricine–Tris, pH 8.3; constant current: 16 μA (6.2 kV); injection: 5 kV, 30 s.

reported silane [14–20], we can only immobilize the gels at the capillary tips (procedure B). The question arises: whether the gels which are immobilized over such a short section are stable enough?

To examine the running stability, the resulting capillaries are run continuously at about 200 V/cm until current drop occurs, with $poly(Asp)_{5400}$ as a testing sample (60–90 min per separation). The results (Fig. 2) show that the capillaries with gels immobilized at the tips by procedure B (both of CapB and CapBB) can be used for more than 20 injections. The gels may crack (from large voids) unexpectedly after about 25 injections as shown in Fig. 2B where the 27th separation failed because a current drop occurred at about 25 min after injection. CapB and CapBB are therefore less stable than the isotachophoretically produced capillaries (up to 7 days [4]) but are comparable to the low-concentration gel-filled capillaries without immobilization (10–30 h [6,7]).

The stability of the capillaries can be improved

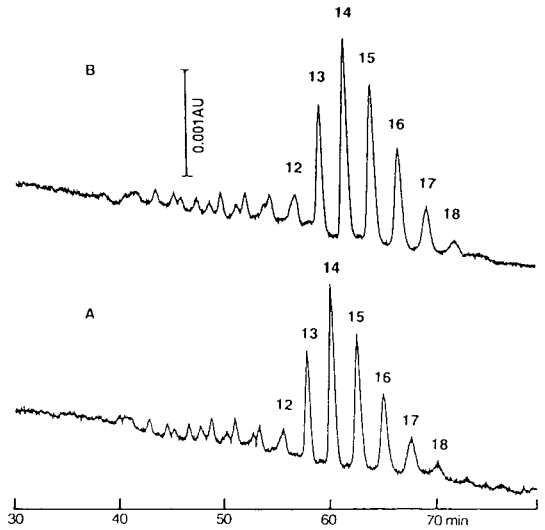

Fig. 4. Electrophoresis of $poly(A)_{12\text{-}18}$ with a newly prepared (A) and a 6-month-stored (B) capillary. The numbers show the estimated size of the peaks; the first part of the peaks (before peak 12) seemed to be impurities and/or a partial hydrolysate of the sample. Capillary: 27 cm (effective length 7 cm) × 25 μm I.D.; gel: 30% T + 5% C; buffer: TT15; constant voltage: 5.4 kV (*ca.* 0.9 μA); injection: 5 kV, 10 s.

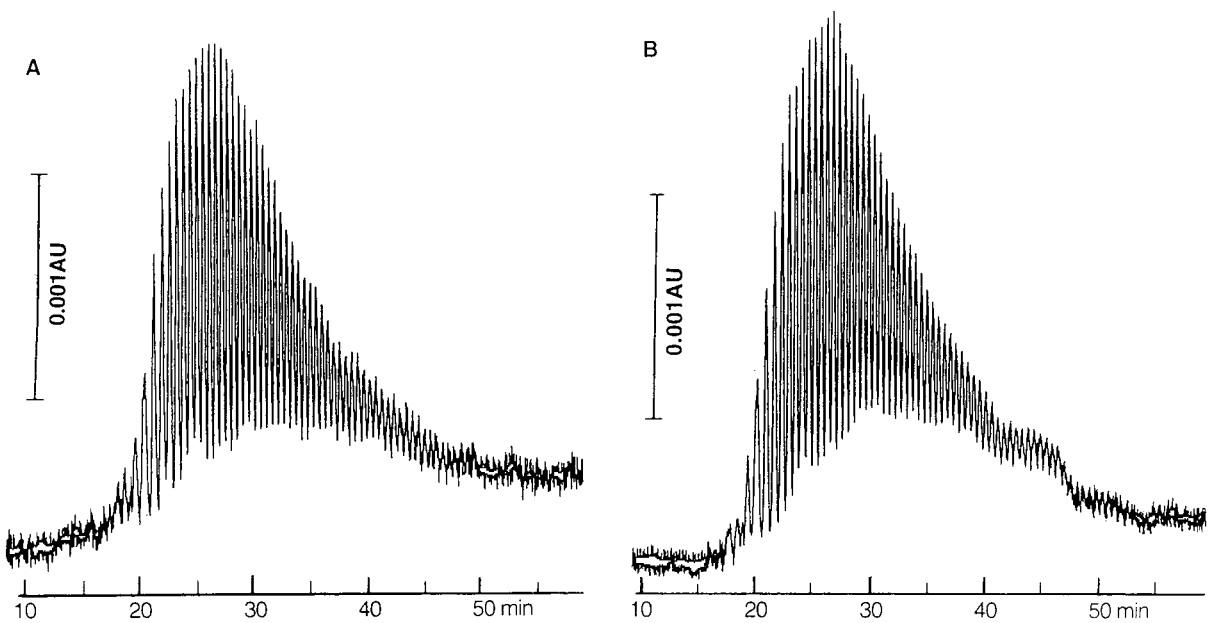

Fig. 3. A comparison of the 10th (A) and 75th (B) separation with CapA. Capillary: 37 cm (effective length 30 cm) × 75 μm I.D.; gel: 15% T + 5% C; buffer: TT15; constant voltage: 7.4 kV (7.9 μA); injection: 5 kV, 15 s.

for up to more than 70 injections by immobilization of the gels over a longer section of at least 0.5 cm with procedure A (CapA and CapAB). Fig. 3 shows that, for the tested capillary, the resolution loss at the 75th injection (Fig. 3B) is less than 10% compared to the 10th injection (Fig. 3A). Interestingly, the stability of CapA is similar to CapAB if positive voltage is applied to the longer immobilized end. When negative voltage is applied to this end, the current may drift in the first several runs but no gel cracking in the tube has been observed. (This orientation phenomenon was also observed for CapB). After running for one week, the gels may crack at the tube end which had been cooled during polymerization. In this case, the capillaries can be repaired by cutting off the damaged end.

The storage time or shelf-life of the prepared capillaries is generally 2 to 3 months, but may be up to more than 6 months, which is comparable with the isotachophoretically produced capillaries (between 1 and 2 months [4]). Fig. 4 shows a comparison between a newly prepared and 6-month-stored capillary of 25 μm I.D. The testing sample is poly(A)$_{12-18}$ instead of poly(Asp)$_{5400}$ which has much more poorer detection sensitivity.

3.2. Polymerization considerations

Reducing the gel immobilization length is only a prerequisite condition to producing void-free capillaries, the elimination of the voids finally depends on how to polymerize the acrylamide inside the capillaries. There are a number of polymerization conditions which can suppress the formation of voids, but the most effective ones seem to be the polymerization pressure and the control of gelatinization direction.

The gelatinization direction can be controlled in several ways [5], of which the axial-programmed-temperature polymerization is the simplest one. By assuming that a radical induced polymerization, once it starts, may quickly spread from one region to a neighbouring region, we simplified the procedure by just keeping the capillary ends at different temperatures (see polymerization process). No strict axial thermal gradient could be developed by this control but about 30% of the voids were eliminated. The data were obtained as following: ten unmodified capillaries of 45 cm × 75 μm I.D. cm with a 20% T + 5% C/TT15 gel were prepared without the application of pressure, of which five were controlled by temperature but the other five not. The voids were counted under a microscope and averaged.

It also seems possible to control the radial gelatinization direction by a radial thermal gradient. We hence cooled the tubing wall by washing it with an ice-cooled monomer solution. About 10% of the voids were eliminated by this procedure. Further study showed that, using a 0.5% HPMC solution instead of the monomer solution, about 12% of the voids were eliminated. This means that this is probably due to a coating effect but not due to the radial thermal gradient. When the capillary wall is coated by a viscous material, the lateral gelatinization can clearly be inhibited for a certain time until the polymerizing solution diffuses into or replaces this coating layer. To keep this coating effective, the injection of the polymerizing solution into the capillary should be very quick and once the solution reaches the outlet, the injection should be stopped immediately.

The thermal and coating controls can eliminate only under 50% of the voids. However, when a slight pressure is applied to the column, the voids can be eliminated nearly completely. Pressurizing polymerization was first developed by Bente and Myertson [8] who used high pressure to pre-compress the polymerizing solution. In our method, the pressure is reduced to *ca.* 5 atm and is applied only to the upper end of the tubes. Our purpose is not to compress the solution but to force the unpolymerized or partially polymerized solution and/or gel to move towards the polymerized end in order to compensate for the volumetric loss. By our simple temperature control, an irregular polymerization easily occurs between the two tube ends where the capillary wall is in contact with air. The irregularly formed gels resist or block the solution flow. Even if there is no irregular gel formed in the tube, the highly viscous solution does not

necessarily flow toward the polymerized end without pressure. Interestingly, a slight pressure associated with isotachophoretic polymerization can also improve the success rate of the preparation.

In addition, capillary position during polymerization influences the elimination of voids. A vertical position yields the best result. In an arched position, voids accumulate in the bend, and in a horizontal position, voids form mostly in the centre of the tube and partially at the upper wall side. The vertical position can also accumulate liquid in the upper capillary end. Under a microscope, the liquid movement in the upper end of a 100 μm I.D. capillary with a 5% T + 5% C gel, newly prepared by setting the upper end at a higher level than the water in the vial to prevent the water from flowing into the tube, was clearly observed by warming and cooling this end during observation. This movement was not observed in the ends of an arched or horizontally positioned capillary. About 2–4 cm of this end should be cut off to eliminate the liquid and empty space resulting from gel shrinkage. This liquid is possibly exuded due to the volumetric losses of the gels. If irregularly accumulating somewhere inside the tube, it will disrupt the applied electric field although it may not cause

Table 1
The success rate in producing CapA with x% T + 5% C gels

	Gel (% T)	Buffer[a]	TEMED[b] (%, v/v)	APS[b] (%, w/v)	Capillary[c]			Success rate (%)
					Dimension	Tatol	Usable	
A	10	TT15	0.05	0.05	45 cm × 50 μm	20	20	100
	15		0.05	0.05		36	35	97.2
	20		0.05	0.05		33	30	90.9
	25		0.05	0.04		7	6	85.7
	30		0.05	0.05		10	6	60.0
	30		0.04	0.035		15	13	86.7
B	20	TT15	0.05	0.05	45 cm × 100 μm	11	10	90.9
					45 cm × 75 μm	20	19	95.0
					45 cm × 50 μm	20	18	90.0
					35 cm × 25 μm	5	4	80.0
C	20	TT15	0.05	0.05	45 cm × 75 μm	20	19	95.0
		BT21	0.05	0.05		8	3	37.5
		BB25	0.05	0.05		17	6	35.3
		BB25	0.05	0.035		15	11	73.3
		BB25	0.04	0.03		20	17	85.0
D	15	TT15	0.03	0.03	45 cm × 50 μm	20	20	100
			0.05	0.05		36	35	97.2
			0.03	0.10		20	15	75.0
			0.05	0.10		20	11	55.0
			0.07	0.10		20	9	45.0
			0.10	0.10		20	5	25.0
			0.10	0.07		20	10	50.0
			0.10	0.05		20	12	60.0
			0.10	0.03		20	16	80.0

[a] TT15 = 0.1 *M* Tricine + 0.05 *M* Tris; BT21 = 0.2 *M* boric acid + 0.1 *M* Tris; BB25 = 0.25 *M* boric acid/borax, pH 8.3.
[b] At the total concentration (TEMED + APS) of < 0.08%, the hanging time of the capillaries was prolonged to 8 h.
[c] A usable capillary for CapA is defined as a void-free capillary with gel immobilized for ≥ 0.5 cm and a total length of ≥ 27 cm which is the shortest manageable length using the Beckman CE system.

current problems. It is thus better to prevent the liquid from accumulating inside the tube.

3.3. Success rate

Void-free capillaries can successfully be prepared with an I.D. as small as 25 μm and gel concentrations of up to more than 30% T. For the gels immobilized after polymerization, the success rate is 95–100%. If the gels are immobilized during polymerization, the success rate typically ranges between 85 and 100% as shown in Table 1, parts A and B. The success rate depends largely on buffer components (Table 1, part C) and on the concentrations of TEMED and APS (Table 1, part D). Generally, organic buffers such as Tricine–Tris can prevent the formation of voids much more effectively than inorganic buffers such as boric acid and phosphate in the same polymerization conditions. When inorganic

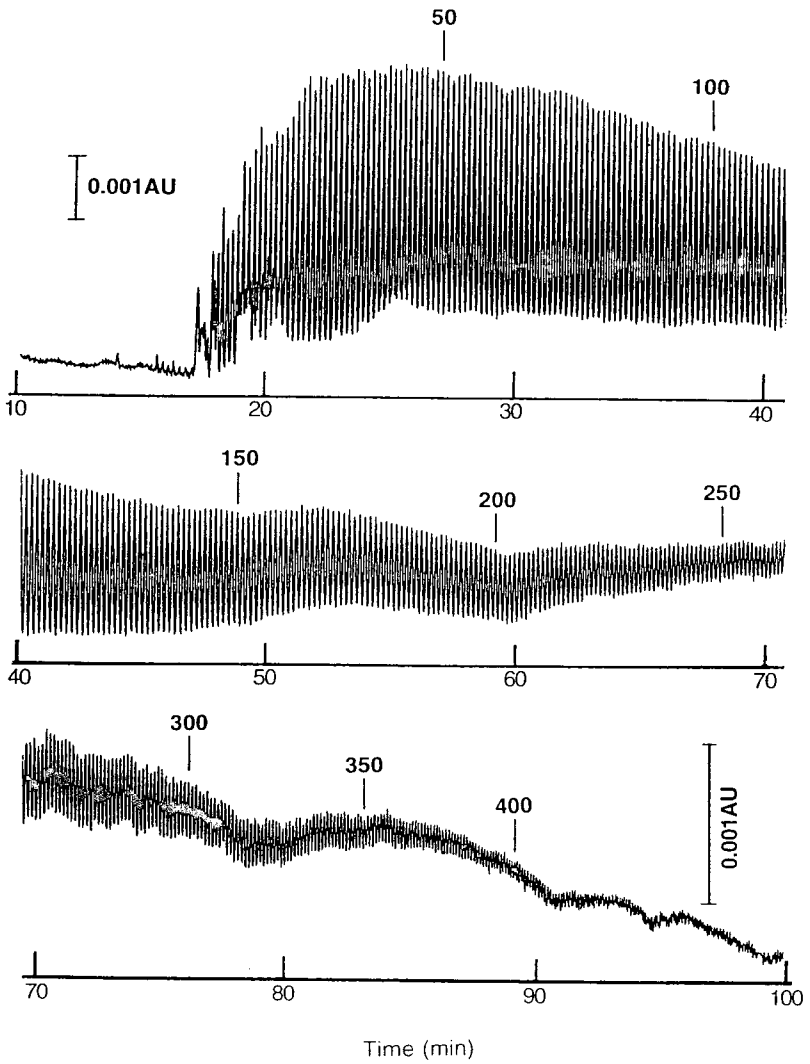

Fig. 5. Electrophoresis of partially hydrolyzed poly(A) with entirely immobilized low-concentration gel-filled capillary. The numbers show the size of the bands measured with poly(A)$_{12\text{-}18}$ as a reference. Capillaries: 37 cm (effective length 30 cm) × 100 μm I.D.; gel: 5% T + 5% C; buffer: 7 *M* urea, 0.1 *M* Tris–0.25 *M* boric acid; voltage: 7.4 kV (8.7 μA); injection: 5 kV, 3 s.

buffers such as boric acid are used, low concentrations of TEMED and APS are preferred to improve the success rate (Table 1, part C). TEMED and APS control the polymerization speed or the starting point of gelatinization. High concentration of TEMED or APS speeds up the preparation but increases the possibility of forming voids. In contrast, low concentration reduces the voids but raises the polymerization time and also the exuding of liquid from gels. At too low concentrations of TEMED and APS, polymerization may not occur. The suggested total concentration of TEMED + APS is 0.06–0.14%. These studies show that, besides the pressure and the control of the gelatinization direction, the buffer components and the concentrations of catalyst and radicals are very important in preparing the highly condensed gel-filled capillaries.

Finally, we would like to mention that the suggested polymerization method can also be used for producing the capillaries with gels of below 8% T + 5% C, immobilized along the entire capillary wall. Fig. 5 shows a separation of poly(A) in a highly denatured gel (5% T + 5% C/7 *M* urea). A 30-cm separating length can yield 400 bands in 90 min without any optimization of the separating conditions. The plate number $[5.54(t_R/w_{1/2})^2$, $w_{1/2}$ = peak width at the half height, t_R = elution time] of 150mer is $1.2 \cdot 10^7$ plates/m. This is comparable to the high performance gel-filled capillaries without immobilization [7].

Acknowledgements

We thank Victoria Kastner for improving the English of the manuscript and the financial support of the Alexander von Humboldt foundation is gratefully acknowledged by Y.C.

References

[1] J. Liu, O. Shirota and M. Novotny, *J. Chromatogr.*, 559 (1991) 223–235.
[2] J. Liu, O. Shirota and M. Novotny, *Anal. Chem.*, 64 (1992) 973–975.
[3] J. Liu, V. Dolnik, Y.-Z. Hsieh and M. Novotny, *Anal. Chem.*, 64 (1992) 1328–1336.
[4] V. Dolnik and M. Novotny, *Anal. Chem.*, 65 (1993) 563–567.
[5] V. Dolnik, K.A. Cobb and M. Novotny, *J. Microcol. Sep.*, 3 (1991) 155–159.
[6] Y. Baba, T. Tsuhako, S. Enomoto, A.M. Chin and R.S. Dubrow, *J. High Resolut. Chromatogr.*, 14 (1991) 204–206.
[7] Y. Baba, T. Matsuura, K. Wakamoto, Y. Morita, Y. Nishitsu and M. Tsuhako, *Anal. Chem.*, 64 (1992) 1221–1225.
[8] P.F. Bente and J. Myertson, *Eur. Pat. Appl.*, EP272925 (June 29, 1988); *US Pat.*, 4 810 456 (March 7, 1989).
[9] H.F. Yin, J.A. Lux and G. Schomburg, *J. High Resolut. Chromatogr.*, 13 (1990) 624–627.
[10] D.Y. Chen, H.P. Swerdlow, H.R. Harke, J.Z. Zhang and N.J. Dovichi, *J. Chromatogr.*, 559 (1991) 237–246.
[11] M.-J. Rocheleau and N.J. Dovichi, *J. Microcol. Sep.*, 4 (1992) 449–453.
[12] H. Drossman, J.A. Luckey, A.J. Kostichka, J. D'Cunha and L.M. Smith, *Anal. Chem.*, 62 (1990) 900–903.
[13] S. Hjertén, *J. Chromatogr.*, 270 (1983) 1–6.
[14] S. Hjertén, *J. Chromatogr.*, 347 (1985) 191–198.
[15] H. Swerdlow and R. Gesteland, *Nucleic Acids Res.*, 18 (1990) 1415–1419.
[16] A. Paulus and J.I. Ohms, *J. Chromatogr.*, 507 (1990) 113–123.
[17] A.S. Cohen, D.R. Najarian and B.L. Karger, *J. Chromatogr.*, 558 (1991) 273–284.
[18] A.S. Cohen, D.R. Najarian, A. Paulus, A. Guttman, J.A. Smith and B.L. Karger, *Proc. Natl. Acad. Sci. U.S.A.*, 85 (1988) 9660–9663.
[19] D.N. Heiger, A.S. Cohen and B.L. Karger, *J. Chromatogr.*, 516 (1990) 33–48.
[20] B.L. Karger and A.S. Cohen, *Eur. Pat.*, EP324539 (July 19, 1989); *US Pat.*, 4 865 706 (Sept. 12, 1989); *US Pat.*, 4 865 707 (Sept. 12, 1989).

ELSEVIER

Journal of Chromatography A, 680 (1994) 73–83

JOURNAL OF CHROMATOGRAPHY A

Separation of very hydrophobic compounds by hydrophobic interaction electrokinetic chromatography

Eric S. Ahuja, Joe P. Foley*

Department of Chemistry, Villanova University, Villanova, PA 19085-1699, USA

Abstract

Separations of very hydrophobic neutral analytes were achieved using hydrophobic interaction electrokinetic chromatography (HI-EKC). Alkyl aryl ketone homologues dodecanophenone (C_{18}), tetradecanophenone (C_{20}), hexadecanophenone (C_{22}) and octadecanophenone (C_{24}) were separated via hydrophobic interactions between free sodium dodecyl sulfate (SDS) monomers and the analytes. The first running buffer consisted of 50 m*M* SDS and 50% acetonitrile (pH 7.0). A complete reversal in the elution order of these analytes was obtained with the second running buffer, 20 m*M* cetyltrimethylammonium bromide (CTAB) and 50% acetonitrile (pH 2.8). With the second running buffer, electroosmotic flow was suppressed and the free CTAB monomers migrated toward the detector. Through hydrophobic interactions between the free CTAB monomers and the analytes, separations of these very hydrophobic alkyl aryl ketones were obtained in less than 10 min; analysis times were less than 5 min with the SDS-based separations.

1. Introduction

The introduction of capillary electrophoresis (CE) [1–3] in 1979 enabled the high-resolution separation of charged analytes with rapid analysis times. The separation power of CE was further enhanced with the development of micellar electrokinetic chromatography (MEKC) [4,5] in 1984. In this technique, the addition of micelles to the running buffer creates a pseudo-stationary phase by which neutral analytes can differentially partition. Since the advent of CE and MEKC, there has been considerable research in both the method development and application of these two powerful separation techniques.

CE has been used to successfully separate a diverse range of compounds such as drug-related impurities [6], warfarin enantiomers in human plasma [7], B vitamins [8], DNA fragments [9] and sulphonamides in pharmaceuticals [10]. A more complete review of CE-related applications can be found in the numerous review articles and books that have been published [11–14].

MEKC has been devoted primarily to the analysis of small molecules. The applications involving MEKC are considerably less than those accomplished with CE but are still numerous and span a broad range of analytes. To date MEKC has been utilized in the analysis of cardiac glycosides [15], mycotoxins [16], β-blockers [17],

* Corresponding author.

0021-9673/94/$07.00
SSDI 0021-9673(94)00500-9

explosive residues in soils [18], herbicides [19], water- and fat-soluble vitamins [20–23], polymycins [24] and priority substituted phenols [25] just to mention a few. A recently published book provides a much more in depth review of the applications performed with MEKC [26].

It is easy to see the impact that CE and MEKC have had in separations. There are other modes of separation utilizing the basic principles of CE some of which include isoelectric focusing, capillary gel electrophoresis and isotachophoresis. These techniques are all employed for the analysis of ionic species. The separation of neutral compounds falls under the technique titled electrokinetic capillary chromatography (EKC). In EKC, additives to the running buffer, such as the micelles utilized in MEKC, provide the pseudophase by which the neutral molecules through their varying affinities for the pseudophase can be separated. Electrokinetic separations have been exclusively used for the analysis of small solutes.

Larger and more hydrophobic neutral analytes have been difficult to separate with EKC and more specifically MEKC. One of the primary problems with the analysis of very hydrophobic compounds by MEKC is that these very hydrophobic compounds tend to remain in the inner hydrophobic core of the micelle and eventually coelute with the micelle itself. One way to increase the affinity of the hydrophobic analytes for the aqueous mobile phase is the addition of organic modifiers to the running buffer. Although this method is effective in enhancing the resolution of more moderately hydrophobic analytes, the "cost" is often much longer analysis times and higher operating currents. Another limitation in dealing with very hydrophobic molecules is their minimal solubility in aqueous media. Sample matrixes often consist solely of organic solvent and introduction of the sample into a predominantly aqueous running buffer leads to the precipitation of the analyte in the capillary and of course this leads to capillary reconditioning procedures. As a result of a blocked capillary, organic solvents are often used to clear the capillary followed by purges with a base. This sort of treatment changes the chemistry on the surface of the capillary and often the result is a change in the electroosmotic velocity. This is an undesirable effect in terms of run-to-run reproducibility. Given these types of disadvantages associated with the existing EKC techniques, there is a strong need to develop new techniques which are specifically suited for the analysis of very hydrophobic neutral analytes.

In 1986 Walbroehl and Jorgenson [27] demonstrated the separation of aromatic ring compounds through proposed "solvophobic interactions" in systems consisting of tetrahexylammonium salts in water–acetonitrile mixtures. When the analytes are dissolved in this separation medium, they undergo a solvophobic interaction with the tetrahexylammonium ion (THA^+) and form positively charged species which can then migrate in an electric field. Although a solvophobic interaction mechanism was proposed, it was also hypothesized [26] that the π-electrons of the aromatic analytes may be attracted to the THA^+ ion in which case the separation mechanism would be based more on electrostatic interactions than true hydrophobic interactions. More recently Bullock [28] demonstrated the separation of Triton X-100 oligomers using hydrophobic interactions between free sodium dodecyl sulfate (SDS) monomers and the different poly(ethylene oxide) chains. The individual oligomers are separated based on differences in the length of these chains.

Based on the success of these studies and the need to develop a viable method by which very hydrophobic neutral analytes can be separated, we formally introduce a new mode of electrokinetic capillary chromatography: hydrophobic interaction electrokinetic capillary chromatography (HI-EKC). In this investigation we report the separation of some very hydrophobic alkyl aryl ketone homologues (C_{18}, C_{20}, C_{22}, C_{24}) using HI-EKC. Fast, high-resolution separations of these analytes, which differ by only two methylene groups, were achieved. The results of this report further support the need to develop a

gradient elution mode for MEKC similar to that found in high-performance liquid chromatography (HPLC).

2. Experimental

2.1. Apparatus

A Waters Quanta 4000 capillary electrophoresis system (Millipore, Waters Chromatography Division, Milford, MA, USA) equipped with fixed-wavelength UV detection at 254 or 214 nm was employed for all the separations performed in this study. HI-EKC was performed in either a 30 cm or 35 cm (injection to detection) × 50 μm I.D. × 370 μm O.D. fused-silica capillary tube (Polymicro Technologies, Tucson, AZ, USA). The total capillary length was 37.5 or 42.5 cm. Injections were made in the hydrostatic mode. The applied voltage ranged from 5 to 30 kV with operating currents less than 50 μA unless otherwise noted in the text. The data were collected at a rate of 20 points/s and analyzed with a Macintosh IIci computer (Apple, Cupertino, CA, USA) using a MacLab 4 channel ADC with the appropriate vendor software (ADInstruments, Milford, MA, USA). All experiments were done at ambient temperature (ca. 25°C).

2.2. Materials

The alkyl aryl ketone homologues (C_8–C_{24}) were purchased as a kit from Aldrich (Milwaukee, WI, USA). The alkylbenzenes (C_{13}, C_{14}, C_{16}) were purchased from Alltech (Deerfield, IL, USA). Anthracene, naphthalene, and phenanthrene were obtained from Aldrich. SDS was purchased from Sigma (St. Louis, MO, USA), while cetyltrimethylammonium bromide (CTAB) was obtained from Aldrich. Both surfactants were used as received. The concentration of SDS ranged from 2–50 m*M* for all the HI-EKC separations. Separations performed in utilizing CTAB were done at concentrations of 20 and 40 m*M*. Stock buffer solutions were prepared with $NaH_2PO_4 \cdot H_2O$ and sodium hydroxide to give a 100 m*M* phosphate buffer at pH 7.0 for the SDS-based separations. A phosphate buffer with pH 2.8 was used with the CTAB-based separations. A phosphate buffer concentration of 5 or 10 m*M* was used in all the experiments. Acetonitrile was obtained from Mallinckrodt (Paris, KY, USA). The non-micellar solutions were made by weighing appropriate amounts of SDS or CTAB and diluting with the stock buffer solution, in some cases 40 to 50% acetonitrile, and distilled water in a 100-ml volumetric flask to obtain the desired concentrations. All the running buffer solutions were filtered through 0.20-μm membrane filters obtained from Alltech and degassed before use. HPLC-grade distilled water used in the makeup of the micellar buffer solutions was obtained from J.T. Baker (Phillipsburg, NJ, USA). Sample solutions were made up of 100% acetonitrile with solute concentrations at or below 2.5 mg ml^{-1}.

2.3. Methods

The capillary was activated using a modification of a previously described procedure [29]. The capillary was first rinsed with 1 *M* potassium hydroxide for 20 min followed by subsequent rinses of 0.1 *M* KOH and distilled water for 20 min each. A final 20-min rinse was performed with the operating buffer before the capillary was used. Purges with the operating buffer were done after each run for 5 min using a vacuum of ca. 16.5 in.Hg (1 in.Hg = 3386.4 Pa) at the detector reservoir.

Electroosmotic velocities were measured where applicable using a method previously published [30].

3. Results and discussion

Hydrophobic interaction chromatography (HIC) has been utilized in many successful fractionations of both water-soluble proteins and membrane proteins [31]. In theses cases, gel beds consisting of uncharged amphiphilic agarose

derivatives were used although charged gels [32] can also be employed. Bonded phase HIC utilizes a hydrophilic polymeric layer that totally covers a silica or polymer support surface and into this layer are incorporated short alkyl or aryl chains in low density. The mild conditions of this type of HIC separate by selectivity based on the hydrophobicity of the surface amino acids and usually render proteins intact [33,34]. Unlike these forms of HIC, HI-EKC is performed in the free solution mode. All hydrophobic interactions take place between solubilized analytes and the hydrophobic portions of free (non-micellized) surfactant monomers in solution.

In this investigation, the surfactants SDS and CTAB were used with high amounts of acetonitrile such that micelles were not formed. Only the free surfactant monomers were present in the running buffer. Initial studies, however, focused on utilizing SDS at concentrations below the critical micelle concentration (CMC) in totally aqueous solutions. In these studies, very hydrophobic alkylbenzenes (C_{13}, C_{14}, C_{16}) were used as the probe analytes as well as the polyaromatic hydrocarbons anthracene, naphthalene and phenanthrene. Table 1 provides the structures, CMCs and aggregation numbers of these two surfactants as well as the general structure of the analytes studied, i.e., the alkyl aryl ketones, alkylbenzenes, and the three polyaromatic hydrocarbons.

The first attempts of achieving separations of very hydrophobic compounds by HI-EKC involved utilizing SDS at concentrations ranging from 2–5 m*M* with 10 m*M* phosphate buffer. Under these experimental conditions, no micelles were present. This was verified by performing runs with hydrophilic to moderately hydrophobic alkyl aryl ketones (C_8–C_{14}). If micelles had been present there would have been some retention of these analytes. This was not observed as all of the analytes eluted with the

Table 1
Structures, critical micelle concentrations and aggregation numbers of the surfactants; general structures of the analytes

Surfactants		
SDS $(CH_3(CH_2)_{11}0S0_3^-Na^+$	CMC = 0.008 *M*	Aggregation number 62
CTAB $(CH_3(CH_2)_{15}N^+(CH_3)_3Br^-)$	CMC = 0.0013 *M*	Aggregation number 78
Analytes		
Alkylbenzenes (n = 7, 8, 10)	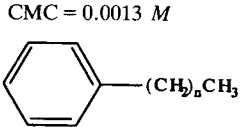	
Alkyl aryl ketones (n = 10, 12, 14, 16)	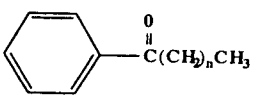	
Polyaromatic hydrocarbons	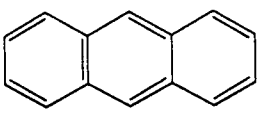 Anthracene	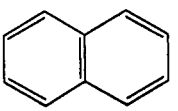 Naphthalene
	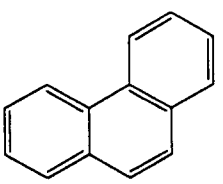 Phenanthrene	

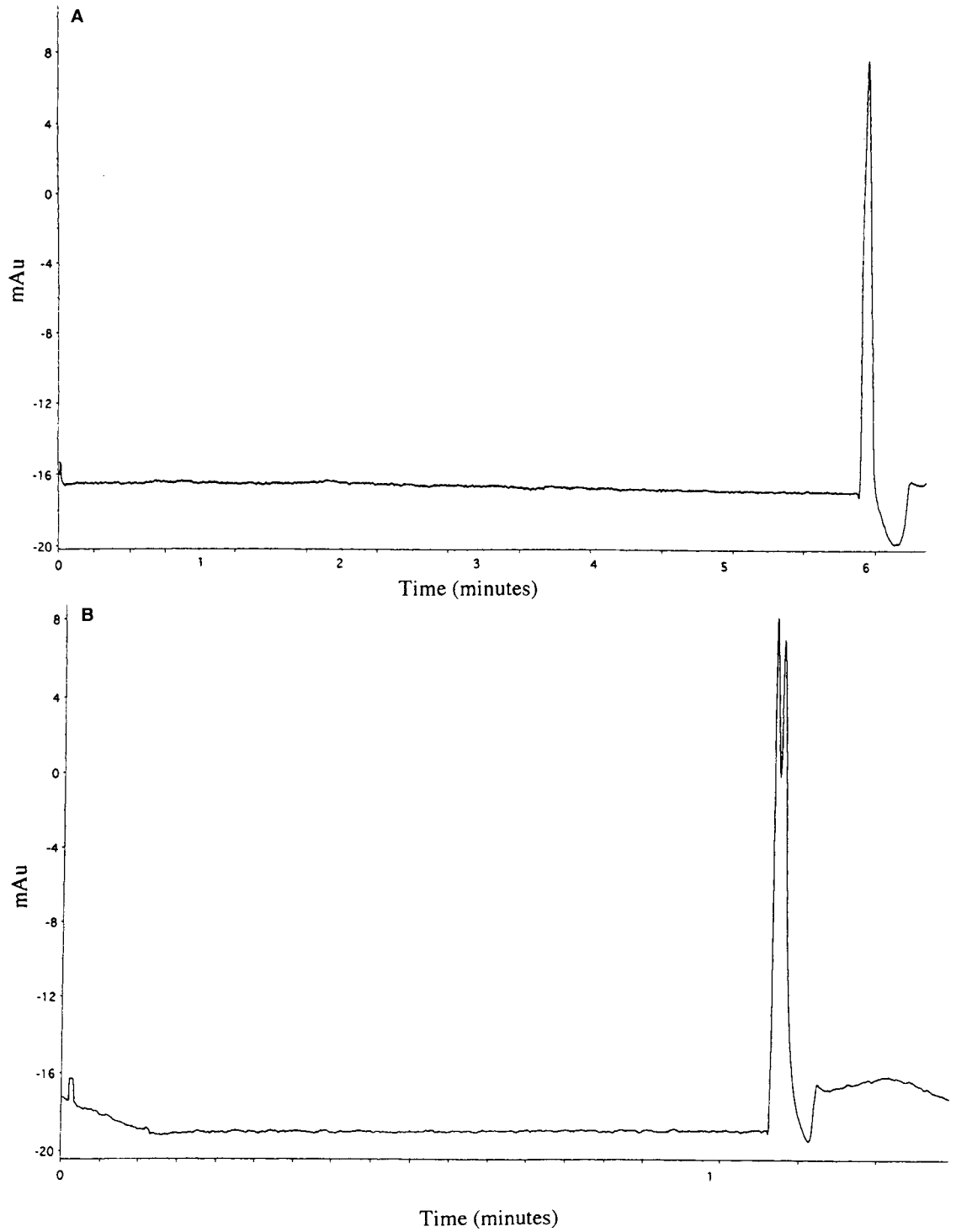

Fig. 1. Elution of very hydrophobic alkylbenzenes (*n*-heptyl-, *n*-octyl- and *n*-decylbenzene) with the electroosmotic flow marker under non-micellar electrokinetic conditions and an applied voltage (current) of (A) 5.0 kV (4.2 μA) and (B) 20.0 kV (27.8 μA). Running buffer: 3 m*M* SDS–10 m*M* phosphate buffer (pH 7.0). Other conditions as in the Experimental section.

electroosmotic flow marker (t_0). In order to test the theory of possible hydrophobic interactions between the free SDS monomers and the compounds of interest, separations of very hydrophobic alkylbenzenes were attempted. Since the alkylbenzenes chosen for this part of the investigation possessed long alkyl chains, it was hoped that these long chains would interact with the hydrophobic moiety of the SDS monomer and result in separation with the elution order following that of MEKC with the most hydrophobic analyte experiencing the greatest retention.

Fig. 1 shows the results obtained with a running buffer system containing 3 m*M* SDS. The operating voltage for this run was 5 kV (Fig. 1A). As can be seen all the alkylbenzenes elute with the electroosmotic flow marker. When the operating voltage was raised to 20 kV, a slight separation was observed as shown in Fig. 1B; reproducibility of this separation was verified with triplicate runs. When the operating voltage was raised to 30 kV no real improvement was observed in the resolution. Similar separations were tried with higher SDS concentrations (3.5, 4 and 5 m*M*) in an attempt to increase the number of free surfactant monomers available for hydrophobic interactions, but the results were similar to that attained with 3 m*M* SDS. The results indicated that there was an insufficient amount of free SDS monomers to achieve the amount of hydrophobic interactions necessary to obtain the desired separations.

Fig. 2 displays the results obtained for the three polyaromatic hydrocarbon compounds. As

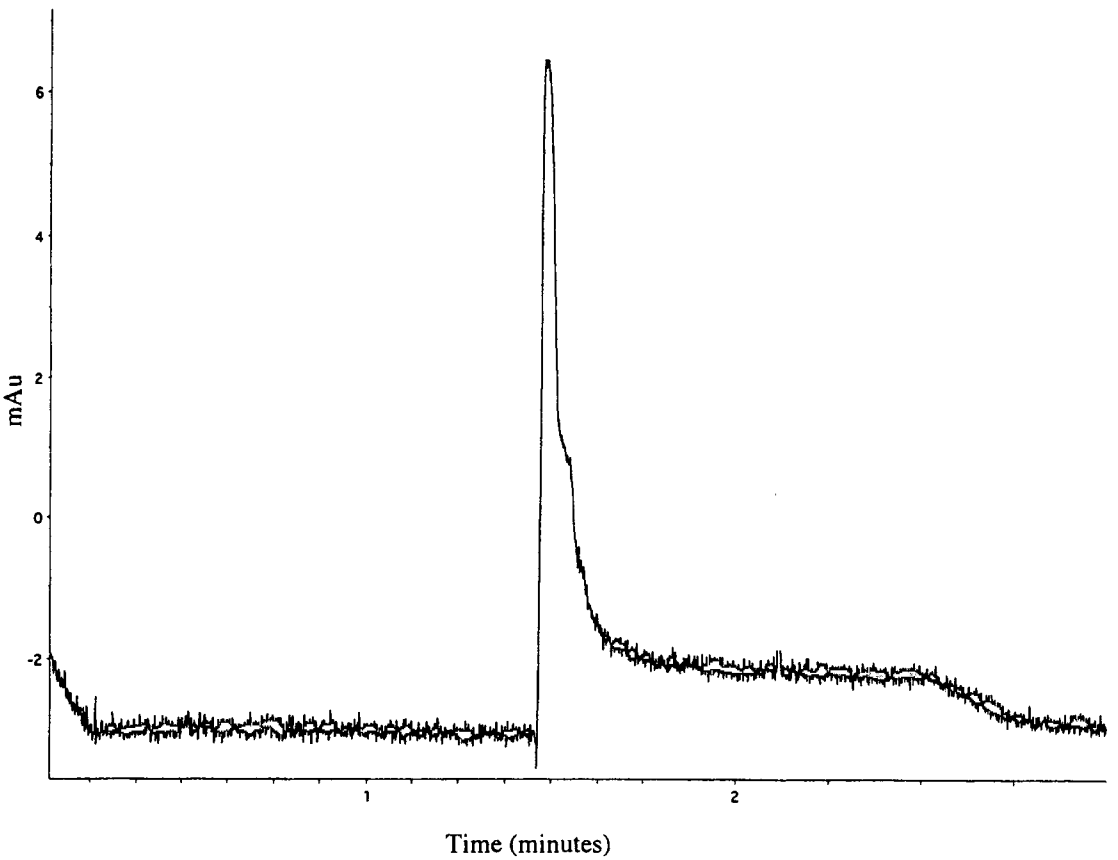

Fig. 2. Elution of three polyaromatic hydrocarbons (naphthalene, anthracene and phenanthrene) with the electroosmotic flow marker. Conditions as in Fig. 1B.

can be seen, all the analytes elute with the electroosmotic flow marker. The separation of these compounds was attempted in order to determine if a better separation could be obtained when the analyte structure contained more aromatic rings as opposed to the long alkyl chains of the alkylbenzenes. The results in Fig. 2 support the findings obtained with the alkylbenzene separations since even a change in solute structure did not produce the desired separation.

In an effort to increase the number of free SDS monomers, separations were attempted with running buffer solutions consisting of 50 m*M* SDS, 50% acetonitrile and 5 m*M* phosphate buffer. In order to ensure that no SDS micelles were present in the running buffer, separations of small neutral molecules were tried. As before, all the solutes eluted with the electroosmotic flow marker which indicated that no SDS micelles were present. Separations of C_{18} and C_{20} alkyl aryl ketones were then attempted (see Fig. 3) using applied voltages of 20, 25 and 30 kV; and hydrodynamic injection times of 5, 3 and 1 s,

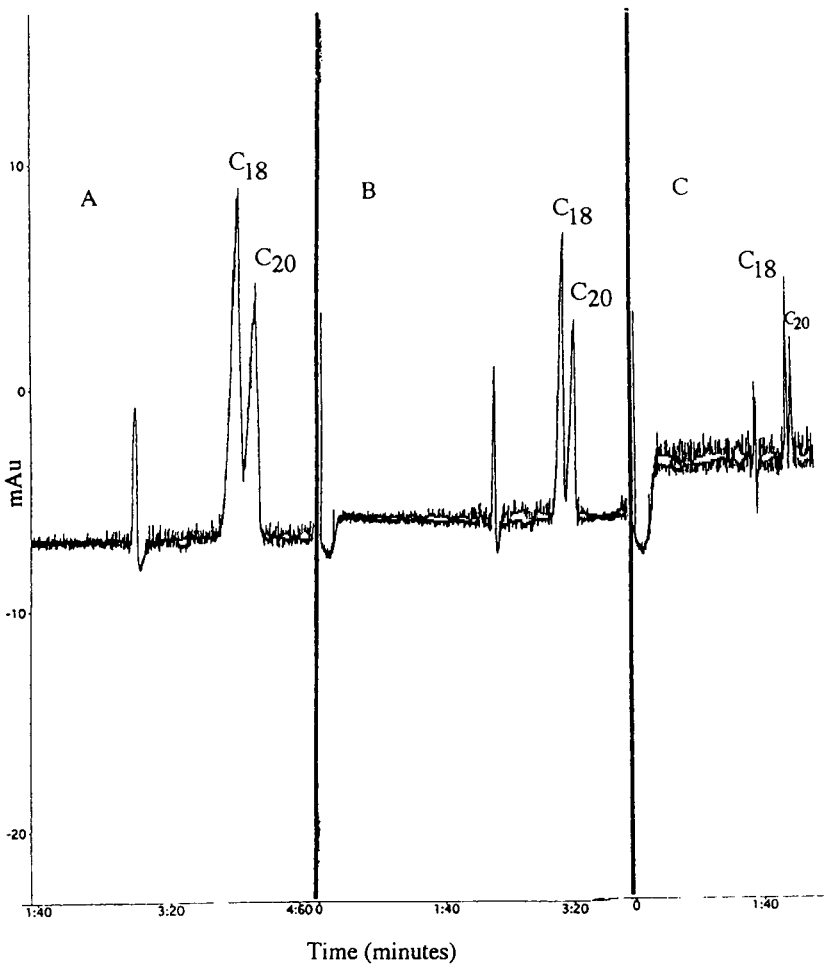

Fig. 3. Separation of alkyl aryl ketones, C_{18} and C_{20}, using a high concentration of *non*-micellized SDS (50 m*M* SDS–50% acetonitrile–5 m*M* phosphate buffer, adjusted to pH 7.0). Other conditions: (A) applied voltage: 20 kV, 5 s injection; (B) applied voltage: 25 kV, 3 s injection; (C) applied voltage: 30 kV, 1 s injection.

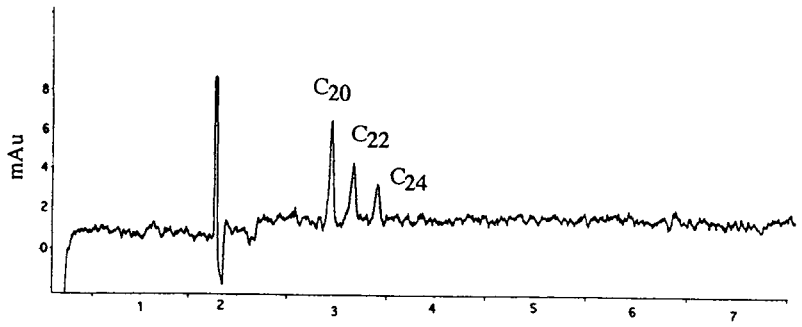

Fig. 4. Separation of C_{20}, C_{22}, C_{24} alkyl aryl ketone homologues using a high concentration of *non*-micellized SDS. Current = 106 μA, other conditions as in Fig. 3C.

respectively. As the operating voltage was increased from 20 to 30 kV with a simultaneous decrease in injection volume, complete resolution of these hydrophobic compounds was achieved in less than 2 min. The elution order followed that seen in MEKC as the less hydro-

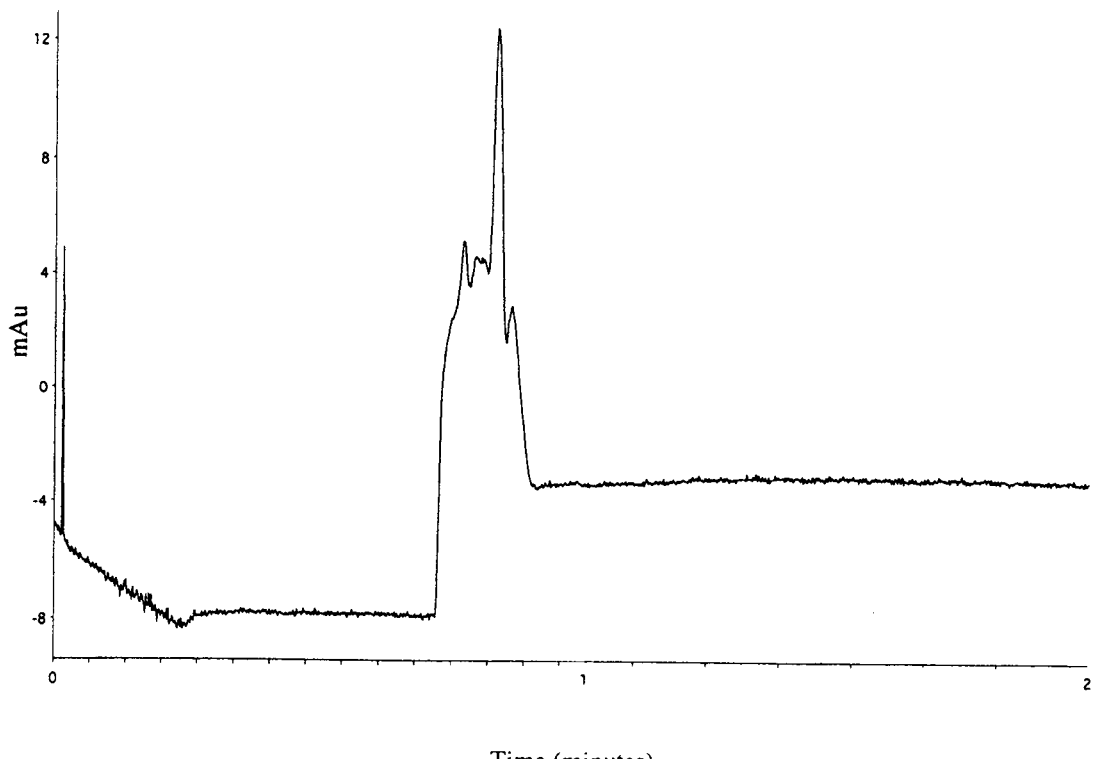

Fig. 5. Elution (but minimal separation) of C_{20}, C_{22}, C_{24} alkyl aryl ketone homologues using a micellar CTAB phase. Experimental conditions: 40 m*M* CTAB–40% acetonitrile–5 m*M* phosphate buffer (pH 7.0); applied voltage 30 kV; operating current <60 μA.

phobic analyte experiences weaker interactions with the free SDS monomers and consequently elutes closer to the electroosmotic flow marker as opposed to the more hydrophobic analyte which experiences a stronger hydrophobic interaction and therefore increased retention. Fig. 4 shows the separation obtained of the three most hydrophobic alkyl aryl ketones (C_{20}, C_{22}, C_{24}) with this running buffer system. The analysis time for this separation is equally impressive. It is important to note that these homologues would have formed precipitates in a totally aqueous medium. The samples injected were dissolved in 100% acetonitrile and since the running buffer consisted of 50% acetonitrile, no precipitation took place in the capillary. Clearly this is an advantage as this had been a problem with MEKC separations where the amount of organic modifier in the running buffer is much less.

With the success of the SDS-based HI-EKC separations, the next logical approach was to attempt separations using a cationic surfactant instead of an anionic surfactant. A surfactant system consisting of 40 m*M* CTAB–40% acetonitrile was first tried. However, as seen in Fig. 5, all the alkyl aryl ketones elute in less than 1 min. This indicated the presence of CTAB micelles because these hydrophobic analytes would reside in the inner regions of the micelle and elute together. In addition, if CTAB micelles were present, one would expect the very quick traversion through the capillary, and indeed this was observed. We then tried a running buffer system consisting of 20 m*M* CTAB–50% acetonitrile. A separation of hydrophilic to moderately hydrophobic alkyl aryl ketone homologues with this system did not result in the elution of any of the analytes after a run time of 30 min, indicating that there were no CTAB

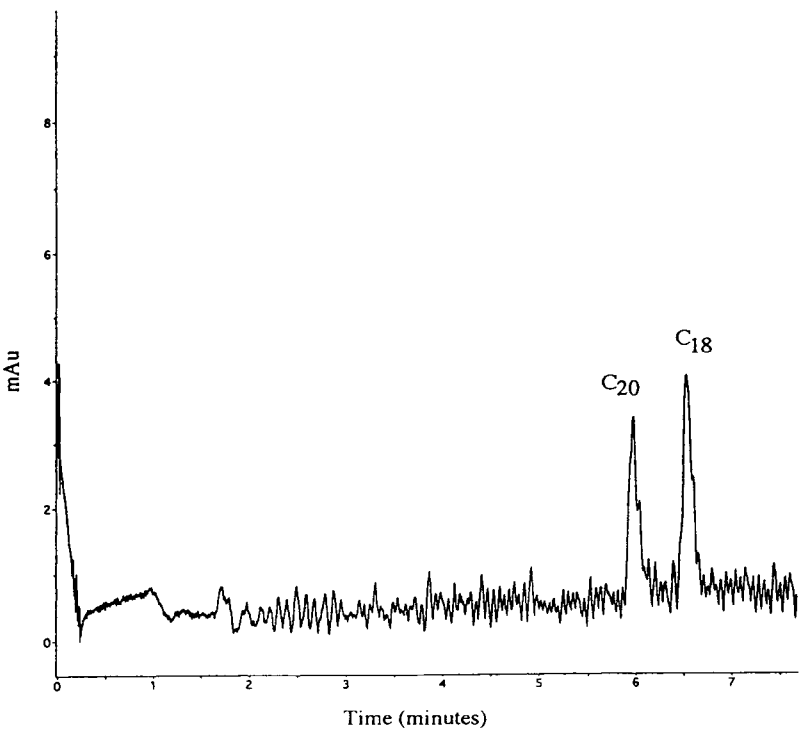

Fig. 6. Separation of alkyl aryl ketones, C_{18} and C_{20}, using a high concentration of *non*-micellized CTAB. Experimental conditions: 20 m*M* CTAB–50% acetonitrile–5 m*M* phosphate buffer (pH 2.8); applied voltage 30 kV; operating current < 40 μA; 1 s injection.

micelles present. Fig. 6 displays the separation of the C_{18} and C_{20} alkyl aryl ketones using the 20 m*M* CTAB–50% acetonitrile system. By comparison of these results with Fig. 3, it is easy to deduce the reversal in elution order of these two analytes. The buffer pH for the separations was 2.8. This was done to decrease the electroosmotic flow such that the positively charged CTAB monomers would serve as the mobile phase and the partially aqueous buffer would serve as the stationary phase. If the pH of the running buffer had been 7.0, both the CTAB monomers and buffer system would rapidly traverse the capillary before any significant hydrophobic interactions, i.e. separation could take place and consequently all the analytes would quickly exit the capillary. By operating at a low buffer pH with the CTAB system, any separations based on hydrophobic interactions result in a completely reversed elution order as the more hydrophobic analytes experience stronger hydrophobic interactions with the free CTAB monomers and travel toward the detector at a faster velocity. The analysis time was less than 7 min for this separation and operating currents were considerably lower than that observed with the SDS-based HI-EKC separations. In Fig. 7, separation of the three most hydrophobic alkyl aryl ketones (C_{20}, C_{22}, C_{24}) is shown. Once again, the reversal in elution order is easily seen in comparison to that observed in Fig. 4 with the SDS-based separations.

In addition, when HI-EKC separations are performed, the alkyl aryl ketone homologues

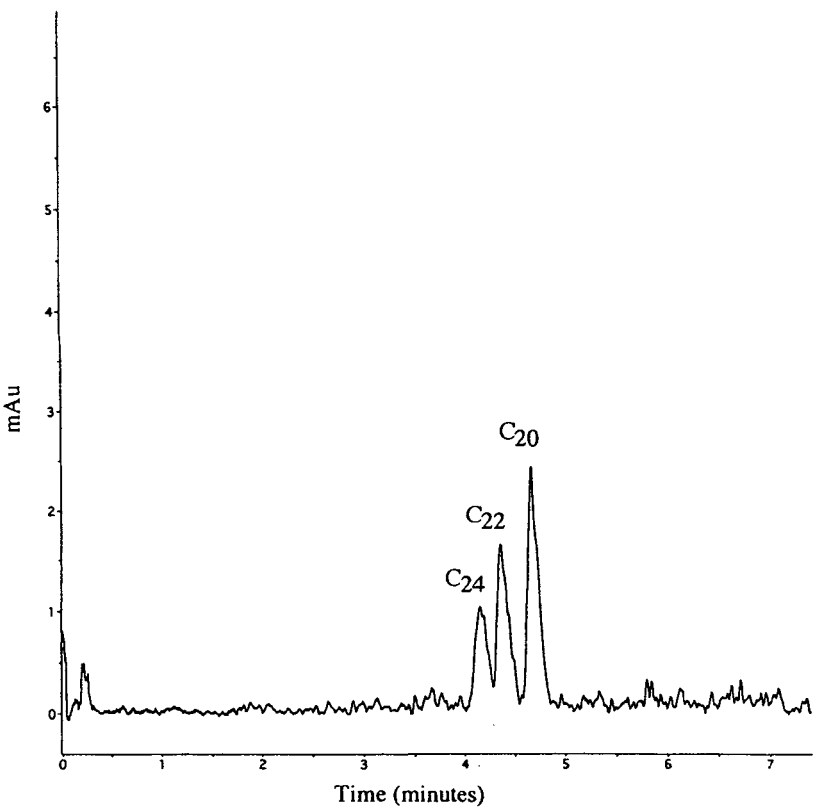

Fig. 7. Separation of C_{20}, C_{22}, C_{24} alkyl aryl ketone homologues using a high concentration of *non*-micellized CTAB. Conditions as in Fig. 6.

(C_{18}, C_{20}, C_{22}, C_{24}) could be used as retention index standards for the calculation of retention indices of very hydrophobic analytes.

4. Conclusions

Clearly, the combination of both the SDS- and CTAB-based HI-EKC methods represent a powerful new way to analyze very hydrophobic analytes. The rapid analysis times and high resolution seen in HI-EKC are very advantageous. If an organic solvent gradient system were available, one could easily run MEKC to separate the hydrophilic to moderately hydrophobic compounds in a sample and then increase the percentage of organic solvent to eliminate the micelles so that the very hydrophobic compounds could be separated as described here. Our approach may serve to bridge the gap between MEKC with predominately aqueous buffer systems and MEKC with non-aqueous buffers, the latter of which has yet to be explored.

Acknowledgements

The authors wish to thank Waters Chromatography Division of Millipore Corporation for the loan of the Quanta 4000 capillary electrophoresis system, the continuing support of Merck Research Laboratories, and the Department of Chemistry at Villanova University for partial travel support.

References

[1] S. Hjertén, *J. Chromatogr.*, 270 (1983) 6.
[2] J.W. Jorgenson and K.D. Lukacs, *Anal. Chem.*, 53 (1981) 1298–1302.
[3] F.E.P. Mikkers, F.M. Everaerts and Th.P.E.M. Verheggen, *J. Chromatogr.*, 169 (1979) 11.
[4] S. Terabe, K. Otsuka, K. Ichikawa, A. Tsuchiya and T. Ando, *Anal. Chem.*, 56 (1984) 111–113.
[5] S. Terabe, K. Otsuka and T. Ando, *Anal. Chem.*, 57 (1985) 834–841.
[6] K.D. Altria, *J. Chromatogr.*, 636 (1993) 125–132.
[7] P. Gareil, J.P. Gramond and F. Guyon, *J. Chromatogr.*, 615 (1993) 317–325.
[8] R. Huopalahti and J. Sunell, *J. Chromatogr.*, 636 (1993) 133–135.
[9] K. Kleparnik, S. Fanali and P. Boček, *J. Chromatogr.*, 638 (1993) 283–292.
[10] C.L. Ng, H.K. Lee and S.F.Y. Li, *J. Chromatogr.*, 632 (1993) 165–170.
[11] P.D. Grossman and J.C. Colburn, *Capillary Electrophoresis —Theory And Practice*, Academic Press, San Diego, CA, 1992.
[12] W.G. Kuhr, *Anal. Chem.*, 62 (1990) R403.
[13] W.G. Kuhr and C.A. Monnig, *Anal. Chem.*, 64 (1992) R389–R407.
[14] S.F.Y. Li, *Capillary Electrophoresis —Principles, Practice, and Applications*, Elsevier, Amsterdam, 1992.
[15] H.J. Gaus, A. Treumann, W. Kreis and E. Bayer, *J. Chromatogr.*, 635 (1993) 319–327.
[16] R.D. Holland and M.J. Sepaniak, *Anal. Chem.*, 65 (1993) 1140–1146.
[17] P. Lukkari, H. Siren, M. Pantsar and M.L. Riekkola, *J. Chromatogr.*, 632 (1993) 143–148.
[18] W. Kleibohmer, K. Cammann, J. Robert and E. Mussenbrock, *J. Chromatogr.*, 638 (1993) 349–356.
[19] Q. Wu, H.A. Claessens and C.A. Cramers, *Chromatographia*, 34 (1992) 25–30.
[20] D.E. Burton, M.J. Sepaniak and M.P. Maskarinec, *J. Chromatogr. Sci.*, 24 (1986) 347–351.
[21] S. Fujiwara, S. Iwase and S. Honda, *J. Chromatogr.*, 447 (1988) 133–140.
[22] H. Nishi, N. Tsumagari, T. Kakimoto and S. Terabe, *J. Chromatogr.*, 465 (1989) 331–343.
[23] C.P. Ong, C.L. Ng, H.K. Lee and S.F.Y. Li, *J. Chromatogr.*, 547 (1991) 419–428.
[24] H.K. Kristensen and S.H. Hansen, *J. Chromatogr.*, 628 (1993) 309–315.
[25] C.P. Ong, C.L. Ng, N.C. Chong, H.K. Lee and S.F.Y. Li, *Environ. Monit. Assess.*, 19 (1991) 93–103.
[26] P. Sandra and J. Vindevogel, *Introduction to Micellar Electrokinetic Chromatography*, Hüthig, Heidelberg, 1992.
[27] Y. Walbroehl and J.W. Jorgenson, *Anal. Chem.*, 58 (1986) 479–481.
[28] J. Bullock, *J. Chromatogr.*, 645 (1993) 169–177.
[29] H.H. Lauer and D. McManigill, *Anal. Chem.*, 58 (1986) 166.
[30] E.S. Ahuja, E.L. Little and J.P. Foley, *J. Liq. Chromatogr.*, 15 (1992) 1099–1113.
[31] S. Hjertén, *Adv. Chromatogr.*, 19 (1981) 111–121.
[32] R.J. Yon, *Int. J. Biochem.*, 2 (1978) 373.
[33] D.L. Gooding, M.N. Schmuck and K.M. Gooding, *J. Chromatogr.*, 296 (1984) 107–114.
[34] E. Shansky, S.L. Wu, A. Figueroa and B.L. Karger, in K.M. Gooding and F.E. Regnier (Editors), *HPLC of Biological Macromolecules*, Marcel Dekker, New York, 1990.

ELSEVIER

Journal of Chromatography A, 680 (1994) 85–92

JOURNAL OF CHROMATOGRAPHY A

α,ω-Bis-quaternary ammonium alkanes as effective buffer additives for enhanced capillary electrophoretic separation of glycoproteins

R.P. Oda, B.J. Madden, T.C. Spelsberg, J.P. Landers*

Department of Biochemistry and Molecular Biology, Mayo Clinic and Mayo Foundation, Rochester, MN 55905, USA

Abstract

The egg white glycoprotein, ovalbumin, is known to be microheterogeneous as a result of its varied glycan content. The use of 1,4-diaminobutane (DAB) as a buffer additive has been shown to be key in the high-resolution capillary electrophoretic separation of "glycoforms" of this protein [*Anal. Biochem.* 205 (1992) 115]. Although a separation buffer consisting of 100 m*M* borate and 1 m*M* DAB allowed for adequate separation of ovalbumin glycoforms, prolonged separation times of 35–45 min were undesirable. In the present study, the α,ω-bis-quaternary ammonium alkanes, hexamethonium bromide (C_6MetBr), hexamethonium chloride (C_6MetCl) and decamethonium bromide (C_{10}MetBr) were tested as buffer additives for their effectiveness in the separation of ovalbumin glycoforms. Where 1 m*M* DAB gave optimal separation in *ca.* 45 min, 100 μM C_6MetCl or C_{10}MetBr yielded comparable resolution in less than 20 min. Results with the C_{10}MetBr were better than those obtained with C_6MetBr, indicating that there may be a correlation between effectiveness and alkyl chain length. Use of the chloride salt of C_6Met afforded the same resolution as the bromide salt in slightly shorter analysis time. The rank order for their effectiveness was found to be C_{10}MetBr > C_6MetCl > C_6MetBr > DAB. These results allow for speculation on the mode through which these additives exert their effect on resolution. Included in these are additive-wall coating interactions, protein–additive interactions, protein-wall interactions or any combination of these.

1. Introduction

High-performance capillary electrophoresis (HPCE), a relatively new analytical tool, has been shown to be capable of attaining separation efficiencies superior to those with high-performance liquid chromatography (HPLC). Electrophoretic separation carried out in 75 μm I.D. (or less) capillaries allows for the efficient dissipation of Joule heat and, therefore, non-denaturing electrophoretic separations can be carried out in simple buffers under high fields (up to 30 000 V). HPCE has been shown to be useful for the separation of a diverse array of molecules including ions [1], small organic molecules [2], carbohydrates [3,4], peptides [5] and oligonucleotides [2].

One of the areas where HPCE has had a dramatic impact is with the analysis of glycoproteins. Surface carbohydrates on proteins, once thought to be artifacts, are now known to impart a number of important biological functions including antigenicity, transport, folding and biological activity. HPCE has been shown to be

* Corresponding author.

0021-9673/94/$07.00
SSDI 0021-9673(94)00219-Y

useful for resolving the glycoforms of a variety of proteins including ribonuclease [5], recombinant T4 receptor [7], human recombinant erythropoietin [8], leech-derived O-linked glycopeptides [9], and transferrin [10,11].

Determining conditions for the electrophoretic separation of proteins in uncoated fused-silica capillaries has been problematic, mainly due to the inherent nature of proteins for interacting with the capillary wall or other proteins. One of the main ways in which this problem has been circumvented is through the use of buffer additives that either coat the inner wall or augment the buffer to reduce protein–wall interactions [12–16]. We [17] and others [18] have demonstrated the utility of alkyl diamines for the analysis of glycoprotein microheterogeneity. In the present study, a similar class of alkyl compounds, in which the terminal diamino groups have been replaced with quaternary ammonium moieties, is tested. It will be shown that α,ω-bis-quaternary ammonium alkanes not only allow for analysis of microheterogeneity, but are much more efficient than their diamino counterparts.

2. Experimental

2.1. Materials

Sodium hydroxide was purchased from Fisher Scientific. All chemicals for peptide sysnthesis were purchased from Applied Biosystems (Foster City, CA, USA). Borax (sodium tetraborate), boric acid, hexamethonium bromide (C_6MetBr), hexamethonium chloride (C_6MetCl), decamethonium bromide (C_{10}MetBr) and diaminobutane (DAB) were purchased from Sigma (St. Louis, MO, USA). Dimethylformamide (DMF) was purchased from Aldrich (Milwaukee, WI, USA). Ovalbumin was purchased from Pharmacia (Piscataway, NJ, USA) or Sigma.

2.2. Buffer and sample preparation

Borate buffer was made by titrating 25 m*M* sodium tetraborate with 100 m*M* boric acid until the desired pH was obtained. For use in the separation buffer (100 m*M* borate), C_6MetBr and other additives were diluted from a stock solution (1 *M*, in Milli-Q purified water) to the desired concentration. All buffers were made with Milli-Q (Millipore) water, and filtered through an 0.2-μm filter (Gelman) before use. Proteins were dissolved in the running buffer without modifier and filtered through an 0.22-μm micro-centrifuge filter (Millipore).

2.3. Instrumentation

HPCE was carried out on a Beckman P/ACE System 2100 interfaced with an IBM 55SX computer utilizing System Gold software (version 7.1) for instrument control and data collection. All peak information (migration time) was obtained through System Gold software.

Reversed-phase (RP) HPLC of 25 μg of ovalbumin was carried out on an ABI 130A microseparation system with an ABI RP-300 C_8 reverse-phase column (100 × 2.1 mm) (Applied Biosystems).

2.4. HPCE separation conditions

Capillaries were bare fused-silica (Polymicro Technologies, Phoenix, AZ, USA) of 87 cm (80 cm to the detector) × 375 μm O.D. × 50 μm I.D. For analyses, the following method was typically used: a three column-volume rinse with separation buffer, 3-s pressure injection of a protein solution in separation buffer or water (3.3 nl; 0.5–1.5 mg/ml), followed by a 3-s pressure injection of the neutral marker, DMF (1:5000 in water); separation at 25 kV (constant voltage with the inlet as the anode and the outlet as the cathode), a three column-volume wash with 0.1 *M* NaOH followed by a three column-volume rinse with separation buffer. All electrophoretic separations were carried out at constant voltage (typically 25 kV) and capillary temperature was maintained at 28°C. Detection was by absorbance at 200 nm.

3. Results and discussion

Ovalbumin is a glycoprotein found in avian egg white and has a M_r of ca. 43 000. It has two

potential asparagine-linked glycosylation sites, one on amino acid 292 and the other on 312 (total of 385 amino acids). Studies have demonstrated that only the Asn_{292} is glycosylated *in vivo* [19] and that Asn_{312} can be glycosylated *in vitro* [20]. As with the carbohydrate component of many glycoproteins, the glycan structure of ovalbumin is heterogeneous [21]. A total of nine different oligosaccharide chains have been identified [22–26], all of which have been classified as high-mannose or hybrid structures. The hybrid and high-mannose forms are present at approximately a 1:1 ratio.

The RP-HPLC separation of ovalbumin on a C_8 column is shown in Fig. 1A. The resolution is relatively poor and the presence of multiple broad peaks is suggestive of glycoprotein heterogeneity. The profile in Fig. 1B represents the electrophoretic separation of the same ovalbumin solution in an 87 cm capillary (effective length of 80 cm) in 100 m*M* borate, pH 8.4. While the analysis time is decreased significantly in comparison with RP-HPLC, the resolution has only been moderately enhanced. Electrophoretic separation of the same sample in the same capillary with borate buffer containing 1 m*M* DAB results in the resolution of the multitude of components present in the sample (Fig. 1C). Decreasing the DAB concentration below 1 m*M* has been shown to lead to loss of resolution [17]. Concomitant with the enhanced resolution is a decrease in electroosmotic flow (EOF), consistent with observations reported in earlier studies [17,27]. It is reasoned that the enhanced resolution results from an increase in analyte residence time brought about by the combination of decreased EOF (from addition of 1 m*M* DAB) and a longer than normal effective capillary length (80 cm *vs.* 40–50 cm capillaries typically used in HPCE) [17]. The type of buffer used also appeared to play a key role in the resolution. Although the details of the mechanism are not completely understood, DAB has been postulated to exert its effect on the separation through a masking of silanol groups. This affects the ζ potential and, subsequently, the EOF.

In a study aimed at understanding the mechanism through which α,ω-diaminoalkanes like DAB function, both the bifunctional character

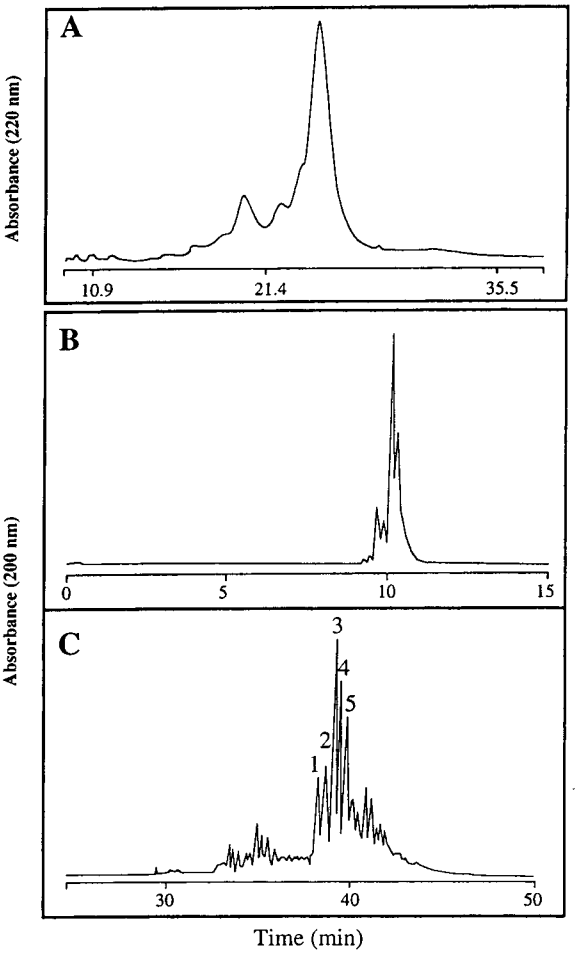

Fig. 1. The effectiveness of DAB for the resolution of ovalbumin isoforms. (A) RP-HPLC of ovalbumin (1 mg/ml; 25-μl injection). Column: ABI RP-300 (C_8, 100 × 2.1 mm). Buffers: A = 5% acetonitrile in water, 0.1% trifluoroacetic acid (TFA); B = 70% acetonitrile in water, 0.1% TFA. Flow-rate: 0.2 ml/min with a gradient of 50% to 100% B over 50 min. (B) Capillary electrophoresis of ovalbumin [1 mg/ml, 3-s pressure (0.5 p.s.i., 1 p.s.i. = 6894.76 Pa) injection]. Buffer: 100 m*M* borate, pH 8.4, no additives. (C) Capillary electrophoresis of ovalbumin [1 mg/ml, 3-s pressure (0.5 p.s.i.) injection]. Buffer: 100 m*M* borate, pH 8.4, 1 m*M* DAB. Capillary: bare silica, 87 cm (80 cm to the detector) × 50 μm I.D. Separation: 25 kV (17 μA); 28°C.

and the length of the alkyl chain were found to play a role in their effectiveness for glycoform resolution [6]. Furthermore, there was an excellent correlation between those alkyl diamines which effected ovalbumin resolution and those which optimally affected EOF. It was, therefore,

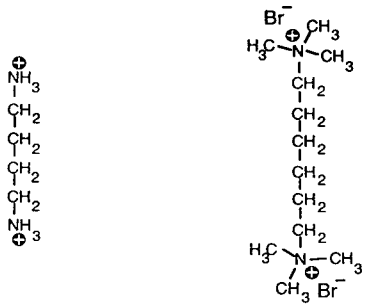

1,4-Diaminobutane Hexamethonium bromide

Fig. 2. Structures of DAB and C_6MetBr.

of interest to determine whether similar compounds containing α,ω-quaternary ammonium groups (*vs.* protonatable amines) were capable of similar effects. Fig. 2 illustrates the structure of the two classes of compounds, highlighting the differences in charge at the termini of each molecule. In theory, quaternary ammonium compounds are advantageous over the α,ω-diaminoalkanes as a result of two properties: their ionization state is not pH-dependent and addition does not alter the buffer pH.

The electropherograms in Fig. 3 show the effect on ovalbumin resolution of hexamethonium bromide (C_6MetBr) added to 100 m*M* borate buffer, pH 8.3 (micromolar values on the *z*-axis represent the final concentration in the separation buffer). Under these conditions, baseline resolution of all peaks could be achieved with 1 m*M* C_6MetBr at the expense of undesireably long analysis times (> 60 min). The optimal concentration for adequate resolution within a reasonable analysis time-frame was 300 μM C_6MetBr (25–35 min). These results were somewhat surprising since faster separation was attained with an additive concentration 3-fold

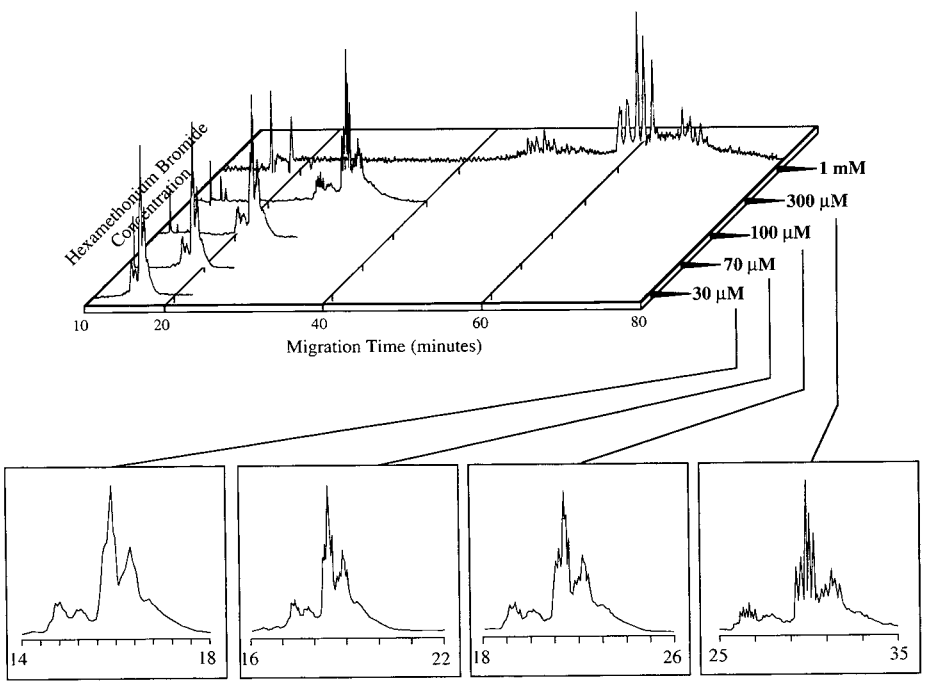

Fig. 3. The dependence of ovalbumin resolution on hexamethonium bromide concentration in the separation buffer. The top part shows the separations on the same time scale. The lower panels, which are expanded time scales (min) profiles of the upper traces, depict the enhanced resolution with increasing concentrations of hexamethonium bromide. From left to right, 30, 70, 100 and 300 μM C_6MetBr final concentration in 100 m*M* borate, pH 8.4. Sample: ovalbumin [1 mg/ml, 3-s pressure (0.5 p.s.i.) injection]. Capillary: bare silica, 87 cm (80 cm to the detector) × 50 μm I.D. Separation: 25 kV (17 μA); 28°C.

lower than DAB. Reproducibility for replicate analyses with 300 μM C_6MetBr in the separation buffer ($n = 3$) was found to be 0.53, 0.53, 0.54, 0.54 and 0.54% R.S.D. for peaks 1–5 (as labelled in Fig. 1C), respectively. The level of reproducibility and resolution associated with C_6MetBr addition to the separation buffer make it ideal for preparative-scale analyses. This contrasts with the use of higher concentrations of DAB (*e.g.*, 3–5 mM) where baseline resolution was associated with significant band broadening and extremely lengthy migration times [17].

The importance of the counterion in the overall separation was evaluated by comparing separations carried in the presence of C_6MetCl and C_6MetBr (Fig. 4). It was interesting to find that the dependence on concentration with C_6MetCl was significantly different than that with C_6MetBr. One significant difference is the fact that adequate separation is attained with 100 μM, a concentration 3-fold lower than that required with C_6MetBr and 10-fold lower than that required with DAB. More important is that adequate resolution is attained in less than 20 min (in comparison with 300 μM C_6MetBr in 33 min and 1 mM DAB in 40 min). This is suggestive of the chloride salt being more effective than bromide salt and may be the result of the higher mobility of chloride as a counterion.

To determine whether the α,ω-quaternary ammonium compounds shared some of the chain length-dependent structure–activity relationships observed with the α,ω-diaminoalkanes [6], C_{10}MetBr was tested for its ability to effect ovalbumin separation (Fig. 5). Similar to the C_6MetCl, resolution of the ovalbumin isoforms was achieved with a concentration of 100 μM C_{10}MetBr. Adequate resolution is attained in

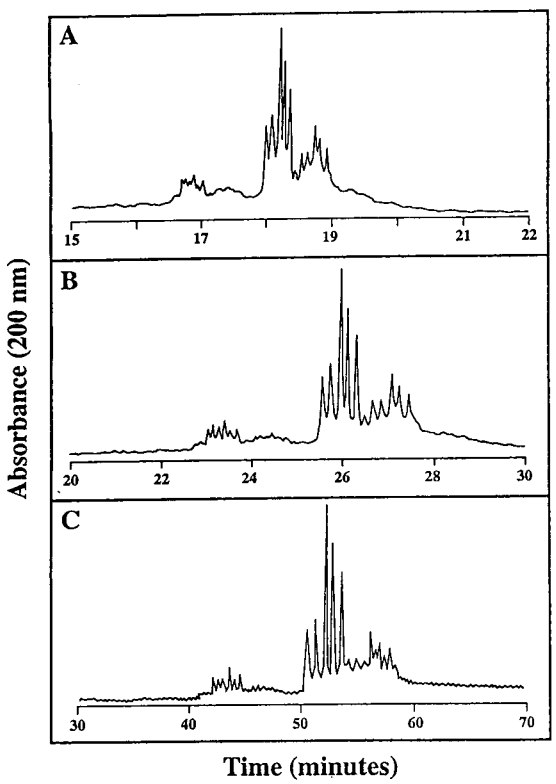

Fig. 4. The dependence of ovalbumin separation on C_6MetCl concentration. (A) 100 μM, (B) 300 μM and (C) 1 mM C_6MetCl. Sample and other conditions as in Fig. 3.

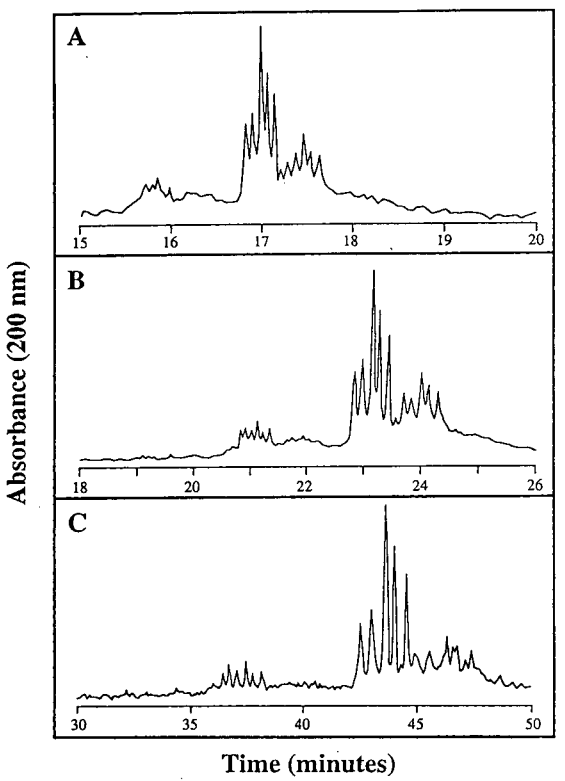

Fig. 5. The dependence of ovalbumin separation on C_{10}MetBr concentration. (A) 100 μM, (B) 300 μM and (C) 1 mM C_{10}MetBr. Sample and other conditions as in Fig. 3.

slightly less time (18 min) than observed with C_6MetCl (20 min) with a reproducibility ($n = 3$) of 0.37, 0.37, 0.38, 0.38 and 0.38% R.S.D. for peaks 1–5, respectively. Comparison of the migration times obtained with a 300 μM concentration of each of the additives in separation buffer shows the order of effectiveness to be C_{10}MetBr > C_6MetCl > C_6MetBr (Fig. 6). This suggests that the alkyl chain length may be a more important parameter than the counterion in effecting resolution.

Based on the markedly shorter analysis times required for resolution of the isoforms in the presence of C_{10}MetBr (18 min) and C_6MetBr (33 min), it was assumed that these additives would have less effect on the slowing of EOF than that observed with DAB (45 min). EOF was monitored in each analysis by the co-injection of DMF with the sample. Surprisingly, the effect of C_6MetBr and C_{10}MetBr on the slowing of EOF was found to be similar to that of DAB (Fig. 7). This indicates that, despite a significant repression of EOF, quaternary ammonium alkane additives allow for ovalbumin glycoforms to be resolved in less than half the analysis time (18 min with C_{10}MetBr *vs.* 40 min with DAB). This is suggestive that alteration in EOF is *not* the only parameter involved in the additive-induced enhancement of resolution.

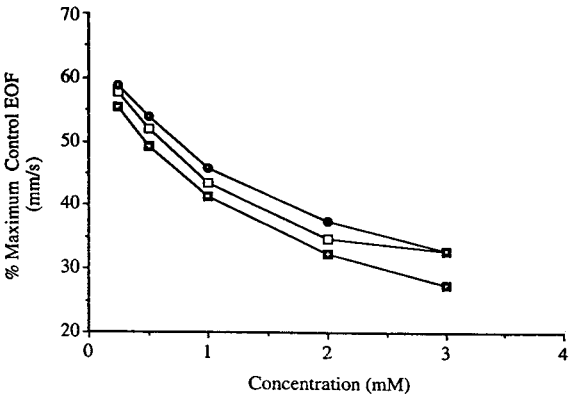

Fig. 7. The effect of DAB (□), C_6MetBr (■) and C_{10}MetBr (●) on EOF. The two amines were added to 100 mM borate buffer, pH 8.4 at the indicated final concentrations. The effect on EOF was determined by the migration time of a neutral marker, DMF. Capillary: bare silica, 87 cm (80 cm to the detector) × 50 μm I.D. Separation: 25 kV (17 μA); 28°C.

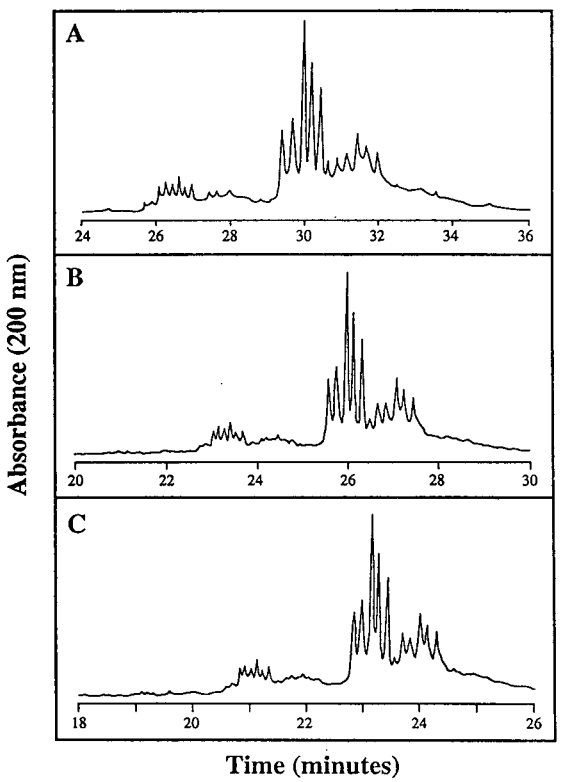

Fig. 6. A comparison of effect of 300 μM concentration of each of the bis-quaternary ammonium additives on ovalbumin resolution. (A) 300 μM C_6MetBr, (B) 300 μM C_6MetCl, (C) 300 μM C_{10}MetBr. Sample and other conditions as in Fig. 3.

As a final step in the evaluation of the quaternary ammonium compounds as additives, we determined whether they could effect the separation of other microheterogenous glycoproteins. Fig. 8 shows the resolution of the isoforms of human chorionic gonadotropin (hCG) with 1 mM hexamethonium bromide and 25 mM borate buffer, pH 8.4. Seven of the eight isoforms are clearly resolved. This presents the possibility that bis-quaternary ammonium alkyl compounds may be effective buffer additives for the resolution of isoforms of other glycoproteins.

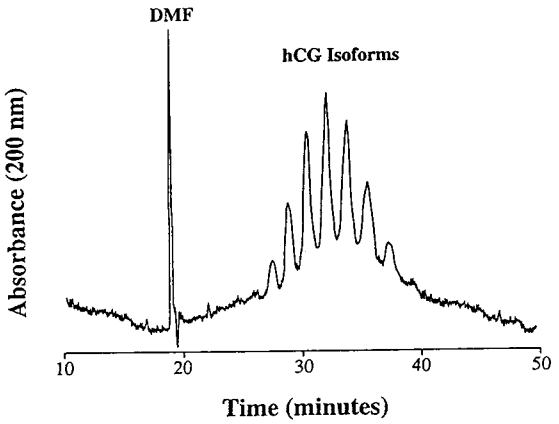

Fig. 8. Effect of hexamethonium bromide on the resolution of hCG isoforms. Human chorionic gonadotropin [5 mg/ml, 5-s pressure (0.5 p.s.i.) injection]. Buffer: 25 m*M* borate, pH 8.4 containing 1 m*M* hexamethonium bromide. Capillary: bare silica, 87 cm (80 cm to the detector) × 50 μm I.D. Separation: 25 kV (8.5 μA); 28°C.

4. Conclusions

This study has demonstrated that bis-quaternary ammonium alkyl compounds appear to be more effective at resolving glycoprotein isoforms than their alkyl diamine counterparts. This stems not only from the fact that resolution is obtained at lower concentrations, but that adequate resolution is obtained in dramatically shorter analysis times. The observed order of effectiveness (C_{10}MetBr > C_6MetCl > C_6MetBr > DAB) indicates that the ideal quaternary ammonium additive possesses a long alkyl chain (C_{10}) and has chloride as a counterion (*i.e.*, decamethonium chloride). From a mechanistic perspective, the fact that similar resolution from two different additives with a greater than 2-fold difference in analysis time and minimal differences in EOF is suggestive that the magnitude of EOF is not the only factor leading to the enhanced resolution. One likely difference between the alkylamines and the quaternary ammonium-type compounds is that the latter tend to be better "ion exchangers". The fact that both classes of amines have a tendency for wall (silanol) interaction suggests that additional parameters, such as the interaction of the additive with protein analytes or interaction of the protein with wall-bound additive (chromatography?) should be considered.

Acknowledgements

The authors wish to thank Collen Allen for her expert clerical assistance and acknowledge the support of the Canadian Medical Research Council (J.P.L.) for financial support.

References

[1] W.R. Jones, P. Jandik and R. Pfeifer, *Am. Lab.*, 23 (1991) 40.
[2] B.L. Karger, A.S. Cohen and A. Guttman, *J. Chromatogr.*, 585 (1989) 492.
[3] J. Liu, O. Shirota, D. Wiesler and M. Novotny, *Proc. Natl. Acad. Sci. U.S.A.*, 88 (1991) 2302.
[4] J. Liu, O. Shirota and M. Novotny, *Anal. Chem.*, 63 (1991) 413.
[5] P.D. Grossman, J.C. Colburn, H.H. Lauer, R.G. Nielsen, R.M. Riggin, G.S. Sittampalam and E.C. Rickard, *Anal. Chem.*, 61 (1989) 1186.
[6] J.P. Landers, R.P. Oda, B.J. Madden and T.C. Spelsberg, *Anal. Chem.*, (1994) submitted for publication.
[7] S.-L. Wu, G. Teshima, J., Cacia and W.S. Hancock, *J. Chromatogr.*, 516 (1990) 115.
[8] A.D. Tran, S. Park, P.J. Lisi, O.T. Huynh, R.R. Ryall and P.A. Lane, *J. Chromatogr.*, 542 (1991) 459.
[9] V. Steiner, R. Knecht, O. Bornsen, E. Gassmann, S.R. Stone, F. Raschdorf, J.-M. Schlaeppi and R. Maschler, *Biochemistry*, 31 (1992) 2294.
[10] F. Kilar and S. Hjertén, *J. Chromatogr.*, 480 (1989) 351.
[11] F. Kilar and S. Hjertén, *Electrophoresis*, 10 (1989) 23.
[12] M.J. Gordon, K.-J. Lee, A.A. Arias and R.N. Zare, *Anal. Chem.*, 63 (1991) 69.
[13] J.E. Wiktorowicz and J.C. Colburn, *Electrophoresis*, 11 (1990) 769.
[14] J.K. Towns and F.E. Regnier, *Anal. Chem.*, 63 (1991) 1126.
[15] J.R. Mazzeo and I.S. Krull, *Biotechniques*, 10 (1991) 638.
[16] C.A. Bolger, M. Zhu, R. Rodriguez and T. Wehr, *J. Liq. Chromatogr.*, 14 (1991) 895.
[17] J.P. Landers, R.P. Oda, B.J. Madden and T.C. Spelsberg, *Anal. Biochem.*, 205 (1992) 115.

[18] E. Watson and F. Yao, *Anal. Biochem.*, 210 (1993) 389.
[19] L.W. Cunningham, B.J. Nuenke and R.H. Nuenke, *Biochim. Biophys Acta.*, 26 (1957) 660.
[20] C.G. Glabe, J.A. Hanover and W.J. Lennarz, *J. Biol. Chem.*, 255 (1980) 9236.
[21] C.-C. Huang, H.E. Mayer and R. Montegomery, *Carbohydr. Res.*, 13 (1970) 127.
[22] T. Tai, K. Yamashita, M. Ogata-Arakawa, N. Koide, T. Muramatsu, S. Iwashita, Y. Inoue and A. Kobata, *J. Biol. Chem.*, 250 (1975) 8569.
[23] T. Tai, K. Yamashita, S. Ito and A. Kobata, *J. Biol. Chem.*, 252 (1977) 6687.
[24] K. Yamashita, Y. Tachibana and A. Kobata, *J. Biol. Chem.*, 253 (1978) 3862.
[25] B.T. Sheares and P.W. Robbins, *Proc. Natl. Acad. Sci. U.S.A.*, 83 (1986) 1993.
[26] Y. Kato, H. Iwase and K. Hotta, *Arch. Biochem. Biophys.*, 244 (1986) 408.
[27] H. Lauer and D. McManigill, *Anal. Chem.*, 58 (1986) 166.

ELSEVIER

Journal of Chromatography A, 680 (1994) 93–98

JOURNAL OF CHROMATOGRAPHY A

Pressurized gradient electro-high-performance liquid chromatography

Beate Behnke, Ernst Bayer*

Institut für Organische Chemie, Universität Tübingen, Auf der Morgenstelle 18, 72076 Tübingen, Germany

Abstract

A microbore liquid chromatographic system was developed for gradient elution using capillary columns with inner diameters of 50 and 100 μm. In addition, voltage gradients up to 30 000 V can be applied across the length of the column. The dramatic improvement of reversed-phase separations of charged analytes is demonstrated by a separation of detritylated oligonucleotides on 5 μm C_{18} reversed-phase silica gel. Several examples are given, illustrating the influence of applied voltage gradients up to 400 V/cm upon the separation in both isocratic and gradient elution modes.

1. Introduction

Liquid chromatography in capillary columns is a fast developing technique offering the potential of increased performance in comparison to the well established wide-bore methods. Three modes can be distinguished: conventional pressure-driven chromatography [1–4], electroosmotic flow-driven electrochromatography [5–8] and combinations of these [9–11]. The use of packed and open-tubular columns in all three modes has been investigated. Electroosmotic flow arising from an electrical field provides eluent transport with a nearly flat flow profile thus increasing the efficiency. In addition, the electroosmotic flow is independent of the particle diameter, as has been experimentally verified for particle diameters as small as 1.5 μm in packed capillary columns of up to 0.6 m length. The resulting very high efficiency in chromatographic performance has recently been demonstrated [7,8]. The combination of pressure and voltage gradients has been investigated by Tsuda [11], who showed that bubble formation could be diminished by applying pressure to the system.

So far all electrochromatographic techniques use the isocratic approach with capillary columns with very small inner diameters. However, gradient elution is a necessity for many HPLC separations and restriction to isocratic separations greatly limits the range of practical applicability. We have developed a gradient system for liquid chromatographic techniques with packed columns of 50 to 100 μm inner diameter and evaluated the performance of this system in electro-HPLC.

2. Experimental

2.1. Preparation of slurry-packed capillary columns

Fused-silica capillaries of 50 and 100 μm I.D. and 360 μm O.D. were obtained from Polymicro

* Corresponding author.

0021-9673/94/$07.00
SSDI 0021-9673(94)00606-7

Technology (Phoenix, AZ, USA). The frits were prepared by sintering 5-μm spherical silica gel (Gromsil; Grom, Herrenberg, Germany) using a self-made heater. For the packing procedure of either silica gel or reversed-phase material, a slurry of 5-μm particles (Gromsil ODS-2, Grom) in acetone (1:10, w/v) was ultrasonicated for 5 min and transferred to a stainless-steel slurry chamber (25 mm × 1 mm I.D.). The capillary protruded about 5 mm into the chamber which was placed into an ultrasonic bath during packing. The slurry was pumped into the capillary at 400 bar using a liquid chromatographic pump (Model S1100; Sykam, Gilching, Germany).

The production of a packed capillary column proceeded as follows. First a temporary end-frit was prepared by tapping the capillary into silica gel wetted with water, drying and heating. The capillary was then packed with silica gel. The outlet frit was formed by sintering at a distance of approximately 20 cm from the end of the capillary, after which the end-frit was cut off and the capillary emptied on both sides of the frit by flushing with water under ultrasonication. After packing the column with the 5-μm reversed-phase particles ca. 1 cm stationary phase was removed by heating the tip of the capillary, thus causing rapid solvent evaporation and ejection of slurry. Finally this end of the capillary was filled up with silica gel and an inlet-frit sintered after drying.

2.2. Apparatus

In order to use the electrochromatographic system in the gradient mode a modular capillary electrophoresis system (Grom) was combined with a gradient HPLC system (Sykam) as shown in Fig. 1. A stainless-steel six-port rotary valve including an injection port (Rheodyne, Cotati, CA, USA) was used for sample injection. The splitting of eluent was achieved by a stainless-steel T-piece connected to a narrow-bore microparticle-packed column functioning as a flow resistance. The splitter was grounded to protect the pump from any damage that may be caused by the high voltage. The electrolyte block on the inlet side of the capillary column was connected

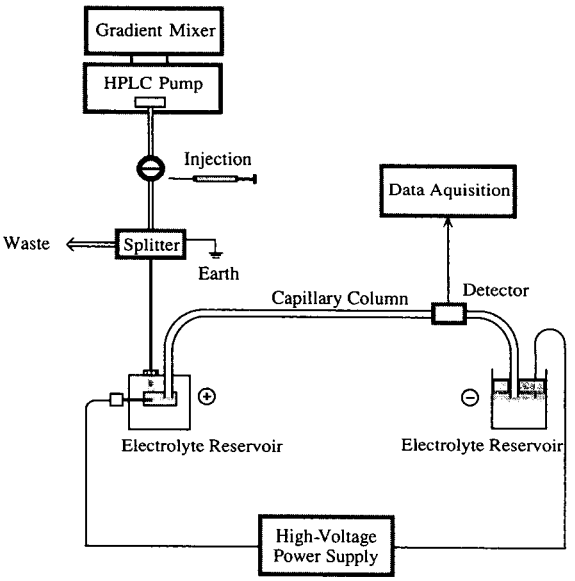

Fig. 1. Schematic representation of an electrochromatographic system.

to the splitter by a laboratory-made interface. A Chromatopac C-R6A (Shimadzu, Kyoto, Japan) was used for data processing.

2.3. Electrochromatography

The chromatographic columns of 50 cm overall length were packed with 5-μm reversed-phase particles to a length of 30 cm. Removal of the polyimide coating allowed on-line UV absorbance detection (260 nm) at 30.2 cm. The flow-rate was 0.5 ml/min at 200 bar. The mobile phase used under isocratic conditions was acetonitrile–buffer containing 10 m*M* triethylammonium acetate (TEAA) (12:88). In the gradient elution mode the buffer was 10 m*M* ammonium acetate at pH 8 containing (A) 0% and (B) 10% acetonitrile. The gradient was 0 to 100% B in 30 min. The buffers were prepared from double-distilled water and thoroughly degassed. The pH was adjusted with a 0.01 *M* triethylamine solution.

Two modes of injection were used. By injection of the sample into the rotary valve only a small fraction entered the chromatographic column after splitting. A second approach was accomplished by filling the electrolyte reservoir

on the inlet side of the capillary with 5 μl sample and pressurizing for 15 s at 200 bar. The reservoir was then flushed with eluent. The concentrations of deoxyoligonucleotides were 5 mg/ml in the split injection mode and 300 μg/ml by injection directly from the electrolyte reservoir.

2.4. Micellar electrokinetic capillary chromatography (MECC)

For electrophoresis the modular capillary electrophoresis system (Grom) was used. Capillaries of 50 μm I.D. and 360 μm O.D. (Polymicro Technology) were flushed for 10 min with 1 *M* NaOH, water and buffer. Overall length of the capillaries was 0.7 m with on-line UV absorbance detection at 0.5 m. The buffer for MECC consisted of 5 m*M* tris(hydroxymethyl)aminomethane, 5 m*M* borate, 7 *M* urea and 50 m*M* sodium dodecyl sulfate at pH 8.9 (HCl). Sample solutions were injected by hydrostatic loading (30 s, 0.1 m). Electrophoresis was performed at 17 kV and 20 μA.

2.5. Chemicals

Oligodeoxyribonucleotides were synthesized on an ABI 38m0B DNA synthesizer using the phosphoramidite approach. The chemicals were purchased from MWG-Biotech (Ebersberg, Germany), Roth (Ulm, Germany) and Merck (Darmstadt, Germany). All chemicals for buffer preparation were of research grade (Merck).

3. Results and discussion

3.1. Microbore HPLC system

Packed fused-silica capillaries used as chromatographic columns provide several advantages. The high mechanical strength allows inlet pressures of up to 800 bar so that long columns can be packed with particles of smaller diameters down to 1.5 μm and used in chromatography [7,8]. Due to the flexibility of the fused-silica capillaries even very long columns can be handled easily. The good optical transparency allows on-column detection in the UV–Vis absorption range. The most important feature for their optional use in electro-HPLC is the isolating property of the fused silica.

A microbore HPLC system was constructed combining a capillary electrophoresis system with an HPLC pump and gradient mixer. The use of capillary columns with inner diameters of 50 to 100 μm demanded a solvent splitter.

Two different injection modes were developed. Split injection via a rotary valve was reproducible but was wasteful of analyte because only a small fraction of the sample volume entered the capillary after splitting. A better approach was the direct injection of sample into the electrolyte reservoir followed by pressurization of the chamber for several seconds. This proved to be an appropriate injection mode although some difficulties were encountered in reproducing the injected amount of the sample.

The development of an interface with minimized dead volume between the HPLC system and the electrolyte reservoir allowed micro-HPLC separations in the gradient mode with columns of 50 μm I.D. While isocratic separations are limited in their application range, the gradient mode offers the tremendous advantage of tuning the selectivity by eluent composition in the same separation. The gradient elution mode also offers the opportunity of easy access to sample enrichment.

This microbore HPLC system allows the scale-down of well established HPLC separations to micro dimensions. In addition, the advantages of plug flow, characteristic of electroosmotically driven systems, upon the chromatographic efficiency can be realized.

3.2. Micro-HPLC separation of oligonucleotides

A comparison of the different modes of micro-HPLC is made on the basis of the separation of oligonucleotides. With isocratic micro-HPLC using 12% acetonitrile only the 9- and 10-mers of a mixture of 1–10-mers could be separated (Fig. 2A). Using 14% acetonitrile the 10-mer oligonucleotide mixture was not retarded at all, while at 10% acetonitrile it was not eluted within 2 h.

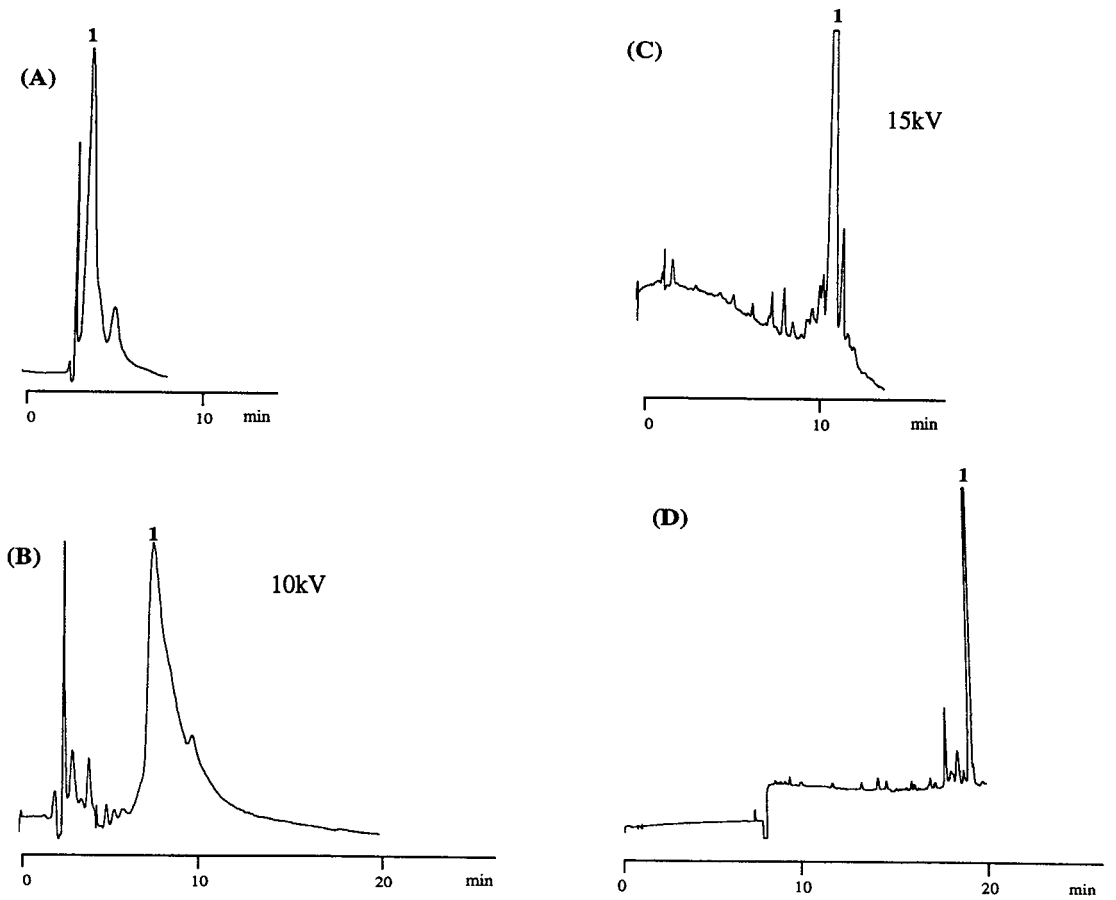

Fig. 2. Comparison of the different modes of micro-HPLC and MECC in analysis of a 10-mer oligonucleotide d(GATGCATAGG–OH) and its by-products. (A) Isocratic micro-HPLC; (B) isocratic electro-HPLC, applied voltage 10 kV; (C) gradient electro-HPLC, applied voltage 15 kV; (D) MECC. Conditions as described in the Experimental section. Peak 1 is the main synthesis product d(GATGCATAGG–OH), all other peaks are by-products.

A variation of the concentration of acetonitrile in the eluent mixture by only 4% under isocratic conditions had a great effect on the selectivity. However it did not result in a decent separation. By ways of contrast, the separation of the mixture of 1–11-mers was easily obtained in the gradient mode (Fig. 3A) thus demonstrating the advantages of the gradient system.

3.3. Electro-HPLC

Electro-HPLC is the combination of microbore HPLC with an applied voltage gradient. Depending on the electric field strength, electroosmotic flow can occur and charged analytes show electrophoretic behavior. There are several advantages arising from the combination of pressure and high voltage. The applied pressure provides stability and reproducibility of the chromatographic performance and prevents bubble formation. Therefore one of the major drawbacks of electrochromatography solely driven by electroosmotic flow, is diminished. Even if some bubbles are formed they are simply swept out thus preventing breakdown of the electric current. Columns with inner diameters up to 150

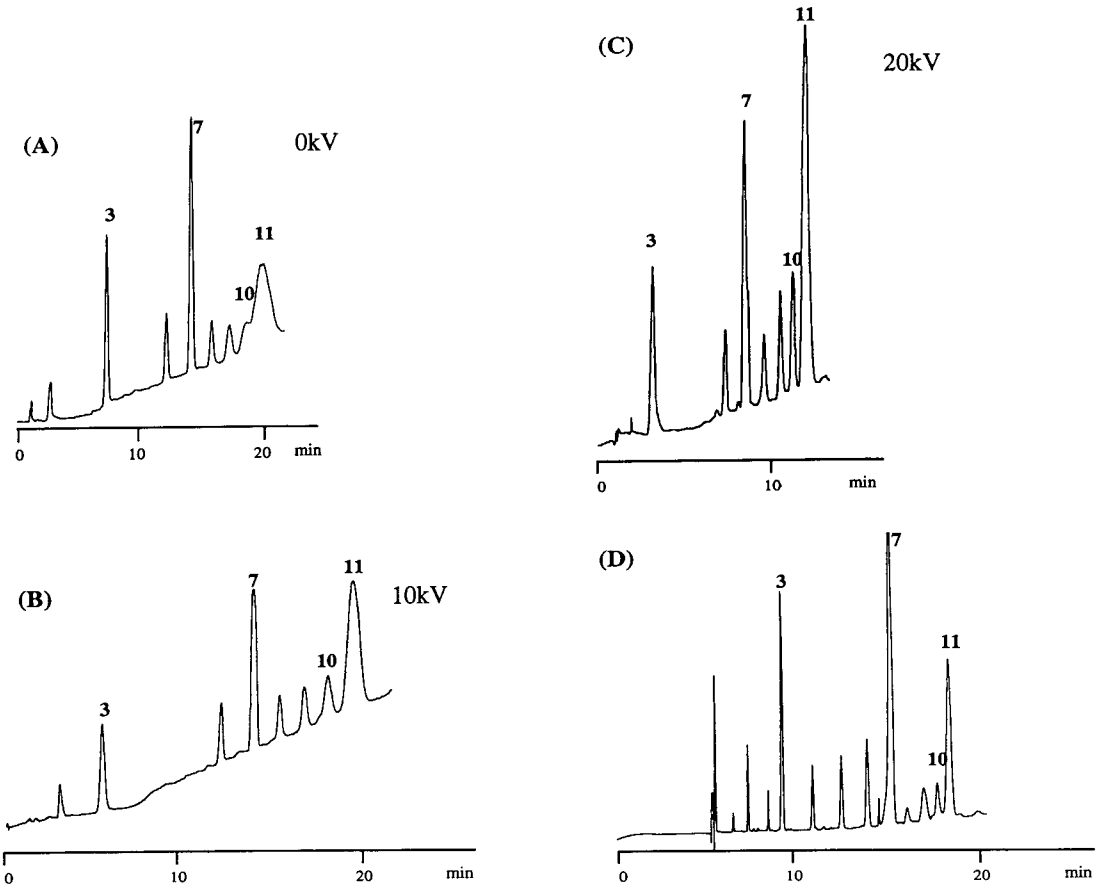

Fig. 3. Influence of applied voltage on the chromatographic separation of oligonucleotides (dC_3–dC_{11}) and comparison with MECC. (A) Gradient micro-HPLC; (B) electro-HPLC, applied voltage 10 kV; (C) electro-HPLC, applied voltage 20 kV; (D) MECC. Conditions as described in the Experimental section. Peaks 3, 7, 10 and 11 correspond to dC_3, dC_7, dC_{10} and dC_{11}, respectively.

μm can be used with a field strength of 400 V/cm in the pressurized system providing high loading capacity and detection sensitivity.

Applying a high-voltage gradient to the chromatographic column results in electroosmotic flow. Its contribution to the overall velocity of the eluent increases with the electric field strength. Using this technique analysis time is shortened and efficiency increases dramatically.

Electric field strength, direction of the voltage gradient, pH, applied pressure, eluent composition and gradient are the most important among various parameters that can be varied to optimize the performance of this highly selective and efficient separation technique.

3.4. Electro-HPLC of oligonucleotides

The higher oligonucleotide homologues in the range 1–11-mer have increasing capacity factors in reversed-phase chromatography and increasing electrophoretic mobility. The direction of the electric field can be used to retard the elution of the higher homologues in order to optimize the selectivity of the separation.

With an electric field strength of 200 V/cm

(Figs. 2B and 3B) the contribution of the electroosmotic flow to the overall velocity was still negligible compared to the pressurized flow (Figs. 2A and 3A). The isocratic electro-HPLC analysis of a 10-mer oligonucleotide mixture (Fig. 2B) revealed the improved separation due to the upstream migration of the analyte molecules resulting in longer retardation and higher selectivity in comparison to the mere HPLC separation (Fig. 2A).

The gradient electro-HPLC separations of an oligonucleotide mixture (dC_3–dC_{11}) shown in Fig. 3B and C demonstrated the optimization of efficiency and speed with increasing participation of electroosmotic flow. Applying a voltage gradient improved drastically the efficiency of the gradient microbore separation of a 10-mer oligonucleotide (Fig. 2C).

These separations were compared with MECC. As in electro-HPLC, MECC discriminates between analytes by a combination of both chromatographic and electrophoretic mechanisms [12]. Both methods show similarly excellent resolution and selectivity (Figs. 2D and 3D), above that which can be accomplished by micro-HPLC.

4. Conclusions

Electro-HPLC combines the advantages of the two basic analytical techniques, chromatography and electrophoresis. The excellent selectivity of gradient-mode chromatography adds to the high efficiency of electrophoretic separations. Using supplementary pressure stable flow conditions are readily obtained, overcoming one of the major problems of chromatography solely driven by electroosmotic flow. Electro-HPLC provides an easy access to dramatically improved HPLC separations optimized in resolution and analysis time by simple scale-down to a micro system and application of a high-voltage gradient.

Acknowledgements

The authors gratefully acknowledge the valuable technical assistance of E. Grom and H. Wohlbold, Tübingen, and the advice of M. Maier for the synthesis of oligonucleotides.

References

[1] F.J. Yang, *J. Chromatogr.*, 236 (1982) 265.
[2] R.T. Kennedy and J.W. Jorgenson, *Anal. Chem.*, 61 (1989) 1128.
[3] M. Novotny, *Anal. Chem.*, 60 (1988) 500A.
[4] N. Djordjevic, D. Stegehuis, G. Liu and F. Erni, *J. Chromatogr.*, 629 (1993) 135.
[5] J.W. Jorgenson and K.D. Lukacs, *J. Chromatogr.*, 218 (1981) 209.
[6] G.J.M. Bruin, P.P.H. Tock, J.C. Kraak and H. Poppe, *J. Chromatogr.*, 517 (1990) 557.
[7] H. Yamamoto, J. Baumann and F. Erni, *J. Chromatogr.*, 593 (1992) 313.
[8] J.H. Knox and I.H. Grant, *Chromatographia*, 32 (1991) 317.
[9] E.R. Verheij, U.R. Tjaden, W.M.A. Niessen and J. van der Greef, *J. Chromatogr.*, 554 (1991) 339.
[10] T. Tsuda and Y. Muramatsu, *J. Chromatogr.*, 515 (1990) 645.
[11] T. Tsuda, *LC·GC*, 5 (1992) 32.
[12] A.S. Cohen, S. Terabe, J.A. Smith and B.L. Karger, *Anal. Chem.*, 59 (1987) 1021.

ELSEVIER

Journal of Chromatography A, 680 (1994) 99–107

JOURNAL OF CHROMATOGRAPHY A

Microcolumn sample injection by spontaneous fluid displacement

Harvey A. Fishman[a], Richard H. Scheller[b], Richard N. Zare[a,*]

[a]*Department of Chemistry, Stanford University, Stanford, CA 94305, USA*

[b]*Howard Hughes Medical Institute, Department of Molecular and Cellular Physiology, Stanford University, Stanford, CA 94305, USA*

Abstract

The withdrawal of a capillary structure from a sample solution causes a droplet to be formed at the end of the capillary. Because of the interfacial pressure difference across the curved surface of the droplet, the droplet is driven into the entrance of the capillary, thereby causing injection of the sample. Assuming negligible sample penetration by diffusive or convective mixing, this injection is intrinsically the smallest possible for a capillary. Moreover, the injection volume can be varied by changing the shape of the capillary structure, specifically the outer diameter of the capillary. This injection method eliminates the need for external pressure differences, applied fields across the capillary, or precise timing, thus offering several advantages over conventional procedures. Studies using capillary electrophoresis as the separation procedure show that approximately 3.5 nl (66 μm I.D. capillary) sample volumes can be injected by hand with a reproducibility of $5.8 \pm 0.7\%$ R.S.D. Parameters that affect the variability of the injection are discussed.

1. Introduction

Microchannel separation techniques, such as capillary electrophoresis (CE) and open tubular liquid chromatography, are emerging as powerful methods for analyzing complex mixtures in subnanoliter volumes [1]. In CE, sample can be introduced into the column by either electrokinetic or hydrodynamic injection [2,3]. Electrokinetic injection discriminates among the sample ions based on differences in the electrophoretic mobility and complicates quantitation [4]. Hydrodynamic injection based on pressure differences between the inlet and outlet buffer reservoirs is more reproducible but requires timing among pressure valves and moving parts [3]. In both methods, a reduction in the injection length improves the separation efficiency but tends to lower the run-to-run reproducibility [5–7].

We describe a method for injection called spontaneous fluid displacement that offers several advantages over conventional injection procedures. Briefly, the injection is based on the formation of a curved meniscus (droplet) at the inlet of a capillary as it is removed from a sample solution [8]. Interfacial pressure differences across the curved surface provide the driving force to inject the sample into the column. In previous work, we identified that this spontaneous injection was largely responsible for the phenomenon called "ubiquitous injection" [8] and offered ways to minimize it. Here, we demonstrate

* Corresponding author.

0021-9673/94/$07.00
SSDI 0021-9673(94)00628-8

that spontaneous fluid displacement, previously considered an extraneous injection effect, can itself be used as a reproducible injection method. Because no externally applied pressure or electric field is required for injection, this method may simplify automated injection, and may be useful for a miniaturized CE system or for applications where electric fields or external pressure differences cannot be used. Furthermore, precise timing is unimportant because the entire injection process occurs spontaneously and is complete when the sample has penetrated into the column. This injection method makes possible smaller injection lengths for improvement in separation efficiency in CE [9]. Although the method is applicable to all microcolumn separations of liquid samples, we demonstrate its feasibility as an injection method in CE.

2. Theory

The action of removing a capillary from a solution has been shown to result in the attachment of a small droplet and its subsequent spontaneous penetration into the column [8]. By considering the mechanism involved, we can identify parameters that should affect the reproducibility of sample injected into the column. The injection mechanism can be divided into two steps: (a) liquid thread breakup to form the droplet, and (b) droplet penetration into the column by spontaneous fluid displacement (Fig. 1).

2.1. Solution breakup

When the capillary is removed from the sample solution, a thread of liquid spans from the capillary inlet surface to the bulk solution. Eventually, the thread of liquid becomes unstable toward the necking and breaks to form a droplet that adheres to the capillary inlet surface [8]. Rigorous theories to explain mechanisms for solution breakup have been developed for long cylindrical fluid bodies such as liquid jets [10–16] and liquid films supported by fibers (analogous to a liquid thread supported by a capillary column) [17]. Because the breakup process of a necking liquid thread supported by a thin fiber shares some of the physical characteristics of that of a liquid jet, considering the more general process of liquid jet instability is useful.

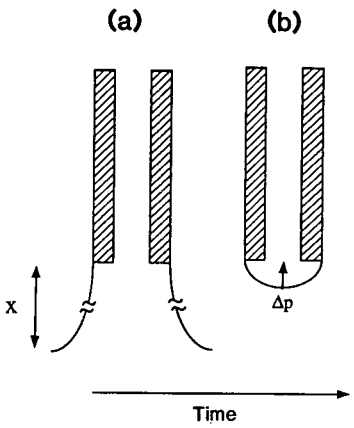

Fig. 1. Schematic depiction of an injection by spontaneous fluid displacement: (a) liquid thread breakup and (b) droplet penetration.

Liquid thread breakup can result from capillary instability [10–17] (Rayleigh instability) or extensional necking [18], and theory describing each phenomenon has been verified experimentally. Moreover, these two breakup processes do not necessarily act independently. For a given set of conditions, the mechanism that causes earlier liquid breakup will determine the droplet volume.

For a cylindrical thread of liquid, small disturbances on the free surface can generate axisymmetric deformations (surface waves) [10]. Because the total surface area is reduced, the resulting liquid structure is thermodynamically more stable than that of a cylinder. The cross-sectional radius, r, of the surface of the thread is then given by [11]

$$r = r_0 + \epsilon \cos \frac{2\pi X}{\lambda} \quad (1)$$

where r_0 is the initial radius of the liquid thread, ϵ is the amplitude of the surface wave of length λ and X is the distance measured along the axis of

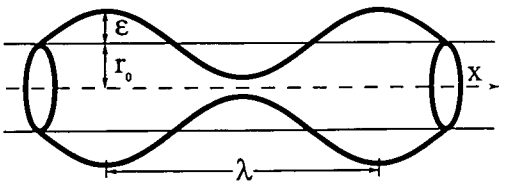

Fig. 2. Schematic illustration of the structure of a liquid jet during breakup by capillary instability. Note the sinusoidal, axisymmetric surface waves.

the thread (Fig. 2). When λ is greater than the circumference of the thread ($2\pi r$), the amplitude of the surface wave grows spontaneously until it equals the radius, r_0, which causes the thread to pinch off into droplets [10]. Based on this analysis, the drop shapes are determined by a single harmonic waveform [16]. Experiments using stroboscopic photography [16] show, however, that small satellite drops form between the main drops. A refined theoretical model based on a nonlinear analysis can be used to predict this satellite drop behavior [14,16]. As a first approximation though, the amplitude, ϵ, of the wave grows in magnitude according to the expression [11,15]:

$$\epsilon = \epsilon_0 \exp \sigma t \tag{2}$$

where σ is the characteristic growth rate and t is the time. If there are axisymmetric wavelike disturbances of equal amplitude distributed over all wavelengths at the start (white noise), the fastest growing mode (wave) will dominate the breakup and occur at its characteristic growth rate [11,15]. The growth rate for the mode of maximum disturbance has been determined in dimensional form as [15]:

$$\sigma = 0.3433 \cdot \left(\frac{\gamma}{r^3 \rho}\right)^{1/2} \tag{3}$$

where γ is the surface tension, r is the radius of the liquid thread and ρ is the density. The characteristic time for liquid thread breakup is given by $1/\sigma$.

If there is a large enough applied tensile force on the liquid thread, then solution breakup can occur by extensional necking, also called cohesive fracture [18]. During extensional necking, a cohesive fracture results when the applied tensile force exceeds some critical level of stored elastic energy. In the presence of a small tensile force on the liquid, breakup by capillary wave instability does not act independently of this cohesive mechanism; in particular, once the diameter of the thread at the node decreases sufficiently, the liquid cohesively fractures because of the tensile forces acting on it, before it separates into complete droplets.

Presently, the exact mechanism for solution breakup of the thread of liquid supported by a capillary column in this work is unknown. Nevertheless, some conclusions can be drawn from the above discussion. For a given solution, the extensional velocity of removing the capillary from the sample solution favors one mechanism over the other, and may result in a different droplet volume. The extensional velocity, v, can be expressed as:

$$v = \dot{e}x \tag{4}$$

where $\dot{e}$ is the extensional rate and x is the maximum distance spanned between the capillary inlet surface and the bulk solution before a cohesive breakup (Fig. 1a). Breakup will most likely occur by capillary instability as long as the capillary is removed from the sample solution at an extensional rate, $\dot{e}$, slower than the growth rate, σ. For a capillary with 360 μm O.D. and a 20 mM phosphate sample solution, the characteristic time for breakup is approximately 3 ms. As an approximation, breakup is more likely to occur by capillary instability if the extensional velocity of the capillary inlet does not exceed 10 cm/s.

In practice, the actual wavelength that forms on the liquid thread is affected by background noise [11] as well as satellite drop formation [16]. In a typical laboratory, noises (from pump sources or other vibrations) can create surface disturbances at any wavelength and prevent breakup at the mode of maximum instability. To overcome random noise and achieve better wavelength control, audio frequency disturbances can be imposed on the thread and tuned

to the mode of maximum instability [11]. For a liquid jet, when experimental parameters are constant and the amplitude of the applied disturbance is controlled using audio modulations, solution breakup can be made reproducible to better than 10% [11]. In fact, this high level of regularity of droplet formation has been used in ink-jet printing [16].

Still other factors may contribute to droplet formation in liquid structures supported by a fiber (or capillary). For instance, refinements in liquid instability theory that take into account experimental differences between breakup in a liquid jet and breakup in a liquid thread that is supported by a fiber have been developed [17]. Because droplet formation may be affected by any factor that distorts the structure of the liquid thread, reproducibility of this structure is expected to require care. Parameters that may be important include how the capillary is cleaved (because overall surface morphology affects fluid attachment), the wetting properties of the surface surrounding the inlet (which affects the contact angle of fluid attachment), the position and angle of the capillary upon removal, and the radius of curvature of the sample solution into which the capillary is inserted. The precise control of these parameters would therefore be expected to improve reproducibility.

2.2. Spontaneous fluid displacement

Injection of the droplet results from an interfacial pressure difference formed across the curved droplet surface (meniscus) [8]. This pressure difference is large enough to support a 4 cm × 50 μm column of buffer. If similar droplets are formed, then reproducible injection should occur if the droplet is localized to the tip of the capillary, and sample is not lost from spreading or sticking to the surface or from effects of solvent evaporation [8]. Several key factors that may affect reproducibility of droplet volume and shape include surface tension of the sample solution, surface wettability of the inlet end of the capillary, and vapor pressure surrounding the capillary [8].

The penetration kinetics of the injection are characterized by an initial high penetration velocity, followed by a leveling off until the droplet has completely entered the column [8]. Allowing the droplet to completely penetrate causes less dependence on precise timing, which should afford high run-to-run reproducibility. For a given capillary structure, penetration kinetics are governed by the surface tension of the sample solution. Thus, two different samples may have slightly different penetration kinetics. In each case, however, equivalent injection volumes will result from waiting until the sample droplet has completely penetrated into the column. More importantly, differences in surface tension between samples will have a greater differentiating affect on losses from surface spreading or from non-uniformities in droplet formation during solution breakage.

3. Experimental

3.1. Chemicals and reagents

All solutions were prepared from a Millipore water-filter system (Milli-Q Plus/UV, Milli-RO 6 Plus; Waters, Bedford, MA, USA). For the CE runs, a 20 m*M* phosphate buffer, pH 8.7 (Mallinckrodt, San Francisco, CA, USA), was filtered through 0.2-μm pore size syringe filters and used for all studies. Imaging studies were carried out using a 0.4 m*M* 2′,7′-dichlorofluorescein solution (Kodak, Rochester, NY, USA) dissolved in 15 m*M*, pH 8.9 phosphate buffer. Stock solutions of N^{ϵ}-dansyl-L-lysine, N^{α}-dansyl-L-tryptophan, and dansyl-L-alanine, (Sigma, St. Louis, MO, USA) prepared in the phosphate running buffer were stored in the refrigerator and serially diluted as needed.

3.2. Capillary treatments

The inlet end of a fused-silica capillary column (52 μm I.D. × 131 μm O.D., 50 μm I.D. × 345 μm O.D., 66 μm I.D. × 352 μm O.D.) (Polymicro Technologies, Phoenix, AZ, USA) was cleaved by first scoring the polyimide coating with a ceramic cleaving square (Polymicro Tech-

nologies) and then carefully bending the capillary to fracture it. With care, this procedure consistently produced a nearly flat surface (as observed under a stereomicroscope) with an angle of $87 \pm 3°$. A 5-mm section of the polyimide coating at the inlet end was removed with a Bunsen burner flame. All capillaries were preconditioned with 0.1 *M* sodium hydroxide (Mallinckrodt), and buffer was then electrophoresed through the column for 1 h. For some studies, the outer surface of the capillary was silanized by holding an air-filled column in a solution of dimethyldichlorosilane in toluene (silanization solution from Supelco, Bellefonte, PA, USA) for 40 min. Afterward, the column was purged with nitrogen and air dried for several minutes. The outer diameter of some capillaries was chemically etched with 0.1 *M* hydrofluoric acid (Sigma) for 40 min. To maintain a constant inner diameter, the other end of the column was attached to a pressure-regulated nitrogen tank, thereby creating a constant flow of nitrogen through the column to prevent acid from entering the inside of the column. The capillary was rinsed with water before use.

To maintain uniform wetting on the outside surface of the capillary (i.e., to reproduce the surface conditions), excess water-droplet formation on the outside surface was minimized. For the charge-coupled device (CCD) imaging experiments, excess water formation could be reduced by slowly withdrawing the analyte solution from contact with the capillary. Only runs with no noticeable surface spreading after sample contact were used in the CCD imaging studies. Using video imaging of the injection, we found that silanating the outside walls of the capillary inlet helped prevent both excess water drop formation and surface spreading onto the sides upon capillary removal. We silanated the outer walls of the capillary inlet as a preventative measure for the CE experiments.

3.3. CE detection system

Separations were performed using a laboratory-built CE system with an absorbance detector (Isco CV4, Lincoln, NE, USA). The detector wavelength was set at 340 nm with a time constant of 0.2 s. The voltage control is described elsewhere [19]. The inlet of the capillary was manually transferred from the sample solution (contained in a 1-ml vial) to the inlet reservoir. The capillary was in contact with the sample solution no longer than 5 s. Timing for the transfer was accomplished using either a stopwatch or an alarm timer. During the injection, the sample solution was held approximately 5 mm below the level of the outlet reservoir to prevent inadvertent hydrodynamic injection. Similarly, to prevent loss of the sample from inadvertent hydrodynamic outflow when the capillary was reinserted into the inlet buffer reservoir, we held the outlet reservoir approximately 5 mm below the inlet. A delay of approximately 10 s occurred between reinserting the capillary into the inlet vial and applying the voltage across the capillary. Data were collected with a 486 computer (Adisys, Santa Clara, CA, USA) using Lab Calc data-acquisition software and a Chrom-1AT data acquisition board (Galactics, Salem, NH, USA). Peak areas and heights were determined using Lab Calc.

3.4. Imaging system

Spontaneous fluid displacement injections were quantitated using a fluorescence imaging system described elsewhere [8]. Briefly, the inlet end of a fused-silica capillary column was fixed in position and imaged by a stereomicroscope onto the focal plane of a liquid-nitrogen-cooled (-126°C), scientific-grade CCD camera equipped with a 512×512 CCD chip (PM512, Photometrics).

3.5. CCD image processing

Image dimensions were estimated by using the premeasured outer diameter of the capillary as an internal calibration. Images of the capillaries had similar cross-sectional profiles. From these images we could estimate the position of the edge of the outer capillary wall with an uncertainty of 3 pixels, thus making the absolute internal calibration distances accurate to within 6 pixels (final injection lengths ranged from 50 to

165 pixels). The front end of the capillary was identified by a bright spot that appeared at the front end of all capillaries before and after the fluorescein solution entered the column. The fluorescence response from the channel of the capillary filled with a homogeneous solution of fluorescein was roughly uniform and varied linearly with the concentrations used in these studies.

To determine spontaneous injection lengths, a plot of the fluorescence intensity along the length of the capillary channel was obtained. First, pixels across the width of the channel were averaged. This averaging resulted in a single intensity value for each point along the length of the column, which yields a one-dimensional image slice along the capillary. These slices were converted to one-dimensional text file arrays and then analyzed on a Macintosh IIci using programs written in Igor (WaveMetrics, Lake Oswego, OR, USA). Plots of the image slice showed the concentration profile along the length of the injection plug. For clarity of presentation, the bright spot present in all of these image slices was removed.

4. Results and discussion

4.1. Injection volume

Spontaneous fluid displacement establishes the feasibility of successively injecting small, fixed volumes in a reproducible manner. A particular capillary inlet has an inherent maximum injection volume that is dependent on its physical characteristics (for, e.g., its morphology, size, etc.). Within this maximum value, the injection volume can be varied in several ways. One method is to reinsert the capillary into the inlet vial at different times during the penetration process, thus placing a larger demand on timing but providing more flexibility for injection. A potentially more reproducible way to vary volume is illustrated in Fig. 3. By changing the outer diameter of the capillary, the amount of droplet formed can be altered.

Fig. 4 shows a comparison of the longitudinal

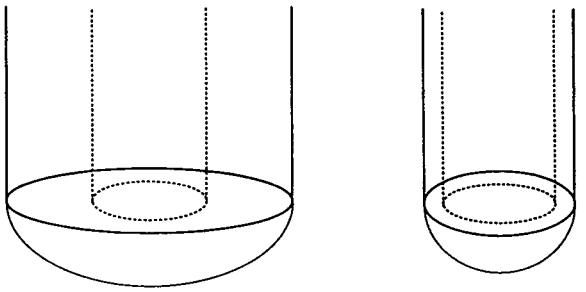

Fig. 3. Schematic diagram of droplet formation at the inlet end of two capillaries with different outer diameters but the same inner diameter.

fluorescence image "slice" of injections from capillaries with different outer diameters but approximately the same inner diameter. The intensity (concentration) profiles along the length of 345 μm O.D. × 50 μm I.D. and 131 μm O.D. × 52 μm I.D. capillaries are shown in Fig. 4a and b, respectively. The capillary inlet was surrounded by a saturated vapor atmosphere in both cases. The complete injection for the thin-

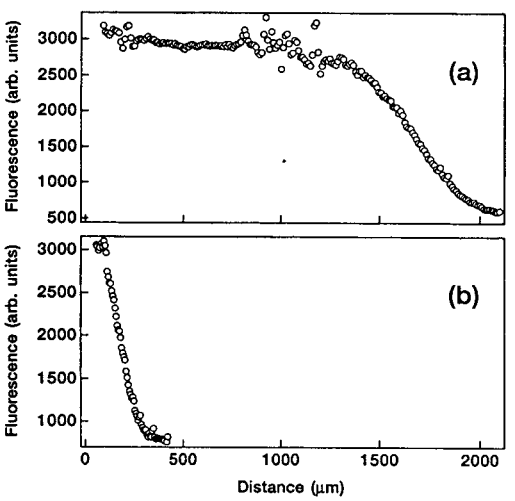

Fig. 4. Fluorescence intensity profiles along the length of an injection by spontaneous fluid displacement. The capillary is surrounded by a vapor-saturated environment. Shown are injections from (a) 50 μm I.D. × 345 μm O.D. capillary and (b) 52 μm I.D. × 131 μm O.D. capillary. The sample consisted of 0.4 m*M* 2',7'-dichlorofluorescein dissolved in 15 m*M* pH 8.9 phosphate buffer; the column length was ca. 58 cm for each case and was filled with 15 m*M* pH 8.9 phosphate buffer.

walled capillary occurred within approximately 5 s after the capillary was removed from the sample solution but required approximately 70 s for the thick-walled capillary. As the O.D. of the capillary becomes smaller, so does the radius of curvature of the resulting droplet, which causes the penetration velocity to increase [8]. For a smaller injection, sample entry by diffusive or convective mixing adds a larger component of extraneous injection error [8]. Varying the size between larger-O.D. capillaries is therefore important to minimize error from these mixing processes.

Shown in Fig. 5 are electropherograms that compare spontaneous fluid displacement injection that results from varying the O.D. of a single capillary column (66 μm I.D.). Fig. 5 shows a separation of three dansylated amino acids after a 10-s delay in transfer (between removing the capillary from the sample to inlet reservoir) for an untreated 352 μm O.D. capillary (Fig. 5a), and then for the same capillary whose O.D. was reduced by etching the capillary in hydrofluoric acid for 40 min (Fig. 5b). Although etching the capillary was used here to demonstrate the concept of varying the injection volume by changing the outer diameter, it did not result in a completely uniform annular surface region, and better methods for manipulating the O.D. should be used.

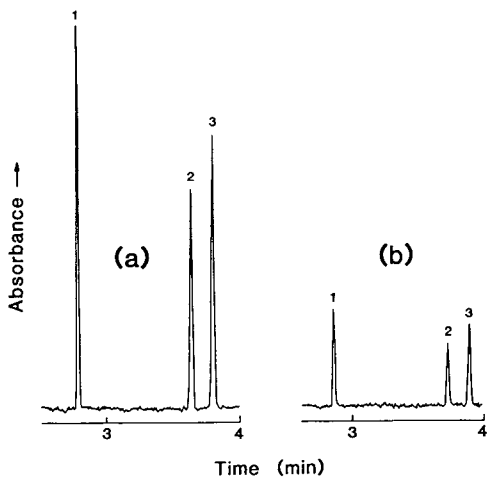

Fig. 5. Electropherograms that demonstrate different injection amounts as a result of varying the outer diameter of a capillary column. Shown are injections from a 66 μm I.D. × 345 μm O.D. capillary (a) untreated and (b) etched in hydrofluoric acid (0.1 *M*) for 40 min. The delay time between transferring the capillary inlet from the sample solution and reinserting it into the inlet reservoir was 15 s. The capillary was transferred in an ambient atmosphere. Each electropherogram shows a separation of ca. 0.5 m*M* each of (1) dansyl-lysine, (2) dansyl-tryptophan and (3) dansyl-alanine. The separation conditions are: capillary length, 60 cm (27 cm to detector); buffer, 20 m*M* phosphate, pH 8.7; voltage, 20 kV.

4.2. Reproducibility

Table 1 shows an initial demonstration of the variability for an injection volume of approximately 3.5 nl (66 μm I.D. × 352 μm O.D. capillary) by spontaneous fluid displacement. Reproducibility in peak areas and peak heights was 5.8 ± .7% R.S.D. ($n = 11$) for manual injections using a 15-s injection transfer time with the capillary surrounded by an ambient atmosphere. It is difficult to make valid comparisons between different published reports on injection reproducibility because of significant variations in the components and run conditions used. It is useful, however, to mention a range of the best reported values. According to several studies on injection reproducibility [3], variability in peak area ranged from 1–3% R.S.D. for hydrodynamic injection using an automated instrument and from 4–11% R.S.D. using manual injection [7,20]. Moreover, a comparatively higher variability occurred when using electrokinetic injection [3] or when injecting smaller volumes [7,20]. Given that the small injections in this study were performed manually, automated control is expected to significantly reduce the spread. Automated injection would be particularly important for reproducing the extensional necking velocity.

5. Conclusions

We have described an injection method based on spontaneous fluid displacement. Although the injections were made by hand, the reproducibility was approximately 6 ± 1% R.S.D. Improve-

Table 1
Comparison of peak area and peak height reproducibility for spontaneous fluid displacement injection of three dansylated amino acids

Run	Lys		Trp		Ala	
	Area[a]	Height[a]	Area	Height	Area	Height
1	1.89	103.00	2.11	71.21	2.21	73.00
2	1.87	98.76	2.13	68.45	2.29	76.41
3	1.97	102.99	2.17	70.72	2.28	75.39
4	2.09	112.36	2.29	76.43	2.37	78.27
5	1.91	102.63	2.10	70.79	2.20	73.15
6	1.97	107.06	2.18	74.38	2.30	76.16
7	2.08	111.25	2.29	74.63	2.44	80.39
8	1.73	95.20	1.99	64.81	2.10	70.98
9	1.94	108.57	2.22	71.78	2.26	76.59
10	2.19	115.05	2.42	77.06	2.57	83.54
11	2.17	117.44	2.35	77.72	2.41	80.40
Mean	1.98	106.76	2.20	72.54	2.31	76.75
S.D.	0.138	6.93	0.125	3.94	0.130	3.71
R.S.D. (%)	6.98	6.49	5.66	5.43	5.61	4.83

Lys = Dansylated lysine; Trp = dansylated tryptophan; Ala = dansylated alanine.
[a] Arbitrary units.

ments are suggested for lowering the variability. Specifically, we expect that reproducibility will be improved by (1) automating the injection, (2) providing a controlled atmosphere surrounding the capillary entrance, (3) providing a flat, uniform cut at the inlet end of the capillary, (4) isolating the injection process from external vibrations, and (5) preventing the droplet from spreading onto the outside walls of the capillary.

This injection method should be applicable to any microcolumn separation technology and does not require the use of an electric field or application of a pressure difference to the buffer reservoirs. Because some limits exist to the flexibility of injection volumes, this method would be complementary to present forms of injection for more conventional uses of CE. By definition, whenever a capillary is removed from a sample solution into the air, spontaneous fluid displacement represents the smallest injection for a capillary structure (assuming negligible sample penetration by diffusion or convection). Injection by spontaneous fluid displacement could therefore be extremely useful in applications for which small, reproducible injections are needed, such as calibration and sampling for single-cell analysis. Moreover, for specialized injections, such as sampling human tear film from the eye [21], or for a miniaturized, portable CE system [22,23], injection by spontaneous fluid displacement may be distinctly advantageous over injection by other means.

Acknowledgements

We thank Professor George Homsy, Department of Chemical Engineering, Stanford University, for numerous helpful discussions on the theory of liquid drop formation. We also thank Dr. Shuming Nie, Rajeev Dadoo, and Jason B. Shear for many helpful comments on the manuscript. H.A.F. is a W.R. Grace Foundation fellow. This work was supported by Beckman Instruments, Inc., and the National Institutes of Mental Health (Grant No. NIH 5RO1 MH45423-03).

References

[1] J.W. Jorgenson and K.D. Lukacs, *Science*, 222 (1983) 266.
[2] S.F.Y. Li, *Capillary Electrophoresis*, Elsevier, London, 1992.
[3] R. Weinberger, *Practical Capillary Electrophoresis*, Academic Press, Boston, MA, 1993.
[4] X. Huang, M. Gordon and R.N. Zare, *Anal. Chem.*, 60 (1988) 375.
[5] H.E. Schwartz, M. Melera and R.G. Brownlee, *J. Chromatogr.*, 480 (1989) 129.
[6] E.V. Dose and G. Guiochon, *Anal. Chem.*, 64 (1992) 123.
[7] D.J. Rose, Jr. and J.W. Jorgenson, *Anal. Chem.*, 60 (1988) 642.
[8] H.A. Fishman, N.M. Amudi, T.T. Lee, R.H. Scheller and R.N. Zare, *Anal. Chem.*, 66 (1994) 2318.
[9] X. Huang, W.F. Coleman and R.N. Zare, *J. Chromatogr.*, 480 (1989) 95.
[10] L. Rayleigh, *Proc. London Math. Soc.*, 10 (1878) 4.
[11] R.J. Donnelly and W. Glaberson, *Proc. Roy. Soc. A*, 290 (1966) 547.
[12] F.D. Rumscheidt and S.G. Mason, *J. Colloid Sci.*, 17 (1962) 260.
[13] S.L. Goren, *J. Fluid Mech.*, 12 (1962) 309.
[14] S.L. Goren, *J. Colloid Sci.*, 19 (1964) 81.
[15] P.G. Drazin and W.H. Reid, *Hydrodynamic Stability*, Cambridge University Press, Cambridge, 1981, pp. 1–27.
[16] D.B. Bogy, *Ann. Rev. Fluid Mech.*, 11 (1979) 207.
[17] B.J. Carroll and J. Lucassen, *J. Chem. Soc., Faraday Trans. I*, 70 (1974) 1228.
[18] A. Ziabicki and R. Takserman-Krozer, *Roczniki Chem.*, 37, (1963) 1511.
[19] J.V. Sweedler, J.B. Shear, H.A. Fishman, R.N. Zare and R.H. Scheller, *Anal. Chem.*, 63 (1991) 496.
[20] S. Honda, S. Iwase and S. Fujiwara, *J. Chromatogr.*, 404 (1987) 313.
[21] R. Dadoo, R.N. Zare, S.T. Lin and R.B. Mandell, presented at the *1992 Pittsburgh Conference on Analytical Chemistry and Applied Spectroscopy, New Orleans, LA, 9–12 March 1992*, abstract 301.
[22] D. J, Harrison, K. Fluri, K. Seiler, Z. Fan, C.S. Effenhauser and A. Manz, *Science*, 261 (1993) 895.
[23] C.S. Effenhauser, A. Manz and H.M. Widmer, *Anal. Chem.*, 65 (1993) 2637.

ELSEVIER

Journal of Chromatography A, 680 (1994) 109–116

JOURNAL OF CHROMATOGRAPHY A

Extended path length post-column flow cell for UV–visible absorbance detection in capillary electrophoresis

Suhyeon Kim, Weonseop Kim, Jong Hoon Hahn*

Center for Biofunctional Molecules, Department of Chemistry, Pohang University of Science and Technology, San 31 Hyoja Dong, Pohang 790–784, South Korea

Abstract

A new type of post-column flow cell with extended optical path length has been developed to improve sensitivity of UV–visible absorbance detection for capillary electrophoresis. In this flow cell, the outlet of the capillary column is connected vertically to the middle of a 3-mm microchannel. Auxiliary flows are employed to flush substances eluted from the outlets of the microchannel. The optical path length is the full length of the microchannel. An 8-fold signal-to-noise ratio improvement over on-column detection has been demonstrated. However, the post-column flow cell suffered 44% loss in resolution. A limit of detection of $3.2 \cdot 10^{-7}$ M has been obtained for fluorescein isothiocyanate.

1. Introduction

Capillary electrophoresis (CE) is an elegant separation technique for the analysis of a wide variety of complex mixtures [1–6]. Typically, CE uses fused-silica capillary columns with inner diameters of 25–100 μm. The narrow diameter columns provide CE with several advantages such as short analysis times, remarkably high separation efficiency, and minimal sample volume requirements. However, in the case of conventional on-column UV–visible absorbance detection, the short optical path length available in such small capillaries limits the detection sensitivity and typically results in limits of detection (LOD) of 10^{-5}–10^{-6} M.

Recently, several interesting methods have been employed to increase the path length for UV–visible absorbance detection in CE [7–12]. Tsuda et al. [9] investigated the use of transparent rectangular borosilicate glass capillaries as an alternative to cylindrical capillaries. Dimensions of the rectangular capillaries ranged from 16 μm × 195 μm to 50 μm × 1000 μm. Detection across the long cross-sectional axis provided up to 15-fold increase in sensitivity. Xi and Yeung [10] devised a means of axially illuminating the full length of the capillary, and obtained a 7-fold increase in sensitivity for a 50-μm I.D. capillary and 3-mm injection plugs. Chervet et al. [11] extended the short optical path lengths in microcapillaries by bending the capillary into a Z shape and illuminating through the bend. A 6-fold improvement in signal-to-noise ratio (S/N) has been demonstrated with Z-shaped flow cells where light is transmitted through a 3-mm bend. The sensitivity of the Z-shaped flow cells has been greatly enhanced by optimizing light throughput in a 3-mm capillary section using a quartz ball lens [12].

* Corresponding author.

0021-9673/94/$07.00
SSDI 0021-9673(94)00679-2

Moring et al. [8] analyzed ray traces of light in the capillary bend of Z-shaped flow cells. This work has shown that the curved structure of the Z-cells requires focusing incident light with a special optics such as a quartz ball lens and offsetting the lens from capillary axis to maximize the light path length and the total light transmission through a bend. Moreover, the maximum effective path length for light transmitted through the bend was found to be much shorter than the length of the optical segment of a Z-cell. For example, the effective path length for a 75-μm capillary with outer diameter of 280 μm was at best 1.33 mm corresponding to 44% of the length of the optical segment (3 mm) of the cell. Therefore, avoiding any bent parts along the capillary's longitudinal axis in the optical segment of flow cells with extended optical path length is a logical extention of the Z-shaped cells for enhancing further the sensitivity of UV–visible absorbance detection in CE.

In this paper, we propose a new method of increasing path length for UV–visible absorbance detection in CE. Fig. 1 schematically shows the proposed extended path length flow cell with a post-column configuration. At the outlet of the capillary column, the eluted solution is splitted into two flows that travel in opposite directions through the microchannel positioned vertically to the column. The microchannel is connected to the column outlet at the middle of the channel. Accumulation of eluted substances at both outlets of the channel is prevented by continuously flushing the outlets with a buffer solution. The optical segment of the proposed flow cell is the straight microchannel. Illuminating the microchannel with light collimated to the direction of the longitudinal axis of the channel allows us to utilize the full length of the channel as the optical path length.

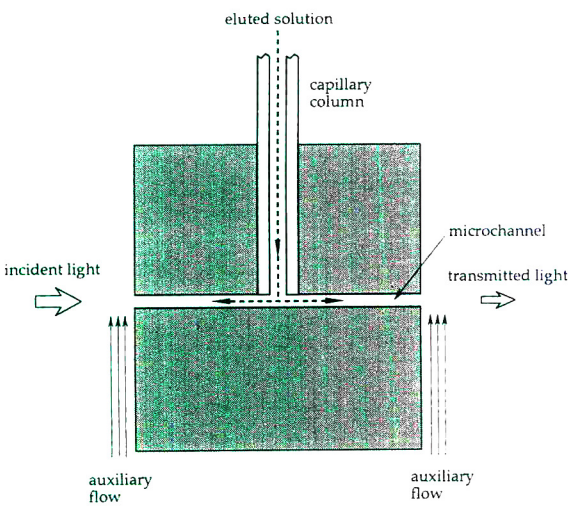

Fig. 1. Schematic of the post-column microchannel flow cell.

In addition to the extended optical path length, our post-column microchannel flow cells enjoy several other potential advantages for optical detection in CE. First, in the case of extended path length on-column flow cells, such as Z-shaped ones [11,12], the bent configuration requires special optical couplings to optimize light throughput [12]. However, the unbent configuration of the post-column flow cells can make the optical coupling easier. Secondly, if the proposed post-column flow cells are provided with an additional influent branch channel for a derivatizing reagent around the outlet of the capillary column, post-column derivatization and sensitive detection can be accomplished at the same time. Finally, because actual shapes and materials of the flow cells can be changed, while keeping essential features for the extended path length post-column detection, the flow cells can be adopted to nearly all kinds of coherent or incoherent optical detection techniques (e.g., absorption, fluorescence and thermo-optical absorption). The purpose of this paper is to demonstrate the feasibility of the extended path length post-column flow cells for UV–visible absorbance detection in CE.

2. Experimental

2.1. Reagents

All chemicals were of analytical-reagent grade and used without further purification. Deionized water was prepared with a Mega-Pure system (Barnstead, Dubuque, IA, USA). Dansyl-amino acids, fluorescein isothiocyanate (FITC) and all

inorganic chemicals were purchased from Sigma (St. Louis, MO, USA). Buffer solutions were filtered through 0.2-μm membrane filters (cellulose nitrate; Whatman, Maidstone, UK) and degassed by sonication for 5 min just before using. Samples for CE analysis were prepared by dissolving pure compounds in the buffer used for running electrolyte solution.

2.2. Post-column microchannel flow cell

The flow cell consists of two parts (Fig. 2a). One is a cylindrical rod-shaped (27 mm × 3 mm diameter) structure. Inside the structure, there is an "upside-down T" shaped channel formed by connection of the end part of the capillary column and the post-column microchannel. The column capillary extends from this assembled structure to the buffer reservoir where (+) high voltage is applied. The other is assembled with a square quartz tubing (20 mm × 10 mm square I.D.; Wale Apparatus, Hellertown, PA, USA) and two square stainless-steel plates. The bottom plate has an inlet for the buffer solution for flushing substances eluted from the microchannel. At the center of the cover plate, there is a 3-mm diameter hole into which the rod structure fits. The cover plate has two additional small holes; one is for the outlet of waste solution and the other is for the mount of a Pt electrode used to hold the cell at ground potential. The counter-gravity flow of the flushing buffer helps bubbles escape from the cell. The flow cell was constructed by putting all pieces together using various kinds of epoxy resins. Great care was taken of making the microchannel aligned vertically to a pair of opposite faces of the square quartz tubing.

Fig. 2b anatomically shows the cylindrical rod-shaped assembly that also consists of two parts. On the top of the lower part, the microchannel is formed along the cross-sectional axis of a borosilicate glass rod (10 mm × 3 mm diameter). The body of the channel is a piece of bisected fused-silica capillary. The procedure of making the channel is as follows. First, a groove of 0.4 mm width and 2 mm depth is made on the top surface of the rod using a diamond wafering blade. A 3-mm long fused-silica capillary (100 μm I.D. and 375 μm O.D.; Polymicro Technologies, Phoenix, AZ, USA) is placed in the groove and fixed with epoxy resin so that the

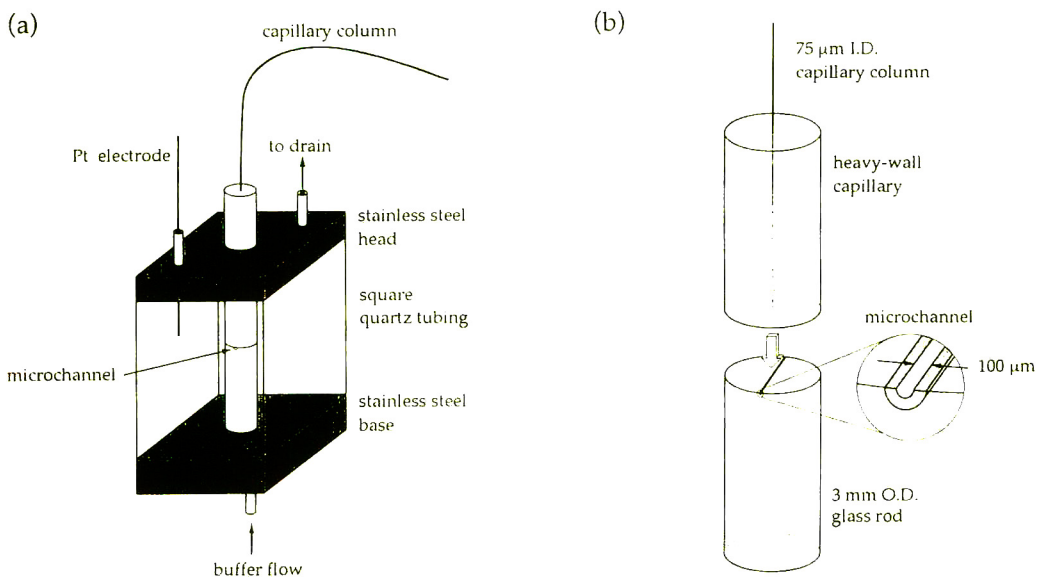

Fig. 2. (a) Whole construction of the post-column flow cell. (b) Anatomic view of the cylindrical rod-shaped assembly in the flow cell.

piece can be positioned vertically to the longitudinal axis of the rod. Finally, the top of the rod is finely ground until half of the cross section of the capillary is remained evenly along the length of the piece.

In the upper part of the cylindrical rod-shaped assembly, the end part of the capillary column (75 μm I.D. and 375 μm O.D.; Polymicro Technologies) is inserted through a piece of heavy-wall capillary (17 mm length, 0.4 mm I.D. and 3 mm O.D.; Wale Apparatus). The capillary column is fixed with epoxy resin and the bottom surface of the upper part is ground to form a fine and flat surface.

The construction of the assembly is completed by putting the two parts together using epoxy resin so that the cross-sectional center of the capillary column can sit on the middle of the longitudinal axis of the bisected capillary. Glass rod surfaces around the outlets of the microchannel are painted with an optically opaque epoxy (Epo-Tek 320; Epoxy Technology, Billerica, MA, USA), which ensures that the only light passing through the channel is detected by a light sensor.

2.3. CE apparatus with the post-column detection scheme

Fig. 3 represents a schematic of the homemade CE setup with the post-column UV–visible absorbance detector. A set of a deuterium (D_2) lamp and a monochromator built in the detector component (SP8480XR; Spectra-Physics, San Jose, CA, USA) of a commercial high-performance liquid chromatograph has been utilized as the light source of our CE system. A monochromatic light from the source is focused onto one end of the microchannel using a quartz plano-convex lens of 15.5 mm focal length. Temporal changes of the transmitted light intensity are transduced into corresponding voltage signals by a photomultiplier tube (PMT) module (HC120-01; Hamamatsu, Bridgewater, NJ, USA). The output signal from the PMT module is converted to the corresponding current signal via a 50-kΩ resistor. A current amplifier (428; Keithley, Cleveland, OH, USA) converts the current signal to an amplified voltage signal. The amplified output signal is then digitized by a 14-bit analog-to-digital (A/D) converter, and the

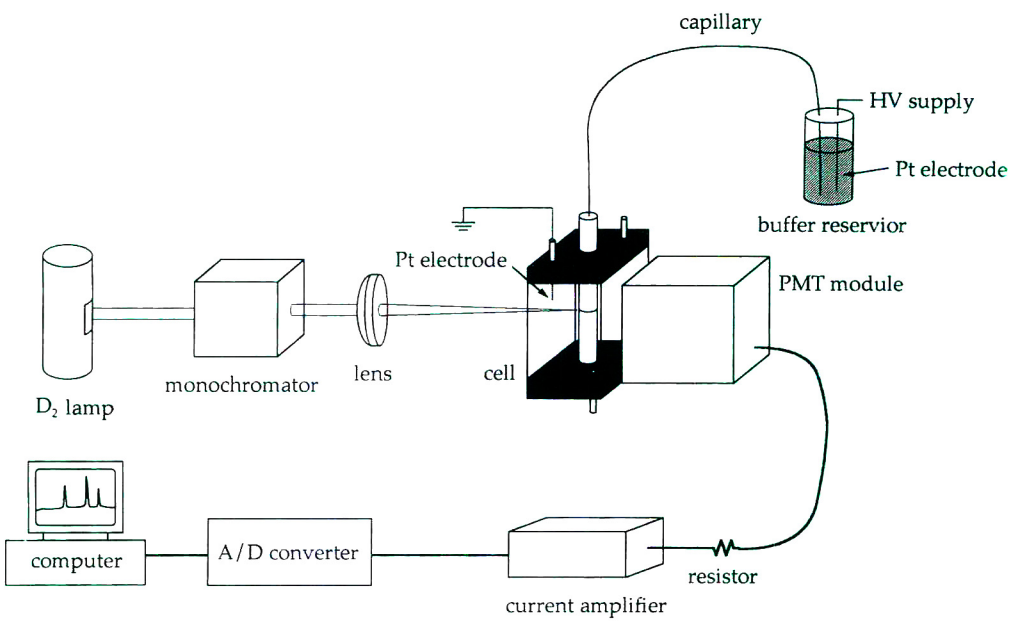

Fig. 3. CE setup with a UV–visible absorbance detector employing the post-column flow cell.

digitized signal is stored and processed using an IBM XT-compatible computer. Electropherograms are smoothed using the 7-point Savitzky-Golay algorithm before plotting them out.

A high-voltage power supply (EH60R1.5CT10; Glassman, Whitehouse Station, NJ, USA) is used to apply (+) high voltage across the fused-silica capillary column of 40 cm length. The buffer solution for auxiliary flows is fed into the flow cell by a HPLC pump (Spectroflow 4000; Kratos Analytical, Lancashire, UK).

2.4. CE apparatus with the on-column detection scheme

The CE setup built for the on-column UV absorbance detection is essentially the same as that for the post-column detection except for some differences. A neutral density (N.D.) filter of 1.0 N.D. (NDQ-100-1.00; CVI Laser, Albuquerque, NM, USA) is placed between the light source and the focusing lens. A 0.5-mm pinhole is used to confirm the dimension of the incident light on the detection window that is 40 cm from the injection end of the capillary column.

2.5. Capillary electrophoresis

The capillary columns were pretreated with 0.1 *M* sodium hydroxide solution, deionized water and running buffer solution in sequence. Each solution was pumped into the capillary for 3 min at a flow-rate of 15 μl/min using a syringe pump (Syringe Infusion Pump 22; Harvard Apparatus, South Natick, MA, USA). After each CE run, the column was rinsed with running buffer solution for 3 min.

Sample injection was accomplished manually by siphoning with a height of 20 cm for 10 s. To carry out CE separation, a high voltage was applied to the injection end of the capillary so that average electric field strength would be 300 V/cm. In the post-column detection method, auxiliary flow was maintained at a flow-rate of 0.7 ml/min after the high voltage was applied to the capillary for each CE run.

3. Results and discussion

According to Beer's law, the magnitude of absorbance for the same solution in absorbance detection is proportional to the optical path length of detection cell. In the case of the conventional on-column detection in CE, the effective path length of a parallel beam of light through a capillary of diameter d is equal to $\pi d/4$, which is due to the cylindrical cross section of capillaries [13]. However, the detection scheme using the post-column microchannel flow cell can utilize the full length of the microchannel as the optical path length.

Ideally, performance evaluation of the post-column microchannel flow cell should be carried out on commercial CE systems. Since no commercial CE instruments, however, were available to us, a simple homemade CE system was built for the evaluation. The system is easily interchangeable between on-column and post-column detection schemes without any changes in instrument except for the cells. Although the system has not performed as good as commercial ones, comparison of the post-column detection method with the on-column one gave us some qualitative information on the performance of the post-column flow cell.

Fig. 4 shows two electropherograms of FITC, which were obtained using the on-column and the post-column detection systems, respectively. The split peak top in Fig. 4b was attributed to superposition of noise signals on the FITC band. Since the I.D. of capillaries used was 75 μm and the length of the microchannel was 3 mm, the theoretical limit of sensitivity gain of the post-column detection over the on-column one would be 50. LODs (at S/N = 2) of FITC in the on-column and the post-column detection methods were $2.6 \cdot 10^{-6}$ *M* and $3.2 \cdot 10^{-7}$ *M*, respectively. Therefore, only an 8-fold enhancement of S/N was achieved by using the post-column microchannel flow cell.

As shown in the enlarged circle of Fig. 2b, the upper flat surface of the microchannel is a part of the bottom surface of the heavy-wall capillary. Because the refractive index of the heavy wall is greater than that of the buffer in the channel,

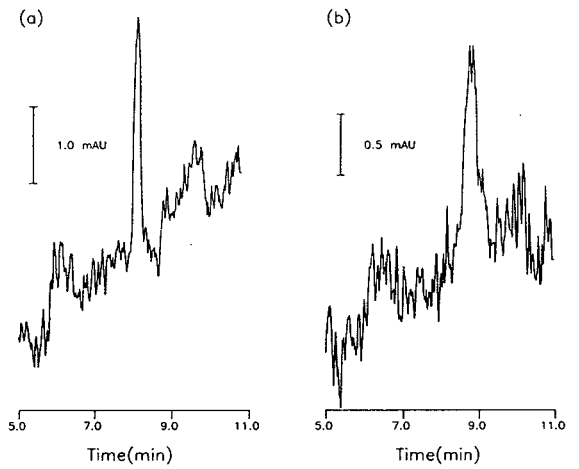

Fig. 4. Electropherograms of FITC. Capillary 75 μm I.D.; buffer, 10 mM phosphate (pH 6.9); sample injection, 10 s at 20 cm height difference; detection wavelength, 488 nm. (a) On-column detection system; sample concentration, $5.5 \cdot 10^{-6}$ M; separation column, 60 cm total length (40 cm to detector); applied voltage, 18 kV (300 V/cm). (b) Post-column detection system; sample concentration, $5.5 \cdot 10^{-7}$ M; separation column, 40 cm length; applied voltage, 12 kV (300 V/cm).

rays of light which are not parallel to the longitudinal axis of the channel can not experience any total internal reflections on the upper surface of the channel. Therefore if incident light is not collimated well, only a small portion of it can be transmitted through the channel. In consequence, probably, high background noise caused by the low light transmission through the microchannel resulted in the poor S/N gain obtained with the post-column design. Therefore a more intense light source and collimation of the light into a small-diameter beam are required to approach the theoretical limit of sensitivity of the post-column detection method. Because the post-column flow cells need collimated incident light to obtain greater sensitivities, coherent optical techniques, such as laser-induced fluorescence, would be better detection methods to which the cells can be applied.

The number of theoretical plates (N) was 10 000 for the on-column detection and 3500 for the post-column detection, which were obtained from the migration times and the full width at half maximum of peaks in both electropherograms of Fig. 4. Thus compared with the on-column detection, the post-column detection suffers 65% loss in efficiency, which corresponds to 44% loss in resolution ($R_S \approx N^{1/2}$). The detection volume of the post-column flow cell is very close to that of the 3-mm Z-cell with 75-μm I.D. Therefore if the influence of cell configuration on the electrophoretic process is similar to each other, it is expected that the maximum N and the loss in efficiency should not be very different in both cases. Much greater loss in efficiency with the post-column design, compared with the Z-shaped flow cells (less than 14% [12]), indicates that there must exist other sources of band broadening in the post-column microchannel flow cell. The auxiliary flows fed into the flow cell can cause some pressure effects which in turn can break the plug flow of electroosmosis. In addition to this, the T-connection between the capillary column and the microchannel may produce turbulence in flow, which could also cause band broadening.

The migration times of FITC in Fig. 4a and b are 8.2 min and 8.8 min, respectively. Although the length from the injection end of capillary columns to the detection window is the same (40 cm) in both cases, the longer migration time was obtained when the post-column microchannel flow cell was used. The difference in migration times may also be explained with the pressure effect mentioned above.

Linearity and reproducibility of the flow cell were evaluated with FITC electropherograms. Fig. 5 shows that linearity covers the range from $5.5 \cdot 10^{-7}$ M to $1.0 \cdot 10^{-5}$ M with the linear correlation coefficient r of 0.992. The flow cell provides a rather disappointing linear dynamic range, compared with linearity over 4.0 orders of magnitude for the ball lens-modified Z-shaped cells [12]. Since the detector compartment of our homemade CE system is not so light-tight as commercial ones, deviation from Beer's law could begin at lower concentrations. Although not shown in Fig. 5, the calibration curve begins to flatten at about $1 \cdot 10^{-5}$ M. However, any band broadening and tailing have not been observed up to about $1 \cdot 10^{-4}$ M, which indicates that the upper limit of the linearity of the post-

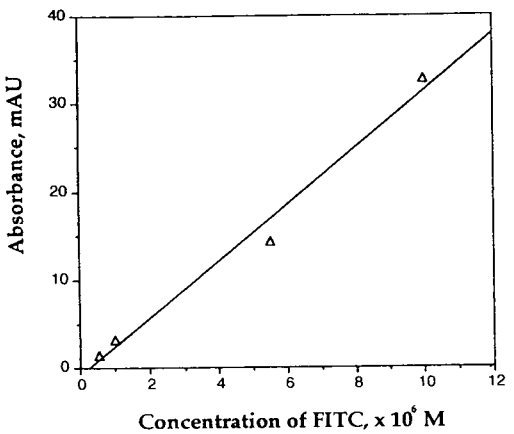

Fig. 5. Linear relationship between concentrations and peak heights of FITC for CE analysis using the post-column flow cell. Linearity covers sample concentrations from $5.5 \cdot 10^{-7}$ M to $1.0 \cdot 10^{-5}$ M and linear correlation coefficient r is 0.992.

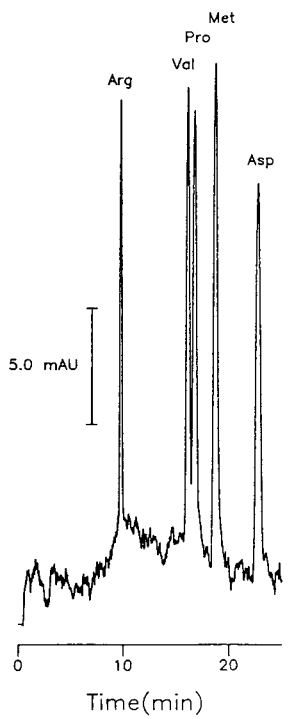

Fig. 6. Electropherogram of dansyl-amino acids obtained using the post-column flow cell. Capillary, 75 μm I.D., 58 cm length; buffer, 30 mM phosphate (pH 4.3); sample concentrations, $1.0 \cdot 10^{-5}$ M for each dansyl-amino acid; sample injection, 10 s at 20 cm height difference; detection wavelength, 216 nm; applied voltage, 17 kV (293 V/cm); Arg = dansyl-arginine; Val = dansyl-valine; Pro = dansyl-proline; Met = dansyl-methionine; Asp = dansyl-aspartic acid.

column flow cells is mainly attributed to stray light. The lower limit of the linearity is due to LOD that is limited by the high background noise caused by low light transmission. Reproducibilities in migration times and peak heights were 3.7% and 5.7%, respectively, in terms of relative standard deviation.

Fig. 6 demonstrates CE separation of a mixture of dansyl-amino acids using the setup equipped with the post-column flow cell. An equimolar mixture of five dansyl-amino acids was successfully separated by the system. LODs of dansyl-amino acids (216 nm) were the same as that of FITC (488 nm).

In the present design, the light incident to the post-column flow cell travels through a 1-cm thick buffer solution confined in a square quartz tubing (Fig. 2a). Although the same solution has been used for the running and the flushing buffers, in order to prevent attenuation of light intensity from scattering around the outlets of the microchannel, absorption by solvent and solute species (especially at short wavelengths) may cause low light transmission to some extent. Minimizing the distance between the flat optical windows and the outlets of the channel will be considered in future designs to improve performance of the cell. In this study for evaluating performance of the post-column flow cell as an absorbance detector cell, the contribution of absorption by buffer solutions to low light transmission would be negligible, because a visible wavelength of 488 nm has been mainly used. Also, to minimize the possibility of this contribution, phosphate buffers that are useful even below 215 nm, where the effect of background absorption is often significant [14], have been used throughout this study.

4. Conclusions

The post-column microchannel flow cell provides CE with an enhanced sensitivity for UV–visible absorbance detection. An 8-fold S/N improvement over on-column detection has been demonstrated, but it is far smaller than the expected 50-fold gain in sensitivity from the

extended optical path length. Optimizing light throughput, minimizing stray light and improving cell design are demanded to realize and expand practical usefulness of our post-column flow cell. It is expected that refined detection techniques employing the post-column microchannel flow cell will utilize all potential advantages of the cell, such as extended optical path length, easy optical coupling, easy modification to post-column derivatization/sensitive detection, and applicability to nearly all kinds of optical detection techniques for CE analysis.

Acknowledgements

The authors are grateful to the Korea Research Foundation and the Center for Biofunctional Molecules for the financial support of this work.

References

[1] J.W. Jorgenson and K.D. Lukacs, *Science*, 222 (1983) 266.
[2] M.J. Gordon, X. Huang, S.L. Pentoney, Jr. and R.N. Zare, *Science*, 242 (1988) 224.
[3] A.G. Ewing, R.A. Wallingford and T.M. Olefirowicz, *Anal. Chem.*, 61 (1989) 292A.
[4] H.H. Lauer and J.B. Ooms, *Anal. Chim. Acta*, 250 (1991) 45.
[5] D. Perrett and G. Ross, *Trends Anal. Chem.*, 11 (1992) 156.
[6] J.P. Landers, R.P. Oda, T.C. Spelsberg, J.A. Nolan and K.J. Ulfelder, *BioTechnology*, 14 (1993) 98.
[7] M. Albin, P.D. Grossman and S.E. Moring, *Anal. Chem.*, 65 (1993) 489A.
[8] S.E. Moring, J.C. Colburn, P.D. Grossman and H.H. Lauer, *LC · GC*, 8 (1990) 34.
[9] T. Tsuda, J.V. Sweedler and R.N. Zare, *Anal. Chem.*, 62 (1990) 2149.
[10] X. Xi and E.S. Yeung, *Appl. Spectrosc.*, 45 (1991) 1199.
[11] J.P. Chervet, R.E.J. van Soest and M. Ursem, *J. Chromatogr.*, 543 (1991) 439.
[12] S.E. Moring, R.T. Reel and R.E.J. van Soest, *Anal. Chem.*, 65 (1993) 3454.
[13] G.J.M. Bruin, G. Stegeman, A.C. van Asten, X. Xu, J.C. Kraak and H. Poppe, *J. Chromatogr.*, 559 (1991) 163.
[14] D.N. Heiger, *High Performance Capillary Electrophoresis—An Introduction*, Hewlett-Packard, Waldbronn, 1992, p. 95.

ELSEVIER

Journal of Chromatography A, 680 (1994) 117–123

JOURNAL OF CHROMATOGRAPHY A

Micellar electrokinetic chromatography using high-molecular surfactants
Use of butyl acrylate–butyl methacrylate–methacrylic acid copolymers sodium salts as pseudo-stationary phases

Hiroto Ozaki[a,*], Shigeru Terabe[a], Akinobu Ichihara[b]

[a]*Faculty of Science, Himeji Institute of Technology, Kamigori, Hyogo 678-12, Japan*

[b]*Dai-ichi Kogyo Seiyaku Co., Ltd., 55, Nishi-shichijo, Higashi-kubocho, Shimogyo-ku, Kyoto 600, Japan*

Abstract

Butyl acrylate–butyl methacrylate–methacrylic acid copolymers sodium salts (BBMA), high-molecular surfactants ($M_r \approx 40\,000$), were utilized in micellar electrokinetic chromatography. Non-ionic test solutes were successfully separated with a 2% BBMA solution in a borate–phosphate buffer (pH 8.0). BBMA showed significantly different selectivity for naphthalene derivatives in comparison with sodium dodecyl sulfate. The capacity factors were proportional to the concentration of BBMA, and the critical micelle concentration was found to be substantially close to zero, suggesting that one BBMA molecule forms one micelle. Effects of the pH, the composition and the molecular mass of BBMA were studied.

1. Introduction

Micellar electrokinetic chromatography (MEKC) [1–4], which uses an ionic micellar solution as the separation solution, is a mode of capillary electrophoresis (CE). CE is a separation technique of ionic analytes only, whereas MEKC is capable of separating both ionic and non-ionic analytes. Almost all advantages of CE apply to MEKC as well and many applications of MEKC separations have been reported [3,4].

The MEKC separation is based on the differential partitioning of an analyte between the micelle, which is a pseudo-stationary phase, and the surrounding aqueous phase, and therefore the choice of surfactants and modifiers of the aqueous phase is important for manipulating separation selectivity [5]. The effect of surfactant structure on selectivity has been discussed elsewhere [5]. It is generally recognized that different surfactants show different selectivity. In particular, the polar group of the surfactant affects selectivity more significantly than the hydrophobic group. Most surfactants have a long alkyl chain as a hydrophobic group but some have different structures: semiplanar structures such as bile salts or multiple-chain structures such as lecithins or some synthetic surfactants [6]. These surfactants are known to have some advantages over the single-alkyl-chain surfactants: bile salts have low solubilizing capability [7–9] and can recognize chirality [10–14]; a

* Corresponding author. Permanent address: Kaneka Techno Research Co. Ltd., 1-2-80, Yoshida-cho, Hyogo-ku, Kobe 652, Japan.

0021-9673/94/$07.00
SSDI 0021-9673(94)00607-5

double-chain surfactant has shown significantly different selectivity [6].

The micelle is in equilibrium with the monomeric surfactant, whose concentration is called critical micelle concentration (CMC) and is constant irrespective of the concentration of the surfactant. Since the micelle works as the pseudo-stationary phase in MEKC, the volume of the micelle, V_{mc}, is directly related to the capacity factor, k', through

$$k' = K(V_{mc}/V_{aq}) \quad (1)$$

where K is the distribution coefficient and V_{aq} is the volume of the aqueous phase excluding the volume of the micelle. The volume of the micelle is given as

$$V_{mc} = \bar{v}(C_{srf} - CMC) \quad (2)$$

where $\bar{v}$ is the partial specific volume of the surfactant forming the micelle and C_{srf} is the concentration of the surfactant. CMC depends on experimental conditions such as temperature, salt concentration and other additives.

When a high voltage is applied across the capillary length, the temperature inside the capillary will rise due to Joule heating even with a thermostated capillary [15–18]. The temperature rise of the running solution inside the capillary probably causes a change in CMC, the distribution coefficient and hence the capacity factor in addition to the viscosity. Therefore, the effect of the temperature rise on the migration time will be more serious in MEKC that in capillary zone electrophoresis (CZE).

High-molecular surfactants called oligo-soaps or poly-soaps are oligomers of monomeric surfactants or polymers that show surface active properties as a whole. The high-molecular surfactant is considered to form the micelle from a single molecule, which may be called a *molecular micelle*. The CMC can be zero or meaningless. Therefore, we can expect a constant concentration of the micelle for the high-molecular surfactant irrespective of the experimental conditions. Although the micelle formed from low-molecular surfactants exists in a dynamic equilibrium and has a limited life time less than 1 s, the molecular micelle is stable. Therefore, the high-molecular surfactant is expected to show different characteristics for the use in MEKC.

The size of the micelle has a distribution, which contributes to the band broadening in MEKC [19]. The effect of the size distribution on efficiency is significant only for analytes having a large capacity factor [19]. The effect of the size distribution can be leveled out by the dynamic exchange of the micellar size in the case of low-molecular surfactants. The distribution of the micellar size of the high-molecular surfactant will be wider than that of the low-molecular surfactant and may adversely affect efficiency of MEKC. However, the high-molecular surfactant will have other advantages over the low-molecular surfactant: a high content of organic solvent will not break down the micelle; very low concentrations of the micelle will be available; no monomeric surfactant that does not contribute to the separation is present.

So far, only one high-molecular surfactant has been reported for MEKC; Palmer et al. [20,21] synthesized undecylenate oligomer by polymerizing micellized sodium 10-undecylenate in aqueous solution. The oligomer was successful for the separation of hydrophobic compounds with relatively high concentrations of acetonitrile.

Butyl acrylate–butyl methacrylate–methacrylic acid copolymers sodium salts (BBMA) are a group of high-molecular surfactants, whose molecular structure is shown in Fig. 1. We tried to utilize BBMA as a pseudo-stationary phase for MEKC [22]. This paper describes some characteristics of BBMA as the pseudo-stationary phase in MEKC. Some other natural or synthetic high-molecular surfactants were also examined for use as pseudo-stationary phases in MEKC.

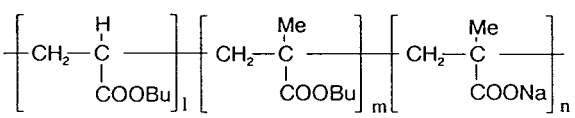

Fig. 1. Molecular structure of BBMA. Me = Methyl; Bu = butyl.

2. Experimental

2.1. Reagents

BBMAs were supplied by Dai-ichi Kogyo Seiyaku (Kyoto, Japan) as aqueous solutions. Most of this work was performed with a grade of BBMA, which was a 23% aqueous solution having a viscosity of 170 cP at 25°C. The molecular mass of the BBMA was about 40 000 from gel permeation chromatography (GPC) using standard polyethylene glycols. Since BBMA contained a minor amount of low-molecular components, it was purified by a reprecipitation method as follows: a portion of the BBMA solution was mixed with 50 portions of acetone; a precipitated polymer was separated by decantation and dried in vacuo at room temperature. Thus purified BBMA was used in this work if it is not mentioned otherwise. Three grades of BBMA having a different content of methacrylic acid (MAA) were used: 50, 40 and 30% of MAA with the same composition of butyl acrylate–butyl methacrylate. BBMAs having different viscosities are also employed: 3300, 250 and 60 cP.

Alginic acid, carboxymethylcellulose sodium salt and poly(N-vinyl-2-pyrrolidone) were purchased from Tokyo Kasei Kogyo (Tokyo, Japan). SDS and Chitosan were from Nacalai Tesque (Kyoto, Japan). Other reagents were of analytical grade and water was purified with a Milli-Q system.

Phenanthrene was used as a tracer of the micelle. Sample solutes were dissolved in 25% aqueous methanol, which was also a marker of the electroosmotic flow.

2.2. Apparatus

MEKC was performed with a Bio-Rad BioFocus 3000 (Hercules, CA, USA) using a fused-silica capillary of 36.5 cm (32 cm to the detector) × 50 μm I.D. obtained from Polymicro Technologies (Phoenix, AZ, USA). The temperature of the capillary was thermostated at 30°C. Samples were injected by the pressurization method and detected at 210, 250 and 280 nm simultaneously under the multi-wavelength mode. The electropherograms were recorded at 210 nm.

GPC was carried out with a Shimadzu LC-9A liquid-delivery pump (Kyoto, Japan) and a Shodex RI SE-51 refractive index (RI) detector (Tokyo, Japan) using Tosoh (Tokyo, Japan) TSK-gel G3000SW (60 cm × 8 mm I.D.) and G2000SW (60 cm × 8 mm I.D.) columns in series at room temperature. A sodium chloride solution (50 m*M*) containing 20% acetonitrile was employed as a mobile phase.

3. Results and discussion

3.1. GPC of BBMA

A gel permeation chromatogram of BBMA is shown in Fig. 2. The main peak was eluted early and assigned to BBMA. The peak is relatively sharp and hence the molecular mass will not be widely distributed. The weak negative peak was due to the sample solvent, water. The low and broad peak between the two peaks was considered to show a low-molecular compound. Almost the same chromatogram was observed for

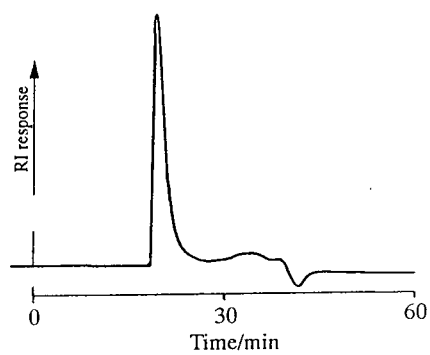

Fig. 2. Gel permeation chromatogram of BBMA. Column, TSK-gel G3000SW + G2000SW; mobile phase, 50 m*M* NaCl containing 20% acetonitrile; flow-rate, 1 ml min^{-1}; temperature, ambient; detector, refractometer.

the purified BBMA as described in the Experimental section.

3.2. Separation by MEKC with BBMA and other high-molecular surfactants

MEKC separations of three test mixtures, benzene derivatives, cold medicines, and naphthalene derivatives, are shown in Fig. 3, obtained with unpurified BBMA. The benzene derivatives were successfully separated, as shown in Fig. 3A, and the migration order was the same as that obtained with SDS [2]. The separation of the cold medicines was not very successful, as shown in Fig. 3B. The capacity factors were too small for the cold medicines but the migration order was the same as that observed with SDS. The naphthalene derivatives were well resolved, as shown in Fig. 3C. The migration order of the

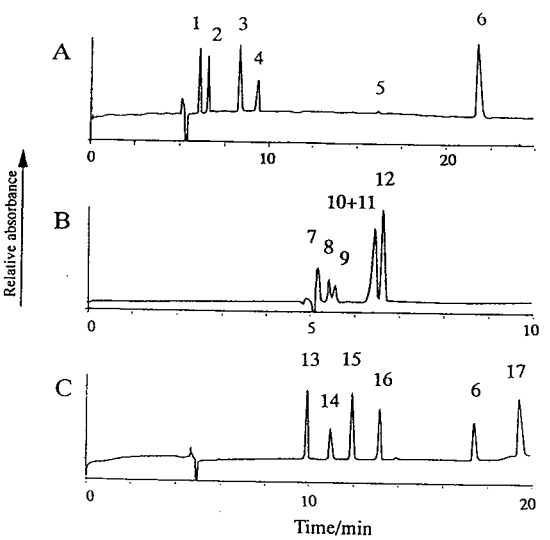

Fig. 3. MEKC separations of benzene derivatives (A), cold medicines (B) and naphthalene derivatives (C) using BBMA. Peaks: 1 = resorcinol; 2 = phenol; 3 = *p*-nitroaniline; 4 = nitrobenzene; 5 = toluene; 6 = 2-naphthol; 7 = acetaminophen; 8 = caffeine; 9 = guaifenesin; 10 = ethenzamide; 11 = isopropylantipyrine; 12 = trimetoquinol; 13 = 1-naphthalenemethanol; 14 = 1,6-dihydroxynaphthalene; 15 = 1-naphthylamine; 16 = 1-naphthaleneethanol; 17 = 1-naphthol. Conditions: capillary, 36.5 cm (32 cm to the detector) × 50 μm; running solution, 2% unpurified BBMA in 50 m*M* phosphate–100 m*M* borate buffer (pH 8.0); applied voltage, 20 kV; detection wavelength, 210 nm.

naphthalene derivatives was significantly different from that obtained with SDS. Efficiency was slightly lower than that usually obtained with low-molecular-mass surfactants, but it was still high enough for most purposes. The high efficiency shown in Fig. 3 suggests that the distribution of the molecular mass of BBMA does not cause a serious loss of efficiency.

The separation selectivity was extremely different especially for naphthalene derivatives in comparison with that observed using SDS. In particular, it is interesting that 1-naphthol migrated much slower than 1-naphthalenemethanol or 1-naphthaleneethanol. This has also been observed with a double-chain surfactant, 5,12-bis(dodecylmethyl) - 4,7,10,13 - tetraoxa - 1,16 - hexadecanedisulfonate (DBTD) [6]. The cold medicines had lower capacity factors than those with SDS, which is probably due to the difference in the polar group of the surfactants: a carboxyl group in BBMA, whereas a sulfate group in SDS. A similar difference in selectivity has also been observed between SDS and sodium trioxyethylene alkyl ether acetate (ECT), which has a carboxyl group [23]. Timepidium bromide, which is often used as a good tracer of the SDS micelle [24], migrated faster than Sudan IV and phenanthrene, which had the same migration times. Therefore, timepidium bromide cannot be used as a tracer of the BBMA micelle.

Solutions (2%) of alginic acid and carboxymethylcellulose in the phosphate–borate buffer (pH 8.0) were viscous and not suitable for use in MEKC. A 0.5% solution of chitosan in 0.33 *M* phosphoric acid was employed in MEKC. No resolution was obtained for the test mixtures but only a broad single peak was observed by applying −5 kV. Polyvinylpyrrolidone solution (2%) in the buffer (pH 7.0) was not effective for the separation of the test mixtures. Only a single peak was observed at about 10 min by applying 10 kV (40 μA).

3.3. Effects of concentration of BBMA and pH on migration time

The dependence of the capacity factors of naphthalene derivatives on the concentration of

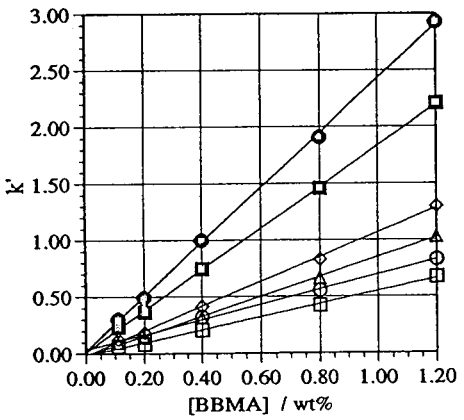

Fig. 4. Dependence of the capacity factor (k') on the concentration of BBMA. Solutes: □ = 1-naphthalenemethanol; ○ = 1,6-dihydroxynaphthalene; △ = 1-naphthylamine; ◇ = 1-naphthaleneethanol; ■ = 2-naphthol; ● = 1-naphthol. Conditions as in Fig. 3 except for the concentration of BBMA.

BBMA is shown in Fig. 4. The capacity factors were proportional to the BBMA concentration and the plotted line for each analyte passed the origin closely when it was extrapolated. The results clearly demonstrate that the CMC of BBMA is virtually zero, as deduced from Eq. 2. Thus, the micelle of BBMA can be assumed to be formed from one molecule by considering the molecular mass of BBMA.

The dependence of the migration-time window (t_{mc}/t_0, where t_{mc} and t_0 are migration times of the micelle and the aqueous phase) on pH is given in Fig. 5. The concentration of BBMA was 0.17%, because the solubility of BBMA was low at low pH. The migration-time window became wider with increasing pH values and it was almost constant between pH 7 and 9, although the results were not shown in Fig. 5. BBMA precipitated below pH 4 probably due to the decrease of the surface charge. The capacity factors of the naphthalene derivatives decreased with an increase in pH as shown in Fig. 6, which means that the solubilizing power of BBMA is reduced probably due to the increased surface charge or ionization of the carboxyl group. The results strongly suggest that although the solutes are neutral, the surface charge of the micelle significantly affects the distribution coefficient.

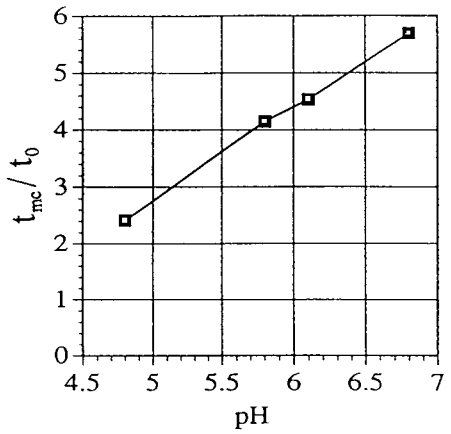

Fig. 5. Dependence of the separation window (t_{mc}/t_0) on pH. Running solution was 0.17% BBMA in 50 mM phosphate buffer. Other conditions as in Fig. 3.

3.4. *Effects of the composition and molecular mass of BBMA on the separation*

Three BBMAs having different contents of MAA were employed to study the effects of the composition on separation. Fig. 7 shows the separations of the naphthalene derivatives at pH 8.0 and Fig. 8 gives the dependence of their capacity factors on the MAA content. The migration-time window increased with an increase in the MAA content, as is clearly seen from Fig. 7, which was ascribed to an increase of

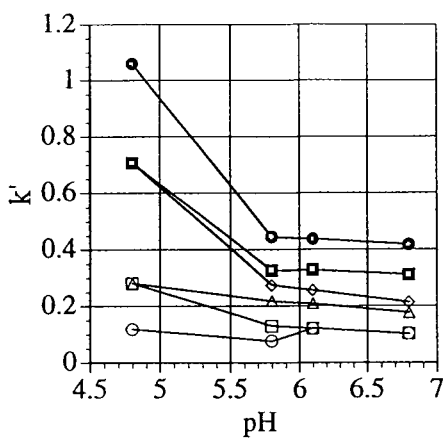

Fig. 6. Dependence of the capacity factors (k') of naphthalene derivatives on pH. Solutes and conditions as given in Fig. 4.

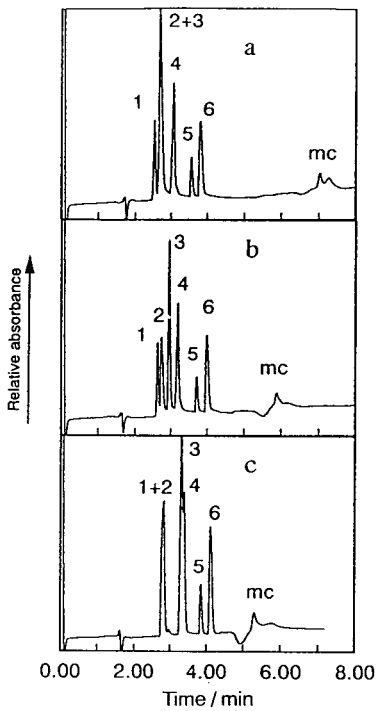

Fig. 7. Separation of naphthalene derivatives using BBMAs having different contents of MAA: (a) 50%, (b) 40% and (c) 30%. Peaks: 1 = 1-naphthalenemethanol; 2 = 1,6-dihydroxynaphthalene; 3 = 1-naphthylamine; 4 = 1-naphthaleneethanol; 5 = 2-naphthol; 6 = 1-naphthol. Running solution, 2% BBMA in a 100 m*M* borate–50 m*M* phosphate buffer (pH 8.0). Other conditions as in Fig. 3.

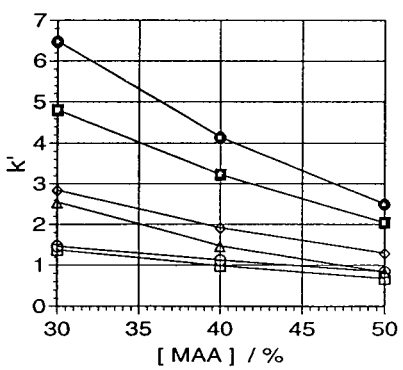

Fig. 8. Dependence of the capacity factor (k') of naphthalene derivatives on the content of MAA in BBMA. Solutes as in Fig. 4; conditions as in Fig. 7.

the surface charge owing to the increased number of carboxyl groups. The capacity factors decreased with an increase of the MAA content. The dependence of the capacity factor on the content of MAA was very similar to that on the pH described above. Both dependencies can be superficially explained in terms of surface charge. However, it should be mentioned that the electroosmotic flow is independent of the MAA content, whereas it is significantly dependent on the pH in the acidic region. Therefore, the use of BBMAs having different MAA contents is more advantageous than varying the pH to manipulate the migration-time window or capacity factor. One more disadvantage of the pH change is that BBMA tends to precipitate below pH 5.

Three BBMAs with different viscosities but same composition were employed to see the effect of molecular mass on the separation of naphthalene derivatives. The three BBMAs gave almost the same chromatograms for the naphthalene derivatives, which suggests that the solubilizing power and the electrophoretic mobilities of the BBMAs are independent of the molecular mass provided the composition is unchanged. Therefore, we can conclude that the molecular mass distribution will not be critical for the reproducibility of the migration time and selectivity, although a wider distribution of molecular mass values may cause lower efficiency.

4. Conclusions

BBMA has been found to be a useful high-molecular surfactant for the use in MEKC and has some advantages over low-molecular surfactants: zero CMC or molecular micelle; different selectivity; and possible manipulation of the migration-time window and capacity factor by changing the pH or content of MAA. The molecular micelle is characteristic of high-molecular surfactants and ensures the constant concentration of the micelle irrespective of the conditions. Although its constant concentration was not confirmed in this study, the advantage of constant concentration will be taken to produce

highly reproducible migration time data in a further work. The molecular micelle will be stable in a running solution containing a high concentration of an organic solvent. Since BBMA has carboxyl groups, it does not dissolve in acidic solution below pH 4. However, other high-molecular surfactants having phosphate or ammonium groups are expected to be usable in a wider pH range, and the use of such high-molecular surfactants is under investigation.

References

[1] S. Terabe, K. Otsuka, K. Ichikawa, A. Tsuchiya and T. Ando, *Anal. Chem.*, 56 (1984) 111–113.

[2] S. Terabe, K. Otsuka and T. Ando, *Anal. Chem.*, 57 (1985) 834–841.

[3] J. Vindevogel and P. Sandra, *Introduction to Micellar Electrokinetic Chromatography*, Hüthig, Heidelberg, 1992.

[4] S. Terabe, in N. Guzman (Editor), *Capillary Electrophoresis Technology*, Marcel Dekker, New York, 1993, pp. 65–87.

[5] S. Terabe, *J. Pharm. Biomed. Anal.*, 10 (1992) 705–715.

[6] M. Tanaka, T. Ishida, T. Araki, A. Masuyama, Y. Nakatsuji, M. Okahara and S. Terabe, *J. Chromatogr.*, 648 (1993) 468–473.

[7] H. Nishi, T. Fukuyama, M. Matsuo and S. Terabe, *J. Chromatogr.*, 513 (1990) 279–295.

[8] R.O. Cole, M.J. Sepaniak, W.L. Hinze, J. Gorse and K. Oldiges, *J. Chromatogr.*, 557 (1991) 113–123.

[9] R.D. Holland and M.J. Sepaniak, *Anal. Chem.*, 65 (1993) 1140–1146.

[10] S. Terabe, M. Shibata and Y. Miyashita, *J. Chromatogr.*, 480 (1989) 403–411.

[11] H. Nishi, T. Fukuyama, M. Matsuo and S. Terabe, *J. Microcolumn Sep.*, 1 (1989) 234–241.

[12] H. Nishi, T. Fukuyama, M. Matsuo and S. Terabe, *J. Chromatogr.*, 515 (1990) 233–241.

[13] H. Nishi, T. Fukuyama, M. Matsuo and S. Terabe, *Anal. Chim. Acta*, 236 (1990) 281–286.

[14] R.O. Cole, M.J. Sepaniak and W.L. Hinze, *J. High Resolut. Chromatogr.*, 13 (1990) 579–582.

[15] H. Wätzig, *Chromatographia*, 33 (1992) 445–448.

[16] M.S. Bello, M. Chiari, M. Nesi, P.G. Righetti and M. Saracchi, *J. Chromatogr.*, 625 (1992) 323–330.

[17] S. Terabe, T. Katsura, Y. Okada, Y. Ishihama and K. Otsuka, *J. Microcolumn Sep.*, 5 (1993) 23–33.

[18] J.H. Knox and K.A. McCormack, *Chromatographia*, 38 (1994) 207–214.

[19] S. Terabe, K. Otsuka and T. Ando, *Anal. Chem.*, 61 (1989) 251–260.

[20] C.P. Palmer, M.Y. Khaled and H.M. McNair, *J. High Resolut. Chromatogr.*, 15 (1992) 756–762.

[21] C.P. Palmer and H.M. McNair, *J. Microcolumn Sep.*, 4 (1992) 509–514.

[22] S. Terabe, H. Ozaki and Y. Tanaka, *J. Chin. Chem. Soc.*, 41 (1994) 251–257.

[23] H. Nishi, T. Fukuyama, M. Matsuo and S. Terabe, *J. Pharm. Sci.*, 79 (1990) 519–523.

[24] H. Nishi, N. Tsumagari and S. Terabe, *Anal. Chem.*, 61 (1989) 2434–2349.

ELSEVIER

Journal of Chromatography A, 680 (1994) 125–135

JOURNAL OF CHROMATOGRAPHY A

Novel chiral surfactant for the separation of enantiomers by micellar electrokinetic capillary chromatography

Jeffrey R. Mazzeo*, Edward R. Grover, Michael E. Swartz, John S. Petersen

Waters Chromatography, 34 Maple Street, Milford, MA 01757, USA

Abstract

A novel chiral surfactant was prepared as both enantiomeric forms, (*R*)- and (*S*)-N-dodecoxycarbonylvaline, and employed for the separation of enantiomeric mixtures by micellar electrokinetic capillary chromatography (MECC). The enantioselectivities (α) obtained for twelve typical pharmaceutical amines using the (*S*)-surfactant were compared to those obtained with (*S*)-N-dodecanoylvaline, a chiral surfactant described in the literature. Higher enantioselectivities were seen for ten of the twelve compounds using (*S*)-N-dodecoxycarbonylvaline. Furthermore, (*S*)-N-dodecoxycarbonylvaline had significantly less background absorbance in the low UV. It is shown that *exact* enantiomer migration order reversal can be obtained by individually employing both enantiomeric forms of the surfactant. For ionizable compounds like the amines examined here, enantioselectivity can be optimized by changing the pH of the MECC buffer. Partitioning is optimized through surfactant concentration, organic additives and pH. The ability to achieve fast chiral separations is shown. A separation of ephedrine enantiomers in urine is shown, with the only sample preparation being filtration.

1. Introduction

An emerging trend in the pharmaceutical industry is the development of drugs as pure enantiomers (enantiopure drugs) rather than as racemic mixtures [1]. This change is due to the realization that the two enantiomers of a chiral compound can have widely different biological activities. The common analgesic, ibuprofen, now marketed by several firms as the racemic mixture, is a case in point. It has been determined that (*S*)-ibuprofen takes effect three times faster than (*R*)-ibuprofen. In other cases, the undesired enantiomer can lower the efficacy of the beneficial enantiomer, and in the worst case it can have adverse side effects. Regulatory agencies worldwide have realized the potential benefits of enantiopure drugs and have published guidelines for the development of chiral drugs [2]. It is expected that many commercial racemic drugs will soon be available as the "pure" enantiomer. As a result, there exists a tremendous need for improved methods of determining optical purity. Since most "enantiopure" drugs have optical purity in excess of 95%, enantioselective chromatographic methods are required.

The use of LC chiral stationary phases is currently the predominant method for the separation of enantiomeric mixtures [3]. Pirkle-type, cyclodextrin, protein, cellulose and ligand-exchange chiral stationary phases are the most common. The 40–50 commercially available columns reflect the major problem associated with

* Corresponding author.

0021-9673/94/$07.00
SSDI 0021-9673(94)00602-4

chiral LC. Specifically, because total plate numbers in chiral LC range from 1000–10 000, the minimum α value required to achieve baseline separation of an enantiomeric mixture is large. For example, with $N = 5000$ and $k = 1$, the minimum α required for baseline separation ($R_s = 1.5$) is 1.20. Since a given chiral phase only shows this α for a small number of compounds, it is typically necessary to screen several different types of chiral columns to achieve separation of a single enantiomeric mixture. Furthermore, simple changes in the mobile phase, such as concentration and type of modifiers, pH and ionic strength, often lead to unpredictable changes in enantioselectivity. Therefore, methods development in chiral LC is a tedious, empirical process.

Given a limit of 5000–10 000 plates, the goal in chiral LC has been to develop phases with higher α values. However, in view of the large number of chiral columns available, the goal of finding a single chiral phase which shows sufficient α for a broad range of compounds is likely to remain elusive. To achieve an improved situation whereby two to five chiral phases can separate the majority of chiral compounds, a separation format affording significantly higher efficiencies than LC is required.

Capillary electrophoresis (CE) is an attractive system for chiral separations because plate counts for small molecules are typically 100 000 or greater. In the example above, if $N = 100\,000$, with $k = 1$ and $R_s = 1.5$, the required α drops to 1.04. Therefore, a given chiral selectand will resolve a significantly higher percentage of enantiomeric mixtures in a CE versus an LC format. Furthermore, because the chiral selectand is dissolved in the CE buffer, several selectands and conditions can be automatically screened with a single CE instrument and capillary.

Many of the chiral separations by CE have employed natural products as the chiral selectand. These selectands include cyclodextrins [4–9] and proteins [10]. Cyclodextrin-containing electrolytes have successfully separated many different types of enantiomeric mixtures. However, both cyclodextrins and proteins are only available as the single enantiomer, making exact enantiomer migration order reversal impossible. This ability is important to both improve quantitation of optical purity and to confirm if a resulting separation is a chiral one.

Micellar electrokinetic capillary chromatography (MECC), introduced by Terabe et al. [11] and recently reviewed [12], is a form of CE which has the ability to separate charged and uncharged compounds simultaneously. It is a very powerful separation method because high efficiencies are generally obtained (100 000 plates or more) and many parameters can be varied to optimize resolution.

Chiral CE separations have been achieved by MECC through the use of bile salts [13–15], which are naturally occurring surfactants. Only limited applications with bile salts have been reported so far. Like cyclodextrins and proteins, bile salts do not allow enantiomer migration order reversal. Furthermore, because of their low aggregation number, bile salts have only found use for hydrophobic analytes.

In 1989, Dobashi et al. [16,17] described the synthesis of (*S*)-N-dodecanoylvaline and its use to separate neutral enantiomeric mixtures by CE. Subsequently, Terabe and co-workers [18–20] performed enantiomeric separations in MECC with the same surfactant. In both cases, the analytes were neutral amino acid derivatives. Otsuka and Terabe [19] found that adding methanol and/or urea to the MECC buffer improved the peak shape of the phenylthiohydantoin-amino acids investigated. A mixed micellar system with sodium dodecyl sulfate was employed to increase both the migration-time window and analyte capacity factors [20].

In principle, a chiral MECC system using synthetic chiral surfactants offers several advantages as a chiral separation system. These advantages include high efficiency, the ability to exactly reverse enantiomer migration order, tolerance of complex sample matrices, and simultaneous chiral and non-chiral separations. Because of the high efficiencies of MECC, we believe that only a few chiral surfactants will be needed to separate the majority of chiral compounds. To demonstrate these potential benefits, we have begun a program to synthesize novel chiral surfactants

and test their ability to separate enantiomeric mixtures in an MECC mode. Here, we report the results obtained using one of these chiral surfactants, (*S*)- and (*R*)-N-dodecoxycarbonylvaline.

2. Experimental

All CE separations were performed on either a Quanta 4000 or 4000E CE system (Waters, Milford, MA, USA). Buffers were prepared with surfactant and disodium phosphate and/or disodium tetraborate. The pH was then adjusted with either sodium hydroxide or phosphoric acid (J.T. Baker). Prior to use, AccuSep (Waters) capillaries, 60 cm (52.5 cm effective length) × 50 μm I.D., were rinsed for 5 min with 0.5 *M* NaOH. Between injections, the capillaries were rinsed with 0.1 *M* NaOH (3 min) and buffer (3 min). Unless indicated separations were performed with UV detection at 214 nm and a voltage of +12 kV. Hydrostatic injection times ranged from 2 to 20 s. All buffers and samples were filtered through a 0.45-μm filter (Millipore, Bedford, MA, USA). Separations were performed at ambient temperature. Samples were prepared as 10 mg/ml stock solutions in methanol and then diluted to 0.1 mg/ml in buffer. The micelle migration time was measured with the hydrophobic compound sulconazole. Racemates and the individual enantiomers (when possible) were purchased from Sigma (St. Louis, MO, USA) and Aldrich (Milwaukee, WI, USA).

2.1. Synthesis of (S)-N-dodecanoylvaline

(*S*)-N-Dodecanoylvaline was prepared according to the procedure of Miyagishi and Nishida [21] by adding dodecanoyl chloride (Aldrich) to a 1 *M* sodium hydroxide solution containing (*S*)-valine (Aldrich). The structure was confirmed by ^{1}H NMR spectroscopy and HPLC analysis showed the product to be pure (≥95%). ^{1}H NMR ($C^2H_3O^2H$, 300 mHz) δ 0.90 (t, J = 6.7 Hz, 3H), 0.965 (d, J = 6.9 Hz, 3H), 0.973 (d, J = 6.9 Hz, 3H), 1.29 (bs, 16 H), 1.62 (m, J = 7.1 Hz, 2H), 2.15 (m, J = 6.8 Hz, 1H), 2.28 (t, J = 7.5 Hz, 2H), 4.32 (d, J = 5.8 Hz, 1H).

2.2. Synthesis of dodecyl chloroformate

Dodecyl chloroformate was prepared according to the procedure of Eckert and Forster [22] by reacting 1-dodecanol with triphosgene. The product was used without further purification. The structure was confirmed by ^{1}H NMR (C^2HCl_3, 300 MHz) δ 0.88 (t, J = 6.6 Hz, 3H), 1.26 (bs, 18H), 1.72 (m, J = 7.0 Hz, 2H), 4.31 (t, J = 6.7 Hz, 2H).

2.3. Synthesis of (S)- and (R)-N-dodecoxycarbonylvaline

The (*S*)- and (*R*)-isomers of N-dodecoxycarbonylvaline were synthesized according to the procedure of Miyagishi and Nishida [21] by adding dodecyl chloroformate to individual 1 *M* sodium hydroxide solutions containing (*S*)- and (*R*)-valine (Aldrich), respectively. The structure was confirmed by ^{1}H NMR spectroscopy and HPLC analysis showed the product to be pure (≥99.5%). ^{1}H NMR ($C^2H_3O^2H$, 300 mHz) δ 0.09 (t, J = 7.0 Hz, 3H), 0.94 (d, J = 6.9 Hz, 3H), 0.98 (d, J = 6.9 Hz, 3H), 1.29 (bs, 18 H), 1.63 (m, J = 6.85 Hz, 2H), 2.14 (m, J = 6.5 Hz, 1H), 4.04 (m, 3H).

3. Results and discussion

The enantiomeric surfactants (*R*)- and (*S*)-N-dodecoxycarbonylvaline were readily soluble in typical MECC buffers (i.e. phosphate–borate and phosphate). At pH < 6.5, the surfactants precipitated from solution. Consequently, they were only used at pH ≥ 7.0 in this work. Tests showed the surfactants to be soluble at 200 m*M*. Since joule heating effects became severe (even at low voltages) above this concentration, an upper solubility limit was not determined.

MECC is a true chromatographic technique. Thus, chromatographic figures of merit such as capacity factor (k) and selectivity (α) can be used

to describe analyte interactions with the micelles. Enantioselectivity (α) is an important parameter which allows comparison of different chiral surfactants. Thus, accurate α measurements must be obtained.

In MECC, k is defined as [23]:

$$k = \frac{t_r - t_{aq}}{t_{aq}\left(1 - \frac{t_r}{t_{mc}}\right)} \quad (1)$$

where t_r is the observed migration time of the solute, t_{mc} is the migration time of a solute which is completely partitioned into the micelle ($k = \infty$) and t_{aq} is the migration time of the solute if it does not interact with the micelle. We have substituted t_{aq}, or the time in the aqueous phase, for the more commonly used t_o, or electroosmotic flow time, to account for the fact that charged compounds will not migrate with the electroosmotic flow when in the aqueous phase.

For a neutral solute, t_{aq} is equal to the electroosmotic flow time (t_o) (usually obtained by injecting methanol or other organic solvent). In the case of charged solutes, t_{aq} is more difficult to measure. Khaledi and co-workers [24,25] have developed equations to determine the capacity factors of both anionic and cationic compounds in MECC. The important factor is that in capillary zone electrophoresis, cationic compounds will migrate before the electroosmotic flow marker, with an apparent mobility equal to the sum of the electroosmotic mobility and electrophoretic mobility:

$$\mu_{apparent} = \mu_{osmosis} + \mu_{electrophoretic} \quad (2)$$

For a given buffer, the electroosmotic flow in the presence vs. the absence of micelles will be different. This difference is due to differences in viscosity and ionic strength. Thus, the strategy employed to calculate t_{aq} of the amines in this study involved two experiments. First, the *electrophoretic* mobilities of the compounds were measured in the same buffer (without the micelles) as used in MECC. This value was calculated by subtracting the electroosmotic mobility from the apparent mobility. Then, the electroosmotic mobility obtained in the MECC separation of the compound was added to its electrophoretic mobility to obtain an apparent mobility in MECC as if there were no interaction with the micelles. The apparent mobility can be converted into a migration time to obtain t_{aq}. Since the two enantiomers of any compound will have the same electrophoretic mobility in the absence of a chiral selectand, they will have the same t_{aq} value as well. The major assumption of this approach is that the cationic compounds will not ion-pair with free surfactant molecules [24,25]. Experiments performed below the critical micelle concentration (CMC) of the surfactants indicated that ion-pairing was minimal.

The solute migration time, t_r, is obtained from the resulting electropherogram, while t_{mc} is obtained by injecting a very hydrophobic marker, such as Sudan III, and measuring the migration time [23]. Initially, Sudan III was used as the micelle marker. However, we found that the chiral compound sulconazole migrated at the same time as Sudan III at all surfactant concentrations examined. Because it was more soluble than Sudan III, sulconazole was used in most cases.

The separation of pseudoephedrine enantiomers using 50 m*M* (*S*)-N-dodecoxycarbonylvaline is shown in Fig. 1. The baseline disturbance at 8.650 min is the electroosmotic flow marker (methanol), and the peak at 46.550 min is the micelle marker (sulconazole). Pseudoephedrine is positively charged at this pH, and in

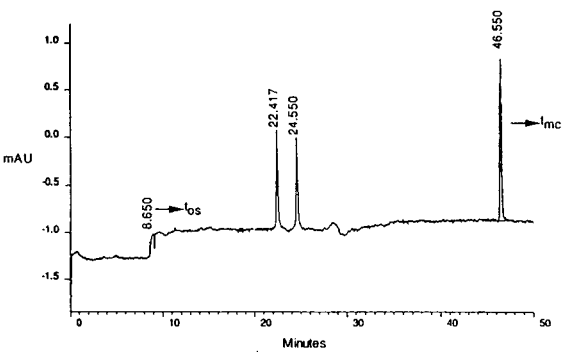

Fig. 1. Separation of pseudoephedrine enantiomers. Sample: 100 μg/ml racemic pseudoephedrine and 50 μg/ml sulconazole dissolved in buffer. Buffer: 50 m*M* (*S*)-N-dodecoxycarbonylvaline, 25 m*M* Na_2HPO_4–25 m*M* $Na_2B_4O_7$, pH 8.8.

free solution migrates before the electroosmotic flow marker. Thus, using the calculation described above, t_{aq} was assumed to be 6.389 min, its migration time in the absence of micelles. From this data and the migration time of the enantiomers, the capacity factor of the first enantiomer (k_1) was 4.84, and the capacity factor of the second enantiomer (k_2) was 6.01. The value of α (k_2/k_1) was 1.24. The average plate count for the two peaks was 104 000, and the resolution was 5.12.

The separation in Fig. 1 was obtained using a simple phosphate–borate buffer, with no urea or methanol required to obtain symmetrical peaks. Symmetrical peaks were also obtained using (*S*)-N-dodecanoylvaline in the same buffer system. We found that adding urea and/or methanol to the buffer did not improve peak shapes for the amines investigated. The migration-time window for a neutral solute in Fig. 1 (t_{aq}/t_{mc}) was 0.19. This result compares favorably with the value of 0.16 reported by Terabe [19] for a buffer containing (*S*)-N-dodecanoylvaline, sodium dodecyl sulfate, urea and methanol. In summary, we found that a simple MECC system led to excellent peak shape and resolution for the analytes tested.

One of the initial motivations for synthesizing (*S*)-N-dodecoxycarbonylvaline was to obtain a chiral surfactant which had lower UV absorbance than (*S*)-N-dodecanoylvaline. A 25 m*M* solution of each surfactant was prepared in 25 m*M* disodium phosphate–25 m*M* disodium tetraborate buffer. The pH was adjusted to 8.8 with either sodium hydroxide or phosphoric acid. These solutions were drawn into a 50 μm I.D. capillary, and the absorbance at 214 nm measured. The absorbance of (*S*)-N-dodecanoylvaline was 30 mAU while that of (*S*)-N-dodecoxycarbonylvaline was 12 mAU. Since the phosphate–borate buffer also had an absorbance of 12 mAU, it was concluded that (*S*)-N-dodecoxycarbonylvaline led to no additional absorbance at 214 nm. This property is very important at high surfactant concentrations, i.e. >100 m*M*, where high backgrounds decrease the effective linear dynamic range of the detector.

The difference in structure between (*S*)-N-dodecanoylvaline and (*S*)-N-dodecoxycarbonylvaline is the replacement of an amide group in (*S*)-N-dodecanoylvaline with a carbamate group in (*S*)-N-dodecoxycarbonylvaline (see Fig. 2). Since the two groups are adjacent to the chiral center in the surfactant, we tested the differences in enantioselectivity (α) between the two surfactants using twelve pharmaceutical amines as test probes. The data are summarized in Table 1. Unexpectedly, there was a large difference in enantioselectivity between the two surfactants. Specifically, (*S*)-N-dodecoxycarbonylvaline afforded higher α values for ten compounds. A separation of norephedrine enantiomers using the two surfactants is shown in Fig. 3. Other structural variations also impact enantioselectivity, and these results will be reported shortly.

To determine the influence of pH on partitioning, experiments were conducted at pH 7.0 and 8.8 using 25 m*M* (*S*)-N-dodecoxycarbonylvaline. All the amines investigated showed higher partitioning at pH 7.0. For instance ketamine, pK_a 7.5, had a capacity factor of 12.5 at pH 7.0 versus 2.2 at pH 8.8. The twelve test compounds in Table 1 all contain one or more amine groups, most of which have pK_a values between 7 and 10. Thus at pH 7.0 they were more positively

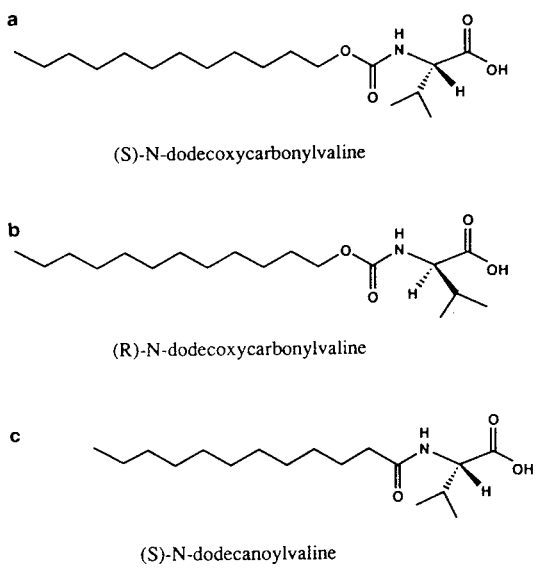

Fig. 2. Structures of the chiral surfactants.

Table 1
Comparison of enantioselectivities (α) obtained at pH 8.8 with 25 m*M* (*S*)-N-dodecoxycarbonylvaline vs. 25 m*M* (*S*)-N-dodecanoylvaline

Analyte	α	
	(*S*)-N-Dodecanoylvaline	(*S*)-N-Dodecoxycarbonylvaline
Atenolol	1	1.04
Bupivacaine	1.06	1.05
Ephedrine	1.05	1.10
Homatropine	1.02	1.03
Ketamine	1.05	1.01
Metoprolol	1.01	1.06
N-Methylpseudoephedrine	1.05	1.32
Norephedrine	1.04	1.10
Norphenylephrine	1.03	1.09
Octopamine	1	1.05
Pindolol	1.02	1.06
Terbutaline	1	1.01

Conditions: UV detection at 214 nm; 2-s hydrostatic injection; 60 cm × 50 μm capillary; +12 kV; pH 8.8 buffer: 25 m*M* Na_2HPO_4–25 m*M* $Na_2B_4O_7$.

charged (as reflected in the difference in free solution mobilities between the two pH values). Since the micelles are anionic, it was not surprising that increased positive charge led to increased partitioning. Values of α were also measured for the twelve test compounds using (*S*)-N-dodecoxycarbonylvaline at pH 7.0 and pH 8.8. The α values for nine compounds were higher at pH 7.0 (Table 2). For some compounds, such as bupivacaine, metoprolol and ketamine, enantioselectivity was significantly higher at pH 7.0. These results point to the importance of electro-

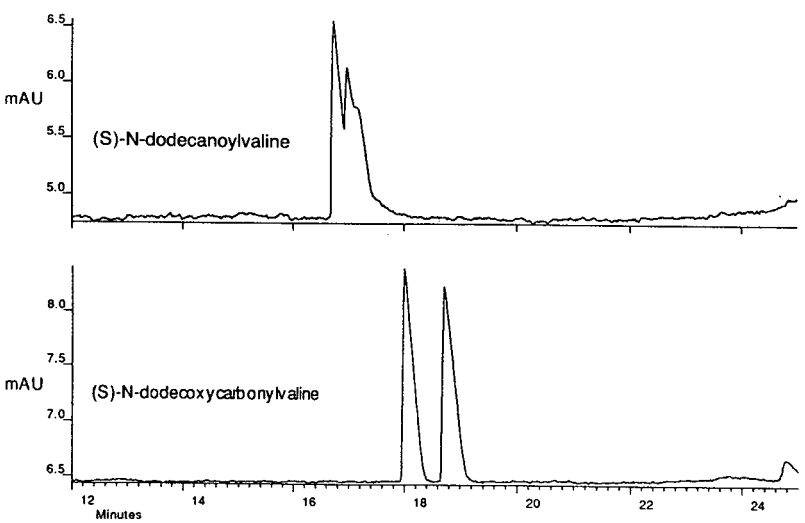

Fig. 3. Comparison of the separation of norephedrine enantiomers with (*S*)-N-dodecoxycarbonylvaline versus (*S*)-N-dodecanoylvaline. Sample: 100 μg/ml racemic norephedrine dissolved in buffer. Buffer: 25 m*M* (*S*)-N-dodecoxycarbonylvaline or (*S*)-N-dodecanoylvaline, 25 m*M* Na_2HPO_4–25 m*M* $Na_2B_4O_7$, pH 8.8.

Table 2
Comparison of enantioselectivities (α) obtained at pH 7.0 vs. pH 8.8 with 25 m*M* (*S*)-N-dodecoxycarbonylvaline

Analyte	α	
	pH 7.0	pH 8.8
Atenolol	1.05	1.04
Bupivacaine	1.26	1.05
Ephedrine	1.14	1.10
Homatropine	1.03	1.03
Ketamine	1.06	1.01
Metoprolol	1.19	1.06
N-Methylpseudoephedrine	1.38	1.32
Norephedrine	1.12	1.10
Norphenylephrine	1.09	1.09
Octopamine	1.05	1.05
Pindolol	1.09	1.06
Terbutaline	1.02	1.01

Conditions: UV detection at 214 nm; 2-s hydrostatic injection; 60 cm × 50 μm capillary; + 12 kV; pH 7.0 buffer: 50 m*M* Na_2HPO_4; pH 8.8 buffer: 25 m*M* Na_2HPO_4–25 m*M* $Na_2B_4O_7$.

static interactions in determining enantioselectivity of the system.

Generally, we have found that under typical MECC operating conditions, (i.e. uncoated capillaries at pH $\geq$ 7,) an α of 1.02, with sufficient optimization of k (see below), will allow baseline resolution. At pH 7, there was sufficient α on all but one of the compounds to allow baseline resolution, as opposed to three unresolved compounds at pH 8.8.

In MECC, k is related to surfactant concentration by the following equation [23]:

$$k = \frac{K\nu_s([\text{surf}] - \text{CMC})}{1 - \nu_s([\text{surf}] - \text{CMC})} \quad (3)$$

where K is the thermodynamic partition coefficient of the solute, ν_s is the partial molar volume of the surfactant, and CMC is the critical micelle concentration of the surfactant. As previously discussed [23], there is an optimum k value in MECC, which is determined by the ratio of t_{mc}/t_{aq} according to the following equation [26]:

$$k_{optimum} = \left(\frac{t_{mc}}{t_{aq}}\right)^{1/2} \quad (4)$$

where t_{mc} is the migration time of a solute completely partitioned into the micelle and t_{aq} is the migration time of the solute if there is no partitioning. (Note again that we have substituted t_{aq} for t_o.) Thus k, and hence resolution, can be optimized by changing the surfactant concentration.

Generally, 25 m*M* surfactant was first tested for separating an analyte. Then, if partitioning was too low, the surfactant concentration was increased. Fig. 4 shows the separation of atenolol enantiomers at surfactant concentrations of 25 and 100 m*M*. At 25 m*M*, k was 0.6 and resolution 0.8. Optimum k for these conditions was calculated to be 2.8. Thus, the surfactant concentration was increased to 100 m*M*; k increased to 2.5, thereby affording a resolution of 2.7.

An important aspect of the separations shown in Fig. 4 is that in both cases, α was 1.04 (while partitioning was significantly different). This result illustrates a large advantage of MECC over LC in methods development. The ability to optimize partitioning *independent of* α makes methods development much more straightforward in MECC. For a given column in LC, if partitioning is not optimum, the strength of the mobile phase must be altered. However, selectivity may change as well.

If partitioning is too high at 25 m*M*, lower surfactant concentrations may be employed.

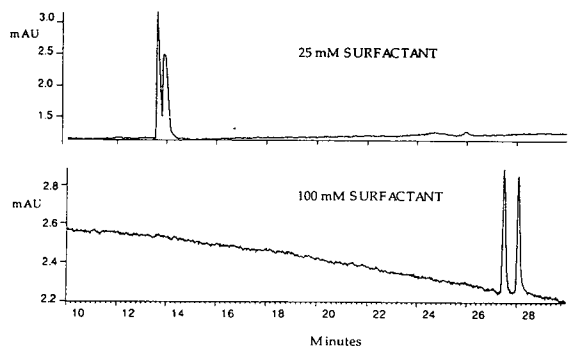

Fig. 4. Influence of surfactant concentration on the separation of atenolol enantiomers. Sample: 100 μg/ml racemic atenolol dissolved in buffer. Buffer: 25 or 100 m*M* (*S*)-N-dodecoxycarbonylvaline, 25 m*M* Na_2HPO_4–25 m*M* $Na_2B_4O_7$, pH 8.8.

However, the practical lower limit of surfactant concentration was 15 m*M*. Below this level, symmetrical peaks could not be obtained. In cases where k is still too large at 15 m*M*, organic solvent may be employed in order to decrease the analyte's thermodynamic partition coefficient. Fig. 5A and B show the separation of propranolol enantiomers at surfactant concentrations of 25 and 10 m*M*. At 25 m*M*, k was 50, and no resolution was apparent. At 10 m*M*, k decreased to 17, resulting in resolution. However, peak tailing and low plates were evident. At 25 m*M* surfactant with 30% acetonitrile, close to baseline resolution was obtained (Fig. 5C). Note that altering the analyte's thermodynamic partition coefficient by adding organic solvent, unlike changing the surfactant concentration, may change selectivity.

The ability to perform fast separations is one of the attractive features of CE. Analysis time is reduced by increasing the applied electric field. However, there is a limit to how much the field can be increased before excessive Joule heating leads to band broadening and decreased resolution. To minimize the conductivity of the MECC buffer, the phosphate–borate buffer system at pH 8.8 was replaced with the zwitterionic buffer, 2-(N-cyclohexylamino)ethanesulfonic acid (CHES). This buffer permits the separation of N-methylpseudoephedrine enantiomers in less than 90 s using an electric field of 860 V/cm and a 30 cm capillary (Fig. 6).

The ability to exactly invert the chirality of the system is an important feature of any chiral separation system. To this end, (*S*)- and (*R*)-N-dodecoxycarbonylvaline (Fig. 2a and b) were used to separate a 3:1 ratio of (*S*):(*R*) benzoin. As expected, the migration order of the two enantiomers was reversed (Fig. 7). When the (*R*)-surfactant was employed, the (*R*)-enantiomer of benzoin migrated first (top separation), while with the (*S*)-surfactant, the (*S*)-enantiomer

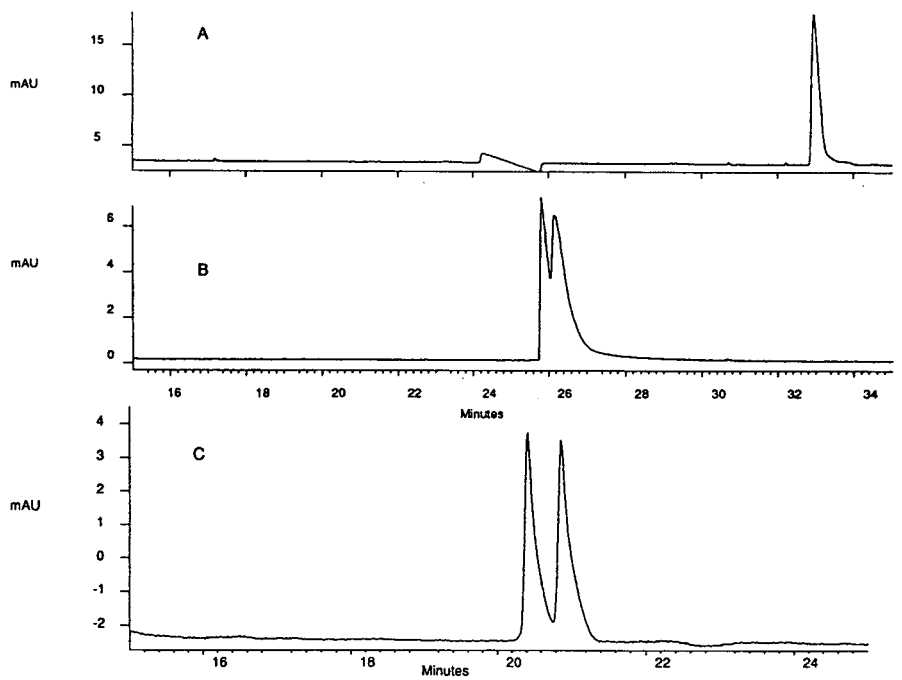

Fig. 5. Influence of surfactant concentration and acetonitrile on the separation of propranolol enantiomers. Sample: 100 μg/ml racemic propranolol dissolved in buffer. Buffers: (A) 25 m*M* (*S*)-N-dodecoxycarbonylvaline, 25 m*M* Na_2HPO_4–25 m*M* $Na_2B_4O_7$, pH 8.8; (B) 10 m*M* (*S*)-N-dodecoxycarbonylvaline, 25 m*M* Na_2HPO_4–25 m*M* $Na_2B_4O_7$, pH 8.8; (C) 25 m*M* (*S*)-N-dodecoxycarbonylvaline, 25 m*M* Na_2HPO_4–25 m*M* $Na_2B_4O_7$, pH 8.8, 30% acetonitrile.

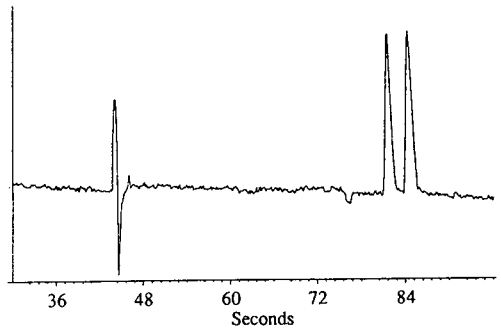

Fig. 6. Fast separation of N-methylpseudoepherine enantiomers. Sample: 100 μg/ml racemic N-methylpseudoephedrine dissolved in buffer. Buffer: 25 m*M* (*S*)-N-dodecoxycarbonylvaline, 50 m*M* CHES, pH 8.8. Capillary: 35 cm × 50 μm I.D. Voltage: +30 kV.

of benzoin migrated first. These two separations were performed sequentially on the same capillary. The α value was 1.05 and efficiencies were greater than 100 000 for both peaks.

In Fig. 7, the migration times of the first and second peaks of each separation are the same (2% difference). Migration order inversion of this nature can only be realized when the two enantiomers of the chiral selectand are employed separately and all other parameters kept constant. The migration order of enantiomers can sometimes be reversed with cyclodextrins in CE, but it requires the development of a new set of separation conditions. Thus, the amount of methods development time is significantly increased without the guarantee of enantiomer migration order reversal.

An experiment was performed in which the total concentration of surfactant was constant (25 m*M*) but different ratios of (*R*)-:(*S*)-N-dodecoxycarbonylvaline were used to separate an analyte with a large α value (N-methylpseudoephedrine, $\alpha = 1.30$). As seen in Fig. 8, α changed linearly with the % (*R*)-N-dodecoxycarbonylvaline. At 100% (*R*)- and 0% (*R*)-surfactant, α was 1.30, although the migration order of the two enantiomers was reversed. At 50% (*R*)-surfactant, no enantioselectivity was seen. At intermediate percentages, the resulting α was linear with % (*R*)-surfactant. These data suggest that the chiral recognition process involves one surfactant molecule interacting with one analyte molecule. Otherwise the α data might not be linear with surfactant optical purity. We are investigating the mixing of other chiral surfactants to improve our understanding of the chiral recognition process.

MECC has been used to perform separations of complex sample matrices such as urine, because micelles can solubilize proteinaceous

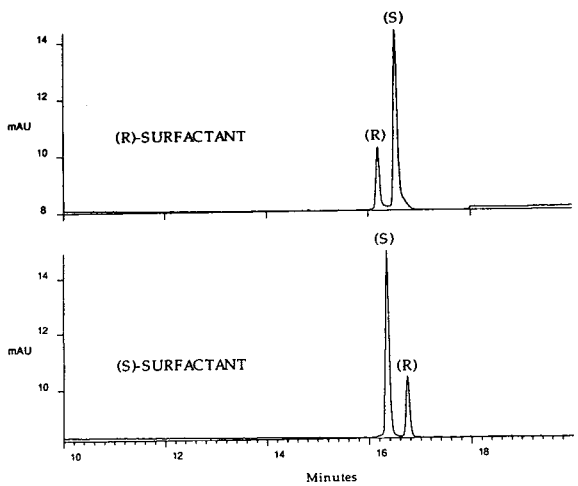

Fig. 7. Migration order reversal of benzoin enantiomers. Sample: 3:1 ratio of (*S*)- to (*R*)-benzoin dissolved in buffer. Buffer: 25 m*M* (*R*)- or (*S*)-N-dodecoxycarbonylvaline, 25 m*M* Na_2HPO_4–25 m*M* $Na_2B_4O_7$, pH 8.8.

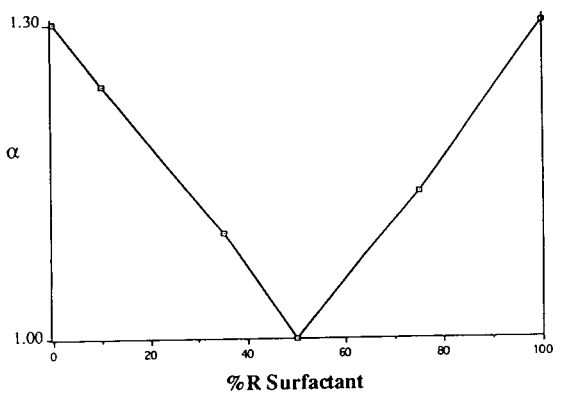

Fig. 8. Graph of enantioselectivity vs. % (*R*)-N-dodecoxycarbonylvaline. Sample: 100 μg/ml racemic N-methylpseudoephedrine dissolved in buffer. Buffer: 25 m*M* N-dodecoxycarbonylvaline, different ratios of (*R*):(*S*), 25 m*M* Na_2HPO_4–25 m*M* $Na_2B_4O_7$, pH 8.8.

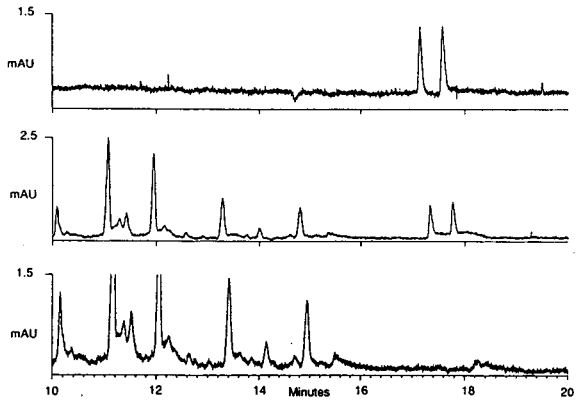

Fig. 9. Separation of ephedrine enantiomers spiked into urine. Samples: 100 μg/ml racemic ephedrine in buffer (top), 100 μg/ml racemic ephedrine in urine (middle), blank urine (bottom). Buffer: 50 m*M* (*S*)-N-dodecoxycarbonylvaline, 25 m*M* Na_2HPO_4–25 m*M* $Na_2B_4O_7$, pH 8.8.

material [27,28]. Fig. 9 shows the separation of 100 μg/ml racemic ephedrine spiked into urine using 50 m*M* (*S*)-N-dodecoxycarbonylvaline. At 25 m*M* surfactant, one of the ephedrine enantiomers co-migrated with a urine matrix peak. Increasing the surfactant concentration to 50 m*M* resolved the ephedrine enantiomer from the urine matrix peak. The only sample preparation in this case was a simple filtration step. This separation is an excellent example of the ability to perform non-chiral and chiral separations simultaneously in MECC with synthetic chiral surfactants.

4. Conclusions

MECC using synthetic chiral surfactants shows great promise as a solution to many chiral separation problems. The chiral surfactant described here can be prepared as both enantiomers, (*S*)- and (*R*)-N-dodecoxycarbonylvaline, allowing *exact* enantiomer migration order reversal. Enantioselectivity data obtained when different ratios of the (*R*)- and (*S*)-surfactants were mixed suggested that the chiral recognition process was based on one surfactant molecule recognizing one analyte molecule. For twelve pharmaceutical amines investigated, (*S*)-N-dodecoxycarbonylvaline was able to exceed a resolution objective of 1.5 for eleven. Resolution was maximized through optimization of surfactant concentration. For charged compounds, like the amines examined here, pH could be used to alter enantioselectivity and partitioning. Rapid chiral separations could be obtained by using zwitterionic buffers and high electric fields. Chiral separations in complex matrices could also be performed, with non-chiral and chiral separations occurring simultaneously. Future communications will report the performance of additional chiral surfactants as well as separation of additional compound classes.

References

[1] S.C. Stinson, *C & EN*, September 27 (1993) 38.
[2] *Chirality*, 4 (1992) 338.
[3] M. Zief and L.J. Crane (Editors), *Chromatographic Chiral Separations*, Marcel Dekker, New York, 1988.
[4] A. Guttman, A. Paulus, A.S. Cohen, N. Grinberg and B.L. Karger, *J. Chromatogr.*, 448 (1988) 41.
[6] M. Swartz, *J. Liq. Chromatogr.*, 14 (1991) 923.
[7] A. Pluyum, W. van Ael and M. de Smet, *Trends Anal. Chem.*, 11 (1992) 27.
[8] S. Wren, *J. Chromatogr.*, 636 (1993) 57.
[9] M. Nielen, *Anal. Chem.*, 65 (1993) 885.
[10] S. Busch, J. Kraak and H. Poppe, *J. Chromatogr.*, 635 (1993) 119.
[11] S. Terabe, K. Otsuka, K. Ichikawa, A. Tsuchiya and T. Ando, *Anal. Chem.*, 56 (1984) 113.
[12] K.R. Nielsen and J.P. Foley, in P. Camilleri (Editor), *Capillary Electrophoresis: Theory and Practice*, CRC Press, Boca Raton, FL, 1993, Ch. 4, p. 117.
[13] S. Terabe, M. Shibata and Y. Miyashita, *J. Chromatogr.*, 480 (1989) 403.
[14] H. Nishi, T. Fukuyama, M. Matsuo and S. Terabe, *J. Microcol. Sep.*, 1 (1989) 234.
[15] R. Cole, M. Sepaniak and W. Hinze, *J. High Resolut. Chromatogr.*, 13 (1990) 579.
[16] A. Dobashi, T. Ono, S. Hara and J. Yamaguchi, *Anal. Chem.*, 61 (1989) 1984.
[17] A. Dobashi, T. Ono, S. Hara and J. Yamaguchi, *J. Chromatogr.*, 480 (1989) 413.
[18] K. Otsuka and S. Terabe, *J. Chromatogr.*, 515 (1990) 221.
[19] K. Otsuka and S. Terabe, *Electrophoresis*, 11 (1990) 982.
[20] K. Otsuka, J. Kawahara, K. Tatekawa and S. Terabe, *J. Chromatogr.*, 559 (1991) 209.
[21] S. Miyagashi and M. Nishida, *J. Colloid Interface Sci.*, 65 (1978) 380.

[22] H. Eckert and B. Forster, *Angew Chem., Int. Ed. Engl.*, 26 (1987) 894.
[23] S. Terabe, K. Otsuka and T. Ando, *Anal. Chem.*, 57 (1985) 834.
[24] M.G. Khaledi, S.C. Smith and J.K. Strasters, *Anal. Chem.*, 63 (1991) 1820.
[25] J.K. Strasters and M.G. Khaledi, *Anal. Chem.*, 63 (1991) 2503.
[26] J. Foley, *Anal. Chem.*, 62 (1990) 1302.
[27] H. Nishi, T. Fukuyama and M. Matsuo, *J. Chromatogr.*, 515 (1990) 245.
[28] P. Lukkari, H. Siren, M. Pantsar and M. Riekkola, *J. Chromatogr.*, 632 (1993) 143.

ELSEVIER

Journal of Chromatography A, 680 (1994) 137–146

JOURNAL OF CHROMATOGRAPHY A

Use of β-cyclodextrin polymer as a chiral selector in capillary electrophoresis

Zeineb Aturki, Salvatore Fanali*

Istituto di Cromatografia del CNR, Area della Ricerca di Roma, P.O. Box 10, 00016 Monterotondo Scalo (Rome), Italy

Abstract

Enantiomers of several basic compounds of pharmaceutical interest were successfully separated by capillary electrophoresis using a modified β-cyclodextrin polymer. As the cyclodextrin contained carboxylic groups, the chiral selector could be used in either an uncharged or a charged mode, selecting the appropriate pH of the background electrolyte. The effect of the pH of the background electrolyte on the effective mobility, resolution and selectivity was studied in the range 2.6–6.2 for the enantiomer resolution of β-hydroxyphenylethylamine, norphenylephrine, terbutaline, ephedrine, norephedrine, ketamine, epinephrine and propranolol. Very good enantiomeric resolution was achieved for all the compounds except for ephedrine and norephedrine ($R < 0.5$). An increase in the pH of the electrolyte caused an inversion of mobility for either terbutaline and propranolol owing to strong complexation with the negatively charged polymer.

1. Introduction

The resolution of enantiomers is a growing field of interest in analytical chemistry, especially for biomedical and pharmaceutical analysis, because often two enantiomers of the same drug show different pharmacological or bioactive effects. Therefore, rapid, sensitive, selective and high-resolution analytical methods are required for, e.g., chiral purity control of drugs, pharmacokinetic studies and drug metabolism analysis [1].

Among the different methods used for this purpose, high-performance liquid chromatography (HPLC) has often been applied in this field using a wide variety of chiral columns in which different resolution mechanisms have been applied [2].

In recent years, capillary electrophoresis (CE) with its high resolving power has attracted great interest for the analysis of different classes of compounds including enantiomers [3–6]. Owing to the similar physico-chemical properties of enantiomers, they cannot be separated by CE unless a chiral environment is used in order to modify selectively their properties and thus the effective mobility. A chiral compound is either added to the background electrolyte [7–12] or bonded to the capillary wall [13] and the method is called the direct resolution method. Here labile diastereomeric complexes are formed during the electrophoretic process and if they exhibit different stability constants the effective mobility is selectively modified and their sepa-

* Corresponding author.

0021-9673/94/$07.00
SSDI 0021-9673(94)00531-D

ration is achieved. So far, chiral surfactants, proteins, chiral metal complexes and cyclodextrins have been used as chiral selectors for enantiomeric resolution by CE [3–6,8–10].

Cyclodextrins (CDs) are chiral compounds with the shape of a truncated cone; they are neutral and natural oligosaccharides that possess a hydrophobic cavity and a hydrophilic exterior. The presence of chiral carbons in their structure allows enantioselective interactions with several analytes. Inclusion complexation between analytes and the CD cavity stabilized by hydrogen bonds with hydroxyl groups of the CD is the main interaction involved in the enantioseparation mechanism [6,14].

Modified CDs have been shown to give a greater possibility of resolution for those compounds which cannot be resolved using the native CD, e.g., sympathomimetic drug enantiomers were completely separated with di-O-methyl-β-CD [11] and α-hydroxy acid enantiomers with methyl amino β-CD [12].

Another approach for improving the selectivity of enantiomer separation when CDs are used as chiral selector is the addition of non-chiral compounds, e.g. organic solvents [15,16] or urea [16], or the use of polymers in the chiral environment [17].

Gels in capillaries, mainly used for the separation of biopolymers [18], have been employed either as support matrices or as modified gels of CD [19,20].

Being interested in enantiomer resolution by CE and encouraged by recent results using modified CDs [12,21], we extended our study to the use of a β-CD polymer containing carboxylic groups. The polymer was added to background electrolytes at different pH values for the enantiomer separation of several basic compounds of pharmaceutical interest.

2. Experimental

2.1. Apparatus

Electrophoretic experiments were performed on a Biofocus 3000 system (Bio-Rad, Hercules, CA, USA) equipped with a UV–visible multi-wavelength detector operating either at a single wavelength (206 nm) or in the scanning mode (190–360 nm). Fused-silica capillary tube [40 cm (effective length 35.5 cm) × 50 μm I.D.] was obtained from Polymicro Technologies (Phoenix, AZ, USA) and a coated capillary cartridge (17 cm × 25 μm I.D.) from Bio-Rad. The polyimide coating of the former was removed from the capillary to create a window at the appropriate position with several drops of concentrated H_2SO_4 at 100°C. The capillary was then positioned in the cartridge. An applied voltage of 15 kV was used and the grounded compartment (close to the detector) was negative. The capillary cartridge was thermostated with circulating liquid at 25°C. The temperature of the carousel compartment was 25°C. Injection of samples was done by the electrokinetic method except for the measurements of the electroosmotic flow, which were done by pressure 5 p.s.i. s, corresponding to $35 \cdot 10^{-3}$ MPa for 1 s.

The new capillary (uncoated) was pressure-rinsed with 0.5 *M* NaOH for 10 min and then water (30 min) in order to activate the silica on the wall.

The following washing steps were used prior to each electrophoretic run: (1) water for 60 s; (2) 0.010 *M* NaOH for 60 s; (3) water for 200 s; (4) background electrolyte for 60 s.

2.2. Chemicals

Soluble anionic β-CD polymer (for its characteristics see Table 1) was purchased from Cyclolab (Budapest, Hungary). (±)-Epinephrine, D,L-β-hydroxyphenethylamine, D,L-pro-

Table 1
Characteristics of anionic β-cyclodextrin polymer

Polymer type	Carboxymethylated-β-cyclodextrin
Producer	Cyclolab (Budapest, Hungary)
Molecular mass	6000–8000
Solubility in water	>20%
CD content	50–60%
COO^- content	3–4%
COO/CD	2
Cross-linking	1-Chloro-2,3-epoxypropane

pranolol, ketamine, (±)-ephedrine, (±)-terbutaline, (+)-ephedrine, (−)-ephedrine and (−)-epinephrine were obtained from Sigma (St. Louis, MO, USA) (±)-norphenylephrine from Aldrich (Steinheim, Germany) and methanol, sodium dihydrogenphosphate, sodium acetate, acetic acid and phosphoric acid from Carlo Erba (Milan, Italy).

The background electrolyte (BGE) composition was 0.065 *M* phosphate buffer (pH 2.5), 0.051 *M* phosphate buffer (pH 3.5), 0.05 *M* sodium acetate–acetic acid (pH 4.5) and 0.075 *M* phosphate buffer (pH 6.2). The buffers of pH 2.5 and 3.5 were prepared by dissolving the appropriate amount of NaH_2PO_4 in 50 ml of doubly distilled water, titrating the mixtures with tenfold diluted H_3PO_3 (85%) and adjusting the volume to 100 ml, while for the buffer at pH 6.2 Na_2HPO_4 was used.

CD polymer was dissolved daily in the buffer and the solutions were filtered through a 0.45-μm filter.

Stock solutions of $2 \cdot 10^{-3}$ *M* racemic standard were prepared and stored at 4°C and diluted with doubly distilled water to $2 \cdot 10^{-5}$ *M* or as otherwise described.

3. Results and discussion

One of the main drawbacks encountered when β-CD is used as a chiral additive in capillary electrophoresis is its low solubility in water (about 1.8%, w/v). One solution to this could be to use a modified β-CD with a higher solubility than the parent compound. The modification is achieved by changing one or more hydroxyl groups on the rim of the CD by introducing other groups, e.g., sulphate, phosphate, carboxylate, methylamino, by chemical reaction.

As shown previously, the use of modified CDs in CE not only allows the application of larger amounts of CD but can also markedly improve the selectivity of enantiomer separation [11,12,18]. Chemical modification of a CD can change the hydrophobicity of the cavity and can allow the formation of other stereoselective bonds (polar, hydrophobic) between substituent groups on the CD cavity and on the chiral centre of the analytes.

β-CD polymer was used as a chiral selector additive to the BGE for the enantiomeric separation of several basic compounds. The analysed compounds (for the structures see Fig. 1) were run in a BGE at different pH in the range 2.5–6.2. They moved in the direction of the cathode owing to the protonation of the amino group. The apparent mobility, $\mu_{app} = \mu_e + \mu_{eof}$ (where e and eof represent effective and electroosmotic flow, respectively) was calculated using the following equation:

$$\mu_{app} = \frac{lL}{t_x V} + \frac{lL}{t_0 V} \quad (1)$$

where l and L are the effective and total length of the capillary, respectively, V the applied voltage and t_x and t_0 the migration time of the sample and the electroosmotic marker, respectively.

Different amounts of β-CD polymer (0–20 mg ml^{-1}) were added to the BGE in order to study the effect of the concentration of the chiral selector on the electrophoretic mobility and resolution of the analysed compounds.

Fig. 2 illustrates the electrophoretic process at pH 2.5 and 4.5. At a low pH the carboxylic groups of the CD polymer are protonated and therefore the chiral selector is moving with the velocity of the electroosmotic flow as a quasi-stationary phase. An increase in pH will cause the polymer to be negatively charged owing to the dissociation of the carboxylic groups; in this case the velocity of the chiral selector is influenced not only by the charge of the analyte and the electroosmotic flow but also by the electrophoretic mobility of the complex formed between the analyte and the polymer.

3.1. Effect of concentration of β-cyclodextrin polymer and pH on effective mobility

Fig. 3 shows the effect of β-CD polymer on the effective mobility of the analysed drugs when a BGE at pH 2.5 was used. On increasing the concentration of the chiral selector on the BGE,

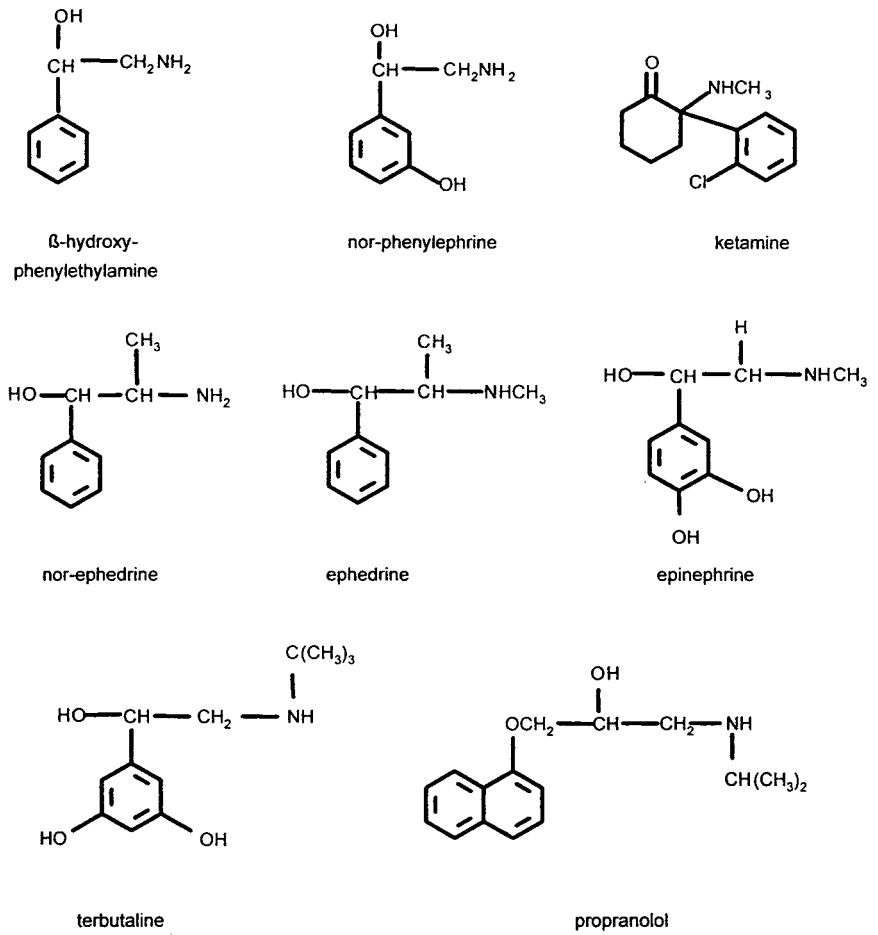

Fig. 1. Structures of the standard compounds used in the electrophoretic study.

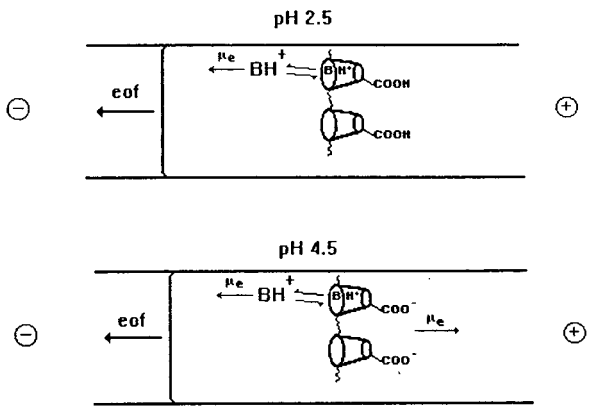

Fig. 2. Illustration of the electrophoretic process when a chargeable β-CD polymer is used as a chiral additive to the background electrolyte.

a general decrease in mobility was recorded owing to complexation between the analytes and β-CD polymer. The affinity of the CD polymer towards the analytes was found to be propranolol > terbutaline > norphenylephrine > β-hydroxyphenylethylamine = ephedrine = norephedrine > epinephrine, considering the estimated difference of effective mobility $\Delta\mu_e = \mu_{e20} - \mu_{e0}$, where μ_{e0} and μ_{e20} are the effective mobilities of the sample in absence and presence of 20 mg ml^{-1} of CD, respectively (μ_{e20} is referred to the enantiomer with lower mobility). The electroosmotic flow was measured by separately injecting benzyl alcohol and methanol (195 nm) and no noticeable change was found on increasing the concentration of the CD in the BGE

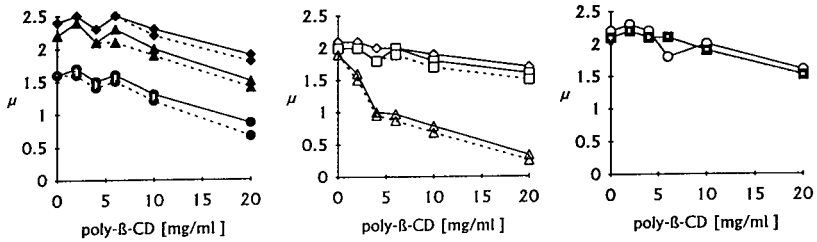

Fig. 3. Effect of β-CD polymer concentration on the effective mobility of the studied compounds. Run conditions: capillary, 40 cm (35.5 cm to detector) × 0.050 mm I.D., uncoated; background electrolyte, 0.065 *M* phosphate buffer (pH 2.5) containing the appropriate amount of β-CD polymer; detection wavelength 206 nm; applied voltage, 15 kV; current, 38 μA; temperature, 25°C; injection, electrokinetic, 5 kV, 5 s. ◆ = β-Hydroxyphenylethylamine; ▲ = norphenylephrine; ● = terbutaline; ◇ = ketamine; □ = epinephrine; △ = propranolol; ■ = ephedrine; ○ = norephedrine. μ in 10^{-4} cm^2 V^{-1} s^{-1}.

($0.64 \cdot 10^{-4}$ and $0.52 \cdot 10^{-4}$ cm^2 V^{-1} s^{-1} at 0 and 20 mg ml^{-1} of CD, respectively).

In order to verify the effect of pH on the effective mobility of the compounds studied, electrophoretic experiments were performed using the BGE at pH 3.5, 4.5 and 6.2. Fig. 4 shows the effect of the pH on the electroosmotic flow, μ_{eof}, with and without 10 mg ml^{-1} of poly-β-CD. As expected, the electroosmotic flow rose on increasing the pH of the BGE. However, the addition of the β-CD polymer to the BGE at the operating pH did not markedly influence the electroosmotic flow.

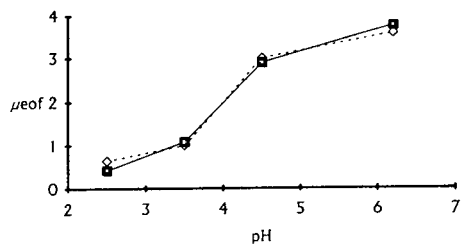

Fig. 4. Effect of pH of the background electrolyte on the electroosmotic flow (μ_{eof}) when the background electrolyte was used in (◇) the absence and (■) the presence of 10 mg ml^{-1} of chiral polymer; μ_{eof} in 10^{-4} cm^2 V^{-1} s^{-1}.

Fig. 5 shows the influence of the concentration of poly-β-CD added to the BGE at pH 4.5 on the effective mobility of the compounds studied. When the analysis was performed in the BGE at pH 4.5 in the absence of chiral polymer, the migration time of the analysed compounds decreased with increase in pH owing to the increase in the electroosmotic flow. The addition of the chiral additive to the BGE caused a general decrease in effective mobility owing to the complexation of the analytes with the polymer additive. At pH 4.5 we observed a stronger complexation than that obtained at lower pH, which can be ascribed to the charge of the β-CD polymer. This effect is markedly observed when 6 mg ml^{-1} of poly-β-CD was used for propranolol enantiomers that are moving behind the electroosmotic flow. This means that their complexation is so strong that the diastereomeric complexes are negatively charged, but the two

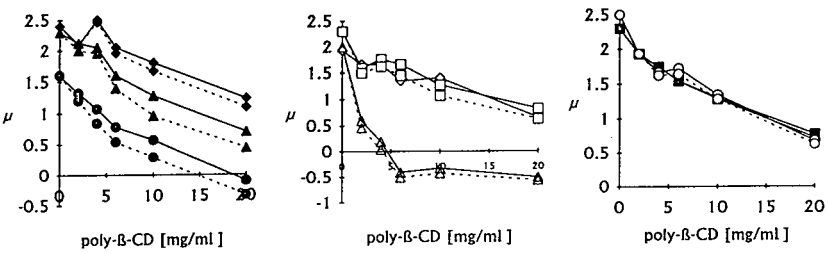

Fig. 5. Effect of the concentration of poly-β-CD on the effective mobility of the studied compounds at pH 4.5. Run conditions: background electrolyte, 0.05 *M* sodium acetate (pH 4.5); applied voltage, 15 kV; current, 39 μA; other experimental conditions as in Fig. 3. For symbols, see Fig. 3; μ in 10^{-4} cm^2 V^{-1} s^{-1}.

isomers are moving in the direction of the cathode owing to the presence of a relatively strong electroosmotic flow.

The same effect was recorded for terbutaline enantiomers but when 20 mg ml^{-1} of poly-β-CD were added to the BGE at pH 4.5. A similar effect was recently observed using chargeable cyclodextrins [18].

Inversion of the electrophoretic mobility was also obtained at pH 3.5 when the BGE was supported with 10 mg ml^{-1} of poly-β-CD but only for propranolol (results not shown).

Fig. 6 shows as an example the separation of a standard mixture containing β-hydroxyphenylethylamine, terbutaline and propranolol, where inversion of the mobility of propranolol and terbutaline can be observed.

Electrophoretic runs performed at pH 6.2 with different amounts of chiral polymer showed a general decrease in the electrophoretic mobility for all the compounds analysed that was more evident than at lower pH. We conclude that the affinity of the analysed compounds for poly-β-CD is as follows [after considering $\Delta\mu_{e(20-)}$]: propranolol > terbutaline > norphenylephrine > norephedrine > β-hydroxyphenylethylamine > epinephrine > ketamine. It is clear that the complexation is strongly influenced by the pH of the BGE, increasing concomitantly.

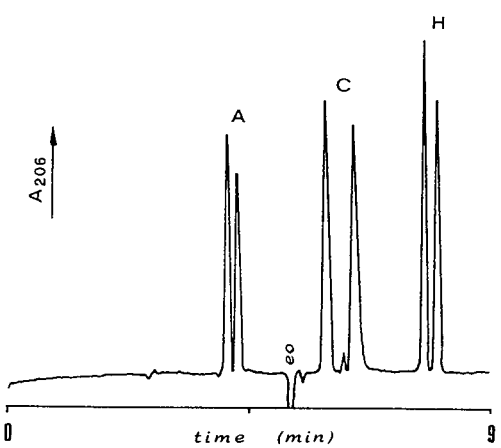

Fig. 6. Electropherogram of the separation of enantiomers of (A) norphenylephrine, (C) terbutaline and (H) propranolol. Background electrolyte, 0.05 *M* acetate buffer (pH 4.5) and 20 mg ml^{-1} of poly-β-CD; applied voltage, 15 kV; current, 39 μA; sampling, 5 kV, 5 s of (A, B) $5 \cdot 10^{-5}$ *M* and (C) $5 \cdot 10^{-6}$ *M*.

3.2. Effect of concentration of β-cyclodextrin polymer and pH on enantiomer resolution

The resolution, *R*, was calculated using the following equation:

$$R = 2\left(\frac{t_2 - t_1}{w_2 + w_1}\right) \quad (2)$$

where t_2 and t_1 are the migration times and w_2 and w_1 the widths at the baseline of the two enantiomers of lower and higher mobility, respectively.

Fig. 7 shows the effect of the amount of poly-β-CD added to the BGE at pH 2.5, 3.5, 4.5 and 6.2 on the resolution of the studied racemic mixtures.

At low pH (2.5) the enantiomers were not resolved for either ketamine or norephedrine, even if the concentration of the chiral additive was increased, while ephedrine enantiomers showed poor resolution ($R < 0.5$) at 20 mg ml^{-1} of poly-β-CD. This was not surprising considering that previously we did not resolve these compounds with β-CD at pH 2.4 [11].

Considering that inclusion complexation is probably a stereoselective resolution mechanism, we can assume that the aromatic groups of the three analysed compounds fit the cavity of the β-CD and hydrogen bonds are formed between hydroxyl and nitrogen groups in the chiral centres of ephedrine and norephedrine with hydroxyl and carboxyl groups on the rim of the CD. In the case of ketamine these possibilities are reduced because no hydroxyl substituents are in the chiral centre.

The chemical structure of epinephrine is similar to that of ephedrine, the difference being in the presence of hydroxyl groups at position 3 and 4 of the aromatic ring. When epinephrine was analysed at pH 2.5, poor enantiomer resolution was obtained when the BGE was supplemented with 6 mg ml^{-1} of poly-β-CD. The resolution was improved by increasing the amount of chiral additive ($R = 1$ and 2.4 at 10 and 20 mg ml^{-1} of

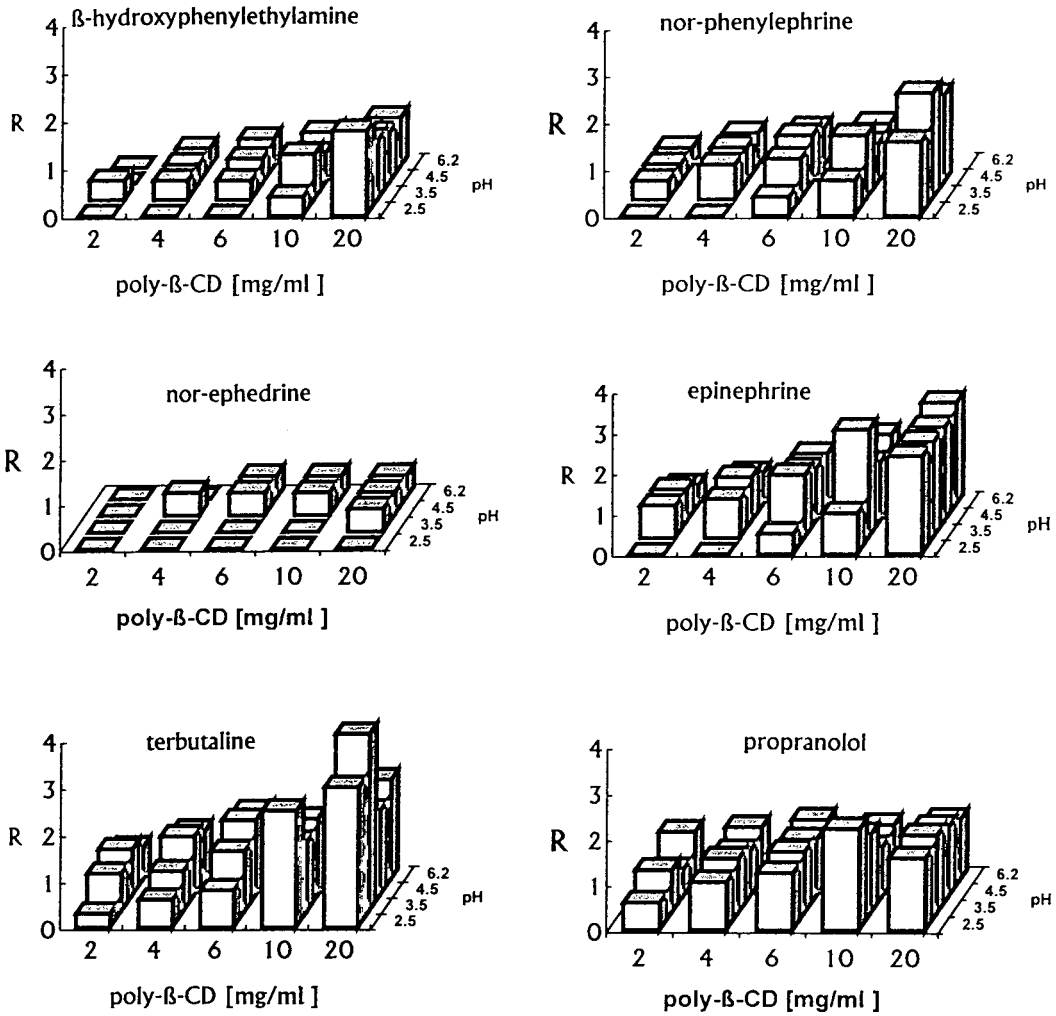

Fig. 7. Effect of the concentration of β-CD polymer on the resolution of the sample compounds at different pH. Applied voltage, 15 kV; current, 38–62 μA. For other experimental conditions, see text.

poly-β-CD, respectively). In order to explain the higher resolution of the two enantiomers of epinephrine compared with the results obtained for ephedrine, we can assume that the two hydroxyl groups on the aromatic ring form stabilizing bonds with the chiral polymer.

In order to obtain a baseline resolution of norphenylephrine and β-hydroxyphenylethylamine, it was necessary to use 6 and 10 mg ml^{-1} of poly-β-CD at pH 4.5 and 3.5, respectively. Also in this instance the resolution was influenced by the amount of chiral selector added to the BGE and by the pH. The maximum resolution, $R = 2.25$, was recorded at pH 3.5 for norphenylephrine and $R = 1.77$ at pH 2.5 for β-hydroxyphenylethylamine when the BGE was supported with 20 mg ml^{-1} of polymer. For both compounds an increase in the pH of the BGE caused a decrease in R when the same amount of chiral additive was used.

The enantiomer resolution of norphenylephrine at pH 6.2 (20 mg ml^{-1} of poly-β-CD) could not be measured owing to the migration of one of the two resolved enantiomers with the

electroosmotic flow. This is, of course, a limitation for quantitative analysis when charged poly-β-CD is used as a chiral additive for enantiomer separation. The same drawback was observed for terbutaline and epinephrine at pH 6.2 (10 and 20 mg ml^{-1} of polymer, respectively). This effect is depicted in Fig. 8b while Fig. 8a shows a good separation of (+)- and (−)-epinephrine obtained at the same pH but at a lower concentration of chiral additive.

Terbutaline and propranolol showed maximum resolution at pH 3.5 ($R = 3.8$) and 2.5 ($R = 2.22$) with 20 and 10 mg ml^{-1} of poly-β-CD, respectively. The two compounds were baseline resolved even when 2 mg ml^{-1} of chiral polymer was added to the BGE at pH 6.2 (propranolol) and 4.5 (terbutaline). At relatively high concentrations of poly-β-CD (10 and 20 mg ml^{-1}) an increase in pH caused a decrease in resolution for terbutaline and propranolol whereas at lower concentration the resolution increased. Also in this instance the amount of polymer had a very important effect on the resolution; in fact, R_s generally increased with increasing amount of chiral additive. The results indicated that the use of a pH lower than 4.5 resulted in a better resolution of both propranolol and terbutaline enantiomers when the concentration of the chiral selector was 10 and 20 mg ml^{-1}. It seems that the strong ion-pairing effect slightly deteriorates the resolution. To explain the stronger complexation of terbutaline and propranolol with the additive in comparison with the other analytes studied we have to consider the inclusion complexation with the β-CD in the polymer, the ion-pair interaction and probable adsorption.

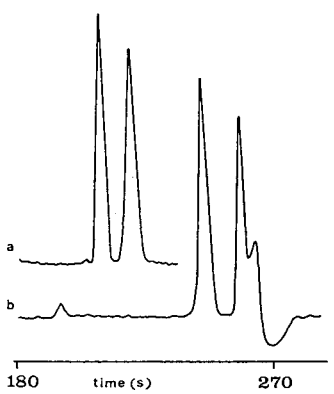

Fig. 8. Electrophoretic separation of a racemic mixture of epinephrine at pH 6.2. The background electrolyte contained (a) 10 and (b) 20 mg ml^{-1} of poly-β-CD. Run conditions: applied voltage, 15 kV; current, 60 μA; injection, 7 kV, 7 s of $5 \cdot 10^{-5}$ *M* racemic epinephrine; capillary, 40 cm × 0.05 mm I.D. (uncoated).

Further, a general decrease in *R* was obtained at pH 6.2 for terbutaline and propranolol probably owing to the strong electroosmotic flow that caused a decrease in migration time compared with those obtained at lower pH. The chiral recognition is a result of dynamic equilibrium between the enantiomers and the chiral selector; thus at pH 6.2 the number of dynamic exchanges is smaller owing to the shorter time. Hence we can stress the importance of the control of the electroosmotic flow for the optimum experimental separation conditions when such a polymer is used in CE.

Experiments performed by injecting the enantiomers of propranolol showed that the *R*-isomer forms more stable diastereomeric complexes than the *S*-isomer with the poly-β-CD; in fact, in all instances the *R*-isomer moved with a longer migration time. As can be seen in Fig. 1, the charged CD polymer moves in the opposite direction to the electroosmotic flow, decreasing the effective mobility of the two isomers. With epinephrine the (+)-isomer moved with a lower effective mobility than its enantiomer, showing a higher affinity for the chiral selector.

Experiments performed in a coated capillary (17 cm × 0.025 mm I.D.) allowed rapid enantiomeric resolution even with a relatively small amount of chiral polymer. At pH 2.5 no noticeable electroosmotic flow was recorded but very broad peaks were obtained for propranolol and terbutaline enantiomers, probably owing to adsorption of the analytes. The negative effect was more evident when the amount of chiral selector was increased. An increase in the pH of the BGE caused a strong electroosmotic flow and poor reproducibility of the migration time, probably owing to adsorption of poly-β-CD on the

capillary wall, which will be negatively charged. Unfortunately, the nature of the coating of the capillary is not known (this is a Bio-Rad patent), so it is not possible to understand the interactions between the polymer used as the chiral selector and the capillary wall.

Fig. 9a shows, as an example, the electrophoretic separation of a standard mixture containing (*R*) and (*S*)-propanolol (enriched in the *R*-isomer) using a coated capillary. By reversing the polarity (the analytes were moving as anions towards the anode) we obtained inversion of the migration order of the two enantiomers (see Fig. 9b).

So far the use of coated capillaries has been hindered by the irreproducibility of the analytical results obtained. We have been trying to improve these results by different approaches such as washing the capillary.

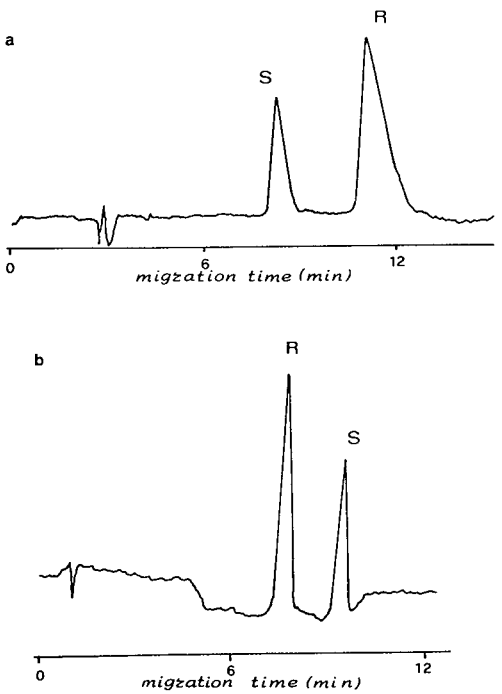

Fig. 9. Electrophoretic separation of a mixture containing (*S*)- and (*R*)-propranolol (1:2). Capillary: 17 cm × 0.025 mm I.D. (coated); background electrolyte 0.05 *M* acetate buffer (pH 4.5) and (a) 10 and (b) 20 mg ml^{-1} of poly-β-CD; applied voltage, 12 kV; current, 20 μA; injection, pressure 10 psi corresponding to $35 \cdot 10^{-3}$ MPa for 2 s. Analytes were moving towards (a) the cathode (−) and (b) the anode (+).

4. Conclusions

We have demonstrated that a chargeable β-CD polymer can be advantageously employed for the enantiomeric resolution of basic compounds of pharmaceutical interest in a relatively short time (less than 5 min). Resolution and complexation are influenced by the amount of chiral polymer (generally increasing with increasing amount of chiral additive), the shape of the analyte molecule and the pH of the background electrolyte. The chiral additive can be easily used in a wide pH range, giving the opportunity to control both the electroosmotic flow and the charge of the cyclodextrin polymer. The latter effect is very important in order to enhance the ion-pairing effect with the analytes and reverse the migration order, which is important when the minor component in a enantiomeric mixture has to be determined.

In order to select the optimum electrophoretic separation conditions, the composition of the BGE has to be selected so as to avoid the use of a pH and a poly-β-CD concentration such that the mobility of the enantiomers is close to that of the electroosmotic flow.

Owing to the use of a limited amount of electrolyte (vials of 500 μl are used with the electrophoresis apparatus), this method is cheap in comparison with others where expensive stationary phases are required.

Further studies will be carried out in order to verify the effect of organic modifiers on the resolution of enantiomeric compounds.

References

[1] J. Gal, in I.W. Wainer (Editor), *Drug Stereochemistry: Analytical Methods and Pharmacology*, Marcel Dekker, New York, 1993, pp. 65–106.

[2] I.W. Wainer, in I.W. Wainer (Editor), *Drug Stereochemistry: Analytical Methods and Pharmacology*, Marcel Dekker, New York, 1993, pp. 139–182.

[3] J. Snopek, I. Jelinek and E. Smolkova-Keulemansova, *J. Chromatogr.*, 609 (1992) 1.
[4] R. Kuhn and S. Hoffstetter-Kuhn, *Chromatographia*, 34 (1992) 505.
[5] K. Otsuka and S. Terabe, in N. Guzman (Editor), *Capillary Electrophoresis Technology*, Marcel Dekker, New York, 1993, pp. 617–629.
[6] S. Fanali, in N. Guzman (Editor), *Capillary Electrophoresis Technology*, Marcel Dekker, New York, 1993, pp. 731–752.
[7] S. Terabe, *Trends Anal. Chem.*, 8 (1989) 129.
[8] S. Terabe, M. Shibata and Y. Miyashita, *J. Chromatogr.*, 480 (1989) 403.
[9] S. Busch, J.C. Kraak and H. Poppe, *J. Chromatogr.*, 635 (1993) 119.
[10] L. Valtcheva, J. Mohammed, G. Pettersson and S. Hjertén, *J. Chromatogr.*, 638 (1993) 263.
[11] S. Fanali, *J. Chromatogr.*, 474 (1989) 441.
[12] A. Nardi, E. Eliseev, P. Boček and S. Fanali, *J. Chromatogr.*, 638 (1993) 247.
[13] S. Mayer and V. Schurig, *J. High Resolut. Chromatogr.*, 15 (1992) 129.
[14] J. Szejtli, *Cyclodextrins and Their Inclusion Complexes*, Akadémiai Kiadó, Budapest, 1982.
[15] S.A.C. Wren and R.C. Rowe, *J. Chromatogr.*, 609 (1992) 363.
[16] S. Fanali, *J. Chromatogr.*, 545 (1991) 437.
[17] D. Belder and G. Schomburg, *J. High Resolut. Chromatogr.*, 15 (1992) 686.
[18] A.S. Cohen, A. Paulus and B.L. Karger, *Chromatographia*, 24 (1987) 15.
[19] A. Guttman, A. Paulus, A.S. Cohen, N. Grinberg and B.L. Karger, *J. Chromatogr.*, 488 (1988) 41.
[20] I.D. Cruzado and G. Vigh, *J. Chromatogr.*, 608 (1992) 421.
[21] T. Schmitt and H. Engelhardt, *Chromatographia*, 37 (1993) 475.

ELSEVIER

Journal of Chromatography A, 680 (1994) 147–155

JOURNAL OF CHROMATOGRAPHY A

Systematic approach to treatment of enantiomeric separations in capillary electrophoresis and liquid chromatography. I. Initial evaluation using propranolol and dansylated amino acids

Sharron G. Penn[a], Gaoyuan Liu[a], Edmund T. Bergström[a], David M. Goodall[a,*], John S. Loran[b]

[a] *Department of Chemistry, University of York, York, YO1 5DD, UK*
[b] *Pfizer Central Research, Sandwich, Kent, CT13 9NJ, UK*

Abstract

A systematic approach is outlined for treatment of enantiomeric separations in capillary electrophoresis (CE) and liquid chromatography (LC) using chiral mobile phase additives. General equations and data analysis methods are presented to relate mobilities or capacity factors to equilibrium constants in binding equilibria, and to maximise mobility or retention time differences as a function of selector concentration. The use of cyclohexanol as a competitor is shown to be beneficial in optimising chiral separations of species which bind strongly to β-cyclodextrins. This general treatment has been applied with the test systems 1: propranolol and β-cyclodextrin and 2: dansylated amino acids and β-cyclodextrin. Chiral separations and binding constants, determined using LC with β-cyclodextrin as a mobile phase additive or a chiral stationary phase, are compared with results using the same selector in CE for system 2. Mobile phase equilibria defined by CE reveal more complex stationary phase binding equilibria in LC. Our studies make a link between LC and CE which may allow rational separation strategies to be transferred between the two fields.

1. Introduction

Chiral analysis in the separation sciences has become increasingly important in recent years due to differences in biological activity of the enantiomers of pharmacologically active compounds [1]. In liquid chromatography (LC) analysis of the different enantiomers is brought about by use of either a chiral stationary phase, or by the addition of chiral additives in the mobile phase. Sybilska and co-workers [2,3] have developed a systematic treatment for use with cyclodextrins (CDs) acting either via complexation in the mobile phase or as a dynamically generated stationary phase. Equations giving the dependence of capacity factors on the CD concentration have been used to determine enantioselective binding constants for a series of chiral barbiturates with β-CD. Similar equations have been used for considering variation of separation factor with β-CD concentration for some positional isomers [4]. In the emerging field of chiral capillary electrophoresis (CE) separation is carried out by adding to the run-

* Corresponding author.

0021-9673/94/$07.00
SSDI 0021-9673(94)00404-W

ning buffer additives such as bile salts [5], chiral surfactants [6], and cyclodextrins [7]. Some recent papers have looked for a strategy to optimise chiral CE with the use of cyclodextrin additives. Wren and Rowe [8] have developed a theoretical model relating mobility to the concentration of a cyclodextrin selector. Their analysis suggested that an optimum CD concentration exists for a particular chiral separation, and this was observed using propranolol and methyl-β-cyclodextrin (Me-β-CD) as a model system. In our previous paper we have extended this treatment [9], showing how binding constants could be derived and giving an application to the system tioconazole and hydroxypropyl-β-cyclodextrin (HP-β-CD). Maximum mobility difference was shown to occur when the selector concentration equalled the reciprocal of the average binding constant. Rawjee and co-corkers [10–12] have developed a multiple-equilibria-based model to account for separation of chiral weak acids and bases as a function of both pH and β-CD. In this paper we aim to find a master approach linking the methods of processing results from chiral CE, and chiral LC methods through the use of both mobile phase additives and chiral stationary phases. In short, can CE methods of optimisation be applied to LC?

2. Theory

2.1. Determination of binding constants, and prediction of resolution in CE

Chiral separations can take place in CE by the addition of a chiral selector, such as cyclodextrin, to the mobile phase. Binding constants can be determined from the dependence of mobility of the analyte on the selector concentration,

$$KC = \frac{\mu_0 - \mu}{\mu - \mu_\infty} \tag{1}$$

where K is the binding constant, and μ, μ_0, μ_∞ are the mobilities of the analyte at concentration of free selector C, mobility of free analyte, and mobility of the analyte:selector complex, respectively. Whilst μ and μ_0 are measured experimentally, μ_∞ and K are obtained by a non-linear least squares fit of the data to Eq. 1 [13]. The experimental set of data for a pair of enantiomers gives the values of binding constants K_1 and K_2 for the two enantiomers. When viscosity varies with selector concentration, observed mobilities, μ_{eff}, should be converted to corrected mobilities before fitting to Eq. 1 [8].

$$\mu = \mu_{\text{eff}} \frac{\eta}{\eta_0} \tag{2}$$

where η_0 and η are viscosities at selector concentration zero and C, respectively.

The selectivity α can be calculated from,

$$\alpha = \frac{K_2}{K_1} \tag{3}$$

The mobility difference $\Delta\mu$ for the enantiomers is dependent on ΔK, the difference of binding constants via the relationship [9,13],

$$\frac{\Delta\mu}{\mu_0 - \mu_\infty} = \frac{-\Delta K}{\bar{K}} \cdot \frac{\bar{K}C}{(1 + \bar{K}C)^2} \tag{4}$$

where $\bar{K}$ is the average binding constant $(K_1K_2)^{1/2}$. Fitting data to this equation allows the difference in binding constants of the two enantiomers to be determined with greatest precision. By differentiation of Eq. 4 with respect to C, it can be shown that the maximum value of the mobility difference occurs when the concentration of cyclodextrin is the reciprocal of the average binding constant, allowing prediction of the optimum concentration to use. An equation for predicting the concentration for maximum resolution has also been developed [13]. Whilst previous treatments of resolution have assumed μ to be a function of concentration, whilst D, the diffusion coefficient is constant, we adopt a self-consistent approach in which Eq. 1 is used to give the variation of both μ and D with concentration of free selector C.

Resolution R_s, is given by,

$$R_s = \frac{F\,\Delta K(\mu_0 - \mu_\infty)}{4\sqrt{2}\bar{K}} \left[\frac{Vlze}{LkT\mu_\infty(\mu_\infty + \mu_{\text{eo}})}\right]^{1/2} \tag{5}$$

where V is the applied voltage, L the length of the capillary, l the length to the detector, z the charge on the analyte, e the electronic charge, k the Boltzmann constant, T the absolute temperature, μ_{eo} the electroosmotic mobility and,

$$F = \frac{\bar{K}C}{(1 + \bar{K}C)(\beta + \bar{K}C)^{1/2}(\gamma + \bar{K}C)^{1/2}}$$

$$\gamma = \frac{\mu_0 + \mu_{eo}}{\mu_\infty + \mu_{eo}}$$

$$\beta = \frac{\mu_0}{\mu_\infty}$$

Differentiation of Eq. 5 with respect to $\bar{K}C$ gives the condition for maximising R_s. Thus with a knowledge of the electroosmotic flow and electrophoretic mobility of the analyte and analyte–selector complex, a prediction of resolution can be made at any selector concentration.

2.2. LC, with and without chiral mobile phase additives

Various cases for chiral discrimination in LC can be considered. The following treatment builds on that given by Sybilska et al. [2]. They gave equations relating capacity factors and selector concentration, for our cases 1 and 4, and we extend this to discuss optimisation of selector concentration and links with CE.

Case 1. Chiral mobile phase additives and achiral stationary phase. All discrimination in the mobile phase. *Case 2.* Chiral mobile phase additives partially bound to achiral stationary phase. Discrimination in both mobile and stationary phase. *Case 3.* Dynamically coated chiral stationary phase. All discrimination in the stationary phase. *Case 4.* Covalently bonded chiral stationary phase. All discrimination in the stationary phase.

Case 1

This is analogous to CE with mobile phase additives as discussed in section 2.1, and therefore an identical rational separation strategy applies for optimising the selector concentration in the two techniques. In this case, k', the capacity factor (or retention factor [14]), versus C, the concentration of the free selector, is a binding curve analogous to the CE binding curve of μ vs. C, with equations for the curve

$$k'_1 = \frac{k'_A}{1 + K_1 C}$$

$$k'_2 = \frac{k'_A}{1 + K_2 C} \quad (6)$$

where k'_1 and k'_2 are capacity factors for the two enantiomers and k'_A the capacity factor for the free analyte. Data fitting of k' as a function of C allows binding constants to be determined.

Upon rearrangement we obtain,

$$\frac{\Delta t}{t_A - t_0} = \frac{\Delta K \quad \bar{K}C}{\bar{K}\ (1 + \bar{K}C)^2} \quad (7)$$

where t_0 is the time for unretained species to elute, t_A the elution time for the free analyte A, and Δt the difference in enantiomer elution times. It should be noted that the right hand side of this equation is identical in magnitude to Eq. 4 for CE, and predicts that Δt will go through a maximum at a concentration of free selector equal to the reciprocal of the average binding constant.

Case 3 and 4

We assume that all binding to the stationary phase occurs at the chiral selector sites. Whilst individual binding constants cannot be obtained directly from LC without knowledge of phase ratios, the ratio of capacity factors is equal to the ratio of binding constants,

$$\frac{k'_2}{k'_1} = \frac{K_2}{K_1} = \alpha \quad (8)$$

This equation will hold using a dynamically coated or covalently bonded chiral selector, either in LC or electrochromatography.

Case 2

This is intermediate between case 1 and cases 3 and 4. In general, competition between chiral discrimination in the mobile and stationary phase

is expected to lead to overall discrimination less than cases 3 and 4.

3. Experimental

Capillary electrophoresis experiments were carried out on a P/ACE 2100 system (Beckman, High Wycombe, UK), thermostatted at 25°C. Each experiment was run in triplicate, with mesityl oxide as a neutral marker. Relative viscosity was determined by taking the ratio of the current I, at [CD] = 0 and at [CD] = C ($I_0/I = \eta/\eta_0$) [8].

Methyl-β-cyclodextrin was a gift from Wacker Chemicals (Halifax, UK). All other materials were from Aldrich (Gillingham, UK). The fused-silica separation capillary for the propranolol work had an internal diameter of 50 μm, a total length of 57 cm and a length of 50 cm from inlet to detector. A voltage of 20 kV was used for the separation, and detection was at 200 nm. The samples were loaded by a 1-s pressure injection (corresponding to 1 nl) from a 0.6 mM solution in run buffer. The pH 7.4 buffer was prepared by titrating 200 mM Na_2HPO_4 with 5 M phosphoric acid, and diluting 5-fold. The pH 3.0 buffer was prepared by titrating 40 mM LiOH with 5 M phosphoric acid.

The fused-silica separation capillary for the dansyl-amino acid work had an internal diameter of 20 μm, a total length of 27 cm and a length of 20 cm from inlet to detector. Separation voltage was 30 kV, and detection at 254 nm. The samples were loaded by a 3-s pressure injection (corresponding to 0.2 nl) from a 0.5 mM solution of dansyl-amino acid in run buffer that had been diluted by a factor of 10 with water, to induce stacking. The pH 6.8 buffer (total final ionic strength = 200 mM) was prepared by mixing 50 mM Na_2HPO_4 and 50 mM NaH_2PO_4; methanol was added in the ratio methanol:buffer (20:80), and then cyclodextrin was added in varying amounts.

The HPLC system consisted of a ternary gradient pump (ACS, Model 352), an injection valve (Rheodyne 7152) with a 20-μl loop, and a variable-wavelength UV detector (ACS, 750/12) operating at 254 nm. The UV data were collected and analysed on an integrator (Trivector Trio). The column was thermostatted at 25°C. In direct chiral analysis a β-CD bonded chiral stationary phase (244 × 4 mm I.D., ChiraDex, E. Merck, Darmstadt, Germany) was used. A mixture of methanol–phosphate buffer, 200 mM, pH 6.8 (20:80) was used as the mobile phase at a flow-rate of 0.8 ml min^{-1}. The concentration of 0.9 mM of Dns-Glu in mobile phase was injected on column. For the mobile phase additive method, a C_{18} column (250 × 4.6 mm I.D.; HPLC Technology, Macclesfield, UK) was used. The mobile phase additive was a mixture of methanol–phosphate buffer, 200 mm, pH 6.8 (20:80) containing a specified concentration of β-CD.

4. Results and discussion

4.1. Competitive binding of cyclohexanol for β-CD

Fig. 1 shows the dramatic difference in separation of tioconazole enantiomers brought about by addition of 0.1% v/v cyclohexanol to a running buffer containing 5 mM β-CD. Whereas little resolution is evident without the cyclohexanol, near baseline resolution is seen in its presence. Cyclohexanol has a high association constant with β-cyclodextrin ($K = 501\ M^{-1}$) [15] and is thus an effective competitor for analyte binding to cyclodextrin. For the separation of enantiomers of tioconazole with β-CD by CE, the binding constants for (−)- and (+)-tioconazole were measured to be $1.32 \cdot 10^3$ and $1.60 \cdot 10^3\ M^{-1}$, respectively. Addition of just 0.1% cyclohexanol to the background electrolyte with all other conditions being identical resulted in an apparent binding constant for (−)- and (+)-tioconazole from data fitting to Eq. 1 of 223 and 259 M^{-1}, respectively. Using a quantitative treatment of competitive binding [13], this six-fold decrease was shown to be consistent with competition between cyclohexanol and tioconazole for β-CD. From Eq. 5 we can calculate that in the absence of cyclohexanol we would require 0.9 mM β-CD concentration in

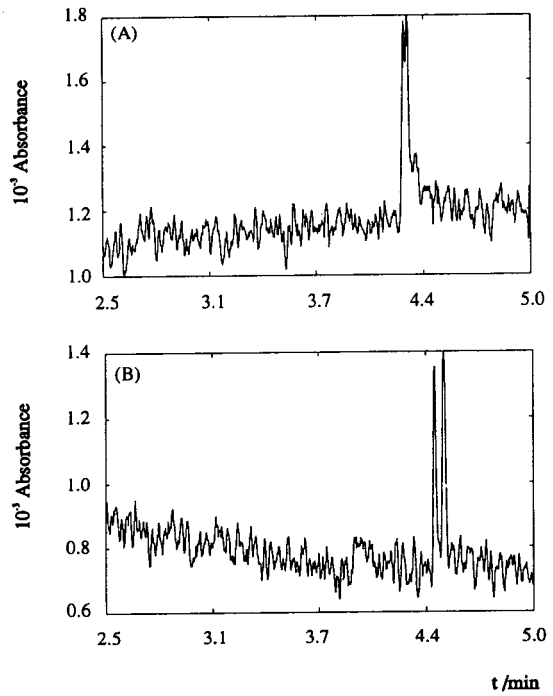

Fig. 1. Effect of competitive inhibition on the separation of tioconazole enantiomers. (A) No cyclohexanol, (B) 0.1% (v/v) cyclohexanol in the running buffer. Buffer: 20 m*M* phosphate/citrate pH 4.3 with 5 m*M* β-cyclodextrin; temperature: 25°C; injection: 1 s pressure injection (1 nl); sample: 0.1 m*M* tioconazole in run buffer; capillary: 50 μm internal diameter, 57 cm length; detection: 230 nm.

the background electrolyte for maximum resolution, but that with 0.1% (v/v) cyclohexanol we would require 5.3 m*M* β-CD (the concentration in Fig. 1) for maximum resolution. Eq. 1 shows that mobility is dependent upon the concentration of free selector, and an excess of selector over analyte is required. Due to the short pathlength of the on-column UV detection in CE, relatively high concentrations of analyte are required when working with weakly absorbing species such as tioconazole. Thus, with the use of cyclohexanol it is possible to bring very strongly binding species that require micromolar [CD] for optimum separation to a more convenient millimolar CD concentration.

4.2. Propranolol: β-cyclodextrin

Nicole et al. [16] determined the binding constant for propranolol binding to β-cyclodextrin to be $K = 220 \pm 20\ M^{-1}$, using an LC method with pH 7.4 phosphate buffer as the mobile phase. Using the same buffer conditions as in LC, we have determined the binding constant by CE from the variation of electrophoretic mobility with β-CD concentration (Fig. 2). Electrophoretic mobilities observed were corrected for buffer viscosity changes as discussed in sections 2.1 (Eq. 2) and 3. The value from CE obtained

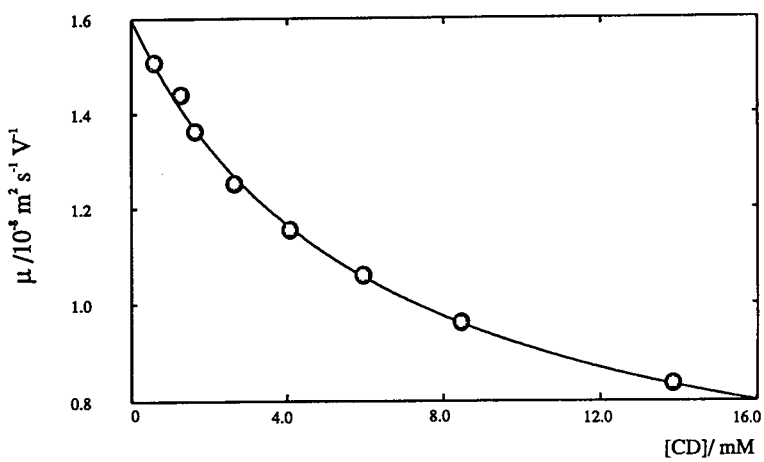

Fig. 2. Electrophoretic mobility of propranolol, corrected for buffer viscosity variation, as a function of [β-CD]. Data fitted to binding equilibrium curve giving $K = 160.4 \pm 3.1\ M^{-1}$. Buffer: 20 m*M* aqueous phosphate buffer pH 7.4; temperature: 25°C; voltage: 20 kV; capillary: 50 μm internal diameter, 57 cm length; detection: 200 nm.

for K, $160 \pm 3\ M^{-1}$, is comparable to that from LC.

Under the HPLC buffer conditions no chiral resolution was achieved in CE, due to the electroosmotic flow being too high at pH 7.4. Chiral resolution, although not baseline, was achieved using the conditions developed by Wren and Rowe [8] with Me-β-CD, at pH 3.0 in a lithium phosphate buffer. Binding constants under these conditions were found to be similar, although with larger errors than at pH 7.4, this being due to the inability to measure the low electroosmotic flow accurately. Both sets of experiments at pH 3.0 and pH 7.4 were under conditions well below the pK_a of propranolol ($pK_a = 9.5$), and no change in binding constant or selectivity was expected on changing the pH for a fully charged species.

4.3. Dansylated amino acids: β-CD

Fujimara et al. [17] used CD-bonded stationary phases in LC to chirally resolve dansylated amino acids. With the use of a 20-μm I.D. capillary it was possible to directly transfer the LC buffer conditions to CE (Fig. 3a). Using β-CD the binding constants between (D,L)-dansylated-glutamate (Dns-Glu) and β-CD were determined to be $K_2 = 220 \pm 4\ M^{-1}$ and $K_1 = 187 \pm 4\ M^{-1}$, and between (D,L)-dansylated-leucine (Dns-Leu) and β-CD $K_2 = 170 \pm 4\ M^{-1}$ and $K_1 = 141 \pm 4\ M^{-1}$. By spiking mixtures with pure L-Dns-amino acids assignments were made as L = 1, D = 2.

Comparison of mobile phase additives in LC (Fig. 3b), bonded phase LC (Fig. 3c) and CE in Table 1 reveal a number of interesting features. Firstly in the *mobile phase additive* work k'_A for Dns-Leu cannot be measured ($k'_A \geq 50$) but it can for Dns-Glu ($k'_A = 8$). This may be due to a partition into the non-polar stationary phase favouring a singly charged analyte (Dns-Leu) in comparison with a doubly charged analyte (Dns-Glu). As previously mentioned, the right hand sides of Eqs. 4 and 7 have the same magnitude, predicting that the left hand sides should be identical. This is indeed the case when looking at the data for Dns-Glu with 7 mM β-CD in LC and CE; $\Delta t/(t_a - t_0) = 0.042$, and under the same conditions in CE $\Delta\mu/(\mu_0 - \mu_\infty) = 0.041$. The data points of k' for Dns-Glu with β-CD as a mobile phase additive do not fit smoothly over the full range of β-CD concentration to the expected theoretical curve predicted by Eq. 6, revealing a more complex binding behaviour. This suggests that it may be a case 2 situation.

When comparing resolution (Fig. 3, Table 1), CE is revealed to be the technique to give the highest resolution for Dns-Glu. The high resolution attainable in CE is due to the electroosmotic flow and the electrophoretic mobility (which feature in the denominator of the resolution Eq. 5) being in opposing directions but of similar magnitude [13]. Table 1 also shows that there is good agreement between experimentally observed resolution at optimum cyclodextrin concentration and values calculated from Eq. 5.

In the case of β-CD bonded *chiral stationary phases* in LC using Dns-Glu and Dns-Leu, the α values obtained by Fujimara et al. [17], and in the present work under the same buffer conditions on the ChiraDex column, differ. For Dns-Glu, α from CE is greater than α from both chiral stationary phases. The situation is reversed when comparing results for Dns-Leu, where a particularly high value of α is seen on the ChiraDex stationary phase. All these results imply that the binding at the critical points for selectivity in a chiral stationary phase may be affected by the tether to the support.

CE reveals that the ratio of the average binding constant for Dns-Glu and Dns-Leu is approximately equal to unity. However, the ratio of k' for Dns-Leu and Dns-Glu is ca. 6. It has been noted that Dns-Glu is strongly bound to a C_{18} stationary phase, and we may postulate a possible contribution to k' for Dns-Glu from bonding interactions to the hydrophobic spacer material of the CD tether. It should also be significant that Dns-Glu is doubly negatively charged, whereas Dns-Leu is singly charged. In the paper by Fujimara et al. use of a high ionic strength buffer was observed to be particularly

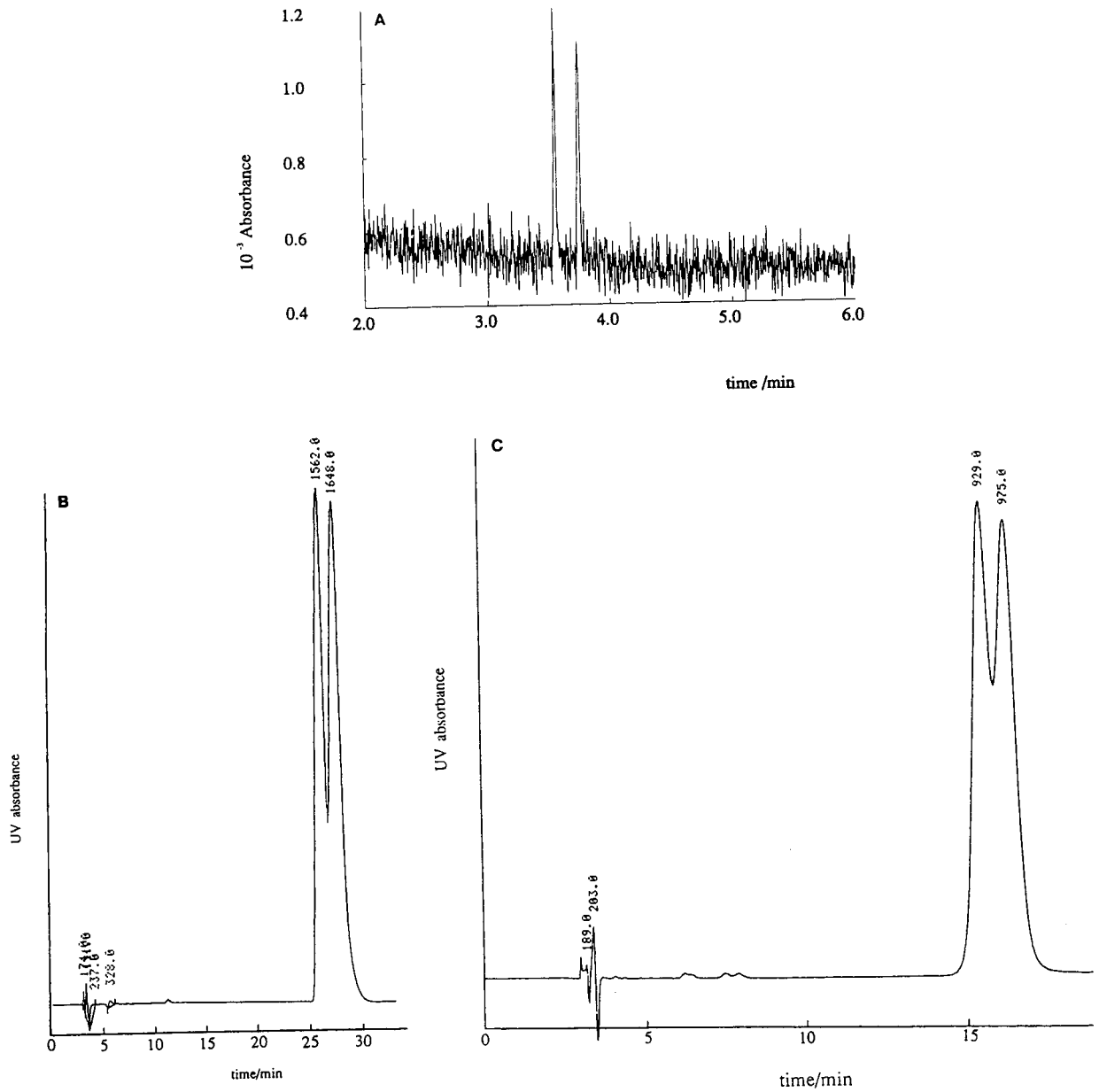

Fig. 3. Comparison of the chiral separation of dansyl-glutamate by: (A) capillary electrophoresis with mobile phase additive, (B) liquid chromatography with mobile phase additive and (C) liquid chromatography using a chiral stationary phase. Conditions: (A) 200 m*M* phosphate buffer pH 6.8, 20% methanol, with 10 m*M* β-CD in mobile phase, (B) 200 m*M* phosphate buffer pH 6.8, 20% methanol, with 7 m*M* β-CD in mobile phase and (C) 200 m*M* phosphate buffer pH 6.8, 20% methanol, no mobile phase additives, ChiraDex β-CD chiral stationary phase. Other conditions as in text.

beneficial in binding and chiral resolution of Dns-Glu, implying the need for charge screening for optimum bonding of Dns-Glu. All of these results have allowed CE to define the binding conditions and selectivity appropriate for free cyclodextrin, showing that the situation is made

Table 1
Comparison of resolution and selectivity data for Dns-Glu and Dns-Leu

Technique	Parameter	Dns-Glu	Dns-Leu
CSP[a]	k'_L	2.79	17.1
	k'_D	3.12	19.7
	α	1.12	1.15
	R_s^b	1.19	0.88
CSP: ChiraDex	k'_L	3.84	13.17
	k'_D	4.11	22.14
	α	1.07	1.68
	R_s^b	0.79	4.34
HPLC-mpa[d]	k'_D	8.34	≥ 50
	k'_L	8.84	≥ 50
	α^c	1.06	–
	R_s^b	0.83	–
CE	K_D	$220 \pm 4\ M^{-1}$	$170 \pm 4\ M^{-1}$
	K_L	$187 \pm 4\ M^{-1}$	$141 \pm 4\ M^{-1}$
	α	1.18	1.21
	R_s^b	6.7	5.4
	R_s theoretical	6.6	8.0

[a] Data from Fujimura et al. [17].
[b] R_s calculated using: $(x_2 - x_1)/\frac{1}{2}(w_1 + w_2)$.
[c] k'_D/k'_L at 7 mM β-CD.
[d] mpa = Mobile phase additive.

more complex by cyclodextrin bound to a chiral stationary phase.

5. Conclusions

By measuring mobility as a function of selector concentration in CE, analyte–selector binding constants can be obtained. In enantioselective binding, a general treatment allows mobility difference and resolution at any selector concentration to be calculated. Similar equations apply to determining binding constants and retention time differences in LC using mobile phase additives, provided that all discrimination is in the mobile phase. This is the first of four general cases identified for chiral separations in LC. The other cases which allow simple treatment in terms of single equilibria are when all binding occurs at an immobilised selector, held either by dynamic coating or covalent bonding to a stationary phase support. Here the ratio of capacity factors of the enantiomers is the ratio of the binding constants.

Application of these ideas using β-cyclodextrin as selector shows satisfactory agreement between binding constants measured for propranolol as analyte in CE and LC. Using Dns-D/L-Glu as analytes, chiral resolution in CE is shown to be in excellent agreement with theoretical prediction, and resolution is considerably better in CE than in LC. When comparing a β-CD bonded stationary phase with β-CD as mobile phase additive in LC and CE, more complex binding equilibria are revealed in the LC situations.

In future work we plan to use CE to define mobile phase equilibria and develop a rational strategy for selector choice and concentration to optimise a separation which can be transferred to

LC, where both mobile and stationary phases are involved, and several binding modes have to be considered.

Acknowledgements

We wish to thank the SERC and Pfizer Central Research for a CASE award (SGP); Zeneca Specialties (ETB); Zeneca Fine Chemicals Manufacturing Organisation, Zeneca Agrochemicals, Pfizer Central Research (GL); and Merck Chromatography for the loan of a ChiraDex LC column.

References

[1] S.G. Allenmark, *Chromatographic Enantioseparations*, Ellis Horwood, Chichester, 1988.
[2] D. Sybilska and J. Zukowski, in A.M. Krstulovic (Editor), *Chiral Separations by HPLC —Applications to Pharmaceutical Compounds*, Ellis Horwood, Chichester, 1989, Ch 7.
[3] D. Sybilska, J. Zukowski and J. Bojarski, *J. Liq. Chromatogr.*, 9 (1986) 591.
[4] K. Fujimara, T. Ueda, M. Kitagawa, H. Takayanagi and T. Ando, *Anal. Chem.*, 58 (1986) 2668.
[5] R.O. Cole, M.J. Sepaniak and W.L. Hinze, *J. High Resolut. Chromatogr.*, 13 (1990) 579.
[6] K. Otsuka and S. Terabe, *J. Chromatogr.*, 515 (1990) 221.
[7] S. Fanali, M. Flieger, N. Steinerova and A. Nardi, *Electrophoresis*, 13 (1992) 39.
[8] S.A.C. Wren and R.C. Rowe, *J. Chromatogr.*, 603 (1992) 235.
[9] S.G. Penn, D.M. Goodall and J.S. Loran, *J. Chromatogr.*, 636 (1993) 149.
[10] Y.Y. Rawjee, R.L. Williams and G. Vigh, *J. Chromatogr.*, 635 (1993) 291.
[11] Y.Y. Rawjee, R.L. Williams and G. Vigh, *J. Chromatogr. A*, 652 (1993) 233.
[12] Y.Y. Rawjee and G. Vigh, *Anal. Chem.*, 66 (1994) 619.
[13] S.G. Penn, D.M. Goodall, E.T. Bergstrom and J.S. Loran, *Anal. Chem*, in press.
[14] L.S. Ettre, *Pure Appl. Chem.*, 65 (1993) 819.
[15] Y. Matsui and K. Mochida, *Bull. Chem. Soc. Jpn.*, 52 (1979) 2808.
[16] T. Nicole, B. Sebille, A. Deranti and G. Lelievre, *J. Chromatogr.*, 503 (1990) 453.
[17] K. Fujimura, S. Suzuki, K. Hayashi and S. Masuda, *Anal. Chem.*, 62 (1990) 2198.

ELSEVIER

Journal of Chromatography A, 680 (1994) 157–162

JOURNAL OF CHROMATOGRAPHY A

Practical aspects of chiral separations of pharmaceuticals by capillary electrophoresis
I. Separation optimization

Andras Guttman*, Nelson Cooke

Beckman Instruments, Inc., 2500 Harbor Boulevard, Fullerton, CA 92634, USA

Abstract

Capillary electrophoresis employing chiral selectors has been shown to be a useful analytical method to separate enantiomers. In our model system hydroxypropyl-β-cyclodextrin was used as chiral selector for the separation of racemic propranolol. Results are presented regarding the effect of different operational variables such as buffer pH, concentration of chiral selector, applied electric field and temperature on the chiral separation. Based on the experimental data, the operational variables were optimized to attain maximum resolving power with minimal analysis time.

1. Introduction

Conventionally, instrumental chiral separations have been achieved by gas chromatography (GC) [1] and by high-performance liquid chromatography (HPLC) [2,3]. In recent years, there has been considerable activity in the separation and characterization of racemic pharmaceuticals by high-performance capillary electrophoresis (HPCE) with particular interest paid to using this technique in modern pharmaceutical analytical laboratories [4–9]. HPCE represents an instrumental approach to electrophoresis with the advantages of fast analysis time, automation, on-column injection and detection. The method is similar to HPLC in that analytes are detected as they pass through the detection window, allowing for quantitation [10]. The great resolving power of this method is based on the high separation efficiency, *i.e.* high theoretical plate counts inherent with CE. It is important to note here, that CE-based chiral separation methods were just recently accepted in inter-company cross-validation reported by Altria *et al.* [11].

As in GC [1,12] and HPLC [2,3], the versatility of HPCE can be extended via incorporation of chiral selectivity into the electromigration process. It has previously been shown that native and derivatized cyclodextrins can be successfully employed in chiral separations using isotachophoresis [13–16], capillary zone electrophoresis [17–20], micellar electrokinetic chromatography [21,22] and capillary gel electrophoresis [23,24]. Cyclodextrins (CDs) are non-ionic cyclic polysaccharides containing glucose units shaped like a toroid or hollow truncated cone. The cavity is relatively hydrophobic while the external faces are hydrophilic, with the edge of the torus of the larger circumference containing secondary hydroxyl groups connected to the chiral carbons

* Corresponding author.

0021-9673/94/$07.00
SSDI 0021-9673(94)00283-F

[25]. These secondary hydroxyl groups can be derivatized in order to increase the size of the cavity or the solubility of the cyclodextrin, *e.g.*, via permethylation, hydroxypropylation.

In the chiral recognition process it is believed that the non-polar portion of the solute molecule *i.e.*, the naphthyl group in the propranolol, distributes inside the cavity of the cyclodextrin and form hydrophobic interactions with the inner hydrophobic moiety. The hydroxyl and amino groups of the propranolol form hydrogen bonds with the hydroxyl groups at the rim of the toroid. Enantioselective recognition arises from these hydrogen bonds at the entrance of the cavity with the chiral glucose moiety, while the complex is stabilized by the host–guest complexation in the cyclodextrin cavity [23].

According to the theory of Rawjee and Vigh [26], when gels or polymer networks are used in CE of enantiomers using CDs as chiral selectors, better separation can be achieved when only the dissociated form of the solute (Type II) or both the dissociated and non-dissociated form of the solute (Type III) complex selectively with the chiral selector. To take advantage of this phenomenon a non-cross-linked hydrophilic polymer network was used in our experiments as a buffer additive using hydroxypropyl-β-cyclodextrin (HP-β-CD) as chiral selector for the separation of racemic propranolol (Type III with HP-β-CD). The use of a polymer network is also advantageous in that suppresses the ζ potential of the inner capillary wall, thus reducing the electroosmotic flow. In this way, the tendency of bulk electroosmotic flow to decrease electrophoretic mobility differences can be minimized [27]. In chiral separations with very low selectivity values this can be an important factor in achieving better enantiomeric separation.

The research described in this report details the effects of the different operational variables such as separation buffer pH, chiral selector concentration, applied electric field strength and separation temperature on the resolution of racemic propranolol. Based on our results, we propose a new optimization scheme that involves changing the electrophoretic operating variables systematically to attain the best available enantiomeric separation in CE of racemic molecules.

2. Materials and methods

2.1. Apparatus

All of the experiments on P/ACE System 2210 capillary electrophoresis apparatus (Beckman Instruments, Fullerton, CA, USA) were performed with the anode on the injection side and the cathode on the detection side. Capillary columns of 25 μm I.D. (Polymicro Technologies, Phoenix, AZ, USA) were used in these experiments in order to achieve the highest available efficiency, thus, good resolution due to the small injected amount of the dilute sample. Capillaries with 20 cm effective length (27 cm total length) were used in the experiments (Beckman). The separations were monitored on column at 230 nm wavelength. The temperature of the coolant liquid in the P/ACE instrument was controlled from 20–50°C to $\pm$ 0.1°C. The samples were injected by the pressure injection mode of the system, typically for 5 s at 0.5 p.s.i. (1 p.s.i. = 6894.76 Pa). The electropherograms were acquired and stored on an IBM 486/66 computer using the System Gold software package (Beckman).

2.2. Chemicals

The racemic (*R*,*S*) propranolol (pK = 9.47) (Sigma, St. Louis, MO, USA) was dissolved in deionized water at a concentration of 10 μg/ml. Ultrapure-grade ϵ-aminocaproic acid, 2-(N-morpholino)ethanesulfonic acid (MES), 3-[N-tris-(hydroxymethyl)methylamino] - 2 - hydroxypropanesulfonic acid (TAPSO), 3-[(1,1-dimethyl-2-hydroxyethyl)amino] - 2 - hydroxypropanesulfonic acid (AMPSO), methanesulfonic acid and tetrabutylammonium hydroxyde (TBAH) were used in the experiments (ICN, Costa Mesa, CA, USA). Buffers were prepared of ϵ-aminocaproic acid, and MES, TAPSO AMPSO adjusted to the proper pH of 3 or 4 by methanesulfonic acid and pH 5, 6, 7, 8 or 9 by TBAH, respectively. HP-β-CD with an average substitution rate of 4.9, was purchased from American Maize Products, Hammond, IN, USA. All buffer solutions contained 0.4% hydrophilic polymeric additive

and were filtered through a 0.8-μm pore size filter (Schleicher & Schuell, Keene, NH, USA) and carefully vacuum degassed at 100 mbar before use.

3. Results and discussion

Rawjee and Vigh's three-dimensional peak resolution model [26] has been put into practice in a simple optimization scheme, where the effects of the major operation parameters; pH, chiral selector concentration, applied electric field strength and separation temperature were consecutively studied in capillary gel electrophoresis. According to this theory, when performing chiral separation of enantiomeric drugs containing one asymmetric center and having only one charged functional group in the molecule (acidic or basic [28,29]), separation buffer pH and the chiral selector concentration are the two most important parameters defining chiral selectivity. Using *R,S*-propranolol as a test compound, the effect of the running buffer pH was first studied on the enantiomeric separation. All the other separation variables were maintained at the starting level of 15 m*M* HP-β-CD, 700 V/cm, applied electric field strength and 20°C running temperature, over the range of pH optimization experiments. Thus, pH buffers containing 15 m*M* HP-β-CD were prepared as described in section 2. In this way, gel-buffer solutions with pH ranging from 3 to 9 were formulated. In order to get the closest mobility match between the solute ions and the buffering and co-ions, buffer pH values were adjusted by using TBAH and methanesulfonic acid [30]. As seen in Fig. 1, the resolution shows a maximum at pH 7.0 for the racemic mixture of propranolol ($R_s = 1.7$), using the starting conditions were given above. As Fig. 1 shows, care needs to be taken in adjusting the pH of the separation buffer solution around the pH optimum of 7.0 since even a minor shift to lower or higher pH values can cause significant differences in the resolution of the enantiomers. The larger decrease in resolution that occurs below pH 6 and above pH 8 might be due to the lack of chiral selectivity at those pH values. It is important to note that

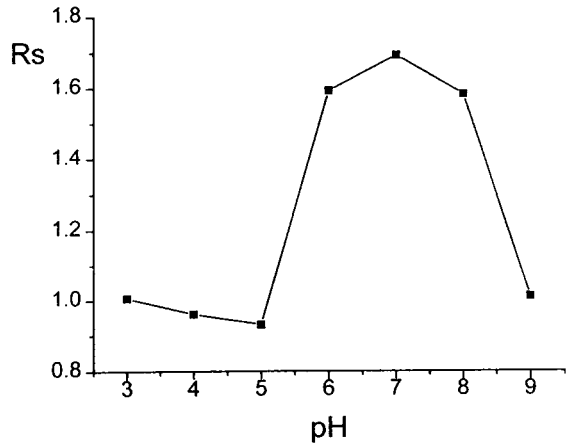

Fig. 1. Separation of *R* and *S* propranolol as a function of the pH ranging from 3 to 9. Conditions: column length: 20 cm (effective, 27 cm total); gel–buffer: 200 m*M* ϵ-aminocaproic acid–methanesulfonic acid (pH 3, 4) and MES–, TAPSO– and AMPSO–tetrabutylammonium hydroxide (pH 5, 6, 7, 8, 9) with 15 m*M* HP-β-CD, containing 0.4% hydrophilic polymeric additive; field strength: 700 V/cm; temperature: 20°C; detection: UV 230 nm.

when phosphate buffers are used significantly lower resolution values ($R_s = 0.8–1.0$) were attained in the pH 6–8 range. This lower resolution might be caused by a drop in efficiency due to the mobility mismatch between the solute and the higher mobility running buffer ions and the competition between the HPO_4^{2-} ions and the solute molecules for binding to the chiral selector [30].

The effect of the concentration of the chiral selector on enantiomeric resolution was investigated next, keeping the pH of the running buffer at the previously defined optimal value of pH 7.0 and maintaining all the other separation parameters constant as described above. The migration times increase with rising HP-β-CD concentration due to two simultaneously occurring phenomena. One is that the solute resides longer in the complex, so it moves slower than the free solute because of its increased mass-to-charge ratio. The other is that the viscosity of the buffer increases with the elevating HP-β-CD concentration [5] which decreases mobility of the solute. Fig. 2 shows the relationship between the

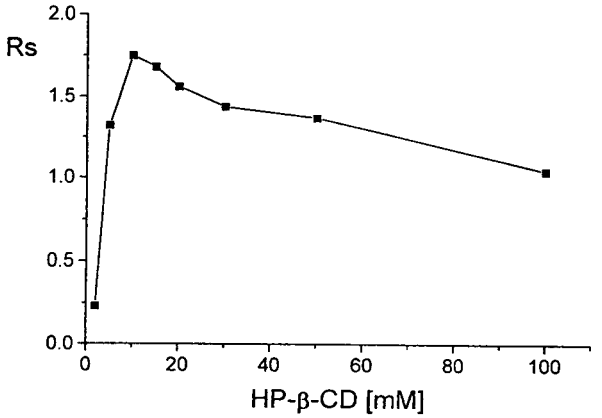

Fig. 2. Relationship between the chiral selector concentration and the resolution of the propranolol enantiomers. Conditions as in Fig. 1, with pH 7.0 gel–buffer and HP-β-CD concentration 2.5–100 m*M*.

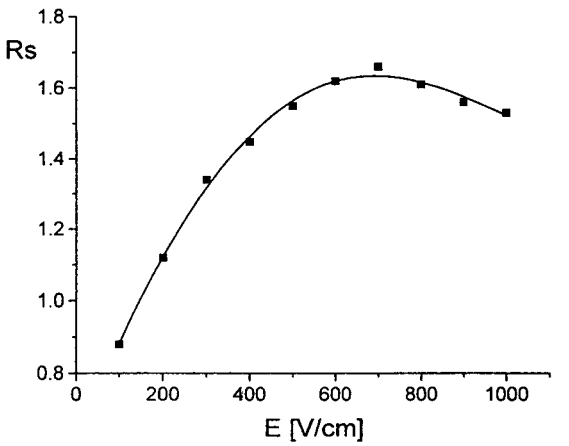

Fig. 3. Effect of the applied field strength on the resolution of propranolol enantiomers. Conditions as in Fig. 2, but HP-β-CD concentration is 10 m*M*; applied electric field 100–1000 V/cm.

resolution and the HP-β-CD concentration in the CE separation of *R* and *S* propranolol. As Fig. 2 shows, there is an optimum in the HP-β-CD concentration at 10 m*M* in the separation of the racemic propranolol. This is the point where a further increase in the chiral selector concentration leads to a resolution decrease. The same effect was found earlier by Wren and Rowe [5] using permethylated β-CDs for the separation of several important β-blockers.

The resolution drop caused by the mobility mismatch and competition of buffer components for the chiral selector is not considered here and in the remaining optimization experiments since the running buffer concentration and pH were maintained at the same level.

Considering the two optimum values found above for the running buffer pH (pH 7.0) and the chiral selector concentration (10 m*M* HP-β-CD), the effect of the applied electric field on the chiral resolving power was studied next (Fig. 3). The plot in Fig. 3 follows the theoretical resolution versus square root electric field strength (*E*) relationship in capillary electrophoresis, reported earlier by Karger *et al.* [10]. Note that resolution starts to decline beyond 700 V/cm, where the excessive Joule heat probably cannot be removed efficiently from the capillary column. This curve suggests the use of a maximum of 700 V/cm field strength for the separation of this particular solute and buffer composition. The resulting migration time is still very short, less than 5 min.

Fig. 4 shows the effect of the separation temperature on the resolution of the propranolol enantiomers, maintaining all the other running variables at the previously recognized optimal levels, *i.e.*, pH 7.0, 10 m*M* HP-β-CD. However, at elevated temperatures with the use of 700 V/cm applied electric field strength in these

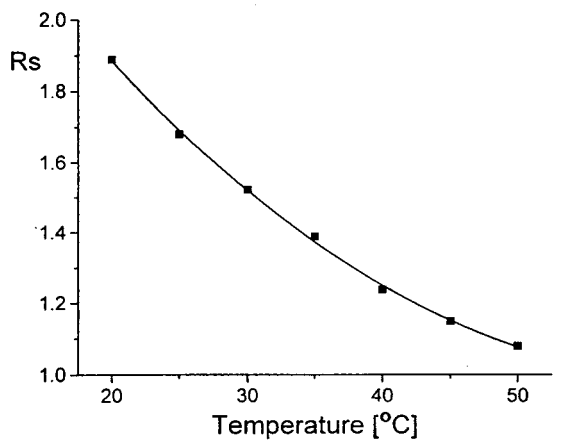

Fig. 4. Relationship between the separation temperature and the resolution of the propranolol enantiomers. Conditions as in Fig. 3, but electric field strength 700 V/cm, temperature 20–50°C.

experiments, one should take into account the running buffer conductivity increase resulting in higher current, caused by the elevated temperature, thus increasing the Joule heat is being developed. In Fig. 4, the temperature *versus* resolution plot suggests that with this particular solute the best resolution can be attained at the lowest running temperature used; in this case 20°C. The use of a lower separation temperature is also favorable for the solute–chiral selector complexation [25] and also decreases diffusion. However, further decrease in separation temperature would increase significantly the analysis time. It is important to note here that temperature has quite a remarkable effect on the separation of the propranolol enantiomers. The resolving power drops almost by 50% over the 30°C temperature window while analysis time decreased only by 28%.

4. Conclusions

We describe a general systematic approach to optimize enantiomeric separations in CE which involves pH, chiral selector, field strength and temperature optimization steps. It is shown that using this approach for the separation of propranolol enantiomers, the use of pH 7.0 running buffer with 10 m*M* HP-β-CD concentration, applying 700 V/cm field strength at 20°C were found to be as optimal separation conditions (Fig. 5). Using these parameters resolution of $R_s = 1.75$ was attained in less than 5 min using a 20 cm polymer network-filled capillary column. Extension of this method to other compounds will be reported in future papers.

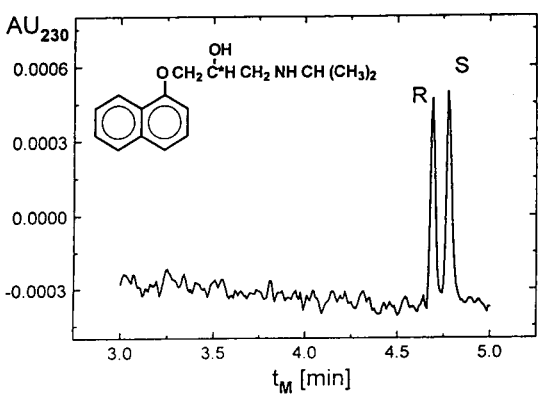

Fig. 5. Optimized CE separation of *R* and *S* enantiomers of propranolol. Conditions: column length: 20 cm (effective); separation gel–buffer: 200 m*M* TAPSO–tetrabutylammonium hydroxide (pH 7.0) with 10 m*M* HP-β-CD, containing 0.4% hydrophilic polymeric additive; electric field strength: 700 V/cm; temperature: 20°C; detection UV 230 nm. t_M = Migration time.

Acknowledgement

The authors wish to acknowledge Professor Gyula Vigh for his stimulating discussions. The authors also thank Ms. Julie Ficke and Dr. Jeff Allen for reviewing the manuscript before submission.

References

[1] E. Smolkova-Keulemansova, *J. Chromatogr.*, 251 (1982) 17.
[2] D. Armstrong, *Anal. Chem.*, 59 (1987) 84A.
[3] S. Ahuja, *Chiral Separations by Liquid Chromatography*, American Chemical Society, Washington, DC, 1991.
[4] K.D. Altria, A.R. Walsh and N.W. Smith, *J. Chromatogr.*, 645 (1993) 193.
[5] A.C. Wren and R.C. Rowe, *J. Chromatogr.*, 635 (1993) 113.
[6] R. Kuhn, F. Stoecklin and F. Erni, *Chromatographia*, 33 (1992) 32.
[7] S. Fanali, *J. Chromatogr.*, 545 (1991) 437.
[8] S. Fanali, *J. Chromatogr.*, 470 (1989) 123.
[9] J. Snopek, I. Jelinek and E. Smolkova-Keulemansova, *J. Chromatogr.*, 609 (1992) 1.
[10] B.L. Karger, A.S. Cohen, A. Guttman, *J. Chromatogr.*, 492 (1989) 585.
[11] K.D. Altria, R.C. Harden, M. Hart, J. Hevizi and P.A. Hailey, *J. Chromatogr.*, 641 (1993) 147.
[12] V. Schurig and H.P. Nowotny, *J. Chromatogr.*, 441 (1988) 155.
[13] I. Jelinek, J. Snopek and E. Smolkova-Keulemansova, *J. Chromatogr.*, 439 (1988) 386.
[14] J. Jelinek, J. Snopek and E. Smolkova-Keulemansove, *J. Chromatogr.*, 438 (1988) 211.
[15] S. Fanali and M. Sinibaldi, *J. Chromatogr.*, 442 (1988) 371.
[16] J. Jelinek, J. Dohnal, J. Snopek and E. Smolkova-Keulemansova, *J. Chromatogr.*, 464 (1989) 139.
[17] S. Terabe, *Trends Anal. Chem.*, 8 (1989) 129.

[18] A. Fanali, *J. Chromatogr.*, 474 (1989) 441.
[19] A.C. Wren and R.C. Rowe, *J. Chromatogr.*, 603 (1992) 235.
[20] J. Snopek, I. Jelinek and E. Smolkova-Keulemansova, *J. Chromatogr.*, 452 (1988) 571.
[21] S. Terabe, H. Ozaki,K. Otsuka and T. Ando, *J. Chromatogr.*, 332 (1985) 211.
[22] H. Nishi and M. Matsuo, *J. Liq. Chromatogr.*, 14 (1991) 973.
[23] A. Guttman, A. Paulus, A. Cohen, N. Grinberg and B.L. Karger, *J. Chromatogr.*, 448 (1988) 41.
[24] I.D. Cruzado and Gy. Vigh, *J. Chromatogr.*, 608 (1992) 421.
[25] J. Szejtli, *Cyclodextrins and their Inclusion Complexes*, Akademia Kiadó, Budapest, 1982.
[26] Y.Y. Rawjee and Gy. Vigh, *Anal. Chem.*, 66 (1994) 416.
[27] M.J. Sepaniak, R.O. Cole and B.K. Clark, *J. Liq. Chromatogr.*, 15 (1992) 1023.
[28] Y.Y. Rawjee D. Staerk and Gy. Vigh, *J. Chromatogr.*, 635 (1993) 291.
[29] Y.Y. Rawjee, R. Williams and Gy. Vigh, *J. Chromatogr. A*, 652 (1993) 233.
[30] Y.Y. Rawjee and Gy. Vigh, *J. Chromatogr. A*, 680 (1994) 599.

ELSEVIER

Journal of Chromatography A, 680 (1994) 163–173

JOURNAL OF CHROMATOGRAPHY A

Comparison of micellar electrokinetic chromatography (MEKC) with capillary gas chromatography in the separation of phenols, anilines and polynuclear aromatics Potential field-screening applications of MEKC

William C. Brumley*, William J. Jones[1]

US Environmental Protection Agency, Environmental Monitoring Systems Laboratory, P.O. Box 93478, Las Vegas, NV 89193-3478, USA

Abstract

Capillary electrophoresis (CE) is known to be complementary to liquid chromatography, but comparison of CE with capillary gas chromatography (GC) for applicable analytes has not been extensive. Capillary GC has been the preeminent separation technique for environmental analysis, but CE has yet to be applied systematically to the determination of environmental analytes. We present data on separations of three classes of semivolatile analytes of interest to environmental analysis: phenols, anilines and polynuclear aromatic hydrocarbons (PNAs). Standard GC conditions were used to illustrate typical separations observed on 30-m and 40-m columns. Rapid analyses were addressed using a high-temperature 15-m column of thinner film. CE separations employed borate buffer with sodium cholate as the micellar agent in micellar electrokinetic chromatography (MEKC). The effects of organic additives were studied using methanol, acetone and tetrahydrofuran. γ-Cyclodextrin was also used in MEKC to enhance the separation of polynuclear aromatic hydrocarbons and to examine its effects on separations of phenols and anilines. Short capillaries effected very rapid (< 3 min) compound-class characterization, an approach which has potential use in site characterization/remediation (field-screening) studies

1. Introduction

Capillary gas chromatography (cGC) is the preeminent separation technique in environmental analysis, especially for volatile and semivolatile analytes. For example, US Environmental Protection Agency (EPA) Methods 625 [1] and 8270 [2] use cGC for separation of analytes. The Environmental Monitoring Systems Laboratory in Las Vegas has a continuing interest in improving methodology based on cGC–mass spectrometry (MS) [3,4] and in investigating new analytical techniques such as high-performance capillary electrophoresis (HPCE) for target analytes [5–7].

Analytical interest in the environmental field has also been focused on liquid chromatographic techniques because of the need to determine non-volatile analytes or very polar compounds. Some results of this interest include EPA Methods 553 [8] and 8321 [2]. Sometimes reversed-

* Corresponding author.

[1] Fellow in the National Network for Environmental Management Studies (NNEMS) program; present address: Department of Chemistry, University of Nevada at Reno, Reno, NV 89507, USA.

SSDI 0021-9673(94)00414-5

phase high-performance liquid chromatography (HPLC) offers unique selectivity for compounds usually separated by cGC such as polynuclear aromatic hydrocarbons (PNAs) [2].

Liquid chromatographies are the more universally applicable separation techniques since they do not depend on volatility and have no molecular mass limitations. In addition, coextractives, metabolites and alteration products of analytes that increase polarity or molecular mass are less likely to create problems for subsequent sample runs because they can be, ideally, washed off the column between runs. Advances in the design of LC–MS interfaces have hastened the application of LC to environmental analysis [9–13].

Recently, interest has heightened in the area of very rapid analyses, in "quick turnaround methods", and in field-screening methods [14]. The emphasis on speed is driven on one hand by the requirements of real-time multidimensional analysis. Monnig and Jorgenson [15] have reported analysis times in the seconds using HPCE. Another consideration is the economics of large volume sampling and analysis in Superfund cleanup efforts. Field-screening methods are one approach to this problem, and they have been the subject of an international symposium held every other year since 1988 in Las Vegas [16].

The high efficiency of micellar electrokinetic chromatography (MEKC) makes it attractive for a variety of separations and suggests its applicability to high-speed analyses. Environmental applications of HPCE are on the increase [17–25].

As a capillary column electrophoretic technique, HPCE employs complete column rinsing between sample runs. Even the pseudochromatographic phase (micelles) in MEKC is regenerated before each run by way of buffer rinsing and equilibration. The low cost of fused silica and the rapid changeouts thus make MEKC attractive for field-screening applications.

In this work we compare the separations obtained using MEKC with those obtained using cGC for three representative compound classes of environmental interest: phenols, anilines and PNAs. Very rapid separations are effected on short capillaries under MEKC. These results are discussed in terms of the applicability of MEKC to field screening methods in environmental analysis.

2. Experimental[2]

2.1. Chemicals

All compounds were obtained from Aldrich (Milwaukee, WI, USA) unless otherwise indicated. Solutions of analytes were made up to appropriate concentrations in methanol or tetrahydrofuran (THF). Acetone, THF and methanol were obtained from Burdick & Jackson (Muskegon, MI, USA). Deionized water (ASTM Type II) was produced (Barnstead/Thermolyne, Dubuque, IA, USA) for all aqueous solutions.

2.2. Soil extraction

A creosote-contaminated soil from Spotsylvania, VA, USA was extracted by sonication extraction using standard EPA methodology [2]. This soil had been previously characterized for PNAs and nitrogen-containing aromatic compounds [3].

2.3. HPCE

A Beckman P/ACE 5000 was used for obtaining separations by MEKC. Capillaries were 57 cm or 27 cm × 0.050 mm I.D. (50 cm or 20 cm to the detector, respectively). Buffer systems used were either a 50 m*M* boric acid/sodium borate (pH 8.35), 100 m*M* sodium cholate, 10% acetone, THF or methanol system; or a 50 m*M* boric acid/sodium borate, 100 m*M* sodium cholate, 30 m*M* γ-cyclodextrin system. Voltage was 25 kV under MEKC for 57-cm capillaries and 20 kV for 27-cm capillaries. UV detection was at 214 nm, and acridine was used as an internal standard for migration-time corrections.

2.4. cGC

A Hewlett-Packard (Avondale, PA, USA)

[2] Mention of trade names or commercial products does not constitute endorsement or recommendations for use.

5890 Series II gas chromatograph with flame ionization detector and electronic pressure control was used. Separations were obtained using a DB-5 capillary column of 30 m × 0.25 mm I.D. (0.25 μm film thickness) and a DB-5HT capillary column of 15 m × 0.25 mm I.D. (0.10 μm film thickness) (J & W, Folsom, CA, USA). Temperature program for DB-5 was 60°C for 3 min followed by a rate of 20°C/min to 300°C. Temperature program for DB-5HT was 60°C for 3 min followed by a rate of 30°C/min to 380°C. All injections were on-column using a retention gap of 3 m × 0.53 mm I.D.

2.5. GC–MS

Additional separations were obtained using a Finnigan-MAT TSQ-45 mass spectrometer operated in the electron impact mode and fitted with a DB-5MS capillary column of 40 m × 0.18 mm I.D. (0.1 μm film thickness). The temperature program was 60°C for 3 min followed by a rate of 20°C/min to 300°C. All injections were on-column with a retention gap of 3 m × 0.53 mm I.D. MS operating parameters included an emission current of 0.27 mA, source temperature of 180°C, and multiplier, pre-amplifier and conversion dynode at −1100 V, 10^{-8} A/V, and −3000 V respectively. The instrument was scanned repetitively at 0.5 s/scan under computer control of an INCOS 2300 data system (Nova 4×, software rev. 6.6).

Table 1
Corrected MEKC migration times for phenols (10% acetone–cholate–borate buffer)

Compound	t_m (min)
Resorcinol	5.98
o-Cresol	6.89
m-Cresol	6.92
p-Cresol	7.16
Catechol	9.77
2-Nitrophenol	10.18
4-Chloro-3-methylphenol	10.54
4-Nitrophenol	10.58
2,4-Dichlorophenol	10.88
2,4,6-Trichlorophenol	11.91
2,4,5-Trichlorophenol	12.05
2,4-Dinitrophenol	12.27
Pentachlorophenol	12.83
Acridine (IS)	10.50

Table 2
Corrected MEKC migration times for anilines (γ-CD–cholate–borate buffer)

Compound	t_m (min)
m-Toluidine	4.68
N-Methylaniline	4.71
p-Toluidine	4.98
3,5-Dimethylaniline	4.99
o-Toluidine	5.01
o-Chloroaniline	5.06
3,4-Dimethylaniline	5.29
4-Methyl-3-nitroaniline	5.58
2-Chloro-4-methylaniline	5.65
2-Methyl-6-nitroaniline	5.76
2-Methyl-4-nitroaniline	5.78
3-Chloro-2-methylaniline	5.91
5-Chloro-2-methylaniline	5.95
4-Methyl-2-nitroaniline	6.01
2,6-Dichloro-3-methylaniline	6.95
2,4,5-Trichloroaniline	7.45
Acridine (IS)	7.00

3. Results and discussion

3.1. MEKC conditions

Several conditions under MEKC were investigated for the separation of phenols, anilines and PNAs. In each case, the micellar agent chosen was sodium cholate. In our study, the sodium cholate concentration was fixed at 100 m*M* and organic additives of acetone, THF and methanol were added to a 10% (90% water) level to examine their effects on separations. Methanol and THF tended to bunch peaks, whereas acetone appeared to add selectivity. An alternative additive investigated was γ-cyclodextrin (γ-CD) at 30 m*M*. Terabe [26] previously indicated the use of this additive for highly hydrophobic compounds.

Tables 1–4 tabulate observed corrected [5] migration times relative to the internal standard (IS) acridine. Figs. 1 –4 illustrate electropherograms of the three classes of compounds and an extract of a creosote-contaminated soil.

3.2. Phenols

Phenols represent a class of compounds that are weakly acidic. They were best separated under 10% acetone–cholate–borate buffer conditions (Fig. 1). The use of γ-CD–cholate buffer also gave good separations. Acetone, by reducing electroosmotic flow (EOF), allowed a better definition between the EOF peak and the very polar, early eluting cresols.

Fig. 1 may be compared to cGC separations found in the literature [27] in terms of resolving power, efficiency and time of run. Although the separation mechanism of cGC depends on both volatility and polarity, there are some similarities in the order of elution in comparing MEKC with cGC. For example, cresols elute first in both MEKC and cGC, and pentachlorophenol is last. The efficiency of both techniques is high, but MEKC does not suffer peak tailing with the polar nitrophenols and pentachlorophenol, a problem that is often evident with cGC when real sample extracts are injected.

It is evident from the migration times in Table 1 that not all phenols are resolved under these conditions. In our hands, not all of the phenols were resolved on a 40-m capillary column as well. Incomplete resolution was observed between *m*- and *p*-cresol, resorcinol and 2,4-dichlorophenol, 2,4,6-trichlorophenol and 2,4,5-

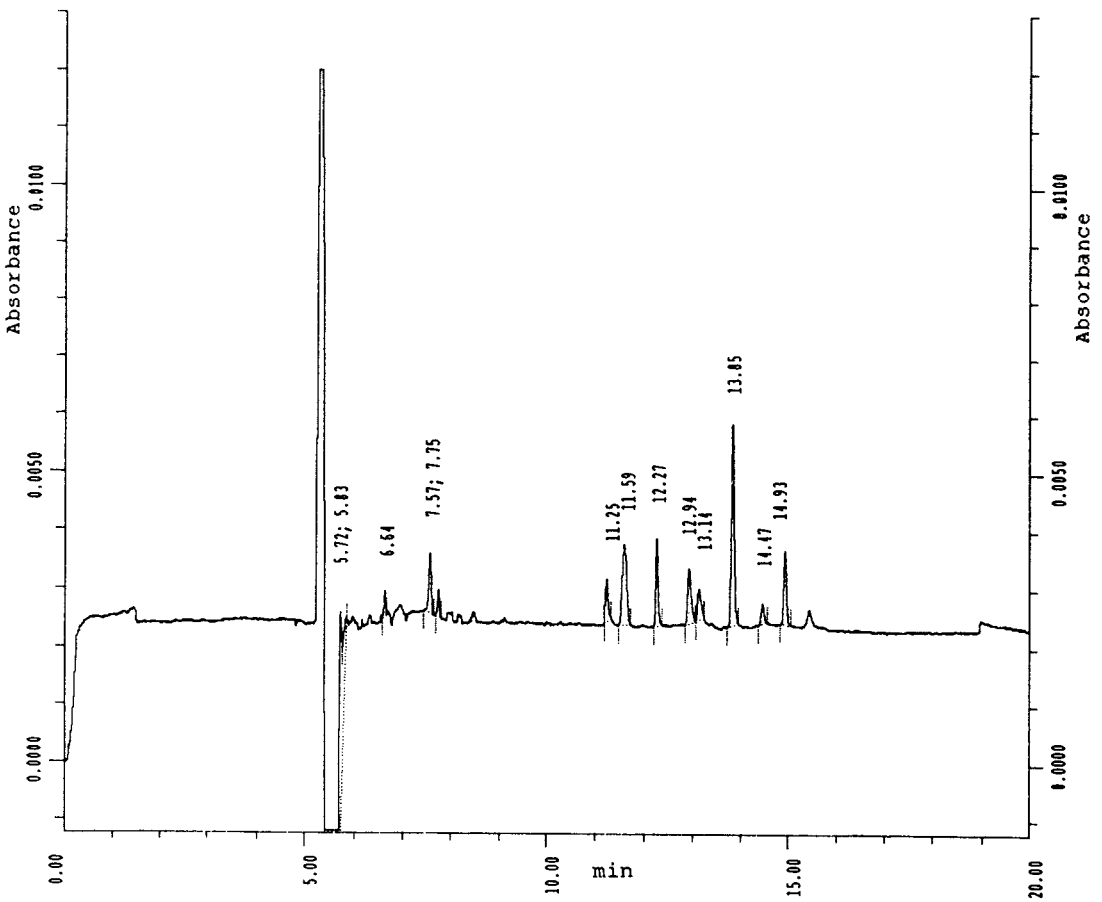

Fig. 1. Electropherogram of 13 phenols under MEKC (10% acetone–cholate–borate buffer). Acridine (IS), migration time (t_m = 11.59 min).

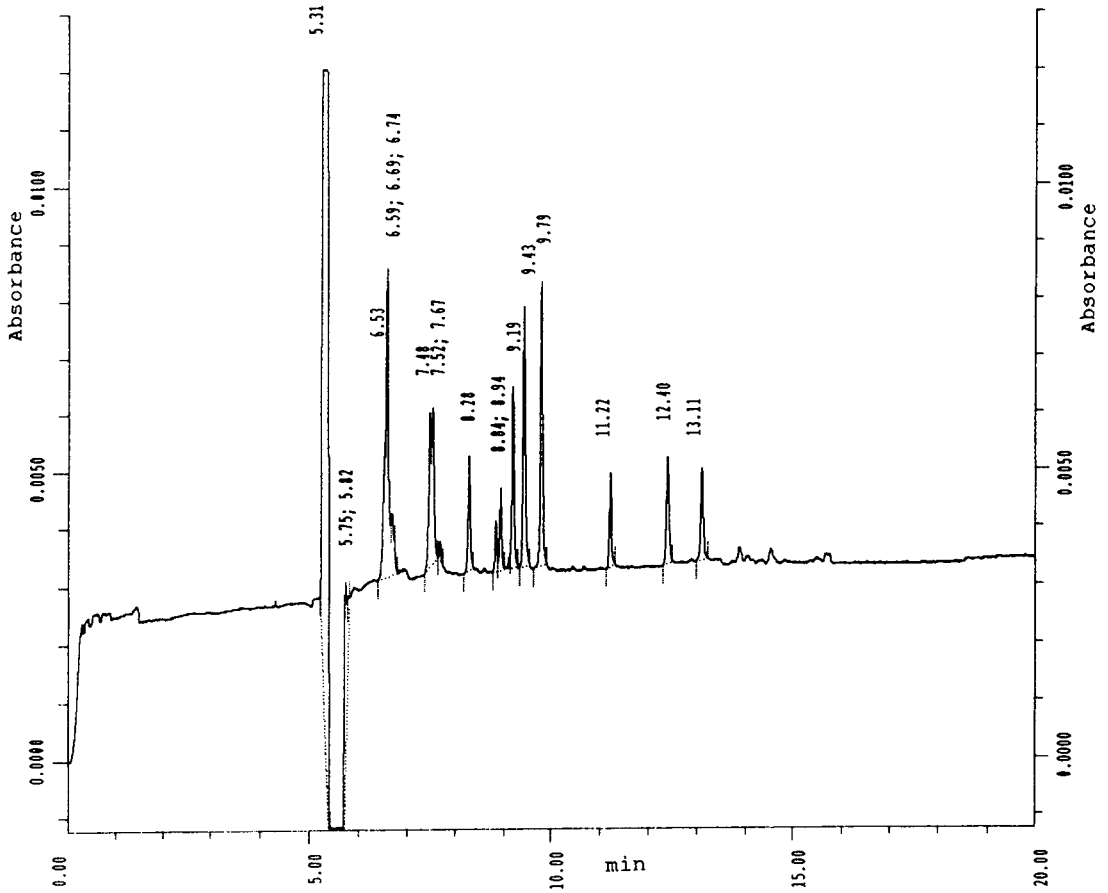

Fig. 2. Electropherogram of 16 anilines under MEKC (10% acetone–cholate–borate buffer). Acridine (IS), $t_m = 11.22$ min.

trichlorophenol, and 4-nitrophenol and 2,4-dinitrophenol.

3.3. Anilines

Anilines were well separated under 10% acetone–cholate–borate (Fig. 2) and CD–cholate–borate conditions. Symmetrical peaks were obtained for these relatively polar compounds under MEKC. As an illustration of selectivity changes as a function of additives, Tables 2 and 3 tabulate corrected migration times for both MEKC conditions. There are obvious changes in elution order in comparing the results in the two tables. Such changes may be useful in particular separation problems. It is also evident from the tables that not all of the compounds are resolved under the conditions studied.

Comparison of MEKC to cGC (Fig. 5) separation indicates relatively high efficiency and selectivity for both techniques. The presence of numerous impurities and alteration products in the solution of anilines was detected by MS, and they appear on the chromatogram as peaks beyond trichloroanilines. Very polar polymerization products are unlikely to be detected by cGC and probably remain on the retention gap where they may be pyrolyzed. Such alteration products are probably observed as late-eluters (e.g., $> t_m = 14$ min) in MEKC, and are flushed from the capillary between runs if not eluted during determination.

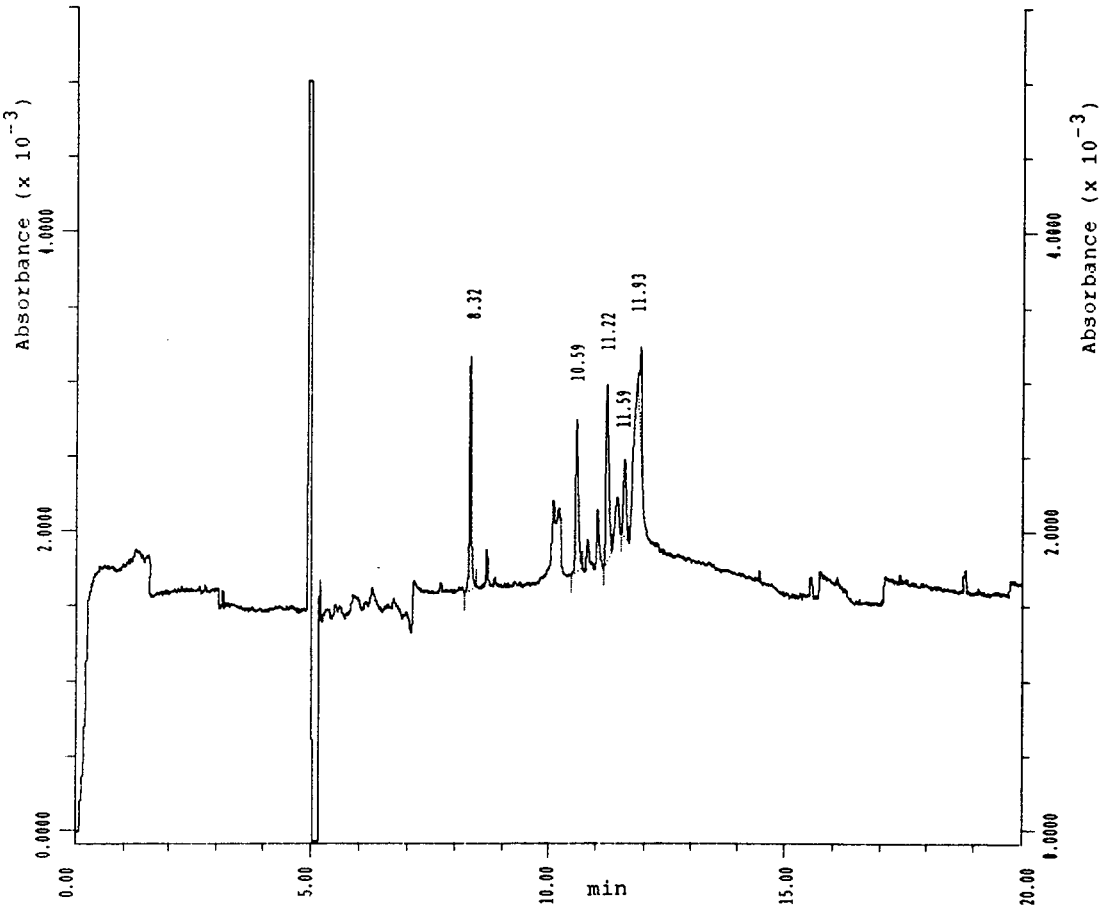

Fig. 3. Electropherogram of 16 PNAs under MEKC (CD–cholate–borate buffer). Acridine (IS), $t_m = 8.32$ min.

3.4. PNAs

PNAs were best separated under CD–cholate–borate conditions (Fig. 3). Some bunching of the higher-molecular-mass PNAs is evident in Fig. 4 and in Table 4. Additional separation of the late-eluting compounds may be effected by the addition of acetonitrile [28] or acetone to the γ-CD-containing buffer. Even so, with 15% acetonitrile, complete separation of all 16 compounds was not obtained under these conditions. Fig. 4 illustrates the electropherogram of an extract of a creosote-contaminated soil using the 10% acetone–CD–cholate–borate conditions. The complexity of this sample is reflected in the large number of polar and hydrophobic compounds present [3].

All 16 PNAs are completely or almost completely resolved by cGC [27]. Thus, for the MEKC conditions investigated, cGC exhibited better resolution for PNAs. However, the range of applicability of MEKC for weakly acidic, basic and neutral compounds was demonstrated in the data presented.

3.5. Short-column, rapid separations

One of the issues we wanted to address in our

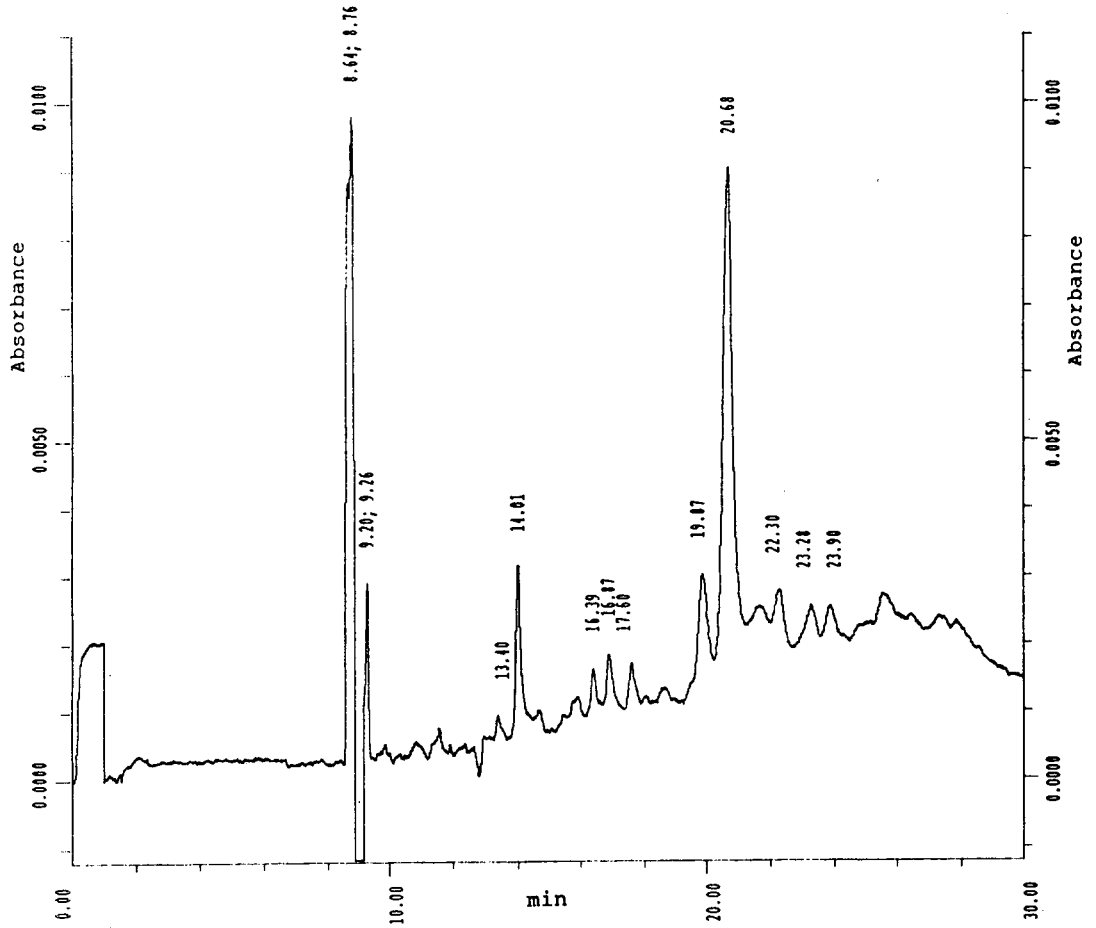

Fig. 4. Electropherogram of an extract of creosote-contaminated soil (10% acetone–CD–cholate–borate buffer). Acridine would elute at t_m = 12.99 min in this electropherogram.

work was the use of MEKC in very rapid compound-class separations. Very rapid determinations in conjunction with rapid extraction [e.g., via supercritical fluid extraction (SFE)] and rapid sample cleanup [e.g., via solid-phase extraction (SPE) cartridges] are of great interest in rapid site characterization/remediation studies and in field-screening methodology.

As an example of this potential, we illustrate a short capillary MEKC separation of PNAs (Fig. 6). Partial separations are obtained in 2–3 min for each compound class. Although incomplete resolution of all compounds is observed, rapid assessment of contaminant plumes or remediation progress could be obtained from these determinations. Only partial resolution of all target analytes is also observed with most field-screening methods that involve cGC. As an example, a rapid separation of PNAs by cGC is illustrated in Fig. 7 using a high-temperature column and operating conditions. All PNAs elute in less than 11 min; compare this result to runs of 44 min in normal work and 18 min in field-screening applications literature [27]. Incomplete separation of analytes is common in field-screening methods.

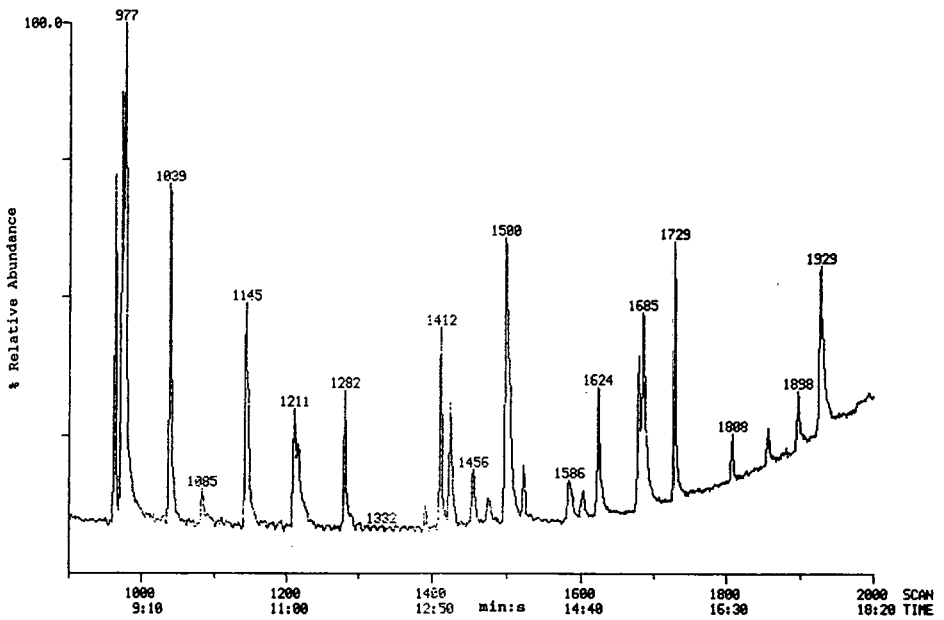

Fig. 5. cGC separation of anilines (40-m DB-5MS, GC–electron impact MS). Acridine, scan 1729; toluidines and N-methylaniline, scans 964, 975 and 977; *o*-chloroaniline, scan 1039; 3,5-dimethylaniline, scan 1085; chloromethylanilines, scans 1145 and 1211; 2,6-dichloro-3-methylaniline, scan 1282; methylnitroanilines, scans 1412 and 1425; 2,4,5-trichloroaniline, scan 1456.

Table 3
Corrected MEKC migration times for anilines (10% acetone–cholate–borate buffer)

Compound	t_m (min)
o-Toluidine	6.93
m-Toluidine	7.06
N-Methylaniline	7.13
p-Toluidine	7.16
o-Chloroaniline	7.87
3,5-Dimethylaniline	7.89
3,4-Dimethylaniline	8.03
4-Methyl-3-nitroaniline	8.72
2-Methyl-4-nitroaniline	9.32
2-Methyl-6-nitroaniline	9.41
2-Chloro-4-methylaniline	9.54
4-Methyl-2-nitroaniline	9.87
5-Chloro-2-methylaniline	9.90
3-Chloro-2-methylaniline	10.25
2,6-Dichloro-3-methylaniline	13.08
2,4,5-Trichloroaniline	14.43
Acridine (IS)	11.70

Table 4
Corrected MEKC migration times for polynuclear aromatics (γ-CD–cholate–borate buffer)

Compound	t_m (min)
Acenaphthylene	7.23
Naphthalene	7.40
Fluorene	9.93
Phenanthrene	10.32
Anthracene	10.64
Pyrene	10.83
Fluoranthene	10.96
Chrysene	11.17
Benzo[*a*]pyrene	11.44
Benzo[*ghi*]perylene	11.57
Benzo[*b*]fluoranthene	11.63
Dibenz[*a*,*h*]anthracene	11.64
Indeno[1,2,3-*c*,*d*]pyrene	11.68
Acridine (IS)	8.20
Acenaphthene	N.D.
Benzo[*a*]anthracene	N.D.
Benzo[*k*]fluoranthene	N.D.

N.D. = Not determined.

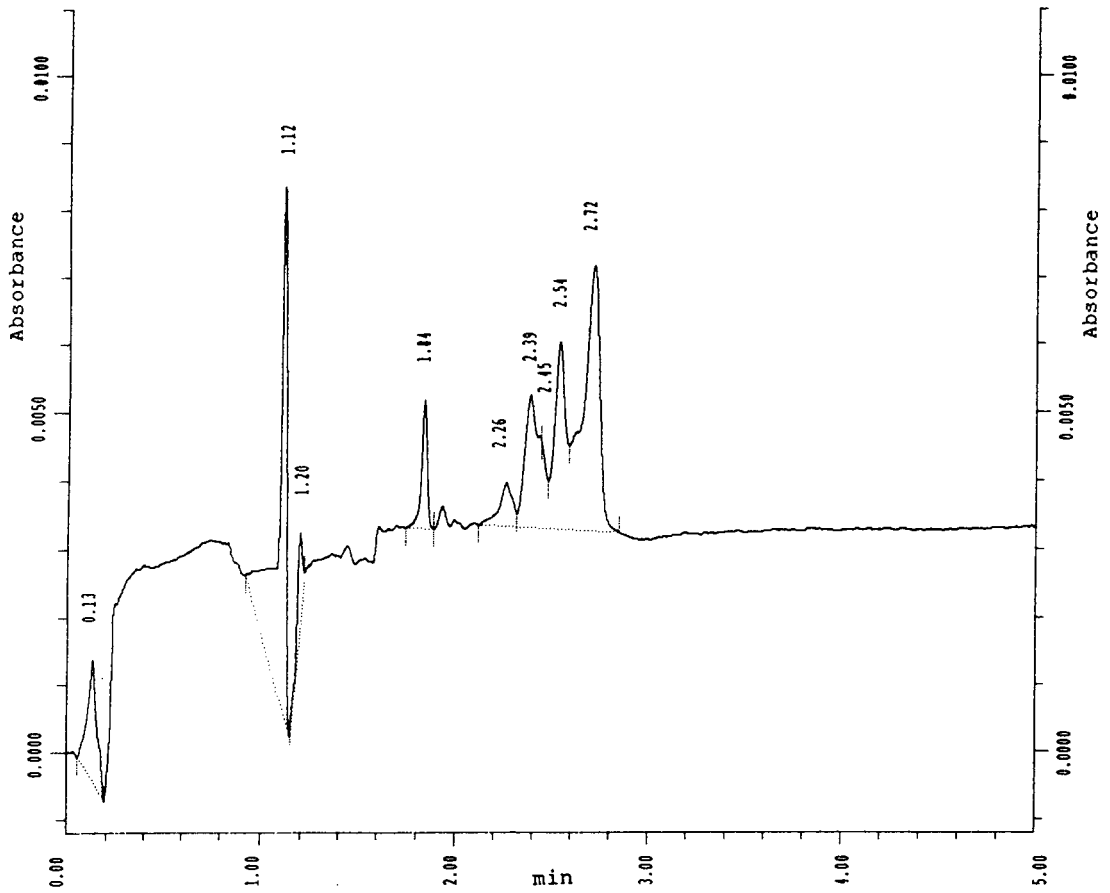

Fig. 6. Short capillary (27-cm) separation of PNAs (γ-CD–cholate–borate buffer). Acridine (IS), t_m = 1.84 min.

We envision a combined SFE–SPE–HPCE instrument that could be automated with an average analysis time per sample of 6 min. This represents a novel application of MEKC to field-screening approaches and would represent at least a 10-fold reduction in analysis time over the usual methodology. Efforts at improving sensitivity and selectivity of detection under MEKC such as by using laser-induced fluorescence (LIF) detection are important to the ultimate application of this potential. Improved sensitivity lowers detection limits and allows injection of more dilute samples. Improved selectivity reduces the amount of cleanup required and increases ruggedness in the determination when a variety of matrices are encountered.

4. Conclusions

MEKC exhibits selectivity that is comparable to that of cGC for polar analytes, but PNAs are best separated by cGC under the conditions used in this work. With regard to rapid determinations, partial separations can be accomplished in about 2–3 min and this compares very favorably with cGC. Applications of this rapid separation capability are envisioned in combination with

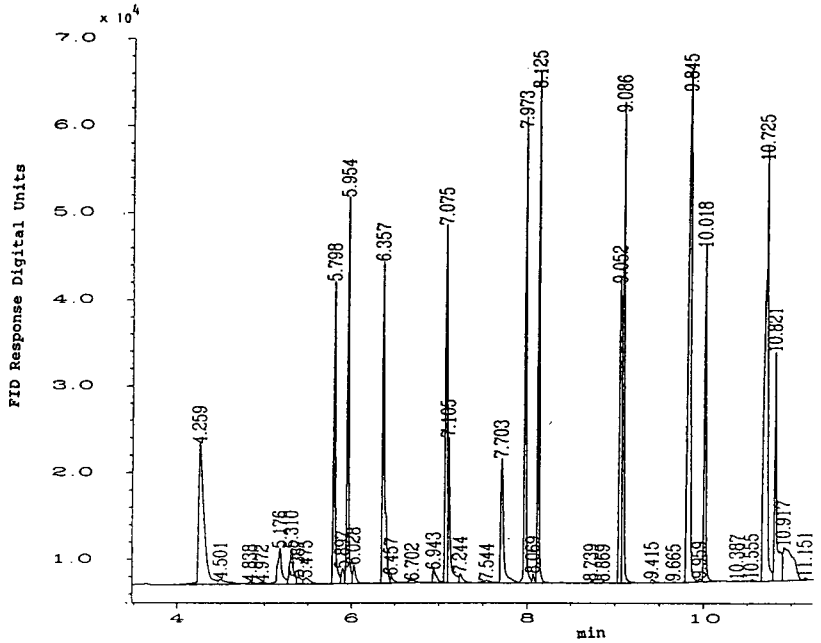

Fig. 7. Rapid separation of PNAs by use of high-temperature column and conditions [15-m DB-5HT, flame ionization detection FID)]. Naphthalene, $t_R = 4.259$ min; benzo[*ghi*]perylene, $t_R = 10.821$ min.

rapid extraction (e.g., SFE) and cleanup techniques (e.g., SPE sorbents). The approach would be particularly useful as an SFE–SPE–MEKC unified instrument with selective and sensitive detection by LIF.

Notice

The U.S. Environmental Protection Agency, through its Office of Research and Development, funded and performed the research described here. It has been subjected to the Agency's peer review and has been approved as an EPA publication.

References

[1] J.W. Eichelberger, E.H. Kerns, P. Olynyk and W.L. Budde, *Anal. Chem.*, 55 (1983) 1471–1479.
[2] *Test Methods for Evaluating Solid Waste (SW-846)*, Vol. IB, US Environmental Protection Agency, Washington, DC, 3rd ed., November 1986; Proposed Update II, Rev. 2, November 1992.
[3] W.C. Brumley, C.M. Brownrigg and G.M. Brilis, *J. Chromatogr.*, 558 (1991) 223–233.
[4] W.C. Brumley, C.M. Brownrigg and A.H. Grange, *J. Chromatogr.*, 633 (1993) 177–183.
[5] W.C. Brumley and C.M. Brownrigg, *J. Chromatogr.*, 646 (1993) 377–389.
[6] W.C. Brumley and C.M. Brownrigg, *J. Chromatogr. Sci.*, 32 (1994) 69–75.
[7] *EPA Report 600/R-92/129, Methods for the Determination of Organic Compounds in Drinking Water*, Supplement II, August 1992, Method 553, Rev. 1.1.
[8] W.C. Brumley, *J. Chromatogr.*, 603 (1992) 267–272.
[9] E.C. Huang and J.D. Henion, *Anal. Chem.*, 63 (1991) 732–739.
[10] M.A. Mosely, L.J. Deterding, K.B. Tomer and J.W. Jorgenson, *Anal. Chem.*, 63 (1991) 1467–1473.
[11] R.M. Caprioli, W.T. Moore, M. Martin, B.B. DaGue, K. Wilson and S. Moring, *J. Chromatogr.*, 480 (1989) 247–257.
[12] R.D. Smith, J.A. Olivares, N.T. Nguyen and R.H. Udseth, *Anal. Chem.*, 60 (1988) 436–441.
[13] T. Nohmi and J.B. Fenn, *J. Am. Chem. Soc.*, 114 (1992) 3241–3246.
[14] *Field Methods Compendium (FMC), OERR 9285.2-11*, Hazardous Site Evaluation Division, Analytical Operations Branch, US Environmental Protection Agency, Washington, DC, July 1993.
[15] C.A. Monnig and J.W. Jorgenson, *Anal. Chem.*, 63 (1991) 802–807.

[16] *Proceedings of the 1st International Symposium, Field Screening Methods for Hazardous Waste Site Investigation, US Environmental Protection Agency, Las Vegas, NV, October 11–13, 1988*, U.S. EPA, Environmental Monitoring Systems Laboratory, Las Vegas, NV.
[17] P. Jankik, W.R. Jones, A. Weston and P.R. Brown, *LC·GC*, 9 (1991) 634–645.
[18] K. Utasuka, S. Terabe and T. Ando, *J. Chromatogr.*, 348 (1985) 39–47.
[19] S. Terabe, Y. Miyashita, O. Shibata, E.R. Barnhart, L.R. Alexander, D.J. Patterson, B.L. Karger, K. Hosoya and N. Tanaka, *J. Chromatogr.*, 516 (1990) 23–31.
[20] C.P. Ong, H.K. Lee and S.F.Y. Li, *J. Chromatogr.*, 542 (1991) 473–481.
[21] F. Foret, V. Sustacek and P. Boček, *Electrophoresis*, 11 (1990) 85–97.
[22] S. Terabe, K. Otsuka, K. Ichikawa and A. Tsuchiya, *Anal. Chem.*, 56 (1984) 111–113.
[23] S. Terabe, K. Otsuka and T. Ando, *Anal. Chem.*, 57 (1989) 834–841.
[24] W.G. Kuhr and C.A. Monnig, *Anal. Chem.*, 64 (1992) 389R–407R.
[25] H. Nishi, T. Fakuyama, M. Matsuo and S. Terabe, *J. Chromatogr.*, 513 (1990) 279–295.
[26] S. Terabe, *Micellar Electrokinetic Chromatography*, Beckman Instruments, Fullerton, CA, 1992.
[27] *Products Catalog and Reference Guide 1992–1993*, J & W Scientific, Folsom, CA, 1992.
[28] P. Camilleri, *Capillary Electrophoresis: Theory and Practice*. CRC Press, Boca Raton, FL, 1993, p. 57.

ELSEVIER

Journal of Chromatography A, 680 (1994) 175–179

JOURNAL OF CHROMATOGRAPHY A

Optimization of separation selectivity in capillary electrophoresis of flavonoids

P.G. Pietta*[,a], P.L. Mauri[b], L. Zini[a], C. Gardana[a]

[a]*Università degli Studi di Milano, Via Celoria 2, 20133 Milan, Italy*

[b]*ITBA–CNR, Via Ampère 56, 20131 Milan, Italy*

Abstract

The migration behaviour of selected flavonoids differing in their degree of hydroxylation was investigated. The influence of the solvent in the injected sample, the surfactant [sodium dodecyl sulphate (SDS)] and pH on the separation selectivity was studied. The organic solvent (methanol or 2-propanol) modifies the interaction between micelles and analytes, thus reducing migration times and resolution. SDS improves the separation at pH 8.3, whereas it has less or no effect at higher pH. At pH 10.5 the separation is mainly regulated by ionization of the hydroxyl groups and borate complexation of the carbohydrate residues.

1. Introduction

Flavonoids are ubiquitous secondary plant metabolites which occur in the free state (aglycone) or as glycosides. These compounds have the basic skeleton of 2-phenylbenzopyrone, and differ in their degree of saturation and the position of hydroxyl, methoxyl and sugar residues. Flavones and flavonols are widespread in different vegetables, fruits and medicinal plants [1], and their analysis has mainly been performed by reversed-phase high-performance liquid chromatography (HPLC) [2]. Recently, capillary electrophoresis (CE) has been proposed as a complementary technique, and the micellar mode introduced by Terabe *et al.* [3] is one of the most widely used CE modes. Micellar electrokinetic chromatography (MEKC) is a hybrid of electrophoresis and chromatography, as micelles originated by the surfactant added to a buffer provide both ionic and hydrophobic interactions. This technique has been applied to the separation of a number of flavonoid-containing drugs [4], and integration of the CE apparatus with UV diode-array detection (DAD) has permitted "on-line" structural information to be obtained as for HPLC [5]. So far, the migration behaviour of flavonoids has received little attention, mainly concerning the role of buffer concentration and sampling time [6,7]. In this work, the influence of pH, the surfactant [sodium dodecyl sulphate (SDS)] and the amount of organic solvent injected on the electrophoretic mobilities and resolution of selected flavonol glycosides was studied.

2. Experimental

2.1. Reagents

Methoxylflavonols (**8**, **9** and **10**) were isolated

* Corresponding author.

0021-9673/94/$07.00
SSDI 0021-9673(94)00285-H

from *Arnicae flos* according to ref. 8. Quercetin, kaempferol and isorhamnetin glucosides (**2**, **3**, **6** and **7**) and rutinosides (**1**, **4** and **5**) were purchased from Extrasynthese (Genay, France).

SDS and sodium tetraborate were purchased from Sigma (St. Louis, MO, USA). Methanol and 2-propanol were of HPLC grade.

The sample mixtures were prepared dissolving 0.5 mg of each standard in various percentages (10–100%) of organic solvent. Replicate injections ($n = 5$) were made.

2.2. Apparatus and conditions

Capillary electrophoretic separations were carried out using a Model 270A apparatus from Applied Biosystems (San Jose, CA, USA) equipped with a 58 cm (to the detector) × 50 μm I.D. fused-silica capillary and a ^{3D}CE system from Hewlett-Packard (Waldbronn, Germany) equipped with a 50 cm (to the detector) × 50 μm I.D. fused-silica capillary. The running buffer was 20 m*M* tetraborate (pH range 8.3–10.5, SDS concentration range 0–100 m*M*). The voltage was 270–300 V/cm; the injection was by aspiration for the Model 270A and by positive pressure for the ^{3D}CE system. The temperature was 30°C and detection was performed at 260 nm.

3. Results and discussion

Quercetin, kaempferol and isorhamnetin are very common flavonols and they occur mainly as glycosides, where the sugar moiety is either a monosaccharide residue (3-O-glucosyl, 3-O-galactosyl) or a disaccharide residue such as 3-O-rutinosyl (Fig. 1). For this reason, compounds **1–10** were considered for investigating the effect of the injected solvent, SDS and pH on electrophoretic mobilities and separation.

3.1. Influence of the organic solvent

Sample preparation is a crucial step in the analysis of flavonoid-containing drugs, and often after a solid-phase purification step the samples are dissolved in solvents, such as methanol or

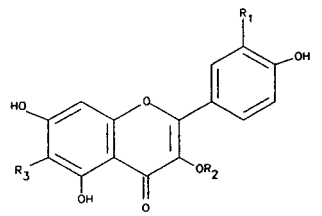

	R_1	R_2	R_3	Compound
1	OH	Rutinose	H	Quercetin-3-O-Rutinoside
2	H	Glucose	H	Quercetin-3-O-Glucoside
3	OH	Galactose	H	Quercetin-3-O-Galactoside
4	H	Rutinose	H	Kaempferol-3-O-Rutinoside
5	OCH_3	Rutinose	H	Isorhamnetin-3-O-Rutinoside
6	H	Glucose	H	Kaempferol-3-O-Glucoside
7	OCH_3	Glucose	H	Isorhamnetin-3-O-Glucoside
8	OH	Glucose	OCH_3	Quercetin-6-methoxy-3-O-Glucoside
9	H	Glucose	OCH_3	Kaempferol-6-methoxy-3-O-Glucoside
10	OCH_3	Glucose	OCH_3	Isorhamnetin-6-methoxy-3-O-Glucoside

Fig. 1. Structures of the investigated flavonol-3-O-glycosides.

2-propanol. The presence of this organic modifier may cause problems in the separation, and its effect on migration time and resolution needs to be known.

Rutin (**1**) was chosen as a reference standard, and several injections were made keeping constant either the sampling time or the percentage of the solvent present in the sample. As shown in Fig. 2, the migration times decrease linearly with increasing amount (0.2–2 nl) of injected solvent. The organic solvent influences the resolution, as exemplified in Fig. 3, which shows how the separation of quercetin-3-O-glucoside (**2**) and quercetin-3-O-galactoside (**3**) is related to the percentage of methanol used to dissolve the sample. For an injection time of 1 s (about 4 nl of sample), optimum resolution of this critical pair is achieved using less than 30% methanol. Analogous results can be obtained by injecting decreasing volumes (less than 4 nl) of a 100% methanolic solution, as the amount of methanol injected is an essential parameter for the resolution.

For routine analysis of flavonoid drugs, it may be suggested that the sample is dissolved in 30%

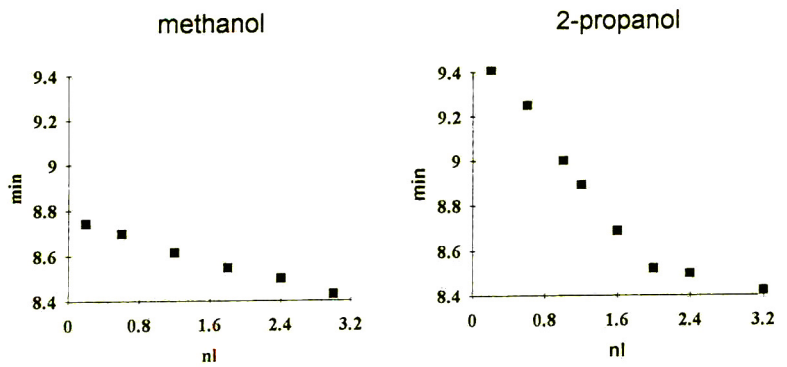

Fig. 2. Influence of the solvent injected on migration times. CE conditions: apparatus, Model 270A equipped with a 58 cm (to the detector) × 50 μm I.D. fused-silica capillary; running buffer, 20 m*M* borate–70 m*M* SDS (pH 8.3); voltage, 270 V/cm; standard, rutin (**1**).

methanol with injection times of 0.5–1.5 s (volumes ca. 2–6 nl).

3.2. *Influence of the surfactant*

A standard mixture of six flavonol-3-O-glucosides was analysed using running buffers with or without SDS. The presence of SDS is crucial for the separation of all components (Fig. 4), as its effect is related to the degree of hydroxylation. SDS decreases the mobilities of kaempferol and isorhamnetin glycosides as compared with quercetin glycosides (Fig. 5), the migration order being Q-Rut (**1**) > Q-Glu (**2**) > K-Rut (**4**) > I-Rut (**5**) > K-Glu (**6**) > I-Glu (**7**). In contrast, in the absence of SDS, kaempferol and isorhamnetin derivatives migrate faster than quercetin derivatives, and with the same sugar moiety [*i.e.*,

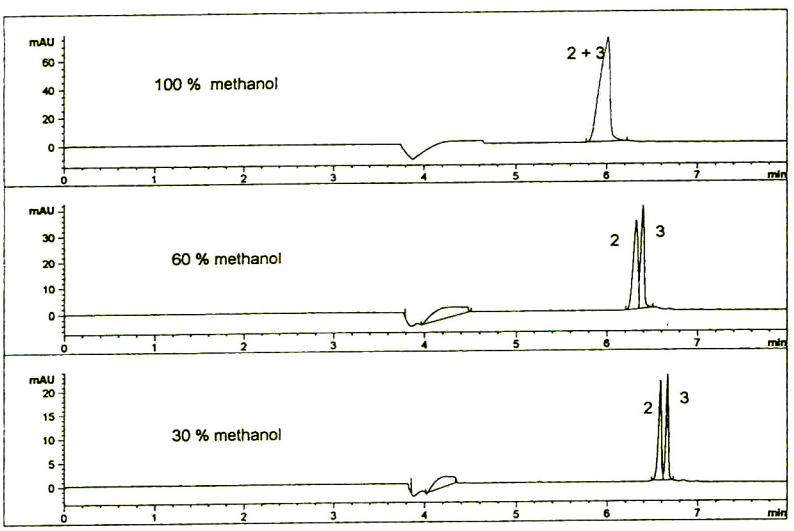

Fig. 3. Influence of percentage of solvent in the sample on resolution. CE conditions: apparatus, ^{3D}CE equipped with a 50 cm (to the detector) × 50 μm I.D. fused-silica capillary; running buffer, 20 m*M* borate–50 m*M* SDS (pH 8.3); voltage, 300 V/cm; injection, 50 mbar, 1 s; for peak identification, see Fig. 1.

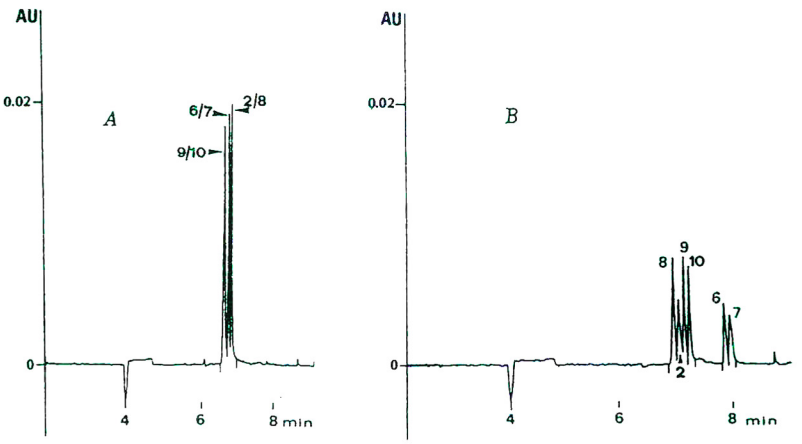

Fig. 4. Influence of the surfactant (SDS) on resolution and mobilities of glucosylflavonols: (A) without SDS and (B) with 50 m*M* SDS. For CE conditions, see Fig. 2; for peak identification, see Fig. 1.

K-Glu (**6**), I-Glu (**7**) and K-Rut (**4**), I-Rut (**5**)] they are not resolved.

3.3. Influence of pH

The pH range 8–11 was chosen to exploit better the influence of the electroosmotic flow on the electrophoretic mobility. At pH 8.3 both the aglycone structure and the sugar type have an impact on migration, whereas at pH 9.3 the electrophoretic behaviour is mainly influenced by the linked carbohydrate. At this pH the presence of SDS is less important, and the order of migration of K-Glu (**6**) and I-Glu (**7**) is inverted. On increasing the pH to 10.5, the migration order depends on linked sugars and changes substantially (Fig. 6); the surfactant has no influence on mobilities and resolution.

From these data, it may be concluded that the amount of the organic solvent injected influences the separation as a consequence of modified partitioning of the analytes between micelles and buffer. Further, the surfactant plays an important role at pH 8.3, as it interacts preferentially with highly hydrophobic kaempferol and isorhamnetin derivatives. Higher pH values improve the complexation of flavonols by tetra-

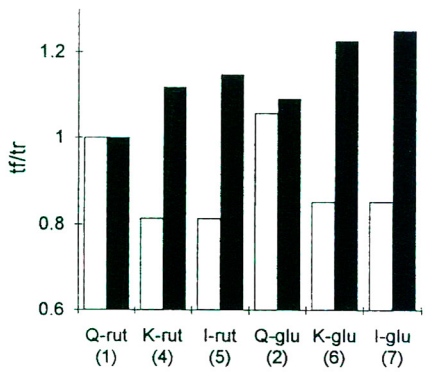

Fig. 5. Effect of SDS on mobilities and resolution of flavonol glucosides and rutinosides at pH 8.3 with 20 m*M* borate: (□) without SDS and (■) with 50 m*M* SDS. t_t = Migration time of the investigated flavonol; t_r = migration time of rutin (**1**).

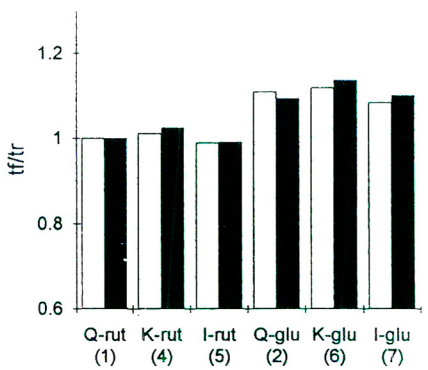

Fig. 6. Electrophoretic behaviour of flavonol glucosides and rutinosides at pH 10.5 with 20 m*M* borate: (□) without SDS and (■) with 50 m*M* SDS.

borate, and the effect of the surfactant is reduced (pH 9.3) or cancelled (pH 10.5).

Acknowledgement

The authors are grateful to CNR–P.F. "Chimica Fine" for providing funds (U.O.P.L. Mauri).

References

[1] J.B. Harbone (Editor), *The Flavonoids, Advances in Research Since 1986*, Chapman & Hall, London, 1994.
[2] P.G. Pietta, P.L. Mauri, E. Manera and P.L. Ceva, *J. Chromatogr.*, 513 (1990) 397.
[3] S. Terabe, K. Otsuda and T. Ando, *Anal. Chem.*, 57 (1985) 834.
[4] P.G. Pietta, P.L. Mauri, A. Rava and G. Sabbatini, *J. Chromatogr.*, 549 (1991) 367.
[5] P.G. Pietta, P.L. Mauri, A. Bruno and L. Zini, *J. Chromatogr.*, 638 (1993) 357.
[6] U. Seitz, P. Oefner, S. Nathakarnkitkool, M. Popp and G. Bonn, *Electrophoresis*, 13 (1992) 35.
[7] P. Morin, F. Villard and M. Dreux, *J. Chromatogr.*, 628 (1993) 153.
[8] I. Merfort, *Phytochemistry*, 31 (1992) 2111.

ELSEVIER

Journal of Chromatography A, 680 (1994) 181–185

JOURNAL OF CHROMATOGRAPHY A

Analysis of isoflavones by capillary electrophoresis

Z.K. Shihabi*, T. Kute, L.L. Garcia, M. Hinsdale

Pathology Department, Bowman Gray School of Medicine, Wake Forest University, Winston-Salem, NC 27157, USA

Abstract

A simple capillary electrophoresis method is described for the assay of several isoflavones and coumestrol isolated from plant extracts. The method has good reproducibility; it compares well to HPLC, and it can be performed in less than 10 min.

1. Introduction

Phytoestrogens are common in many plant species. They resemble estrogens and mimic some of their functions. Recently, interest in these compounds has increased considerably because many of them have been found to inhibit tumor growth *in vitro* [1–3] and *in vivo* [4,5]. For example, the isoflavone genistein specifically inhibits tyrosine kinase [6] and DNA topoisomerase [7]. However, analysis of these compounds from plant extracts is difficult, often requiring a prior derivatization of the compounds before analysis. Some of the methods used to analyze these compounds include HPLC [8] and GC–MS [9,10]. Here, we show that these compounds can be analyzed from plant extracts easily and rapidly by capillary electrophoresis (CE).

2. Materials and methods

2.1. Chemicals

3-Methyl-1-isobutylxanthine was obtained from Aldrich (Milwaukee, WI, USA). Coumestrol was obtained from Eastman Kodak (Rochester, NY, USA). The isoflavone standards were gifts from Dr. S. Barnes, University of Alabama, Birmingham, AL, USA. The HPLC column was obtained from E. Merck (Gibbstown, NJ, USA).

2.2. CE Equipment

A CE instrument (Beckman Instruments, Fullerton, CA, USA), was set at 254 nm. The capillary, 50 cm × 50 μm I.D., was rinsed after each run with 1 *M* NaOH for 1 min, and filled for another minute with 200 m*M* borate buffer, pH 8.6 (the running buffer). The voltage was set at 13 kV, and the sample was introduced by pressure injection for 10 s.

2.3. Sample extraction

Soy beans or other plant parts were homogenized to a fine powder, and 15-mg samples were vortex-mixed in a centrifuge tube with 1 ml of extracting solution. The extracting solution consisted of 66% acetonitrile, 0.4% NaCl and 30 mg/l of methyl isobutyl xanthine, as an internal standard, in water. The sample was centrifuged for 15 s at 14 000 *g* in a Model B Microfuge

* Corresponding author.

0021-9673/94/$07.00
SSDI 0021-9673(94)00307-U

(Beckman Instruments, Palo Alto, CA, USA), and the aliquot was introduced into the instrument. The isoflavones are not very soluble in aqueous or organic solvents; however, we found that a mixture of water and acetonitrile improved their solubility.

2.4. HPLC Equipment

For comparison studies, samples were also measured by HPLC. A Model 110 A pump (Beckman Instruments, Fullerton, CA, USA), was used to deliver the mobile phase at 1.2 ml/min through a C_8, 5-μm cartridge column, 125 mm × 4 mm I.D. The sample was introduced through a 20-μl loop and eluted isocratically for daidzin and genistin with a mobile phase of 16% acetonitrile in 20 m*M* phosphate buffer, pH 7.2. To elute daidzein and genistein, the mobile phase was 23% acetonitrile in the same phosphate buffer.

3. Results and discussion

A good baseline separation of five different isoflavones, in addition to coumestrol, is achieved in less than 10 min as illustrated in Fig. 1A. Fig. 1B shows the electropherogram from a soy bean extraction. It indicates the presence of isoflavones, as well as, other UV-absorbing compounds. Optimum separation occurs at a pH range of 8.5–8.8. Above this range, the migration time increases, and the daidzin peak becomes very broad. At lower pH, daidzein and genistein migrate very close to biochanin A (4′-methoxygenistein). The linearity of the test was determined using genistein. The response is linear from 0.4 to 60 mg/l (Fig. 2). The minimum detectable limit (3 S.D. above baseline) for genistein is 0.4 mg/l. The reproducibility of the migration time and the peak height for all of these compounds is good as summarized in Table 1. The table shows that the R.S.D. for both the migration time and peak height improves, in general, when the calculation is based on the internal standard. For example, the R.S.D. (n = 10) for the peak height of daidzein is 4.46%,

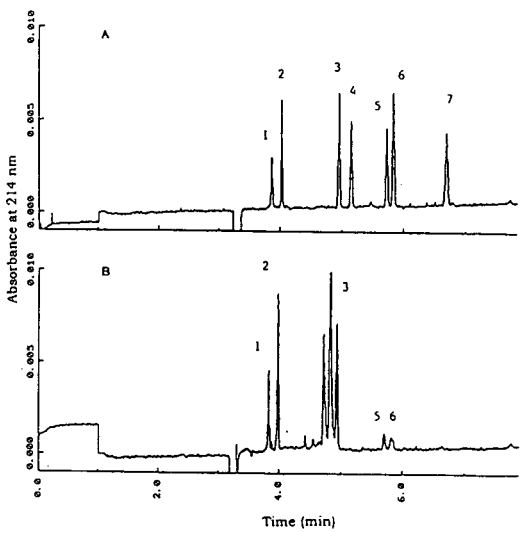

Fig. 1. Separation of the following compounds: 1 = daidzin; 2 = genistin; 3 = internal standard (methylxanthine); 4 = biochanin A; 5 = daidzein; 6 = genistein; 7 = coumestrol. (A) Standards in the extracting solution at a concentration of 6 mg/l, (B) soy bean seeds extract in the presence of 0.4% NaCl.

while the R.S.D. is 1.54% when the calculation is based on the internal standard.

Fig. 3 illustrates how the concentration of different isoflavones varies among different varieties of soy beans. Among the isoflavones present in soy beans are genistein and daidzein, which inhibit tumor growth directly in tissue cultures [1–3]. However, their sugar conjugates, daidzin and genistin, do not exhibit this effect [1–3]. The concentration of these four isoflavones measured by CE from soy beans is very

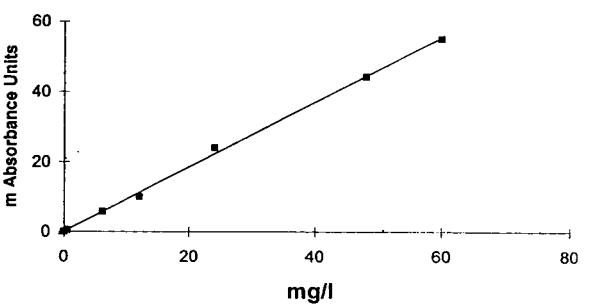

Fig. 2. Genestein calibration on the CE apparatus.

Table 1
The relative standard deviation (R.S.D.) of the different compounds

Compound	R.S.D. (%) (n = 10)			
	Peak height (mm)	Peak height/ I.S.	Migration time (min)	Migration time/ I.S.
Internal standard (I.S.)	5.21	0.00	0.75	0.00
Daidzin	3.29	3.60	1.19	0.71
Genistin	4.62	2.70	1.02	1.06
Biochanin A	5.68	1.09	1.05	1.10
Genistein	3.02	2.64	1.02	1.08
Daidzein	4.46	1.54	1.20	0.91
Coumestrol	3.66	3.67	1.28	1.14

close to that measured by HPLC (Fig. 4), and also close to that reported in the literature [11].

The kudzu plant, which grows wild in the southern parts of the USA, is a rich source of daidzein, as indicated by the electropherogram produced by root extracts of this plant (Fig. 5). The daidzein peak was verified by spiking the sample with pure daidzein. On the other hand, daidzin has been found, recently, to inhibit human mitochondrial aldehyde dehydrogenase [12]. Interestingly, root extracts of this plant in pill form have been used in the orient as treatment for alcoholism.

We have found this CE method to be very useful in following the isolation and purification of these compounds. The advantages of this

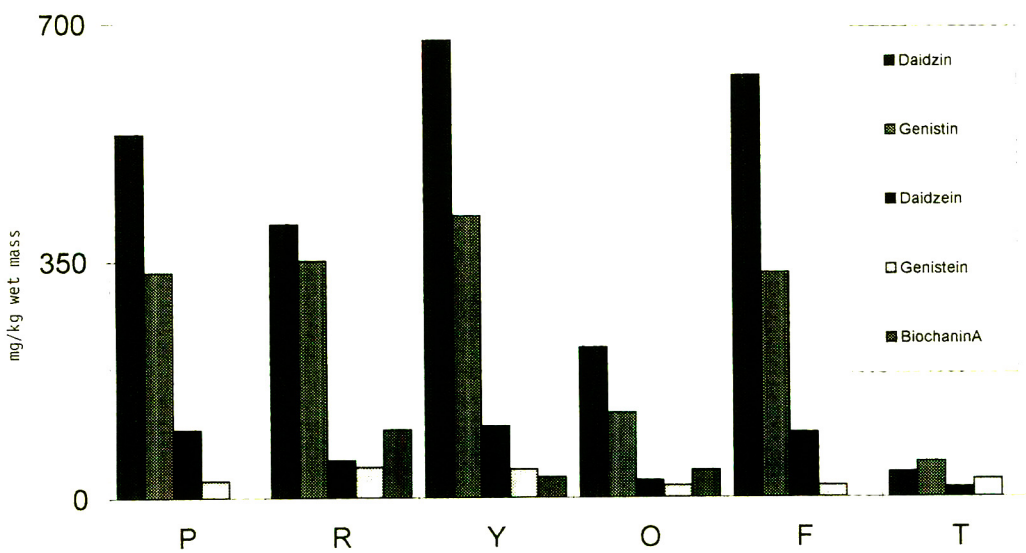

Fig. 3. Content of isoflavones in different varieties of soy bean seeds obtained locally. P = Powder; R = roasted; Y = yellow; O = organic; F = flakes; T = Tofu.

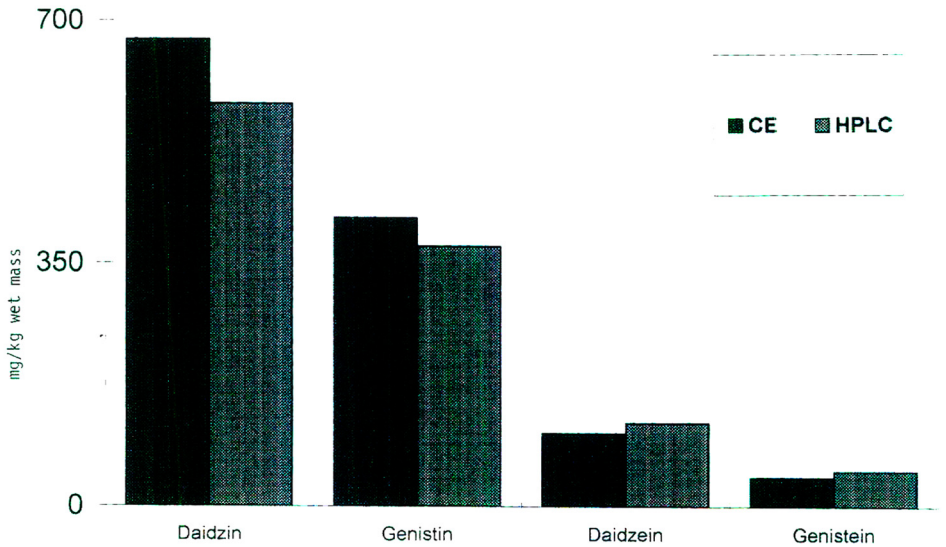

Fig. 4. Comparison of isoflavones by HPLC and CE extracted from yellow soy beans.

method over HPLC are: it is rapid; it does not require solvent gradient and column equilibration, and it does not consume organic solvents for elution. In addition, the capillaries for CE are much less expensive than the columns for HPLC.

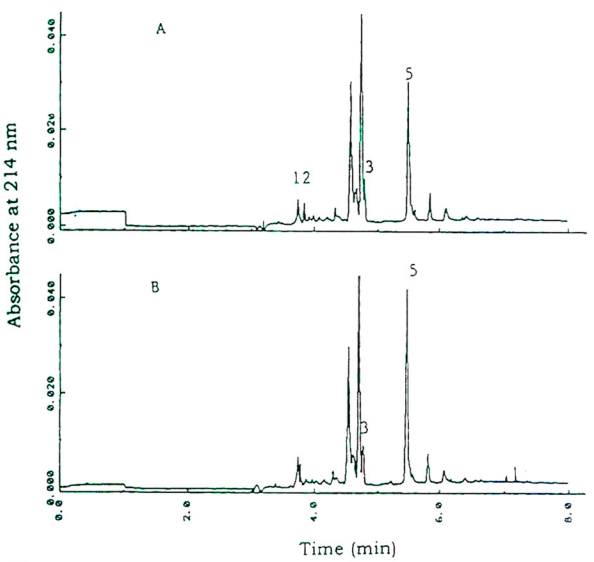

Fig. 5. Daidzein content of (A) kudzu roots (15 mg of the roots were homogenized in 1 ml of the extracting solvent) and (B) after spiking with daidzein (6 mg/l).

Acknowledgement

We thank Dr. S. Barnes from the University of Alabama at Birmingham, for supplying the isoflavone standards.

References

[1] G. Peterson and S. Barnes, *Biochem. Biophys. Res. Commun.*, 179 (1991) 661.
[2] Y. Matsukawa, N. Marui, T. Sakai, Y. Satomi, M. Yoshida, K. Matsumoto, H. Nishino and A. Aoike, *Cancer Res.*, 53 (1993) 1328.
[3] F. Traganos, B. Ardelt, N. Halko, S. Bruno and Z. Darzynkiewicz, *Cancer Res.*, 52 (1992) 6200.
[4] S. Barnes, C. Grubbs, K.D.R. Setchell and J. Carlson, *Progr. Clin. Biol. Res.*, 347 (1990) 239.
[5] H. Adlecreutz, in P. Rozen (Editor), *Frontiers of Gastrointestinal Research*, Karger, Basel, 1988, pp. 165–176.
[6] T. Akiyama, J. Ishida, S. Nakagawa, S. Ogawara, S. Watanabe, N. Itoh, M. Shibuya and Y. Fukami, *J. Biol. Chem.*, 262 (1987) 5592.

[7] Y. Yamashita, S.-Z. Kawada and H. Nakano, H., *Biochem. Pharmacol.*, 39 (1990) 737.
[8] A.C. Eldridge, *J. Chromatogr.*, 234 (1982) 494.
[9] M. Naim, B. Gestetner, I. Kirson, Y. Birk and A. Bondi, *Phytochemistry*, 12 (1973) 169.
[10] M. Naim, B. Gestetner, S. Zilkah, Y. Birk and A. Bondi, *J. Agric. Food Chem.*, 22 (1974) 806.
[11] K.R. Price and G.R. Fenwick, *Food Addit. Contam.*, 2 (1985) 73.
[12] W.-M. Keung and B.L. Vallee, *Proc. Natl. Acad. Sci. U.S.A.*, 90 (1993) 1247.

ELSEVIER

Journal of Chromatography A, 680 (1994) 187–200

JOURNAL OF CHROMATOGRAPHY A

Determination of carbohydrates in fruit juices by capillary electrophoresis and high-performance liquid chromatography

A. Klockow[a,b], A. Paulus[a,*], V. Figueiredo[c], R. Amadò[b], H.M. Widmer[a]

[a]*Ciba, Corporate Analytical Research, CH-4002 Basle, Switzerland*

[b]*Swiss Federal Institute of Technology (ETH Zurich), Institute of Food Science, CH-8092 Zurich, Switzerland*

[c]*Kantonales Laboratorium Basel Stadt, Kannenfeldstrasse 2, CH-4012 Basle, Switzerland*

Abstract

A capillary zone electrophoresis (CZE) method with indirect UV detection was adapted for the routine determination of carbohydrates in a variety of fruit juices. The method was optimized with respect to the effect of buffer pH, temperature and capillary length. Potassium sorbate was chosen as the background electrolyte and chromophore for UV detection at 256 nm. Optimum separation conditions were found with a buffer of a pH of 12.2–12.3 and a subambient temperature of 15°C. The optimized CZE method was compared with a routine method for the determination of sugars in fruit juices, a high-performance anion-exchange chromatographic method with pulsed amperometric detection (HPAEC–PAD), with respect to separation efficiency, sensitivity, linearity and repeatability. The CZE method showed a 10–20-fold increase in separation efficiency compared with the HPAEC–PAD method, but the amperometric detection in the latter proved to result in detection limits of 2–3 orders of magnitude lower than those obtained by indirect UV detection. Both methods showed good linearity in the investigated concentration ranges and good repeatability for migration times and peak areas. CZE with commercial instrumentation was applied to the routine determination of carbohydrates in fruit juices such as orange, apple and grape juice. The quantitative CZE results with internal calibration showed no significant differences from those for the HPAEC–PAD reference method. It was demonstrated that capillary electrophoresis (CE) can be applied in a routine food testing laboratory. The method is simple, inexpensive and easy to implement and will further broaden the application range of CE in food analysis.

1. Introduction

In recent years, capillary electrophoresis (CE) has attracted increasing interest and its successful use in different application fields such as biochemistry, biotechnology, pharmacy and clinical chemistry has been demonstrated in a variety of studies [1–3]. However, the impact that CE can have in food science and particularly in quality control of food and food additives is today only starting to be recognized. So far, less than 100 CE applications in food science have been published. Among them, the analysis of hop bitter acids in beer [4], the differentiation and determination of milk proteins [5] and the identification of different sulfonamides in pork meat as a means to ascertain the use of animal drugs [6] are worth mentioning. CE can also be very helpful for the determination of ascorbic acid [7] and other organic acids [8] in fruit juices.

Currently, the most popular techniques for the determination of carbohydrates in food stuff are

* Corresponding author.

0021-9673/94/$07.00
SSDI 0021-9673(94)00454-H

thin-layer chromatography (TLC), gas chromatography (GC) of volatile carbohydrate derivatives and high-performance liquid chromatography (HPLC). Although TLC is a simple and rapid method for the identification of carbohydrate compositions, the analysis times are long and the separation efficiency is often not satisfactory [9]. GC exhibits good sensitivity, but the formation of stereochemical isomers during the necessary derivatization with, for example, trimethylsilane to yield volatile sugar derivatives results in very complex chromatograms and remains a major problem [10]. Other derivatization procedures, such as the formation of alditolacetate or aldonitriloacetate derivatives, also lead to problems in the interpretation of the resulting chromatograms [11].

Another possibility for the rapid determination of simple sugars and also for polysaccharide hydrolysates is electrophoretic separation on supporting media such as paper [12] or silylated glass-fibre paper [13,14]. However, similarly to TLC, slab electrophoretic methods only provide qualitative information. Among the methods mentioned above, HPLC is certainly the most important method for carbohydrate determinations in both research applications and routine analysis. HPLC separations can be carried out on different stationary phases such as alkylated or aminoalkylated silica gels or ion-exchange resins [15]. The latter, in combination with pulsed amperometric detection (PAD) [16,17], represents a selective and sensitive system for carbohydrate determinations with the additional advantage that no derivatization step is required. A disadvantage of this HPLC method is its limited separation efficiency, especially when analysing higher oligosaccharides. In addition, HPLC can be time consuming when column equilibration procedures are necessary. Overall, the analysis costs are high owing to the expensive instrumentation, stationary phase material and solvent consumption.

CE has the potential to be an alternative method to HPLC and also to the other methods because it can bring speed, quantification and reproducibility combined with a high separation efficiency to the routine quality control of carbohydrates. At first sight, an electrophoretic method does not seem appropriate to carbohydrate determinations because the solutes lack both charge (a prerequisite for electrophoretic separation) and a suitable chromophore (necessary for on-column UV detection). To overcome these problems, several strategies can be pursued.

To attach a charge to the sugar solutes, ionization at high pH [18], complexation of their vicinal hydroxyl groups with borate, resulting in an anionic complex [19], and derivatization with a charged label [20] have been described.

On-line detection of sugars without precolumn labelling can be accomplished in the UV region at 195 nm after borate complexation, as the UV absorbance of complexed sugar molecules is increased to allow detection at the millimolar level [19]. Indirect photometric detection [18,21] represents a second possibility. Several procedures for labelling sugars with a suitable labelling reagent for sensitive UV and fluorescence detection have been described, those with 2-aminopyridine [22], 3-methyl-1-phenyl-2-pyrazolin-5-one [23] and 8-aminonaphthalenetrisulfonic acid [24] being the most popular. Other attempts to determine sugars involve different detection schemes, such as amperometric [25] and refractive index detection [26]. By freely combining these different means of charging and detecting sugars, a variety of methods for the determination of carbohydrates using CE can be explored.

Indirect photometric detection of underivatized carbohydrates represents a simple, easy and time-efficient approach. As the pK_a of monosaccharides is generally >12, this method requires a background electrolyte with a pH >12 to ensure the formation of negatively charged sugar molecules. Further, a carrier electrolyte anion with a high molar absorbance will allow adequate detection sensitivities. Although the sensitivity of indirect UV detection methods generally does not reach the levels achieved by direct UV measurements, sugar detection in the low millimolar range is possible, with sorbic acid as an absorbing additive [18].

The aim of this work was the improvement of

a CZE method for the determination of sugars in a high-pH separation system with indirect UV detection [18]. This method was then subsequently applied to the determination of sucrose, glucose and fructose in three different fruit juices. To validate the method, the quantitative CZE results were compared with results obtained for a routine control series in a government food control laboratory applying a certified HPLC method, based on anion-exchange chromatography coupled with pulsed amperometric detection (HPAEC–PAD). Both methods were submitted to a statistical analysis to demonstrate that the CZE method with indirect UV detection is suitable for routine food testing laboratories.

2. Experimental

2.1. Chemicals

All chemicals and sugar standards were of analytical-reagent grade.

For the CE experiments, sugar standards of D-fructose (Fru), L-fucose (Fuc), D-galactose (Gal), D-glucose (Glc), D-mannose (Man), D-raffinose, N-acetyl-D-glucosamine (GlcNAc), N-acetyl-D-galactosamine (GalNAc), N-acetylneuraminic acid (NANA) and D-sucrose (Suc) were purchased from Fluka (Buchs, Switzerland), D-glucoronic acid (GlcA) from Serva (Heidelberg, Germany) and D-galacturonic acid (GalA) from Merck (Darmstadt, Germany). Buffer chemicals were supplied by either Sigma (St. Louis, MO, USA) or Fluka (Buchs, Switzerland). All buffers were prepared with water purified with a Milli-Q system (Millipore, Bedford, MA, USA) and used throughout all analyses.

The three sugar standards (Glc, Fru, Suc) used in the HPAEC analysis were purchased from Merck. Sodium hydroxide (NaOH), necessary for the preparation of the LC eluent, was supplied by Baker (Gross Gerau, Germany).

2.2. Sample pretreatment

For CE separations, the fruit juices were diluted 50–100-fold with Milli-Q-purified water. Whereas the orange juice had to be filtered through a 0.22-μm Millipore filter, the other juices could be applied without further pretreatment. For HPAEC analyses, the juices were diluted 2000–10 000-fold and filtered through a 0.45-μm filter before injection.

2.3. Procedures

The CZE background electrolyte was prepared by dissolving an appropriate amount of potassium sorbate in Milli-Q-purified water to yield a final concentration of 6 m*M*. The pH was adjusted to 11.9–12.4 by titration with 1 *M* NaOH at room temperature. The sugar standard solutions for the method development experiments contained between 0.25 and 0.4 mg ml^{-1} of each sugar. A stock standard solution of 8 mg ml^{-1} of Suc and 4 mg ml^{-1} of Glc and Fru was used for the external calibration in juice analysis. This solution was diluted to concentrations of 0.2–2.0 mg ml^{-1} for Suc and 0.1–1.0 mg ml^{-1} for the two monosaccharides.

For the determination of the response factors, samples containing 0.8 mg ml^{-1} of Suc and 0.4 mg ml^{-1} of Glc and Fru were used. Glucuronic acid was added as an internal standard, resulting in a final concentration of 0.22 mg ml^{-1} GlcA in standard samples and 0.12 mg ml^{-1} GlcA in fruit juices.

To prepare the 200 m*M* sodium hydroxide HPAEC eluent, 26 ml of 50% (w/w) sodium hydroxide solution were mixed with 1000 ml of degassed water. It was necessary to keep the eluent free of carbonate. Sugar mixtures containing 2, 10 and 50 mg l^{-1} of each sugar were used as standard solutions for external calibration.

2.4. Instrumentation

CE separations were performed on a Spectra Phoresis 1000 capillary electrophoresis system (Thermo Separation Products, Freemont, CA, USA). For data acquisition and data handling an OS/2 compatible 486 computer combined with a Spectra Phoresis software package for individual peak integration was used. Fused-silica capil-

laries of 50 μm I.D. from Polymicro Technologies (Phoenix, AZ, USA) were cut to the appropriate length of 42 or 90 cm. The detection window was placed 7 cm from the cathodic end, resulting in an effective separation distance of 35 and 83 cm, respectively. UV detection was carried out at 256 nm throughout all experiments. Injection was accomplished by applying a pressure of 105 mbar for a preset time (1 or 2 s). Unless indicated otherwise, the capillary was thermostated at 15°C. Before starting a series of analyses, the fused-silica capillaries were conditioned by flushing them with running buffer for at least 10 min, followed by an equilibration time of 15 min. Overnight, the capillaries were stored in 1 m*M* NaOH.

HPAEC analyses were accomplished on a Model 4000i ion chromatographic system (Dionex, Sunnyvale, CA, USA) with a 50-μl injection loop and a pulsed amperometric detector (PAD-1). All separations were carried out at room temperature on a Carbopac PA1 column (250 × 4 mm I.D.) combined with a Carbopac PA1 guard column (both from Dionex) at an eluent flow-rate of 1 ml min^{-1}. The detector consisted of a gold working electrode and an Ag/AgCl reference electrode. The pulse sequence used for the carbohydrate analysis consisted of three steps: sampling (50 mV, 480 ms), cleaning (600 mV, 120 ms) and reduction of the electrode surface (−600 mV, 60 ms). To ensure a carbon dioxide-free eluent during analysis, an EDM-2 degassing module (Dionex) was necessary. Data acquisition was carried out on a Maxima 820 work station (Millipore).

3. Results and discussion

3.1. CZE method development

A recently published paper by Vorndran *et al.* [18] served as the basis of the CZE method development. The reasons for choosing sorbate as the carrier electrolyte anion and chromophore for indirect photometric detection, at a concentration of 6 m*M*, are discussed therein.

Separation in CZE is based on differences in the electrophoretic mobilities (μ_{ep}) of the analytes. As the electrophoretic mobility depends mainly on the pH of the separation system, optimization of the buffer pH is important for reaching the optimum separation conditions. Because the pK_a values of sugars are in the range of 12–14 [27], the buffer pH must be >12 to ionize the sugar molecules.

In Fig. 1, the influence of pH on the experimentally determined electrophoretic mobility of four sugars in the pH range 11.9–12.4 is shown. By closely inspecting the experimental data, we could not confirm the previously published [18] linear behaviour between electrophoretic mobility and pH owing to the increased dissociation rate of the sugars with increasing pH. It should be pointed out that those monosaccharides with pK_a values within the investigated pH range (12.1–12.4) exhibit a relatively steep increase in electrophoretic mobility, indicating their higher degree of ionization. Raffinose, with a reported pK_a of 12.74 [27], shows a linear relationship.

Surprisingly, the electroosmotic flow inside the capillary decreased continuously from pH 11.9 to 12.4, resulting in longer analysis times for all solutes. This can be explained by an increase in the ionic strength of the background electrolyte, resulting in a thinner double layer and thus a lower zeta potential [28].

The temperature of the buffer system is also an important parameter that has a pronounced influence on the separation of low-molecular-mass carbohydrates. According to the literature, an increase in temperature of 1°C should increase the electrophoretic mobility by approximately 2% [29]. However, in our experiments, an increase in the electrophoretic mobilities with decreasing temperature was observed. This behaviour is due to a change in pH rather than to a temperature effect alone. At lower temperature, the dissociation of water molecules is dictated by a smaller ion-product value, resulting in a lower proton concentration and thus in a higher pH.

Table 1 demonstrates the effects that pH and temperature changes have on the resolution of various sugar pairs. From these values it can be concluded that, in order to increase the dissocia-

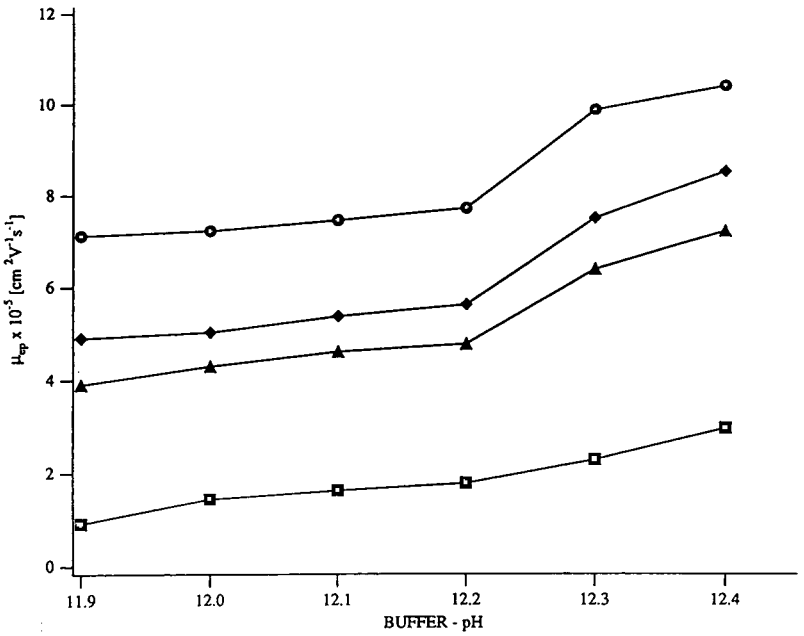

Fig. 1. Experimentally determined electrophoretic mobilities of carbohydrates as a function of pH. Running conditions: buffer 6 m*M* sorbate adjusted to different pH; capillary, 42 cm (35 cm effective length) × 50 μm I.D.; 230 V cm^{-1}; 15°C; indirect UV detection at 256 nm; 2-s injection. Solutes: ○ = mannose; ◆ = glucose; ▲ = galactose; □ = raffinose.

tion and improve the resolution of the sugars, it is best to choose a temperature as low and a pH as high as possible for the separation. However, there are instrumental limitations. Above pH 12.3, fluctuations in the UV baseline were observed, rendering an analysis impossible. Consequently, for practical purposes a buffer pH of 12.2–12.3 and a temperature of 15°C were chosen. All subsequent experiments were carried out under these conditions.

Table 1
Resolution as a function of pH and temperature

	Resolution			
	μ_{eo}–Raf	Raf–Gal	Gal–Glc	Glc–Man
pH 11.9	0.41	1.49	0.44	1.69
pH 12.0	0.77	1.75	0.54	1.77
pH 12.1	1.00	2.10	0.59	1.82
pH 12.2	1.31	2.43	0.71	1.76
pH 12.3	1.49	3.10	1.10	2.18
pH 12.4	1.90	3.73	1.15	2.12
40°C	0.47	0.86	0	0.84
30°C	0.60	1.27	0.28	1.07
25°C	0.79	1.48	0.46	1.29
20°C	0.93	1.97	0.64	1.47
15°C	1.19	2.55	0.85	1.81

Theory predicts that the separation efficiency in CZE is proportional to capillary length when the electric field is kept constant [30]. In addition, a contribution from injection to band broadening can be observed, which has an impact on the separation efficiency and resolution. This influence of capillary length on the separation is demonstrated in Fig. 2. Fig. 2a shows the separation of the eight monosaccharides expected to occur in glycoproteins. It can be calculated that a 1-s injection at 105 mbar into a 42-cm capillary will result in an injection plug of

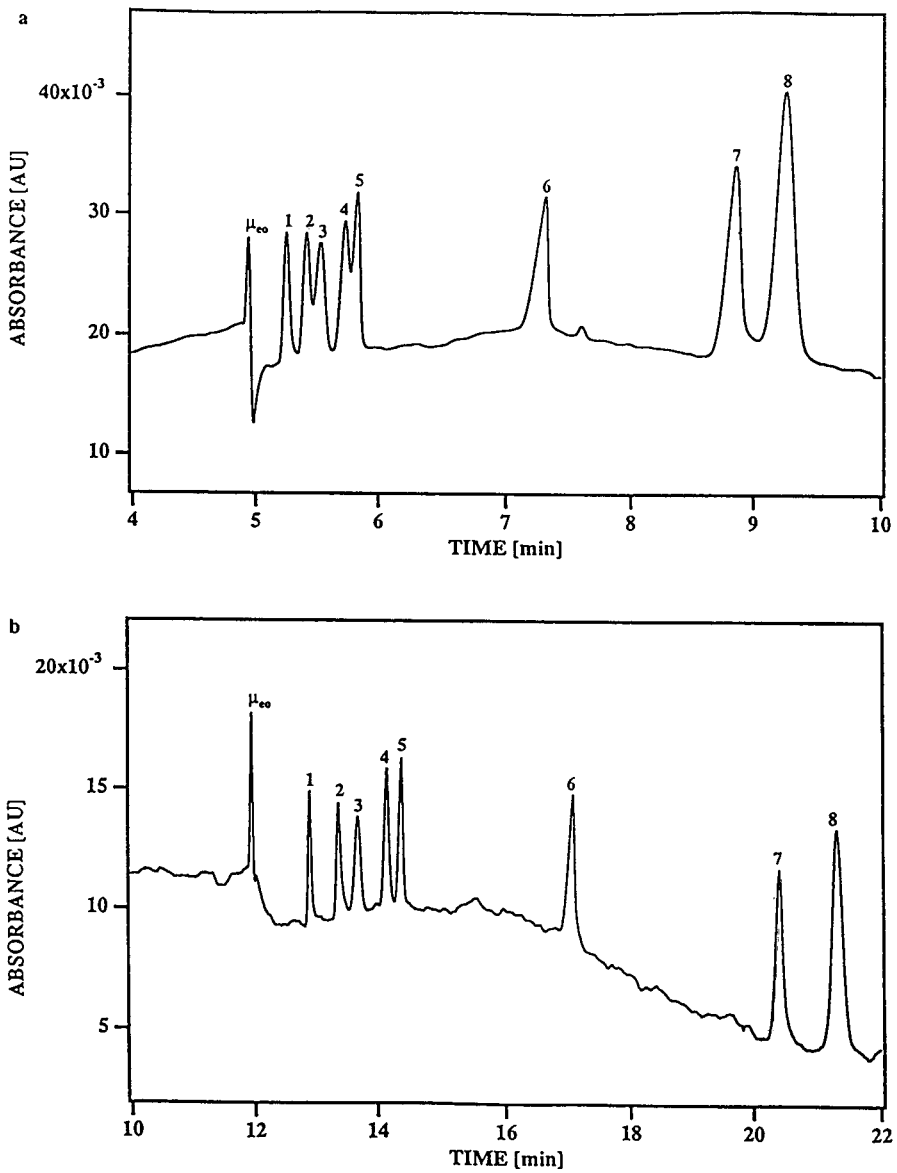

Fig. 2. Capillary zone electrophoresis of carbohydrates. Running conditions: buffer 6 m*M* sorbate adjusted to pH 12.2; 230 V cm^{-1}; 15°C; indirect UV detection at 256 nm; 1-s injection. Sugars, 0.97–1.55 m*M*; 1 = fucose; 2 = galactose; 3 = glucose; 4 = N-acetylgalactosamine; 5 = N-acetylglucosamine; 6 = N-acetylneuraminic acid; 7 = galacturonic acid; 8 = glucuronic acid. (a) Capillary 42 cm (35 cm effective length) × 50 μm I.D.; (b) capillary 90 cm (83 cm effective length) × 50 μm I.D.

1.95 mm. This leads to an incomplete resolution of the sugar pairs Gal–Glc and GalNAc–GlcNAc, because more of the capillary volume was occupied by the injection plug compared with a longer capillary, resulting in a shorter effective separation length. If the same experiment was performed in a 90-cm capillary, as shown in Fig. 2b, the separation efficiency more than doubled, resulting in baseline resolution of these sugar pairs, but at the cost of doubling the analysis time. The better resolution can be attributed to two effects: the smaller contribution of the shorter injection plug of 0.9 mm, which results from a higher pressure drop at the longer capillary, and the longer separation distance with the same electric field strength.

As the resolution of the three sugars Glc, Fru and Suc, occurring in fruit juices, proved to be sufficient with the shorter capillary, the 42-cm capillary was chosen for further separations.

3.2. Comparison of CZE with HPAEC

In order to evaluate the usefulness of the above-described CZE method, the results of the CZE experiments were compared with those obtained with the state-of-the-art method for carbohydrate analysis in routine work, HPAEC–PAD. The comparison was made with respect to separation efficiency, sensitivity, linearity and repeatability.

Separation efficiency

The separation power of two analytical systems can be evaluated by the separation efficiency, expressed by the number of theoretical plates (N). N describes the band broadening in a given analysis system and can be calculated by the expression

$$N = 5.54(t_m / w_h)^2$$

where t_m is the migration time and w_h the peak width at half-height [31]. As shown in Table 2, typical plate numbers for the sugar solutes in the HPAEC system are in the range 3000–4000. In CZE, the separation efficiency proved to be 10–20 times higher with theoretical plate numbers of 30 000–70 000 (Table 2). This is important, because a high separation efficiency has a positive effect on the resolution of the analytes.

Although the number of theoretical plates in CZE is more than one order of magnitude higher than in HPAEC, even higher plate numbers, up to 400 000, would be expected with indirect UV detection [32]. However, this requires an effective mobility of the analyte ions close to that of the background electrolyte co-ion, in order to avoid a concentration overload [33]. In the separation system discussed here, the electrophoretic mobility of the sorbate anion was measured at pH 12.2 to be $42.8 \cdot 10^{-5}$ cm^2 V^{-1} s^{-1} whereas the sugars showed the following, much lower mobilities: Suc, $2.24 \cdot 10^{-5}$; Glc, $7.12 \cdot 10^{-5}$; and Fru, $8.89 \cdot 10^{-5}$ cm^2 V^{-1} s^{-1}. Therefore, the separation efficiency was relatively low compared with other CE separations, but still compares favourably with the HPAEC results.

Limit of detection (LOD)

The LOD has an impact on the degree of sample dilution and the reproducibility of the

Table 2
Comparison of separation efficiency and limits of detection in CZE and HPAEC

Sugar	Separation efficiency (N)		Limit of detection (LOD)	
	CZE	HPAEC	CZE (mM)	HPAEC (μM)
Sucrose	49 700	4 350	0.29	0.58
Glucose	29 300	3 400	0.23	1.11
Fructose	69 600	3 100	0.24	1.11

measurements because of the decreased matrix effects at higher dilutions. The LOD was calculated as the concentration that gave a signal three times greater than the baseline noise. As shown in Table 2, indirect UV detection with sorbate resulted in LODs of 0.23–0.29 m*M*, whereas PAD was able to detect as little as 0.5–1 μM concentrations of sugars. Thus PAD resulted in detection limits of 2–3 orders of magnitude better than those with indirect UV detection.

Concentration detection limits in the 10^{-4} *M* range for carbohydrates are not very impressive. Assuming a 50-μm capillary and molar absorptivities (ε) of 10 000–100 000 l mol^{-1} cm^{-1}, concentration detection limits in the 10^{-5}–10^{-7} *M* range can be expected according to the Lambert–Beer law. If, in a separation method, labelling of the carbohydrates should be avoided, indirect detection is the only alternative. In that event, the spectroscopic characteristics of the indirect UV absorber is responsible for the detection limits. The chosen compound should match the mobilities of the solutes and be compatible with the separation buffer, e.g., between pH 12 and 13. Up to now, only sorbate has been reported to come close to these requirements. With $\varepsilon = 26\,000$ l mol^{-1} cm^{-1}, measured at pH 12.3 and 256 nm, low micromolar detection concentrations seem possible. Joule heat effects resulting in high baseline noise and non-ideal peak shapes originating from a mismatch of the electrophoretic mobilities of solutes and the indirect UV absorber are the reasons why the theoretical limits could not be realized.

In terms of mass detection, the comparison is in favour of CE. Assuming a 50-μl injection for HPAEC and a ca. 4-nl injection for CE, the absolute amounts detectable are 25–50 pmol for HPAEC and 0.9–1.1 pmol for CE.

Linearity

The linearity describes the molar range in which the detector signal depends linearly on the analyte concentration. The correlation coefficients for the HPAEC calibration graphs were 0.9999 for all three standard sugars in the concentration range 1–50 mg l^{-1}. The calculated correlation coefficients for the extremal CE calibration are given in Table 3. For Suc, calibration was carried out in the concentration range 0.2–2.0 g l^{-1} and for Glc and Fru in the range 0.1–1.0 g l^{-1}. In summary, both methods resulted in good linearity in the investigated concentration ranges.

Repeatability

To determine the repeatability, a sugar mixture, as given in Table 4, was injected several times into the CE and the HPAEC systems. In CZE experiments, the peak-area repeatability was found to be between 2.0 and 2.4% and the migration time repeatability was <0.3% (Table 4). HPAEC showed a better peak-area repeatability, mainly owing to lower noise and automated peak integration and almost the same repeatability for migration time as CE. It can therefore be concluded that both methods are suitable for routine application.

Although the repeatability of the CZE separations on a single day is satisfactory, the day-to-day analysis resulted in scattered values, leading to relative standard deviations (R.S.D.s) of 10–

Table 3
Linearity of carbohydrate determination with CZE and HPAEC

Sugar	Method	Concentration range	Correlation coefficient
Sucrose	CZE	0.2–2.0 g l^{-1}	0.9993
	HPAEC	1–50 mg l^{-1}	0.9999
Glucose	CZE	0.1–1.0 g l^{-1}	0.9977
	HPAEC	1–50 mg l^{-1}	0.9999
Fructose	CZE	0.1–1.0 g l^{-1}	0.9934
	HPAEC	1–50 mg l^{-1}	0.9999

Table 4
Repeatability in CZE and HPAEC [R.S.D. (%)]

Sugar	CZE concentration (m*M*)	HPAEC concentration (m*M*)	CZE (area) ($n = 7$)	HPAEC (area) ($n = 10$)	CZE (t_m)[a] ($n = 7$)	HPEAC (t_R)[b] ($n = 10$)
Sucrose	2.2	0.3	2.0%	1.5%	0.2%	0.9%
Glucose	2.2	0.6	2.2%	0.6%	0.3%	0.5%
Fructose	2.2	0.6	2.4%	0.5%	0.3%	0.5%

[a] t_m = Migration time.
[b] t_R = Retention time.

18% for peak areas. The main reason lies in the characteristics of the inner capillary wall, which are very difficult to keep constant in the high pH range over several days and which have a considerable effect on the electroosmotic flow and therefore on the overall mobilities of the analytes.

In addition, a background electrolyte with buffering capacity is necessary to keep the degree of dissociation of the sugars constant. However, at pH > 12, sorbic acid with a pK_a of 4.8 [34] has no buffering properties at all, resulting in pH shifts due to ion depletion. As demonstrated in Fig. 1, even a small change in pH of 0.1 unit has a strong effect on the electrophoretic mobility of the sugars. Because the peak area of any analyte in CZE depends on its electrophoretic mobility, a shift in the pH of the background electrolyte results in a change in the peak-area measurements [32].

3.3. Comparison of CZE fruit juice analysis with HPAEC

As shown above, the described CZE method allows a rapid separation of sugars with sufficient selectivity, within a linear range from 0.1 to 1.0 g l^{-1}. As it can be generally expected that sugar contents in fruit juices will be in the range 10–100 g l^{-1} [35], a dilution of 1:50 to 1:100 should allow a CE analysis.

To show that CE can be applied in routine analysis, three fruit juices, apple, orange and grape juice, were analysed with respect to their sugar compositions and contents. The applicability of the CZE method was demonstrated by its comparison with an HPLC method for carbohydrate determination, the HPAEC–PAD method. The HPLC analyses were carried out in the Kantonales Laboratorium, Basle, a government food control laboratory, within the scope of its daily routine work on fruit juices control.

Examples of CZE and HPAEC separations are shown in Figs. 3 and 4. Three main sugars, Suc, Glc and Fru, are expected to be present in fruit juices. The CZE separation of a standard mixture of these sugars under optimum conditions is shown in Fig. 3a. Fig. 3b shows the analysis of an apple juice, which was diluted 1:50 with water prior to injection. The analysis of the orange and grape juices yielded very similar electropherograms. Therefore, only the quantitative results are summarized in Table 5. It is important to note that in Fig. 3b no matrix peaks interfere with the sugar separation. The same is true for diluted orange and grape juices. For comparison, Fig. 4 displays a typical HPAEC trace from an orange juice analysis.

Most striking is the difference in the elution and migration order of the sugars in the two separation systems. From the basic principles of both methods, a separation according to the differences in pK_a of the sugars is expected. Therefore, the sugar molecules should be eluted in the order of their pK_a values, viz., Fru > Glu > Suc [27]. In CZE, the expected migration order is reversed owing to the strong electroosmotic flow (EOF) inside the capillary at pH 12.2. The EOF is generated at high pHs by the negatively charged silica surface of the inner capillary wall and causes a bulk flow inside the capillary towards the cathode. Because the EOF

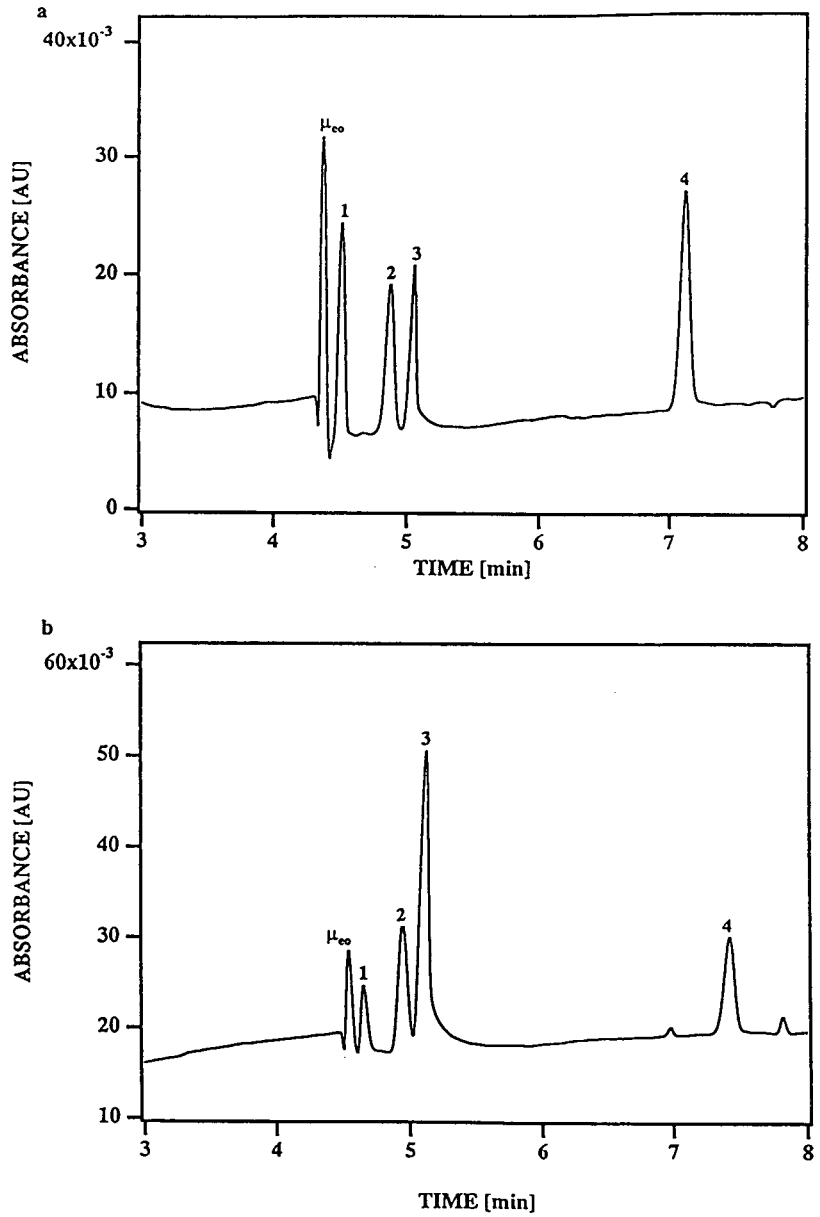

Fig. 3. Capillary zone electrophoresis of fruit juices: (a) standard mixture (sugars, 2.22–2.42 m*M*) and internal standard (GlcAc, 1.15 m*M*); (b) apple juice (diluted 1:50). Running conditions as in Fig. 1; 1-s injection. 1 = Sucrose; 2 = glucose; 3 = fructose; 4 = glucuronic acid.

is stronger than the electrophoretic mobility of the negatively charged sugars, the latter are also directed to the cathode. As a consequence, Suc, less dissociated at the separation pH, elutes first because it is less able to migrate against the direction of the EOF towards the anode, whereas the higher dissociation of Glc and Fru causes them to elute later.

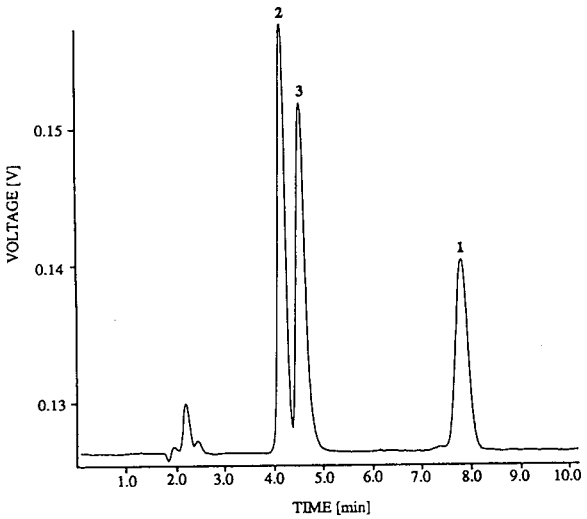

Fig. 4. HPAEC analysis of an orange juice (diluted 1:2000) on a Carbopac PA1 column with 200 m*M* NaOH as eluent at a flow-rate of 1 ml min^{-1}. Other separation conditions are described under 'Experimental'. Peak assignment as in Fig. 3.

The HPAEC separation is also based on the pK_a differences of the sugars, which influence the interaction of the analytes with the stationary phase, in this instance an anion–exchange material. This interaction depends on a dissociation equilibrium between the ionized and the non-ionized forms of the sugar molecules, as only the former is able to interact with the stationary phase. Therefore, an analyte with a lower pK_a is more strongly retained on the stationary phase than an analyte with a higher pK_a. Consequently, Glc is eluted before Fru, as shown in Fig. 4. However, Suc does not follow this separation principle. Although its pK_a is higher than that of Glc, it elutes later. The reason for that is a greater anion-exchange affinity of disaccharides compared with monosaccharides and therefore a higher retention [36].

Table 5 summarizes the results of the sugar determinations in apple, orange and grape juice. Each value represents the mean of at least three injections. The HPAEC data were evaluated only with external calibration. This proved to be satisfactory, as the injection volume of 50 μl with the appropriate injection loop was expected to be reproducible within less than 1% R.S.D. Owing to the strong dilution of at least 1:2000, no matrix effects were observed.

As no quantitative data on the determination of sugars in fruit juices with CE and indirect UV detection are available, the CZE method was validated with both external and internal calibration, with GlcA as the internal standard.

Usually, R.S.D.s in liquid chromatographic determinations are expected to be up to 3%. This holds true for the determination of sugars in apple and grape juice, although their absolute sugar contents differ by a factor of 3–4 (Table 5). An exception is the orange juice analysis, which shows R.S.D.s up to 6%. This could possibly be explained by the temperature sensitivity of the HPAEC system. In three consecutive runs, increasing peak areas for the individual sugars were observed. This could partly be a consequence of an increase in room temperature due to malfunctioning of the air conditioning system.

In CE, exact control of the injection volume, which is in the range 5–10 nl, is difficult to achieve. Nevertheless, typical R.S.D.s for both external and internal calibration are between 1% and 3%, except for the determination of Fru in orange juice and the determination of Suc in apple juice.

From the data in Table 5, it is obvious that all measured values were in the expected range. However, values obtained with CZE by external calibration differed by up to 15% from the corresponding HPAEC data. Internal calibration results in sugar concentrations much closer to those measured by HPAEC. The main reason for the larger deviations of the external CZE calibration results might be the poor reproducibility of the nanolitre injection volumes in CE. It is also possible that the silica surface of the inner capillary wall changed during a series of experiments, thus slightly changing the separation conditions from the first to the last injection.

The results of the CZE and HPAEC experiments were evaluated statistically for a correlation by the *t*-test [37]. The *t*-test is a means of proving that the mean values of two independent series of data originate from the same normal

Table 5
Sucrose, glucose and fructose contents in fruit juices

Sample	Sugar	Method	Calibration	Concentration found (g l^{-1})	R.S.D. (%)	Expected range[a] (g l^{-1})
Apple juice	Sucrose	CZE	External	16.6 ± 0.42	2.5	12.0–23.0
			Internal	17.1 ± 0.83	4.9	
		HPAEC	External	19.2 ± 0.50	2.6	
	Glucose	CZE	External	23.3 ± 0.50	2.2	17.0–30.0
			Internal	22.7 ± 0.74	3.3	
		HPAEC	External	24.3 ± 0.23	1.0	
	Fructose	CZE	External	56.5 ± 0.35	0.6	51.0–77.0
			Internal	62.8 ± 2.04	3.3	
		HPAEC	External	59.8 ± 1.29	2.2	
Orange juice	Sucrose	CZE	External	31.9 ± 1.03	3.2	27.0–48.0
			Internal	34.6 ± 0.70	2.0	
		HPAEC	External	36.6 ± 1.49	4.1	
	Glucose	CZE	External	21.5 ± 0.50	2.3	23.0–29.0
			Internal	22.0 ± 0.10	0.5	
		HPAEC	External	24.3 ± 1.42	5.8	
	Fructose	CZE	External	19.5 ± 1.10	5.6	27.0–48.0
			Internal	25.6 ± 0.90	3.5	
		HPAEC	External	26.6 ± 1.64	6.2	
Grape juice	Glucose	CZE	External	87.1 ± 0.76	0.9	81.0
			Internal	73.5 ± 1.01	1.4	
		HPAEC	External	74.3 ± 1.06	1.4	
	Fructose	CZE	External	86.5 ± 1.79	2.1	83.0
			Internal	81.2 ± 1.57	1.9	
		HPAEC	External	79.1 ± 2.93	3.7	

[a] Values from Ref. [35].

distribution with the same mean value. If this is the case, the difference in the mean values of the two series should not be significant. However, in order to apply the *t*-test to two sets of data, the standard deviations of both sets of data must be comparable, indicated by the *F*-value [37]. As can be seen from the *t*-values in Table 6, the differences between the HPAEC results and the results of the CZE analyses obtained by internal calibration are not significant for all data sets at the 99% confidence level. In contrast, the data for the external CZE calibration differed significantly in all except two instances from those obtained by HPAEC, indicating that external calibration of CZE did not yield the same values as HPAEC and is therefore an invalid method. This again confirms the previous statement, that the results from the internal CE calibration are much closer to the HPLC results than those from the external CE calibration. Therefore, the internal calibration method is to be preferred when working with CE.

In summary, good agreement between the sugar contents declared on the fruit juice packaging and the sugar contents determined by CZE and the HPAEC method was found (Table 7). On inspecting the CZE and HPAEC results closely, it is striking that only the data for the orange juice are lower than the declared values. This could be due to partial adsorption of soluble sugars on haze particles, such as polyphenols, polysaccharides and proteins, which are removed by filtration, resulting in an underestimation of the sugar content in this juice.

It is evident from these results that the described CZE method is suitable as a routine method for the determination of soluble carbohydrates in fruit juices.

Table 6
Statistical evaluation of the results obtained by CZE and HPAEC

Juice	Sugar	Method[a]	*F* value	*t* value	Difference CZE–HPAEC
Apple	Sucrose	CZE ext. cal.	1.42	7.88	Significant
		CZE int. cal.	2.76	4.34	Not significant
	Glucose	CZE ext. cal.	4.73	3.57	Not significant
		CZE int. cal.	3.22	4.10	Not significant
	Fructose	CZE ext. cal.	13.58	4.93	Significant
		CZE int. cal.	2.50	2.03	Not significant
Orange	Sucrose	CZE ext. cal.	2.09	5.16	Significant
		CZE int. cal.	4.53	2.44	Not significant
	Glucose	CZE ext. cal.	8.07	3.73	Not significant
		CZE int. cal.	201.60	3.42	Not significant
	Fructose	CZE ext. cal.	2.22	7.17	Significant
		CZE int. cal.	3.32	1.06	Not significant
Grape	Glucose	CZE ext. cal.	1.95	19.69	Significant
		CZE int. cal.	1.10	1.10	Not significant
	Fructose	CZE ext. cal.	2.68	4.30	Not significant
		CZE int. cal.	3.48	1.27	Not significant

Test conditions: for $F\ (P = 0.95;\ f_1 = f_2 = 2) \leq 19.00 \Rightarrow t(P = 0.99;\ f = 4) \leq 4.60$; for $F\ (P = 0.95;\ f_1 = f_2 = 2) > 19.00 \Rightarrow t(P = 0.99;\ f = 2) \leq 9.92$. P = confidence level; f = degrees of freedom.
[a] Ext. cal. = external calibration; int. cal. = internal calibration.

4. Conclusions

A simple, reproducible and inexpensive CZE method for the separation of soluble, low-molecular-mass carbohydrates with indirect UV detection was adapted to fruit juice analysis. The sensitivity proved to be sufficient to measure levels of sugars in common fruit juices. In principle, other foodstuffs with similar carbohydrate concentrations such as jellies, honey, candies or soft drinks could also be within the scope of this method. The CZE method was compared with the routine HPLC method, yielding similar results in terms of resolution, reproducibility and recovery. A statistical comparison (*t*-test) showed that there is no significant difference in the results obtained by the two independent methods, provided the internal calibration method was used for CZE.

Therefore, it can be concluded that CE with the additional advantages of a short analysis time, high separation efficiency and low running costs is attractive for routine work. Additionally, CE provides the possibility of validating HPLC results or results from any other carbohydrate analysis with a second independent analytical method.

Although CE is still a relatively young analytical technique, it certainly will continue to grow in the future and find more and more applications in the area of food science. Eventually, validated CE methods should provide fast, automated and high-resolution assays in food control laboratories.

Table 7
Total carbohydrate content

Juice	Concentration (g l^{-1})		
	Declared	Found	
		CZE[a]	HPAEC
Apple	110.0	102.6	102.4
Orange	100.0	82.2	86.8
Grape	150.0	154.7	152.6

[a] Results from internal calibration.

References

[1] B.L. Karger, A.S. Cohen and A. Guttmann, *J. Chromatogr.*, 492 (1989) 585.
[2] H. Nishi and S. Terabe, *Electrophoresis*, 11 (1990) 691.
[3] Y. Xu, *Anal. Chem.*, 65 (1993) 425R.
[4] J. Vindevogel and P. Sandra, *J. High Resolut. Chromatogr.*, 14 (1991) 795.
[5] N. de Jong, S. Visser and C. Olieman, *J. Chromatogr. A*, 652 (1993) 207.
[6] M.T. Ackermans, J.L. Beckers, F.M. Everaerts, H. Hoogland and M.J.H. Tomassen, *J. Chromatogr.*, 596 (1992) 101.
[7] B. Lin Ling, W.R.G. Baeyens, P. van Acker and C. Dewaele, *J. Pharm. Biomed. Anal.*, 10 (1992) 717.
[8] B. Kenney, *J. Chromatogr.*, 546 (1991) 423.
[9] R. Macrae, *HPLC in Food Analysis*, Academic Press, London, 2nd ed., 1988.
[10] M.H. Gordon, *Principles and Applications of GC in Food Analysis*, Ellis Hoorwood, Chichester, 1990.
[11] I.B. Niederer, *Diss. ETH*, No. 10070, ETH, Zürich, 1993.
[12] H. Weigel, *Adv. Carbohydr. Chem.*, 18 (1963) 61.
[13] B. Bettler, R. Amadò and H. Neukom, *J. Chromatogr.*, 498 (1990) 213.
[14] H. Schäfer and H. Scherz, *Z. Lebensm.-Unters.-Forsch.*, 177 (1983) 193.
[15] S. Honda, *Anal. Biochem.*, 140 (1984) 1.
[16] *Technical Note 20*, Dionex, Sunnyvale, CA, 1989.
[17] C. Corradini, A. Cristalli and D. Corradini, *J. Liq. Chromatogr.*, 16 (1993) 3471.
[18] A.E. Vorndran, P.J. Oefner, H. Scherz and G.K. Bonn, *Chromatographia*, 33 (1992) 163.
[19] S. Hoffstetter-Kuhn, A. Paulus, E. Gassmann and H.M. Widmer, *Anal. Chem.*, 63 (1991) 1541.
[20] W. Nashabeh and Z. El Rassi, *J. Chromatogr.*, 514 (1990) 57.
[21] T.W. Garner and E.S. Yeung, *J. Chromatogr.*, 515 (1990) 639.
[22] S. Honda, S. Iwase, A. Makino and S. Fujiwara, *Anal. Biochem.*, 176 (1989) 72.
[23] S. Honda, S. Suzuki, A. Nose, K. Yammamoto and K. Kakehi, *Carbohydr. Res.*, 215 (1991) 193.
[24] C. Chiesa and Cs. Horváth, *J. Chromatogr.*, 645 (1993) 337.
[25] L.A. Colon, R. Dadoo and R.N. Zare, *Anal. Chem.*, 65 (1993) 476.
[26] B. Krattiger, G.J.M. Bruin and A.E. Bruno, *Anal. Chem.*, 66 (1994) 1.
[27] J.A. Rendleman, Jr., *Adv. Chem. Sci.*, 117 (1972) 51.
[28] J.H. Knox and I.H. Grant, *Chromatographia*, 24 (1987) 135.
[29] H.H. Lauer and J.B. Ooms, *Anal. Chim. Acta*, 250 (1991) 45.
[30] J.W. Jorgenson and K. Lukacs, *Science*, 222 (1983) 266.
[31] Cs. Horváth and W.R. Melander, in E. Heftmann (Editor), *Chromatography —Fundamentals and Applications of Chromatographic and Electrophoretic Methods, Part A: Fundamentals and Techniques* (*Journal of Chromatography Library*, Vol. 22A), Elsevier, Amsterdam, 1983, p. A44.
[32] M.W.F. Nielen, *J. Chromatogr.*, 588 (1991) 321.
[33] F. Foret, S. Fanali and L. Ossiani, *J. Chromatogr.*, 470 (1989) 299.
[34] A. Bergholdt, J. Overgaard, A. Colding and R.B. Frederikson, *J. Chromatogr.*, 644 (1993) 412.
[35] S.W. Souci, W. Fachmann and H. Kraut, *Die Zusammensetzung der Lebensmittel, Nährwerttabellen 1989/90*, Wissenschaftliche Verlagsgesellschaft, Stuttgart, 4th ed., 1989.
[36] R.D. Rocklin and C.A. Pohl, *J. Liq. Chromatogr.*, 6 (1983) 1577.
[37] K. Doerfel, *Statistik in der Analytischen Chemie*, Deutscher Verlag für Grundstoffindustrie, Leipzig, 5th ed., 1990.

ELSEVIER

Journal of Chromatography A, 680 (1994) 201–208

JOURNAL OF CHROMATOGRAPHY A

Application of capillary ion electrophoresis and ion chromatography for the determination of O-acetate groups in bacterial polysaccharides

Robert W. Hepler, Charlotte C. Yu Ip*

Department of Virus and Cell Biology, Merck Research Laboratories, West Point, PA 19486, USA

Abstract

Many bacterial polysaccharides possess O-linked acetate groups as constituents of their repeating units which often can serve as immunological determinants. It is therefore important to develop analytical methods for process monitoring as well as product characterization when such O-acetylated polysaccharides are used as components of vaccines. This is the case in a polysaccharide conjugate vaccine under development for treatment of diseases caused by *Streptococcus pneumoniae*. An ion chromatographic (IC) method utilizing suppressed conductivity detection (SCD) was developed to quantitatively measure O-acetate groups in the capsular polysaccharides from *S. pneumoniae* types 18C and 9V following hydrolytic release of O-acetate from the polysaccharide backbones using 2 m*M* sodium hydroxide. IC was carried out using an OmniPac PAX-500 column and 0.98 m*M* NaOH in 2% methanol as the mobile phase. Capillary ion electrophoresis (CIE) with indirect photometric detection was evaluated as an alternative method. The CIE method utilized a 72 cm × 75 μm I.D. fused-silica capillary and an electrolyte composed of 5 m*M* potassium hydrogenphthalate, 0.5 m*M* tetradecyltrimethylammonium bromide, and 2 m*M* sodium tetraborate, pH 5.88. A comparison of CIE and IC–SCD in terms of reproducibility, accuracy, linearity, and sensitivity will be presented.

1. Introduction

Purified type-specific capsular polysaccharides from *Streptococcus pneumoniae* are currently used in the preparation of a commercially available vaccine against pneumococcal (Pn) disease. The Pn polysaccharides are also conjugated to carrier proteins as a Pn conjugate vaccine for the prevention of pediatric Pn diseases [1]. Until recently, routine characterization of the carbohydrate composition of the vaccine was accomplished by colorimetric assay. Currently, the technique of high-pH anion-exchange chromatography (HPAEC) using pulsed amperometric detection (PAD) is used for the analysis of the carbohydrate composition of acid-hydrolyzed Pn polysaccharide types [2]. HPAEC–PAD allows for the detection of subnanomole amounts of the monosaccharide components of these Pn polysaccharides. However, the constituent side chain

* Corresponding author.

0021-9673/94/$07.00
SSDI 0021-9673(94)00329-08

groups such as O-acetate in Pn polysaccharide 9V and Pn polysaccharide 18C cannot be detected by HPAEC–PAD. The objective of this work was to investigate analytical methods for the separation and quantitation of O-linked acetate in Pn polysaccharides and to determine the optimal hydrolysis conditions for the release of O-acetate from Pn polysaccharide types 9V and 18C.

Determination of the O-acetyl content of bacterial polysaccharides has traditionally been accomplished by chemical assay [3] or, more recently, by NMR techniques [4]. The application of ion chromatography (IC) coupled with suppressed conductivity detection (SCD) for the quantitative analysis of O-linked acetate in Pn polysaccharides has not been reported, although the technique of IC–SCD has been used to quantitate inorganic and organic anions with sensitivity in the parts-per-billion range [5]. We initially investigated the use of IC–SCD as a quantitative tool to monitor hydrolytic release of O-acetate from Pn polysaccharides.

Recent developments in the use of capillary ion electrophoresis (CIE) using indirect photometric detection [6–9] provided an alternative method for the detection and quantitation of O-acetate groups in hydrolyzed Pn polysaccharide types 9V and 18C. This method involves the incorporation of a cationic surfactant in the running buffer to cause a reversal of the normal electroosmotic flow [9,10]. The method also involves the reversal of the polarity of the CE system to cause the migration of anions from the site of injection (cathode) past the detector window to the anode. Detection is accomplished by incorporation of a highly-UV absorbing species in the buffer. Analyte ions displace chromophoric buffer ions as they pass the detector, causing a reduction in absorbance which can be recorded as a positive peak by reversing the polarity of the detector output.

In this article, we will investigate the applicability of the recently developed CIE methodologies for the analysis of O-acetate in bacterial polysaccharides and compare this new method with the IC method.

2. Experimental

2.1. Ion chromatographic systems and eluents

Ion chromatography (IC) was performed on a Dionex (Sunnyvale, CA, USA) BioLC equipped with a gradient pump module and connected to a pulsed electrochemical detector operating in the conductivity mode. Separation was accomplished using Omnipac-PAX 500 guard and analytical columns (250 mm × 4 mm I.D., 8.5 μm bead diameter) and an anion trap column (ATC-1) which was placed between the gradient pump and injection valve to remove anionic contaminants from the eluent. Chemical suppression of background conductivity was accomplished using a Dionex Anion Micro Membrane Suppressor (AMMS-II) operated via an AutoRegen pump with 50 m*M* sulfuric acid as the regenerant. Samples were injected via a Spectra Physics SP8880 autosampler equipped with a PEEK stator and rotor seal (Rheodyne) and a 100-μl PEEK sample loop. Data were collected by a PE Nelson A/D converter (Cupertino, CA, USA) and analyzed using PE Nelson Turbochrom software version 3.3.

IC was performed by isocratic elution with 0.98 m*M* sodium hydroxide in 2% methanol for 15 min at a flow-rate of 1 ml/min. This was followed by a 10-min wash in 50 m*M* NaOH, 2% methanol, and a 12.5-min re-equilibration with the starting buffer. The conductivity detector was set to a range of 3 μS. The background conductivity for the isocratic buffer was less than 1 μS at a regenerant flow-rate of approximately 10 ml/min.

2.2. Capillary ion electrophoresis system

Capillary ion electrophoresis (CIE) was performed on an Applied Biosystems (Foster City, CA, USA) Model 270A CE unit equipped with an 72 cm × 75 μm I.D. (50 cm separation length) fused-silica capillary (Polymicro Technologies, Phoenix, AZ, USA) and an UV detector. The electrophoresis buffer was composed of 5 m*M* potassium hydrogenphthalate, 4 m*M* sodium

tetraborate, and 0.5 m*M* tetradecyltrimethylammonium bromide (TTAB) pH 5.88. The buffer was filtered through a 0.45-μm filter prior to use. Each run consisted of a 3-min wash with 0.1 *M* sodium hydroxide, a 3-min wash with high purity water, and an equilibration with running buffer for 5 min prior to sample injection. Samples were loaded using a 5-s vacuum injection at 127 mm of mercury. The detector was set at 254 nm with the output polarity reversed. The detector range was set at 0.004 OD units. The samples were separated over a period of 10 min at an applied voltage of −15 kV.

2.3. Reagents and preparation of standards and samples

Moisture corrected samples of type-specific Pn polysaccharides were prepared from purified Pn polysaccharide powders obtained from the Merck Manufacturing Division (West Point, PA, USA). An EM Sciences Aquastar V3000 volumetric Karl Fisher titrator was used for moisture content analysis. Moisture corrected samples of polysaccharide powder (2.5 mg/ml) were dissolved in pyrogen-free water over a period of 24 h at room temperature on a rotating platform.

Sodium hydroxide, sodium acetate trihydrate, and HPLC-grade methanol were purchased from Fisher Scientific (Pittsburgh, PA, USA). Sodium tetraborate, TTAB, potassium hydrogenphthalate, and N-acetylmannosamine were purchased from the Sigma (St. Louis, MO, USA).

An acetate standard was prepared by dissolving sodium acetate in water at a concentration of 10 m*M*. This standard was stored at −20°C in 1-ml aliquots; 100 μl of this concentrated standard was diluted in a total volume of 2 ml of water for a concentration of 500 μM. Five serial 2-fold dilutions of this standard were performed to prepare the remaining concentrations of the standard curves.

2.4. Alkaline hydrolysis of bacterial polysaccharides

For the assay validation studies, 100 μl of a 2.5-mg/ml solution of moisture corrected Pn polysaccharide type 18C was mixed with 250 μl of pyrogen-free water and 50 μl of freshly prepared and helium sparged 16 m*M* sodium hydroxide for a final concentration of 0.625 mg/ml polysaccharide and 2 m*M* NaOH. The samples were incubated overnight at room temperature and diluted in water 1:1.3, 1:5, and 1:15 prior to analysis.

For the quantitation of O-acetate in Pn 9V and 18C, 50 μl of a 2.5-mg/ml solution of polysaccharide was mixed with 125 μl of pyrogen-free water and 25 μl of 16 m*M* sodium hydroxide for a polysaccharide concentration of 0.625 mg/ml and a hydroxide concentration of 2 m*M*. The samples were incubated at room temperature for 16 h, diluted 1:10, and 1:5 (type 9V, and 18C, respectively) in water, and analyzed by CIE and IC using the methods outlined above.

3. Results and discussion

The repeating units of Pn polysaccharides types 9V and 18C are shown in Fig. 1 and are based on structures published by previous investigators [11–14]. Repeat unit molecular masses of 968 and 1006 for Pn polysaccharides 9V and 18C, respectively, were used for conversion of mass to moles. While Pn polysaccharide 18C was found to contain one O-acetate group per polysaccharide repeating unit [11], the reported number of O-acetate groups per repeating unit in Pn polysaccharide 9V has varied from 1.2 using NMR [13] to 1.6 using a colorimetric assay [12], suggesting either inaccuracy in determination, or more likely the existence of a mixed population of singly and doubly-acetylated molecules. For this report, alternative methods for the quantitation of O-acetate in Pn polysaccharides 9V and 18C which require little sample and are relatively easy to perform were investigated for the characterization of these components of a Pn conjugate vaccine. Both methods involve the release of O-acetate from the polysaccharide backbone followed by chromatographic or electrophoretic

Pn Ps Type 9V

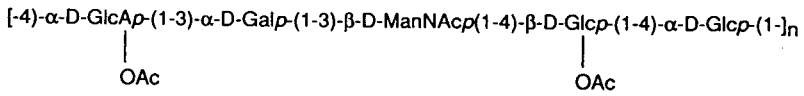

Pn Ps Type 18V

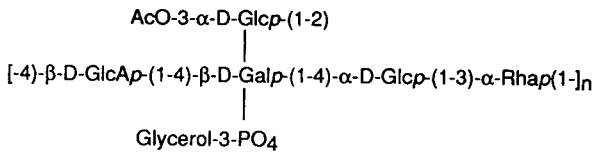

Fig. 1. Structures of the repeating units of the capsular polysaccharides (Ps) of *Streptococcus pneumoniae* types 9V and 18C.

separation and detection. A typical example of an electropherogram and chromatogram using the methods outlined in the experimental section are shown in Figs. 2 and 3. Fig. 2 is a CIE electropherogram of a sample of hydrolyzed Pn polysaccharide 18C in which the acetate migrates as a sharp peak with a migration time of 7.2 min, the broad (9.0 min) peak following acetate is caused by the presence of carbonate in the sample. Fig. 3 is the IC chromatogram of the same hydrolyzed Pn polysaccharide 18C sample in which acetate elutes as a sharp peak with a retention time of 5.8 min.

3.1. Optimization of the hydrolysis conditions for the release of O-acetate from Pn polysaccharidess 9V and 18C

Preliminary experiments were performed using IC to determine the hydrolysis conditions necessary for the removal of O-acetate from these polysaccharides. Various concentrations (1 m*M* to 50 m*M*) of sodium hydroxide were used for different lengths of time (0.5 h to 48 h) at different temperatures (4°C to 65°C). It was determined that 2 m*M* sodium hydroxide at room temperature for 16 h provided optimum

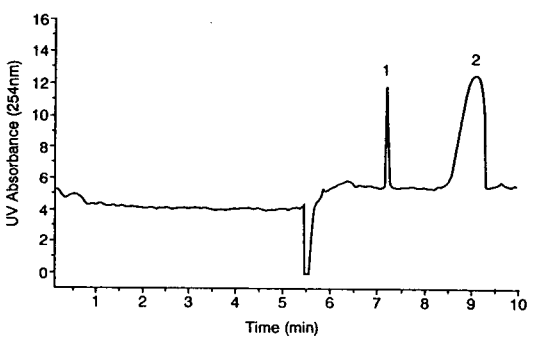

Fig. 2. Typical electropherogram of an alkaline hydrolyzed Pn polysaccharide 18C showing O-acetate released from the sample. Peaks: 1 = acetate; 2 = carbonate.

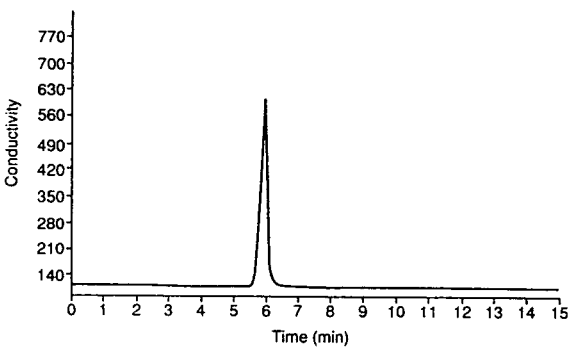

Fig. 3. Typical chromatogram of an alkaline hydrolyzed Pn polysaccharide 18C showing O-acetate released from the sample.

release of O-acetate from Pn polysaccharide 9V and Pn polysaccharide 18C. A time-course study was also performed using CIE in which samples were incubated in 2 m*M* NaOH for 0.5 h to 48 h at room temperature. The results of this study are shown in Fig. 4. Again, 16 h at room temperature in 2m*M* sodium hydroxide were sufficient to provide maximum release of O-acetate from Pn polysaccharide 9V and Pn polysaccharide 18C.

In order to verify that the hydrolysis conditions chosen for O-acetate removal did not release N-linked acetate (Pn polysaccharide 9V contains an N-acetate group in addition to the O-acetate groups, see Fig. 1), we also subjected N-acetylmannosamine (N-acetylated monosaccharide) and Pn polysaccharide type 4 (which contain both N-acetylmannosamine and N-acetylfucosamine as part of the constituents in the repeating unit [15]) to the hydrolysis conditions outlined above. No acetate was detected in either the Pn polysaccharide 4 or N-acetylmannosamine samples after 48 h of hydrolysis in 2 m*M* NaOH (see Fig. 4).

One disadvantage of the IC method for O-acetate quantitation was the inability to quantitate background levels of acetate (free residual acetates from purification process) in samples.

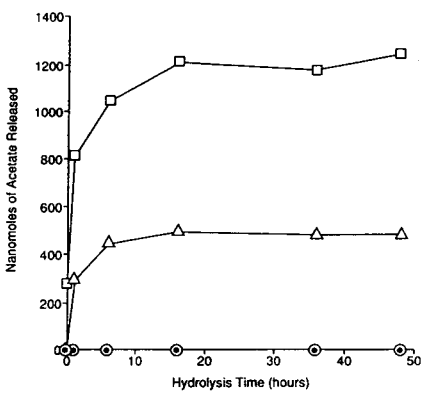

Fig. 4. Time course of O-acetate released from Pn polysaccharide 9V, □; Pn polysaccharide 18C, ○; N-acetylmannosamine, △; and Pn polysaccharide type 4, ●.

This was due to the fact that the IC buffer contained 0.98 m*M* sodium hydroxide, which resulted in on-column hydrolysis of O-acetate in the samples during the chromatographic procedure. This was not a problem with CIE because the CIE buffer did not contain sodium hydroxide and therefore did not hydrolyze the samples during analysis. For these reasons, the IC method is limited to the analysis of final purified samples or samples which have been dialyzed free of acetate prior to hydrolysis and IC.

3.2. Linearity

Table 1 gives the linearity data as obtained using CIE and IC. Standard curves were generated using a sodium acetate standard at concentrations of 500, 250, 125, 62.5, 31.25, and 15.6 μM in both the CIE and IC assay. Peak area by CIE appears linear (on a linear scale) throughout the range of acetate concentrations used in this study, and preliminary data showed peak areas to be linear through acetate concentrations as high as 5 m*M*. Peak area by IC is linear (on a linear scale) up to a concentration of 250 μM acetate.

Fig. 5 shows the relationship between acetate concentration and migration time for CIE. The data show that migration time decreased with increasing concentrations of acetate. This is due to electromigrative dispersion of the sample [7]. We therefore chose to limit the standard curve in a typical assay to 500 μM in order to minimize excessive broadening of the migration zones.

Table 1
Linearity data for CIE and IC

Method	r^a	Linear range (μM)
CIE	0.9999	15.6–500
IC	0.9988	15.6–250

[a]Linear correlation coefficient.

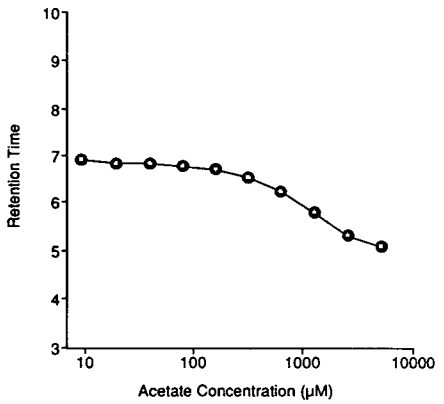

Fig. 5. Effect of acetate concentration on capillary ion electrophoretic retention time.

3.3. Limit of detection and sensitivity

Limits of detection for both assays were calculated based on a method [16] wherein the limit of detection, y, is equal to the blank (equivalent to the y intercept or y_B), plus three times the standard deviation of the blank, S_B. The limits of detection for CIE and IC determined by this method were 7 μM and 12 μM, respectively. It should be noted at this point that although the limits of detection for both methods appear similar, the absolute amount of acetate detected is much smaller using capillary electrophoresis. Assuming that a volume of 3.5 nl/s (value provided by the manufacturer) is taken up by the capillary, the mass amount of acetate applied to the capillary at the lowest standard concentration is $1.1 \cdot 10^{-3}$ nmol. The mass of acetate applied to the IC column at the lowest standard concentration is $1.56 \cdot 10^{-1}$ nmol so that overall CIE is two orders of magnitude more sensitive than IC on a mass basis.

3.4. Repeatability and reproducibility

In order to arrive at estimates of assay repeatability (intra-day precision) and reproducibility (inter-day precision), a hydrolyzed sample of Pn polysaccharide 18C was assayed at three dilution levels; corresponding to the upper (480 μg/ml), mid (125 μg/ml), and lower (42 μg/ml) regions of the standard curve using five sequential injections on three days. The relative standard deviations (R.S.D.) for intra- and inter-day variability were calculated and are presented in Table 2.

The 3-day averages of the within-run variability for CIE at the 1:1.3, 1:5, and 1:15 dilutions were 4.6, 4.5, and 4.3%, respectively. The 3-day average within-run values for IC were 0.7, 0.6, and 0.9% for the 1:1.3, 1:5, and 1:15 dilutions, respectively. As shown in Table 2, the results indicate that the total variability for these two assays are similar.

The reproducibility of the migration/retention time for each of the methods was also determined from the data outlined above. The average R.S.D. for the migration time of acetate by CIE ($n = 15$) on each of three days was 1.2%, while the overall variability in migration time across three days of analyses was 1.6%. The corresponding data for IC retention time was 0.6% and 1.0% for the 3-day average R.S.D. and overall variability, respectively.

Table 2
Assay variability (% R.S.D.) data for CIE and IC

Dilution level	Day 1		Day 2		Day 3		Total (inter-day)	
	CIE	IC	CIE	IC	CIE	IC	CIE	IC
1:1.3	6.5	0.3	2.3	1.0	5.1	0.7	7.2	3.4
1:5	5.1	0.5	5.3	0.5	3.0	0.8	6.2	1.1
1:15	3.7	1.1	5.5	0.8	3.7	0.9	2.6	5.0

3.5. Assay comparison

In order to compare the two assays, a sample of sodium hydroxide-hydrolyzed Pn polysaccharide 18C was diluted to achieve an equivalent acetate concentration of approximately 250 nM/ml. This solution then was used to prepare dilutions equal to 90, 80, 70, 60, 50, 40, 30, 20, and 10% of the stock. Each sample was then assayed in duplicate by CIE and IC along with acetate standards. Interpolated concentrations for each sample then were calculated based on the acetate standards normalized to the point of each curve, and compared by plotting the values obtained from IC on the x axis and the values from CIE on the y axis. The slope of the line is 0.997 ± 0.023, and the y intercept is 0.92, indicating that each method yields equivalent results over this concentration range.

3.6. Matrix effects

In order to identify potential effects of the sample matrix on the outcome of routine analyses, a spiking experiment was performed on each of three days. In this experiment, a hydrolyzed Pn polysaccharide 18C sample or water was spiked with five levels of acetate, 20, 40 80 160 and 320 μM. The slope of the lines representing the acetate standard in water and the acetate standard spiked into the sample matrix were calculated and shown in Table 3. The data showed that the slopes were the same (within-assay variability) for the total acetate content in either matrix using CIE or IC. This result indicates that the recovery of acetate in water is the same as in a sample matrix containing hydrolyzed Pn polysaccharide 18C and that there are no detectable matrix effects in either assay under these conditions.

Table 3
Matrix effect data for CIE and IC

Matrix	Slope	
	CIE	IC
H_2O	232 ± 1	20407 ± 527
Hydrolyzed sample	237 ± 5	20959 ± 481

3.7. Quantitation of O-acetate in Pn 9V and 18C

In order to determine the molar ratio of O-acetate to polysaccharide in the Pn polysaccharides 9V and 18C, triplicate hydrolyses were performed and analyzed in duplicate by both CIE and IC. The μM of acetate determined in these assays were divided by the μM amount of each of the polysaccharide to provide a ratio of O-acetate to polysaccharide repeating unit. The CIE data shows that Pn polysaccharide 9V contains 1.4 mol of O-acetate per mole of polysaccharide repeating unit. Pn polysaccharide 18C was found to contain 0.8 mol of O-acetate per mole of polysaccharide repeating unit. These values are in general agreement with structural studies of Pn polysaccharides 9V and 18C as reported by previous investigators [12–13]. IC provides essentially the same information; however, because IC cannot be used to determine free acetate in the samples prior to hydrolysis, the values obtained by IC in cases where samples contain free acetate would overestimate the actual O-acetate content. Free acetate values can be determined by CIE and were taken into account in the calculations used to provide the data presented above.

4. Conclusions

Alternative methods for rapid determination of the O-acetate content of two type specific polysaccharides from *S. pneumoniae* using both IC and CIE following alkaline hydrolysis have been described and compared. Both IC and CIE demonstrate similar levels of performance in terms of sensitivity, repeatability, reproducibility and accuracy. However, to avoid the over-estimation of acetate for those Pn polysaccharide samples containing traces of free acetate, the IC method requires that the samples be dialyzed prior to the alkaline hydrolysis procedure. This is due to on-column hydrolysis of O-acetate from

the Pn polysaccharides in the NaOH containing IC eluent. The CIE method is linear to 5 m*M* acetate while the IC method is linear to 250 μM. In addition, CIE has several advantages over IC, which include the elimination of the expensive IC columns which require extensive cleaning and regeneration resulting the generation of large volumes of hazardous waste. Overall run times for each method are 21 and 37.5 min for CIE and IC, respectively. Therefore, we conclude that the CIE method is faster, easier to use and cost effective, and that CIE should be the method of choice for the quantitation of O-acetate in bacterial polysaccharides following alkaline hydrolysis.

Acknowledgements

The authors thank Drs. Ronald W. Ellis and Paul Keller for their critical review and helpful suggestions in this work. We also thank members of the Merck manufacturing division for providing Pn polysaccharide samples for the analyses.

References

[1] P.P. Vella, S. Marburg, J.M. Staub, P.J. Kniskern, W.J. Miller. A. Hagopian, C. Ip, R. Tolman, C.M. Rusk, L.S. Chupak and R.W. Ellis, *Infect. Immun.*, 60 (1992) 4977.
[2] C.C. Yu Ip, V. Manam, R. Hepler and J.P. Hennessey, Jr., *Anal. Biochem.*, 201 (1992) 343.
[3] S. Hestrin, *J. Biol. Chem.*, 180 (1949) 249.
[4] M. Moreau, J.C. Richards and M.B. Perry, *Carbohydr. Res.*, 182 (1988) 79.
[5] R.D. Rocklin, C.A. Pohl, and J.A. Schibler, *J. Chromatogr.*, 411 (1987) 107.
[6] F. Foret, S. Fanali, L. Ossicini and P. Bocek, *J. Chromatogr.*, 470 (1989) 299.
[7] F. Foret, S. Fanali, A. Nardi and P. Bocek, *Electrophoresis*, 11 (1990) 780.
[8] W.R. Jones and P. Jandik, *J. Chromatogr.*, 546 (1991) 445.
[9] L. Kelly and R.J. Nelson, *J. Liq. Chromatogr.*, 16 (1993) 2103.
[10] X. Huang, J.A. Luckey, M.J. Gordon and R.N. Zare, *Anal. Chem.*, 61 (1989) 766.
[11] C. Lugowski and H.J. Jennings, *Carbohydr. Res.*, 131 (1984) 119.
[12] M.B. Perry, V. Daoust and D.J. Carlo, *Can. J. Biochem.*, 59 (1981) 524.
[13] L.R. Phillips, O. Nishimura and B.A. Fraser, *Carbohydr. Res.*, 121 (1983) 243.
[14] T.J. Rutherford and C. Jones, *Carbohydr. Res.*, 218 (1991) 175.
[15] C. Jones, F. Currie and M. Forster, *Carbohydr. Res.*, 221 (1991) 95.
[16] J.C. Miller and J.N. Miller, *Statistics for Analytical Chemistry*, Ellis Horwood, New York, 2nd ed, 1988, p. 101.

ELSEVIER

Journal of Chromatography A, 680 (1994) 209–215

JOURNAL OF CHROMATOGRAPHY A

High-performance capillary electrophoresis of O-glycosidically linked sialic acid-containing oligosaccharides in glycoproteins as their alditol derivatives with low-wavelength UV monitoring

Kazuaki Kakehi, Akiyo Susami, Atsushi Taga, Shigeo Suzuki, Susumu Honda*

Faculty of Pharmaceutical Sciences, Kinki University, Kowakae 3-4-1, Higashi-osaka 577, Japan

Abstract

Several O-glycosidically linked monosialooligosaccharides from glycoproteins were separated as their alditol derivatives in ca. 10 min in borate buffer (pH 9.6) containing sodium dodecyl sulfate (SDS), and sensitively detected at the 10^{-4} *M* level by measuring absorption at 185 nm. Oligosaccharides having higher degree of polymerizations migrated faster, and N-acetyl- and N-glycolylneuraminic acid-containing oligosaccharide analogues could be resolved from each other under the conditions employed. Good linearity was demonstrated between 0.9 and 20 m*M* concentrations for relative response of N-acetylneuraminyllactose as a model compound to lactobionic acid as an internal standard. The detection limit was 0.2 m*M*, which corresponded to 0.80 pmol as the injected amount. The relative standard deviation of relative response at 9 m*M* was 1.97% ($n = 7$). The established system was successfully applied to microanalysis of sialooligosaccharides in bovine submaxillary mucin and swallow nest material.

1. Introduction

The analysis of oligosaccharides and polysaccharides is important for understanding their biological roles in bioactive glycoproteins, and particular attention has been paid for the analysis of sialooligosaccharides to elucidate the physiological role of the sialic acid residues.

There are a few established methods, such as hydrazinolysis and digestion with glycopeptidase, for the release of N-glycosidically linked sialooligosaccharides from glycoproteins [1]. The released oligosaccharides may be analyzed directly by high-performance anion-exchange chromatography [2] or high-performance capillary electrophoresis (HPCE) [3]. They may be also analyzed by high-performance liquid chromatography (HPLC) or HPCE after derivatization with some chromogenic or fluorogenic reagents [4,5].

On the other hand, there are no good methods for the release of O-glycosidically linked oligosaccharides to give free oligosaccharides. Treatment with alkali in the presence of borohydride can liberate O-glycosidically linked oligosaccharides [6], but the released oligosaccharides are converted concurrently to the corresponding alditols. Such alditols may be analyzed by high-performance-anion exchange chromatography with pulsed amperometric detection [7,8], but they cannot be sensitively detected by UV or visible light absorption in intact state and they cannot be detected by fluorescence at all. Conversion to absorbing or fluorescent derivatives is

* Corresponding author.

0021-9673/94/$07.00
SSDI 0021-9673(94)00625-3

also hampered, because they lack the aldehyde group as the key functional group.

Under these circumstances, HPCE is expected to become an alternative to high-performance-anion exchange chromatography, since sensitive low-wavelength monitors have been recently developed. Some simple mono- and oligosaccharides have been separated as their borate complexes in basic conditions and detected at 195 nm [9]. Sialooligosaccharides from glycoproteins are considered to absorb such low-wavelength UV light more strongly, because of the presence of N-acyl groups in both sialic acid and hexosamine residues.

This paper presents a study of the analysis of O-glycosically linked sialooligosaccharides as their alditols, based on HPCE with low-wavelength UV detection.

2. Materials and methods

Bovine submaxillary mucin was prepared from bovine submaxillary glands according to the literature [10]. The nest material of Chinese swiftlet was commercially available from a Chinese foodstuff shop (Kobe, Japan). N-Acetylneuraminyllactose (NeuAc-Lac) was obtained from Sigma (St. Louis, MO, USA). Lactobionic acid used as the internal standard for calibration was obtained from Tokyo Kasei Kogyo (Tokyo, Japan). ^{1}H NMR spectra were recorded in deuterium oxide at room temperature with a JEOL JNM GSX-500 spectrometer (JEOL, Tokyo, Japan) at 500 MHz. The proton signals were referenced to the methyl proton signal of the internal acetone (2.225 ppm) in δ (ppm). Negative ion fast-atom bombardment mass spectra were obtained in glycerol matrix using a JEOL SX102 mass spectrometer. The energy of the primary xenon beam was 8 kV. Calibration of mass number was carried out by using Ultramark (available from JEOL) as the mass reference. Evaporation of small volume of solutions (smaller than 1 ml) was carried out by a centrifugal concentrator CC-101 (Tomy, Tokyo, Japan) at room temperature. The reagents and solvents for chromatography were of the highest grade commercially available. Deionized water double distilled in a glass-made apparatus was used throughout the work.

2.1. Isolation of sialooligosaccharide alditol standards from bovine submaxillary mucin

Bovine submaxillary mucin (100 mg) was treated with 50 m*M* sodium hydroxide (10 ml) containing sodium borohydride to a concentration of 1 *M* for 72 h at 37°C. Acetic acid was carefully added to the mixture to destroy the excess amount of sodium borohydride, and the mixture was centrifuged. The supernatant solution was collected and lyophilized to dryness. Methanol (50 ml) was added to the residue, and the mixture was evaporated to dryness. The procedures were repeated five times to remove boric acid completely. The residue was then dissolved in a small volume of water (3 ml), and applied to a column (100 cm × 3.0 cm I.D.) of Sephadex G-50 (Pharmacia, Uppsala, Sweden) equilibrated with 30 m*M* ammonium hydrogen carbonate. The column was eluted with the same solution, and 10-ml fractions were collected. The fractions containing sialic acids, as monitored by the resorcinol–hydrochloric acid assay [11], were collected and lyophilized.

Reduced oligosaccharides (**1**, **2**, **3** and **4** in Fig. 1) were isolated by preparative HPLC in the following manner [12].

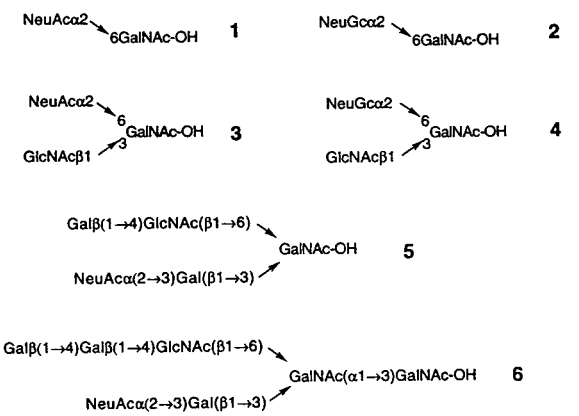

Fig. 1. List of the sialooligosaccharide alditol standards employed in the present work.

The residue obtained from the resorcinol-positive Sephadex G-50 fractions was applied to a column (250 mm × 4.6 mm I.D., 5 μm) of Takara PalPak-N (Takara Shuzo, Kyoto, Japan) and the column eluted isocratically with a mixture of acetonitrile–15 m*M* potassium dihydrogenphosphate solution (pH 5.2) (80:20, v/v) for 15 min, followed by gradient elution by changing the volume ratio of acetonitrile and the phosphate buffer linearly from 80:20 to 50:50 during 45 min at a flow-rate of 0.8 ml/min. The effluent was monitored at 210 nm. The effluents giving peaks at 25, 28, 33 and 37 min were collected and evaporated to dryness at room temperature. Each of the residues was dissolved in a small amount of water, and desalted on a small column (30 cm × 1 cm I.D.) of Sephadex G-25. The fractions which showed positive reaction to resorcinol were collected and lyophilized, to afford the sialooligosaccharide alditol standards.

2.2. Isolation of monosialooligosaccharide alditol standards from Chinese swiftlet

The procedure for isolation of monosialooligosaccharide alditols (**5** and **6** in Fig. 1) was similar to that described by Wieruszeski et al. [12]. Edible bird's nest material (1 g) was added in 50 m*M* sodium hydroxide (50 ml) containing sodium borohydride to a concentration of 1 *M*, and the mixture was incubated for 72 h at 37°C. The reaction was stopped by dropwise addition of acetic acid for neutralization. The resultant solution was centrifuged, the supernatant was lyophilized, a small volume of methanol (30 ml) was added to the residue, and the mixture was evaporated to dryness. The process of the addition and evaporation of methanol was repeated four times more. The residue was dissolved in a small volume of 30 m*M* aqueous ammonium bicarbonate, the solution was applied to a column (110 cm × 2.5 cm I.D.) of Sephadex G-50, and the column was eluted with the same solution. Fractions of 10 ml were collected, and assayed for sialic acid by the resorcinol–hydrochloric acid method. The 320–400-ml fraction was collected and lyophilized to dryness. The residue was dissolved in a small volume of pyridine acetate buffer (1 m*M* pyridine and 2 m*M* acetic acid, pH 5.6), and applied to a column (25 cm × 1.5 cm I.D.) of DEAE-Sephadex A-25 (Pharmacia), equilibrated with the same buffer. The column was eluted by a linear gradient made by the 1 m*M* pyridine–2 m*M* acetic acid buffer and the 150 m*M* pyridine–300 m*M* acetic acid buffer at a flow-rate of 10 ml/h. The volume of the starting and final buffers was 300 ml. Fractions of 5 ml were collected and assayed by the resorcinol–hydrochloric acid method. The fractions eluted between 250 and 325 ml were collected and lyophilized to dryness. The fractions showed the presence of three major peaks at 36, 42 and 45 min in HPLC on the amine-bonded silica column under the conditions described above for the isolation of sialooligosaccharides from bovine submaxillary mucin. The oligosaccharides giving peaks at 36 min and 45 min were isolated as pure state. These oligosaccharides showed molecular masses of 1406 and 1040, respectively, in negative fast atom bombardment-MS, and their ^{1}H NMR spectra were the same as those of oligosaccharides **5** and **6** (Fig. 1), respectively, described by Wierunszeski et al. [12].

2.3. Micro scale analysis of sialooligosaccharides in bovine submaxillary mucin and Chinese swiftlet

A sample of bovine submaxillary mucin (100 μg) was dissolved in 50 m*M* sodium hydroxide (100 μl) containing sodium borohydride to a concentration of 1.0 *M* in a polypropylene tube (1.5 ml), and the mixture was incubated for 72 h at 37°C. The excess amount of sodium borohydride was decomposed by careful addition of acetic acid (10 μl). The mixture was then passed through a small column of Amberlite CG-120 (H^+ form, 2 ml), and the column was washed with water (20 ml). The eluate and the washing fluid were combined and evaporated to dryness at 30°C by a rotary evaporator. The residue was dissolved in a small volume of methanol (5 ml) and the solution was evaporated to dryness. The methanol addition-dry up procedures were repeated four times more to remove boric acid

completely. The residue was dissolved in water (50 μl), and an aliquot was analyzed by HPCE.

A mixture of O-linked sialooligosaccharide alditols from Chinese swiftlet (10 μg) was also obtained similarly as described above. The amounts of the reagents and the volume of the solvent were reduced to one tenth of those used for the analysis of oligosaccharides in bovine submaxillary mucin.

2.4. HPCE

A Waters Quanta 4000 model (Millipore Japan, Tokyo, Japan) was used to carry out electrophoresis. An uncoated open tubular fused-silica capillary tube (50 cm × 360 μm O.D.; 50 μm I.D.), obtained form Polymicro Technologies (Phoenix, AZ, USA), was used in all experiments. The tube was fixed to the detector at the 7 cm position from the cathodic end of the capillary. The polyimide coating (2 mm section) was burned off to make a window for UV detection. For all experiments, absorbance at 185 nm was used for monitoring oligosaccharide alditols. All samples were introduced by hydraulic pressure for 10 s at a 10 cm height, and analysis was performed at 17 kV. The carrier solution was made from 200 m*M* borate buffer (pH 9.6) and contained sodium dodecyl sulfate (SDS) to a concentration of 100 m*M*.

3. Results and Discussion

3.1. Separation of monosialooligosaccharide alditols by HPCE

The electroosmotic flow is toward the cathode, since an uncoated capillary tube of fused silica having a negative charge on its inner wall is used in this work. On the other hand, sialooligosaccharides have the carboxyl groups which are dissociated to give anions under neutral and alkaline conditions. Therefore, they are expected to be held back when introduced from the anodic end. Thus, the combined effects of electroosmosis and electrostatic phenomenon will give peaks in the order of increasing charge to size ratios.

We investigated conditions for separation of the six oligosaccharide alditol standards, **1–6** (Fig. 1). Alkaline borate buffer gave basically a similar migration profile to that in alkaline phosphate buffer, indicating no significant contribution of borate complex formation. At pH 9.6, separation was optimal, but resolution was not satisfactory for the N-acetyl and N-glycolylneuraminic acid containing pairs, **1–2** and **3–4**. Addition of SDS to a concentration of 100 m*M*, however, resulted in baseline resolution of these pairs, as shown in Fig. 2. Table 1 lists the electrophoretic mobilities of **1–6** together with those of N-acetyl- and N-glycolylneuraminic acids.

N-Glycolylneuraminic acid-containing oligosaccharides (peaks **2** and **4**) showed slightly longer migration times than the N-acetylneuraminic acid-containing analogues (peaks **1** and **3**). Under the alkaline conditions employed, the carboxyl groups in these sialooligosaccharides are considered to be almost completely dissociated. Therefore, the operating mechanism of separation is exclusively zone electrophoresis. For these reasons the improvement of resolution by addition of SDS should be attributable to alteration of the electric charge to molecular size

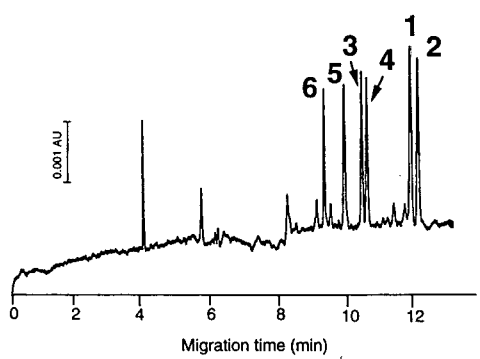

Fig. 2. Separation of an equimolar mixture of sialooligosaccharide alditol standards. Peak numbers refer to compounds in Fig. 1. Analytical conditions: capillary, fused silica (50 cm × 50 μm I.D.); carrier, 200 m*M* borate buffer (pH 9.6) containing SDS (0.1 *M*); applied voltage, 17 kV; detection, UV absorbance at 185 nm.

Table 1
Electrophoretic mobilities of some sialooligosaccharides

Sialooligosaccharide	μ_{ep} ($cm^2\ min^{-1}\ V^{-1}$, $\times 10^3$)
NeuAc	14.44
NeuGc	14.66
NeuAcα(2→6)GalNAcOH	13.04
NeuGcα(3→6)GalNAcOH	13.26
GalNAcβ(1→3) [NeuAcα(2→6)]GalNAcOH	11.39
GalNAcβ(1→3) [NeuGcα(2→6)]GalNAcOH	11.57
Galβ(1→4)GlcNAcβ(1→6)GalNAcOH	10.67
NeuAc(α2→6)Galβ(1→3)/ Galβ(1→4)GlcNAcβ(1→6)GalNAc(α1→3)GalNAcOH	9.73
NeuAc(α2→6)Galβ(1→3)/	

Ac = Acetyl; Gal = galactose; Gc = glycol; Neu = neuraminic acid.

ratio. If the electric charge is significantly different between the pairs, they should have been resolved even without addition of SDS. Consequently the most probable mechanism will be alteration of molecular size. It is anticipated that the addition of SDS might change the conformation of these oligosaccharides to different magnitudes resulting in variation of molecular size.

3.2. Quantitative analysis of sialooligosaccharide alditols by HPCE at 185 nm

The calibration curve of N-acetylneuraminyllactose was prepared by using a commercially available authentic specimen. Fig. 3 shows the separation of this model sialooligosaccharide and lactobionic acid used as an internal standard.

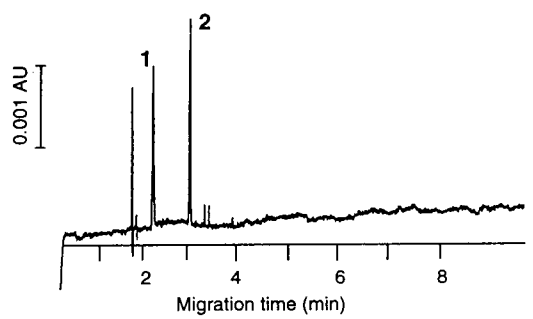

Fig. 3. Analysis of N-acetylneuraminyllactose by using lactobionic acid as an internal standard. Analytical conditions as in Fig. 2, except that the applied voltage was 25 kV. Peaks: 1 = N-acetylneuraminyllactose; 2 = lactobionic acid (internal standard).

In this case, a higher voltage (25 kV) was applied, hence the separation was rapid (in ca. 3 min). The plot of the relative peak response vs. the concentration of N-acetylneuraminyllactose showed good linearity between 0.9 and 20 m*M*. The lower limit of concentration (0.9 m*M*) in quantitative analysis corresponded to 3.6 pmol as the absolute injected amount, as the injected volume was 4.0 nl. This volume was obtained as $\pi r^2 l$, where r and l are the radius and the length of the plug of diluted rede ink introduced hydrodynamically in the same manner as sample solutions of reduced oligosaccharides. The minimum detectable concentration was 0.2 m*M* (signal-to-noise ratio 3). This is corresponding to 0.80 pmol as injected amount. We employed a 5-μl volume for the sample solutions, and the minimum sample amount in this volume was 1.0 nmol, since the lowest detectable concentration was 0.2 m*M*. This limit is higher than that obtained by high-performance anion-exchange chromatography (20 pmol, [13]), but the minimum amount injected to the capillary tube (0.8 pmol) was by far smaller than this amount. In addition, it was an advantage of the present method that greater portion of the sample could be recovered after analysis. The relative standard deviation of the relative peak response at 10 m*M* was 1.97% ($n = 7$).

3.3. Micro scale analysis of sialooligosaccharides in mucin samples

On the basis of the foregoing results the O-glycosidically linked sialooligosaccharides were released as alditol derivatives from a minute amount (100 μg) of bovine submaxillary mucin, and the derivatives were analyzed under the optimized conditions. The result is shown in Fig. 4.

Two predominant peaks due to NeuAcα-(2→6)GalNAc-OH (peak 1) and GalNAcβ(1→3)[NeuAcα(2→6)]GalNAc-OH (peak 3) were observed, accompanied by the peaks of the corresponding N-glycolyl analogues, NeuGcα(2→6)GalNAc-OH (peak 2) and GalNAcβ(1→3)[NeuGcα(2→6)]GalNAc-OH (peak 4). The total amounts of these major oligosaccharides were 91% of the overall peak areas. The broad peaks observed between 7 and 9 min were not identified in the present study, but these are presumably due to larger sialooligosaccharides having smaller charge to size ratio under these conditions.

Another example for analysis of the oligosaccharides in Chinese swiftlet is shown in Fig. 5.

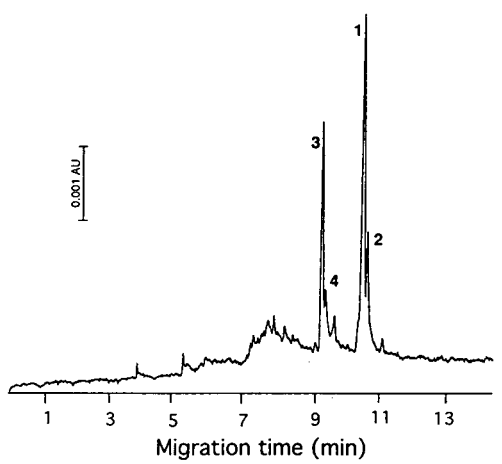

Fig. 4. Micro scale analysis of O-glycosidically linked sialooligosaccharides in bovine submaxillary mucin. Analytical conditions as in Fig. 2; peak numbers refer to compounds in Fig. 1. For the procedure for the release of oligosaccharides, see Materials and methods section.

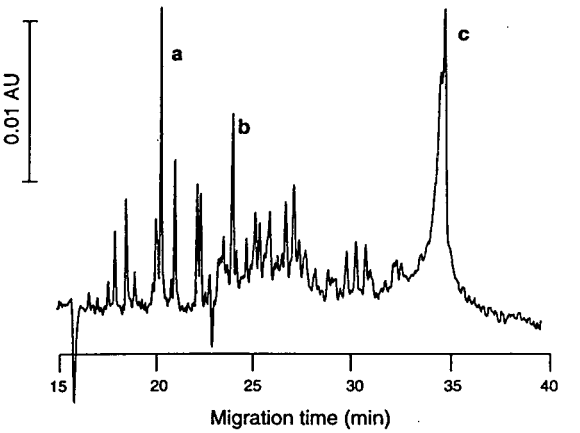

Fig. 5. Micro scale analysis of O-glycosidically linked sialooligosaccharides in Chinese swiftlet. Analytical conditions as in Fig. 2 except that the tube length was 100 cm. Peaks a, b and c were assigned to oligosaccharide alditols **5** and **6**, and N-acetylneuraminic acid, respectively. Concerning the procedure for the release of oligosaccharides, see the Materials and methods section.

Complex patterns were observed. Peaks a and b were identified as oligosaccharide alditols **6** and **5**, respectively, by co-migration with the standards. The large peak (peak c) observed at 35 min is due to that of N-acetylneuraminic acid introduced as the internal marker. In this case, a longer capillary (1 m) than that used for the analysis of oligosaccharides in bovine submaxillary mucin was used to obtain better separation, hence longer analysis time (35 min) was required.

The series of operations in these analyses are simple, because the processes of the release of oligosaccharides and reduction to alditols are conducted in one-pot fashion. Although considerable interference should be taken into consideration in cases of impure glycoprotein samples, the overall procedure is quite practical and convenient.

References

[1] T. Mizuochi, in E.F. Hounsell (Editor), *Glycoprotein Analysis in Biomedicine*, Humana Press, Totowa, NJ, 1993, p. 55.
[2] Y.C. Lee, *Anal. Biochem.*, 189 (1990) 151.

[3] P. Hermentin, R. Witzel, R. Doenges, R. Bauer, H. Haupt, T. Patel, R.B. Parekh and D. Brazel, *Anal. Biochem.*, 206 (1992) 419.
[4] K. Kakehi, S. Suzuki, S. Honda and Y.C. Lee, *Anal. Biochem.*, 199 (1991) 256.
[5] S. Honda, A. Makino, S. Suzuki and K. Kakehi, *Anal. Biochem.*, 191 (1990) 222.
[6] D.M. Carlson, *J. Biol. Chem.*, 243 (1968) 616.
[7] S. Honda, S. Suzuki, S. Zaiki and K. Kakehi, *J. Chromatogr.*, 523 (1990) 189.
[8] T. Hayase, M. Skeykhanazari, V.P. Bhavanandan, A.V. Savage and Y.C. Lee, *Anal. Biochem.*, 211 (1993) 72.
[9] H.S. Kuhn, A. Paulus, E. Gassmann and H.M. Widmer, *Anal. Chem.*, 63 (1991) 1541.
[10] G. Tettamanti and W. Pigman, *Arch. Biochem. Biophys.*, 124 (1968) 41.
[11] L. Svennerholm, *Biochim. Biophys. Acta*, 24 (1957) 604.
[12] J.M. Wieruszeski, J.-L. Michalski, J. Montreuil, G. Strecker, J.P.-Katalinic, H. Egge, H. van Halbeek, H.G.M. Mutsaers and J.F.G. Vliegenthardt, *J. Biol. Chem.*, 262 (1987) 6650.
[13] K. Kakehi, S. Suzuki and S. Honda, unpublished results.

ELSEVIER

Journal of Chromatography A, 680 (1994) 217–224

JOURNAL OF CHROMATOGRAPHY A

Analysis of the microheterogeneity of the glycoprotein chorionic gonadotropin with high-performance capillary electrophoresis

Dean E. Morbeck, Benjamin J. Madden, Daniel J. McCormick*

Department of Biochemistry and Molecular Biology, Mayo Clinic, Rochester, MN 55905, USA

Abstract

Human chorionic gonadotropin (hCG) is a heteromeric glycoprotein hormone with a molecular mass of *ca.* 38 000. The carbohydrate side chains terminate with sialic acid and account for roughly 30% of the mass of the hormone. Glycoforms of hCG have been routinely identified with conventional methods of isoelectric focusing or chromatofocusing and exhibit varied bioactivity. In the present report, high-performance capillary electrophoresis (HPCE) was used to separate the glycoforms of hCG and its subunits. Optimal conditions for obtaining near-baseline resolution of the glycoforms were 25 m*M* borate, pH 8.8 containing 5 m*M* diaminopropane. The samples were separated in a 100 cm fused-silica capillary with an internal diameter of 50 μm at 25 kV and 28°C. In its native form, hCG migrated in less than 50 min as 8 distinct, highly resolved peaks. In the absence of diaminopropane, hCG migrated as a single, broad peak. When analyzed individually, the α subunit separated into four peaks and the β subunit resolved as seven peaks. The two subunits could also be separated when the heterodimer was incubated in 0.25% trifluoroacetic acid for 1 h prior to injection into the capillary. To illustrate the potential clinical application of this technique, four different sources of hCG were analyzed. The number of different isoforms was constant among the four samples; however, the relative concentration (amounts) of the isoforms varied. These results illustrate the potential utility of HPCE in the clinical diagnostic analysis of hCG microheterogeneity.

1. Introduction

Human chorionic gonadotropin (hCG) is a member of a family of glycoprotein hormones [1] which includes thyroid-stimulating hormone (TSH) and the gonadotropins luteinizing hormone (LH) and follicle-stimulating hormone (FSH). hCG is produced by the trophoblasts of the normal placenta and of choriocarcinoma tissue [2–4] and by non-trophoblastic neoplasia [5,6]. The hormone has an approximate molecular mass of 38 000 and consists of an α and β subunit that are non-covalently associated. Whereas both subunits have two N-glycosylated asparagines, the β-subunit contains an additional four O-glycosylated serine residues located within the C-terminal region. These carbohydrate modifications account for 30–35% of the mass of the hormone and result in several different glycoforms of the hormone [7].

The microheterogeneity of hCG and related glycoproteins has been examined by the methods of chromatofocusing and isoelectric focusing (IEF). The overall charge of hCG is acidic with a

* Corresponding author.

0021-9673/94/$07.00
SSDI 0021-9673(94)00182-9

p*I* around 4 but it is comprised of 6 to 8 isoforms with p*I* values ranging between 3 and 6 [7]. The significance of the various isoforms is manifest in biological activity. More acidic variants of each of the hormones in this family tend to be more biologically active due to slower clearance from the circulation [7]. This relationship between the glycosylation pattern and the hormone's potency may be important in certain endocrine disorders and during the normal course of pregnancy. Studies of hCG from patients with trophoblastic disease have revealed that the glycosylation pattern is different from that of normal hCG [8–11]. These changes present an opportunity to develop diagnostic screening methods which discriminate choriocarcinoma from non-malignant trophoblastic diseases [12].

Although methods for analyzing heterogeneity of glycoproteins have provided valuable information, they are not without limitations. Both chromatofocusing and IEF are labor-intensive analyses and neither technique has provided quantitative or qualitative resolution of the different isoforms needed to obtain pure isoform preparations. In addition, with chromatofocusing a significant amount of the hormone remains on the column until elution with 1 *M* NaCl. The chemical nature of this highly charged material is not clear.

An alternative to the traditional methods of separation is the use of high-performance capillary electrophoresis (HPCE). This technique combines the advantages of simplicity, speed and reproducibility with high separation efficiency. Wide [13,14] used zone electrophoresis in agarose gel to analyze the heterogeneity of FSH, LH and TSH. Although the resolution was poor due to the limitations of the apparatus, Wide estimated that each of the hormones was composed of at least 20 different isoforms with minor differences in charge. The significance of this finding *versus* the number of isoforms identified with IEF is not known.

Recently, Landers *et al.* [15] reported a method for the efficient, high-resolution separation of the glycoprotein ovalbumin. In this method, the buffer additive diaminobutane was utilized to enhance separation that otherwise yielded a single broad peak. These studies present, for the first time, a facile method for the reproducible separation of hCG by HPCE and the improved baseline separation of its isoforms using a diaminoalkane as a buffer additive.

2. Materials and methods

2.1. Materials

Boric acid, sodium tetraborate and 1,3-diaminopropane (DAP) were obtained from Sigma (St. Louis, MO, USA). The neutral marker, dimethylformamide (DMF), was purchased from Aldrich (Milwaukee, WI, USA).

Four different preparations of hCG were used. The reference batch hCG CR127 was kindly supplied by the National Hormone and Pituitary Program (University of Maryland School of Medicine). Two separate batches of crude urinary hCG (Diosynth, Chicago, IL, USA) were purified using a previously published method [16]. This purification scheme results in the separation of nicked hCG and hCGβ fragment from intact hCG [17]. The resulting preparations were designated hCG 2292 and hCG 393. The fourth preparation of hCG, AK930, was purified from urine of a patient with metastatic choriocarcinoma using the method referenced above.

Pure subunits were obtained by treating hCG 2292 with 6 *M* guanidine hydrochloride for 18 h. The dissociated subunits were purified by reversed-phase HPLC on a Vydac C_8 column (Hesperia, CA, USA) in 0.1% aqueous trifluoroacetic acid (TFA) and a gradient of 5% to 48% acetonitrile in 0.1% aqueous TFA. Two major peaks were obtained, the first was the α subunit and the second was the β subunit (Fig. 1).

2.2. Capillary electrophoresis

All separations were performed on an Applied Biosystems Model 270A capillary electrophoresis system (Foster City, CA, USA) interfaced with a personal computer utilizing Beckman System Gold software (version 5.0; Beckman, Fullerton,

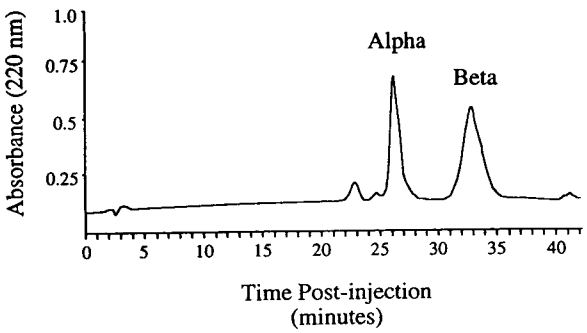

Fig. 1. Analysis and purification of hCG 2292 with reversed-phase HPLC following treatment with 6 *M* guanidine · HCl for 18 h. Conditions were 0.1% aqueous TFA with a gradient of 5 to 48% acetonitrile in 0.1% aqueous TFA.

CA, USA). Separations were performed with fused-silica capillaries which were 100 cm in length (78 cm to the detector) with an internal diameter of 50 μm. All electrophoretic separations were carried out at 25 kV constant voltage (inlet as the anode and outlet as the cathode) and the capillary temperature was maintained at 28°C. Detection was by absorbance at 200 nm.

Prior to each electrophoretic separation, the capillary was washed with 2 column volumes of 0.1 *M* NaOH followed by a 8-column-volume rinse with running buffer. The neutral marker DMF (1.5 m*M*) was then vacuum-injected for 1 s followed by the vacuum injection of each sample for 2 s. The estimated concentration of each hCG solution used for analysis was about 4 mg/ml.

In order to determine optimal conditions for the separation of hCG and its isoforms, several buffers of varying ionic strength and pH were analyzed. Six borate buffers at ionic strengths of 25 and 100 m*M* and pH values of 8.2, 8.8 and 9.2 were examined. In addition, 50 m*M* Tris–384 m*M* glycine, pH 8.3 and 20 m*M* ammonium formate, pH 8.8 were also tested. The buffer additive DAP was tested at various concentrations. All buffers were made with HPLC-grade water (EM Science, Gibbstown, NJ, USA) and filtered through a 0.2-μm filter (Gelman Science, Ann Arbor, MI, USA) before use.

2.3. Data analysis

In order to compare the distribution of the isoforms of the different preparations of hCG, the integration functions of System Gold were used to determine the area under the curve of the major peaks. Eight peaks were identified and the percent of the total area under the curve was calculated for each. Each of the four preparations of hCG was analyzed at least three times and the average percent of the total area for each peak was determined. Percent of total area for each peak were analyzed by ANOVA and the means were compared with the Scheffe *F*-test using the statistical program Statview (version 1.0.3).

3. Results and discussion

Addition of diaminopropane to the running buffer was necessary for the successful separation of hCG isoforms. When hCG was analyzed without DAP, a single peak with a broad tail and a migration time of under 20 min was observed (Fig. 2A). Adding DAP at various concentrations (Fig. 2B–E) resulted in the detection of multiple, well resolved peaks with a concomitant increase in the total migration time. Resolving power increased with additional DAP used; 1 m*M* DAP resulted in the appearance of multiple peaks with poor resolution, whereas the addition of 2.5 and 5.0 m*M* DAP led to the separation of eight clearly defined peaks in less than 50 min. Increasing the DAP concentration to 10 m*M* did not result in an increase in the number of peaks or improved resolution (data not shown).

Based on these results, all subsequent experiments were conducted with 5 m*M* DAP added to the running buffer. The improvement in resolution with 5 *versus* 2.5 m*M* DAP was sufficient to justify the additional migration time required for the analysis. The optimal conditions for separation were then determined and resulted in the choice of 25 m*M* borate buffer, pH 8.8 with 5 m*M* DAP as the running buffer. The current generated with this buffer in a 100 cm × 50 μm

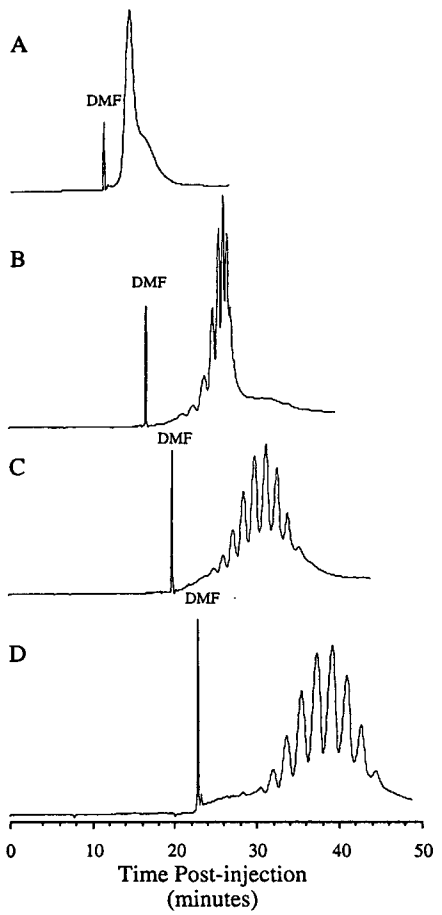

Fig. 2. Effect of various concentrations of diaminopropane on the electrophoretic migration and separation of hCG 2292 (4 mg/ml). Separations were carried out in a 100 cm × 50 μm fused-silica capillary with 25 m*M* borate, pH 8.8, 2 s injection of sample (4 mg/ml), 25 kV and 28°C. The DAP concentrations used were 0 (A), 1.0 (B), 2.5 (C) and 5.0 m*M* (D).

I.D. capillary at 28°C and 25 kV was 6 to 7 μA. Although borate was the buffer of choice, Tris-glycine and ammonium formate buffers containing 5 m*M* DAP yielded similar separations of hCG that had the same number of isoforms but without the enhanced baseline resolution obtained with borate buffer (data not shown).

It has been hypothesized that diaminoalkanes such as DAP enhance the separation of the glycoforms by decreasing the endoosmotic flow (EOF). This decrease in EOF results from the cationic amines interacting with the negatively charged capillary wall and thereby increasing the migration time of the sample. This increase in migration time allows for enhanced resolution of the different glycoforms. Other diaminoalkanes such as putrescine (1,4-diaminobutane) have been utilized as buffer additives for the analysis of microheterogeneity of glycoproteins, including tissue plasminogen activator (tPA) [18], ovalbumin and pepsin [15] and human recombinant erythropoietin [19]. Landers *et al.* [20] compared diaminoalkanes of different chain lengths (C_2–C_6) and demonstrated that diaminopropane and diaminobutane modified EOF and improved the resolution of ovalbumin to the same degree. In the present study, we also tested diaminobutane and diaminopentane and observed similar results (data not shown).

The choice of buffer may be critical for optimizing resolution of the different glycoforms. In their analysis of ovalbumin, Landers *et al.* [15] found that borate was superior to phosphate at putrescine concentrations of 1 m*M*. However, separation of the isoforms was possible in phosphate with a higher concentration of putrescine (5 m*M*). In contrast, Taverna *et al.* [18] found that putrescine was not efficient with borate but was with tricine for the analysis of tPA glycopeptides. In the present study, 25 m*M* borate, pH 8.8 containing 5 m*M* DAP provided the best results in terms of the resolution of hCG glycoforms. Tris-glycine and ammonium formate, on the other hand, yielded separation of the isoforms, albeit with resolution that was inferior to that seen with borate. Since we did not attempt to optimize the conditions with Tris-glycine and ammonium formate buffers it is not known if under different conditions these buffers would perform similar to borate. The borate ion may be inherently better for analyzing glycoproteins [15] because of its potential to form a borate–sugar diol complex as proposed by Novotny and co-workers [21,22]. The carbohydrates on hCG are of the high-mannose variety [23–26] which would allow for this type of complexation. Use of borate *versus* other buffers for the analysis of glycoproteins warrants further study.

The pattern of isoform separation is interest-

ing and merits discussion. Because HPCE separates molecules based on their charge-to-mass ratio, unlike IEF which separates proteins based on isoelectric point, the identity of the isoforms that correspond to each peak is not inherently obvious. Since the isoforms separated into peaks with a normal distribution, it suggests that the predominant forms are those with an "average" charge-to-mass ratio. The minor forms thus deviate from this ratio in both directions. Unfortunately, it is not possible to label each peak with a corresponding p*I*; this will require additional studies using fraction collection to obtain the individual forms and then determining the p*I* with IEF.

In addition to the high-resolution separation of the native heterodimer, the purified subunits were also analyzed for heterogeneity (Fig. 3). The α subunit is 92 residues in length and contains two sites for N-linked glycosylation whereas the β subunit is 145 residues long and has four sites for O-linked glycosylation in addition to two sites for N-linked glycosylation. Upon electrophoresis, the HPLC-purified α subunit resolved into four discernable peaks with migration times between 25 and 32 min (Fig. 3A). The first peak was detected in less than 3 min after the neutral marker DMF and appeared to be heterogeneous. Altogether, four major species of the α subunit were separated.

The separation pattern for the β subunit of hCG had a similar profile to the one for the intact dimer with fewer peaks (Fig. 3B *vs.* 3C). There were five major and two minor peaks (a total of seven) arranged in the same Gaussian or normal distribution as the native heterodimer; however, the peaks for the β subunit migrated faster than those for the intact dimer.

Since the subunits of hCG are not covalently linked, it was possible to dissociate them in acid and show that the separation profiles from the subunits analyzed individually were similar to the profile of the hormone following dissociation. Fig. 4 illustrates the effect of 0.25% TFA on the disassociation of the hCG subunits. The dissociation profiles represent 0, 60 min and 5 h after the addition of 0.25% TFA. As the amount of time increased following the addition of TFA, the

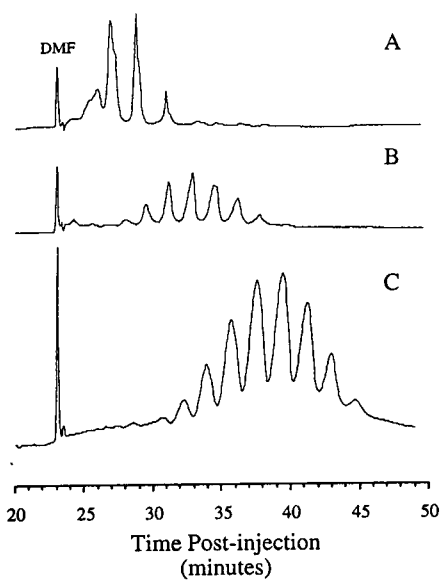

Fig. 3. Electropherograms of the individual α (A) and β (B) subunits of hCG 2292 (C). Separations were carried out in a 100 cm × 50 μm fused-silica capillary, with 25 m*M* borate plus 5 m*M* DAP, pH 8.8, 2 s injection of sample (4 mg/ml), 25 kV and 28°C.

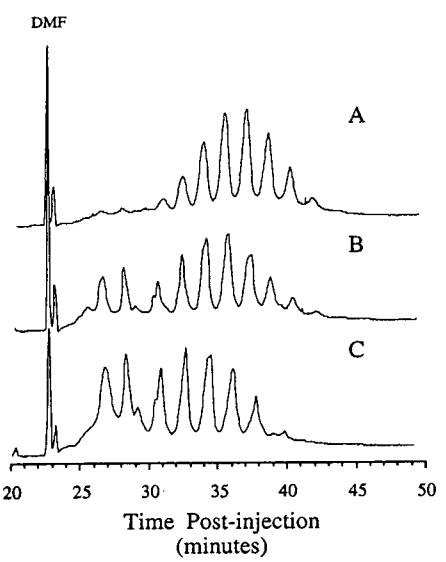

Fig. 4. Separation and analysis of microheterogeneity of the α and β subunits of hCG 2292 following addition of 0.25% TFA to the intact dimer. Figures represent 0 (A), 60 min (B) and 5 h (C) after the addition of TFA. Conditions as in Fig. 3.

magnitude of the peaks in Fig. 4C clearly decreased whereas peaks in positions similar to those for α and β appeared and increased in magnitude. The dissociation of hCG was examined after 24 h and did not exhibit any significant changes from the profile at 5 h.

The behavior and number of isoforms of the α subunit were expected based on its known glycosylation pattern. An important distinction to make, however, is that the results obtained here are for α subunit isolated from the dimer and are not the free subunit isolated from urine. This is a significant point because free subunit produced during pregnancy is more acidic than dimer α, may have a sialylated, serine-linked oligosaccharide, and consequently cannot form a heterodimer with the β subunit [27].

The oligosaccharides of the α subunit are characterized by a lack of fucosylation and exist predominantly in the monosialylated (50%) and asialylated (30%) forms [23]. The relative low amount of sialylation indicates that amount of acidity due to the oligosaccharides is minimal. In addition, based on the limited number of different possibilities that exist for oligosaccharides on the α subunit, Grotjan and Cole [7] estimated that two to three major isoforms of α exist. Results of the present study confirm these observations and predictions. The fact that the α subunit isoforms migrated more quickly than the β subunit and the intact dimer is probably due to the fact that it is smaller and less negatively charged than the other species. In addition, the number of peaks agrees nicely with Grotjan and Cole's estimate. In contrast, studies of the microheterogeneity of the α subunit using IEF have reported the presence of seven to eight peaks [27–29]. The reason for the differences between these reports and the present study is not known.

The similarity between the separation pattern for the β subunit and the one for the intact dimer is intriguing although not surprising. In general, the number of glycoforms should be influenced by the number of sialic acids present on the oligosaccharides. Since the β subunit contains six glycosylation sites and most of these contain oligosaccharides with one or two sialic acids, most of the heterogeneity of the dimer should be the result of the β subunit. Indeed, Cole [25] proposed this very idea based on studies of the O-glycosylation of the β subunit. The number of major peaks is in agreement with earlier IEF studies [30–32] and estimates by Grotjan and Cole [7]. Since the shape of the electropherogram is similar to that of the dimer, the contribution of the α subunit to dimer heterogeneity appears to be small, possibly increasing the total number of dimer isoforms by one or two.

In order to further investigate the nature of the separations, four unique preparations of hCG were analyzed and the results compared. Fig. 5 depicts the profiles of the four different

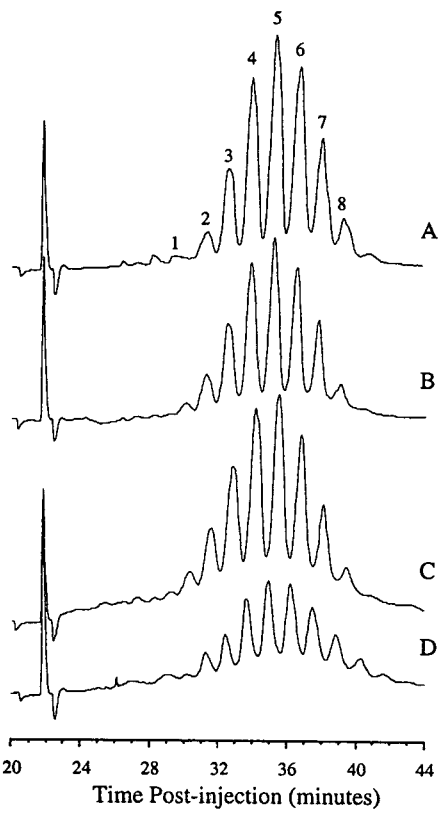

Fig. 5. Comparison of microheterogeneity among four separate preparations of hCG. (A) hCG CR127, (B) hCG 393, (C) hCG 2292 and (D) hCG AK930. Conditions as in Fig. 3. Peak numbers are referred to in Table 1.

preparations and illustrates an overall similar pattern of separation. Thus it appears that each of the four samples consists of roughly the same eight major isoforms. However, the relative amounts of each of the different isoforms, as manifested in the size of the peaks, was different among the different preparations. In order to compare the relative proportions of each of the peaks, it was necessary to quantitate them. The data in Table 1 shows the average peak area for each of the eight isoforms isolated from four different hCG samples. The data shown are the mean of three separate analyses for each preparation and are expressed as a percentage of the total area for all eight peaks. For the sake of comparison, Table 1 also depicts the mean values for the first four and last four peaks. Overall, the data show that there is a remarkable difference in the composition of the different hCG preparations. Nearly two thirds (64.9) of the isoforms of CR127 migrate as peaks 5–8, whereas peaks 5–8 represent 57.2% of hCG 393 and 51.7% of hCG 2292. The peaks for the choriocarcinoma preparation, AK930, migrated in a manner that did not allow an accurate comparison to the peak isoforms of the other hCG samples. If the data are calculated for AK930 in two ways so that the peaks align with either the previous or subsequent peak, then the relative amount of AK930 that is represented by peaks 5–8 is either 48.2% or 65.5%. Future studies using fraction collection and determination of the p*I* values of the different isoforms will provide a more complete picture of the characteristics of these different preparations.

In summary, seven to eight isoforms of hCG were separated with baseline resolution but only in the presence of the EOF modifier, DAP. Isoforms of the individual subunits were also separated with this procedure. Although we have not determined the p*I* of the different forms, variances in the different isoforms among differ-

Table 1
Comparison of the relative amounts of the glycoforms identified for each of four different preparations of hCG (%)

Sample[a]	Peak[b]							
	1	2	3	4	5	6	7	8
CR127	0.7 ± 0.1[c]	2.6 ± 0.1	10.5 ± 0.1	21.2 ± 0.2	26.6 ± 0.1	22.5 ± 0.1	12.0 ± 0.3	3.8 ± 0.1
		35.1 ± 0.5[d]				64.9 ± 0.6[e]		
393	1.4 ± 0.1	5.6 ± 0.1	13.4 ± 0.3	22.4 ± 0.1	25.1 ± 0.1	19.5 ± 0.1	10.1 ± 0.1	2.6 ± 0.2
		42.8 ± 0.6[d]				57.2 ± 0.5[e]		
2292	2.3 ± 0.1	7.4 ± 0.1	15.4 ± 0.1	23.2 ± 0.1	24.2 ± 0.1	17.5 ± 0.1	8.0 ± 0.1	1.9 ± 0.1
		48.3 ± 0.4[d]				51.7 ± 0.4[e]		
AK930	5.5 ± 0.3	8.7 ± 0.5	16.9 ± 0.5	20.7 ± 0.4	19.9 ± 0.3	15.0 ± 0.6	9.1 ± 0.3	4.2 ± 0.7
		51.8 ± 1.7[d]				48.2 ± 1.9[e]		

[a] Source of hCG (see Materials and methods section).
[b] Peak number in Fig. 5.
[c] Area under the curve for peak 1 divided by the total area under the curve for the entire electropherogram. Expressed as a mean % ± standard error.
[d] Sum of peaks 1–4.
[e] Sum of peaks 5–8.

ent preparations of hCG were clearly present and suggest that HPCE may be of great utility for the comparison of hCG microheterogeneity in normal tissues and neoplasms.

4. Acknowledgement

The authors wish to thank M. Cristine Charlesworth for the purification of the different hCG preparations.

5. References

[1] R.J. Ryan, M.C. Charlesworth, D.J. McCormick, R.P. Milius and H.T. Keutmann, *FASEB J.*, 2 (1988) 2661.
[2] R. Nishimura, Y. Endo, K. Tanabe, Y. Ashitaka and S. Tojo, *J. Endocrinol. Invest.*, 4 (1981) 349.
[3] S. Amr, C. Rosa, R. Wehmann, S. Birken and B. Nisula, *Ann. Endocrinol.*, 45 (1984) 321.
[4] L.A. Cole, F. Perini, S. Birken and R.W. Ruddon, *Biochem Biophys. Res. Comm.*, 122 (1984) 1260.
[5] G.S. Cox, *Biochem. Biophys. Res. Comm.*, 98 (1981) 942.
[6] L.A. Cole, S. Birken, S. Sutphen, R.O. Hussa and R.A. Pattillo, *Endocrinology*, 110 (1982) 2198.
[7] H.E. Grotjan, Jr. and L.A. Cole, in B.A. Keel and H.E. Grotjan, Jr. (Editors), *Microheterogeneity of Glycoprotein Hormones*, CRC Press, Boca Raton, FL, 1989, Ch. 11, p. 219.
[8] R.A. Reisfeld, D.M. Bergenstal and R. Hertz, *Arch. Biochem. Biophys.*, 81 (1959) 456.
[9] R.A. Reisfeld and R. Hertz, *Biochim. Biophys. Acta*, 43 (1960) 540.
[10] L.A. Cole, *J. Clin. Endocrinol.*, 65 (1987) 811.
[11] J. Amano, R. Nishimura, R. Mochizuki and A. Kobata, *J. Biol. Chem.*, 263 (1988) 1157.
[12] T. Endo, K. Iino, S. Nozawa, R. Iizuka and A. Kobata, *Jpn. J. Cancer Res.*, 79 (1988) 160.
[13] L. Wide, *Acta Endocrinol.*, 109 (1985) 181.
[14] L. Wide, *Acta Endocrinol.*, 109 (1985) 190.
[15] J.P. Landers, R.P. Oda, B.J. Madden and T.C. Spelsberg, *Anal. Biochem.*, 205 (1992) 115.
[16] J. Hiyama, A. Surus and A.G. Renwick, *J. Endocrinol.*, 125 (1990) 493.
[17] S. Birken, Y. Chen, M.A. Gawinowicz, J.W. Lustbader, S. Pollak, G. Agosto, R. Buck and J. O'Connor, *Endocrinology*, 133 (1993) 1390.
[18] M. Taverna, A. Baillet, D. Biou, M. Schlüter, R. Werner and D. Ferrier, *Electrophoresis*, 13 (1992) 359.
[19] E. Watson and F. Yao, *Anal. Biochem.*, 210 (1993) 389.
[20] J.P. Landers, R.P. Oda, S. Svedberg and T.C. Spelsberg, *Anal. Chem.*, submitted for publication.
[21] J. Liu, O. Shiruta, D. Wiesler and M. Novotny, *Proc. Natl. Acad. Sci. U.S.A.*, 88 (1991) 2302.
[22] J. Liu, O. Shiruta, M. Novotny, *Anal. Chem.*, 63 (1991) 413.
[23] T. Mizuochi and A. Kobata, *Biochem. Biophys. Res. Comm.*, 97 (1980) 772.
[24] L.A. Cole, S. Birken and F. Perini, *Biochem. Biophys. Res. Comm.*, 126 (1985) 333.
[25] L.A. Cole, *Mol. Cell. Endocrinol.*, 50 (1987) 45.
[26] K. Hard, J.B.L. Damm, M.P.N. Spruijt, A.A. Bergwerff, J.P. Kamerling, G.W.K. van Dedem and J.F.G. Vliegenthart, *Eur. J. Biochem.*, 205 (1992) 785.
[27] R. Nishimura, T. Utsunomiya, K. Ide, K Tanabe, T. Hamamoto and M. Mochizuki, *Endorinol. Jpn.*, 32 (1985) 463.
[28] R. Benveniste, M.C. Conway, D. Puett and D. Rabinowitz, *J. Clin. Endocrinol. Metab.*, 85 (1979) 85.
[29] R. Benveniste, J. Lindner, D. Puett and D. Rabinowitz, *Endocrinology*, 105 (1979) 581.
[30] D. Graesslin, H.C. Weise and W. Braendle, *FEBS Lett.*, 31 (1973) 214.
[31] K. Yazaki, C. Yazaki, K. Wakabayashi and M. Igarashi, *Am. J. Obstet. Gynecol.*, 138 (1980) 189.
[32] N. Nwokoro, H.C. Chen, A. Chrambach, *Endocrinology*, 108 (1981) 291.

ELSEVIER

Journal of Chromatography A, 680 (1994) 225–232

JOURNAL OF CHROMATOGRAPHY A

Determination of the number and distribution of oligosaccharide linkage positions in O-linked glycoproteins by capillary electrophoresis

Paul L. Weber*[,a,b], Christopher J. Bramich[b], Susan M. Lunte[b]

[a]*Department of Chemistry, Briar Cliff College, Sioux City, IA 51104, USA*

[b]*Center for Bioanalytical Research, University of Kansas, Lawrence, KS 66047, USA*

Abstract

O-Linked oligosaccharide chains are found in a wide variety of glycoproteins. Determination of the number of O-linked serine and threonine residues is an important step in glycoprotein characterization. Alkaline release of the oligosaccharide chains from the peptide chain followed by bisulfite addition to the unsaturated residues generates sulfonates. Hydrolysis of treated samples followed by derivatization with naphthalene 2,3-dicarboxyaldehyde and cyanide results in analytes which are separated and quantitated by capillary electrophoresis with UV detection. The utility of the method was demonstrated using bovine submaxillary mucin yielding results that agreed with previously published values.

1. Introduction

A variety of methods exist which can be used to determine oligosaccharide chain structure and peptide structure. However, there are relatively few procedures which can be used to determine the number and distribution of oligosaccharide linkage positions on the peptide chain. The current, most popular approach is to sequence a peptide with a commercial sequencer and note at which position sequencing is terminated. Subsequent comparison of these data to the sequence obtained after the carbohydrate chains have been enzymatically or chemically removed usually gives the desired information [1–3]. Examples of recent reports using this method are those of Schmid et al. [4] and Nakada et al. [5]. Alternative approaches include one which employs a biotinylated lectin/avidin-biotinylated peroxidase on-membrane staining technique [6].

In 1973, Pigman and Moschera [7] reviewed a reductive β-elimination procedure used to release oligosaccharide chains O-linked to serine and threonine residues and effect conversion to alanine and α-aminobutyric acid, respectively. The amino acid residues can then be released by acid hydrolysis and quantitated for compositional information [8]. Alternatively, the treated peptide can be subjected to sequence analysis [9]. One drawback to the reductive β-elimination is that the alanine which is generated in the procedure is also a commonly occurring amino acid in proteins. Therefore it is necessary to analyze

* Corresponding author.

0021-9673/94/$07.00
SSDI 0021-9673(94)00658-X

an untreated sample in order to correct for endogenous alanine.

In a recent review on carbohydrate analysis, a relatively straightforward method similar to reductive β-elimination is given [10]. Originally described by Harbon et al. [11], it involves the treatment of the glycoprotein with a solution of alkaline sulfite in order to cause β-elimination of oligosaccharide chains O-linked to serine and threonine residues and conversion of the resulting unsaturated derivatives to their sulfonates (Fig. 1). The modified protein is then hydrolyzed to produce free amino acids which are then separated and quantitated. Using this procedure, any serine residue which was attached to an oligosaccharide will be converted to a cysteic acid (CA) residue while an O-linked threonine results in an α-amino-β-sulfonylbutyric acid residue (ASBA). Thus, the quantity of these two residues relative to the quantity of serine and threonine residues, respectively, gives the relative number of serines and threonines O-linked to oligosaccharide chains. Note that in this procedure two unique amino acids are formed which are not commonly found in peptide structures.

In order to increase sensitivity, this method has been modified by using radioactively labeled sulfite [12]. Though it gives useful results, it requires the use of radioactive substances. It also suffers from drawbacks common to other techniques which involve quantitation of the amino acid sulfonates in the presence of other amino acids. The sulfonates coelute at the void volume of an amino acid analyzer. The methods are quite tedious and time-consuming requiring desalting, ion-exchange chromatography for separation and then paper chromatography for identification.

With the advent of capillary electrophoresis (CE) it is possible to expedite the separation and quantitation of the amino acids involved in the procedure. Since CE in its simplest form, capillary zone electrophoresis (CZE), separates substances by size and charge, it seems well suited to analyze a reaction such as the alkaline-sulfite reaction in which the products have acquired an additional negative charge. CE also offers the advantages of highly efficient separations, low volume requirements and minimal sample preparation as compared to other separation techniques such as liquid chromatography. Specifically, we have developed a method whereby the amino acids, including the sulfonates, are derivatized and analyzed by CE. The amino acids are reacted with naphthalene-2,3-dicarboxyaldehyde (NDA) in the presence of cyanide to generate the cyanobenzylisoindole (CBI) deriva-

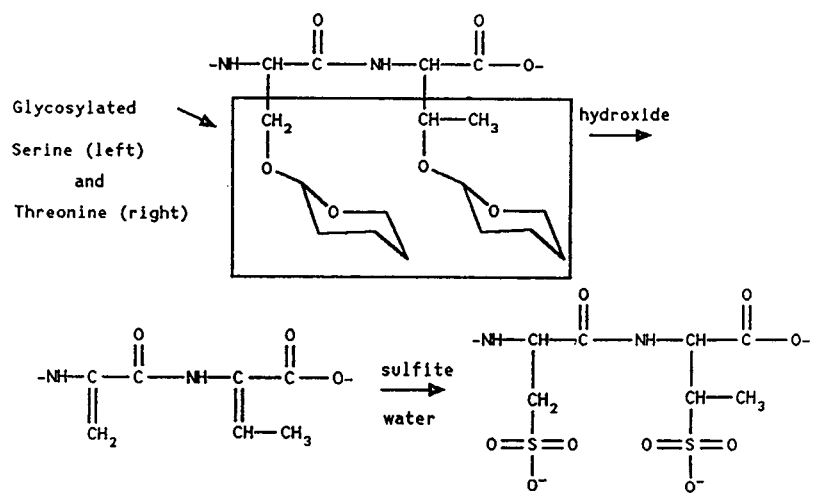

Fig. 1. Alkaline sulfite reaction causing β-elimination of O-linked serine and threonine residues and conversion of the unsaturated intermediates to sulfonates.

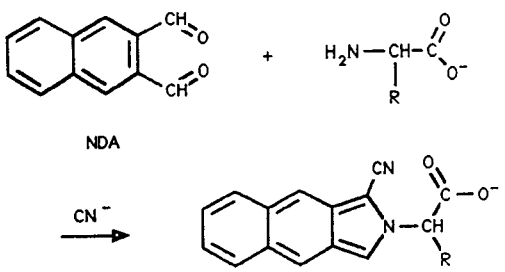

Fig. 2. NDA–cyanide derivatization reaction with primary amino acids.

tives (Fig. 2) and subsequently separated by CZE using UV detection. The separation of the CBI derivatives of selected amino acids by CE has been accomplished previously by us [13]. The CBI derivatives can also be detected with greater sensitivity by fluorescent, electrochemical and chemiluminescence detectors [14].

2. Experimental

2.1. Materials

Amino acids, glycoproteins and sodium dodecyl sulfate were obtained from Sigma (St. Louis, MO, USA). Sodium cyanide (99%) was acquired from Fluka (Ronkonkoma, NY, USA). Sodium borate (ACS), sodium sulfite (ACS), NaOH and concentrated HCl (ACS) were purchased from Fisher Scientific (Fair Lawn, NJ, USA) and NDA was acquired from Oread Labs. (Lawrence, KS, USA). Solutions were prepared in Nanopure water (Sybron-Barnstead, MA, USA).

2.2. Alkaline sulfite reaction (β-elimination and bisulfite addition)

The conditions used in this reaction are adapted from Ref. [12]. Exactly 5.0 mg of glycoprotein were mixed with 100 μl of 5 m*M* α-aminoadipic acid (internal standard, IS). If the sample was a control sample, 300 μl of 6 *M* HCl was then added. Next, 1.5 ml of 0.5 *M* Na_2SO_3 in 0.1 *M* NaOH were added with thorough mixing. The solution is then incubated at 37°C in a recirculating water bath for the indicated amount of time. The reaction is stopped by removing the solution, allowing it to reach room temperature, and combined with 400 μl of concentrated HCl. The mixture was sonicated and then evaporated at 50°C under a stream of dry air to remove HCl. To insure that the reaction was stopped, 400 μl of 6 *M* HCl was added, the mixture sonicated and evaporated.

2.3. Hydrolysis of treated glycoprotein and controls

Approximately 1.0 ml of 6 *M* HCl was mixed with the sample and the mixture sonicated. From the solution 190-μl aliquots were removed, evacuated and sealed to exclude oxygen for the solution. The vials were heated at 105°C for the indicated amount of time, 48 h in the standard protocol. Evaporation of the HCl solution from the cooled sample was followed by a 750-μl wash and evaporation to ensure removal of HCl. The residue was dissolved in 150 μl of water and filtered through a 0.22-μm filter.

2.4. Amino acid derivatization

The sample derivatization procedure used was a modification of that given by Lunte and Wong [14]. For derivatization of sample hydrolyzates, the indicated volume of sample, 10 μl in the standard protocol, was added to 5 μl of 10 m*M* NaOH. Next, 40 μl of 5 m*M* NaCN followed by 40 μl of 5 m*M* NDA in acetonitrile were added and mixed vigorously. The appearance of a fluorescent yellow-green color within a few minutes indicated that the reaction is proceeding. After the indicated amount of time, 1.25 h in the standard protocol, the sample was injected into the CE system.

Standard solutions of amino acids were derivatized in a similar manner. To 20 μl of 20 m*M* sodium borate (pH 9.0) were added 10 μl of a stock amino acid mixture. The mixture contained 0.56 m*M* of each amino acid. Addition of NaCN and NDA solutions were as above and the sample injected 1.25 h later.

2.5. Capillary electrophoresis

The instrument used in this work was an ISCO Model 3140 capillary electropherograph. Uncoated fused-silica columns of 100 cm (75 cm to window) × 50 μm I.D. were employed. The buffer composition in the columns and reservoirs was 20 m*M* sodium borate (pH 9.0). Operating voltage as 30 kV. These conditions are similar to those employed previously [13] for amino acid analysis. Although CBI derivatives exhibit an absorption maximum in the visible range at 420 nm, we found the 254 nm wavelength used for detection in these studies provided greater sensitivity. Samples were vacuum injected for 15 k Pa·s. The column was flushed after every run for 5 min with running buffer and after a maximum of six runs for 3 min each with 0.1 *M* NaOH, then water, then buffer.

Micellar electrokinetic capillary chromatography (MECC), used in the determination of the absolute amount of threonine, was run under identical conditions except that a 50 m*M* sodium dodecyl sulfate in 20 m*M* sodium borate (pH 9.0) buffer was used [15].

The electropherograph was interfaced with an IBM-compatible personal computer and output from the electropherograph was collected and analyzed using ICE software (ISCO).

3. Results and discussion

This method consists of four separate steps. These are: (1) treatment of the glycoprotein with alkaline sulfite to cause β-elimination and subsequent generation of sulfonates (Fig. 1), (2) hydrolysis of the treated glycoprotein, (3) derivatization of the released amino acids (Fig. 2) and (4) CE of the amino acid derivatives.

Optimization of the conditions used in steps 1, 2 and 3 were undertaken using mucin. Separation parameters for step 4 had been optimized previously by Weber et al. [13] and were used as described.

Finally, the method was applied to the analysis of bovine submaxillary mucin. This compound was chosen since it is a glycoprotein with a simple amino acid composition and a high percentage of serines and threonines O-linked to oligosaccharides.

3.1. Optimization of derivatization time (step 3)

Initial studies involved determination of the optimum reaction time for the derivatization procedure. A previous report [15] indicated that a minimum of 20 min is required. Observations in our laboratories indicated that amino acids with negatively charged side chains require additional time for derivatization especially if reagent is not present in large excess. Therefore, solutions obtained from the hydrolysis of an alkaline sulfite treated mucin sample were derivatized and allowed to react various lengths of time from 0.75 to 1.5 h before injection onto the CE system. Though the electropherograms displayed a broader mixture of amino acids, only serine, threonine, CA and ASBA were investigated, since these were the key amino acids for linkage analysis. Glycine in the mixture was also analyzed. It serves as a reference point to which the other four amino acids can be compared since it reacts quickly and the resulting derivative is quite stable. The height of each amino acid was measured and a plot peak height relative to glycine versus reaction time was made (Fig. 3). A reaction time of 1.25 h produces the greatest yield of CBI derivative and was thus chosen as the reaction time to be used for subsequent derivatizations. Note that the yield of the cysteic acid derivative is particularly sensitive to reaction time.

3.2. Hydrolysis time (step 2)

Since proteins vary dramatically in their resistance to acid-catalyzed hydrolysis and since the resultant amino acids also exhibit varying degrees of stability under the hydrolytic conditions, a detailed study was undertaken to see the effect of time of hydrolysis on the recovery of amino acids for both alkaline-sulfite treated (for 24 h) mucin and control mucin. The peak height of each amino acid relative to that of glycine was determined by CE following derivatization.

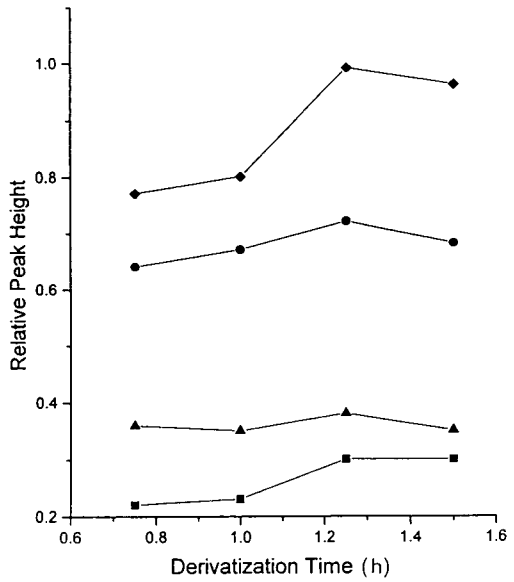

Fig. 3. Effect of derivatization time on the relative peak heights of amino acids in CE. Sample from mucin reacted with alkaline sulfite, hydrolyzed, derivatized and analyzed by CE as described in text. ● = Thr + Val; ▲ = Ser; ■ = ASBA; ◆ = CA.

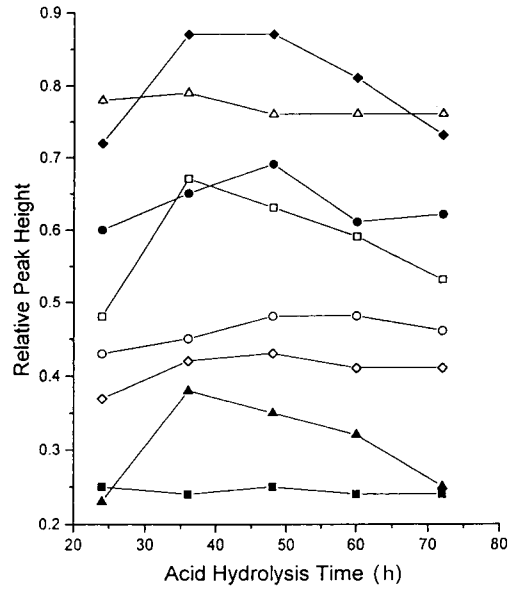

Fig. 4. Effect of acid-catalyzed hydrolysis time on the relative peak heights of amino acids in CE. Sample mucin reacted with alkaline sulfite, hydrolyzed, derivatized and analyzed by CE as described in text. □ = Thr + Val; ○ = Ser; ▲ = ASBA; ◆ = CA; △ = Ala; ■ = IS; ● = Glu; ◇ = Asp.

Glycine in the mixture was chosen as a reference since it is relatively stable to acid hydrolysis. Fig. 4 shows the effect of hydrolysis time on relative peak heights. Generally speaking, most amino acids exhibited an optimum recovery when treated for 48 h, although in the treated mucin samples, threonine, alanine and ASBA showed just slightly higher recoveries at 36 h. Thus, 48 h seems to be the optimum time for acid hydrolysis and this time was used for the standard protocol in all subsequent analysis.

3.3. Alkaline sulfite reaction time (step 1)/ glycosylation percentage

Earlier work involving the alkaline-sulfite reaction reported conflicting times for this reaction [12,16,17]. In order to ascertain the appropriate reaction time, the amino acid recovery as a function of reaction time was studied. Samples of treated mucin and controls were reacted for 24, 36, 48 or 60 h and then analyzed by the standard protocol. A plot of amino acid peak height relative to that of glycine versus reaction time is shown in Fig. 5. In general, reaction time seems to have little affect on amino acid recovery. A notable exception appears to be the 24-h treatment which yields less CA and correspondingly more serine. This effect, which was reproducible, indicates that 24 h does not effectively convert all glycosylated serines to the sulfonate.

A more useful way of visualizing the data given in Fig. 5 is seen in Fig. 6. By using the appropriate response factors listed in Table 1 with the data from Fig. 5, one can determine the percentage of serine O-linked to oligosaccharide in samples at each reaction time. A different situation exists for threonine. In the borate buffer, threonine co-migrates with valine as a single peak. This is expected by CE theory since the amino acids are very close in size and shape [18]. However, in MECC, these amino acids are well separated [15] and MECC was performed on a sample by merely adding sodium dodecyl sulfate to the running buffer prior to analysis. Thus, by including the information provided by the MECC run, one can determine the per-

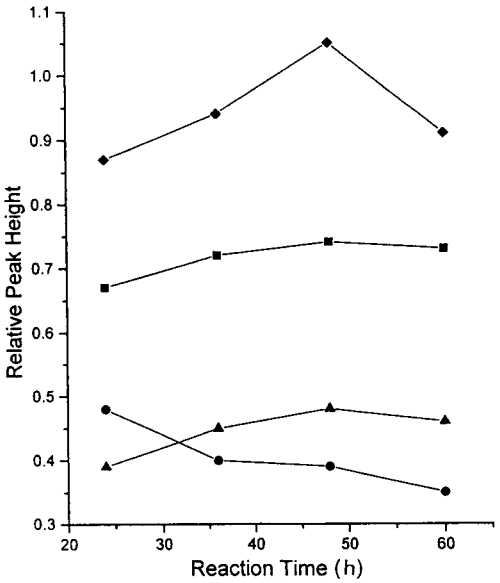

Fig. 5. Effect of alkaline sulfite reaction time on the relative peak heights of amino acids in CE. Sample mucin reacted with alkaline sulfite, hydrolyzed, derivatized and analyzed by CE as described in text. □ = Thr + Val; ○ = Ser; ▲ = ASBA; ◆ = CA.

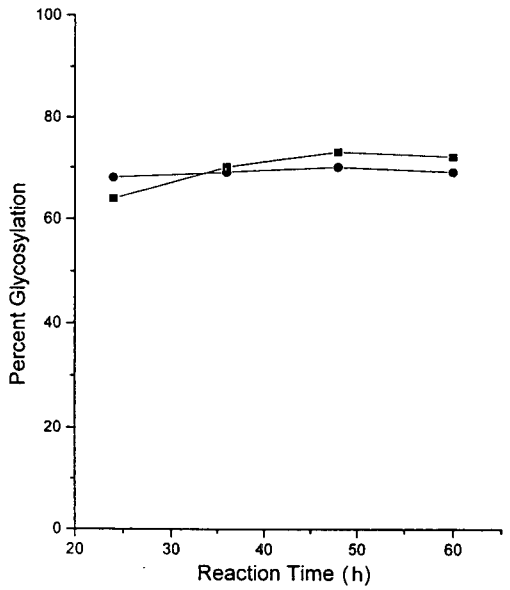

Fig. 6. Effect of alkaline sulfite reaction time on the percent glycosylation of serin and threonine in CE. Sample mucin reacted with alkaline sulfite, hydrolyzed, derivatized and analyzed by CE as described in text. ● = Thr; ■ = Ser. Percent glycosylation for Ser = [CA]/([CA] + [Ser]); Percent glycosylation for Thr = [ASBA]/([ASBA] + [Thr]).

centage of threonine O-linked to oligosaccharide in the same manner as done for serine. The 36-, 48- and 60-h reaction times give values close to each other, averaging 72% glycosylation for serine and 69% for threonine. This compares well to the values of 67% and 73% which we calculated from data reported for a core peptide of mucin [7].

3.4. Compositional analysis of mucin

A sample of bovine submaxillary mucin was subjected to the alkaline sulfite treatment, hydrolysis and derivatization. The mixture was separated by CE to give the electropherogram in Fig. 7B. Note the excellent resolution obtained in less than 20 min. When this electropherogram is compared to a control sample of mucin (Fig. 7A), the appearance of two new sulfonate peaks (migration times 15.7 and 16.8 min) and the corresponding reduction in the threonine and serine peaks (migration times 9.7 and 9.9 min) is noted.

Table 1
Response factors for selected amino acids and composition of bovine submaxillary mucin before and after alkaline sulfite treatment

Amino acid[a]	Response factors[b]	Untreated[c]	Treated[c]	Literature[d]
"Thr"	1.02	0.46	0.33	0.58
Ser	1.01	0.49	0.16	0.54
Ala	0.90	0.36	0.37	0.34
Gly	0.92	0.47	0.49	0.49
IS	1	–	–	–
Glu	1.06	0.27	0.27	0.18
ASBA	1.05	–	0.20	–
Asp	1.03	0.18	0.18	0.07
CA	1.01	–	0.41	–

[a] IS = Internal standard, α-aminoadipic acid; ASBA = α-amino-β-sulfobutyric acid; CA = cysteic acid, "Thr" = threonine and valine which coelute.
[b] Determined using relative peak heights.
[c] Micromole/milligram protein.
[d] Relative values reported by Pigman and Moschera [7].
Conditions as in Fig. 7.

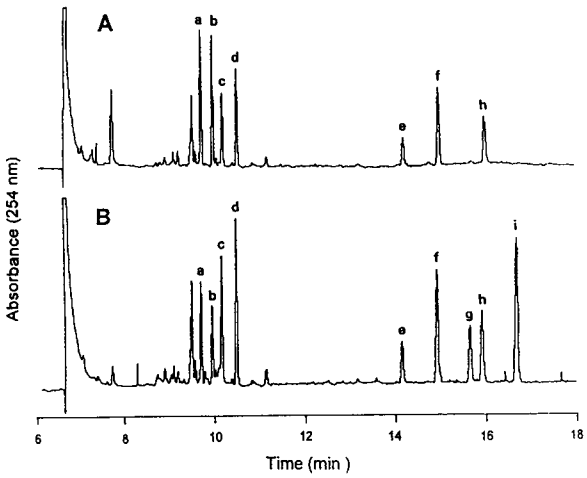

Fig. 7. Electropherogram of NDA-derivatized amino acids obtained from the hydrolysis of untreated (A) and alkaline sulfite treated (B) mucin. CE Conditions: 100 cm (effective length, 75 cm) × 50 μm I.D.; applied voltage, 300 V/cm; detection at 254 nm, 0.002 AUFS, 20 m*M* sodium borate buffer (pH 9.0). Peaks: a = Thr and Val; b = Ser; c = Ala; d = Gly; e = IS; f = Glu; g = ASBA; h = Asp; i = CA.

A solution containing equimolar amounts of eight amino acids found in alkaline sulfite-treated mucin samples and the internal standard was derivatized and separated by CE. This permitted determination of response factors used for the quantitation of amino acids in glycoprotein samples (Table 1). The mixture contains the sulfonated amino acids, CA and ASBA, that would be generated from serine and threonine respectively O-linked to oligosaccharides. Since ASBA is not commercially available, its constitutional isomer, homocysteic acid (HCA), was used instead. This substitution seems acceptable since the migration time of the two should be virtually identical according to CE theory and experimental results reported by Weber and Vaught [18]. Also, peak response factors should be nearly the same since the CBI moiety is the primary chromophore.

Also given in Table 1 is the amino acid composition of both treated and control mucin. Comparison of the amino acid composition for the mucin to reported values [7] shows good agreement except that the amounts of glutamate and aspartate are significantly higher. This could be due to decarboxylation of these amino acids or incomplete deamidation of asparagine and glutamine during hydrolysis in the cited work.

Five consecutive injections of a treated mucin sample gave relative standard deviations from 2 to 5% for the amino acids listed in Table 1.

4. Conclusions

The alkaline sulfite treatment of a glycoprotein, followed by hydrolysis, derivatization and analysis by CE represents a useful alternative to the current methods employed for the determination of O-linked serine and threonine residues. Optimization of procedural conditions yield results comparable to literature values. CE offers a number of advantages over methods which utilize liquid chromatography such as low volume requirements and easy sample preparation. Since limits of detection for the derivatization method had previously been reported [13], this was not studied. However, the procedure could easily be scaled down yielding smaller volumes for CE analysis. Also, the use of a laser-induced fluorescence detector for detection of CBI derivatives [19] would further increase sensitivity.

Acknowledgements

The authors wish to thank Nancy Harmony for her help in preparation of this manuscript. We would also like to thank ISCO, Inc. for the CE system used in this study and Dionex Corp. for financial support.

References

[1] A.J. Mort and D.T.A. Lamport, *Anal. Biochem.*, 82 (1977) 289–309.
[2] S. Hefta and J.E. Shively, in A.L. Burlingame and J.A. McCloskey (Editors), *Biological Mass Spectrometry*, Elsevier, Amsterdam, 1990, pp. 259–284.
[3] M.W. Spellman, *Anal. Chem.*, 62 (1990) 1714–1722.

[4] K. Schmid, M.A. Hediger, R. Brossmer, J.H. Collins, H. Haupt, T. Marti, G.D. Offner, J. Schaller, K. Takagaki, M.T. Walsh, H.G. Schwick, F.S. Rosen and E. Remold-O'Donnell, *Proc. Natl. Acad. Sci. U.S.A.*, 89 (1992) 663–667.
[5] H. Nakada, M. Inoue, Y. Numata, N. Tanaka, I. Funakoshi, S. Fukui, A. Mellors and I. Yamashina, *Proc. Natl. Acad. Sci. U.S.A.*, 90 (1993) 2495–2499.
[6] K. Hsi, L. Chen, D.H. Hawke, L.R. Zieske and P. Yuan, *Anal. Biochem.*, 198 (1991) 238–245.
[7] W. Pigman and J. Moschera, in R.F. Gould (Editor), *Carbohydrates in Solution*, American Chemical Society, Washington, DC, 1973, pp. 220–241.
[8] H. Devaraj, J.W. Griffith, M. Sheykhnazari, B. Naziruddin, G.P. Sachdev and V.P. Bhavanandan, *Arch. Biochem. Biophys.*, 302 (1993) 285–293.
[9] M. Kobayashi, J. Ban, T. Asano, M. Utsunomiya, S. Kusumoto, K. Nishi and K. Kato, *FEBS Lett.*, 302 (1992) 129–132.
[10] A. Kobata and K. Furukawa, in H.J. Allan and E.C. Kisailus (Editors), *Glycoconjugates*, Marcel Dekker, New York, 1992, pp. 33–69.
[11] S. Harbon, G. Herman and H. Clauser, *Eur. J. Biochem.*, 4 (1968) 265–272.
[12] Y. Endo and A. Kobata, *J. Biochem.*, 80 (1976) 1–8.
[13] P.L. Weber, T.J. O'Shea and S.M. Lunte, *J. Pharm. Biomed. Anal.*, 12 (1994) 319–324.
[14] S. Lunte and O. Wong, *Current Separ.*, 10 (1990) 19–26.
[15] P.L. Weber and D.R. Buck, *J. Chem. Educ.*, 71 (1994) 609–612.
[16] T. Arima, M.J. Spiro and R.G. Spiro, *J. Biol. Chem.*, 247 (1972) 1825–1835.
[17] R.G. Spiro and V.D. Bhoyroo, *J. Biol. Chem.*, 249 (1974) 5704–5717.
[18] P.L. Weber and R.N. Vaught, presented at the *5th International Symposium on High Performance Capillary Electrophoresis, Orlando, FL, 1993*, poster M507.
[19] T. Ueda, R. Mitchell, F. Kitamura, T. Metcalf, T. Kuwana and A. Nakamoto, *J. Chromatogr.*, 593 (1992) 265–274.

ELSEVIER

Journal of Chromatography A, 680 (1994) 233–241

JOURNAL OF CHROMATOGRAPHY A

Separation and analysis of cyclodextrins by capillary electrophoresis with dynamic fluorescence labelling and detection

Sharron G. Penn[b], Rick W. Chiu[a], Curtis A. Monnig[a,*]

[a]*Department of Chemistry, University of California, Riverside, CA 92521-0403, USA*

[b]*Department of Chemistry, University of York, Heslington, York YO1 5DD, UK*

Abstract

Mixtures of α-, β- and γ-cyclodextrins were complexed with 2-anilinonaphthalene-6-sulfonic acid (2,6-ANS) and separated by capillary electrophoresis. The enhanced fluorescence emission of 2,6-ANS when complexed with the cyclodextrins allowed isolated zones to be visualized. Detection limits for α-, β- and γ-cyclodextrin were determined to be 62, 2.4, and 24 μM, respectively. Enhanced resolution of cyclodextrin mixtures could be obtained by adjusting the concentration of ANS in the running buffer or by suppressing the electroosmotic flow. Components in 2,6-di-O-methyl-β-cyclodextrin with differing degrees of substitution were separated by this technique and compared with electrospray mass spectra of the same mixture.

1. Introduction

Cyclodextrins (CDs) are toroidally shaped polysaccharides formed from 6, 7 and 8 glucopyranose units for the α, β and γ species, respectively [1]. The interior of the torus is an electron rich, hydrophobic environment while the exterior contains many sites capable of hydrophilic interactions. CDs are used to increase the solubility and bioavailability of hydrophobic pharmaceuticals in aqueous solutions [2,3], and as selectivity reagents for the resolution of structural, positional and stereo isomers in the separation sciences [4–6].

CDs are difficult to analyze as they are uncharged and demonstrate no appreciable UV–Vis absorbance. Furthermore, the reactivity of these compounds is such that they are not easily labelled with a visualizing agent. Methods previously used for the analysis of CD mixtures include thin-layer chromatography [7], high-performance liquid chromatography (HPLC) [8–11] and capillary electrophoresis (CE) [12]. The chromatographic methods typically suffer from poor sensitivity, long analysis times and poor resolution. Electrophoretic separation methods would not normally be considered for separating CDs as the molecules are uncharged except at very high pH. However, Nardi et al. [12] were able to separate mixtures of native cyclodextrins by CE when the CDs were complexed with the benzoate ion. The benzoate anion also served as a means of visualizing the complex via indirect UV absorbance detection. Although this pro-

* Corresponding author.

0021-9673/94/$07.00
SSDI 0021-9673(94)00605-9

cedure was able to fully resolve α-, β- and γ-CD, the resolution was not sufficient to separate more complex mixtures, and the quantity of analyte required for detection was relatively high.

To improve the sensitivity and separating power of the cyclodextrin analysis, improved methods for mobilizing and visualizing these molecules must be employed. One promising method for detecting CDs is to employ a fluorescent probe. CDs are known to dramatically alter the fluorescence quantum efficiency of many fluorophores which form an inclusion complex [13]. This phenomenon has been recently exploited for detection of CDs by HPLC [14]. Steady state fluorescence and anisotropy measurements have been used to determine the binding constant (K) for β-CD and several isomers of anilinonaphthalenesulfonates (ANS) under varying pH and temperature conditions [15]. Of the fluorophores studied, 2-anilinonaphthalene-6-sulfonic acid (2,6-ANS) consistently provided the highest binding constant, 1860 M^{-1} at pH 11.0, and so was judged best for the studies described here. In this work, we exploit the properties of host–guest complexes of CDs and 2,6-ANS to develop a more sensitive means of separating and observing mixtures of CDs by CE.

2. Experimental

2.1. Instrumentation

Fluorescence excitation and emission spectra were acquired using a multifrequency cross-correlation phase and modulation spectrofluorometer (Model K2, ISS, Champaign, IL, USA) with a 300-W Xe arc excitation source. The monochromators on this instrument were adjusted so that both excitation and emission signals had a spectral bandpass of 4 nm. All spectra were collected in the DC excitation and emission mode.

The CE apparatus was constructed from components. A regulated high-voltage DC power supply (Model EH50R02, Glassman High Voltage, White House Station, NJ, USA) operated at 30 kV was used to drive the electrophoretic separation. A platinum wire electrode approximately 6 cm in length was used to establish electrical contact between the high-voltage supply and a 1.5-ml inlet buffer reservoir. The inlet reservoir and high-voltage end of the capillary were enclosed in a Plexiglass box to minimize arcing and to protect the operator from accidental shock. All separations were carried out in a fused-silica capillary (Polymicro Technologies, Phoenix, AZ, USA) of 50 μm I.D., 360 μm O.D., and approximately 1 m in length. The outlet buffer reservoir was grounded through a 1-MΩ resistor to allow the current passing through the capillary to be monitored with a voltmeter.

Fluorescence excitation was performed with an argon ion laser (Innova 90-5, Coherent, Palo Alto, CA, USA) operating at 363.8 nm. To minimize fluctuations in the signal, the intensity of the laser beam was actively regulated with a laser stabilization accessory (Model 50SA, LiCONiX, Santa Clara, CA, USA). An excitation beam of approximately 14 mW was focused with a fused-silica lens (focal length 100 mm, Newport Research Corporation, Irvine, CA, USA) into a region of the separation capillary with the polyimide coating removed. The resulting fluorescence emission signal was collected and imaged on the entrance slit of a double monochromator (Model DH-10, Instruments SA, Edison, NJ, USA) with a microscope objective (15×, Oriel, Stratford, CT, USA). The spectrometer was adjusted to provide a spectral bandpass of 8 nm centered at 424 nm. Output from the photomultiplier tube (Model R1527-03, Hamamatsu, Bridgewater, NJ, USA) was amplified with a current-to-voltage amplifier (Model 428, Keithley Instruments, Cleveland, OH, USA). For these studies, the photomultiplier tube was biased at −700 V and the amplifier gain maintained at $1 \cdot 10^5$ V A^{-1} with a time constant of 300 ms. An Objective C program running on a NeXTCube computer (NeXT Computer, Redwood City, CA, USA) monitored the output from the current amplifier with a 16-bit analog-to-digital converter (Model XL-1900 mainframe with XL-ADC2 ADC, Elexor Associates, Morris Plains, NJ, USA) which digitized the signal at 7

Hz. The column efficiency, theoretical plates, retention time, peak areas, etc. were determined by a program which calculated statistical moments for these data [16].

Electrospray spectra were acquired with a quadrupole mass spectrometer configured with an electrospray interface (Model 201 mass filter with options ES and E2000, Vestec, Houston, TX, USA). The quadrupole mass analyzer was controlled and data recorded by a dedicated processor (Model 900 DSP, Teknivent, Maryland Heights, MO, USA) monitored by a 80486-based computer running commercial software (Vector/Two version 1.4, Teknivent).

Samples solutions were introduced into the electrospray interface by means of a syringe pump (Model 341B, Sage Instruments, Boston, MA, USA) at a flow-rate of 1.4 μl min^{-1}. The electrospray needle was held between 2 and 3 kV for all analyses. The electrospray voltage, distance between the needle and the first skimmer cone, and sample flow-rate were adjusted to achieve a stable spray current of approximately 0.2 μA. Instrument operating temperatures were maintained at the following values for all analyses; spray chamber 50°C, ion lenses 150°C, block 250°C. The repeller voltage was 20 V and the pressure in the analyzer $5 \cdot 10^{-6}$ Torr (1 Torr = $1.3 \cdot 10^{2}$ Pa). Calibration of the mass analyzer was performed while sequentially aspirating solutions of poly(ethylene glycol) with average molecular masses of 400, 900, and 1500 u.

2.2. Reagents and materials

Chemicals and reagents were purchased from the following sources and used without further purification: α-CD, Sigma (St. Louis, MO, USA); 2,6-ANS, Molecular Probes (Eugene, OR, USA); anhydrous disodium hydrogen phosphate, methanol and sodium hydroxide, Fisher Scientific (Pittsburgh, PA, USA); tetrabutylammonium bromide (TBAB), β-CD, γ-CD and heptakis (2,6-di-O-methyl)-β-CD (DM-β-CD), Aldrich (Milwaukee, WI, USA). The DM-β-CD was specified to contain 30% of the 2-6-di-O-methyl substituent by plasma desorption mass spectrometry with the remainder primarily higher and lower O-methyl homologues.

2.3. Procedures

At the start of each day, the capillary was sequentially rinsed with 1 *M* sodium hydroxide, de-ionized water and the running buffer. Buffer solutions were prepared from a 100 m*M* solution of sodium phosphate adjusted to pH 12 with 1 *M* sodium hydroxide. This solution was diluted with deionized water to produce a 30 m*M* buffer. Benzoic acid buffers were prepared from sodium benzoate adjusted with 5 *M* hydrochloric acid to pH 4.0. Just prior to analysis, 2,6-ANS was added to these buffers to produce the stated concentration of fluorophore.

In the initial investigation of 2,6-ANS as a mobile phase additive for CE, it was observed that the inlet buffer reservoir became visibly discolored after a limited exposure to electrophoretic conditions (typically 5 analyses). The fluorescence background signal monitored at the detector increased proportionally with this discoloration and was dramatically reduced when the buffer in the inlet reservoir was replaced with a fresh solution of 2,6-ANS. This reaction only occurred when voltage was applied to the inlet buffer reservoir, so it was inferred that the 2,6-ANS molecule was being electrochemically altered. A reaction consistent with these observations and known chemical properties of the molecule would be the oxidation of 2,6-ANS to form an imine. To minimize the generation of interfering species, the electrode area available for reaction was reduced by covering all but the end of the electrode with a PTFE sleeve. The production of the interfering species was greatly inhibited and more than 20 separations could be performed without significant hindrance from the electrochemical reaction product.

3. Results and discussion

3.1. Anilinonaphthalenesulfonate fluorescence measurements

Fig. 1 shows the steady-state excitation and emission spectra for 2,6-ANS ($6.7 \cdot 10^{-6}$ *M*) in distilled water, and in solutions saturated with α-CD (0.15 *M*), β-CD (0.016 *M*), and γ-CD

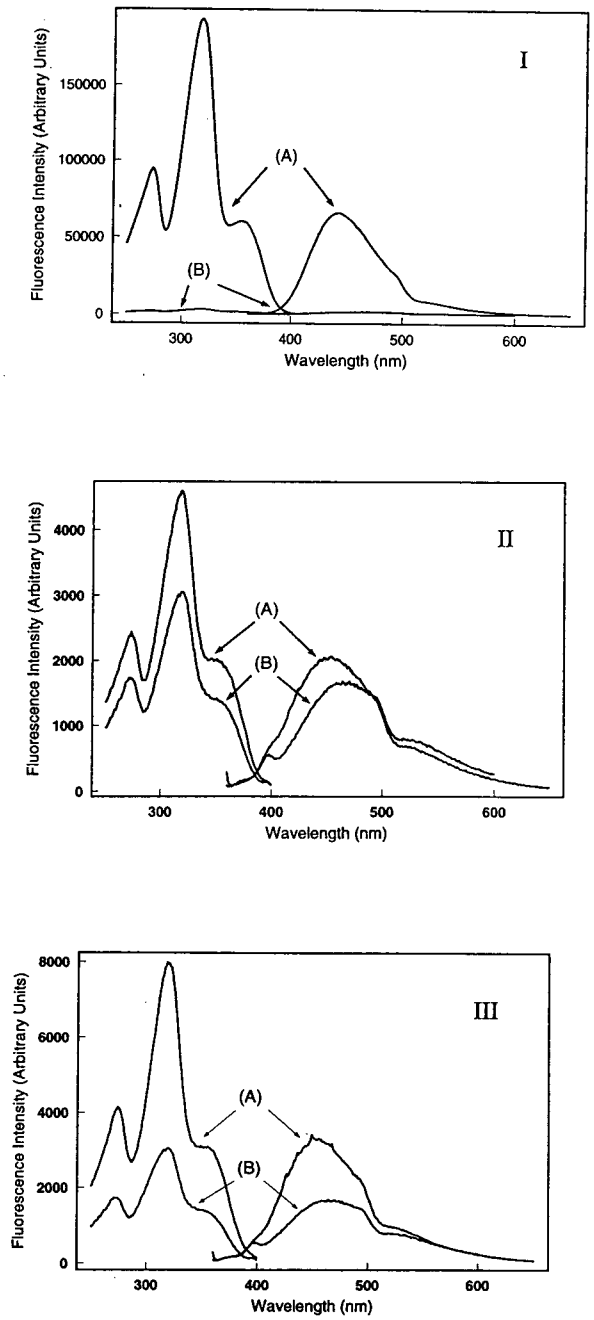

Fig. 1. Fluorescence excitation and emission spectra for $6.7 \cdot 10^{-6}$ M 2,6-ANS. A is the spectrum in a solution saturated with CD, B is the spectrum in distilled water. Figs. I, II and III correspond to β-CD (0.016 M), α-CD (0.15 M), and γ-CD (0.18 M) respectively. All excitation spectra were monitored at 460 nm and emission spectra were excited at 351 nm.

(0.18 M). From these spectra, it is clear that the uncomplexed 2,6-ANS demonstrates a fluorescence signal which is enhanced in the presence of the CDs. For all CDs studied, when an inclusion complex is formed, the fluorescence excitation spectrum remains virtually unchanged but a significant shift to shorter wavelengths is observed in the emission signal. In addition to the shift in the wavelength of maximum fluorescence emission, the CD–2,6-ANS host–guest complex produces a large change in fluorescence emission intensity. This enhancement is as much as a factor of 55 at 422 nm for β-CD, but α- and γ-CD also significantly enhance the fluorescence signal of 2,6-ANS when complexed. Of the CDs investigated, (α-, β-, γ-, hydroxypropyl-β-, methyl-β-, and DM-β-CD), the derivatized β-CDs were found to provide the largest enhancement of fluorescence emission. The fluorescence emission signal for 2,6-ANS complexed with DM-β-CD increased by a factor of 245 at 426 nm. The maximum excitation and emission wavelengths as well as fluorescence enhancement factors are summarized in Table 1. For the work described here, all fluorescence emission measurements were made at 424 nm which was found to give close to maximum enhancement for all the CDs studied.

3.2. Separation of native cyclodextrins

Not only does the 2,6-ANS molecule allow the CDs to be visualized, it also imparts a charge to this otherwise neutral molecule to allow separation in an electric field in much the same way that benzoate was previously used [12]. Fig. 2 shows the molecular species and relative mobilities of these species in the capillary. The uncomplexed CD has no net charge under all but strongly basic conditions [17] and so migrates at the velocity of the electroosmotic flow. The 2,6-ANS molecule and the complex are negatively charged. Since the size of the complex is greater than that of 2,6-ANS, the magnitude of the electrophoretic mobility $|\mu|$ will be lower, as indicated by the relative size of the vectors in Fig. 2. The electroosmotic flow, with mobility

Table 1
Fluorescence signal properties for cyclodextrin–2,6-ANS complexes

	λ^{ex}_{max} (nm)	λ^{em}_{max} (nm)	Fluorescence emission enhancement
Uncomplexed 2,6-ANS	318	464	–
α-CD–2,6-ANS	318	452	1.8 (416 nm)
β-CD–2,6-ANS	317	441	55 (422 nm)
γ-CD–2,6-ANS	318	454	2.3 (426 nm)
Heptakis (2,6-di-O-methyl)-β-CD–2,6-ANS	317	437	245 (426 nm)

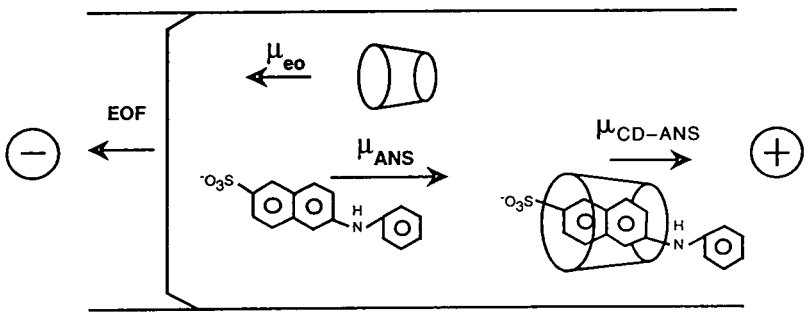

Fig. 2. Schematic diagram showing mobilities of 2,6-ANS, CD and CD–2,6-ANS complex in a bare fused-silica capillary.

μ_{eo}, opposes the movement of 2,6-ANS and the CD–ANS inclusion complex.

Fig. 3 shows a representative separation of a mixture of α-, β-, and γ-CD at pH 12. The peak corresponding to neutral species appears at 6.6 min while those of the CDs appeared shortly thereafter. To account for these data we consider the equilibrium,

$$CD + ANS \leftrightarrows CD\text{–}ANS \quad (1)$$

The equilibrium constant for this reaction, K, is given by:

$$K = \frac{[CD\text{–}ANS]}{[CD][ANS]} \quad (2)$$

The similarity in size between the CD cavity and the fluorophore causes 2,6-ANS to form inclusion complexes with β-CD preferentially, but α- and γ-CD also form complexes to a lesser extent. In previous work, the equilibrium constants for

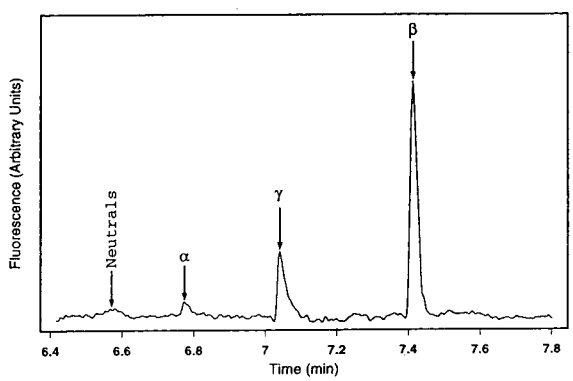

Fig. 3. CE separation of α-, β-, and γ-CD. Analysis buffer: 40 m*M* phosphate, pH 11.76, 1 m*M* 2,6-ANS. The analysis was carried out in a capillary of dimensions 50 μm I.D., 360 μm O.D., and 1 m in length in a field of 300 V cm^{-1}. The sample was introduced into the capillary by electrokinetic injection; 5 kV for 2 s from a sample containing 1.44 mg ml^{-1} α-CD, 0.017 mg ml^{-1} β-CD and 0.24 mg ml^{-1} γ-CD. Detection was by fluorescence excited at 363 nm and monitored at 424 nm.

most β-CD–ANS complexes have been found to show no significant sensitivity to solution pH [15]. From Fig. 3 it can be seen that $|\mu|$ for α-CD–2,6-ANS < γ-CD–2,6-ANS < β-CD–2,6-ANS. These results are consistent with those seen in Fig. 1, where the magnitude of the fluorescence enhancement per unit concentration of CD is observed to be α-CD–2,6-ANS < γ-CD–2,6-ANS < β-CD–2,6-ANS. These observed differences in mobility and fluorescence enhancement must in part be due to differences in the binding constants for CD–2,6-ANS. The mixture of CDs may therefore be separated by differences in the fraction of molecules which are complexed with 2,6-ANS. For β-CD–2,6-ANS, $K = 2 \cdot 10^3$ [15] and therefore in 1 m*M* 2,6-ANS Eq. 2 shows that a fraction 0.67 of the β-CD is complexed if buffer constituents do not interfere with the binding. Although binding constants for α- and γ-CD have not been measured, they are evidently less than that for β-CD and so the fractions complexed to 2,6-ANS will be less than for β-CD. Increasing the 2,6-ANS concentration in the running buffer improves the separation of the native CDs, but also increases the background fluorescence signal, making detection more difficult. In general, the optimum separation/detection conditions were when the minimum amount of 2,6-ANS necessary to achieve the desired separation was added to the analysis buffer.

To demonstrate the quantitative capabilities of this technique, solutions containing pure α-, β- and γ-CD were separated in a buffer containing 1.0 m*M* 2,6-ANS. Both peak height and peak area measurements provided a linear signal response over an extended range of concentration. A linear signal response was observed for β-CD over a concentration range from $5.2 \cdot 10^{-6}$ to $1.6 \cdot 10^{-3}$ *M*. The signals from α- and γ-CD increased linearly with concentration from $2.1 \cdot 10^{-4}$ to $6.3 \cdot 10^{-2}$ *M* and $1.8 \cdot 10^{-5}$ to $6. 1 \cdot 10^{-3}$ *M*, respectively. From these data, the detection limits (signal-to-noise of 3) are estimated to be 62, 2.4, and 24 m*M* for α-, β- and γ-CD, respectively. The limiting noise source in these measurements was fluctuations in the fluorescence background signal from the uncomplexed 2,6-ANS. The upper limits of detection were established either by the solubility of the CD or the non-linear increase in the concentration of the CD–2,6-ANS complex once a significant fraction of the CD was complexed.

3.3. Separation of derivatized cyclodextrins

To demonstrate the potential resolving power of this technique for the analysis of complex mixtures of CDs, a separation of DM-β-CD was performed. Derivatized CDs are usually a mixture of CDs with various degrees of substitution. These derivatized molecules are being investigated by the pharmaceutical industry as possible delivery complexes for very hydrophobic drugs [2] and so monitoring their chemical composition is a critical part of any toxicological study.

Initial attempts to separate DM-β-CD under the conditions used to separate α-, β- and γ-CD provided incomplete resolution of the molecules with different degrees of substitution. From these data and previous reports [12], it was clear that the dominant mobilization mechanism for the inclusion complexes was the electroosmotic flow in the capillary. This flow would not separate the different DM-β-CD species and overwhelmed the electrophoretic processes so that little separation was obtained. To increase the ratio of electrophoretic to electroosmotic mobility, two changes were made to the separation procedure. First, the separation was performed in a benzoate buffer (30 m*M*) which contained a small amount (1 m*M*) of 2,6-ANS. A previous investigation of the complexation of benzoic acid with the CDs suggests that electrophoretic mobility can be enhanced by increasing the concentration of complexing reagent [12]. The presence of this additional charged inclusion species increases the proportion of time the mobility of the CD is influenced by the electric field, without increasing the fluorescence background signal. Addition of benzoate to the buffer did enhance the separation but also interfered with the inclusion of 2,6-ANS, causing detection limits to suffer. This effect can be modeled as a competition between the benzoate anion and the 2,6-ANS for the CD cavity. Under

conditions where [benzoate] >> [2,6-ANS], as used here, binding of the 2,6-ANS will be given by,

$$K_{obs} = \frac{K_{ANS}}{1 + K_B[B]} \quad (3)$$

where K_{obs} is the observed binding constant, K_{ANS} the binding constant for 2,6-ANS, and K_B and [B] the binding constant and concentration of the competitor (the benzoate anion). Drawing from the analogy of chiral separation by CE, the concentration of the competitor can be optimized to provide maximum mobility difference while still providing adequate sensitivity [18]. Modeling of these interactions has found that the maximum mobility difference is found when the product of the binding constant and the concentration (K_{obs}[CD]) is unity. From previous work [12] it can be estimated that the binding constant K for the β-CD–benzoate complex is 50 M^{-1}. As previously mentioned, K_{ANS} for 2,6-ANS–β-CD is $2 \cdot 10^3$ M^{-1}, and the derivatised β-CDs have been inferred from fluorescence studies to have even stronger binding. By applying Eq. 3, K_{obs} in 30 mM benzoate is reduced by a factor of 2.5 in comparison with K_{ANS}, bringing K_{obs}[CD] closer to unity. This explains the action of the benzoate ion on improving the separation, as well as increasing the time the CD–2,6-ANS is influenced by the electric field.

The second method for improving the separation is to alter the analysis buffer to suppress the electroosmotic flow. Reduced electroosmosis increases the time required for the analysis but enhances resolution [19].

One means of suppressing electroosmotic flow in a fused-silica capillary is by the addition of organic solvents to the analysis buffer [20]. Similarly, the addition of small quantities of ammonium salts to the buffer can suppress or even reverse electroosmotic flow [21]. Both of these techniques were used to enhance the separation of DM-β-CD. Representative separations of DM-β-CD are shown in Fig. 4. In Fig. 4A, the separation is performed under conditions similar to those used for the separation in Fig. 3, where the elution time for the molecules

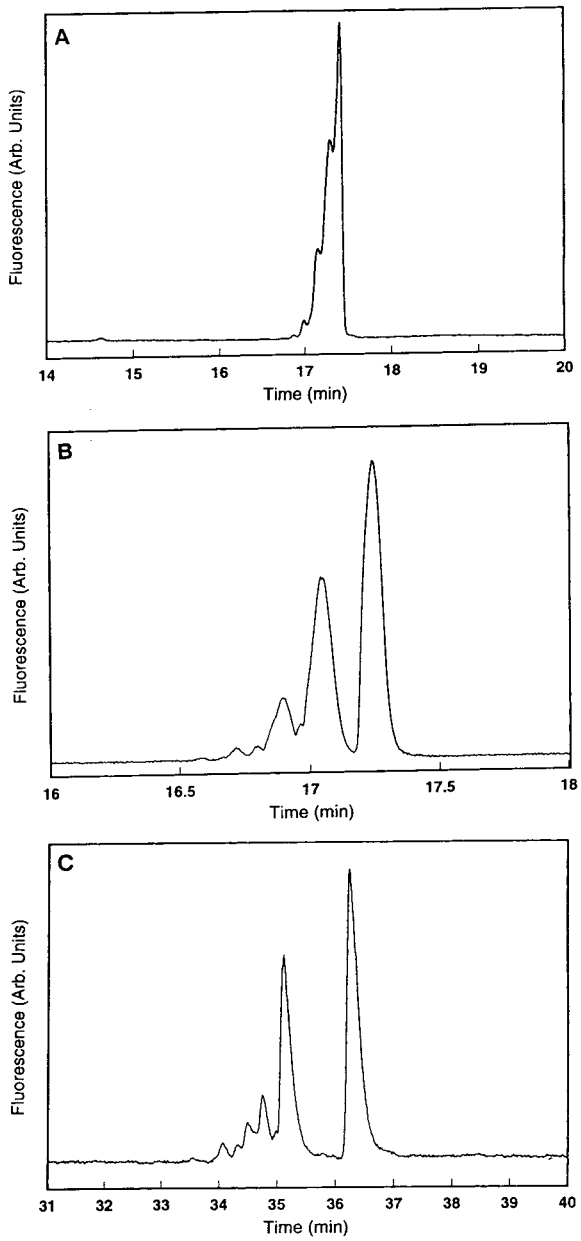

Fig. 4. CE separation of DM-β-CD. Analysis buffers: (A) 1 mM 2,6-ANS in 40 mM phosphate buffer (pH 11.76), (B) 1 mM 2,6-ANS in 30 mM benzoate (pH 8.0) with 20% methanol, (C) 40 μM TBAB and 1 mM 2,6-ANS in a pH 4.0 benzoate buffer (30 mM). The analysis was carried out in a capillary of dimensions 50 μm I.D., 360 O.D., and 1 m in length in a field of 300 V cm^{-1}. The sample was introduced into the capillary by electrokinetic injection; 5 kV for 2 s. Detection was by fluorescence excitation at 363 nm and monitored at 424 nm.

is 6.6 min. Although the electropherogram clearly indicates that the sample is heterogeneous, individual components are not resolved. In Fig. 4B, methanol is added to the running buffer to suppress electroosmosis and sodium benzoate added to enhance electrophoretic migration. A corresponding increase in resolution is observed. For this electropherogram, the time corresponding to the elution of neutral molecules is 14.8 min. Fig. 4C shows that addition of TBAB to the buffer further suppresses electroosmosis (elution time for neutral molecules is 26.9 min) and an additional increase in resolution is observed.

The identification of the species separated was attempted by comparing the separation with the electrospray ionization mass spectrum of DM-β-CD shown in Fig. 5. Three major components can be seen in both figures, with the intensity of the signals in the mass spectrum reversed from the trend in the electropherogram. In the mass spectrum, the charge is imparted to the homologues principally via a sodium adduct ion. The slight shoulder on the high mass side of the peaks is consistent with the formation of a potassium adduct. The three major peaks in the spectrum are assigned to be the β-CD (i) fully methylated on all the 2 and 6 positions of all 7 glucose subunits, (ii) the addition of an extra methyl group on species (i), (iii) the addition of 2 extra methyl groups on species (i). It is interesting to note that for species (i) and (ii) there are no geometric isomers, but for species (iii) there are 3 geometric isomers that have the same statistical weight. The mass spectrometer is *not* able to distinguish the geometric isomers of species (iii). The binding of the species (i), (ii) and (iii) with 2,6-ANS will differ, due to the possibility of steric interference of the extra methyl groups. A lower binding constant of a species in the electropherogram would lead to a shorter migration time. Therefore it is possible that the major peak at 36.4 min in Fig 4C is due to species (i), and the peak at 35.2 min to species (ii). The preceding peaks may all be due to species (iii), being a partial separation of the geometric isomers, to which the binding constant and hence the electrophoresis will be sensitive. This explanation is consistent with 30% of the mixture being the fully substituted 2,6-di-O-methylated-β-CD, species (i). Since in both the electropherogram and the mass spectrum, peak intensity is not necessarily a quantitative indication of the relative abundance of each chemical species, further work needs to be done to substantiate these arguments. The use of on-line CE–mass spectrometry [22] or fraction collection followed by mass spectrometry [23] could be used to conclusively determine whether the CE peaks were of single mass components. Even without this information, this CE separation could be used as a finger print method for the comparison of batch-to-batch and supplier-to-supplier variations in the derivatized CDs.

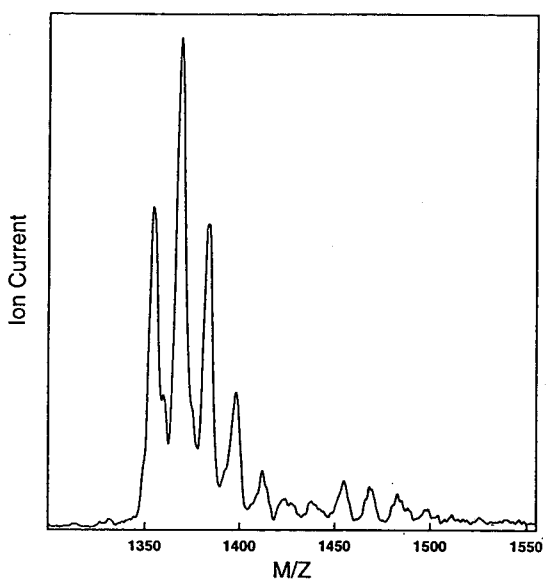

Fig. 5. Electrospray mass spectrum of DM-β-CD (1.2 mg ml^{-1}). Spray current: 0.2 μA. Solvent: 3% aqueous acetic acid–methanol (50:50). Approximately 1.6 μg of the DM-β-CD mixture was consumed for this analysis.

4. Conclusions

This work demonstrates the feasibility of analyzing complex mixtures of cyclodextrins by CE. Dynamic fluorescence labelling provides a simple, sensitive and selective means of monitoring the CD. The increase in fluorescence

associated with 2,6-ANS binding to β-CD allowed sensitive detection of β-CD, while α- and γ-CD demonstrated less of an enhancement and correspondingly higher detection limits. Although the instrument used in these studies employed a laser excitation source, equivalent sensitivity should be possible with less expensive arc-lamp fluorescence detectors as the detection limits are determined by the background fluorescence signal and not by shot noise or the detection electronics. Suppression of the electroosmotic flow increased the time required for the analysis but provided enhanced separation capabilities. Addition of organic modifiers and an ammonium salt allowed components of DM-β-CD with differing degrees of substitution to be separated. Further suppression of the electroosmotic flow with coated capillaries [24,25] or the application of a radial electric field [26,27] should further enhance the separation capability of this technique.

Acknowledgements

The authors would like to thank Dr. David M. Goodall, Dr. Frank V. Bright and Dr. Werner G. Kuhr for their helpful suggestions and comments and Michele Villegas for assistance with the acquisition of fluorescence excitation and emission spectra. Financial support was provided by the Arnold and Mabel Beckman Foundation, the University of California and the Science and Engineering Research Council (United Kingdom) through a CASE award (S.G.P.). Travel support for S.G.P. was provided by Pfizer Central Research.

References

[1] W. Saenger, *Angew. Chem. Int. Ed. Engl.*, 19 (1980) 344.
[2] F. Hirayama, *J. Pharm. Soc. Jpn.*, 113 (1993) 425.
[3] D. Ducheme and D. Wouessidjewe, *J. Coord. Chem.*, 27 (1992) 223.
[4] T.W. Ward and D.W. Armstrong, *J. Liq. Chromatogr.*, 8 (1986) 407.
[5] S. Fanali, *J. Chromatogr.*, 474 (1989) 441.
[6] W.L. Hinze, D.Y. Pharr, Z.S. Fu. and W.G. Burkert, *Anal. Chem.*, 61 (1989) 422.
[7] G. Vigh, I. Cruzado and Y. Rawjee, presented at *the Fourth International Symposium on HPCE, Amsterdam, 1992.*
[8] G. Liu, D.M. Goodall and J.S. Loran, *Chirality*, 5 (1993) 220.
[9] H.L. Jin, A.M. Stalcup and D.W. Armstrong, *J. Liq. Chromatogr.*, 11 (1988) 3295.
[10] K. Koizumi, Y. Kubota, Y. Okada and T. Utamara, *J. Chromatogr.*, 341 (1985) 31.
[11] T. Tacheuchi, M. Murayama and D. Ishii, *J. High Resolut. Chromatogr.*, 13 (1990) 69.
[12] A. Nardi, S. Fanali and F. Foret, *Electrophoresis*, 11 (1990) 774.
[13] R.P. Hangland, *Handbook of Fluorescent Probes and Research Chemicals*, Molecular Probes, Eugene, OR, 1985.
[14] H. Reeuwijk, H. Irth, U.R. Tjaden, F.W.H.M. Merkus and J. van der Greef, *J. Chromatogr.*, 614 (1993) 95.
[15] G. Catena and F.V. Bright, *Anal. Chem.*, 61 (1989) 905.
[16] E. Grushka, *Anal. Chem.*, 41 (1969) 889.
[17] D. Lee and M. Bunker, *J. Chromatogr. Sci.*, 27 (1989) 486.
[18] S.G. Penn, E.T. Bergström, D.M. Goodall and J.S. Loran, *Anal. Chem.*, (1994) in press.
[19] R.A. Wallingford, A.G. Ewing, *Adv. Chromatogr.*, 29 (1989) 1.
[20] C. Schwer and E. Kenndler, *Anal. Chem.*, 63 (1991) 1801.
[21] T. Tsuda, *J. High Resolut. Chromatogr. Chromatogr. Commun.*, 10 (1987) 622.
[22] R.D. Smith, J.H. Wahl, D.R. Goodlett and S.A. Hofstadler, *Anal. Chem.*, 65 (1993) 574A.
[23] J.A. Castoro, R.W. Chiu, C.A. Monnig and C.L. Wilkins, *J. Am. Chem. Soc.*, 114 (1992) 7571.
[24] M. Huang, W.P. Verkink and M.L. Lee, *J. Microcol. Sep.*, 4 (1992) 233.
[25] A. Malik, Z. Zhao and M.L. Lee, *J. Microcol. Sep.*, 5 (1993) 119.
[26] C.S. Lee, W.C. Blanchard and C.T. Wu, *Anal. Chem.*, 62 (1990) 1550.
[27] M.A. Hayes and A.G. Ewing, *Anal. Chem.*, 64 (1992) 512.

ELSEVIER

Journal of Chromatography A, 680 (1994) 243–246

JOURNAL OF CHROMATOGRAPHY A

Capillary zone electrophoretic determination of organic acids in cerebrospinal fluid from patients with central nervous system diseases

Atsushi Hiraoka*[,a], Junichiro Akai[a], Itaru Tominaga[b], Munekazu Hattori[b], Hideki Sasaki[c], Teruyo Arato[d]

[a]*Department of Mental Health, Kyorin University School of Health Sciences, Hachioji, Tokyo 192, Japan*
[b]*Department of Neuropsychiatry, Chiba National Hospital, Chiba, Chiba 260, Japan*
[c]*Nihon Milipore, Waters Chromatography Division, Shinagawa-ku, Tokyo 140, Japan*
[d]*Department of Biochemistry, Kyorin University School of Medicine, Mitaka, Tokyo 181, Japan*

Abstract

Organic acids in cerebrospinal fluid (CSF) from patients with various central nervous system (CNS) diseases were determined by capillary zone electrophoresis (CZE). Under one of the two sets of conditions employed, several anionic components of CSF were separated into corresponding peaks on the electropherograms and determined. The other conditions employed were also useful in measurement of the lactate contents in CSF. The CSF levels of lactate and pyruvate and the ratios of lactate to pyruvate were elevated in patients with cerebral infarction and bacterial meningitis, whereas CSF ascorbate was reduced mainly in inflammatory disorders of the CNS. The results showed that CZE can become a powerful tool in the biochemical diagnosis of CNS diseases.

1. Introduction

Cerebrospinal fluids (CSF) has been examined biochemically for the diagnosis of central nervous system (CNS) diseases. It is known from earlier studies that lactate (LA) is the most abundant among the organic acid components of CSF and that its concentrations are increased in cerebral infarction [1] and bacterial meningitis but not in viral meningitis [2–6]. Such changes in the CSF levels of LA were virtually independent of the serum levels of LA [7], and the CSF contents of LA and pyruvate (PA) were positively correlated with each other [8], indicating that the concentration ratios of LA to PA were greater in CSF with higher LA levels [9]. It is therefore generally accepted that increased LA concentrations in CSF, which are generally accompanied by elevated CSF LA/PA values, can reflect the pathological conditions of the CNS in association with tissue acidosis and/or anaerobic glycolysis caused by ischaemia or bacterial activity. The concentrations of these compounds in CSF have conventionally been measured mainly by high-performance liquid chromatography (HPLC) or enzymatic methods. However, capillary zone electrophoresis (CZE) is a simple and valuable system for the determination of a variety of ionized substances, such as low-molecular-mass cations [10], drugs [11–14], vitamins [15]

* Corresponding author.

0021-9673/94/$07.00
SSDI 0021-9673(94)00362-D

and sugar derivatives [16]. In this work, CZE was applied to the determination of CSF organic acids, including LA and PA, as an aid in neurological diagnosis.

2. Experimental

2.1. Subjects and samples

Forty CSF samples were taken by lumbar puncture from five cerebral infarction, two bacterial meningitis, two viral meningitis, one Guillain–Barré syndrome, three Parkinson's disease, two senile dementia, three multiple sclerosis, six epileptic, two schizophrenic, three depressive illness, five neurosis and six other micellaneous neuropsychiatric disorder patients (17 males and 23 females, 18–79 years old). All the samples were stored at −20°C for up to 2 weeks until analysed. Before the analyses, CSF samples were deproteinized by centrifuging ultrafiltration at 740 *g* for 30 min with Centricon-10 miniconcentrators (Grace Japan), and 20-μl portions each from the ultrafiltrates thus prepared were pipetted into sample vials of the two CZE instruments.

2.2. Conditions of CZE analyses

Two conditions, A and B, were established employing a Waters Quanta-4000 unit equipped with a negative power supply and a Beckman P/ACE 2000 unit, respectively. Under conditions A, samples to be examined, which were obtained from 28 patients, including two acute-phase cerebral infarction, one chronic-phase cerebral infarction, two bacterial meningitis, two viral meningitis, one Guillaine–Barré syndrome and two shizophrenic, were injected by hydrostatic loading for 60 s into a fused-silica capillary (60 cm × 75 μm I.D.), and separation was done at 20 kV using 50 m*M* sodium tetraborate (pH 9.2) containing 2.5% tetradecyltrimethylammonium bromide (TTAB) (Nihon Millipore) as the electrolyte. UV detection was performed at 185 nm and the data were processed with a Waters 825 Data Station. Under conditions B, samples from twelve patients, including two cerebral infarction, were injected by hydrostatic loading for 20 s into a capillary (50 cm × 75 μm I.D.), and separation was done at 20 kV using 100 m*M* borate buffer (pH 8.3) as the electrolyte. UV detection was performed at 200 nm. Under both conditions, the capillaries were conditioned at the start of each analysis by purging with 0.1 *M* potassium hydroxide solution for 1 min, deionized water for 1 min and the electrolytes for 2 min.

3. Results and discussion

A typical electropherogram obtained under conditions A is illustrated in Fig. 1. Several peaks in addition to a large peak of chloride (Cl) were detected on the electropherograms, and peaks with the migration times (t_M) of *ca.* 4.9, 5.2, 5.5, 5.8, 5.9, 6.3, 6.6 and 6.8 min were identified as oxalate, fumarate, inorganic phosphate, acetate, PA, LA, glutamate (Glu) and ascorbate (AsA), respectively, by mixed analyses with the authentic samples. Among these anions, oxalate, acetate and LA, and also two major inorganic anions (Cl and phosphate), were detected in all 28 samples examined, although fumarate, PA, Glu and AsA were detected only in 6, 22, 9 and 23 samples, respectively, out of the 28. In the experiments using standard samples with the concentrations of 1.56–800 μg/ml, the detection limits of these seven organic acids (including Glu) were in the range 1.56–3.12 μg/ml, and linear increases in the peak areas were

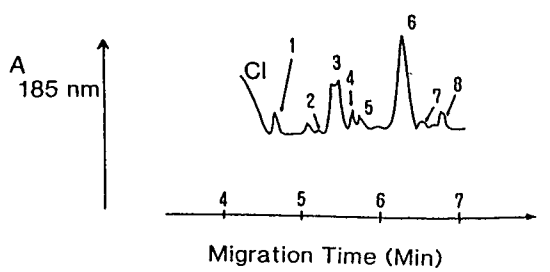

Fig. 1. Typical electropherogram obtained under conditions A. Cl = chloride; 1 = oxalate; 2 = fumarate; 3 = inorganic phosphate; 4 = acetate; 5 = pyruvate; 6 = lactate; 7 = glutamate; 8 = ascorbate.

also confirmed in the concentration ranges 0–800 μg/ml (LA) and 0–100 μg/ml (others). Therefore, the levels of these compounds in the CSF examined could be determined from the ratios of peak areas against the 100 μg/ml standard samples.

The mean ± standard deviation (S.D.) CSF LA concentration was 147.4 ± 83.7 μg/ml (n = 28), and the highest and lowest values were 475 and 66 μg/ml, respectively. Evaluated LA levels above 180 μg/ml were found only in CSF from two acute-phase cerebral infarction patients and two bacterial meningitis patients. All the other 24 CSF samples, including those from a chronic-phase cerebral infarction patient and two viral meningitis patients, had LA concentrations within the range 66–173 μg/ml. The mean ±S.D. CSF PA level (the value for six samples in which this compound was not detected were taken as 0 μg/ml) was 4.1 ± 2.8 μg/ml (n = 28), and the highest value (12.2 μg/ml) observed in a bacterial meningitis patient was associated with the highest level of CSF LA mentioned above.

In 22 CSF samples in which PA was detected, a positive correlation (r = 0.72) was observed between the levels of PA and LA. The mean ±S.D. LA/PA value in above-described four CSF samples with elevated LA levels of 180–475 μg/ml was 36.8 ± 4.4 μg/ml (n = 4), which was significantly greater ($p < 0.05$) than that in other samples (28.0 ± 3.3 μg/ml, n = 18) with non-raised LA levels of 66–173 μg/ml and detectable amounts of PA.

All of these trends in pathological changes in the CSF levels of LA and Pa agreed with those reported by earlier workers who examined CSF by HPLC or enzymatic methods [1–9] (see Introduction). The mean ±S.D. CSF AsA concentration (a value obtained in the same manner as for PA) was 5.2 ± 2.9 μg/ml (n = 28). This compound was not detected in five CSF samples, three of which were taken from patients with inflammatory disorders of the CNS (bacteral meningitis, viral meningitis and Guillain–Barré syndrome). This trend was in agreement with that revealed by our previous work employing HPLC, in which we demonstrated that the relative AsA concentrations in CSF to serum were reduced in various CNS diseases, especially in such inflammatory disorders [17].

Glu was detected in nine CSF samples out of the 28 examined. Kim *et al.* [18] reported that Glu decreased in CSF of patients with schizophrenia, although in CSF samples from two schizophrenic patients treated in this study (see Section 2.1) this compound was detected, suggesting that there is no decrease in its level in CSF in schizophrenia. Virtually no diagnostic value for other CSF organic acids detected by this system was found owing to the small amounts present.

A typical electropherogram obtained under conditions B is illustrated in Fig. 2. Several peaks were detected on the electropherograms, and those with $t_M \approx 4.5$ and 8.8 min were identified as glutamine (Gln) and LA, respectively. Under these conditions, peaks of organic acids other than LA, which were detected and identified under conditions A (Fig. 1), were not so separated well enough for these CSF minor organic acids to be determined. However, the concentrations of LA in twelve CSF samples examined were measured, and the results were essentially the same as those for the other 28 samples examined under conditions A, as the mean ±S.D. CSF LA level in these twelve samples was 112.9 ± 58.6 μg/ml (n = 12) and levels above 180 μg/ml (the highest was 224 μg/ml) were detected only in two cerebral infarction patients.

It was also noteworthy that only under these conditions peaks of Gln, which is a neutral amino acid, and LA, which is an organic acid, appeared on the same electropherograms. The cause of this difference in the electropherogram

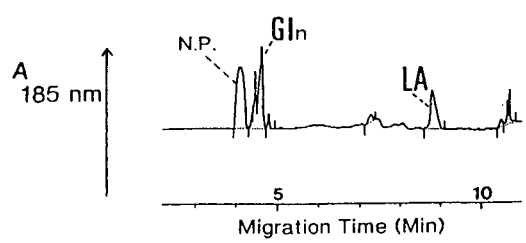

Fig. 2. Typical electropherogram obtained under conditions B. N.P. = neutral peak; Gln = glutamine; LA = lactate.

patterns obtained under conditions A and B was assumed to be as follows. Under conditions B, which do not use TTAB and a negative power supply, the capillary has a cathodic electroosmotic flow (EOF), which carries Gln, having little charge and low mobility at this pH (8.3), to the cathode. On the other hand, LA with a negative charge has a migration potential to the anode, but organic acids have a low net mobility. Therefore, LA was also carried to the cathode with the strong EOF. The CZE analyses under conditions B, which is a capillary isotachophoresis system previously developed by us [19], can become a useful tool for the determination of Gln in CSF, an increase in which is an important marker of hepatic encephalitis [20].

The present results indicate that CZE is a powerful tool for the determination of organic acids in CSF as an aid in the biochemical diagnosis of CNS disease. In analyses under conditions A, a high resolution of peaks which was achieved with the use of a negative power supply, and addition of TTAB to the electrolyte enabled us not only to determine LA, the major organic component of CSF, but also to detect changes in the levels of some other CSF minor organic acids in association with pathological conditions of the CNS. However, in analyses under conditions B, evaluated levels of LA in CSF can be clearly detected. This type of examination of CSF is very valuable for estimating the brain damage in ischaemia of cerebral infarction [1] and also to distinguish between bacterial meningitis and viral meningitis [2–6].

References

[1] R. Zupping, A.E. Kaasick and E. Ravdam, *Arch. Neurol.*, 23 (1971) 33.
[2] G. Controni, W.J. Rodriguez and J.M. Hicks, *J. Pediatr.*, 91 (1977).
[3] I. Brook, K.S. Bricknell and G.D. Overturf, *J. Infect. Dis.*, 137 (1977) 379.
[4] R.A. Koromorowski, S.G. Farmer and G.A. Hanson, *J. Clin. Microbiol.*, 8 (1978) 89.
[5] E. D'Souza, B.K. Mandel and J. Hooper, *Lancet*, 2 (1987) 579.
[6] A. Hiraoka, I. Miura, M. Hattori, I. Tominaga, K. Kushida and M. Maeda, *Biol. Pharm. Bull.*, 17 (1994) 1.
[7] J.B. Posner and F. Plum, *Arch. Neurol.*, 16 (1967) 492.
[8] B.K. Seijo, *Brian Energy Metabolism*, Wiley, New York, 1978, p. 607.
[9] R.A. Fishman, *Cerebrospinal Fluid in Diseases of the Nervous System*, W.B. Saunders, Philadelphia, 1980, p. 231.
[10] A. Weston, P.B. Brownm, P. Jandick, W.R. Jones and A.L. Heckenberg, *J. Chromatogr.*, 593 (1992) 289.
[11] S.K. Yeo, H.K. Lee and S.F.Y. Li, *J. Chromatogr.*, 585 (1991) 133.
[12] M.T. Ackermans, J.L. Beckers, F.M. Everets, H. Hoogland and M.J.H. Thomassen, *J. Chromatogr.*, 596 (1992) 101.
[13] U. Seita, P.J. Oefner, S. Nathakarnkitkkol, M. Popp and G.K. Brown, *Electrophoresis*, 13 (1992) 35.
[14] G.L. Chee and T.S.M. Wan, *J. Chromatogr.*, 612 (1993) 172.
[15] E. Kenndler, C. Schwer and D. Kaniansky, *J. Chromatogr.*, 508 (1990) 203.
[16] S. Honda, S. Iwase, A. Makino and S. Fujisawa, *Anal. Chem.*, 176 (1989) 72.
[17] A. Hiraoka, I. Miura, M. Satô, M. Hattori and I. Tominaga, *J. Anal. Bio-Sci.*, 13 (1990) 176.
[18] J.S. Kim, H.H. Kornhuber, W. Schmid-Burk and B. Holzmüller, *Neurosci. Lett.*, 20 (1980) 379.
[19] A. Hiraoka, I. Miura, M. Hattori and I. Tominaga, *Clin. Biochem.*, 22 (1989) 293.
[20] B.T. Hourani, E.M. Hamlin and T.B. Raymond, *Arch. Intern. Med.*, 177 (1991) 1033.

ELSEVIER

Journal of Chromatography A, 680 (1994) 247–251

JOURNAL OF CHROMATOGRAPHY A

Determination of organic acids in urine by capillary zone electrophoresis

Mika Shirao*,[a], Riko Furuta[a], Sumiko Suzuki[a], Hiroyuki Nakazawa[a], Susumu Fujita[b], Toshihiko Maruyama[c]

[a]*National Institute of Public Health, 6-1 Shirokanedai 4-Chome, Minato-ku, Tokyo 108, Japan*
[b]*Scientific Crime Laboratory, Kanagawa Prefecture Police H.Q., 54 Yamashitacho, Naka-ku, Yokohama-shi 231, Japan*
[c]*Waters Division of Nihon Millipore, 14-10 Nishinakajima 5-Chome, Yodogawa-ku, Osaka 532, Japan*

Abstract

The simultaneous measurement of organic acids was studied using capillary electrophoresis with direct measurement of UV absorption at 185 nm. The organic acids studied were oxalic, formic, malonic, fumaric, succinic, α-ketoglutaric, citric, acetic, pyruvic, lactic, isovaleric and hippuric acid. They were separated in a fused-silica capillary (100 cm × 75 μm I.D.) filled with 50 m*M* borax buffer (pH 10.0) containing cationic surfactant as the electroosmotic flow modifier. The method was successfully applied to the determination of organic acids in urine in comparison with an organic acid analyser.

1. Introduction

Organic acids in the living body are present as intermediate and ultimate metabolites. When metabolic disorders occur, accumulation in the body fluids or tissues and excretion in the urine and stool of particular organic acids are observed. Organic acids have been determined in urine and serum in order to diagnose numerous inborn errors of metabolism known as organic acidurias [1–3]. It is also necessary to measure the concentration of organic acids in foods with respect to quality control of foods and their storage. Organic acid analysers (OAA), a post-labelling HPLC system and gas chromatography–mass spectrometry have been used for the determination of organic acids [4–8]. However, these techniques are time consuming and need tedious operation.

Capillary electrophoresis is a modern analytical technique that permits rapid and efficient separations of charged components present in small sample volumes [6,7]. In conventional capillary electrophoresis, a specimen is injected on to the anodic electrode and detection is performed on the cathodic electrode, as electroosmotic flow (EOF) goes from the anode to the cathode because of the negative electric charge of the capillary wall. In the measurement of particular anions, such as inorganic acids and short-chain carboxylic acids, the reversal of the EOF with cationic surfactants together with sample injection from the anode is reported to give successful separations [9–14]. In those studies, indirect detection of anions using UV-absorbing electrolytes was employed. However,

* Corresponding author.

0021-9673/94/$07.00
SSDI 0021-9673(94)00328-7

the indirect method was not applicable to the trace determination of organic acids in urine as described here. In this study, we developed analytical conditions for the simultaneous determination of organic acids with direct detection at 185 nm. In addition, the method was applied to the measurement of organic acids in urine and compared with an organic acid analyser.

2. Experimental

2.1. Reagents and samples

Oxalic acid, malonic acid, sodium isovalerate and hippuric acid were obtained from Kanto Chemical (Tokyo, Japan), α-ketoglutaric, pyruvic, DL-citric, malic, DL-tartaric and succinic acid and sodium tetraborate (borax) from Wako (Osaka, Japan) and L-lactic, fumaric and methylmalonic acid from Sigma (St. Louis, MO, USA). All solutions were prepared from distilled, deionized water. Stock solutions of the organic acids were prepared at a concentration of $1 \cdot 10^4$ ppm. 2-Nitrophenylhydrazine hydrochloride (ONPH) and 1-ethyl-3-(3-dimethylaminopropyl)carbodiimide hydrochloride (EDC) were obtained from Tokyo Rikakikai (Tokyo, Japan). CIA OFM Anion-BT, the electroosmotic flow modifier, was purchased from Waters Division of Nihon Millipore (Tokyo, Japan).

Human urine was collected from healthy volunteers and stored at −20°C until analysis. The samples were clarified by centrifugation at 800 *g* for 20 min to remove cells and other particulate matter, then passed through a C_{18} solid-phase extraction cartridge (Waters) before injection.

2.2. Instrumentation and analytical conditions

Capillary electrophoresis was carried out with a Quanta 4000 system with a Model 820 data station (Waters). The separations were carried out using an uncoated fused-silica capillary (100 cm × 75 μm I.D.) obtained from Waters. The injection mode used was hydrostatic, urine samples being elevated to a height of 10 cm for 45 s. The injection volume was calculated as approximately 54 nl. Detection was carried out at 254 nm by the indirect method and at 185 nm by the direct method. The applied voltage was 20 kV using a negative power supply.

A Model S300Z organic acid analyser (Tokyo Rikakikai) was used with an HC-5-500 anion-exchange column (50 cm × 5 mm I.D.) (Tokyo Rikakikai) [6]. The conditions for separation and postcolumn reaction for detection were as follows: mobile phase, 0.2 *M* HCl; reaction solution 1, 0.01 *M* ONPH in 0.1 *M* HCl; reaction solution 2, 0.15 *M* EDC in 4% pyridine solution in ethanol; reaction solution 3, 1.5 *M* NaOH; column temperature, 60°C; flow-rate of mobile phase, 0.25 ml/min; flow-rate of reaction solutions, 0.3 ml/min; injection volume, 100 μl; and detection wavelength, 530 nm.

3. Results and discussion

3.1. Assessment of detection wavelength

Kenney [14] and Wildman *et al.* [13] determined organic acids in foods and urine by the indirect method at 254 nm with potassium phthalate buffer and sodium chromate buffer. When we analysed urine samples for trace organic acids using similar methods the phosphate present interfered. The use of borax buffer with direct detection at 185 nm gave satisfactory results for organic acids without interference.

As the pK_a value of each organic acid expected in urine was lower than 7, the pH of the buffer was studied between 6 and 11 with 50 m*M* borax adjusted with sodium hydroxide or hydrochloric acid in the presence of 0.5 m*M* CIA OFM Anion-BT. Satisfactory results were obtained with borax buffer at pH 10 in respect of peak resolution, stability of the baseline and operation time. Similar migration times were obtained with buffers with pH < 8, but both the shape of the peaks and the separation of several acids were far inferior to those at pH 10, while the baseline became labile at pH 11.

Fig. 1 shows the effect of the concentration of borax buffer at pH 10.0 on the migration time of organic acids. While the resolution was improved

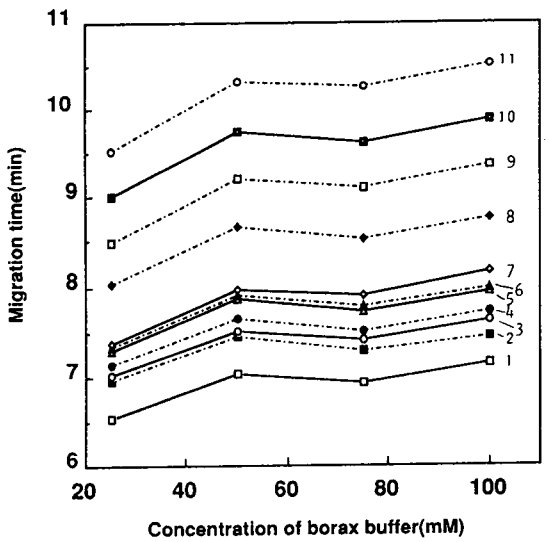

Fig. 1. Effect of concentration of borax buffer (pH 10.0) on migration time. Solutes: 1 = oxalic acid; 2 = formic acid; 3 = malonic acid; 4 = fumaric acid; 5 = succinic acid; 6 = α-ketoglutaric acid; 7 = citric acid; 8 = pyruvic acid; 9 = lactic acid; 10 = isovaleric acid; 11 = hippuric acid. For other conditions, see Experimental.

with increase in concentration, the operation time became longer and the electric current was elevated, as shown in Fig. 2 at higher concentration. As a high electric current should be avoided in order to suppress Joule heat generation [15], the concentration of the buffer adopted was 50 m*M* with an applied voltage of 20 kV.

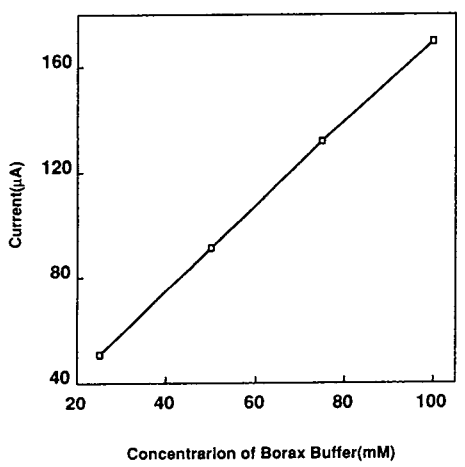

Fig. 2. Effect of concentration of borax buffer (pH 10.0) on electric current. Conditions as in Fig. 1.

Among the cationic surfactants tested, including cetyltrimethylammonium chloride and tetrabutylammonium bromide, CIA-Pak OFM Anion-BT gave the best separation and good peak shapes for simultaneous analysis. Fig. 3 shows the electropherogram of twelve organic acids employing 50 m*M* borax buffer at pH 10.0 with 0.5 m*M* CIA OFM Anion-BT.

It is known that the temperature in the capillary greatly affects electrophoresis [15]. As the instrument used in this study had no temperature control system except the forced cooling of the capillary by a fan, the influence of the temperature of the laboratory on the reproducibility of analysis was investigated. From the results with a standard solution in a laboratory without air conditioning, the migration time was greatly affected, with R.S.D. 9.50% ($n = 8$). In contrast, results obtained in an air-conditioned room (25 ± 1°C) showed good reproducibility, with R.S.D. 0.92% ($n = 8$). Therefore, all subsequent experiments were carried out in an air-conditioned room.

When we analysed urine samples, the delay in the migration times of organic acids became greater; the many impurities in the samples and

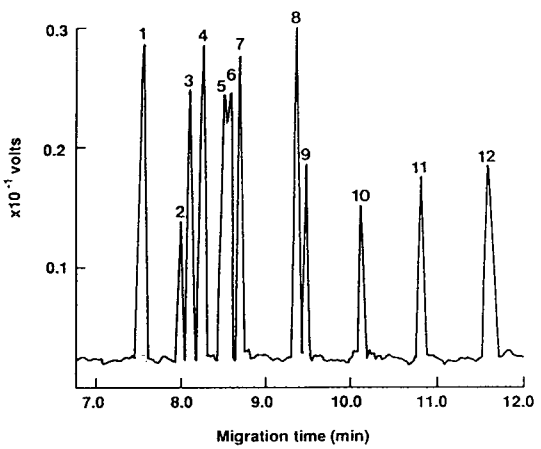

Fig. 3. Electropherogram of standard organic acids. Peaks: 1 = oxalic acid; 2 = formic acid; 3 = malonic acid; 4 = fumaric acid; 5 = succinic acid; 6 = α-ketoglutaric acid; 7 = citric acid; 8 = acetic acid; 9 = pyruvic acid; 10 = lactic acid; 11 = isovaleric acid; 12 = hippuric acid. For conditions, see Experimental.

the possibility of the occurrence of precipitates were thought to be responsible, and the effect of washing the capillary was investigated. Among the solutions studied, successive washing of the capillary with methanolic KOH solution (3 min), distilled water (3 min) and electrophoresis buffer (5 min) was suitable for precise analysis.

3.2. Calibration

The linearity of the method was evaluated between 10 and 250 ppm with respect to both peak-area and peak-height response. As the correlation coefficients for peak height (0.901–0.999) were better than those for peak area (0.878–0.999), calculations were carried out using peak height. The detection limits of oxalic, formic, malonic, fumaric, succinic, α-ketoglutaric, citric, acetic, pyruvic, lactic and isovaleric acid were 5 ppm and that of hippuric acid was 100 ppb.

3.3. Determination of organic acids in urine

Fig. 4 shows the electropherogram of organic acids in human urine using the developed method. The peaks were identified by adding a standard solution to urine according to the procedure of Wildman *et al.* [13]. The amounts of organic acids were different for each urine sample. Oxalic, formic, succinic, citric, pyruvic, lactic and hippuric acid were identified as shown in Fig. 4. The arrows numbered 3, 4 and 7 indicate the migration times of malonic, fumaric and acetic acid. Although the peaks of these acids in this sample did not appear larger than the background noise, they were reproducible and they appeared as peaks in other samples.

This method could also be applicable to urine samples without dilution. A chromatogram of organic acids in the same sample obtained with the organic acid analyser is shown in Fig. 5. The organic acids indicated were identified. Glucuronic acid was appeared in some samples. Under these conditions, it was difficult to determine fumaric and hippuric acid, because they eluted as broad peaks at *ca.* 4.5 and 6.5 h, respectively. The detection limits of other acids were *ca.* 500 ppb with the organic acid analyser.

When the concentrations of some acids that are abundant in urine, such as citric acid, were calculated, the values determined by capillary electrophoresis were similar to those obtained with the organic acid analyser.

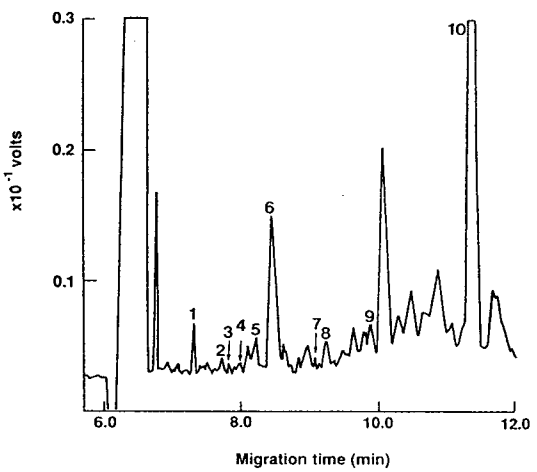

Fig. 4. Electropherogram of organic acids in urine. Peaks: 1 = oxalic acid; 2 = formic acid; 3 = malonic acid; 4 = fumaric acid; 5 = succinic acid; 6 = citric acid; 7 = acetic acid; 8 = pyruvic acid; 9 = lactic acid; 10 = hippuric acid. The arrows numbered 3, 4 and 7 indicate the migration time of malonic, fumaric and acetic acid, respectively. Conditions as in Fig. 4.

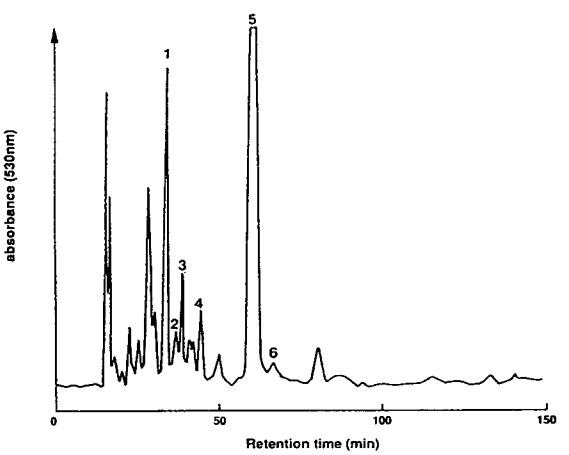

Fig. 5. Chromatogram of organic acids in urine obtained with the organic acid analyser. Peaks: 1 = lactic acid; 2 = acetic acid; 3 = pyruvic acid; 4 = formic acid; 5 = citric acid; 6 = succinic acid. For conditions, see Experimental.

4. Conclusions

We have discussed the fundamental conditions for the determination of organic acids in urine by capillary electrophoresis. Using detection at 185 nm and an applied voltage of 20 kV, favourable separation was achieved in a fused-silica capillary of 100 cm × 75 μm filled with 50 m*M* borax buffer (pH 10) without interference from phosphate present in urine. The capillary electrophoresis method was to an organic acid analyser especially with respect to operating time and the amount of the sample required, but the latter was more sensitive than the former.

The determination of organic acids is also important in food manufacturing and quality control of foods. From our preliminary results for the analysis of food samples, such as wines and soy sauce, the method described was applicable except for a few acids contained in these samples which overlapped others. Slight modification of analytical conditions is necessary and is under study for the determination of organic acids in foods and other samples.

References

[1] Y. Mardens, A. Kumps, C. Planchon and C. Wurth, *J. Chromatogr.*, 577 (1992) 341.
[2] T. Niwa, *J. Chromatogr.*, 379 (1986) 313.
[3] P. Sims, R. Truscott and B. Halpern, *J. Chromatogr.*, 222 (1981) 337.
[4] K. Kidouchi, T. Niwa, D. Nohara, K. Asai, N. Sugiyama, H. Morishita, M. Kobayashi and Y. Wada, *Clin. Chim. Acta*, 173 (1988) 263.
[5] T. Hayashi, T. Sugiura, H. Terada, S. Kawai and T. Ohno, *J. Chromatogr.*, 118 (1976) 403.
[6] R. Horikawa and T. Tanimura, *Anal. Lett.*, A20 (1982) 1629.
[7] R.H. Haas, J. Breuer and M. Hammen, *J. Chromatogr.*, 425 (1988) 47.
[8] L. Bjorkman, C. Mclean and G. Steen, *Clin. Chem.*, 22 (1976) 49.
[9] P. Jandik and G. Bonn, *Capillary Electrophoresis of Small Molecules and Ions*, VCH, New York, 1993, Ch. 5, p. 257.
[10] P. Jandik and W.R. Jones, *J. Chromatogr.*, 546 (1991) 431.
[11] S. Hjertén, K. Elenbering, F. Kilar and J.-L. Liao, *J. Chromatogr.*, 403 (1987) 47.
[12] J. Romano, P. Jandik, W.R. Jones and P.E. Jackson, *J. Chromatogr.*, 546 (1991) 411.
[13] B.J. Wildman, P.E. Jackson, W.R. Jones and P.G. Alden, *J. Chromatogr.*, 546 (1991) 459.
[14] B.F. Kenney, *J. Chromatogr.*, 546 (1991) 423.
[15] H.E. Schwartz, R.H. Palmieri and R. Brown, in P. Camilleri (Editor), *Capillary Electrophoresis. Theory and Practice*, CRC Press, Boca Raton, FL, 1993, Ch. 6, p. 213.

ELSEVIER

Journal of Chromatography A, 680 (1994) 253–261

JOURNAL OF CHROMATOGRAPHY A

Enantiomeric resolution of primary amines by capillary electrophoresis and high-performance liquid chromatography using chiral crown ethers

Yvonne Walbroehl*, Joseph Wagner

Marion Merrell Dow Research Institute, 16 Rue d'Ankara, 67046 Strasbourg, France

Abstract

High-performance liquid chromatography with a chiral crown ether stationary phase and capillary electrophoresis (CE) with a chiral crown ether dissolved in the operating buffer have been used for the separations of enantiomers of a variety of primary amines of pharmaceutical interest, including aminotetralin analogues, aminomethylbenzodioxane, amino derivatives of naphthalene and phenanthrene, and aminodecalin analogues. Interestingly, the enantiomers of many of these compounds were adequately resolved by only one or the other of the two methods, indicating that the techniques are complementary. The influence of the degree of complexation of analyte molecules with the crown ether on chromatographic retention, electrophoretic migration, and chiral recognition is discussed, as well as the relative advantages and disadvantages of the two methods in practical applications.

1. Introduction

High-performance liquid chromatography (HPLC) using various types of chiral stationary phases, mobile phase additives, and derivatizing agents has been used extensively for the analysis of amino acids and amines [1,2]. More recently, capillary electrophoresis (CE) has been applied to chiral separations [3]. Although some work has focused on the use of CE for the separation of diastereomeric derivatives of chiral compounds, much of the work has focused on the use of chiral selectors in the electrophoretic operating buffer. Most commonly, cyclodextrin buffer additives are used for chiral separations by CE. More recently, Kuhn and co-workers [4,5] described the use of a chiral crown ether for chiral resolution of various amino acids, peptides, and optically active amines without prior derivatization. In this work we compare the use of CE with a chiral crown ether in the buffer and HPLC with a crown ether stationary phase for the enantiomeric resolution of primary amines of pharmaceutical interest.

2. Experimental

All CE experiments were carried out using a Beckman P/ACE 2100 CE system. The system was interfaced to an IBM-compatible personal computer and Beckman System Gold software was used for data collection and manipulation. Separations were carried out in a fused-silica

* Corresponding author. Present address: Institute of Analytical Research (R6), Syntex (USA), Inc., 3401 Hillview Avenue, P.O. Box 10850, Palo Alto, CA 94303, USA.

0021-9673/94/$07.00
SSDI 0021-9673(94)00298-N

capillary tube (Beckman Instruments, Neuilly, France). The dimensions of the tube were 57 cm × 75 μm I.D., with the detector located 7 cm from the outlet end of the capillary. A detector slit size of 100 μm × 200 μm was used for experiments with direct detection. The detection wavelength was either 254 or 280 nm, depending on the absorbance spectrum of the analyte. The capillary was thermostatted at 25°C. Most experiments were carried out using a 50 m*M* sodium phosphate buffer at pH 2.2 containing 30 m*M* 18-crown-6 tetracarboxylic acid (18-crown-6 TCA). Sample concentrations were typically 0.5 mg/ml in water. Pressure injections of 2–3 s (approximately 10–15 nl) were made.

For chiral resolutions of compounds which have poor UV absorbance, an electrolyte solution containing 6 m*M* benzyltrimethylammonium chloride (BTMACl) and 30 m*M* 18-crown-6 TCA and the pH adjusted to 3.7 with 1 *M* NaOH was used, with indirect detection. The detector wavelength was set at 214 nm. A slit size of 50 μm × 200 μm was used for measurements with indirect detection. A 57 cm × 75 μm I.D. capillary thermostatted at 25°C was used for these experiments. Sample concentrations were typically 0.5 mg/ml in water. Pressure injections of 5 s (approximately 26 nl) were made.

HPLC experiments were carried out using a conventional HPLC system consisting of a Waters M590 pump, a Waters WISP 710B autosampler, and either a Waters M481 UV detector or a Kratos Spectroflow 773 UV detector. A CrownPak(+) column (15 cm × 4 mm I.D., 5 μm packing) obtained from Daicel (Tokyo, Japan) was used. The column was thermostatted using either a water bath or a methanol bath. A guard column (2.1 cm × 2.0 mm I.D.) containing glass beads (30–50 μm diameter) was used. For those experiments using post-column derivatization with *o*-phthalaldehyde (OPA) and fluorescence detection, a Dosapro minipump from Milton Roy was used to pump the derivatization reagent. A Shimadzu RF530 detector was used, with an excitation wavelength of 360 nm and emission wavelength of 450 nm. The conditions of the OPA derivatization were as described in Ref. 6, except that the ionic strength of the potassium borate buffer used for pH control in these experiments was higher (0.8 *M*). Unless otherwise indicated, the following chromatographic conditions were used for the aminotetralin analogues: mobile phase, 0.013 *M* $HClO_4$, pH 2.04, 15% methanol; temperature, 40°C; flow-rate, 1 ml/min; detector wavelength, 210 nm. The conditions used for the aminonaphthalene analogues were: mobile phase, 0.16 *M* $HClO_4$, pH 1.00, 15% methanol; temperature, 30°C; flow-rate, 1 ml/min; detector wavelength, 254 nm. The conditions used for the aminophenanthrene analogues were, unless otherwise stated: mobile phase, 0.0011 *M* $HClO_4$, pH 2.92, 15% methanol; temperature, 30°C; flow-rate, 1 ml/min; detector wavelength, 280 nm. The chromatographic conditions used for the aminodecalin analogues were: 0.16 *M* $HClO_4$, pH 0.98, 15% methanol; temperature, 30°C; flow-rate, 1 ml/min; detector wavelength; 210 nm. Sample concentrations for all experiments were typically 0.5 mg/ml in water or eluent and injections volumes were 10 μl.

Chemicals were reagent grade, unless otherwise stated. Phosphoric acid, sodium hydroxide, perchloric acid and methanol were obtained from Merck (Darmstadt, Germany). 18-Crown-6 TCA was also obtained from Merck. BTMACl was obtained from ICN Pharmaceuticals (Plainview, NY, USA). Water was purified from laboratory water using a Millipore water-purification system. 1-Aminotetrahydronaphthalene was obtained from Aldrich (Saint Quentin Fallavier, France) The other aminotetralins and aminomethylbenzodioxane were synthesized in our laboratories by published procedures [7,8]. The amino derivatives of naphthalene and phenanthrene were prepared as described in Ref. 9. The 3-amino-2-decalones [10,11] and decalylamine [12] were also prepared in our laboratories.

3. Results and discussion

3.1. Aminotetralins

We investigated a group of aminotetralins, including positional isomers and substituted ana-

logues. Rondelli et al. [13] reported the enantiomeric resolution of a substituted aminotetralin by HPLC, following chiral derivatization with *R*-(+)-α-methylbenzylisocyanate. Witte et al. [14] have done an extensive study of resolution of substituted aminotetralins by HPLC using a cellulose tris-3,5-carbamate stationary phase, but most of the compounds in this study were secondary or tertiary amines. The HPLC retention times, CE migration times, separation factors (α), and resolution (R_s) for the aminotetralins and aminomethylbenzodioxane are given in Table 1. The separation factor in HPLC was calculated as described in Ref. 15. The separation factor for CE was calculated as indicated in Ref. 5. Resolution for both methods was calculated according to Ref. 15.

Structures of the crown ethers used in the HPLC and CE systems are shown in Fig. 1. In the CE system, there are two mechanisms for chiral recognition. These have been previously discussed by Kuhn et al. [5]. Recognition occurs by either a steric barrier mechanism or by hydrogen bonding between the guest molecule and the carboxylic acid groups on the crown

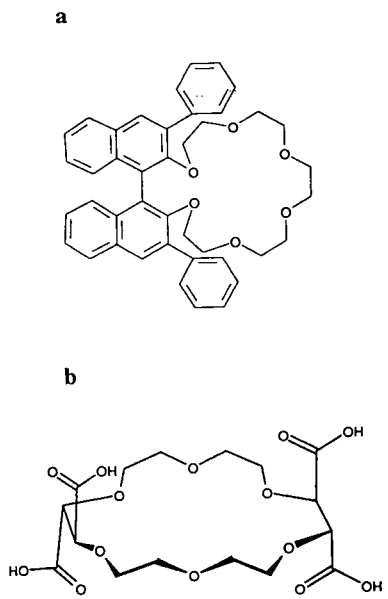

Fig. 1. (a) (*S*)-2,3:4,5-Bis(1,2,3-phenylnaphtho)-1,6,9,12,15,18-hexaoxacycloeicosa-2,4-diene, crown ether incorporated into the stationary phase of the CrownPak(+) HPLC column. (b) (2*R*,3*R*,11*R*,12*R*)-(+)-1,4,7,10,13,16-hexaoxacyclooctadecane-2,3,11,12-tetracarboxylic acid, crown ether used in the CE operating buffer.

Table 1
Results for aminotetralins and aminomethylbenzodioxane

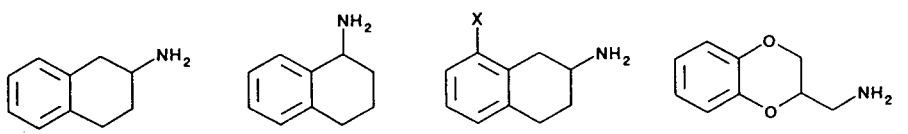

Compound **1** Compound **2** Compounds **3 - 5** Compound **6**

Compound	X	HPLC Results				CE Results			
		t_{R1}	t_{R2}	α	R_s	t_{m1}	t_{m2}	α	R_s
1		9.01	11.53	1.31	2.82	20.56		1.000	0
2		4.61	5.60	1.27	1.27	13.22	17.86	1.351	3.34
3	OCH_3	23.96	28.90	1.21	1.88	17.72	17.91	1.011	0.41
4	C≡N	18.82	19.91	1.06	0.51	20.91	22.94	1.097	6.12
5	Br	–	–	–	–	20.93	22.07	1.054	3.68
6		7.41	11.59	1.56	3.45	24.95	25.45	1.020	1.12

t_{R1}, t_{R2} = HPLC retention times (min) of the first- and second-eluting isomers, respectively; t_{m1}, t_{m2} = CE migration times (min) of the faster- and slower-migrating isomers, respectively.

ether. Similarly, chiral recognition in the HPLC system occurs by either a steric barrier mechanism or through hydrophobic interactions between the guest molecule and the hydrophobic substituents on the crown ether incorporated into the HPLC stationary phase.

The results for compounds **1** and **2** indicate that the position of the amino group is important in chiral recognition for these compounds. By HPLC, 2-aminotetralin (compound **1**) is more strongly retained and better resolved than 1-aminotetralin (compound **2**). In the CE experiment, the opposite result was observed. Compound **1** exhibits a strong affinity for the crown ether in the electrophoresis buffer, as evidenced by its longer migration time, but no chiral resolution is observed. However, compound **2**, while more weakly complexed by the crown ether, is well resolved. The geometry of compound **2** must lead to a larger difference in the stability constants for its enantiomers with the crown ether as compared to its positional isomer, compound **1**. A large number of spikes were observed in the electropherograms for compounds **1** and **2**, indicating that there may be a problem with the solubility of these compounds in the operating buffer.

Results for compounds **3–5** demonstrate the effect of different substituents at the 9-position on chiral resolution for substituted 2-aminotetralins. In the HPLC system, if non-stereospecific interactions such as hydrophobic interactions with the stationary phase are weak, then the retention time can be used as an indicator of the degree of complexation of the analytes with the crown ether. In the CE system, other factors contribute to the overall migration rate of an analyte, such as the molecular size and shape. Complexation with the crown ether effectively retards the migration of analytes in this system. For a group of analytes with similar size and charge, the migration time in CE will be a rough indicator of the degree of complexation. In Fig. 2, the separation factor, α, is plotted as a function of the retention time of the first-eluting isomer in HPLC and the migration time of the first-eluting isomer in CE. These plots indicate that in both systems there is a correlation between the strength of complexation, as measured by the migration time for CE and the retention time for HPLC, and the degree of chiral recognition, as measured by α. Interestingly, we observed that for those compounds which were well resolved by CE (compounds **4** and **5**), poor results were obtained by HPLC. Conversely, compound **3** was well resolved by HPLC, by not by CE. Compound **5** was well resolved by CE, but was not eluted from the CrownPak(+) column. We found no conditions that would elute this compound from the column. No indications of solubility problems, such as spurious spikes, were observed in the electropherograms for compounds **3–5**.

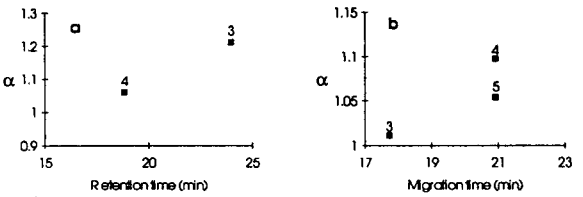

Fig. 2. (a) Correlation between separation factor, α, and HPLC retention time. (b) Correlation between α and CE migration time. Compound numbers refer to Table 1.

One compound with the amine group located two carbons from the chiral center (compound **6**) was also included in this study. This compound was very well resolved by HPLC, most likely because the position of the aromatic portion of the guest molecule with respect to the amino group permits hydrophobic interactions with the aromatic portion of the crown ether in the stationary phase of the CrownPak(+) column. Compound **6** is also adequately resolved by CE. The resolution is less than that observed by HPLC since there is no possibility of hydrophobic interactions assisting in chiral recognition. However, this data is in contrast to results observed by Kuhn et al. [5] in which compounds with the chiral center a the β-carbon were poorly resolved by CE under conditions similar to ours. Kuhn et al. observed better selectivity by CE for compounds with bulky substituents, due to increased steric hindrance. Compound **6** is bulkier than the compounds in Kuhn et al.'s study and thus a better separation is obtained. Representa-

tive chromatograms of compounds **4** and **6** are given in Fig. 3. Corresponding electropherograms are shown in Fig. 4.

3.2. Amino derivatives of naphthalene and phenanthrene

The results for a group of bicyclic and tricyclic aromatic amines are summarized in Table 2. This group of compounds can be divided into two sub-groups, aminonaphthalene analogues (compounds **7–10**) and aminophenanthrene analogues (compounds **11–15**). For the aminonaphthalene analogues (compounds **7–10**), the effect of substitution on chiral recognition by the crown ethers is apparent. Two methyl groups at the 3-position (compound **8**) result in a large increase in retention and resolution by HPLC. Similarly, dimethyl substitution at the 3-position results in increased migration times and resolution in the CE experiment. The substitution of two fluorine atoms at the 3-position (compound **9**) results in decreased retention and resolution by HPLC. But in the CE experiment, increases in migration time and resolution were observed.

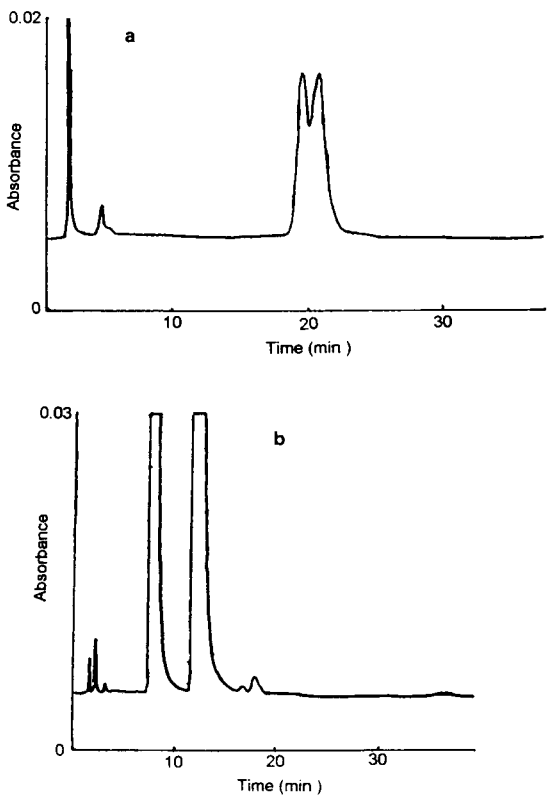

Fig. 3. Chromatograms of (a) compound **4**, 162 ng injected; and (b) compound **6**, 5.7 μg injected. Conditions: Column, CrownPak(+), 15 cm × 4.0 mm; mobile phase, 0.013 *M* $HClO_4$, pH 2.04, 15% methanol; temperature, 40°C; flow-rate, 1 ml/min; detector wavelength, 210 nm; injection volume, 10 μl.

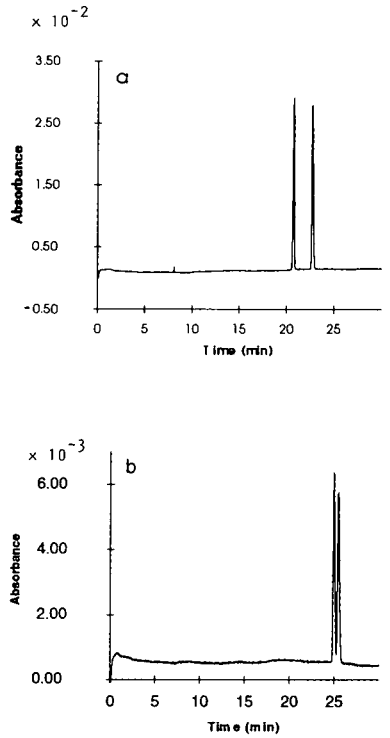

Fig. 4. Electropherograms of (a) compound **4**, 7.5 ng injected; and (b) compound **6**, 5 ng injected. Conditions: capillary, 57 cm × 75 μm I.D.; buffer, 50 m*M* sodium phosphate, pH 2.2, 30 m*M* 18-crown-6 TCA; temperature, 25°C; voltage, + 15 000 V; detector wavelength, 210 nm.

In Fig. 5, the separation factor, α, is plotted versus retention time in HPLC and migration time in CE for compounds **7–10**. The plots indicate that for this group of compounds, there is a correlation between the degree of complexation and the degree of chiral recognition in both systems.

Compound **10** is a secondary amine which does not form complexes with crown ethers. As

Table 2
Results for aminonaphthalenes and aminophenanthrenes

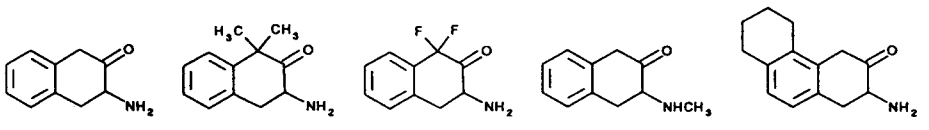

Compound 7 Compound 8 Compound 9 Compound 10 Compound 11

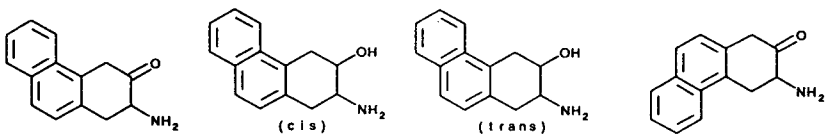

Compound 12 Compound 13 Compound 14 Compound 15

Compound	Eluent	HPLC Results				CE Results			
		t_{R1}	t_{R2}	α	R_s	t_{m1}	t_{m2}	α	R_s
7	A	8.46	16.67	2.16	3.40	18.89	20.76	1.099	1.89
8	A	16.61	38.61	2.45	9.00	25.19	28.34	1.125	4.88
9	A	5.61	6.47	1.20	1.46	19.68	21.73	1.104	2.22
10	A	4.02	–	1.00	0	14.61	–	1.000	0
11	B	47.54	80.18	1.70	2.52	18.00	18.96	1.053	1.07
12	B	31.77	68.61	2.26	3.00	18.50	19.23	1.039	3.00
13	B	17.71	22.75	1.31	1.03	20.87	21.14	1.013	0.73
14	B	31.38	58.07	1.89	2.58	16.64	17.72	1.065	3.36
15	C	37.5	71.4	1.96	1.28	19.84	20.07	1.011	<0.5

Eluents: (A) 0.16 *M* $HClO_4$, pH 1.00, 15% methanol; (B) 0.0011 *M* $HClO_4$, pH 2.92, 15% methanol; (C) 0.0016 *M* $HClO_4$, pH 2.51, 15% methanol. Other experimental conditions given in text. t_{R1}, t_{R2}, t_{m1} and t_{m2} as in Table 1.

expected, the HPLC retention time and the CE migration time are shorter for this molecule than for its demethylated analogue (compound **7**). Also, no chiral resolution was achieved for this compound, which shows that complex formation is required for chiral recognition. Similar results were observed previously by Kuhn et al. [5].

The second sub-group, aminophenanthrene analogues (compounds **11–15**), have three fused rings and are significantly more hydrophobic than the aminonaphthalene analogues. For these compounds, the relationship between HPLC retention time and chiral recognition is less clear (see Fig. 6a). This is probably due to the increased hydrophobicity of these compounds in

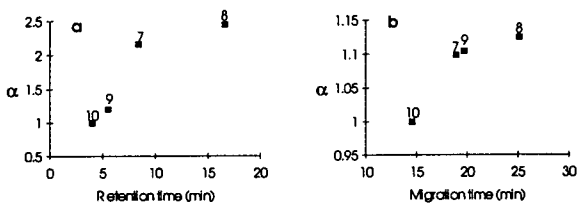

Fig. 5. (a) Correlation between separation factor, α, and HPLC retention time. (b) Correlation between α and CE migration time. Compound numbers refer to Table 2.

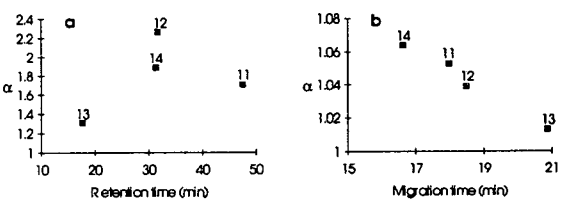

Fig. 6. (a) Correlation between separation factor, α, and HPLC retention time. (b) Correlation between α and CE migration time. Compound numbers refer to Table 2.

comparison to those having only two rings. Increased hydrophobicity contributes to retention, but not to chiral resolution. Thus retention time is no longer a good indication of the degree of complexation in the HPLC system. The chromatographic retention times for most of these compounds were extremely long as 60–80 min in most cases, and the peaks were quite broad. By CE, analysis times are fairly short in comparison to HPLC. Because the peaks in CE are very narrow, good resolution is still achieved for three of the five compounds. The relationship between the CE migration time and the observed separation factor is unclear (see Fig. 6b). This indicates that factors such as molecular size and shape or perhaps a difference in the degree of ionization, are at least as important as complexation with the crown ether in the overall mobilities of the analytes.

For this series of compounds, the structure of the molecule and steric effects leading to a large difference in stability constant appear important for chiral recognition in both the HPLC and CE systems. For example, for compounds **13** and **14**, which are *cis*/*trans* isomers, the *trans* isomer is better resolved in both the HPLC and CE systems. The much shorter retention times by HPLC indicate that when the hydroxyl is *cis* to the amino group, the complex with the crown ether in that system is considerably less stable. The effect in the CE system is more dramatic and can be explained by differences in hydrogen bonding between the hydroxyl group and carboxyl groups on the crown ether. Compounds **12** and **15** are structural isomers, differing only in the orientation of the dibenzo functionality with respect to the amino and carbonyl groups. Although the structural difference in these two compounds is located far from the chiral center, there are significant differences in resolution observed using both techniques. In the HPLC system, the difference in resolution for these two compounds may be a combination of steric and hydrophobic effects. In the CE system, the effect is most likely purely steric, since the carbonyl group is in the same position relative to the amino group in both molecules.

3.3. Aminodecaline analogues

The final group of compounds consists of three structural isomers (compounds **16–18**) and related compound which lacks the carbonyl moiety at the 2-position (compound **19**) (see Table 3).

Table 3
Results for aminodecalin analogues

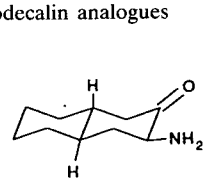

Compound **16**

(trans)

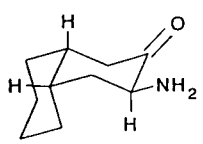

Compound **17**

(cis)

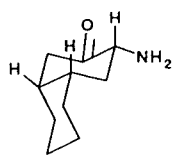

Compound **18**

(cis - 3R,9R,10S)

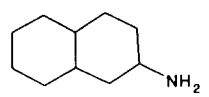

Compound **19**

Compound	HPLC Results				CE Results			
	t_{R1}	t_{R2}	α	R_s	t_{m1}	t_{m2}	α	R_s
16	8.71	16.50	2.06	6.15	12.31	13.07	1.062	1.45
17	7.50	9.29	1.28	2.15	12.85	14.01	1.090	3.34
18	6.03	6.27	1.05	0.42	12.89	13.55	1.051	2.26
19	28.35	–	1.00	0	12.81	–	1.000	0

Experimental conditions given in text. t_{R1}, t_{R2}, t_{m1} and t_{m2} as in Table 1.

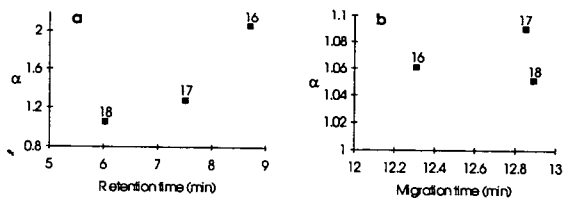

Fig. 7. (a) Correlation between separation factor, α, and HPLC retention time. (b) Correlation between α and CE migration time. Compound numbers refer to Table 3.

In the HPLC experiment, a strong correlation is observed between retention time and α (see Fig. 7a). Under the standard conditions for this series of compounds, compound **18** is only poorly resolved. By adjusting the eluent, it is possible to adequately resolve compound **18**, at the expense of analysis time. Under the eluent conditions required to resolve this compound, retention times for compounds **16** and **17** are expected to be very long. Nevertheless, it is possible to analyze all three compounds in the same run. In the CE system, all three compounds are well resolved, but no correlation between migration time and a was observed (see Fig. 7b). The retention times of all three compounds are within 0.5 min of one another. The *cis* isomers are significantly different in shape from the trans, with probably leads to the larger resolutions observed for these isomers.

A fourth compound (compound **19**) was analyzed by both HPLC and CE. This compound lacks any chromophore whatsoever. In order to detect it by HPLC, post-column derivatization with OPA was employed. Indirect UV detection was used in the CE experiment. No resolution for this compound was observed in either system. Even when the column temperature in the HPLC system was reduced, no resolution was observed. Its retention time in the HPLC system indicates that the compound interacts with the crown ether in that system, at least to some extent. Because the relationship between migration time and complexation in CE is weak, it is difficult to estimate the amount of complexation in that system. The fact that compound **19** was not resolved by either method suggests that the structures of the stereoisomers are so similar that there is no difference in the stability constants for complexes with crown ethers. Compound **19** was the only compound in the entire group of amines studied which was not resolved by either technique.

4. Conclusions

We have demonstrated the utility of crown ethers in the chiral separation of a variety of primary amines of pharmaceutical interest. For all but the most hydrophobic compounds tested, we found that within a series of related compounds, a correlation between the degree of retention on the HPLC column and chiral recognition was observed. For hydrophobic compounds this relationship was less clear, probably due to the more significant contribution of hydrophobic interactions to chromatographic retention. A correlation between CE migration time and chiral recognition was observed within some groups of compounds, but not others. This result is not surprising, since electrophoretic mobility in our system is a complex function of molecular size, shape, and charge, as well the degree of complexation with the crown ether.

In general, for those compounds having a reasonably strong chromophore in the UV, neither CE nor HPLC is clearly advantageous. In cases where both techniques give a good separation, CE is advantageous when the amount of available sample is very small. It may also be advantageous in the area of routine analysis because the high cost of a chiral HPLC column can be avoided. However, when high sensitivity is required, HPLC is advantageous because of the larger detector cell volume. Also, for a few compounds in this study, solubility problems were encountered in the totally aqueous CE electrolyte. For such compounds, HPLC may be more practical, although it may be possible to use an organic modifier in the CE buffer for these compounds. In the analysis of compounds that absorb poorly in the UV, HPLC is clearly advantageous in terms of its sensitivity.

For many of the compounds in this study, only one of the two techniques was successful in

separating the enantiomers. This is because different crown ethers are used in each of the two techniques. The two crown ethers have somewhat different mechanisms for chiral selection. Depending on their structure, some compounds are more easily separated by one or the other of the two systems. Therefore, one should regard CE and HPLC as complementary tools for enantiomeric resolution of primary amines.

Acknowledgements

The authors would like to thank Professor J.-M. Lehn for his interest in this work. We also acknowledge Dr. Marcel Hibert and Dr. Hugues d'Orchymont for providing compounds, Ms. Blanche Heintzelmann and Ms. Laurence Breton for their assistance in the experimental work, and Ms. Laurie Gunther for secretarial work.

References

[1] I.W. Wainer, in A.M. Krstulovic (Editor), *Chiral Separations by HPLC: Applications to Pharmaceutical Compounds*, Ellis Horwood, Chichester, 1989, Ch. 9, p. 194.

[2] H. Brückner and B. Strecker, *J. Chromatogr.*, 627 (1992) 97.

[3] R. Kuhn and S. Hoffstetter-Kuhn, *Chromatographia*, 34 (1992) 34.

[4] R. Kuhn, F. Stoecklin and F. Erni, *Chromatographia*, 33 (1992) 32.

[5] R. Kuhn, F. Erni, T. Bereuter and J. Häusler, *Anal. Chem.*, 64 (1991) 2815.

[6] J. Wagner, C. Gaget, B. Heintzelmann and E. Wolf, *Anal. Biochem.*, 164 (1987) 102.

[7] M. Hibert, J. McDermott, D. Middlemiss, A. Mir and J. Fozard, *Eur. J. Med. Chem.*, 24 (1989) 31.

[8] W. Nelson, M. Powell and D. Dyer, *J. Med. Chem.*, 22 (1979) 1125.

[9] H. d'Orchymont and C. Tarnus, *Eur. Pat.*, 378 456 (1990).

[10] F. Piriou and H. d'Orchymont, *Tetrahedron*, submitted for publication.

[11] A. Pavia, F. Winternitz and R. Wylde, *Bul. Soc. Chim. Fr.*, 8 (1966) 2506.

[12] T. Cohen, A. Botelho and E. Jankowski, *J. Org. Chem.*, 45 (1980) 2839.

[13] I. Rondelli, F. Mariotti, D. Acerbi, E. Redenti, G. Amari and P. Venturo, *J. Chromatogr.*, 612 (1993) 95.

[14] D.T. Witte, J.-P. Franke, F.J. Bruggeman, D. Dijkstra and R.A. de Zeeuw, *Chirality*, 4 (1992) 389.

[15] L.R. Snyder and J.J. Kirkland, *Introduction to Modern Liquid Chromatography*, Wiley, New York, 2nd ed., 1979, pp. 34–35.

ELSEVIER

Journal of Chromatography A, 680 (1994) 263–270

JOURNAL OF CHROMATOGRAPHY A

Dual electrochemical detection of cysteine and cystine in capillary zone electrophoresis

Betty L. Lin*, Luis A. Colón[1], Richard N. Zare

Department of Chemistry, Stanford University, Stanford, CA 94305, USA

Abstract

A method for the simultaneous determination of cysteine and cystine at the submillimolar level is presented based on the capillary zone electrophoretic (CZE) separation of the analytes coupled to a dual electrochemical detection system. The detector uses two gold/mercury amalgam electrodes placed in series and set at −1.00 V and at +0.20 V vs. Ag/AgCl, respectively. The advantages of the proposed method for the analysis of these compounds include direct detection of both analytes, no elaborate sample preparation, no derivatization procedures, and no pathlength dependence. In addition, the small volumes required for CZE analysis make it suitable for clinical studies. The method was applied to human urine samples.

1. Introduction

The separation and detection of sulfur-containing amino acids is a topic of active interest and has medical applications. For example, hepatic cystinuria is an inherited disorder of amino acid transport characterized by high concentrations of cysteine and cystine in urine (usually >1 m*M* levels) [1]. Several analytical methods have been reported for the specific measurement of these species in urine, such as colorimetry [2,3] and high-performance liquid chromatography (HPLC) followed by spectrophotometric [4–6] or fluorimetric detection [7]. These methods usually require, however, a colorimetric or derivatizing reagent that reacts exclusively with the free sulfhydryl group and not with the disulfidic form. Therefore, cystine must be previously reduced to cysteine before detection, for example, by using dithiothreitol [7], KCN [2,4], sodium sulfite [5,6], or KBH_4 [3].

The use of HPLC with electrochemical detection has also been proposed for the determination of thiols. Initial work on this subject was performed by Rabenstein and Saetre [8], who reported the use of a mercury pool electrode. Allison and Shoup [9] developed a dual-electrode detector for the simultaneous determination of thiols and disulfides. This detector used two gold/mercury amalgam electrodes placed in series. The first electrode, or upstream electrode, set at −1.0 V vs. Ag/AgCl, reduces the disulfides to their corresponding thiols. The second electrode, or downstream electrode, set at +150 mV vs. Ag/AgCl, detects thiols that result from the reduction of disulfides at the first electrode as well as free thiols present in the sample. The main advantages of using this dual-electrode detection system are the direct detec-

* Corresponding author.

[1] Present address: Department of Chemistry, State University of New York at Buffalo, Buffalo, NY 14214, USA.

SSDI 0021-9673(94)00533-F

tion of analytes, no need for reduction or derivatization before separation, and the provision of measurements independent of pathlength or cell dimensions. Moreover, the selectivity achieved when using gold/mercury amalgam electrodes is enhanced over that when using glassy carbon or gold electrodes because of the low detection potential (+150 mV) applied. Further applications of this dual-electrode detector coupled to HPLC have been widely reported for various thiolic and disulfidic compounds in complex matrices [10–13].

Another novel method for electrochemical detection of thiols and disulfides in HPLC is based on the formation of silver mercaptides from free sulfhydryl groups with silver ion in an ammoniacal medium [14,15]. This method again requires the conversion of disulfides into thiols with sulfite or by electroreduction. The sample preparation steps are therefore more elaborate than those with the use of gold/mercury electrodes.

As an alternative to HPLC, capillary zone electrophoresis (CZE) provides specific advantages regarding the analysis of thiols. Applications of HPLC to the detection of thiols are characterized by low column efficiency and often irreproducible results [16–19]. For clinical sample analysis, CZE is especially recommended over HPLC for the low volume of sample required, the absence of packing material, and the minimization of metallic instrumentation that would catalyze the conversion of free thiols to disulfidic forms. CZE has actually been proposed for use in the determination of thiols and disulfides coupled to absorbance [20] and to fluorescence [21] detection. A reduction of the disulfide followed by its derivatization with a fluorigenic reagent prior to CZE is again required in both methods proposed. More recently, O'Shea and Lunte [22] reported the use of gold/mercury amalgam microelectrodes for free thiol detection. Considering the previous advantages reported for CZE separations as well as for the dual electrochemical detection system, this paper presents, to our knowledge, the first time that both analytical methods are coupled together. Two gold/mercury amalgam microelectrodes are placed in series to detect simultaneously the thiolic species cysteine together with its disulfide cystine separated by CZE. Our work builds on the use of gold/mercury amalgam electrodes reported by O'Shea and Lunte combined with the use of the dual-electrode detection system proposed by Allison and Shoup for HPLC separations. The method proposed is direct, specific, and selective for the detection of cysteine and cystine. Its successful application to urine samples is also presented.

2. Experimental

2.1. Chemicals and sample preparation

Cysteine, cystine, EDTA and 2-(N-morpholinoethanesulfonic acid) (MES) were obtained from Sigma (St. Louis, MO, USA). All other compounds were chemically pure and used as received. Water purified with an Ultra-Pure water system (Millipore, Bedford, MA, USA) was used to prepare all solutions. The separation buffer consisted of a 10 m*M* MES solution adjusted at a pH of 5.5 with sodium hydroxide. The standard cysteine solutions were prepared daily in the previously mentioned MES buffer containing 2 m*M* EDTA used to prevent metal-catalyzed thiol oxidation. Cystine had to be dissolved in 10 m*M* HCl because of its poor solubility in aqueous solutions. The urine samples were diluted by a factor of ten in the separation buffer containing EDTA and stored at <4°C without further sample pretreatment. All the solutions were passed through a membrane filter (Nalgene syringe filters, 0.4-μm pore size; Baxter Diagnostic, Hayward, CA, USA) before use.

2.2. Apparatus

Capillary zone electrophoresis

The complete CZE system was built in the laboratory and has been described previously [23]. A high-voltage power supply (Hipotronics, Brewster, NY, USA) set at 20 kV was used to drive the electrophoresis in the capillary. Fused-

silica capillaries (360 μm O.D. × 75 μm I.D.) were purchased from Polymicro Technologies (Phoenix, AZ, USA). A hole was drilled through the capillary (Laser Machining, Somerset, WI, USA) leaving a distance of ca. 50 cm length at one side and 1 cm on the other side. The samples were injected electrokinetically. The separation was achieved on a 10 m*M* MES buffer, pH 5.5, through which argon gas was bubbled vigorously for 30 min prior to use [22]. A gas purifier (Oxiclear; Supelco, Bellefonte, PA, USA) was used to ensure the purity of the argon before bubbling. The electrophoretic currents reached were approximately 3.5 μA. All the capillaries were cleaned with sodium hydroxide (100 m*M*) before use, followed by water and separation buffer. Whenever urine samples were injected, the cleaning procedure was repeated between runs.

Detection

Constant-potential amperometric detection in combination with CZE was performed using the end-column approach [24]. A mercury battery (Duracell, 1.4 V) provided the required voltage to the working electrode placed at the end of the separation capillary. The Faraday current was amplified using a two-electrode current amplifier (Model 428; Keithley Instruments, Cleveland, OH, USA). All potentials were referenced to the Ag/AgCl electrode (MI-402, 3 *M* KCl saturated with AgCl; Microelectrodes, Londonderry, NH, USA). Data collection was performed using a Lab Calc program. The electrochemical cell used was similar to those reported previously [25]. To decouple the electrophoretic separation field from the electrochemical detection field, three different strategies were tried: a nafion tubing joint [26], a liquid nafion joint [27], and a palladium connector device [28]. Nafion is a cation-exchange polymer membrane that allows the movement of the ions but not of the bulk solution, whereas the palladium connector is a solid-state field decoupler. The construction of each was similar to that described previously except for the palladium connector. This connector was adapted to the dual-electrode detection system as shown in Fig. 1. On one side of the decoupler was placed a 50 cm long fused-silica capillary tubing. On the other side of the decoupler was placed a capillary piece of ca. 3 cm length. This last capillary piece contains the hole at ca. 1 cm from the protruding end of the capillary. At this point, the generator electrode was built.

Dual gold/mercury microelectrode system

The downstream gold/mercury amalgam working microelectrode was constructed similar to those described previously [25] but using a 25 μm diameter gold wire (California Fine Wire, Grover City, CA, USA). This gold electrode was

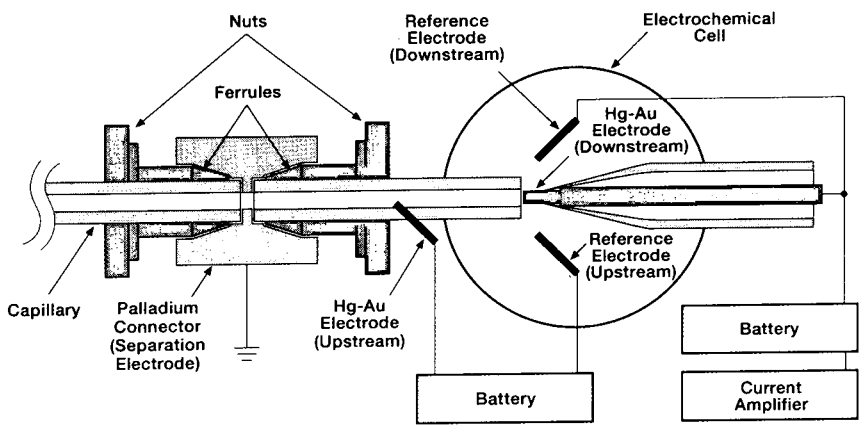

Fig. 1. Schematic diagram of the transversal cross-section of the palladium field decoupler and the dual-electrode detection system.

washed carefully with acetone and deionized water and then dipped into triple-distilled mercury (Aldrich, Milwaukee, WI, USA) for ca. 45 s.

The upstream generator electrode was constructed by inserting a ca. 1 cm piece of gold wire (25 μm diameter) through a hole drilled in the capillary. Epoxy (epoxy 907, Miller Stephenson, Danbury, CT, USA) was applied to seal the wire in place. Once cured, the rest of the protruding gold wire was attached to the end of a 5 cm length copper wire (380 μm diameter) by using conductive silver paint (Epoxy Technologies, Billerica, MA, USA) to achieve electrical connection. Once the silver paint was dry, more epoxy was applied to cover the completed connection. After an overnight curing period, the capillary was flushed with acetone and water to clean the gold electrode. The gold/mercury amalgam was prepared by electrodeposition. A 1.0 *M* KNO_3 with 5.8 m*M* mercurous ion and 0.5% HNO_3 solution was flushed through the column. A deposition potential of -230 mV vs. Ag/AgCl was applied for 5 min. The column was then thoroughly flushed with water to eliminate all traces of the mercurous solution. For the experimental measurements, this electrode was set at -1.0 V vs. Ag/AgCl by means of a mercury battery in a two-electrode configuration. The Ag/AgCl electrode was placed at the outlet buffer vial together with the detection electrodes. For reproducible results, the gold/mercury amalgam required an equilibrium period of ca. 24 h before use, in agreement with previous reports on the use of this electrode [9,22].

3. Results and discussion

3.1. Dual-electrode configuration

We first attempted to optimize the type of microelectrodes used for determining free thiols. According to the literature, gold, glassy carbon and graphite [29] coupled to HPLC have been used to measure thiols. We preferred mercury for the present determinations, however, as the optimum potential for oxidation is relatively low (<0.25 V) so that interferences from other easily oxidized species are avoided. Furthermore, gold/mercury amalgam microelectrodes were recently reported for the successful analysis of free thiols in CZE [22]. The microelectrodes we employed were similar to those reported in the literature except the gold electrode was dipped in mercury for a longer period of time.

Fig. 2 shows the hydrodynamic cyclovoltammogram of the gold/mercury microelectrode with and without cysteine in the buffer electrolyte. A potential of 0.2 V vs. Ag/AgCl was chosen for thiol determination, as it gave the maximum response while it retained the properties of the gold/mercury amalgam. Higher potentials would decrease the selectivity of the determination and remove mercury by electrooxidation.

Various designs were considered for construction of the upstream electrode. The configuration using the palladium connector was shown in Fig. 1. The configurations built at ca. 1 cm after the nafion tubing joint are shown in Fig. 3. In the configuration of Fig. 3a, the upstream electrode and a pseudoreference platinum electrode were placed facing each other on opposite sides of the CZE column. They were both connected to a battery. This first approach did not result in

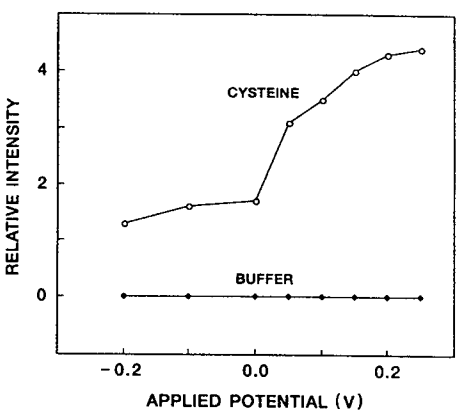

Fig. 2. Hydrodynamic cyclovoltammogram using a gold/mercury microelectrode of (◆) 10 m*M* MES (pH 5.5) and (○) 10 μ*M* cysteine in MES buffer containing 2 m*M* EDTA, CZE capillary: 52 cm × 75 μm I.D., separation voltage: 20 kV, sample injection: electrokinetically 10 s. All potentials are referenced vs. an Ag/AgCl electrode.

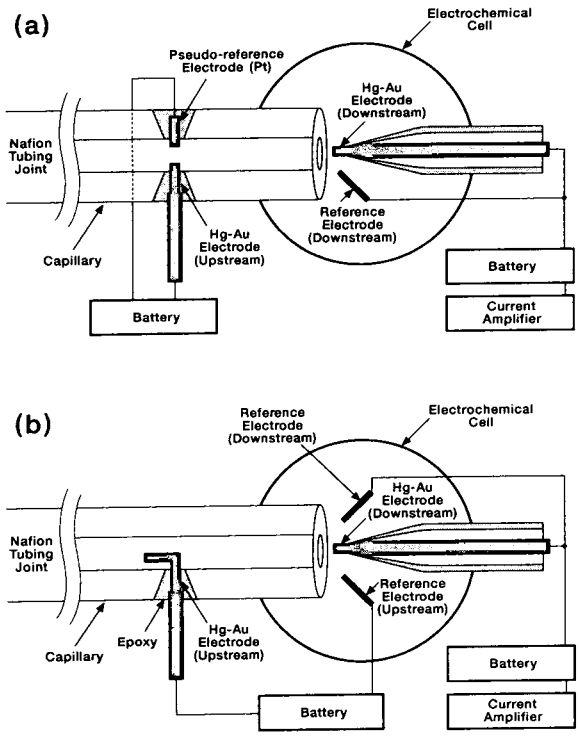

Fig. 3. Schematic diagram of two different designs for the dual-electrode detection system.

any detectable signal for cystine. Apparently, the surface of this upstream electrode was too small for the quantitative reduction of the disulfide into the corresponding thiol.

A second attempt was then made to lengthen the exposed upstream electrode surface. No reference electrode was placed inside the capillary. Instead, only the gold wire was inserted inside the capillary hole, and, with the aid of another gold wire of 50 μm diameter inserted thorough the capillary, it was pushed further inside the capillary to achieve the configuration depicted in Fig. 3b. The Ag/AgCl reference electrode for this upstream electrode was then placed outside the separation capillary, inside the electrochemical cell. This model provided reproducible signals for the determination of both cysteine and cystine and was used in subsequent measurements.

A third design was attempted that used a palladium field decoupler instead of the nafion tubing joint to simplify the handling and construction of the dual electrochemical system. This solid-state decoupler was definitely more useful for the determination of the free thiols by themselves. The selectivity, sensitivity, resolution, and reproducibility of the overall cysteine determination were similar to those of the nafion tubing joint. When this design was applied to the simultaneous determination of thiols and disulfides, however, the upstream electrode had to be placed at the second short piece of the CZE capillary, after the palladium connector and near the electrochemical cell (Fig. 1) so that the separation field would not interfere with the reduction field. All these requirements resulted in the need of at least a ca. 3 cm piece of capillary tubing that protruded through the second part of the connector. Consequently a loss of efficiency resulted from having a distance longer than 2 cm from the separation cathode to the detection cell [30]. No further attempts were therefore made in this direction.

Another approach used liquid nafion in place of nafion tubing to cover the capillary fracture. Liquid nafion was tried out on both configurations depicted in Fig. 3. The need to apply several layers of nafion, coupled with the long periods of solvent drying, made the construction of the capillary field decoupling system relatively troublesome. Moreover, if the capillary was not properly sealed to a support, the nafion could enter through the fracture and block the capillary. As a result, off-column detection using nafion tubing was chosen for the qualitative and quantitative simultaneous determination of cysteine and cystine. This design appeared to be the simplest and provided the most reproducible measurements for our purposes, and the results are reported in detail in the next section.

3.2. Qualitative and quantitative determination of cysteine and cystine

The CZE analysis of both cysteine and cystine was performed in a 52 cm long capillary using 10 m*M* MES buffer, pH 5.5. MES buffer was used because its high resistance provided low detector noise, in accordance with previous reports [30].

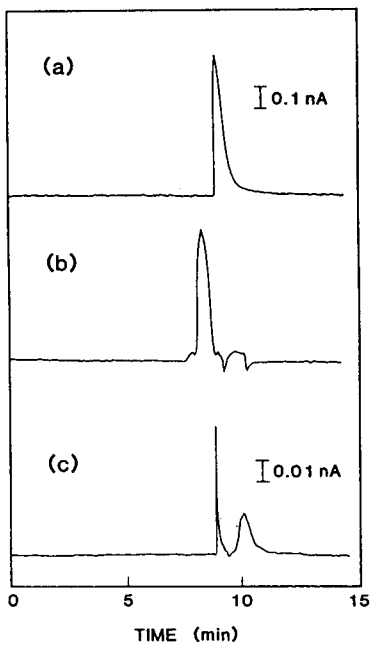

Fig. 4. Electropherograms of (a) 1 m*M* cysteine, (b) 10 m*M* cystine and (c) 10 μM cysteine and 300 μM cystine, all analytes dissolved in 10 m*M* MES pH 5.5 containing 2 m*M* EDTA. Upstream electrode : −1.0 V vs. Ag/AgCl, downstream electrode: + 0.200 V vs. Ag/AgCl. CZE conditions as in Fig. 2.

It was therefore preferred to phosphate, borate and acetate buffers, which were also tried at varying pH values ranging from 3 to 9. Fig. 4 shows the electropherograms of cysteine (a), cystine (b) and a mixture of the two (c). The migration times of the two individual peaks appeared slightly shorter than those of the mixture owing to the difference in time between the injections. After various CZE injections, the heated columns provided shorter migration times for each analyte. The different concentrations of analyte injected accounts for the different peak shapes obtained. A decrease in column voltage improved the separation although it was accompanied by a loss of efficiency and longer analysis times. A separation voltage of 20 kV was used throughout and provided the separation of both analytes in ca. 10 min. Increasing column lengths would result in a similar effect as decreasing the applied separation voltage. An average column length of 52 cm was used. The statistical data obtained from the quantitative study of cysteine and cystine following the proposed method are shown in Table 1. The poor detectability observed for cystine was caused by the low yield of cystine reduction (ca. 8%). The exposed microelectrode surface was relatively small and present only on one side of the capillary. Future work might be aimed at improving the reduction yield of the disulfide by either increasing the exposed upstream electrode surface inside the capillary or by using other dual-electrode designs.

3.3. Application to urine samples

To analyze the potential of this detector for the analysis of cysteine and cystine in real samples, urine samples from healthy volunteers were injected and evaluated. Fig. 5 shows the

Table 1
Statistical data on the quantitative determination of cysteine and cystine following the proposed method

	Cysteine	Cystine
Migration time reproducibility (R.S.D., $n = 10$ runs)	< 1%	< 1%
Migration time reproducibility (R.S.D., $n = 3$ days)	≤ 5%	≤ 5%
Peak height reproducibility (R.S.D., $n = 10$)	4.49%	5.98%
Linearity range (correlation coefficient >0.997, peak height vs. analyte concentration)	5 μM–1 m*M*	100 μM–10 m*M*
Detection limits ($S/N = 3$)	5 μM	100 μM

The specific experimental conditions are described in the text. The reproducibility tests were performed at 100 μM cysteine and 1 μM cystine concentration levels.

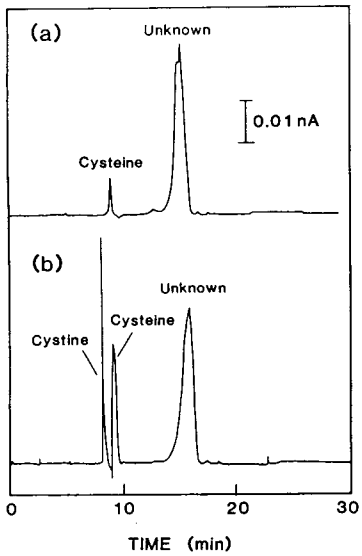

Fig. 5. Electropherogram of (a) urine diluted 1:10 and (b) the same urine sample to which 20 μM cysteine and 500 μM cystine (final concentrations) were added before injection. Conditions as in Fig. 4.

electropherogram of a tenfold dilution of human urine assayed as such (Fig. 5a) and after its spiking with cysteine and cystine at cystine concentration levels of cystinuric patients (Fig. 5b). The mean analytical recovery of spiked cysteine and cystine was 97.5% (S.D. 1.8%, $n = 3$) and 99.3% (S.D. 7.4%, $n = 3$), respectively. In this particular urine sample, a 78 μM concentration of cysteine was found, calculated by standard addition for three different determinations. This concentration is within the normal range reported [7,31]. The second compound of this electropherogram has not yet been identified. Assays from other urine samples diluted and analyzed similarly gave this unidentified peak in 50% of the volunteers. The slight shoulder observed in Fig. 5b and peak splitting observed in Fig. 5a suggests the presence of a rapidly decomposing compound or a mixture of compounds co-migrating at the same time. In any case, the analytes of interest seem to be well resolved from the unknown species. The sensitivity of the disulfide detection may be the subject of further improvement, and the application of this method to urine samples from cystinuric patients as well as to the determination of other thiolic and disulfidic species is envisaged.

Acknowledgements

B.L.L. gratefully acknowledges the Fundación Ramón Areces of Spain for a postdoctoral scholarship. The authors also thank Beckman Instruments, Inc., for support of this work.

References

[1] S. Segal and S.O. Thier in J.B. Stanbury, J.B. Wyngaarden and D.S. Frederickson, J.L. Goldstein and M.S. Brown (Editors), *The Metabolic Basis of Inherited Disease*, McGraw-Hill, New York, 1983, pp. 1774–1791.
[2] W.V. Berg and O. Kilian, *J. Clin. Chem. Clin. Biochem.*, 26 (1988) 223.
[3] S. Kelly, E. Leidhim and L. Desjardins, *Clin. Chim. Acta*, 39 (1972) 4691.
[4] J. Chrastil, *Analyst*, 115 (1990) 1383.
[5] J.C. Crawhall and D. Kalant, *Anal. Biochem.*, 172 (1988) 479.
[6] E.T. Backer, A. van den Ende and W.P. Geus, *Clin. Chim. Acta*, 165 (1987) 351.
[7] H. Birwe and A. Hesse, *Clin. Chim. Acta*, 199 (1991) 33.
[8] D.L. Rabenstein and R. Saetre, *Anal. Chem.*, 49 (1977) 1036.
[9] L.A. Allison and R.E. Shoup, *Anal. Chem.*, 55 (1983) 8.
[10] G.T. Yamashita and D.L Rabenstein, *J. Chromatogr.*, 491 (1989) 341.
[11] J.P. Richie, Jr. and C.A. Lang, *Anal. Biochem.*, 163 (1987) 9.
[12] D. Dupuy and S. Szabo, *J. Liq. Chromatogr.*, 10 (1987) 107.
[13] S.M. Lunte and P.T. Kissinger, *J. Liq. Chromatogr.*, 8 (1985) 691.
[14] T. Kuninori and J. Nishiyama, *Anal. Biochem.*, 197 (1991) 19.
[15] J. Nishiyama and T. Kuninori, *Anal. Biochem.*, 200 (1992) 230.
[16] B.L. Ling, W.R.G. Baeyens and C. Dewaele, *Anal. Chim. Acta*, 255 (1991) 283.
[17] D. Perrett and S.R. Rudge, *J. Pharm. Biomed. Anal.*, 3 (1985) 3.
[18] D. Perrett and S.R. Rudge, *J. Chromatogr.*, 294 (1984) 380.
[19] S.R. Rudge, D. Perret, P.L. Drury and A.J. Swannell, *J. Pharm. Biomed. Anal.*, 1 (1983) 205.

[20] E. Jellum, A.K. Thorsvnd and E. Time, *J. Chromatogr.*, 559 (1991) 455.
[21] B.L. Ling, W.R.G. Baeyens and C. Dewaele, *J. High Resolut. Chromatogr.*, 14 (1991) 169.
[22] T. O'Shea and S.M. Lunte, *Anal. Chem.*, 65 (1993) 247.
[23] M.J. Gordon, X. Huang, S.J. Pentoney Jr. and R.N. Zare, *Science*, 242 (1988) 224.
[24] X. Huang, R.N. Zare, S. Sloss and A.G. Ewing, *Anal. Chem.*, 63 (1991) 189.
[25] L.A. Colón, R. Dadoo and R.N. Zare, *Anal. Chem.*, 65 (1993) 476.
[26] T.J. O'Shea, R.D. Greenhagen, S.M. Lunte, C.E. Lunte, M.R. Smyth, D.M. Radzik and N. Watanabe, *J. Chromatogr.*, 593 (1992) 305.
[27] T.J. O'Shea, S.M. Lunte and W.R. LaCourse, *Anal. Chem.*, 65 (1993) 948.
[28] W.Th. Kok and Y. Sahin, *Anal. Chem.*, 65 (1993) 2497.
[29] E.G. DeMaster and B. Redfern, *Methods Enzymol.*, 143 (1987) 110.
[30] R.A. Wallingford and A.G. Ewing, *Anal. Chem.*, 59 (1987) 1762.
[31] P.R. Parvy, J.I. Bardet, D.M. Rabler and P.P. Kamoun, *Clin. Chem.*, 34 (1988) 2092.

ELSEVIER

Journal of Chromatography A, 680 (1994) 271–277

JOURNAL OF CHROMATOGRAPHY A

Simultaneous detection of thiols and disulfides by capillary electrophoresis–electrochemical detection using a mixed-valence ruthenium cyanide-modified microelectrode

Jianxun Zhou, Thomas J. O'Shea[1], Susan M. Lunte*

Center for Bioanalytical Research, University of Kansas, 2095 Constant Avenue, Lawrence, KS 66047, USA

Abstract

Thiols and disulfides are separated and detected by capillary electrophoresis–electrochemical detection using a mixed-valence ruthenium cyanide-modified microelectrode. A carbon fiber array microelectrode was employed to maximize the signal-to-noise ratio. Detection limits for glutathione disulfide, cystine and homocystine were 2.5, 1.3 and 1.1 fmol, respectively. The response for cystine was linear over two orders of magnitude with a correlation coefficient of 0.992. The long-term stability and overall reproducibility of the electrode were investigated and found to be highly dependent on the cation concentration in the electrophoretic buffer. The selectivity of this technique for disulfides was demonstrated by the detection of cystine in the urine of a patient with kidney stones.

1. Introduction

There is currently a great deal of interest in the detection of oxidized and reduced thiols in biological and chemical systems. Thiols and disulfides play important roles in drug metabolism and protein synthesis, as well as having been used as radio-protective agents and antibiotics. Examples of important thiols and their corresponding disulfides include glutathione (GSH), glutathione disulfide (GSSG), cysteine and cystine. Glutathione plays an important role in drug metabolism and toxicity. The appearance of high levels of GSSG in tissue have been shown to be related to oxidative stress. Cysteine is an amino acid which plays a critical role in protein synthesis and structure. High levels of cystine in the urine are indicative of kidney dysfunction.

The determination of disulfides is a particularly challenging analytical problem because most have no distinguishing chromophores, and the thiol group is no longer available for derivatization. One approach is to separate the thiols and disulfides into fractions, and then chemically reduce the disulfide to its corresponding thiol. The resulting thiol in each fraction is then determined colorimetrically following reaction with Ellman's reagent, 3,3′-dithiobis(6-nitrobenzoic acid) [1]. This wet chemistry is tedious, although relatively sensitive. Utilizing this chemistry, disulfides have also been detected following separation by liquid chromatography using a two-stage solid-phase

* Corresponding author.

[1] Present address: Searle Research and Development, 4901 Searle Parkway, Skokie, IL 66077, USA

0021-9673/94/$07.00
SSDI 0021-9673(94)00626-1

postcolumn reactor [2]. Disulfides have also been determined by liquid chromatography–electrochemical detection (ED) using a dual gold–mercury amalgam electrode [3]. In this case, the disulfides are reduced electrochemically prior to detection of the thiol at the second electrode.

Modified electrodes have been used for the detection of a wide variety of analytes including thiols, carbohydrates and amines [4,5]. In 1989, Cox and Gray [6] reported a new type of modified electrode based on a mixed-valence (mv) ruthenium oxide cross-linked with cyanide. This electrode has been employed for the detection of insulin, cystine and methionine following flow injection analysis [4]. More recently, Kennedy et al. [7] utilized the mv RuCN-modified electrode for direct detection of insulin in pancreatic B cells.

Capillary electrophoresis (CE) is a powerful tool for separation of a wide range of analytes, including both large and small molecules [8,9]. Thiols and disulfides have been separated by using CE prior to UV detection [10]. However, this method of detection yields poor detection limits as a results of the small optical pathlength characteristic of CE (typically less than 100 μm). In addition, the wavelength employed is 200 nm, which limits selectivity in biological matrices. Previously, we demonstrated the use of modified electrodes for ED in CE [11,12]. Since this method of detection is based on a reaction occurring at an electrode surface, the limits of detection are not compromised by the small dimensions characteristic of microcolumn-based separation systems. CE–ED has been extensively applied for the analysis of catecholamines in single cells and for the detection of amino acids and pharmaceuticals in microdialysate samples [13–17].

In this paper, the separation and detection of thiols and disulfides by CE–ED is reported. A carbon fiber array microelectrode modified with a ruthenium-containing inorganic film is employed as the working electrode. The selectivity of the method is demonstrated by the determination of cystine in urine.

2. Experimental

2.1. Chemicals and solutions

L-Cystine, D,L-homocystine and oxidized glutathione were obtained from Sigma (St. Louis, MO, USA) and used as received. Stock solutions of disulfides were prepared daily in 1 *M* HCl to a final concentration of 10 m*M*. They were then immediately diluted in 10 m*M* HCl, 10 m*M* sodium phosphate, pH 2.8, to the appropriate concentration level. Solutions were stored at 4°C until use. All solutions were made with NANOpure water (Sybron-Barnstead, Boston, MA, USA) and passed through a 0.2-μm pore size membrane filter prior to CE.

2.2. Apparatus

The construction of the basic CE system has been described elsewhere [11]. However, in this case end column detection was employed, as described by Huang et al. [18]. A 28 cm × 360 μm O.D. × 20 μm I.D. fused-silica capillary (Polymicro Technologies, Phoenix, AZ, USA) was employed in all separations. The run buffer was 10 m*M* sodium phosphate, 10 m*M* HCl, pH 2.8. Samples were injected using a laboratory-built pressure-injection system. Using the continuous fill mode, the injection volume was calculated to be 440 pl by recording the time required for the sample to reach the detector.

A BAS LC-4C amperometric detector (Bioanalytical Systems, West Lafayette, IN, USA) was used for amperometric detection in a conventional three-electrode mode. A Pt auxiliary and Ag/AgCl reference electrode were used in all studies. Electropherograms were recorded with a Model BD-41 dual-pen strip chart recorder (Kipp and Zonen, Netherlands). The detector potential was set at +850 mV unless otherwise indicated.

Cyclic voltammetry was carried out with a Model CySy-1 computerized electrochemical analyzer (Cypress Systems, Lawrence, KS, USA) in a three-electrode system cell with an

Ag/AgCl reference electrode and a platinum wire auxiliary electrode.

2.3. Construction of microelectrodes

Carbon fiber array microelectrodes were prepared as follows: a bundle (15–20) of 10-μm-diameter carbon fibers (Amoco Performance Products, Greenville, SC, USA) was carefully inserted into a 3 cm piece of fused-silica capillary of 150 μm I.D. × 360 μm O.D., until they protruded approximately 0.5 cm from one end of the capillary and approximately 1 cm out of the opposite end of the capillary. The latter was bonded to a length of copper wire using silver epoxy (Ted Pella, Redding, CA, USA). At the detection end, the carbon fibers (0.5 cm) were cut off along the cross-section of the capillary, which was then filled with epoxy (Miller-Stephenson, Danbury, CT, USA). Once cured, the capillary end was gently polished on fine emery paper until a smooth surface was achieved, with the cross-sections of carbon fibers being clearly observed. The electrode was then ultrasonicated in acetone and NANOpure water for several minutes. A single carbon fiber disk electrode was also made and used for comparison. The same preparation procedure was employed, except that a single 33-μm-diameter carbon fiber was placed in a 50 μm I.D. × 360 μm O.D. fused-silica capillary.

The modification of microelectrodes was performed according to previously reported methods [6,7,19]. Briefly, the electrode was cycled between 500 and 1100 mV vs. Ag/AgCl at a scan rate of 50 mV/s for a total of 50 cycles in a deoxygenated plating solution of 2 m*M* $RuCl_3$, 2 m*M* $K_4Ru(CN)_6$ and 0.5 *M* KCl, which had been adjusted to pH 2.0 with 1 *M* HCl. The initial and final potentials were 500 mV. Following the modification procedures, the electrode was removed from the plating solution, rinsed thoroughly with distilled water, and allowed to air dry for ca. 20 min.

Since problems were encountered with grounding of the Nafion joint at pH values below 3 (presumably due to protonation of the Nafion film), end-column detection was employed. This method, which has been described in detail by Huang et al. [18], mandates the use of capillaries of relatively small internal diameter (20 μm or less) to minimize background current due to the electrophoretic current. In this work, a "wall-jet" design similar to that previously described was used [11].

2.4. Sample preparation

Human urine samples were immediately diluted with the run buffer (1:10 dilution), filtered (2-μm pore) and directly injected onto the CE system.

3. Results and discussion

3.1. Cyclic voltammetry

A cyclic voltammogram of the modified electrode in the supporting electrolyte (solid curve) and in a solution of glutathione disulfide (dashed curve) is presented in Fig. 1. The electrode exhibited only a single redox couple in 10 m*M*

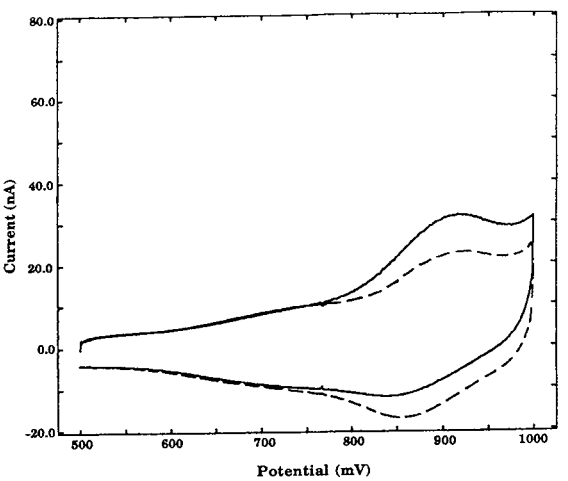

Fig. 1. Cyclic voltammogram of 10^{-4} *M* oxidized glutathione (GSSG) using the mv RuCN-modified carbon fiber array microelectrode in 10 m*M* sodium phosphate–10 m*M* HCl, pH 2.8; scan rate, 50 mV/s. Curve 1 shows the surface waves of the electrode in blank electrolyte.

sodium phosphate buffer, pH 2.8, with the anodic and cathodic peak potentials (E_{pa} and E_{pc}) around 900 and 850 mV, respectively. It has been suggested that these surface waves can be attributed to the reversible oxidation of Ru^{3+} [20,21]. The electrocatalytic oxidation of GSSG using this electrode is apparent in Fig. 1. There is an increase in the oxidation peak current upon addition of the analyte, without any obvious shift in the peak potential. This behavior is characteristic of a typical heterogeneous catalytic oxidation electrode process [5]. As is the case with other modified electrodes containing mixed-valence inorganic films [20–22], the voltammetry was found to be dependent on the cation concentration. However, the voltammetric behavior of the electrode was not dependent on the type of cation used in the supporting electrolyte.

3.2. End-column CE–ED system using a carbon fiber array microelectrode

For these studies, a disk-type microelectrode was employed. Compared to the single carbon fiber electrode, it is much easier to handle and operate and also to align with the separation capillary since it is sealed in a capillary of exactly the same outer diameter as the separation capillary [11]. In addition, its surface can be easily renewed by polishing. This attribute is particularly important for the reproducible modification of the microelectrode. One of the primary advantages of using an array electrode is that it is possible to obtain the higher current responses characteristic of a macroelectrode with these low background currents. Carbon fiber array electrodes have been used effectively as detectors for liquid chromatography [23,24] and flow injection analysis [25]. In all of these applications, the carbon fiber array electrodes have been reported to exhibit low background currents and good reproducibility. In addition, microarray electrodes have been shown to be useful for measurements at extreme positive potentials [26] and have been used in the construction of peroxidase-modified amperometric biosensors for the electrocatalytic reduction of hydrogen peroxide [27]. All of these factors prompted us to investigate the applicability of carbon fiber array electrodes for CE–ED. Therefore, a modified carbon fiber array microelectrode was used for all subsequent work.

Separation of $5 \cdot 10^{-5}$ M each of homocystine, cystine and oxidized glutathione by CE–ED using the carbon fiber array microelectrode-based detector is shown in Fig. 2. All of these homodisulfides were resolved and were easily detected at the micromolar level. Detection limits were 2.5, 3.0 and 6.2 μM for homocystine, cystine and oxidized glutathione, respectively ($S/N = 3$). Based on an injection volume of 440 pl, the mass detection limits correspond to 1.1, 1.3 and 2.5 fmol. The response of cystine was examined over the concentration range of $5 \cdot 10^{-6}$ to 10^{-4} M. Linear regression analysis yielded a slope of 0.027 nA/μM with a correlation coefficient of 0.992.

The stability of the detector response for cystine was examined using a pressure injection flow-through (FIA) system in the same capillary. A comparison of the response of the electrode in two different buffers, one containing 150 mM Na^+ and the other 10 mM Na^+, is shown in Fig. 3A. These data show that both the sensitivity and stability of electrode response are much greater in 150 mM sodium phosphate buffer than in 10 mM sodium phosphate–10 mM HCl at the same pH. This is not unexpected considering the

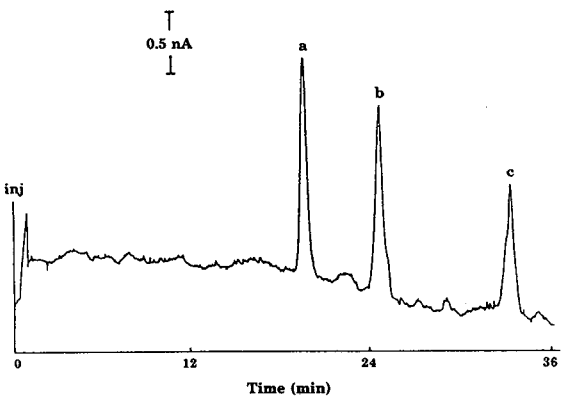

Fig. 2. Electropherogram of $5 \cdot 10^{-5}$ M each of homocystine (a), cystine (b) and GSSG (c). Buffer, 10 mM sodium phosphate–10 mM HCl, pH 2.8. Separation voltage, 20 kV. Detection potential, 850 mV vs. Ag/AgCl.

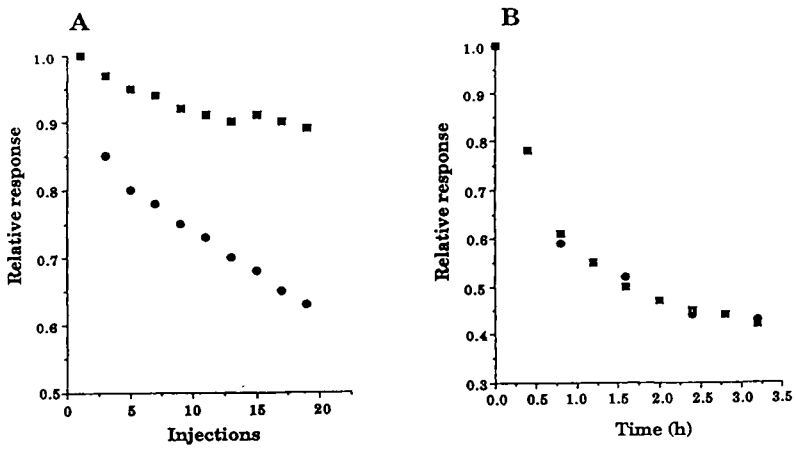

Fig. 3. (A) Relative current response for $5 \cdot 10^{-5}$ *M* cystine at the modified electrode using FIA; carrier phase in FIA is (□) 150 m*M* sodium phosphate, pH 2.8 and (○) 10 m*M* sodium phosphate–10 m*M* HCl, pH 2. Detection potential was fixed at 850 mV vs. Ag/AgCl. (B) Effect of injection frequency of cystine on detector response under CE conditions; run buffer 10 m*M* sodium phosphate; (□) injection of cystine every 15 min and (○) injection of cystine every 45 min.

requirement for a high cation concentration by the mv RuCN-modified electrode to facilitate both the electrochemical process of the deposited film and the catalytic oxidation of disulfides [6,19].

The detector stability under CE–ED conditions is shown in Fig. 3B. It was observed that the current response decreased gradually over time, and that the magnitude was essentially independent of the number of sample injections. This indicates that the reduction in response is not due to passivation of the electrode surface but to a gradual loss of catalytic activity of the film. This observation is in agreement with previous reports in which it has been suggested that the film catalyzes the oxidation of disulfides through the transfer of oxygen as well as electrons, thereby producing a non-passivating product [19].

From all of these observations, it was concluded that the decrease in detector response resulted from the continuous loss of electrochemical activity of the modified electrode due to the use of a buffer solution of inadequate cation concentration. This is confirmed by the observation of the baseline and background noise level in blank run buffer. As can be seen from Fig. 2, the electrode was relatively noisy, and exhibited a baseline drift. These same phenomena were observed in a FIA–ED system using the same buffer conditions. The noise level and baseline drift could be markedly reduced in the FIA–ED by increasing the sodium concentration in the mobile phase to 150 m*M*.

It is clear that the performance of the electrode for the catalytic oxidation of disulfides in the CE–ED system would be significantly improved if a buffer containing a high (>150 m*M*) concentration of cation were used. Unfortunately, a buffer solution of extremely high conductivity is impractical for the present CE–ED system because the high electrophoretic current causes losses in efficiency due to Joule heating and the generation of high background in the electrochemical detector. It was found that the detector response stabilized after 90 min at 850 mV vs. Ag/AgCl in the 10 m*M* sodium phosphate run buffer. Under these conditions, eight successive injections of 10^{-6} *M* cystine produced a R.S.D. value of 8.7% for peak current measurement.

The stability of the electrode can be improved by decreasing the time period at which the detection potential is applied. Only 40% of the initial response for $5 \cdot 10^{-5}$ *M* cystine remained after 4 h of continuous operation of the working electrode in the CE–ED system. On the other hand, the electrode gave 65% of the initial

current response in the same time period, as long as it was held at open circuit between sample injections. The reproducibility of electrode regeneration was also investigated. Responses for $5 \cdot 10^{-5}$ *M* cystine at ten individually modified electrode surfaces using the same electrode (with the surface being renewed by polishing) resulted in a R.S.D. of 13.2%. The catalytic current was measured for the first sample injection after the electrode had been subjected to the applied potential for approximately 30 min.

3.3. Analytical applications

Simultaneous detection of thiols and disulfides

Thiols such as cysteine and reduced glutathione (GSH) are also detected by this modified electrode. An electropherogram showing the simultaneous detection of 10^{-5} *M* GSH and $5 \cdot 10^{-5}$ *M* GSSG obtained with the CE–ED system is shown in Fig. 4A. This is the first report of the simultaneous electrochemical detection of thiols and disulfides by CE. An analytical application is shown in Fig. 4B for the determination of contaminating GSSG in commercially available GSH (Sigma). That GSH from Sigma contains a small amount of the homodisulfide GSSG has been previously demonstrated by CE using UV detection [10]. Calculations by external standard method revealed that there was about 5% of the contaminant present in the GSH sample.

Determination of urinary cystine

The urinary concentrations of cystine in patients with kidney stones are excessively high because the diminished renal tubular resorption of this compound increases its concentration in urine [28]. Cystine is poorly soluble in acid urine and when its concentration exceeds its solubility, precipitation of both crystals and stones in the urinary tract results.

The application of the CE–ED system with a mv RuCN-modified electrode for the analysis of urinary cystine from a kidney stone patient was performed in order to evaluate its performance in real sample analysis. As shown in Fig. 5, a well-defined cystine peak can be clearly iden-

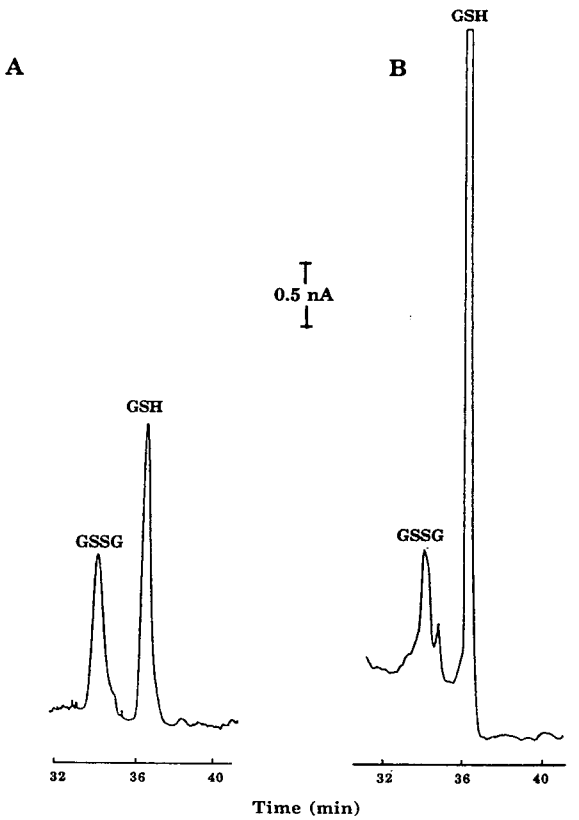

Fig. 4. (A) Electropherograms of $5 \cdot 10^{-5}$ *M* GSSG and 10^{-5} *M* GSH; (B) Electropherogram of GSH sample from Sigma, concentration: 10^{-4} *M*. Conditions as in Fig. 2.

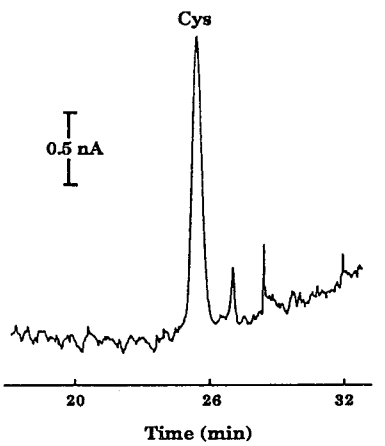

Fig. 5. Electropherogram of a urine sample (1:10 dilute) from a subject with kidney stones. The peak corresponds to $6 \cdot 10^{-4}$ *M* cystine. Conditions as in Fig. 2.

tified from the background of the urine. The concentration of cystine in this urine sample was calculated as approximately 0.6 m*M*. No cystine was detectable in urine obtained from healthy volunteers.

4. Conclusions

A modified electrode based on a mv RuCN film has been evaluated for the simultaneous detection of thiols and disulfides by CE. An end-column CE–ED system using a microarray disk carbon fiber electrode was employed. The divergence in the requirements of buffer (or cation) concentration between CE and ED is still a limiting factor in improvement of the sensitivity and reproducibility of the detection system. Possible solutions to this problem are under investigation.

Acknowledgements

The authors thank Nancy Harmony for assistance in the preparation of this manuscript. Financial support from the Center for Bioanalytical Research and the Kansas Technology Enterprise Corporation is gratefully acknowledged, as is the generous donation of a potentiostat by Bioanalytical Systems, West Lafayette, IN, USA.

References

[1] B. Fowler and A.G. Robins, *J. Chromatogr.*, 72 (1972) 105.
[2] J.F. Studebaker, S.A. Slocum and E.L. Lewis, *Anal. Chem.*, 50 (1978) 1500.
[3] L.A. Allison and R.E. Shoup, *Anal. Chem.*, 55 (1983) 8.
[4] J.A. Cox, R.K. Javorleski and P. Kulesza, *Electroanalysis*, 3 (1992) 869.
[5] R. Baldwin and K. Thomsen, *Talanta*, 38 (1991) 1.
[6] J.A. Cox and T.J. Gray, *Anal. Chem.*, 61 (1989) 2462.
[7] R.T. Kennedy, L. Huang, M.A. Atkinson and P. Dush, *Anal. Chem.*, 65 (1993) 1882.
[8] W.G. Kuhr and C.A. Monnig, *Anal. Chem.*, 64 (1992) 389R.
[9] Y. Xu, *Anal. Chem.*, 65 (1993) 425R.
[10] J.S. Stamler and J. Loscalzo, *Anal. Chem.*, 64 (1992) 779.
[11] T.J. O'Shea and S.M. Lunte, *Anal. Chem.*, 66 (1994) 307.
[12] T.J. O'Shea and S.M. Lunte, *Anal. Chem.*, 65 (1993) 247.
[13] T.M. Olefirowicz and A.G. Ewing, *Anal. Chem.*, 62 (1990) 1872.
[14] T.M. Olefirowicz and A.G. Ewing, *J. Neurosci. Methods*, 34 (1990) 11.
[15] J.B. Chien, R.A. Wallingford and A.G. Ewing, *J. Neurochem.*, 54 (1990) 633.
[16] T.J. O'Shea, M. Telting-Diaz, S.M. Lunte, C.E. Lunte and M.R. Smyth, *Electroanalysis*, 4 (1992) 463.
[17] T.J. O'Shea, P.L. Weber, B.P. Bammell, C.E. Lunte and S.M. Lunte, *J. Chromatogr.*, 608 (1992) 189.
[18] X. Huang, R.N. Zare, S. Sloss and A.G. Ewing, *Anal. Chem.*, 63 (1991) 189.
[19] J.A. Cox and T.J. Gray, *Anal. Chem.*, 62 (1990) 2742.
[20] J.A. Cox and P.T. Kulesza, *Anal. Chem.*, 56 (1984) 1021.
[21] P.J. Kulesza, *J. Electroanal. Chem.*, 220 (1987) 295.
[22] F. Li and S. Dong, *Sci. Sinica (Ser. B)*, 30 (1987) 367.
[23] S.D. Kolev, J.H.M. Simons and W.E. van der Linden, *Anal. Chim. Acta*, 273 (1993) 71.
[24] W.L. Caudill, J.O. Howell and R.M. Wightman, *Anal. Chem.*, 54 (1982) 2532.
[25] F. Belal and J.L. Anderson, *Analyst*, 110 (1985) 1493.
[26] J.L. Anderson, K.K. Whiten, J.D. Brewster, T-Y. Ou and W.K. Nonidez, *Anal. Chem.*, 57 (1985) 1366.
[27] E. Csoregi, L. Gorton and G. Marko-Varga, *Anal. Chim. Acta*, 273 (1993) 59.
[28] R. Berkow (Editor), *The Merck Manual*, Merck & Co., Rahway, NJ, 15th ed., 1987, p. 1959.

ELSEVIER

Journal of Chromatography A, 680 (1994) 279–285

JOURNAL OF CHROMATOGRAPHY A

Improvement of laser-induced fluorescence detection of amino acids in capillary zone electrophoresis

Jürgen Mattusch*, Klaus Dittrich

Department of Analytical Chemistry, UFZ-Centre for Environmental Research Leipzig–Halle Ltd., Permoserstrasse 15, D-04318 Leipzig, Germany

Abstract

Laser-induced fluorescence detection in capillary zone electrophoresis of fluorescein isothiocyanate (FITC I)-derivatized amino acids is a very sensitive detection technique. Unfortunately, the excess of FITC I and additional compounds interferes with the separation and detection of the amino acids. Therefore, the interferences were minimized by using optimal derivatization conditions. A liquid ion-exchange resin LA-2 was used to extract FITC I from the sample solution after derivatization. A better long-term stability was one of the results we obtained from optimizing the extraction step. The separations of the FITC-amino acids were performed in borate buffer solution of pH 9.5. Not all amino acids can be separated completely. The detection limits of two selected compounds, proline and arginine, were 0.3 and 0.5 n*M*, respectively.

1. Introduction

Laser-induced fluorescence (LIF) detection is the most sensitive detection technique [1–4] in capillary zone electrophoresis (CZE). Amino acids and primary amines can react with fluorescein isothiocyanate (FITC) to form highly fluorescent compounds [5–8]. The efficiency of the derivatization reaction depends on many factors; there are many interfering reactions, partly attributed to the impurities in the reagents. Therefore, it is difficult to identify the FITC-amino acid signals unambiguously and to distinguish them from the interfering peaks [5]. Previous results [9] showed that the stability of the derivatives decreases with time, leading to bad reproducibility and high detection limits. The aim of this work was to minimize the interfering effects of the amino acid determination after derivatization in different ways.

First, decreasing interferences implies that the derivatization conditions should be optimized, such as variation of buffer concentration, buffer components, buffer additives, FITC concentration and timing of the preparation.

Second, the reaction of the impurities with the FITC can be stopped by deactivating the derivatives or by minimizing their concentration to a very low level after complete reaction with the amino acids. Furthermore, it should be of interest to improve the reproducibility of the method, too. The basic idea is to decrease the FITC excess by reaction with an water-insoluble ion-exchange resin modified with amine groups simi-

* Corresponding author.

0021-9673/94/$07.00
SSDI 0021-9673(94)00324-3

lar to the derivatization of the amino acids, but differing in the FITC derivative being fixed in the organic phase. The result should be a simple liquid–liquid separation of the aqueous and organic phases.

2. Experimental

2.1. Equipment

A commercial Beckman P/ACE System 2050 with a laser-induced fluorescence detector was used for all experiments. The excitation was performed by an air-cooled argon ion laser (3 mW) at a wavelength of 488 nm. The emission intensities were measured at a wavelength of 520 ± 10 nm filtered by a band pass filter. Unless otherwise specified, the separations took place in a 57 cm (50 cm effective length) $\times$ 75 μm I.D. capillary and a voltage of 20 kV with the cathode on the detector side. The capillary was thermostated at 25°C. Sample injection was accomplished by voltage (5 kV, 5 s) or mainly by pressure (0.5 p.s.i.; 1 p.s.i. = 6894.76 Pa) for a time of 10 s. The instrument was controlled and data were collected with software Gold. The detector signals were amplified by a factor of 10 by the software.

2.2. Materials

The L-amino acids alanine (Ala), arginine (Arg), asparagine (Asn), glutamine (Gln), glutamic acid (Glu), glycine (Gly), histidine (His), isoleucine (Ile), phenylalanine (Phe), proline (Pro) and tyrosine (Tyr) were purchased from Merck (Darmstadt, Germany), the FITC isomer I (FITC I) and the ion-exchange resin Amberlite LA-2 from Fluka (Buchs, Switzerland). The 1 m*M* stock solutions of the amino acids were stored at + 4°C. The FITC I stock solution was prepared by dissolution of 19.5 mg FITC I in 100 ml acetone. After derivatization overnight 9 ml of the solution were mixed (by shaking) with a known volume of resin LA-2.

3. Results and discussion

3.1. Optimization of the derivatization reaction with FITC I

To show the influence of the kind and concentration of the buffer solution on the efficiency of the derivatization reaction L-Arg was selected as a model substance because of its short migration time. The comparison of phosphate and carbonate buffer solutions is shown in Fig. 1. The peak intensity and the peak shape strongly depend on the concentration of the buffer which varied from 4.4 to 133 m*M*. The best results (small and high peaks) were obtained at lower buffer concentrations. Similar results were also observed for disodium hydrogenphosphate solution, which was preferred for the higher sensitivity (expressed as peak area) at a concentration of 0.022 *M* and the shorter derivatization time. Working without any buffer components gives very low derivatization efficiencies and totally disturbed peak shapes. The carbonate and phosphate buffer conditions for maximum sensitivity are shown in Table 1.

Experiments on the time dependence of the derivatization have shown that pyridine recommended as activator [5] for the derivatization had no significant influence on the degree of formation of FITC-amino acid derivatives (Fig. 2). In addition, the pyridine impurities produced additional FITC derivatives which overlapped with the amino acid peaks of interest. This means that derivatization without pyridine is possible without a great decrease of efficiency.

Decreasing FITC concentrations ranging from 55.5 to 0.55 μM also led to decreasing absolute intensities of the components FITC-Arg and FITC but in every case in the same intensity ratios of FITC and FITC-amino acid (Fig. 3). It was not possible to get a high constant intensity of the analyte by decreasing the FITC concentration. Therefore, the higher concentration (55.5 μM) of FITC was used for the following investigations. A additional increase in FITC concentration to improve sensitivity is possible but interfering peaks have to be eliminated more effectively then.

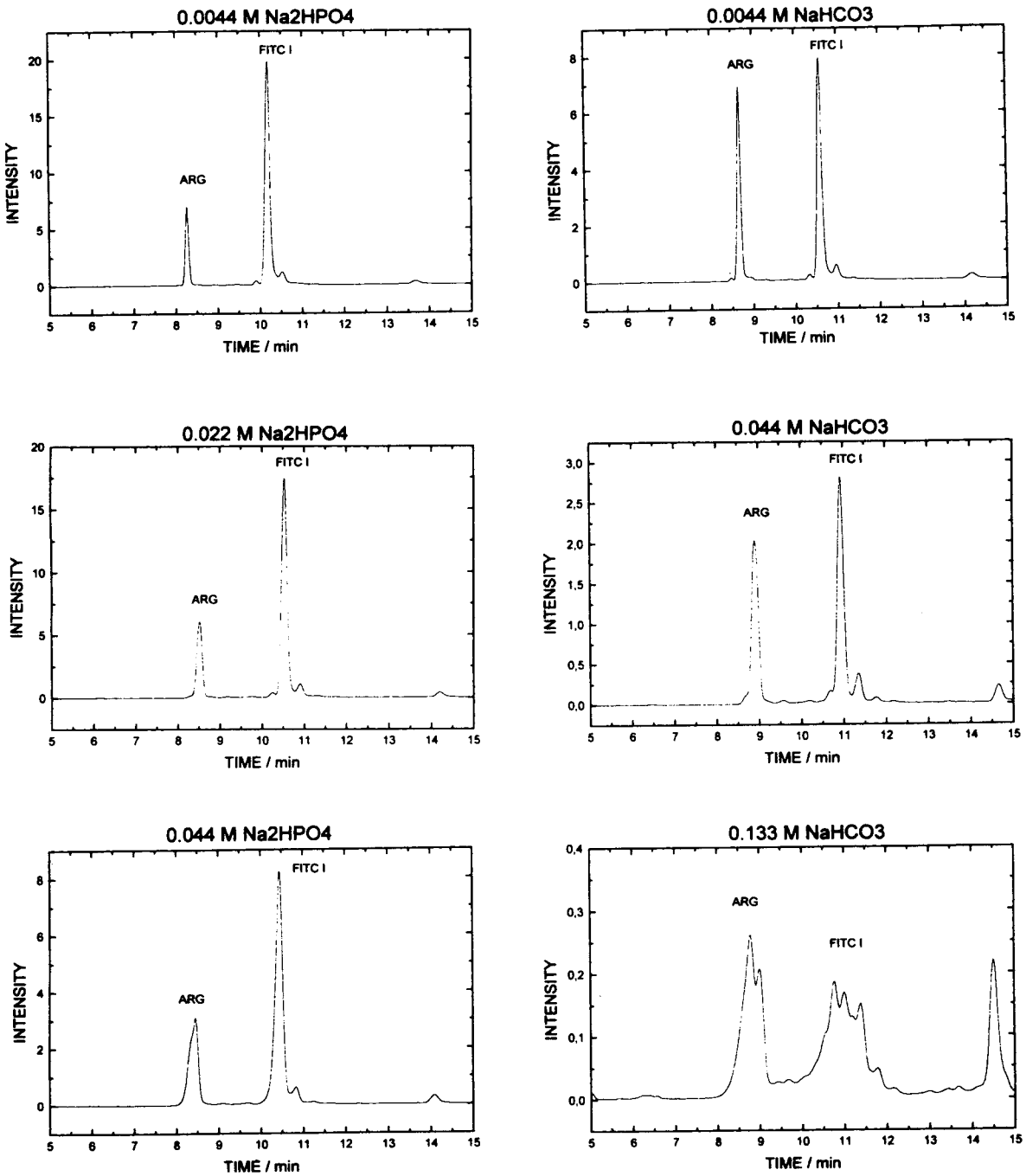

Fig. 1. Electropherograms of FITC-Arg and FITC using different buffer solutions. Derivatization conditions: FITC (11 μM), Arg (10 μM); separation conditions: borate buffer pH 9.

Table 1
Conditions for effective derivatization

Buffer	Concentration (m*M*)	pH	Reaction time (h)
Hydrogencarbonate	4.4	9	14
Hydrogenphosphate	22	9	12

Derivatization stock solutions: sodium hydrogencarbonate (0.2 *M*) and disodium hydrogenphosphate (0.2 *M*), both analytical-reagent grade.

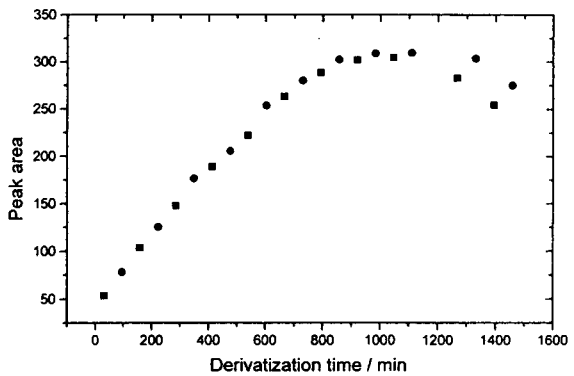

Fig. 2. Plot of peak area of FITC-Arg as a function of derivatization time with (●) and without (□) pyridine. Derivatization conditions: carbonate buffer (0.022 *M*) pH 9, FITC (11 μM), without or 10 μl pyridine/4.5 ml derivatization solution, Arg (10 μM).

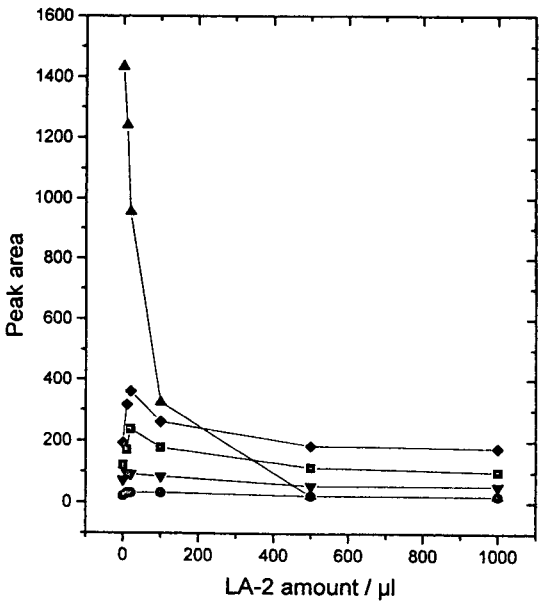

Fig. 4. Plot of peak areas of FITC-Arg (■), FITC-Pro (◆), FITC (▲) and two unknown compounds (●, ▼) as a function of added Amberlite LA-2 amount. LA-2 amount (μl)/6 ml derivatization solution, Pro (10 μM), other conditions as in Fig. 2.

3.2. Elimination of interfering components

To eliminate the interfering components corresponding to the higher FITC concentration for a more effective derivatization an ion-exchange

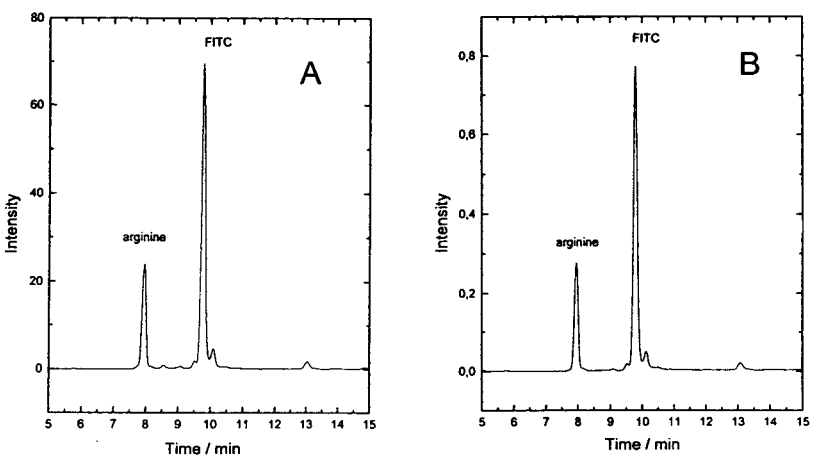

Fig. 3. Electropherograms of FITC-Arg and FITC using different FITC concentrations. Derivatization conditions: 0.022 *M* phosphate buffer pH 9.4, arginine (10 μM), (A) 55.5 μM FITC, (B) 0.55 μM FITC.

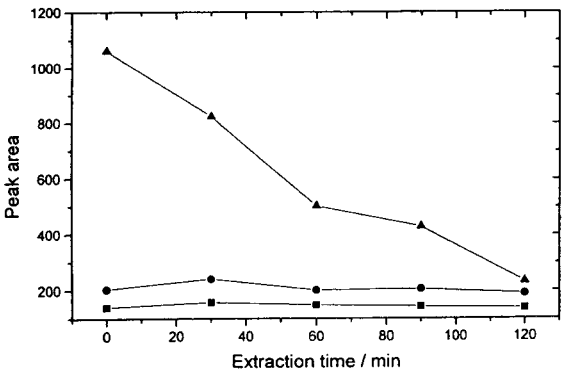

Fig. 5. Dependence of peak area of FITC-Pro (●) and FITC-Arg (■) on extraction time. Extraction condition: 10 μl LA-2/9 ml derivatization solution, other conditions as in Fig. 3. ▲ = FITC.

resin with secondary amine functionalities to react with FITC was tested. This resin was selected for three reasons: (1) the water-insoluble resin reacts with the FITC excess to decrease their concentration in the aqueous solution by liquid–liquid extraction, (2) it may stop the reaction with the amino acids at a specific time and (3) it may prevent further side reactions with impurities. Depending on the amount of the resin LA-2 the FITC intensity (expressed as peak area) is drastically reduced (Fig. 4). Unfortunately, some of the interfering peaks, the two unknowns, do not follow in the same matter. But the peak areas of FITC-Arg and FITC-Pro are unchanged so that a reaction between the derivatives and the resin did not take place. The interfering FITC resin adduct is easily separated by the distribution in the organic phase and/or a simultaneous formation of an orange precipitate in the organic phase. The aqueous phase separated from the resin phase can be used without further pretreatment for analysis. The plot of peak area *versus* extraction time in Fig. 5 with 10 μl LA-2/9 ml aqueous solution shows the reaction of LA-2 and FITC without changes in Arg and Pro intensities. One of the advantages of the FITC excess deactivation by LA-2 is also the improvement of the long-term stability of the amino acid derivatives demonstrated on Arg and Pro in Fig. 6. After a derivatization time of 12 h the liquid phases of the three samples were separated and analyzed over a period of 20 h. Contrary to the continuous increase of the peak intensities of the FITC-amino acids without LA-2 to reach a maximum the peak intensities decreased slightly in the case of LA-2 extracts (100 and 500 μl/9 ml) to reach stable signals over the time. Summarizing the results, the following conditions were selected for the most effective derivatization procedure: 55 μ*M* FITC, 22 m*M* Na_2HPO_4, reaction time 12 h, room temperature, 0.2 ml Amberlite LA-2, 30 min shaking.

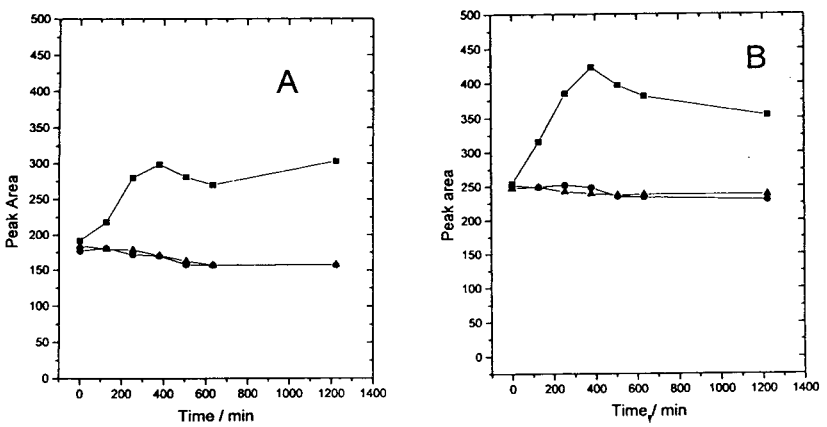

Fig. 6. Dependence of peak area of FITC-Arg and FITC-Pro on time after extraction of FITC with different amounts of LA-2 (long-term stability). LA-2 amounts/6 ml derivatization solution, time was measured after phase separation, other conditions as in Fig. 3. ■ = Without LA-2; ● = 100 μl LA-2; ▲ = 500 μl LA-2.

3.3. Optimization of the electrophoretic separation

To optimize the electrophoretic separation two main parameters were considered, *e.g.* the pH and the concentration of the buffer solution. Our previous investigations shown that the best results for FITC-amino acid separations with respect to short analysis time and high separation efficiency were obtained with a borate buffer. An increase in pH from 8.6 to 9.9 led to longer migration times for all amino acids investigated without drastic changes in sequence (Fig. 7). The elution order of FITC-amino acids depends only on the degree of the electroosmotic flow showing a maximum between pH 8 and 9. For the best combination resolution and migration time a pH value of 9.5 was chosen. By dilution of the original borate solution the migration time can be decreased even further if a complete analysis of all amino acids is not required. The migration times for all amino acids investigated may be found in Table 2. The pressure injection technique (10 s) has produced the highest sensitivity without distortion of peak shape for the FITC-amino acid detection.

The calibration for FITC-Arg and FIT-Pro has given detection limits ($S/N = 3$, 5 s peak width)

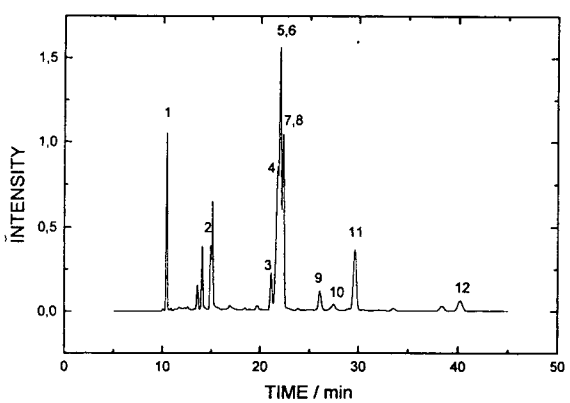

Fig. 7. Electropherogram of selected FITC-amino acids. Separation buffer: 0.4% boric acid, 0.3% sodium tetraborate pH 9.5; derivatization conditions: 0.022 *M* phosphate pH 9.4; extraction: 0.2 ml LA-2/6 ml sample solution. Peaks: 1 = Arg; 2 = $(Cys)_2$; 3 = Ile; 4 = His; 5 = Pro; 6 = Tyr; 7 = Phe; 8 = Gln; 9 = Ala; 10 = $(Cys)_2$; 11 = Gly; 12 = Glu.

Table 2
Migration times of the FITC-amino acids

Derivatives	Migration time (min)[a]	
	A	B
Ala	9.15, 13.25	26.79
Arg	7.36	10.4
Asn	11.8	15.05
$(Cys)_2$	13.45	14.28, 27.73
Gln	13.21	14.72, 22.87
Glu	19.84	41.13
Gly	14.09	31.03
His	12.21	22.12
Ile	12.07	14.51, 21.93
Phe	12.19	22.95
Pro	12.6	22.00
Tyr	12.24	22.49

Borate buffer: A = 0.2% boric acid, 0.15% sodium tetraborate, pH 9.5; B = 0.4% boric acid, 0.3% sodium tetraborate, pH 9.5

of 0.5 and 0.3 n*M*, respectively, with correlation coefficients of 0.999 in both cases. The relative standard deviations are lower then 10% for a concentration of 10 n*M*. The dynamic range is more than three orders of magnitude. The proposed method will be applied to the determination of amino acids in needles of trees and other environmental samples in addition and comparison to the traditional HPLC determination. Further investigations on this subject will be aim at a more effective separation.

Acknowledgement

This work was supported in part by BMFT.

References

[1] L.N. Amankwa, M. Albin and W.G. Kuhr, *Trends Anal. Chem.*, 11 (1992) 114.
[2] M. Albin, R. Weinberger, E. Sapp and St. Moring, *Anal. Chem.*, 63 (1991) 417.
[3] Ch. Toulas and L. Hernandez, *LC·GC Int.*, 5 (1992) 27.

[4] K. Seiler, D.J. Harrison and A. Manz, *Anal. Chem.*, 65 (1993) 1481.
[5] Y. Cheng and N.J. Dovichi, *Science (Washington, D.C.)*, 242 (1988) 562.
[6] S. Wu and N.J. Dovichi, *J. Chromatogr.*, 480 (1989) 141.
[7] B. Nickerson and J.W. Jorgenson, *J. High Resolut. Chromatogr. Chromatogr. Commun.*, 11 (1988) 878.
[8] D.S. Stegehuis, H. Irth, U.R. Tjaden and J. van der Greef, *J. Chromatogr.*, 538 (1991) 393.
[9] J. Mattusch, unpublished results.

ELSEVIER

Journal of Chromatography A, 680 (1994) 287–297

JOURNAL OF CHROMATOGRAPHY A

Capillary electrophoretic determination of amino acids with indirect absorbance detection

Y.-H. Lee, T.-I. Lin*

Department of Chemistry, National Taiwan University, Taipei 106, Taiwan

Abstract

Methods for the capillary electrophoretic (CE) analysis of a mixture of twenty common amino acids with indirect absorbance detection were developed. The suitability of nine background electrolytes (BGEs) was investigated. The effects on the CE separation of the analytes of the BGE, pH, and various additives were evaluated. Metal cations and cationic surfactants were used as buffer additives either to decrease or to reverse the electroosmotic flow in order to improve the resolution. *p*-Aminosalicylic acid and 4-(N,N-dimethyl)aminobenzoic acid are best suited as the carrier buffers and background absorbance providers as they have effective mobilities closer to the mobilities of most amino acids at alkaline pH. The CE separation of 17–19 amino acid peaks could be achieved in 20–40 min. The performance of CE in various BGEs and the influence of pH, divalent metal ions and cationic surfactants are discussed.

1. Introduction

The detection method in the capillary electrophoretic (CE) determination of amino acids is of considerable interest as it dictates whether the determination of amino acids can be routinely performed in most commercial instruments. The most widely used detection method for amino acids developed in the past is via pre- or post-column derivatization of the analytes with fluorescent probes [1–3] and detection by measuring fluorescence or laser-induced fluorescence. The fluorescence method has the advantage of high detection sensitivity, reaching attomolar mass detection limits. However, the derivatization process can be very time consuming and requires considerable additional work. The process also changes the native electrophoretic mobility of analytes. Alteration of the electrophoretic mobility of the analyte is dependent on the nature and reactive group of chemical modifying agents.

The detection of underivatized amino acids can also be accomplished by indirect methods in CE similar to those employed in liquid chromatography. In capillary zone electrophoresis (CZE), indirect fluorescence detection has been developed for a variety of analytes, including amino acids [4,5]. For the best detection limits, often a laser light source is required. Amperometric and refractive index gradient detection methods for the CE of amino acids have also been demonstrated [6,7]. Another very attractive alternative is by indirect absorbance detection, as most commercial CE systems are equipped with a UV–Vis absorbance detector and a wide variety of background absorbers are available.

* Corresponding author.

0021-9673/94/$07.00
SSDI 0021-9673(94)00314-Y

Indirect UV detection in CZE has become popular recently, and has been applied to the detection of a wide variety of analytes, *e.g.*, organic acids and bases, inorganic anions and metal cations. However, only very few studies have been made on the CE of amino acids based on indirect UV detection. Foret *et al.* [8] reported the use of benzoic acid or sorbic acid as background absorbing co-ion [or background electrolyte (BGE)] for separating organic anions including some dicarboxylic amino acids. Bruin *et al.* [9] discussed theoretical and experimental considerations for indirect detection methods in general and reported the indirect CE determination with UV detection of seven amino acids using salicylate as the BGE at pH 11.0. Ma *et al.* [10] reported the use of indirect UV detection in the CE separation of polyamines and some basic amino acids with quinine sulphate as the BGE. Quinine sulphate could also be used for indirect fluorescence detection as its quantum yield is high.

In this work, we investigated the potential use and suitability of nine BGEs for the CE determination of amino acids with indirect UV detection. The BGEs studied were sorbic, salicylic, benzoic, nicotinic, phthalic, *p*-aminosalicylic (PAS), *p*-aminobenzoic (PAB), 4-(N,N′-dimethylamino)benzoic (DMAB) and 7-amino-4-hydroxy-2-naphthalenesulphonic (AHNS) acids. The type and concentration of the BGE and pH all play a role as they influence the separation behaviour of amino acids in CE. Metal cations (Mg^{2+}, Zn^{2+} and Cu^{2+}) and long-chain cationic surfactants were employed as buffer additives either to decrease or to reverse the electroosmotic flow (EOF) in order to improve the resolution. The roles that BGEs, pH and buffer additives play in the CE separation are discussed.

2. Experimental

2.1. Chemicals

BGEs and twenty common amino acids were obtained from Sigma. All other chemicals were of analytical-reagent grade from several suppliers. Doubly deionized water prepared with a Milli-Q system (Millipore, Bedford, MA, USA) or doubly deionized, distilled water was used exclusively for all solutions. Metal cation additives were chloride salts.

Buffers and pH adjustment

Sorbic, nicotinic, benzoic, phthalic, DMAB and AHNS acids and sodium salts of salicylic, PAS and PAB acids were prepared as 0.01 *M* stock standard solutions. These were diluted to 5 or 10 m*M* of BGE and the pH was adjusted as required, by adding aliquots of 1 *M* NaOH, from 10 to 11.2, depending on the experiments, as specified in the figures. As the buffer had a fairly high pH, if exposed to air the pH could be lowered by dissolution of CO_2, hence the vial must be capped tightly immediately after use. The original pH could be maintained for 3–4 days. The pH of the buffer was checked periodically and readjusted if necessary. For the surfactant experiments, dodecyltrimethylammonium bromide (DTAB), tetradecyltrimethylammonium bromide (TTAB) and cetyltrimethylammonium bromide (CTAB) were employed. Surfactant solutions of 10 m*M* were prepared, containing 10 m*M* BGE, and then diluted to the desired concentration.

2.2. Apparatus

CE experiments were carried out in a fully automated Spectra Phoresis Model 1000 instrument (Spectra-Physics, San Jose, CA, USA) as described previously [11]. In most experiments except in the determination of the electrophoretic mobility of BGEs, the detector wavelength was fixed at the optimum value depending on the BGE used (see Table 1). In indirect detection, peaks in the electropherogram appeared originally as negative peaks but were inverted to positive peaks by using the vendor's software. The separation capillaries (bare fused silica) from Polymicro Technologies (Phoenix, AZ, USA) were 75 μm I.D. (365 μm O.D.) × 70 cm (63 cm to the detector) for the determination of the mobilities of BGEs and 75 μm I.D. (365 μm

O.D.) × 90 cm (83 cm to the detector) for the separation of mixtures of amino acids. UV–Vis absorption of the BGEs were measured with a Model U-2000 double-beam scanning spectrophotometer (Hitachi, Tokyo, Japan).

2.3. Electrophoretic procedures

Prior to first use, a new capillary was subjected to a standard wash cycle, and subsequent runs were carried out according to the established procedure [11]. Stock 10 m*M* solutions of amino acids were prepared in deionized water. Equal aliquots of each were mixed to obtain a mixture of twenty amino acids, each with a final concentration of 5×10^{-4} *M*. Sample injection was effected in the hydrodynamic (HD) mode for 1 s. The separation run was carried out at +20 kV constant voltage at 25°C constant temperature and with a current of 7–10 μA. All buffer solutions were filtered through 0.20-μm membranes and degassed under vacuum for 10 min. Between runs, the capillary was post-washed with deionized water for 5 min. As a daily routine, the capillary was prewashed in the following sequence: (a) 0.1 *M* NaOH, (b) deionized water, 10 min each at 60°C, (c) deionized water, 5 min at 25°C and (d) running buffer, 10 min at 25°C.

Peak identification for each analyte was carried out by spiking with known standards and the peaks with increased height were identified.

2.4. Electrophoretic mobility determination

Benzyl alcohol was added to the samples as a neutral marker for the electrophoretic mobility determination. The mobilities of various BGEs under the specified CE conditions were determined in the buffer containing 10 m*M* sodium borate and 10 m*M* sodium phosphate at pH 11.0. A mixture of all BGEs, 0.1 m*M* each in deionized water at pH 11.0, was injected in the HD mode for 1 s. The CE voltage applied was +15 kV. Detection was effected by rapid scanning of the absorbance from 200 to 350 nm, which allowed a positive identification of the background provider. The electroosmotic mobility (μ_{eo}, in $cm^2\ V^{-1}\ s^{-1}$) is calculated by the following equation:

$$\mu_{eo} = l_d l_t / (t_m V)$$

$$\mu_e = \mu_{obs} - \mu_{eo}$$

where l_d and l_t are the length of the capillary to the detector and the total length of the capillary, respectively, V is the running voltage and t_m the migration time of the neutral marker (benzyl alcohol). The electrophoretic mobility of the BGE, μ_e, is obtained by subtracting μ_{eo} from the observed mobility, μ_{obs}.

3. Results and discussion

3.1. General considerations for selecting BGE

In selecting a BGE suitable for CE, the mobility of the BGE and the molar absorptivity of the BGE in the wavelength region where the BGE and amino acids both absorb were taken into consideration. A BGE with a mobility matching those of the majority of the analytes would give a better separation and resolution. The absorbance of the BGE should be high and, ideally, should not overlap with those of the analytes. To avoid the absorbance from the aromatic amino acid residues, the wavelength region 265–285 nm should be avoided. In Fig. 1, a three-dimensional spectral scan of the CE of six BGEs is presented to show the absorption spectral characteristics of various BGEs. The optimum detection wavelengths are summarized in Table 1.

In order to maximize the negative charges carried by the analytes, the pH was set between 10 and 11.2. In this pH range, the amine group is unprotonated and all BGEs carry negative charges. The electrophoretic mobility (in $cm^2\ V^{-1}\ s^{-1} \times 10^3$) of amino acids (not counting the basic amino acids, Arg and Lys) varies from −0.100 (proline) to −0.440 (aspartic acid). The mobilities of the BGEs are in the range −0.249 to −0.329 (Table 1). Hence no single BGE could accommodate all amino acids with good res-

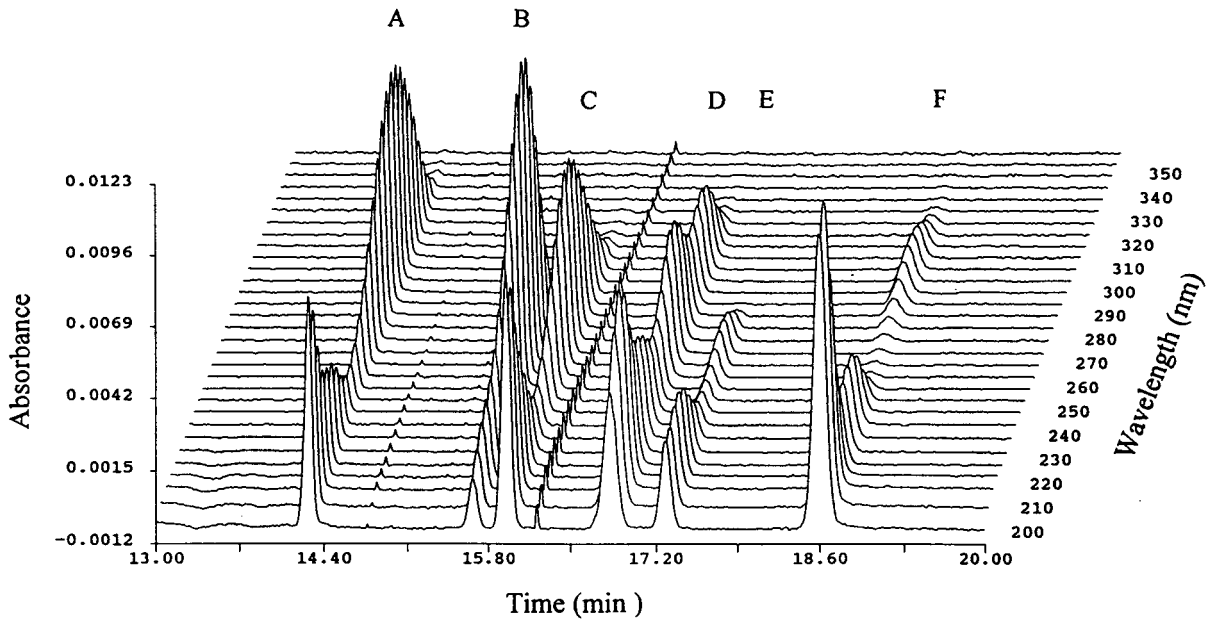

Fig. 1. Three-dimensional spectral view of CE separation of a mixture of six BGEs: (A) DMAB, (B) sorbic, (C) PAB, (D) PAS, (E) nicotinic and (F) salicylic acids. Conditions same as in the mobility determination (see Experimental for details).

olution. Our search with nine BGEs resulted in finding two BGEs that serve better than the others. Under optimum conditions, nineteen peaks could be resolved with at least seventeen peaks completely separated at the baseline level. Among the twenty amino acids, leucine (Leu) and isoleucine (Ile) have the closest structural and charge similarity, and hence are the most difficult to separate.

3.2. Separation of the amino acids in DMAB and PAS

Among the BGEs that were investigated, DMAB and PAS gave the best overall results. Fig. 2a shows the electropherogram of twenty amino acids in 10 m*M* DMAB at pH 11.0. Seventeen amino acid peaks are identified. The Arg peak merged with the system peak (the

Table 1
pK_a values, electrophoretic mobilities, electroosmotic velocities and detection wavelengths for various BGEs

BGE acid	pK_a	Mobility[a] ($cm^2\ kV^{-1}\ s^{-1}$)	μ_{eo}[b] ($cm^2\ kV^{-1}\ s^{-1}$)	Detection wavelength (nm)
Salicylic	2.94	−0.329	0.796	230
Nicotinic	4.82	−0.309	0.770	263
PAS	3.25	−0.301	0.766	266
Benzoic	4.19	−0.290		222
PAB	4.94	−0.285	0.756	266
Sorbic	4.77	−0.281	0.737	254
DMAB	6.03	−0.249	0.714	288

[a] See Experimental for details.
[b] Mean value ($n = 5$); relative standard deviation <0.2%.

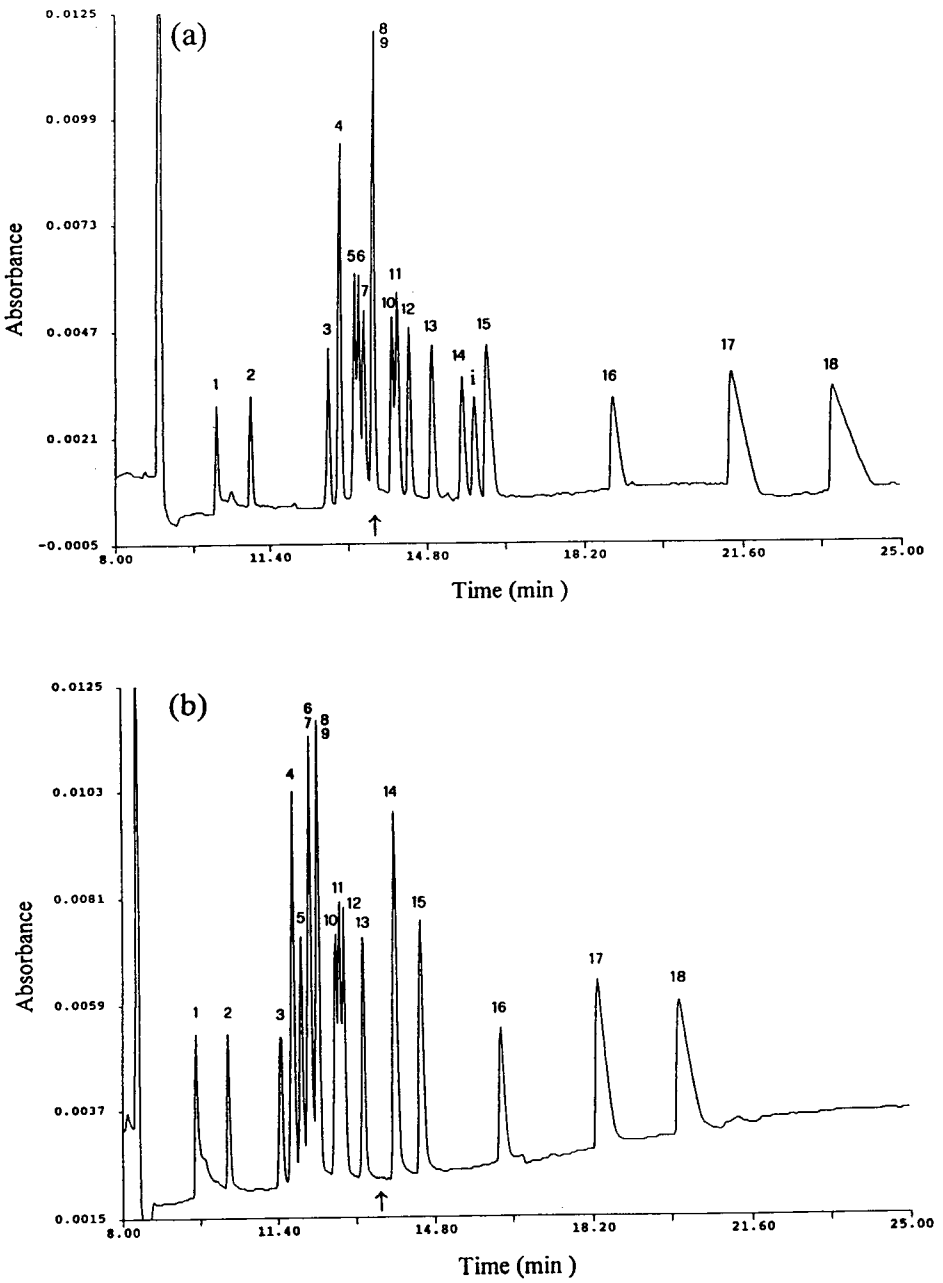

Fig. 2. Electropherograms of twenty common amino acids in 10 m*M* (a) DMAB and (b) PAS at pH 11.0. Concentrations of amino acids, 0.5 m*M* each. Migration order (peaks): 1 = Lys; 2 = Pro; 3 = Trp; 4 = Leu, Ile; 5 = Phe; 6 = Val; 7 = His; 8 = Met; 9 = Gln; 10 = Ala; 11 = Thr; 12 = Asn; 13 = Ser; 14 = Gly; 15 = Tyr; 16 = Cys; 17 = Glu; 18 = Asp. Peak i is the internal marker (benzoic acid). Arg is merged with the system peak (the first peak). The upward arrows indicate the migration positions of the BGEs.

leading peak). The migration order for the twenty amino acids is as follows: (0) Arg, system peak, (1) Lys, (2) Pro, (3) Trp, (4) Leu, Ile (not resolved), (5) Phe, (6) Val, (7) His, (8) Met, (9) Gln, (10) Ala, (11) Thr, (12) Asn, (13) Ser, (14) Gly, (i) internal marker, benzoic acid, (15) Tyr, (16) Cys, (17) Glu and (18) Asp. Peaks are labelled in this way throughout the text and figures.

In DMAB, Met and Gln (peaks 8 and 9) could not be separated; peaks 5–7 and peaks 10 and 11 could not be baseline resolved. Leu and Ile could not be separated at all in any of the BGEs. The electropherogram of the mixtures in PAS is presented in Fig. 2b. The migration pattern is similar to that in DMAB, but the profiles are different in the region where the peaks (peaks 5–12 from 12 to 14 min) are most congested and difficult to resolve. In PAS, only sixteen peaks are resolved. Phe (peak 5) could be separated but Val and His are merged (peaks 6 and 7). Met and Gln (peaks 8 and 9) still could not be separated. The separation among Ala, Thr and Asn (peaks 10–12) is worse.

3.3. Effects of Mg^{2+}, Zn^{2+} and Cu^{2+} as buffer additives

In order to improve the resolution of amino acids in the most congested region (time span between 12 and 14 min.), means to decrease the EOF was sought. Decreasing the EOF would allow the analytes more time to be resolved. Previous studies [12,13] have shown that the addition of metal ions leads to better separations and improves the number of theoretical plates in the micellar CE of oligonucleotides and in the separation of sulphonate and sulphate surfactants. Addition of metal cations could neutralize the negative charges on the bare silica capillary wall, thus decreasing the EOF. However, these cations also form complexes with the BGEs (formation constant $Cu^{2+} > Zn^{2+} > Mg^{2+}$). Because the formation constant of Mg^{2+} is lower, the extent of complex formation with BGE is less. Mg^{2+} is most effective in decreasing the EOF, as shown in Fig. 3. The extent of the decrease in EOF increases as the concentration

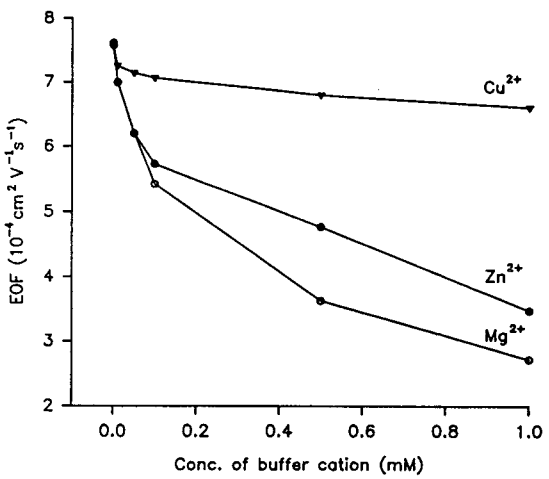

Fig. 3. Effect of divalent metal cations on EOF in 10 m*M* PAS at pH 11.0.

of cation is raised. However, concentrations of cation higher than 0.1 m*M* result in a significant increase in the overall separation time. The optimum Mg^{2+} concentration is about 0.05 m*M*. When the Zn^{2+} concentration is >0.1 m*M*, precipitates will form. Note that complex formation of metals with BGEs also results in alterations of the charge and mobility of the BGE. Of the three metal ions studied, Cu^{2+} is the least suitable.

The electropherogram in 10 m*M* PAS in the presence of 0.05 m*M* Mg^{2+} is presented in Fig. 4. In comparison with Fig. 2b, the addition of Mg^{2+} improves the separation of the peaks in the congested region, particularly for Ala, Thr and Asn (peaks 10–12). However, Val and Phe (peaks 5 and 6) are merged as one peak, and so are Met and Gln (peaks 8 and 9). Note also that the overall separation time is about 8 min longer for the mid-region, and is double for the last three peaks owing to the decrease in EOF.

3.4. Influence of pH

A major factor affecting electrophoretic separations in almost every kind of CE is pH. Its effects are manifested in several ways: (1) in ionizing analytes and BGEs and affecting their mobilities, (2) in altering charges on the capillary

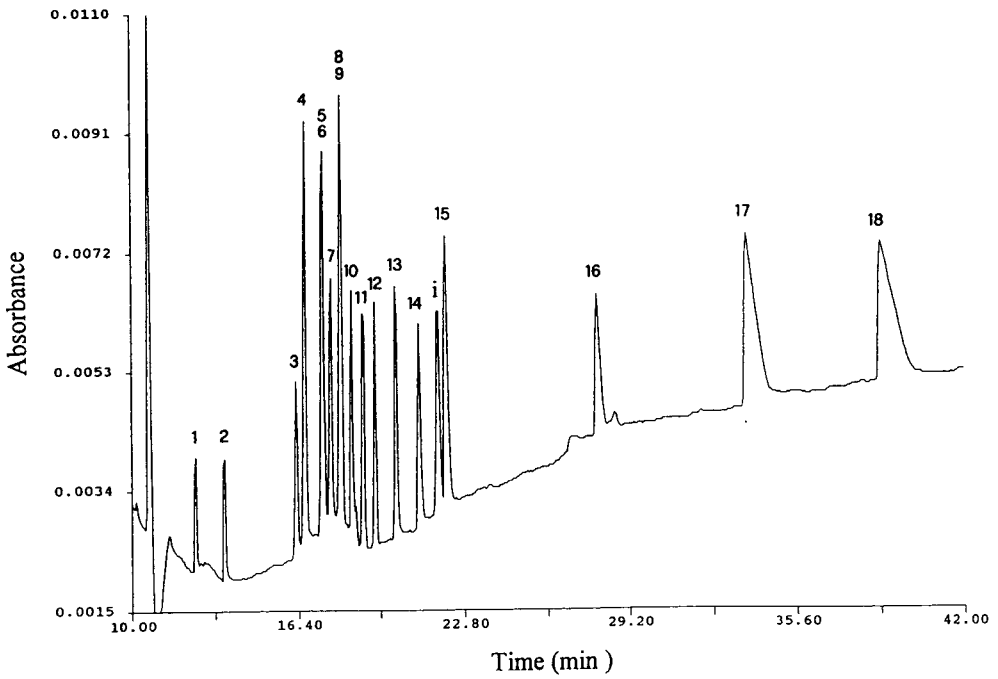

Fig. 4. Electropherogram of twenty common amino acids in 10 m*M* PAS–0.05 m*M* Mg^{2+} at pH 11.1.

surface, thus affecting the EOF, and (3) in changing the extent of complexation between the BGE and metal ion additive. Fig. 5 is a plot of pH *vs.* the electrophoretic mobilities for ten selected amino acids in 10 m*M* PAS–0.05 m*M* Mg^{2+} in the pH range 10.0–11.2. In this range, the change in mobility is associated with the pK_2 or pK_3 of the analytes. In general, the α-amino groups of aliphatic amino acids have larger p*K*s and they are more sensitive to pH. They exhibit a sharper slope in the plot. They are also the analytes in the most congested region, and therefore are the most difficult to separate. At pH 10.3, nineteen peaks could be identified, but the peaks of Met and Gln (peaks 8 and 9) and of Ser and Tyr (peaks 13 and 15) are only partially resolved (Fig. 6). Note that the migration order for peaks 3–10 changes significantly. The last three peaks are also delayed by about 30 min owing to the decrease in EOF.

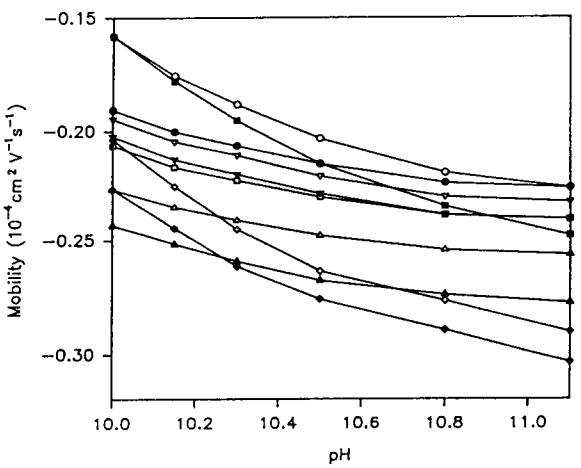

Fig. 5. Effect of pH on the electrophoretic mobility of selected amino acids in 10 m*M* PAS–0.05 m*M* Mg^{2+}. ○ = Val; ▽ = His; □ = Gln; △ = Thr; ◇ = Gly; ● = Phe; ▼ = Met; ■ = Ala; ▲ = Ser; ◆ = Tyr.

3.5. Influence of cationic surfactants on CE

To improve the resolution further, the influence of some cationic surfactants on CE was investigated. Surfactants affect the CE separation mainly by dynamically controlling the EOF [14]. There have been several reports on im-

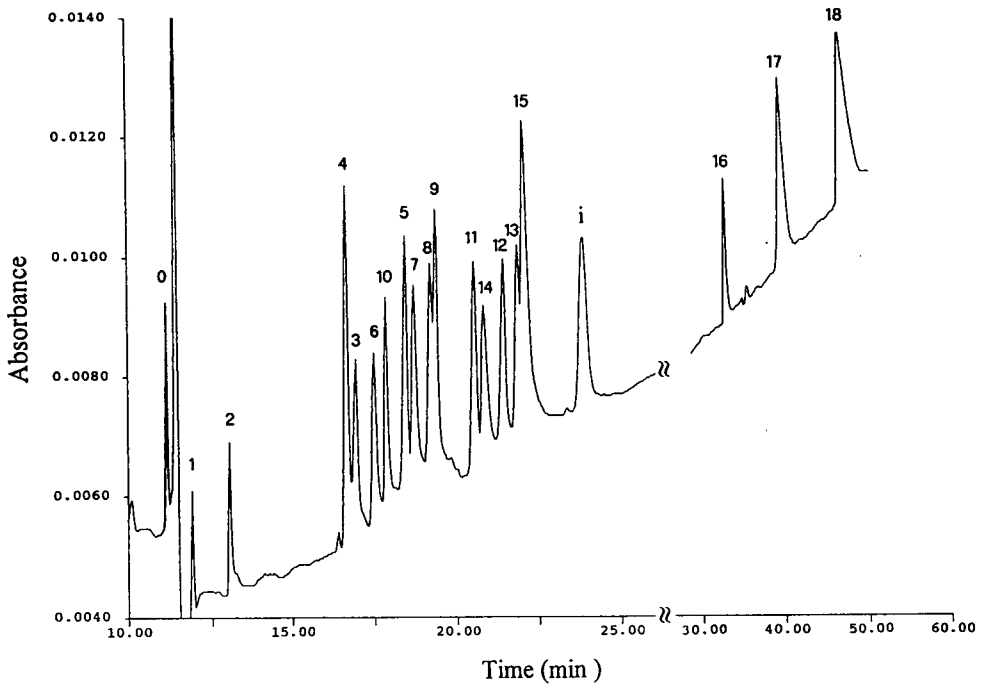

Fig. 6. Electropherogram of twenty common amino acids in 10 m*M* PAS–0.05 m*M* Mg^{2+} at pH 10.3. The leading peak (0) is Arg, separable from the system peak.

provements of resolution in CE separations of catecholamines [15], inorganic anions [16], urea herbicides, alkylbenzenes and phenylalkyl alcohols [17] by the addition of cationic surfactants. The effects of three cationic surfactants, DTAB, TTAB and CTAB, are illustrated in Fig. 7. Surfactants with longer straight alkyl chains, e.g. CTAB and TTAB, are more effective in reversing the EOF. Complete reversal of the EOF is achieved with 0.05 m*M* CTAB or 0.1 m*M* TTAB. On the other hand, 1 m*M* DTAB would be required to obtain a similar decrease in EOF. At these concentrations, the surfactants are well below their critical micelle concentrations (CMC). Above the CMC, the EOF is less affected by the concentration of the surfactant. The electropherogram of a mixture in 10 m*M* PAS in the presence of 0.25 m*M* DTAB at pH 10.9 is displayed in Fig. 8. Seventeen analyte peaks could be detected. However, Phe and Val (peaks 5 and 6), and Met and Gln (peaks 8 and 9) could not be separated. In DTAB, the baseline is flatter and the overall separation time span is about 3 min shorter. In 0.05 m*M* CTAB, the EOF is completely reversed. The CE separation of amino acids could be performed with

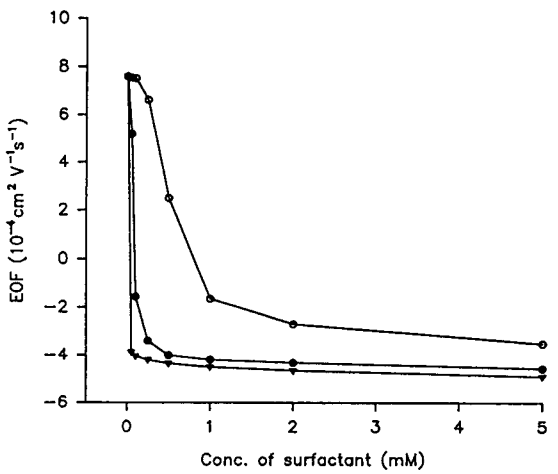

Fig. 7. Effect of cationic surfactants on EOF in 10 m*M* PAS at pH 11.0. ○ = DTAB; ● = TTAB; ▽ = CTAB.

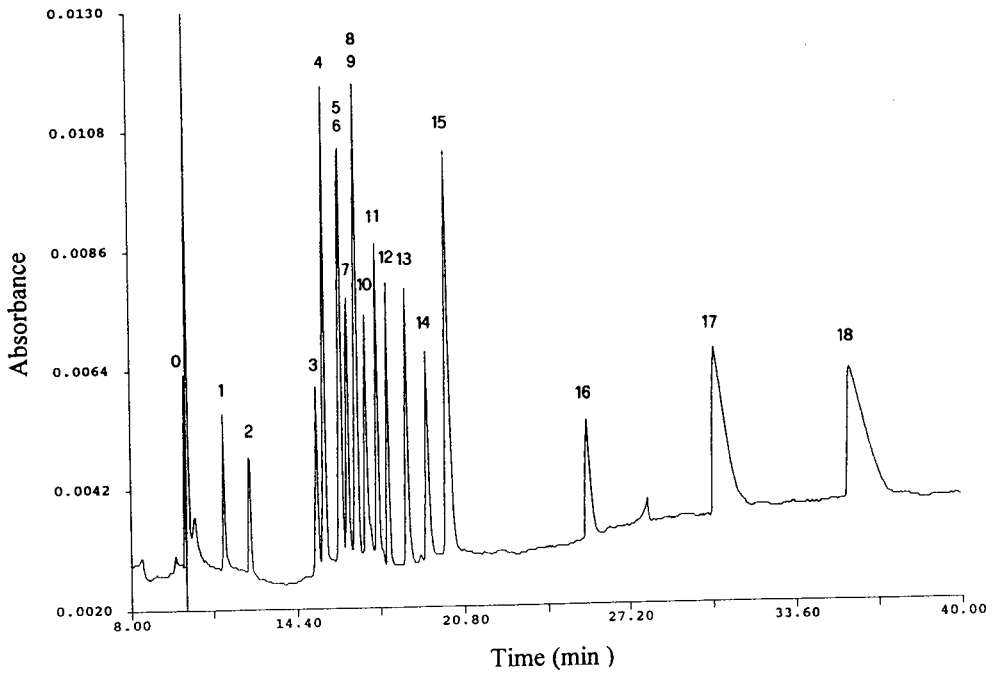

Fig. 8. Electropherogram of twenty common amino acids in 10 m*M* PAS–0.25 m*M* DTAB at pH 10.9. The leading peak (0) is Arg.

reversed polarity (applying a negative voltage); the analytes would then run toward anode. The migration order of all analytes is reversed completely. The negatively charged Asp and Glu (peaks 18 and 17) come out first (Fig. 9). Two advantages could be realized by running with reversed polarity: (1) the separation time span is significantly shorter and (2) acidic analytes exhibit sharper and more symmetric peaks. However, the separation for peaks 5–9 is only partial.

3.6. Separation of amino acids in other BGEs

The use of salicylic acid as the BGE has been reported [9], but the mobility is fairly high (*i.e.*, more negative in value) and its absorptivity at 230 nm is only moderate. When CE is performed in salicylate buffer (electropherogram not shown), only the peaks of the slowly migrating Cys, Glu and Asp are improved by shortening the migration time and narrowing the peak width. Similar results were obtained with nicotinic acid. Hence they are not suitable as BGEs for the complete separation of all amino acids with indirect detection. Phthalic acid is not a good BGE if used alone, but could be mixed with a less mobile (towards the anode) BGE to improve the peak width for the acidic residues. AHNS is a larger molecule and may interact strongly with the analytes and the capillary wall, resulting in peak broadening and baseline drift. Another BGE that has been studied is PAB. Similarly to PAS, CE performed in PAB gives a good separation of at least seventeen peaks (electropherogram similar to Fig. 2b; data not shown). However, PAB is not stable in alkaline solution; a faint brown colour appears in the buffer solution after applying a high voltage. Although sorbic acid has a high molar absorptivity and the CE resolution appears to be as good as with PAS, the sensitivity appears to be only half that in PAS. Therefore, judged from

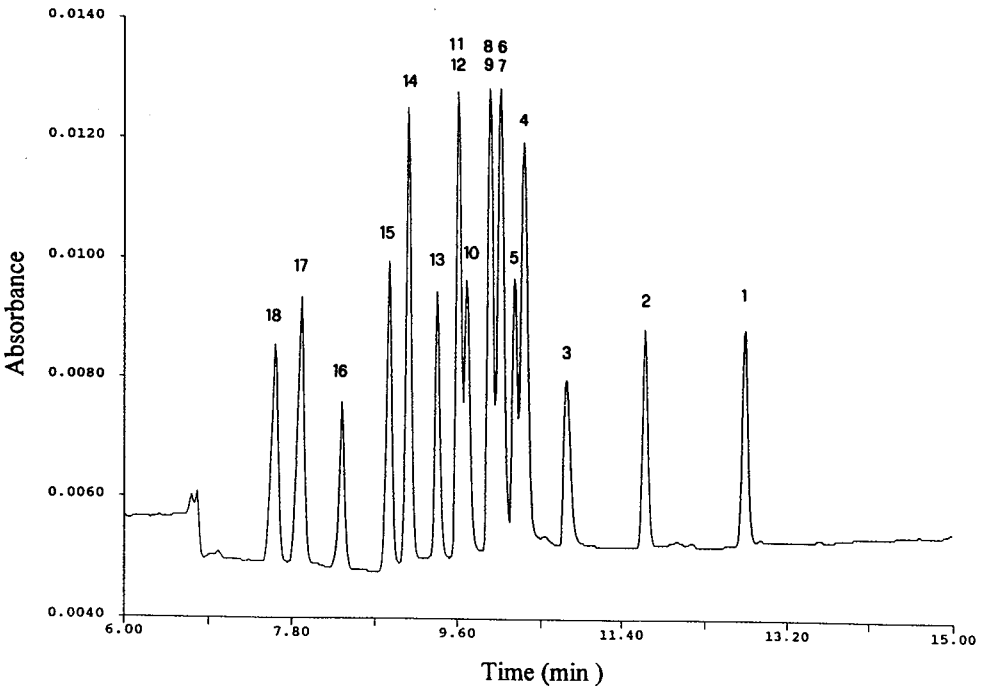

Fig. 9. Electropherogram of twenty common amino acids in 10 m*M* PAS–0.05 m*M* CTAB at pH 11.0 running with reversed polarity (towards the anode).

the overall performance, PAS and DMAB appear to be the best.

4. Conclusions

The effective CE separation and detection of 17–19 peaks for twenty acids could be achieved using commercial CE instruments with indirect UV absorbance methods. Of the nine BGEs studied, PAS and DMAB (10 m*M*) appear to be best suited for the analysis, running at pH 10.3–11.2. Resolution is also improved by the addition of Mg^{2+} (0.05 m*M*), DTAB (0.25 m*M*) or CTAB (0.05 m*M*) as buffer additives.

Acknowledgement

This work was supported by grant NSC83-0208-M002-068 from the National Science Council, Taiwan.

References

[1] S.F.Y. Li, *Capillary Electrophoresis*, Elsevier, Amsterdam, 1992, Ch. 7.
[2] J. Liu, Y.-Z. Hsieh, D. Wiesler and M. Novotny, *Anal. Chem.*, 63 (1991) 408.
[3] M. Albin, R. Weinberger, E. Sapp and S. Moring, *Anal. Chem.*, 63 (1991) 417.
[4] W.G. Kuhr and E.S. Yeung, *Anal. Chem.*, 60 (1988) 1832.
[5] E.S. Yeung and W.G. Kuhr, *Anal. Chem.*, 63 (1991) 275A.
[6] T.M. Olefirowicz and A.G. Ewing, *J. Chromatogr.*, 499 (1990) 713.
[7] J. Pawliszyn, *Anal. Chem.*, 60 (1988) 2796.
[8] F. Foret, S. Fanali, L. Ossicini and P. Bocek, *J. Chromatogr.*, 470 (1989) 299.
[9] G.J.M. Bruin, A.C. van Asten, X. Xu and H. Poppe, *J. Chromatogr.*, 608 (1992) 979.
[10] Y. Ma, R. Zhang and C.L. Cooper, *J. Chromatogr.*, 608 (1992) 93.
[11] T.-I. Lin, Y.-H. Lee and Y.-C. Chen, *J. Chromatogr. A*, 654 (1993) 167.
[12] S. Chen and D.J. Pietrzyk, *Anal. Chem.*, 65 (1993) 2770.
[13] A.S. Cohen, S. Terabe, J.A. Smith and B.L. Karger, *Anal. Chem.*, 59 (1987) 1021.

[14] H.-T. Chang and E.S. Yeung, *Anal. Chem.*, 65 (1993) 650.
[15] T. Kaneta, S. Tanaka and H. Yoshida, *J. Chromatogr.*, 538 (1991) 385.
[16] T. Kaneta, S. Tanaka, M. Taga and H. Yoshida, *Anal. Chem.*, 64 (1992) 798.
[17] D. Crosby and Z. El Rassi, *J. Liq. Chromatogr.*, 16 (1993) 2161.

ELSEVIER

Journal of Chromatography A, 680 (1994) 299–310

JOURNAL OF CHROMATOGRAPHY A

Analysis of dansyl amino acids in feedstuffs and skin by micellar electrokinetic capillary chromatography

Søren Michaelsen*[,a], Peter Møller[b], Hilmer Sørensen[b]

[a] *Department of Research in Small Animals, National Institute of Animal Science, Research Centre Foulum, P.O. Box 39, DK-8830 Tjele, Denmark*

[b] *Chemistry Department, Royal Veterinary and Agricultural University, 40 Thorvaldsensvej, DK-1871 Frederiksberg C, Denmark*

Abstract

Micellar electrokinetic capillary chromatography (MECC) using sodium dodecyl sulphate (SDS) and sodium cholate have been used for analyses of 30 dansylated (Dns) amino acids. The influences of sample preparation, Dns/amino acid ratio, sample solvent composition, and separation conditions including voltage, temperature, pH and buffer composition were investigated. Complete separations of acidic and neutral amino acids were obtained within 45 min in the SDS system. The efficiency expressed as number of theoretical plates for the applied capillary 0.52 m long were between 210 000 and 343 000, and the repeatability was very good with relative standard deviations on relative migration times between 0.09 and 0.70% and on relative normalised peak areas (RNPAs) between 0.85 and 3.41%. The linearity studies gave correlation coefficients between 0.9957 and 0.9993 for RNPAs against concentration. Detection limits were between 3 and 6 fmol or approximately 2 pg of each amino acid. Basic amino acids were separated in a MECC system using sodium cholate. Procedures and problems using Dns derivatisation for amino acids analysed by the MECC methods are described. Finally, examples of analyses of hydrolysates of real complex samples show, that this method can be applied to determine the amino acid composition of proteins in feedstuffs and skin.

1. Introduction

Efficient methods of amino acid analyses are required in connection with determining the nutritional value of proteins in food and feedstuffs including the special non-protein amino acids [1]. Furthermore, studies of the properties of connective tissues such as skin also requires suitable methods of analyses for the amino acids in especially the proteins collagen and elastin. The amino acid composition of such proteins includes Pro, 4-HyPro, 5-HyLys (Hy = hydroxy), desmosine and isodesmosine [2]. Analyses of secondary amines and imino acids like Pro and 4-HyPro demands special derivatisation methods [1,2]. Dansyl (Dns) derivatisation is well suited, as it works on secondary amino groups, and the obtained derivatives are very stable [1].

High-performance capillary electrophoresis (HPCE) methods have gained increasing interest due to their many advantages [3]. Many HPCE papers describing amino acid separations have

* Corresponding author. Present address: Novo Nordisk A/S, Biochemicals, Bygning SMH, Mørkhøj Bygade 28, DK-2880 Søborg, Denmark.

0021-9673/94/$07.00
SSDI 0021-9673(94)00365-G

been published. The methods published include the use of Dns-amino acid derivatives [4–8], phenylthiohydantoin (PTH) [9,10], naphthalene dicarboxaldehyde (NDA) [11,12], dabsyl [13,14], fluorescein isothiocyanate (FITC) [15–17], *o*-phthaldialdehyde (OPA) [17,18], fluorescamine [4,17], 9-fluorenylmethylchloroformate (FMOC) [17] and 3-(4-carboxybenzoyl)-2-quinoline carboxaldehyde (CBQCA) [19]. The HPCE methods described in these papers include free zone and micellar electrokinetic capillary chromatography (MECC) as well as inclusion chromatography for amino acid enantiomers. The MECC methods show the most promising results. However, most papers are only dealing with few amino acids and with purchased amino acid derivatives of various types. Hereby problems with interfering reagent compounds have not been considered, Furthermore, the performance including the qualitative aspects of the methods have not been reported. Finally, results from analyses of amino acids in hydrolysates of complex samples like feedstuffs and skin have not been reported either.

This paper describes the use of MECC with sodium dodecyl sulphate (SDS) and sodium cholate for analysing Dns-amino acids. The influences of sample preparation, Dns/amino acid ratio, sample solvent composition, and separation conditions including voltage, temperature, pH and buffer composition were investigated. Procedures and problems using Dns derivatisation for amino acids analysed by HPCE are reported. Determination of the performance including linearity, repeatability and response factors were performed. Finally, amino acid analyses of real complex samples are shown. The procedure described gives an efficient and reliable determination of amino acids in complex samples.

2. Experimental

2.1. Apparatus

An ABI Model 270 A-HT capillary electrophoresis system and a Model 600 data analysis system was used (Applied Biosystems, Foster City, CA, USA). The fused silica capillary was 720 mm × 50 μm I.D. (J & W Scientific, Folsom, CA, USA), and the detection point was 520 mm from the injection end of the capillary.

2.2. Materials and reagents

Free amino acids including *cis*-4-Hy-L-Pro (C4Hy-L-Pro), *cis*-4-Hy-D-Pro (C4Hy-D-Pro) and δ-Hy-Lys (HyLys) as well as the derivatives Dns-L-Asp (Asp), Dns-L-Glu (Glu), N-Dns-L-Ser (Ser), Dns-Gly (Gly), N-Dns-L-Thr (Thr), Dns-L-Ala (Ala), O-Dns-L-Tyr (Tyr), N,O-di-Dns-L-Tyr (DiTyr), Dns-L-Val (Val), Dns-L-Met (Met), Dns-L-Phe (Phe), Dns-L-Ile (Ile), Dns-L-Leu (Leu), Dns-L-Pro (Pro), N-Dns-*trans*-4-Hy-L-Pro (T4HyPro), N^{α}-Dns-L-Trp (Trp), N,N-di-Dns-L-cystine (Di2Cys), Dns-L-cysteic acid (cysteic acid), Dns-L-Norvaline (Nor), Dns-L-α-amino-*n*-butyric acid (α-ABA), Dns-γ-amino-*n*-butyric acid (γ-ABA), α-Dns-L-Arg (Arg), N^{ϵ}-Dns-L-Lys (Lys), di-Dns-L-Lys (DiLys), Dns-β-Ala (β-Ala), Dns-tryptamine (Trypt), Dns-cadavarine (Cad), di-Dns-cadavarine (DiCad), Dns-spermidine (Sper), di-Dns-1,4-diaminobutane (Putr) and di-Dns-histamine (Hisn) were obtained from Sigma (St. Louis, MO, USA). Desmosine and isodesmosine were obtained from Elastin Product Co. (Owensville, MO, USA).

2.3. Procedure

Buffers for HPCE separations were made in pure water, and buffers were filtered through a 0.2-μm filter prior to use. Dns-Amino acids were dissolved in methanol and diluted to 20% methanol with water. Samples were introduced from the anodic end of the capillary by 1-s vacuum injection. Separations were performed under various separation conditions as described in the text. On-column UV detection was at 216 nm unless otherwise stated. The capillary was washed for 2 min with 1 *M* NaOH, 2 min with water and 5 min with run buffer prior to each analysis. Data processing was performed with the data analysis system and according to Michaelsen *et al.* [20].

Proteins in the samples (10–30 mg) were hydrolysed in 6 *M* HCl (10 ml) at 120°C and for 20 h. The hydrolysate was dried with air, redissolved in water and dried again. The sample was then redissolved in 2.0 ml of water and the internal standards Nor (0.010 mmol/sample) and 3,4-dimethoxyphenylammonium chloride (0.005 mmol/sample) were added. For group separation of amino acids 0.5 ml of the redissolved sample was applied to two connected columns set up vertically on top of each other. From top to bottom the columns were: (A) CM-Sephadex C-25 (H^+; 1.0 ml slurry of water and column material, 1:1), (B) Dowex 50W-X8, 200–400 mesh (H^+; 1.0 ml slurry of water and column material, 1:1) [1]. The columns were washed with 9.5 ml water, separated and eluted with 20 ml 2 *M* acetic acid–methanol (1:1) for the A column and with 10 ml 1 *M* pyridine for the B column. The eluates were dried with air and redissolved in 0.5 ml water. The derivatisation was performed in the dark for 2 h with 50 μl sample added to 1.0 ml 25 m*M* Dns-Cl in acetonitrile and 1.0 ml 40 m*M* $LiCO_3$, pH 9.5. The reaction was then stopped by adding 100 μl 4% ethylamine, and the derivatised sample was dried with air. The derivatised sample was redissolved in 20% aqueous methanol, where most amino acid derivatives are dissolved but not all the products of the reagents. The samples were centrifuged at 2000 *g* for 2 min before analysis by HPCE.

3. Results and discussion

The separation mechanisms which are most likely to give acceptable separations of Dns-amino acids are exploitation of hydrophobic interaction of the amino acid side chain and Dns with surfactant monomers and micelles and differences in electrophoretic mobilities of the negatively charged Dns-derivatives at pH values above 4.5. The most promising results published are obtained by use of MECC with SDS in boric acid [8,21]. This MECC method was therefore tested for our purpose.

Dns-Amino acids and amines were dissolved in methanol (4 mg/ml) and diluted (× 86) to a final concentration in 20% aqueous methanol. Tyr could only be dissolved in a lower concentration of 2 mg/ml. Trypt, Cad, DiCad and γ-ABA precipitated when diluted to 20% aqueous methanol in the standards. Furthermore, Di2Cys, β-Ala and Putr could not be dissolved to acceptable concentrations in other solvents tested (acetonitrile, 1-propanol solutions, dimethyl sulphoxide, formamide, MECC buffers). All other 28 Dns-amino acids were dissolved and diluted without problems in methanol.

3.1. Separation conditions

The influence of separation conditions on the separations expressed as migration times (t_M), relative migration times (RMT), and the number of theoretical plates per meter of capillary (N/m) were investigated. The standard used contained 18 amino acids Asp, Glu, Ser, Gly, Thr, Ala, DiTyr, Val, Met, Phe, Ile, Leu, Pro, T4HyPro, cysteic acid, Trp, Asn and Gln. Not all results are shown here, but the evaluation and determination of the best separation conditions are based on all results. The most important parameters are mentioned here. The initial HPCE conditions were a buffer of 100 m*M* boric acid, 100 m*M* SDS, pH 8.3, a temperature of 27°C and a voltage of 15 kV. Asn and Ser were not completely separated under these conditions, which has also been reported by Miyashita and Terabe [21].

The migration orders changed for Glu, Asp, Val, Gly, Ala, Gln and cysteic acid with increasing SDS concentration from 100 to 180 m*M* (Fig. 1). Asn and Ser coeluted at concentrations between 100 and 140 m*M* as did Glu and Val at 120 m*M* SDS. At a concentration of 150 m*M* SDS all 18 amino acids could be separated, whereas at concentrations from 160 to 180 m*M* the amino acids Asp and Gly, Gly and cysteic acid as well as Glu and Gln were not completely separated. A concentration of 150 m*M* SDS was therefore chosen, as this also resulted in an acceptable migration time of 44 min for the latest appearing amino acid DiTyr. The observed ef-

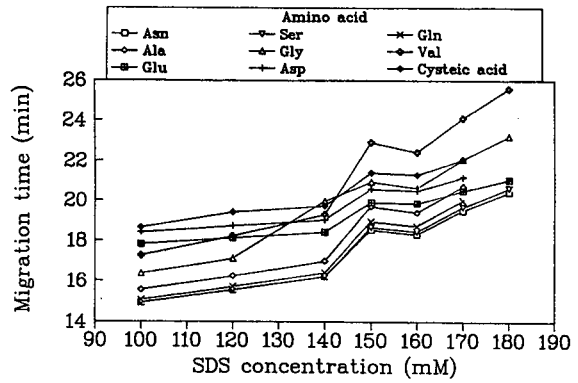

Fig. 1. Influence of SDS concentration on migration times of 9 amino acids. Conditions: 100 m*M* boric acid, pH 8.3, 27°C, 15 kV, 216 nm, vacuum injection 1 s.

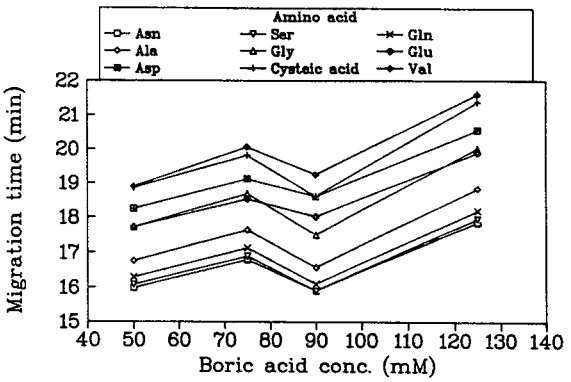

Fig. 2. Influence of boric acid concentration on migration times of 9 amino acids. Conditions: 150 m*M* SDS, other conditions as in Fig. 1.

fects of increasing SDS concentrations are probably a combination of changes in the shape and size of the micelles as well as the surface charge due to the presence of counter ions, increased ratio of the volume of the micellar phase to that of the aqueous phase and decreased electroosmotic flow, due to viscosity changes in the buffer [20]. The effects of SDS in concentrations from 30 to 50 m*M* have been thoroughly described by Ong *et al.* [8]. However, the number of amino acids included in their study was lower and did not include Asn, Gln, T4HyPro, Pro, Ala and Ile. The low concentrations of SDS are not sufficient to separate these amino acids.

Boric acid concentrations of 50, 75, 90, 100 and 125 m*M* gave poor separations of Asn and Ser except at 100 and 125 m*M*. Other amino acids did also coelute at various concentrations except at 100 m*M* (Fig. 2, data for 100 m*M* in Fig. 1). As a consequence hereof a concentration of 100 m*M* boric acid was chosen.

The separations obtained using pH values of 7.5, 8.0, 8.3, 8.5, 8.8, 9.0 and 9.3 were investigated. Increasing pH resulted in changed migration order of Asp, Gly and Glu. The best separations were obtained at pH 7.5 and 8.3. The other pH values of the buffer gave coelution of Gly and Glu or Asn and Ser. A buffer value of pH 8.3 was chosen. A general decrease in migration times with increasing pH was expected due to increased electroosmotic flow [20]. However, this was not seen, and changed properties of amino acids are probably the cause of that [8]. Ong *et al.* [8] also describes the effect of pH, but this is from pH 6.6 to 8.0.

Four voltages of 11, 13, 15 and 17 kV were tested. Good separations were obtained for all amino acids except for Asp and Gly at 17 kV. Furthermore, a small increase in N was observed when going from 11 to 15 kV. A voltage of 15 kV was chosen due to these results and because of a decrease in migration time of the latest appearing amino acid DiTyr from 61 to 43 min when going from 11 to 15 kV.

Temperatures of 22.4, 23.7, 25, 26, 27 and 29°C were also tested. The temperature was found to be very important for the separation of especially Thr, Asn and Ser; Ala and Glu as well as Asp and Gly (Fig. 3). The results clearly showed the best separation at the lowest temperature, and even such small changes in temperature of 1°C had a great effect (Fig. 3). Values of N were generally highest at the lowest temperatures. Values of N obtained with the applied capillary 0.52 m long were for Met, Phe and Trp determined to be 170 000, 210 000 and 190 000 at 22.4°C, 149 000, 168 000 and 165 000 at 25°C, 127 000, 147 000 and 145 000 at 27°C and 123 000, 133 000 and 130 000 at 29°C. Unfortunately, obtaining lower temperatures than 27°C is not possible with the applied ABI instrument, because there is no cooling possibility.

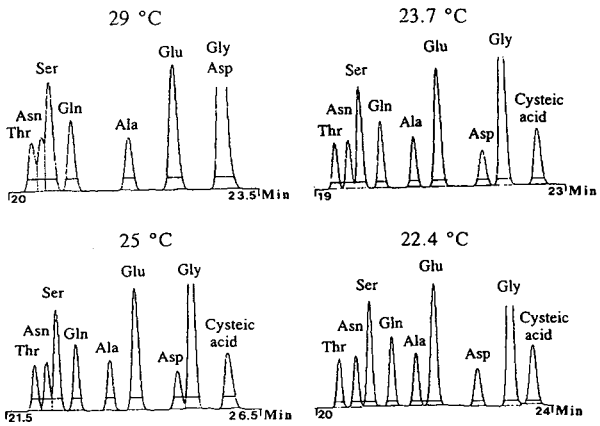

Fig. 3. Influence of temperature on the separation of 9 amino acids. Conditions: 150 m*M* SDS, 13 kV; other conditions as in Fig. 1.

The lowest temperature possible will therefore be determined by the ambient temperature. A temperature of 27°C had to be chosen.

Finally, various concentrations of 1-propanol and tetraethyl ammonium bromide (TEAB) were added to the buffer in order to obtain a higher selectivity of the method, especially for the first appearing amino acids. Addition of 1-propanol had a great influence on migration times, as especially the electroosmotic flow decreased with increasing 1-propanol concentrations. Moreover, changes in migration orders were seen. However, several amino acids co-eluted, and inclusion of 1-propanol can therefore not increase the selectivity. TEAB is supposed to form ion pairs with the amino acid carboxyl group and thereby change selectivity. Furthermore, TEAB may have some influence on the electroosmotic flow, due to interaction with the capillary wall. Addition of 1 to 40 m*M* TEAB to the buffer did also result in changes in migration times and relative migration times, but no general improvement in selectivity was found.

The best detection wavelength was chosen by testing 200, 216 and 245 nm in the optimised method. These values were selected from UV data of the Dns-amino acids. The amino acid peak areas at 216 nm were between 145 and 180% of the areas obtained at 200 nm except for the aromatic amino acids Phe, Trp and DiTyr, which were 0, 138 and 119%, respectively, of the areas at 200 nm. The peak areas at 245 nm were only between 50 and 65% of the areas at 200 nm, except again for the aromatic amino acids. The best sensitivity in UV detection of Dns-amino acids is therefore obtained at 216 nm. However, this wavelength has not been used in any of the previously published papers using UV detection.

The influence of the methanol concentration in Dns-amino acid samples on the separation efficiency was studied. A relatively high methanol concentration in the sample is necessary to dissolve the derivatised amino acids. However, high methanol concentrations in the sample reduced the separation efficiency dramatically (Fig. 4). This may be explained by reduced interaction with SDS or changed stacking conditions in the first minutes after voltage has been applied. The migration time for the tested amino acid Phe slightly decreased from 24.7 to 22.2 min, when the methanol concentration increased from 5 to 50%. This supports the explanation with reduced interaction with SDS. A concentration of 20 to 25% methanol can be used to obtain complete dissolution of Dns-amino acids and only loosing little in separation efficiency. We have used 20% methanol.

The separation obtained by using the optimised conditions on a sample containing 21

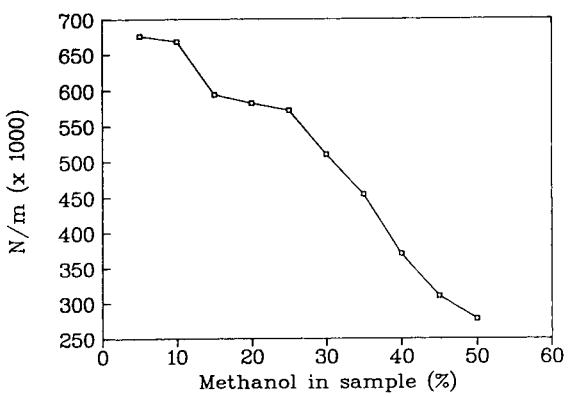

Fig. 4. Influence of the methanol concentration on the separation efficiency (*N*/m) for Phe. Conditions: 150 m*M* SDS, 25°C; other conditions as in Fig. 1.

amino acids is seen in Fig. 5. The migration times were between 17.3 and 44.5 min, and the separation efficiencies were between 403 000 N/m for cysteic acid and 660 000 N/m for Phe, which are considered satisfactory.

3.2. Migration order

The migration order and RMT values relative to mesityl oxide included as a neutral marker are shown for 30 amino acids in Table 1. Most of the amino acids can be separated by the HPCE method at the optimised conditions. However, Glu and α-ABA, Val and γ-ABA, as well as DiLys, Tyr, Trypt, HyLys and Cad are not separated well enough. Tyr and Lys with only one Dns group will not be present, when real samples are analysed, and a relatively large surplus of Dns-Cl is used. This surplus should be 10 times or more of Dns-Cl compared to amino acid [22].

Table 1
Migration order and RMT values (relative to mesityl oxide) for amino acids

Amino acid	RMT	Amino Acid	RMT
T4HyPro	0.824	Nor	1.206
Thr	0.900	Pro	1.215
Asn	0.909	Met	1.236
Ser	0.913	Ile	1.362
Gln	0.930	Leu	1.416
Ala	0.960	Phe	1.571
Glu	0.982	Trp	1.604
α-ABA	0.989	Lys	2.055
Mesityl oxide	1.000	Arg	2.076
Asp	1.015	DiLys	2.138
Gly	1.027	Tyr	2.145
Cysteic acid	1.055	Trypt	2.156
Val	1.104	DiHyLys	2.160
γ-ABA	1.105	Cad	2.176
C4Hy-D-Pro	1.142	DiTyr	2.191
C4Hy-L-Pro	1.144		

Conditions as in Fig. 5. except a temperature of 25°C.

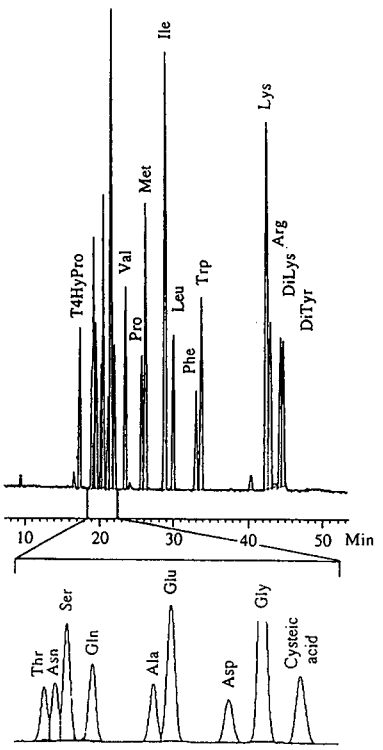

Fig. 5. Separation of 21 amino acids in the optimised method. Conditions as in Fig. 1 except 150 mM SDS.

The separation mechanisms involved are differences in electrophoretic mobility of the Dns-amino acids due to variations in the side chains, hydrophobic interaction of the Dns groups and SDS and the amino acid side chains and SDS in combination with ion repulsion of the negatively charged amino acid carboxyl groups and the negatively charged SDS. The electroosmotic flow will move the amino acids towards the cathode, and the interaction with SDS and the electrophoretic mobility of the amino acids will have a retarding effect on the compounds.

The migration order of *e.g.* Ala, Val and Leu as well as Asn and Gln illustrates the increased hydrophobic interaction with SDS, as the side chain becomes more hydrophobic. The electrophoretic mobilities of the amino acids with the longer side chains are lower, but the increased hydrophobicity has a larger effect. Nor shows a further increased interaction with SDS compared to Val due to the linear side chain of Nor. The appearance of Gly between Ala and Val is probably due to a higher electrophoretic mobility of Gly than of Ala in combination with the hydrophobic interaction. Glu and Asp appears quite early in the electropherograms even though

their electrophoretic mobility is high because of two negative charges. This is probably due to the hydrophilic character of the side chains in combination with increased ion repulsion with SDS. The migration order of α-ABA and γ-ABA is likely to be explained by the increased hydrophobic interaction of γ-ABA compared to α-ABA. This is due to less ion repulsion with SDS of the carboxyl group in γ-ABA than in α-ABA, caused by the position of the carboxyl group compared to the Dns group in the two compounds. T4HyPro migrates faster than C4Hy-L-Pro and C4Hy-D-Pro, and this is likely to be caused by facilitated hydrophobic interaction of HyPro and SDS, when the carboxy and the hydroxy groups of HyPro are on the same side of the cyclic ring of Pro as in the *cis* forms. Pro shows a further increased interaction with SDS, because it lacks the hydroxy group. Met, Leu and Ile have relatively non-polar side chains and appear therefore in the middle of the electropherograms. The aromatic amino acids Phe, Trp and Tyr will interact relatively strongly with SDS, and therefore these compounds appear late in the electropherogram. This is especially seen for DiTyr. Lys has a large and relatively non-polar side chain as well as a net zero charge which both results in strong interaction with SDS. DiLys shows a further increased interaction with SDS, and therefore appears after Lys. Ong *et al.* [8] also describe the migration order in MECC using SDS, but not all amino acids included in this study were included in their study. Moreover, lower concentrations of SDS were used.

3.3. Detection limits

Detection limits have been determined from a signal-to-noise ratio of 2 using dilutions of a sample containing 17 amino acids. The optimised separation conditions were used with vacuum injection for 1 s. The detection limits were found to be between 0.7 and 1.3 μM, except for the aromatic amino acids Trp at 0.5 μM and DiTyr at 0.1 μM. The injected volume is approximately 4.5 nl with the applied temperature of 27°C and assuming a viscosity in the buffer and the sample identical to water [23]. The detection limits are therefore between 3 and 6 fmol or approximately 2 pg of each amino acid. Use of instruments with fluorescence detection will reduce detection limits considerably. The possibility of analysing samples having a lower sample concentration than 0.7 to 1.3 μM by increasing the capillary diameter was investigated. Increasing the diameter increases the injected sample volume and the length of the light pathway in the capillary, and thereby increased peak areas are obtained. Increasing the diameter from 50 to 75 μm resulted in increased normalised peak areas (NPAs) of approximately a factor 5.5 and decreased migration times of a factor 0.7 for Ala and Phe. However, the separation efficiency expressed as N/m decreased a factor 3.4. Increased capillary diameter can therefore only be recommended, when the obtained separation efficiency is not critical.

3.4. Repeatability and linearity

The repeatabilities of the method expressed as relative standard deviation (R.S.D.) of RMT, NPA and relative NPA (RNPA) values are shown in Table 2. R.S.D.s of RMT values were very low lying between 0.09 and 0.70%. This is in the same level as reported for other MECC methods [20,24]. R.S.D.s of NPA values were quite high especially for Glu, Asp and DiTyr. Integration of DiTyr is difficult, and this results in the high R.S.D. Problems with Glu and Asp will be explained elsewhere. Finally, R.S.D.s of RNPA values were much improved compared to the NPA values lying between 0.85 and 3.41% except for Glu, Asp and DiTyr. This improvement compared to NPA values is caused by elimination of variations in injection volumes. Altogether, both qualitative and quantitative analyses can be performed satisfactory in regard to repeatability.

The linearity of the method was determined by using a standard containing 14 amino acids at 6 concentration levels and with 5 repetitions. Linear regression analyses of NPA values against concentrations gave correlation coefficients between 0.9824 and 0.9912 except for DiTyr at

Table 2
Repeatability as relative standard deviation of RMT, NPA and RNPA values for amino acids

Amino acid	R.S.D. (%)		
	RMT	NPA	RNPA
T4HyPro	0.29	6.36	2.32
Thr	0.22	7.26	2.31
Asn	0.24	6.99	2.89
Ser	0.24	6.47	3.41
Gln	0.23	6.48	2.32
Ala	0.16	6.25	1.70
Glu	0.26	8.47	5.85
Asp	0.24	7.53	4.37
Gly	0.14	6.03	1.95
Val[a]		5.62	
Pro	0.09	5.97	0.85
Met	0.12	5.64	1.21
Ile	0.19	6.12	1.22
Leu	0.23	5.93	1.42
Phe	0.31	6.16	1.70
Trp	0.32	5.78	1.71
DiTyr	0.70	14.45	9.92

Conditions as in Fig. 5, 14 repetitions.
[a] Other amino acids relative to Val.

0.9222. Correlation coefficients between 0.9957 and 0.9993 were obtained by using RNPA values. Hereby variations in injection volumes are eliminated, and these variations have nothing to do with linearity. The most correct evaluation of linearity is therefore based on RNPA values, and the linearity of this method is good.

3.5. Relative response factors

Relative response factors (RRF) for 15 amino acids were calculated (Table 3). The RRF values were calculated from response factors (RF) as $RRF = RF_x/RF_{Leu}$, where RF = NPA/concentration in sample. The RRF values were from 0.6881 to 1.5466 and depended strongly on the amino acid, although most of the amino acids have one identical Dns group. However, the amino acids Tyr and Trp have a considerable UV absorption at this wavelength. This accounts for the higher RRF values of these two amino acids [2]. R.S.D.s of RRF values were between 1.8 and 4.8%, with the highest value for Glu. These results show that either complete standards must be included in each series of analyses, or the RRF values for all amino acids under the actual conditions must be determined.

3.6. Derivatisation and examples of analyses

Samples of skin from mink and various feedstuffs were hydrolysed and derivatised (see Experimental). The necessary amount of ethylamine to stop the reaction was determined in a series of derivatisations. Unfortunately, HPCE analyses directly of the reaction mixture after derivatisation gave very bad results. This is due to the high amount of acetonitrile in the sample. Dissolution in methanol–water gives much better results. The amount of 20% methanol in water to dissolve the derivatised amino acids was also

Table 3
Relative response factors (RRF) for amino acids

Amino acid	RRF	R.S.D. (%)	Amino acid	RRF	R.S.D. (%)
T4HyPro	0.730	3.1	Pro	0.743	2.0
Thr	0.834	2.6	Met	0.688	4.6
Asn	0.762	2.2	Ile	1.093	2.6
Ser	1.007	1.9	Leu	1	
Gln	0.779	2.5	Phe	0.784	4.5
Ala	0.801	3.0	Trp	1.547	1.8
Glu	0.911	4.8	DiTyr	1.409	15.9
Val	0.970	1.9			

Conditions as in Fig. 5, 6 concentration levels and 5 repetitions, RRF values calculated relative to Leu.

determined in a series of experiments. The volume had to be at least 800 μl at the applied conditions of derivatisation (see Experimental). A residue is present in all samples, but the residue does not contain amino acids, as the amino acid peak areas do not increase further by increasing the volume of methanol–water. An example of an analysis of acidic and neutral amino acids in a hydrolysed skin sample is shown in Fig. 6. At least three reagent peaks were seen in all derivatised samples. However, amino acids could be separated by the applied method. The amino acids can be quantified in the samples by using RRF values and an internal standard. Nor was used here as internal standard, but Nor and Pro were not completely separated, and therefore another internal standard may be used. Cys can also be determined by the method after oxidation to cysteic acid (Fig. 5). Analyses of acidic and neutral amino acids in samples of feedstuffs as well as the samples of skin have been performed and works well. Furthermore, analyses of desmosine and isodesmosine, which are two special amino acids present only in elastin and responsible for the special properties of elastin, have been tested in the SDS system. Desmosine and isodesmosine consists each of one lysine and three allysine (lysine with an aldehyde group in the sidechain instead of an amino group) units forming a pyridine ring. It was impossible to dissolve sufficient amounts of the Dns derivatives of these amino acids in various solvents, probably due to the presence of at least four Dns groups on each amino acid. However, analysing the underivatised amino acids was possible in the SDS system (Fig. 7). Desmosine has a molecular extinction coefficient of 4750 M^{-1} cm^{-1} at 234 nm and of 3200 M^{-1} cm^{-1} at 268 nm and isodesmosine has a molecular extinction coefficient of 6450 M^{-1} cm^{-1} at 278 nm and a relatively small absorbance at 234 nm. These properties can be used to identify the amino acids, as seen in Fig. 7.

Derivatisation of different amounts of the same sample did not give the expected peak areas for Glu and Asp after HPCE analysis. Furthermore, the larger R.S.D.s of both NPA and RNPA values seen (Table 2) suggests problems in quantifying these amino acids after Dns

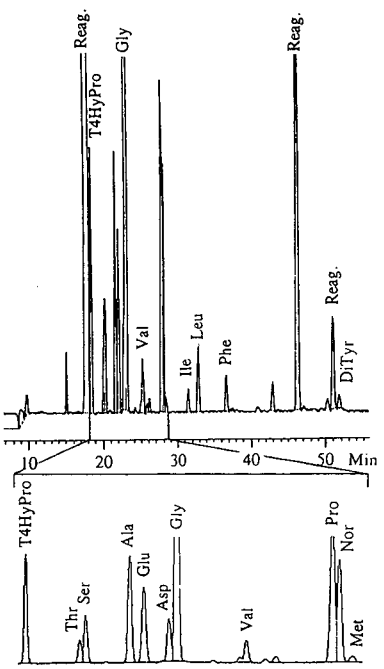

Fig. 6. Separation of Dns-derivatised acidic and neutral amino acids in a hydrolysate of skin from mink. Conditions as in Fig. 1 except 150 mM SDS.

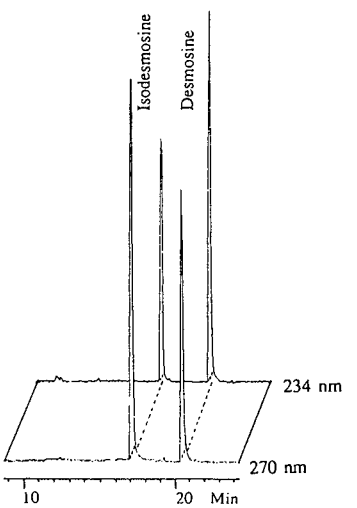

Fig. 7. Separation of underivatised desmosine and isodesmosine in the SDS system. Conditions as in Fig. 1 except 150 mM SDS and the detection wavelength.

Table 4
Peak areas in percent of expected peak areas at decreasing Dns/amino acid ratios in the derivatisation

Dns/amino acid ratio	Area in percent of expected				
	50	20	10	5	2.5
Asp	100	91	86	75	56
Glu	100	94	87	82	70
Ala	100	84	86	90	81
Leu	100	88	99	120	134

Conditons as in Fig. 1 except 150 m*M* SDS. Expected peak areas calculated from the peak areas obtained at the highest Dns/amino acid ratio.

derivatisation. A series of derivatisations with decreasing Dns/amino acid ratio was performed with Asp and Glu, and the results were compared to results obtained with Ala and Leu (Table 4). The expected peak area was calculated from the peak area obtained at the highest Dns/amino acid ratio. The amount of amino acid to be derivatised was increased and the Dns-Cl amount was held constant. The peak areas were much lower than expected for Asp and Glu at low Dns/amino acid ratios, and this was not seen for Ala and Leu. A possible explanation could be the ability of the carboxyl group of especially Glu to form a peptide bond with the amino group of Glu as in pyroglutamic acid, and thereby release Dns. The presence of pyroglutamic acid in the sample prior to derivatisation cannot give these results. However, a lower stability of Dns derivatives of Asp and Glu may be explained by the release of Dns. Furthermore, an additional peak was seen in increasing amounts appearing after Asp and Glu when the Dns/amino acid ratio decreased. This could be the transformation product.

These findings of a dependence of amino acid peak areas on the Dns/amino acid ratio are in contradiction with the results described by Tapuhi *et al.* [22]. They stated that such problems were not seen, when derivatisations with corresponding reaction mixtures were performed. However, using other derivatisation conditions Seiler [25] and Neadle and Pollitt [26] reported a dependence of the yield of the derivatisation on the relative amount of Dns-Cl present. The influence of Dns/amino acid ratio on peak areas of Asp and Glu can be minimised by using high Dns/amino acid ratios and by adjusting the amino acid concentrations in samples to a well defined level.

3.7. Cholate system

Other MECC systems than SDS were investigated due to the fact, that reaction products from the Dns derivatisation interfered with the basic amino acids Lys, DiLys, HyLys and Arg as well as Tyr (Fig. 5 and 6). Furthermore, these amino acids had long migration times. The best results were obtained in buffers containing 50 m*M* disodium hydrogenphosphate and 50 or 80 m*M* sodium cholate at pH 8.0 and analysed at 30°C and 20 kV (Fig. 8). The efficiency was between 228 000 and 428 000 *N*/m for Arg, Lys, Tyr and DiLys at these conditions. Furthermore, HyLys (mixed DL and DL *allo* form) gave two well separated peaks appearing between Tyr and DiLys (Fig. 8B). In electropherograms of hydrolysed protein, with the hydrolysate group separated to obtain the basic amino acids and de-

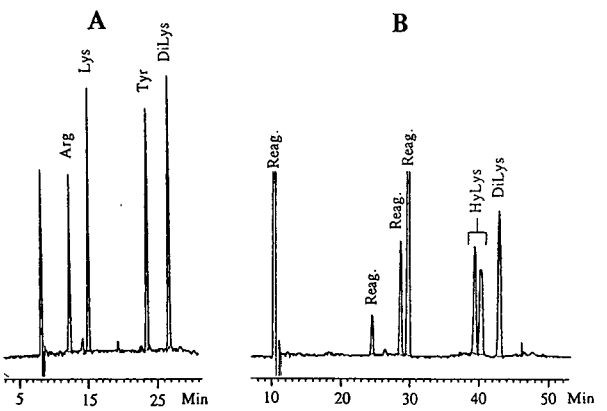

Fig. 8. Separation of amino acids in the cholate system. (A) Basic amino acids and Tyr, 50 m*M* disodium hydrogenphosphate, 50 m*M* sodium cholate, pH 8.0, 30°C, 20 kV, 216 nm, 1 s vacuum injection. (B) DiLys and HyLys forms (derivatised mixed DL and DL *allo* forms), conditions as in (A) except 80 m*M* sodium cholate, 27°C and 18 kV.

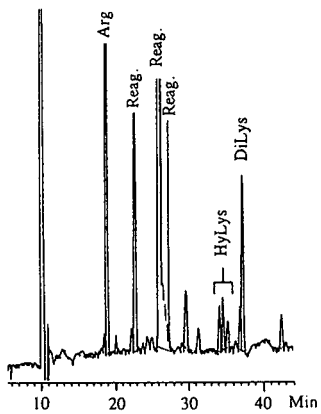

Fig. 9. Separation of derivatised basic amino acids in a hydrolysate of skin from mink. Conditions as in Fig. 8B.

rivatisation of the amino acids these basic amino acids could be seen and their identity tested by spiking (Fig. 9). Further optimisation of parameters and determination of the performance of this method have to be performed, but it seems promising for analyses of the basic amino acids. Apart from Terabe *et al.* [7], who used taurodeoxycholate for chiral separation of six amino acids, no other reports on MECC with cholate for Dns-amino acids have been reported. Analyses of acidic and neutral amino acids were also tested in the cholate system, but many amino acids coeluted. The developed method with SDS is recommended for analyses of these amino acids.

4. Conclusions

The described MECC methods with SDS and cholate can be used to analyse amino acids released from proteins in feedstuffs and skin. The derivatisation step with Dns-Cl is relatively simple and fast. Most amino acids can be dissolved in 20% methanol in water. The optimised SDS method gives complete separations of acidic and neutral amino acids within 45 min, and the efficiency is high with up to 660 000 N/m. Furthermore, the repeatability and linearity are good. The detection limits are in the low femtomole range. Finally, basic amino acids can be separated by the cholate method.

Acknowledgements

The authors gratefully acknowledge support from the Danish Agricultural and Veterinary Research Council, the Danish Ministry of Agriculture and the Danish Fur Breeders Association.

References

[1] B.O. Eggum and H. Sørensen, *Absorption and Utilization of Amino Acids*, CRC Press, Boca Raton, FL, 1989, Ch. 17, pp. 265–295.
[2] A. Negro, S. Garbisa, L. Gotte and M. Spina, *Anal. Biochem.*, 160 (1987) 39.
[3] S. Michaelsen and H. Sørensen, *Polish J. Food Nutr. Sci.*, 1 (1994) in press.
[4] J.W. Jorgenson and K.A. Lukacs, *Anal. Chem.*, 53 (1981) 1298.
[5] P. Gozel, E. Gassmann, H. Michelsen and R.N. Zare, *Anal. Chem.*, 59 (1987) 44.
[6] A. Guttman, A. Paulus, A.S. Cohen, N. Grinberg and B.L. Karger, *J. Chromatogr.*, 448 (1988) 41.
[7] S. Terabe, M. Shibata and Y Miyashita, *J. Chromatogr.*, 480 (1989) 403.
[8] C.P. Ong, C.L. Ng, H.K. Lee and S.F.Y. Li, *J. Chromatogr.*, 559 (1991) 537.
[9] K. Otsuka, S. Terabe and T. Ando, *J. Chromatogr.*, 332 (1985) 219.
[10] K.C. Waldron and N.J. Dovichi, *Anal. Chem.*, 64 (1992) 1396.
[11] M.D. Oates and J.W. Jorgenson, *Anal. Chem.*, 61 (1989) 432.
[12] T. Ueda, F. Kitamura, R. Mitchell and T. Metcalf, *Anal. Chem.*, 63 (1991) 2979.
[13] M. Yu and N.J. Dovichi, *Anal. Chem.*, 61 (1989) 37.
[14] M. Yu and N.J. Dovichi, *Mikrochim. Acta*, III (1988) 27.
[15] Y.-F. Cheng and N.J. Dovichi, *Science*, 242 (1988) 562.
[16] S. Wu and N. Dovichi, *J. Chromatogr.*, 480 (1989) 141.
[17] M. Albin, R. Weinberger, E. Sapp and S. Moring, *Anal. Chem.*, 63 (1991) 417.
[18] J. Liu, K.A. Cobb and M. Novotny, *J. Chromatogr.*, 468 (1988) 55.
[19] J. Liu, Y.-Z. Hsieh, D. Wiesler and M. Novotny, *Anal. Chem.*, 63 (1991) 408.
[20] S. Michaelsen, P. Møller and H. Sørensen, *J. Chromatogr.*, 608 (1992) 363.

[21] Y. Miyashita and S. Terabe, *Beckman Applications Data, DS-767*, Beckman, Palo Alto, CA, 1990.
[22] Y. Tapuhi, D.E. Schmidt, W. Lindner and B.L. Karger, *Anal. Biochem.*, 115 (1981) 123.
[23] J. Harbaugh, M. Collette and H.E. Schwartz, *Beckman Technical Information Bulletin, TIBC-103*, Beckman, Palo Alto, CA, 1990.
[24] S. Michaelsen, M.-B. Schrøder and H. Sørensen, *J. Chromatogr. A*, 652 (1993) 503.
[25] N. Seiler, in D. Glick (Editor), *Methods of Biochemical Analysis*, Vol. 18, Interscience, New York, 1970, pp. 259–337.
[26] D.J. Neadle and R.S. Pollitt, *Biochem. J.*, 97 (1965) 607.

ELSEVIER

Journal of Chromatography A, 680 (1994) 311–315

JOURNAL OF CHROMATOGRAPHY A

Separation of 24 dansylamino acids by capillary electrophoresis with a non-ionic surfactant

Norio Matsubara*, Shigeru Terabe

Faculty of Science, Himeji Institute of Technology, Kamigori, Hyogo 678-12, Japan

Abstract

The separation of 24 dansylamino acids was investigated by capillary electrophoresis with an additive of micelles of a non-ionic surfactant, Tween 20. Although two pairs of peaks, norvaline and methionine derivatives, and didansyltyrosine and solvent (methanol), did not show good resolution, other dansylamino acids were well separated within 70 min using 100 m*M* Tween 20 and pH 2.40. The theoretical plate numbers calculated for dansylamino acids were 28 000–111 000 with a 19-cm capillary column.

1. Introduction

Recently, capillary electrophoresis (CE) has been attracting attention for the separation of ionic analytes because it gives high theoretical plate numbers. Amino acid derivatives separated by CE or micellar electrokinetic chromatography (MEKC) include phenylthiohydantoin [1–3], dansyl [4,5], *o*-phthaldialdehyde [6,7] fluorescein isothiocyanate [7,8,9], fluorescamine [7,10] and 9-fluorenylmethyl chloroformate [7] derivatives. However, separations of twenty or more amino acids were often difficult because of insufficient resolution. We reported previously the separation of closely related peptides by using micelles of a non-ionic surfactant as an additive to buffer solution [11]. In this work, this technique was applied to the separation of 24 dansylated amino acids.

2. Experimental

Dansylamino acid derivatives were purchased from Sigma (St. Louis, MO, USA). All except glycine derivative were L-isomers. Monodansyl-L-tyrosine was purchased from ICN Biomedicals (Costa Mesa, CA, USA). Tween 20 (Fig. 1) was purchased from Wako (Osaka, Japan). These chemicals were used as received.

A fused-silica capillary (Polymicro Technologies, Phoenix, AZ, USA) of 25–50 μm I.D. and 363 μm O.D. was attached to a Spectra Chrom 200 UV detector (Spectra-Physics, San Jose, CA, USA). Detection was carried out by

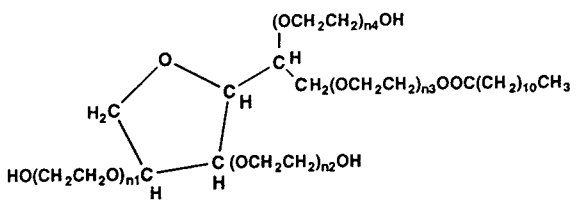

Fig. 1. Structure of Tween 20.

* Corresponding author.

0021-9673/94/$07.00
SSDI 0021-9673(94)00299-O

on-column measurements at a wavelength of 214 nm and a detection rise time of 0.5 s through a 3-mm capillary window without polyimide. The high-voltage d.c. power supply was a Model HCZE-30PNO.25-LDSW (Matsusada Precision Devices, Kusatsu, Japan) delivering up to ±30 kV. For data recording and processing, a Chromatopac Model C-R6A (Shimadzu, Kyoto, Japan) was used. Samples were injected hydrodynamically from the anodic end of a capillary. Before each run, the column was rinsed successively with methanol, water and the separation buffer. The pH of separation solution was measured with a Beckman Φ34 pH meter calibrated at pH 4 and 7 with a commercial pH standard from Beckman.

3. Results and discussion

When Tween 20 was selected as a micellar pseudo-stationary phase to separate dansylamino acids, the most important factor was the concentration of Tween 20, which was varied from 10 to 150 m*M*. At 10 m*M*, some hydrophobic amino acid derivatives were separated but hydrophilic amino acid derivatives were largely overlapped (Fig. 2). At 150 m*M*, dansylamino acids were well separated but a long analysis time was required for the separation of 24 dansylamino acids because dansyl derivatives of hydrophobic amino acids had large capacity factors under these conditions. The concentration range of Tween 20 to achieve simultaneously optimum resolution and a reasonable analysis time was 80–100 m*M* (Fig. 3).

Although most of dansylamino acids did not change their migration order within the investigated pH range, some dansylamino acids changed their migration order depending on the pH of the buffer. The separation of glutamate, glycine, alanine and lysine derivatives was pH sensitive. As shown in Fig. 4, dansyl glutamate eluted between glycine and alanine derivatives at pH 2.19, and eluted earlier than dansylglycine at pH 2.37 or above when the concentration of Tween 20 was 100 m*M*. When the pH was raised to 2.73 in the presence of 100 m*M* Tween 20,

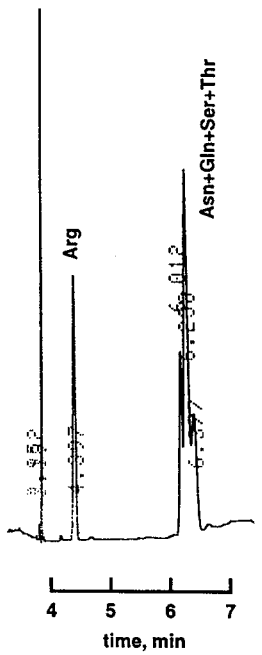

Fig. 2. Separation of dansyl derivatives of arginine, asparagine, glutamine, serine and threonine. Electrophoretic solution, 10 m*M* Tween 20 in 25 m*M* sodium phosphate buffer (pH 2.40); applied voltage, 14 kV; capillary I.D., 50 μm; column length, 35 cm (effective length, 20 cm).

dansyl glutamate and dansylglycine were well separated, but the migration times of glycine and alanine derivatives came closer.

Another pH-dependent separation was found with tryptophan, aspartate and cystine derivatives (Fig. 5). At pH 2.29 aspartate, cystine and tryptophan derivatives eluted in this order, but at pH 2.52 dansyltryptophan eluted first followed by the derivatives of aspartate and cystine.

The separation of dansylglutamine and dansylserine was achieved when the pH of separation buffer was in the range 2.33–2.73 but started to overlap at pH 2.19 and overlapped completely at pH 2.08 when the concentration of Tween 20 was set at 100 m*M*.

Dansylnorvaline and dansylmethionine were only partially resolved at pH 2.4 with 100 m*M* Tween 20, which is an optimized condition for most amino acid derivatives. The peak of didansyltyrosine overlapped with the solvent peak (methanol) caused by electroosmotic flow

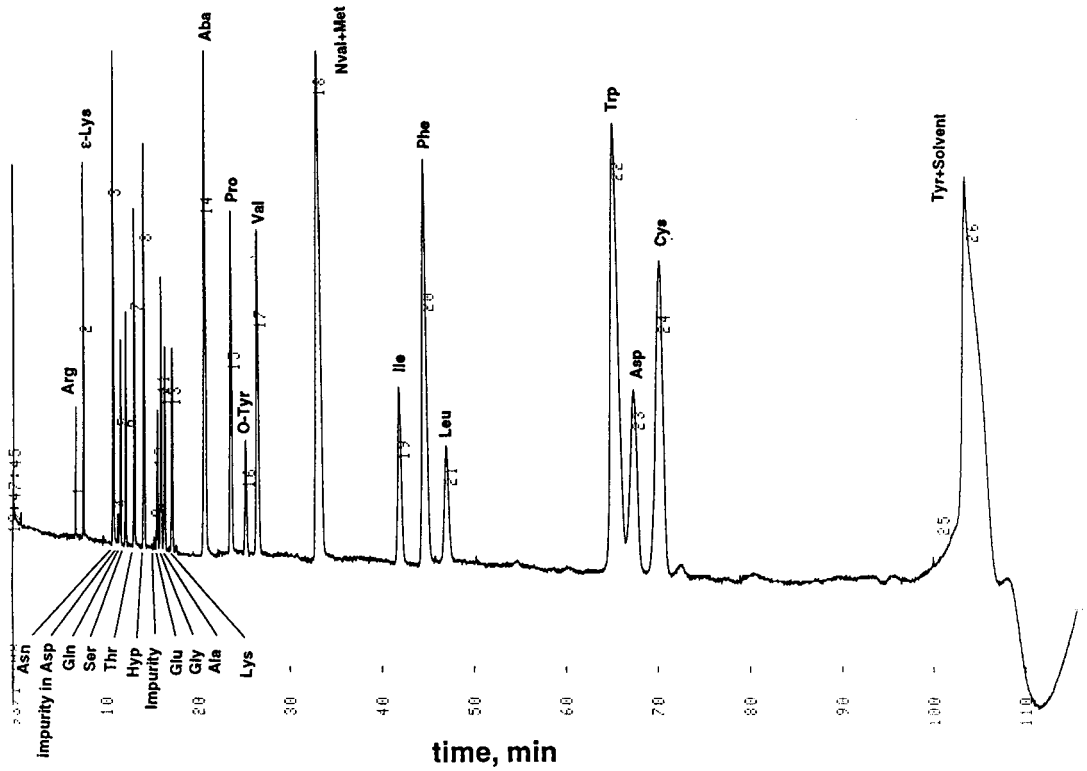

Fig. 3. Separation of 24 dansylamino acids. Dansylamino acids are represented by three-character abbreviations of the corresponding amino acids (ε-Lys is ε-dansyllysine, O-Tyr is O-dansyltyrosine, Cys is didansylcystine and Lys and Tyr are didansyl derivatives). Electrophoretic solution, 100 m*M* Tween 20 in 25 m*M* sodium phosphate buffer (pH 2.40); applied voltage, 16 kV; capillary I.D., 25 μm; column length, 34 cm (effective length, 19 cm).

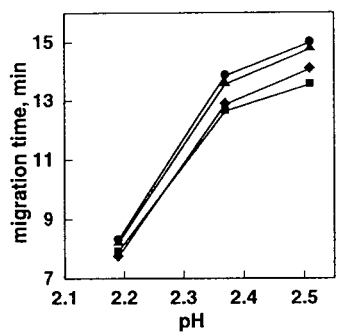

Fig. 4. Effect of pH on the separation of (■) dansyl glutamate, (◆) dansylglycine, (▲) dansylalanine and (●) didansyllysine. Electrophoretic solutions, 100 m*M* Tween 20 in 25 m*M* sodium phosphate buffer; applied voltage, 14 kV; capillary I.D., 50 μm; column length, 34 cm (effective length, 19 cm).

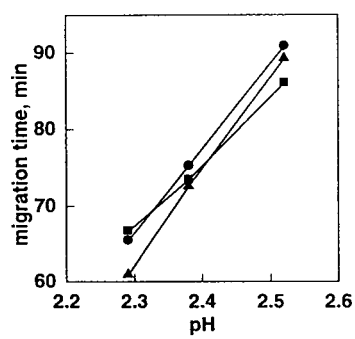

Fig. 5. Effect of pH on the separation of (▲) dansyl aspartate, (■) dansyltryptophan and (●) didansylcystine. Electrophoretic solution, 100 m*M* Tween 20 in 25 m*M* sodium phosphate buffer; applied voltage, 14 kV; capillary I.D., 30 μm; column length, 38 cm (effective length, 22 cm).

because of the slow migration of didansyltyrosine.

The migration times of dansylamino acids were plotted against the hydrophilicity values of free amino acids [12]. As shown in Fig. 6, the migration times increased with decrease in the hydrophilicity of the amino acids. In the pH range 2–3, the dimethylamino group in the dansyl group and the nitrogen atoms of the side-chain of lysine and arginine are positively charged. The carboxyl group of amino acids is hardly charged except for aspartate and glutamate, which have a second carboxyl group. As a result, the total charges of most amino acids without a charged side-chain are almost identical. Hence the migration order of dansylamino acids is regulated not by their charge but mainly by their distribution coefficients into surfactant micelles. As Tween 20 has no electric charge, the interaction is not ionic but mainly hydrophobic. The observed migration order of dansylamino acids is well explained by this hypothesis. The exceptions are the derivatives which have two dansyl groups per an amino acid (lysine, cystine and tyrosine) or those which have a negatively charged side-chain (aspartate and glutamate). Didansyltyrosine (open square in Fig. 6) eluted much more slowly than expected from the hydrophilicity value of the amino acid because of the hydrophobicity of the extra dansyl group. Didansyllysine eluted much later than ε-dansyllysine, which is also explained by the high hydrophobicity of dansyl groups. Although aspartate has a net positive charge at pH 2.4, the migration time of dansyl aspartate was much longer (open triangle in Fig. 6) than expected from its hydrophilicity value, probably owing to the negative charge of the side-chain. The side-chain of arginine not only increases the positive charge of the molecule but also enhances the hydrophilicity, which resulted in its short migration time.

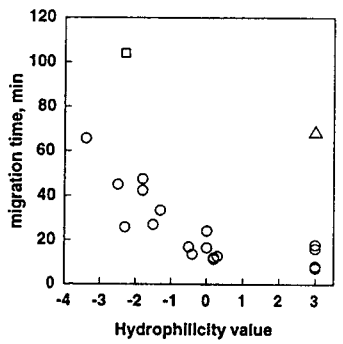

Fig. 6. Relationship between hydrophilicity values of free amino acids and migration times of corresponding dansylamino acids. △ = Dansyl aspartate; □ = didansyltyrosine. Conditions as in Fig. 3.

The migration orders observed with the dansylamino acids are also consistent with those of peptides which have a single amino acid difference [11] if we assume that the migration orders of peptides with a single amino acid difference are decided by the hydrophilicity value of the different amino acids. Human [met^{13}]-motilin eluted earlier than synthetic [leu^{13}]-motilin. Similarly, [val^{5}]-angiotensin II eluted earlier than [leu^{5}]-angiotensin II, and [sar^{1}, gly^{8}]-angiotensin II eluted earlier than [sar^{1}, ala^{8}]-angiotensin II.

4. Conclusions

If SDS is chosen as a surfactant for the separation of dansylamino acids, a problem arises from Joule heating because a relatively high concentration is required for the separation of dansylamino acids. In contrast, increasing the concentration of Tween 20 does not raise the conductivity because it is electrically neutral. The number of theoretical plate of dansylamino acids obtained with the present method (100 m*M* Tween 20 and pH 2.40), 28 000–111 000 with a 19-cm column, is comparable to that of SDS-MEKC. Although non-ionic surfactants have not yet been extensively studied as a micellar phase in CE separations, more investigations on the separation of ionic compounds can be expected.

Acknowledgements

This work was supported in part by a Grant-in-Aid for Scientific Research (No. 05740450)

from the Ministry of Education, Science and Culture, Japan.

References

[1] K. Otsuka, S. Terabe and T. Ando, *J. Chromatogr.*, 332 (1985) 219.
[2] S. Terabe, Y. Ishihama, H. Nishi, T. Fukuyama and K. Otsuka, *J. Chromatogr.*, 545 (1991) 359.
[3] K.C. Waldron and N.J. Dovichi, *Anal. Chem.*, 64 (1992) 1396.
[4] Y. Miyashita and S. Terabe, *Beckman Applications Data DS-767*, Beckman, Fullerton, CA, 1990.
[5] C.P. Ong, C.L. Ng, H.K. Lee and S.F.Y. Li, *J. Chromatogr.*, 559 (1991) 537.
[6] J. Liu, K.A. Cobb and M. Novotny, *J. Chromatogr.*, 468 (1989) 55.
[7] M. Albin, R. Weinberger, E. Sapp and S. Moring, *Anal. Chem.*, 63 (1991) 417.
[8] K.C. Waldron, S. Wu, C.W. Earle, H.R. Harke and N.J. Dovichi, *Electrophoresis*, 11 (1990) 777.
[9] S. Wu and N.J. Dovichi, *Talanta*, 39 (1992) 173.
[10] N.A. Guzman, J. Moschera, C.A. Bailey, K. Iqbal and A.W. Malick, *J. Chromatogr.*, 598 (1992) 123.
[11] N. Matsubara and S. Terabe, *Chromatographia*, 34 (1992) 493.
[12] T.P. Hopp and K.R. Woods, *Proc. Natl. Acad. Sci. U.S.A.*, 78 (1981) 3824.

ELSEVIER

Journal of Chromatography A, 680 (1994) 317–320

JOURNAL OF CHROMATOGRAPHY A

Optical resolution of amino acid derivatives by micellar electrokinetic chromatography with N-dodecanoyl-L-serine

Koji Otsuka[a,*], Kaoru Karuhaka[a], Mitsuo Higashimori[a], Shigeru Terabe[b]

[a]*Department of Industrial Chemistry, Osaka Prefectural College of Technology, Saiwai-cho, Neyagawa, Osaka 572, Japan*

[b]*Department of Material Science, Faculty of Science, Himeji Institute of Technology, Kamigori, Hyogo 678-12, Japan*

Abstract

Optical resolution by micellar electrokinetic chromatography with N-dodecanoyl-L-serine (DSer) was investigated. Similarly to the use of sodium N-dodecanoyl-L-valinate or sodium N-dodecanoyl-L-glutamate, addition of sodium dodecyl sulfate (SDS), urea and organic modifiers such as methanol and 2-propanol (IPA) to DSer micellar solutions could give improved peak shapes and enhance the enantioselectivity. With a DSer–SDS–urea–methanol solution, six phenylthiohydantoin (PTH)DL-amino acids were separated and each enantiomeric pair was optically resolved. By using a DSer–SDS–urea–IPA solution, the same PTH–DL-amino acids were partially resolved, while PTH-DL-Thr was resolved only in this system. N-Dodecanoyl-L-aspartic acid and sodium N-tetradecanoyl-L-glutamate were also investigated, but satisfactory results were not obtained.

1. Introduction

Recently, optical resolution has become one of major applications of high-performance capillary electrophoresis (HPCE) [1–3], especially in pharmaceutical fields. To achieve direct enantiomeric separation by HPCE, cyclodextrin capillary zone electrophoresis (CD-CZE), micellar electrokinetic chromatography (MEKC) with chiral surfactants and cyclodextrin-modified MEKC (CD-MEKC) are usually employed. MEKC is also a popular technique for separating small neutral molecules in addition to charged solutes.

In optical resolution by MEKC with chiral micelles, sodium N-dodecanoyl-L-valinate (SDVal) [4–8], sodium N-dodecanoyl-L-glutamate (SDGlu) [9], various bile salts [10–13], digitonin [6,9] and saponins [14] have been used as chiral selectors. In the present investigation, we used N-dodecanoyl-L-serine (DSer) instead of SDVal and SDGlu. To dissolve this surfactant, basic (pH 11.0–12.0) buffer solutions were employed and sodium dodecyl sulfate (SDS), urea and organic modifiers, such as methanol and 2-propanol (IPA), were also added to DSer solutions to enhance the enantioselectivity of aqueous buffers. Some phenylthiohydantoin-DL-amino acids (PTH-DL-AAs) were successfully resolved with DSer–SDS–urea–methanol and DSer–SDS–urea–IPA solutions. Although the enantioselectivities in these micellar systems were not substantially different from the SDVal or SDGlu systems, PTH-DL-Thr was optically resolved only with the DSer–IPA solution. As other chiral surfactants, N-dodecanoyl-L-aspartic acid (DAsp) and sodium N-tetradecanoyl-L-

* Corresponding author.

0021-9673/94/$07.00
SSDI 0021-9673(94)00481-N

glutamate (STGlu) were also examined, but successful results were not obtained.

2. Experimental

DSer, DAsp and STGlu (Fig. 1) were obtained from Ajinomoto (Tokyo, Japan), SDS and methanol from Nacalai Tesque (Kyoto, Japan) and urea, IPA and PTH-DL-AAs from Wako (Osaka, Japan). Micellar solutions were prepared by dissolving surfactants and urea in 50 m*M* borate buffer adjusted to an appropriate pH with 100 m*M* sodium hydroxide solution. Organic modifiers were added to the micellar solutions when required. Sample solutions were prepared by dissolving enantiomers in acetonitrile. All the chemicals were of analytical-reagent grade and used as received.

Capillary electrophoresis was performed with a laboratory-built system consisting of a Matsusada HCZE-30PN0.25-LDS regulated high-voltage power supply (Kusatsu, Shiga, Japan), a Shimadzu (Kyoto, Japan) SPD-6A UV spectrophotometric detector and a Shimadzu Chromatopac C-R6A data processor. An untreated fused-silia tube purchased from Polymicro Technologies (Phoenix, AZ, USA), 252 or 300 mm (effective length) × 52 μm I.D. was used as a separation capillary and on-column UV detection was employed.

Sample injection was carried out by the hydrodynamic method. Separation was performed at constant voltage and ambient temperature.

3. Results and discussion

As the solubility of DSer in neutral aqueous solutions is low, owing to its free acid form, basic buffer solutions were employed and/or organic modifiers were added to the DSer solutions. By using buffers of pH 7.0–9.0 without organic modifiers, sufficient solubility of DSer was not attained. On the other hand, by using buffers of pH 11.0–12.0, DSer was dissolved completely even without organic solvents. However, at pH 12.0, chiral separation could not be achieved for any enantiomers. In this instance, unstable baselines were always observed, mainly owing to the degradation of the inside wall of the capillary by high-pH solutions, and also no reproducible result was obtained. At pH 11.0, although stable baselines and reproducible separation were obtained, still no enantiomeric resolution was observed.

Addition of organic modifiers, such as methanol and IPA, could enhance the solubility of DSer: even at pH 7.0, a buffer containing 20% (v/v) IPA or methanol could dissolve DSer completely. However, no optical resolution could be obtained, and moreover, the separation of some conventional test solutes [15], a mixture of some neutral compounds, was not successful. These results suggested that sufficient micellar formation did not occur in such a buffer solution. By using a buffer of pH 11.0, addition of IPA could give a partial enantiomeric separation of some PTH-DL-AAs, but the efficiency was still very low.

As reported previously [8,9], addition of SDS,

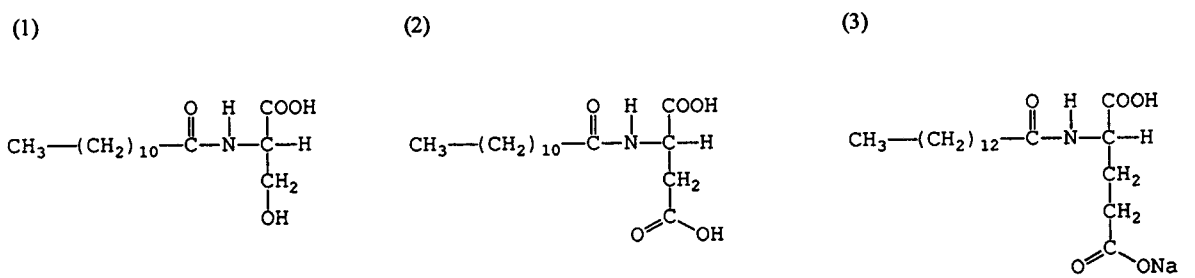

Fig. 1. Structures of (1) DSer, (2) DAsp and (3) STGlu.

urea and methanol to SDVal or SDGlu micellar solutions could give efficient enantiomeric resolution of PTH-DL-AAs and some other enantiomers. Similarly, we used DSer–SDS mixed micellar solutions (pH 11.0) containing urea and methanol or IPA to obtain good peak shapes and enhanced enantioselectivity. These electrolyte systems were stable enough to obtain a good baseline and reproducible separation, although they contained urea in a high-pH region. By using a 75 m*M* DSer–75 m*M* SDS–1 *M* urea (pH 11.0) solution containing 20% (v/v) methanol, six PTH-DL-AAs were separated and each enantiomer was optically resolved, as shown in Fig. 2. Although the order of the migration and the separation characteristic in the DSer–methanol system were very similar to those obtained with SDVal and SDGlu solutions [8,9], PTH derivatives of DL-Met and DL-Val were successfully separated from each other by this DSer–methanol system, whereas these two PTH-DL-AAs could not be separated with SDVal and SDGlu solutions.

By using IPA instead of methanol as an organic modifier, similar results for the optical resolution of the six PTH-DL-AAs were obtained, as shown in Fig. 3, although the efficiency was not comparable to that in the DSer–methanol system. However, as for PTH-DL-Thr, only the DSer–IPA system could give an enantiomeric separation, as shown in Fig. 4: in our previous studies, PTH-DL-Thr has never been optically resolved with any other N-alkanoyl-L-amino acid, i.e., SDVal and SDGlu and DSer–methanol systems. This implies that IPA is effective in enhancing the enantioselectivity of the enantiomeric pair of Thr. In Fig. 4, the peaks are not confirmed as to which corresponds to which enantiomeric form, as we have no authentic compounds of PTH-D- and -L-Thr. However, the DSer–IPA system gave two peaks for PTH-DL-

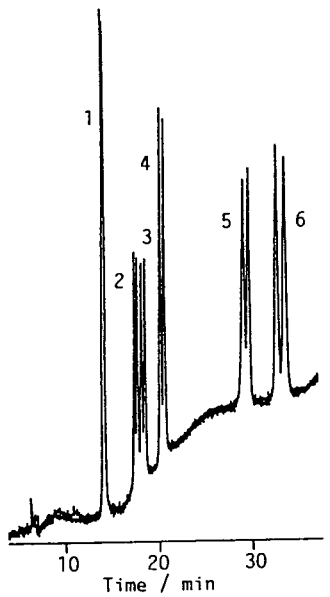

Fig. 2. Chiral separation of six PTH-DL-AAs by MEKC with DSer–methanol. Corresponding AAs: 1 = Aba; 2 = Met; 3 = Val; 4 = Nva; 5 = Trp; 6 = Nle. Micellar solution, 75 m*M* DSer–75 m*M* SDS–1 *M* urea (pH 11.0) containing 20% (v/v) methanol; separation capillary, 300 mm (effective length) × 52 μm I.D.; total applied voltage, 15 kV; electric field strength, 300 V cm^{-1}; detection wavelength, 260 nm; temperature, ambient.

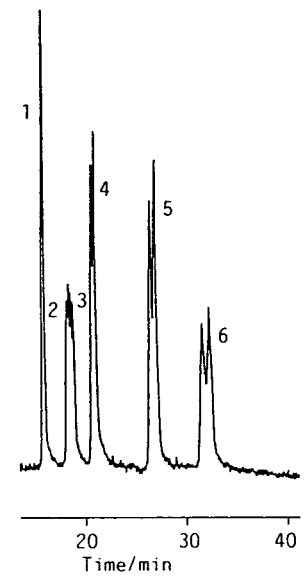

Fig. 3. Chiral separation of six PTH-DL-AAs by MEKC with DSer–IPA. Micellar solution, 75 m*M* DSer–75 m*M* SDS–1 *M* urea (pH 11.0) containing 20% (v/v) IPA; effective length of the separation capillary, 252 mm; electric field strength; 332 V cm^{-1}. Other conditions and peak numbers as in Fig. 2.

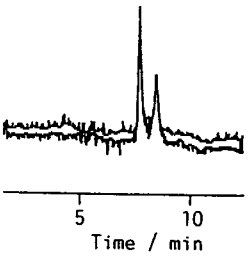

Fig. 4. Optical resolution of PTH-DL-Thr by MEKC with DSer–IPA. Conditions as in Fig. 3.

Thr, whereas only one peak was obtained with DSer–methanol for the same enantiomer.

As for other chiral surfactants, DAsp and STGlu were also examined for enantiomeric separation. The former showed some resolution but the efficiency was always low, and the latter did not show any resolution.

In conclusion, the use of DSer–SDS–urea–methanol solutions could provide a good optical resolution of PTH-DL-AAs, although the resolution was not very different from that with SDVal–SDS–urea–methanol solutions. On the other hand, DSer–SDS–urea–IPA systems were effective only for the enantiomeric separation of PTH-DL-Thr. Further investigations on chiral separations by MEKC with N-alkanoyl-L-amino acids and some other surfactants and additives are in progress.

Acknowledgements

The authors are grateful to Dr. Akio Ishiwata of Ajinomoto for kindly providing various N-alkanoyl-L-amino acids. This work was supported in part by a Grant-in-Aid for Scientific Research (No. 05750729) from the Ministry of Education, Science and Culture, Japan.

References

[1] K. Otsuka and S. Terabe, *Trends Anal. Chem.*, 12 (1993) 125–130.
[2] K. Otsuka and S. Terabe, in N.A. Guzman (Editor), *Capillary Electrophoresis Technology*, Marcel Dekker, New York, 1993, Ch. 20.
[3] S. Terabe, K. Otsuka and H. Nishi, *J. Chromatogr. A*, 666 (1994) 295–319.
[4] A. Dobashi, T. Ono, S. Hara and J. Yamaguchi, *Anal. Chem.*, 61 (1989) 1984–1986.
[5] A. Dobashi, T. Ono, S. Hara and J. Yamaguchi, *J. Chromatogr.*, 480 (1989) 413–420.
[6] K. Otsuka and S. Terabe, *J. Chromatogr.*, 515 (1990) 221–226.
[7] K. Otsuka and S. Terabe, *Electrophoresis*, 11 (1990) 982–984.
[8] K. Otsuka, J. Kawahara, K. Tatekawa and S. Terabe, *J. Chromatogr.*, 559 (1991) 209–214.
[9] K. Otsuka, M. Kashihara, Y. Kawaguchi, R. Koike, T. Hisamitsu and S. Terabe, *J. Chromatogr. A*, 652 (1993) 253–257.
[10] S. Terabe, M. Shibata and Y. Miyashita, *J. Chromatogr.*, 480 (1989) 403–411.
[11] H. Nishi, T. Fukuyama, M. Matsuo and S. Terabe, *J. Microcol. Sep.*, 1 (1989) 234–241.
[12] H. Nishi, T. Fukuyama, M. Matsuo and S. Terabe, *J. Chromatogr.*, 515 (1990) 233–243.
[13] R.O. Cole, M.J. Sepaniak and W.L. Hinze, *J. High Resolut. Chromatogr.*, 13 (1990) 579–582.
[14] Y. Ishihama and S. Terabe, *J. Liq. Chromatogr.*, 16 (1993) 933–944.
[15] S. Terabe, K. Otsuka and T. Ando, *Anal. Chem.*, 57 (1985) 834–841.

ELSEVIER

Journal of Chromatography A, 680 (1994) 321–340

JOURNAL OF CHROMATOGRAPHY A

Simulation and optimization of peptide separation by capillary electrophoresis

Alejandro Cifuentes, Hans Poppe*

Laboratory for Analytical Chemistry, University of Amsterdam, Nieuwe Achtergracht 166, 1018 WV Amsterdam, Netherlands

Abstract

The different mobility equations that have appeared in the literature for predicting peptide mobility were compared. A modified equation that relates the mobility of individual proteolytic species of a peptide to its composition has been obtained: $\mu = 1758 \log(1 + 0.297q)/M^{0.411}$, where μ is the electrophoretic mobility in 10^{-9} $m^2/s \cdot V$, q is the integral value of the charge of the species and M its molecular mass. Also, a rough estimation of the set of pK_a values for a peptide was developed. The usefulness of this equation together with a computer program for predicting separations of compounds by capillary zone electrophoresis is demonstrated, employing real electropherograms of peptides from the literature or from experiments.

1. Introduction

The separation of peptides and proteins by capillary electrophoresis (CE) is one of the most important application fields of this technique [1–4]. The CE analysis of these biopolymers provides valuable information about the identity, purity and structural changes of the peptides themselves and the proteins they constitute [2,5–7]. The high efficiencies normally obtained in these separations and the short analysis times (less than 30 min) have made CE a major laboratory tool for the separation, analysis and characterization of such biomolecules [2,8].

Nevertheless, the analysis and identification of peptides from real samples and the interpretation of peptidic maps resulting from protein hydrolysis are still time consuming [2,5,9]. There is a necessity to develop new approaches that can shorten the long time normally needed to identify peptides, and at the same time to facilitate the improvement of the quality, in terms of efficiency and resolution, of CE peptide separations.

An ab initio method that could predict residence time from structure would be valuable. Correlations of structure with mobility are therefore important. This paper presents a study comparing the different mobility equations that have appeared in the literature for predicting the mobility of peptides, in order to obtain an expression that can be applied in general terms, and consequently able to predict the electrophoretic mobilities of peptides under different separation conditions. Such an equation requires a knowledge of the charge of the species, i.e., a knowledge of pK values. Part of the work was therefore devoted to the development of an a priori estimation of pK values.

* Corresponding author.

0021-9673/94/$07.00
SSDI 0021-9673(94)00363-E

We also describe an approach that allows the prediction of migration times and peak shapes of peptides in different buffer and at different pH values. Predictions of electropherograms are carried out employing a computer program [10] in combination with one of the above-mentioned models that best relates the peptide mobility to its amino acid sequence. The predictions are compared with real separations obtained in our laboratory or from the literature.

2. Experimental

2.1. Instrumentation

Separations were carried out using a laboratory-made electrophoretic system. The apparatus included a Hivolt Model V.C.S 303/1 power supply (Wallis Electronics Worthing, UK) and a Spectroflow 757 variable-wavelength UV–Vis detector (ABI, Ramsey, NJ, USA) with a in-house modified flow cell, operated at 210 nm. Cooling of the capillary to room temperature was achieved with a liquid-thermostated air stream propelled by a fan. During electrophoresis, the current through the capillary was measured using a Metex M-3800 multimeter. A fused-silica capillary (Polymicro Technologies, Phoenix, AZ, USA) of 50 μm I.D. and 360 μm O.D. was used; the total length of the capillary was 68.4 cm and the effective length (from the injection point to the detector) was 43.8 cm. Injection was carried out at the anodic side using electromigration. The computer programs employed were Quattro Pro (Borland International, Scotts Valley, CA, USA) for the optimization of equations, one written at our laboratory for the simulation of the electrophoretic separations and whose characteristics have been described [10] and another custom program to carry out the pK_a calculations. All the programs were used on an 80386SX microprocessor-based PC (Laser 386SX).

2.2. Samples and chemicals

Peptides AGG, GGG and LGF were purchased from Nutritional Biochemicals (Cleveland, OH, USA) and peptides GGP and LGG from Fluka (Buchs, Switzerland). All the long peptides (Table 5) were purchased from Bachem Feinchemikalien (Bubendorf, Switzerland) and used as received. The peptides were dissolved in water, previously purified by passage through a PSC filter assembly (Barnstead, Boston, MA, USA), at the concentrations indicated in each instance. The samples were stored at −20°C and heated to room temperature before use. Ethanolamine, formic acid and acetic acid (E. Merck, Darmstadt, Germany), N-[tris(hydroxymethyl)methyl]glycine (Tricine) and 3-cyclohexylamino-1-propanesulphonic acid (CAPS) (Aldrich, Brunel, Netherlands) were used in the different running buffers. The pH of these solutions was adjusted using sodium hydroxide solution (1 mol/l). The buffers were stored at 4°C and heated to room temperature before use.

3. Results and discussion

3.1. General

The utility of computer programs to predict the electrophoretic behaviour of small molecules and to obtain optimum capillary zone electrophoretic (CZE) separations has been already shown [10–15]. These programs, briefly, describe substance mobility in CZE in terms of fundamental constants of each solute [pK_a and mobility of the dissociated forms (μ_{A^-})] and buffer characteristics [pH, concentration, pK_a and mobility (μ_{B^-}) of the different substances that form the buffer]. However, the possibilities of employing these programs decreases the higher is the analyte complexity in terms of the number of charged groups [16] (e.g., peptides and proteins), as there is a lack of data on the required parameters (pK_a and μ values) for such complex biopolymers.

The computer program that we have employed has been treated in more detail elsewhere [10]. It produces the complete electropherogram, and therefore data on capillary dimensions, injection

time and voltage (or injected plug length), separation voltage, electroosmotic flow and sample concentration are required.

3.2. Prediction of pK_a values of peptides

The parameters for the running buffer are usually easily obtained from the literature [17–19]. Electroosmotic flow is obtained experimentally or taken from the literature. For only very few peptides are pK_a values available in the literature. However, for a fundamental understanding of electrophoretic behaviour this knowledge is essential. Most workers resort to a set of average pK_a values for charged amino acid residues contained in peptides and a set of N-terminal and C-terminal pK_a values. One such a set is given in Ref. [6]. Such sets of values have been shown to be effective, e.g., in calculating the isoelectric point (*IP*) [20,21]. However, it is not likely that such value will lead to accurate predictions of peptide charges at pH values very different from the *IP*, where the charge is larger than unity, for two reasons. First, assigning equal pK_a values to the same type of groups (terminal COOH and NH_2, side-chain groups of the same type) and considering these as pK_a values of the entire molecule neglects the statistical effect that occurs when more than one protolytic group is present [22]. This occurs independent of any (additional) electrostatic or conformational effect of one group on the other, as will be considered later. For example, in a dicarboxylic acid with a large distance between the two carboxyls to exclude these latter effects, each having a "local" pK_a value of 4.7, the compound $COOH\cdots COO^-$ is indistinguishable from $COO^-\cdots COOH$. Therefore, this form is twice as likely to occur, on statistical groups; overall K_{a_1} and K_{a_2} values, as observed with, e.g., titrations or when estimating the charge from the mean mobility, are twice as large and twice as small, respectively, as those of an isolated COOH group; that is, the pK_a values are shifted by log 2 to 4.4 and 5.0, respectively.

In simple peptides, having only a few protolytic groups, this statistical effect may often be smaller than given in the above example because in general the "local" pK_a values differ substantially. However, with larger, multiply charged peptides it may also be greater as so many groups are involved and the likelihood that some are very similar increases. We therefore decided to follow a "brute force" approach and calculated this effect in full detail. The procedure was as follows. Assuming that "local" group pK_a values are available, the formation constant of each individual species (thus distinguishing the two forms given above) can be found as the product of K values of those groups that have given up a proton. The overall $K_{a,n}$ values can then be found by adding all such K values that pertain to a given value of n, the number of protons released.

This calculation turned out to be time consuming, even on a fast PC with a numeric processor, and while truncating the addition given above for forms that contribute very little to the sum. For instance, with eight dissociating groups already a total of $2^8 = 256$ individual forms have to be considered. Nevertheless, it was feasible to carry out the whole calculation is less than 1 min for up to fourteen dissociating groups.

A second complication stems from the mutual electrostatic interaction of charged groups: if the COOH groups in the above example are not far apart, the K value of a given group is smaller when the other group is already ionized. This effect was taken into account in the following crude manner [23]:

$$\Delta pK_{a,i} = Cq_j/D_{i,j}$$

where C is a universal constant, q_j is the charge on the influencing group (0 or 1), and $D_{i,j}$ is the distance of the reaction centres of groups i and j. The C value reflects fundamental constants, such as the elemental charge and the permittivity of the medium. Here it is very empirical in nature. The interaction will take place partly though the solution and partly through the "medium" of the molecule itself. Depending on the nature of the molecule and, e.g., the ionic strength of the solution, these contributions may differ in relative importance. Also, this approach only takes

the enthalpic effect into account; any entropy effect is neglected.

The value to be taken for the distance $D_{i,j}$ is of a similar empirical nature and is difficult to decide for each combination of functional groups in a given molecule. We found the following expression (measuring distances, D, N, Y, in units of one atom–atom bond, of the order of 0.15 nm) to be the most effective in the correlations:

$$(D_{i,j})^2 = 3^2 N_{i,j}/(3^2 + Y_i^2 + Y_j^2)$$

where $N_{i,j}$ is the (contour) distance between the anchoring points of the groups in the main chain of peptide bonds and Y_i and Y_j are the distances from the reaction centres to the anchoring points of the two groups.

This choice reflects the idea that the peptide chain forms a random chain, with random flight segments of length three times the atom–atom distance (= one peptide unit), and that summing of distances should be done quadratically because of the random orientation in space of all the length segments. The choice can be criticized in numerous ways. For example, the randomness (stiffness) of the chain may not be as described, and may not be a constant but rather depend on the charges present and the ionic strength. Also, specific conformations of the chain may be preferred, because of electrostatic and hydrophobic effects, effects that in long chains ultimately lead to folding. We nevertheless worked with these schemes, as this approach allows one to obtain estimates of pK_a values that are in our opinion better than those with the fixed set of group pK_as, and obtaining the necessary data requires only geometrically analysing the chemical formula of the peptide.

Thus, the local pK_a values were corrected with a number of terms such as given by $\Delta pK_{a,i}$, depending on the charge distribution in the form considered, and next the summation described above was carried out.

This approach requires the following data: constant C, pK_a values for twenty terminal NH groups, pK_a values for twenty COOH groups and pK_a values for seven side-chain groups (Arg, Asp, Cys, Glu, His, Lys, Tyr), a total of 48 values. (This large number of parameters may seem excessive. Indeed, a satisfactory correlation can also be obtained by assigning one value to all terminal NH_2 groups, one to proline and one to all terminal COOH-groups. With the seven side-chain values, this would lead to only ten parameters. We decided to use the 48, arguing that we were after a prediction as good as possible for a situation where the structure of the peptide is entirely known. As a result of the large number of parameters there is some triviality in the applied fitting procedure, e.g., some of the amino acids occurring in the training set do not occur in any of the peptides in the training set. As a result for the adaptation of its group pK_a values the only reference point is the amino acid itself: the training pK_a value is just reproduced in the group pK_a value, with a number of degrees of freedom of zero. We did not see this as a disadvantage, through.)

The 48 parameters were obtained by minimizing the sum of squares between predicted pK_a values and those of 43 amino acids and peptides from the literature [24–26] ranging from two to five amino acids, 98 values in total. Literature values for pK_as were corrected for zero ionic strength.

The residual sum of squared deviations (SSQ) was about a factor of 3 smaller (9.35 vs. 24.74) than can be found by just neglecting statistical and electrostatic interaction, e.g., in the way described by Rickard et al. [6].

Some indication of the validity of the procedure can also be derived from the C value obtained, 3.0. An ab initio estimate of C can be found as follows: neglecting all entropy effects, the change in a pK_a value due to a charge e at a distance D (measured in atom–atom distance, $1.5 \cdot 10^{-10}$ m) can be calculated as

$$\Delta pK_a = 0.43e^2/(4\pi\varepsilon_0\varepsilon_r D \cdot 1.5 \cdot 10^{-10})/kT$$

where e is the elementary charge, ε_0 is the permittivity of vacuum, ε_r is the relative permittivity of the medium, k is the Boltzmann constant and T is the absolute temperature. This expression at $T = 300$ K, with ε_r set to that of water, corresponds to a C value of

Table 1
Values used in CZE mobility calculations

Peptide	M	n	q		μ_{exp} [a]	μ_i [b]	μ_a [c]
			This work	From literature			
20 mmol/l sodium citrate, pH 2.5, 30°C [36]							
LEMY	554.7	4	0.89	0.82	13.1	13.2	12.4
GFY	385.4	3	0.90	0.83	15.8	15.6	14.6
GPETLCGAELVDAL	1443.6	14	0.86	0.71	9.0	8.8	7.3
QF	1293.3	2	0.84	0.83	17.4	16.3	16.3
GFYF	532.6	4	0.92	0.83	14.1	13.9	12.7
GPETLCGAELVDAL-QFVCGDR	2305.6	21	1.65	1.61	11.8	12.7	12.4
VCGDR	604.6	5	1.68	1.73	22.5	22.9	22.8
SCDLR	648.7	5	1.67	1.73	22.3	22.1	22.1
LEMYCAPLK	1123.4	9	1.82	1.82	19.1	18.7	18.4
RLEMY	710.9	5	1.79	1.82	21.4	21.8	22.2
PAK	314.4	3	1.78	1.83	26.0	30.3	31.2
CAPLK	586.7	5	1.84	1.83	18.6	25.2	24.1
FNLPTGY	825.9	7	0.95	1.83	19.7	12.0	21.0
RAPQTGIVDECCFR	1706.9	14	2.62	2.73	19.4	21.1	21.3
RLEMYCAPLK	1279.6	10	2.68	2.82	23.1	24.0	24.5
LEMYCAPLKPAKSA	1577.9	14	2.65	2.82	20.3	21.7	22.5
FNLPTGYGSSSR	1300.4	12	1.93	2.83	22.1	18.2	24.4
RLEMYCAPLKPAK	1576	13	3.48	3.82	24.6	26.6	28.1
39 mmol/l ethanolamine, pH 10, 25°C [37]							
AA	160.2	2	−0.97	−0.98	−24.2	−24.0	−24.2
AAA	231.3	3	−0.98	−0.98	−19.8	−20.9	−20.8
AN	203.2	2	−0.97	−0.98	−22.8	−21.8	−18.7
AG	146.1	2	−0.97	−0.98	−25.9	−24.9	−25.1
AGG	203.2	3	−0.98	−0.98	−22.4	−22.0	−22.0
AH	226.2	2	−0.97	−0.98	−19.2	−20.8	−21.0
GGGGG	303.3	5	−0.99	−0.98	−18.9	−18.8	−18.6
AL	207.3	2	−0.97	−0.98	−21.3	−21.8	−22.0
ALG	259.3	3	−0.98	−0.98	−19.0	−19.9	−19.9
AV	188.2	2	−0.97	−0.98	−22.5	−22.5	−22.7
GGGG	246.2	4	−0.99	−0.98	−23.3	−20.4	−20.3
GGGGGG	360.3	6	−0.99	−0.98	−17.2	−17.5	−17.4
20 mmol/l citric acid, pH 2.5, 30°C [27]							
AFDDING	750.8	7	0.75	0.33	10.3	9.9	4.7
KKKKKKK	915.5	7	7.02	7.33	50.7	52.3	53.5
AKKKKKK	858.2	7	6.05	6.33	49.5	49.0	50.3
SYSMEHFRWGKPV	1624	13	3.43	2.98	22.0	25.7	23.2
ILPWKWPWWPWRR	1907.5	13	3.63	3.32	26.7	25.1	23.5
GRTGRRNSIHDIL	1495.6	13	4.12	4.38	32.1	30.2	31.5
AFKAKNG	734.9	7	2.63	2.41	31.3	29.2	27.4
AFKIKNG	777	7	2.63	2.41	30.4	28.5	26.7
GFLRRIRPKLK	1383.9	11	5.19	5.33	37.8	36.5	37.1
AFKADNG	721.8	7	1.68	1.37	21.7	20.5	17.4
AGCKNFFWKTFTSC	1659.8	13	2.79	2.14	21.4	22.0	17.8
YAGFM	587.8	5	0.95	0.38	12.0	13.8	5.9
YVNWLLAQKGKKN-DWKHNITQ	2586.1	21	4.84	5.28	28.1	26.9	28.5

(Continued on p. 326)

Table 1 *(continued)*

Peptide	M	n	q		μ_{exp} [a]	μ_i [b]	μ_a [c]
			This work	From literature			
GGFMTSEKSQTPLVT-LFKNAIIKNAYKKGE	3304.9	30	5.01	5.30	22.9	24.9	25.8
HFRWGKPVGKKRRP-VKVYP	2336.1	19	8.00	8.24	36.8	38.4	39.0
SYSMEHFRWGKPVG-KKRRPVKVYP	2933.9	24	7.29	8.22	33.1	33.1	35.5
RKRSRKE	959.2	7	4.87	5.31	43.8	40.7	43.0
AFKKKKK	877.2	7	5.11	5.33	45.8	43.6	44.7

[a] Experimental mobility in 10^{-9} $m^2/s \cdot V$ obtained from literature.
[b] Theoretical mobility in 10^{-9} $m^2/s \cdot V$ obtained considering the charge of isolated species and Eq. 5.
[c] Theoretical mobility in 10^{-9} $m^2/s \cdot V$ obtained considering an average charge value and Eq. 5.

$$C = 0.43e^2/(4\pi \cdot 8.8 \cdot 10^{-12} \cdot 80 \cdot 1.5 \cdot 10^{-10})/(1.38 \cdot 10^{-23} \cdot 300) = 2.00$$

The value actually found was 2.96. Although this does not coincide exactly with the ab initio estimate, the fact that it is of the right order of magnitude and bearing in mind the uncertainties connected with the choice of the distance expression and the ε_r value (that of the pure water, 80) provides some confidence that the procedure partially reflects physical reality.

The final *SSQ* value, 9.35, corresponds to a

Table 2
Results from optimization for the different equations

Equation No.	Model	$\sigma = \sqrt{\frac{\sum_{i=48pep} (\mu_{iexp} - \mu_{ipre})^2}{48 - n_{parameters}}}$ (10^{-9} $m^2/s \cdot V$)		$\sigma = \sqrt{\frac{\sum_{i=25pep} (\mu_{iexp} - \mu_{ipre})^2}{25}}$ (10^{-9} $m^2/s \cdot V$)
		σ value using q from this work	σ value using average q from literature	
1	$\frac{94.58 \log(1+q)}{n^{0.312}}$	3.13	3.32	2.61
2	$\frac{839.6\ q}{M^{2/3}}$	4.24	4.74	2.51
3	$\frac{486.4\ q}{M^{0.584}}$	3.94	4.64	2.00
4	$\frac{1222\ q}{3.01M^{1/3} + 1.12M^{2/3}}$	4.02	4.70	2.02
5	$\frac{1758 \log(1+0.297\ q)}{M^{0.411}}$	2.23	2.49	1.72

Table 3
Statistical F test of the five equations from Table 3

	$\sigma_1 = 3.13$	$\sigma_2 = 4.24$	$\sigma_3 = 3.94$	$\sigma_4 = 4.02$	$\sigma_5 = 2.23$
$\sigma_1 = 3.13$		–	–	–	+
$\sigma_2 = 4.24$	–		–	–	+
$\sigma_3 = 3.94$	–	–		–	+
$\sigma_4 = 4.02$	–	–	–		+
$\sigma_5 = 2.23$	+	+	+	+	

Significance level 5%; degrees of freedom 45–48; average F value 1.64. Minus signs indicate no significant difference ($\sigma_i^2/\sigma_j^2 < 1.64$) between the equations; plus signs indicate significant difference ($\sigma_i^2/\sigma_j^2 > 1.64$).

root mean squared expected error of $\sqrt{9.35/(98\text{-}48)} = 0.43$. This requires the following comment: this precision is certainly not good enough for the prediction of special pH-induced selectivity effects. One must bear in mind that in the highly efficient CE system substances having a relative overall mobility of only 1.02 are easily separated, whereas of course a value of 1.00 leads to no separation whatsoever. The value 1.02 corresponds to a pH shift (in the middle of a titration branch) of $2 \cdot 0.43 \cdot 0.02 = 0.02$. Hence, the accuracy of the prediction is at least one order of magnitude worse than would be required to predict whether two randomly chosen peptides could be separated due to different pK_a values at some pH.

Table 4
pK_a values and electrophoretic mobilities (μ) used for the simulated electorpherograms of the five peptides in Fig. 4B

No.	Peptide	pK	μ (10^9 m^2/s·V)
1	LGF	8.06	−18.20
			0
		3.47	18.20
2	GGP	8.27	−21.27
			0
		3.21	21.27
3	GGG	8.27	−23.02
			0
		3.30	23.02
4	LGG	8.06	−20.69
			0
		3.30	20.69
5	AGG	8.24	−22.35
			0
		3.30	22.35

Nevertheless, on might hope that for structurally related peptides the prediction of differences in pK_a values is better and the prediction might

Table 5
pK_a values and electrophoretic mobilities (μ) used for the simulated electropherograms of the five peptides in Figs. 5B, 6B and 7B

No.	Peptide	pK	μ (10^9 m^2/s·V)
1	LQAAPALDKL	11.21	−20.49
		7.77	−11.43
			0
		4.16	11.43
		2.97	20.49
2	WAGGDASGE	8.58	−30.43
		5.45	−22.27
		4.23	−12.42
			0
		3.24	12.42
3	FHPKRPWIL	12.42	−10.80
			0
		10.18	10.80
		6.68	19.36
		5.27	26.45
		2.78	32.51
4	SYSMEHPRWG	13.21	−25.96
		10.30	−19.00
		7.36	−10.60
			0
		6.30	10.60
		3.74	19.00
		2.61	25.96
5	ELAGAPPEPA	8.52	−29.04
		5.18	−21.25
		4.22	−11.85
			0
		3.37	11.85

have some limited use in this respect. Also, at pH values where large peptides are multiply charged, an estimate of the total charge q is of great importance. Below we present results to that effect.

3.3. Prediction of mobilities

Next, we need an expression that permits us to obtain the electrophoretic mobilities of individual charged species. Several equations for the electrophoretic mobility of peptides have been published [6,27–30]. These semi-empirical equations relate the electrophoretic mobility (μ) of peptides with structural parameters, such as the charge (q), molecular mass (M) and amino acid numbers (n) of peptides. The equations are as follows:

Grossman's equation [27] (as also used in Ref. [28]);

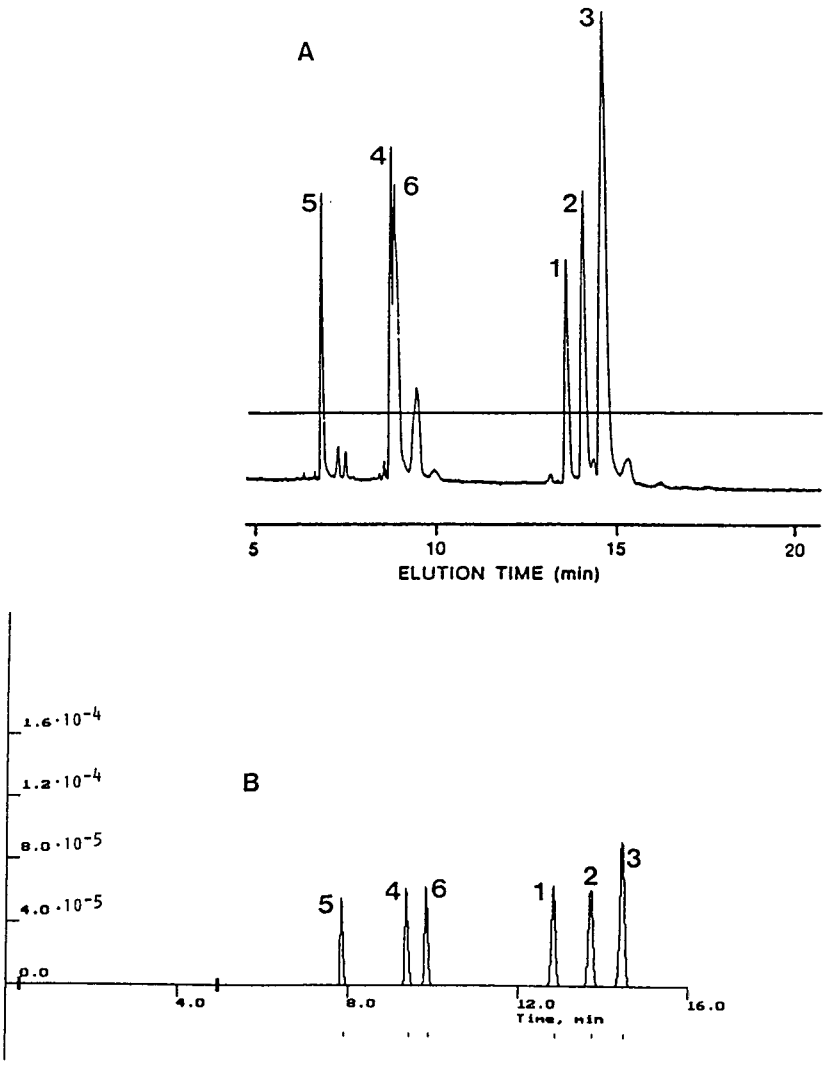

Fig. 1. Electropherogram of six model peptides: 1 = AFAAING; 2 = AFDAING, 3 = AFDDING; 4 = AFKAING; 5 = AFKKING; 6 = AFKADNG. (A) Capillary 65 cm (45 cm to detector) × 50 μm I.D. × 320 μm O.D.; electric field, 277 V/cm; buffer, 20 mM citric acid (pH 2.50); UV detection at 200 nm. Redrawn from Ref. [8]. (B) Simulated electropherogram: injection length, 2 mm; sample concentration, $1.2 \cdot 10^{-4}$–$1.8 \cdot 10^{-4}$ M; electroosmotic flow adjusted to $\mu_{eo} = 9 \cdot 10^{-9}$ m^2/s·V.

$$\mu = \frac{A \log(q+1)}{n^B} \quad (1)$$

Offord's equation [29] (as also used in Refs. [6,30–32]):

$$\mu = \frac{Aq}{M^{2/3}} \quad (2)$$

Compton's equation [33,34]:

$$\mu = \frac{Aq}{M^m} \quad (3)$$

$$\mu = \frac{Aq}{BM^{1/3} + CM^{2/3}} \quad (4)$$

In these equations A, B and C are constants depending on the solvent system used and m

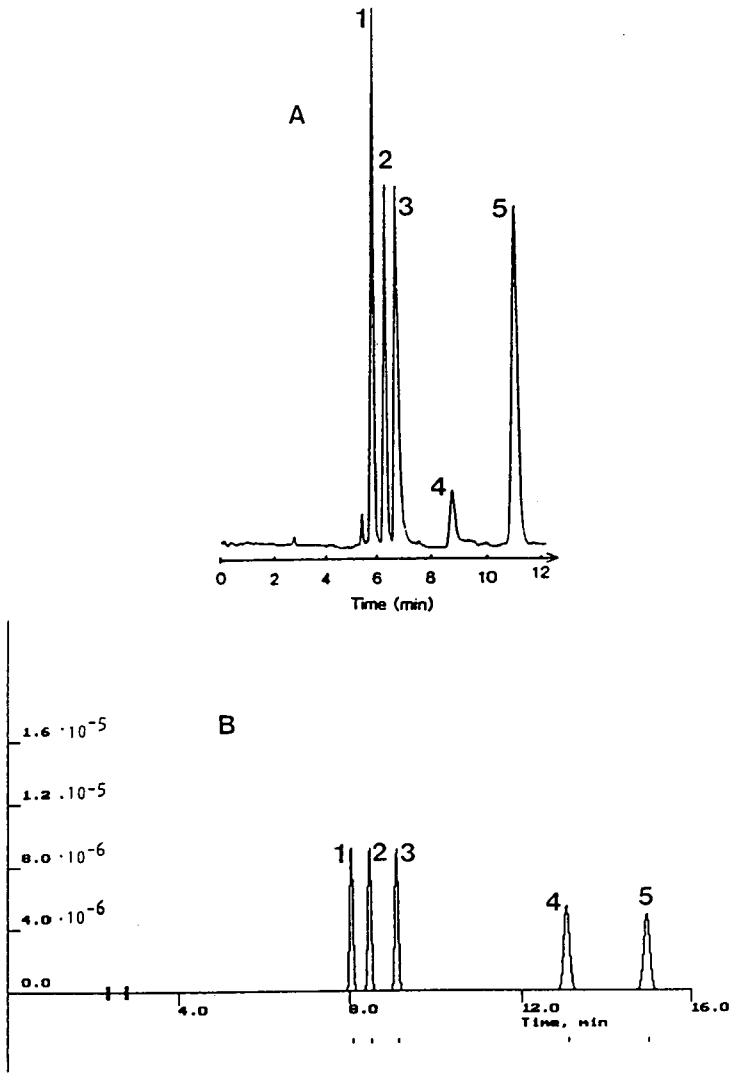

Fig. 2. Electropherogram of substance P degraded by an endopeptidase for 180 min. (A) Non-crosslinked polyacrylamide-coated capillary ($\mu_{eo} = 0$ m^2/s·V), 100 μm I.D., length from injection to detection 20 cm; run voltage, 3000 V; buffer, 30 mM phosphoric acid (pH 2.6); UV detection at 200 nm. Redrawn from Ref. [38]. (B) Simulated electropherogram: injection at 500 V for 30 s; sample concentration considered to be 10^{-5} M.

varies between 1/3 and 2/3 depending on the system and M [34,35]. These equations were used in our work, but Eq. 1 was used in a different way from that used by the originators. They (and others extending their work) inserted average (charge) q values, mostly derived from the application of the Henderson–Hasselbach equation with pK_a values from Ref. [6]. We think that this procedure is inconsistent with a first principle: the average mobility of a peptide occurring in different protolytic forms should be the weighted average of the mobilities of all forms. For mobility correlations that are non-linear in q, such as Eq. 1, this is clearly not the case. For instance, a peptide in two forms, with charges 0 and +1 in equal amounts, thus having $q = 0.5$, would give for the logarithmic factor in Eq. 1 $\log q = \log(1 + 0.5) = 0.176$; weighing of

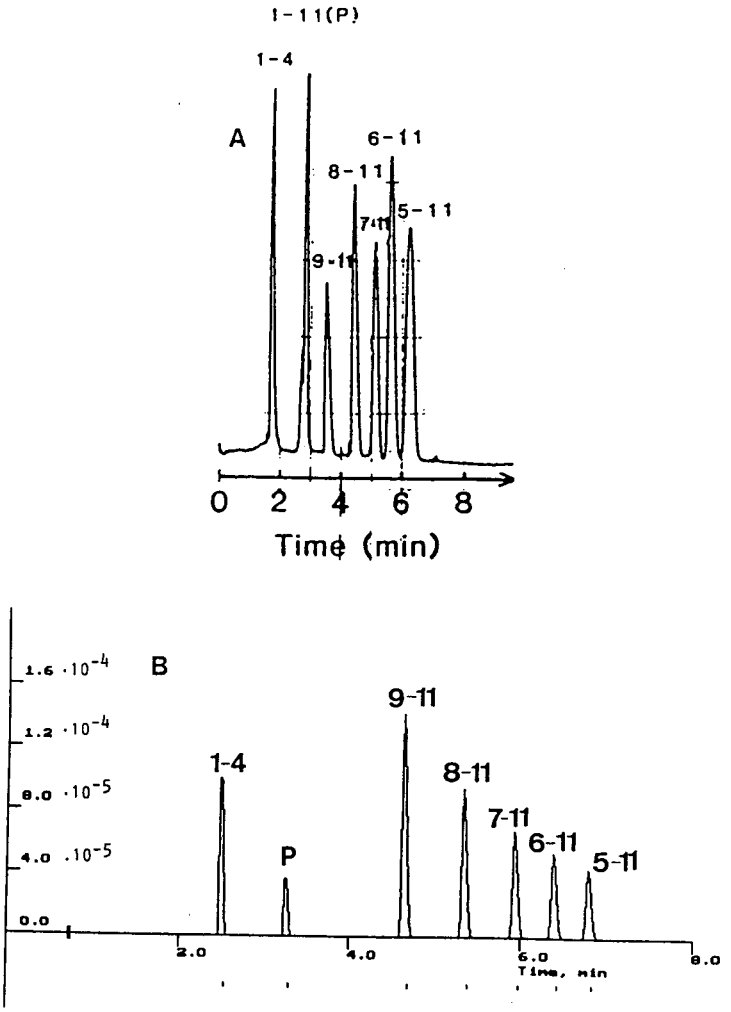

Fig. 3. Electropherogram of an artificial mixture of substance P and its (1–4), (9–11), (8–11), (7–11), (6–11) and (5–11) fragments. Sample concentration, 50 μg/ml of each peptide. (A) Non-crosslinked polyacrylamide-coated capillary ($\mu_{eo} = 0$ $m^2/s \cdot V$), 50 μm I.D., length from injection to detection 16 cm; separation voltage, 6000 V; buffer, 20 mM phosphoric acid (pH 2.6); UV detection at 200 nm. Redrawn from Ref. [38]. (B) Simulated electropherogram: injection at 2000 V for 10 s; sample concentration, 50 μg/ml.

the logarithmic factor for the individual forms yields 0.5 log (1 + 0) + 0.5 log (1 + 1) = 0.151. We remedied this by applying Eq. 1 and our modification Eq. 5 (see below) to the *individual* forms, using integer charge (qn) values instead of q, and next performing the averaging of the mobility with the Henderson–Hasselbach equation. This is numerically more complicated, but, when data are stored in a computer the expense is still negligible compared with that of an experiment.

To test these equations we used electropho-

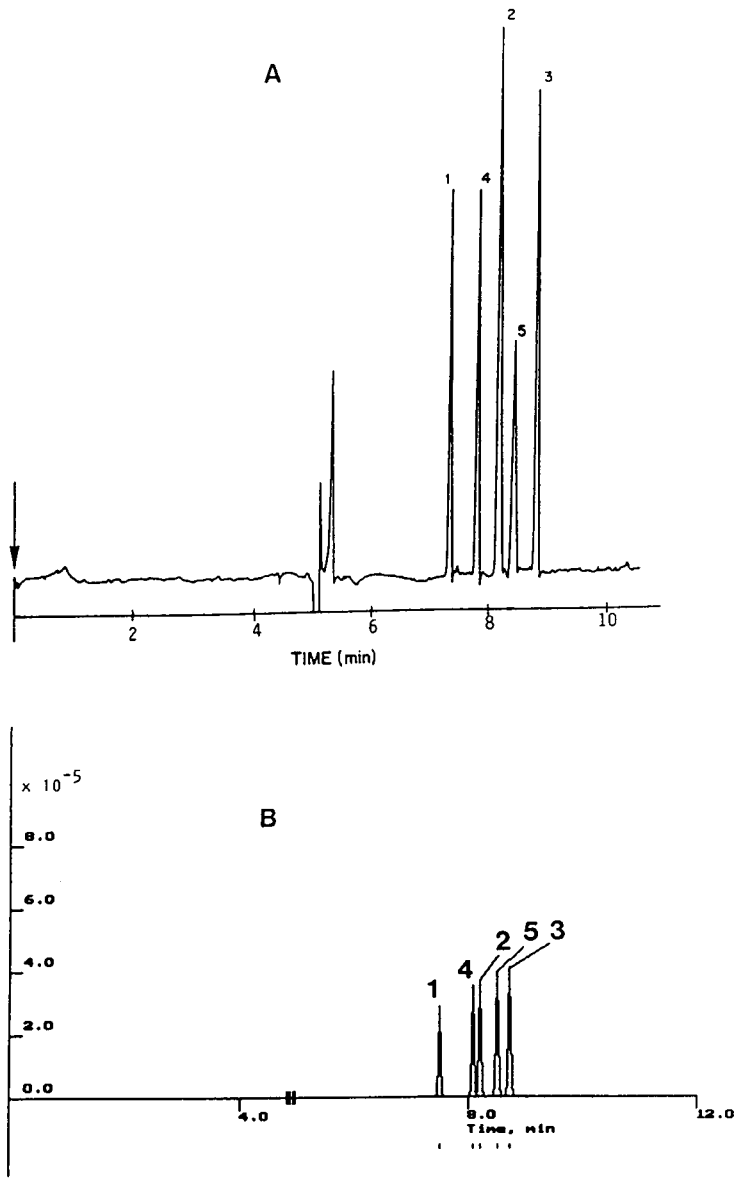

Fig. 4. Electropherograms of peptides from Table 4. Sample concentration, 0.4 mg/ml for each peptide. (A) Capillary, 68.4 cm (43.8 cm to detector) × 50 μm I.D. × 360 μm O.D.; injection at 300 V for 4 s; run voltage, 20 kV; buffer, 0.1 *M* CAPS (pH 10.4) ($\mu_{eo} = 50.8 \cdot 10^{-9}$ m^2/s·V); UV detection at 210 nm. (B) Simulated electropherogram.

retic mobility, charge and molecular mass (M or n) data from different peptides with different pH, ionic strength and buffers. These values, obtained from the literature [27,36,37], are given in Table 1. In addition we considered a modification of Eq. 1:

$$\mu = \frac{A \log(1 + Bq)}{M^C} \quad (5)$$

A logarithmic relationship between charge and mobility was chosen by the authors of Eq. 1, while considering that as the total charge on the peptide increases, the effect of other additional charges on its mobility should decrease [27]. However, the curvature described by $\log(1 + q)$ is entirely arbitrary, and we preferred to have an adjustable (via the parameter B) curvature. Also, we considered that the dependence of mobility on molecular mass could be more precise than the classical dependence on the number of amino acids in a polymer model.

The charge data from the literature given in Table 1 had been calculated employing the Henderson–Hasselbach equation and Rickard et al.'s pK values [6], and they were obtained

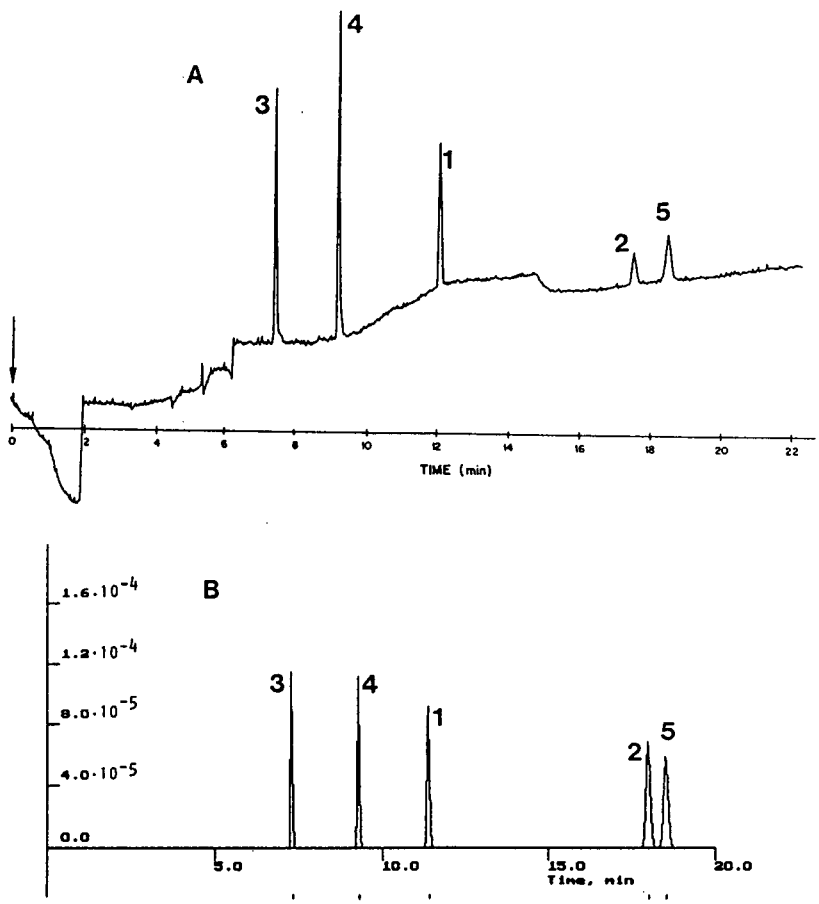

Fig. 5. Electropherograms of peptides from Table 5. (A) Conditions. as in Fig. 4, except buffer, 1.54 M acetic acid–0.66 M formic acid (pH 1.9) ($\mu_{eo} = 0$ m^2/s·V), and injection at 4500 V for 6 s (B) Simulated electropherogram.

directly from Refs. [27] and [36]. Charge data from Ref. [37] were not directly available, so they were calculated employing the same procedure as used in Refs. [27] and [36]. The presently obtained charge values ("q this work" in Table 1) were deduced employing the pK_a values obtained with our program.

The optimization of the parameters A, B, C, etc in Eqs. 1–5 was done by calculating the SSQ values between the experimental electrophoretic

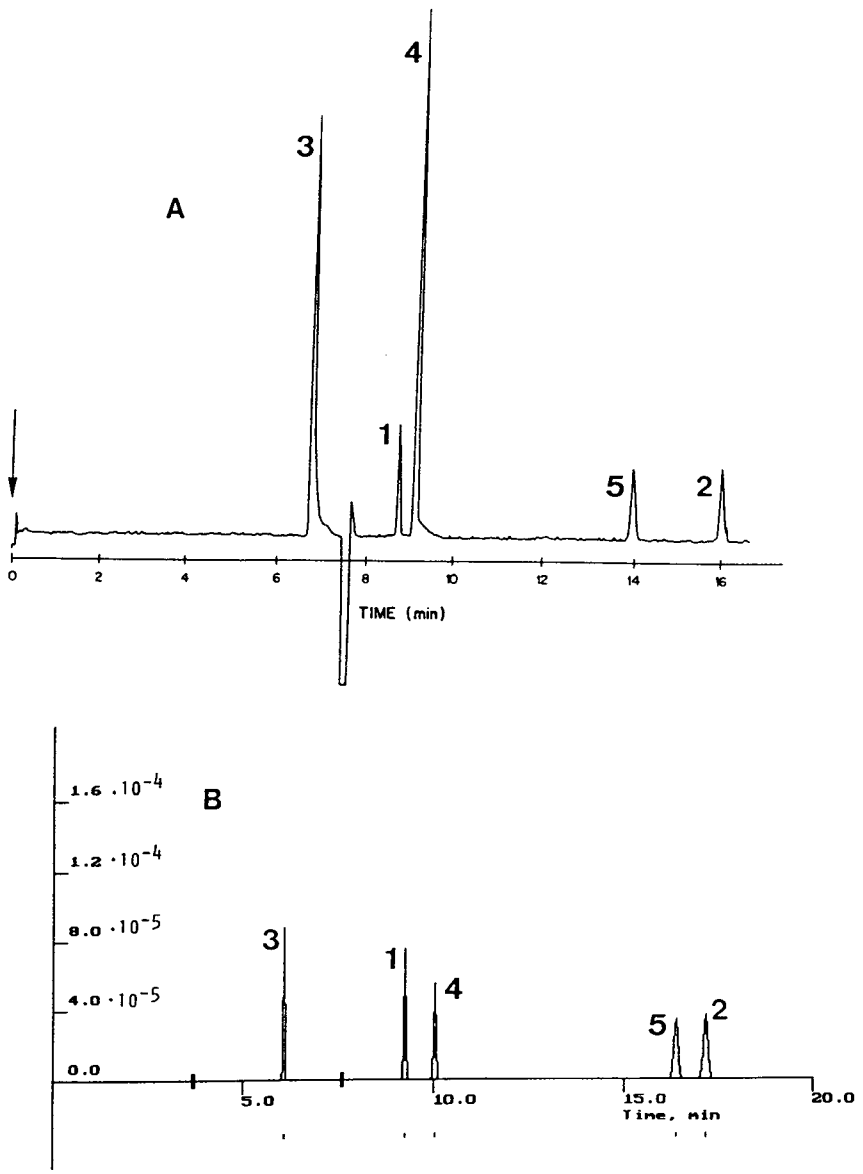

Fig. 6. Electropherograms of peptides from Table 5. (A) Conditions as in Fig. 4, except run voltage, 15 kV, buffer, 0.1 M Tricine–20 mM ethanolamine (pH 8.1) ($\mu_{eo} = 43.7 \cdot 10^{-9}$ $m^2/s \cdot V$) and injection at 2000 V for 5 s. (B) Simulated electropherogram.

mobility of the 48 peptides and their respective predicted values, and adjusting the parameters until a minimum *SSQ* was obtained. The results with this optimization for the five equations were tested by calculating the electrophoretic mobility for two groups of five different peptides. The first group was measured at two values of pH (1.9 and 10.4) and the other at three values (1.9, 8.1 and 11.5). Then, 25 predicted mobility values from each equation were compared with the experimental data.

The results are shown in Table 2 in terms of σ, equal to SSO/α, where α is the number of data minus the number of parameters. The results show lower σ values for all the models when the charge values obtained in this work were employed instead of the average charges from the literature, so all later calculations were carried out employing the first values. To compare the five different equations a statistical F test was applied to theses σ values (Table 3). Considering a significance level of 5%, and a number of degrees of freedom ranging from 45 to 47 depending on the tested equation, we obtained

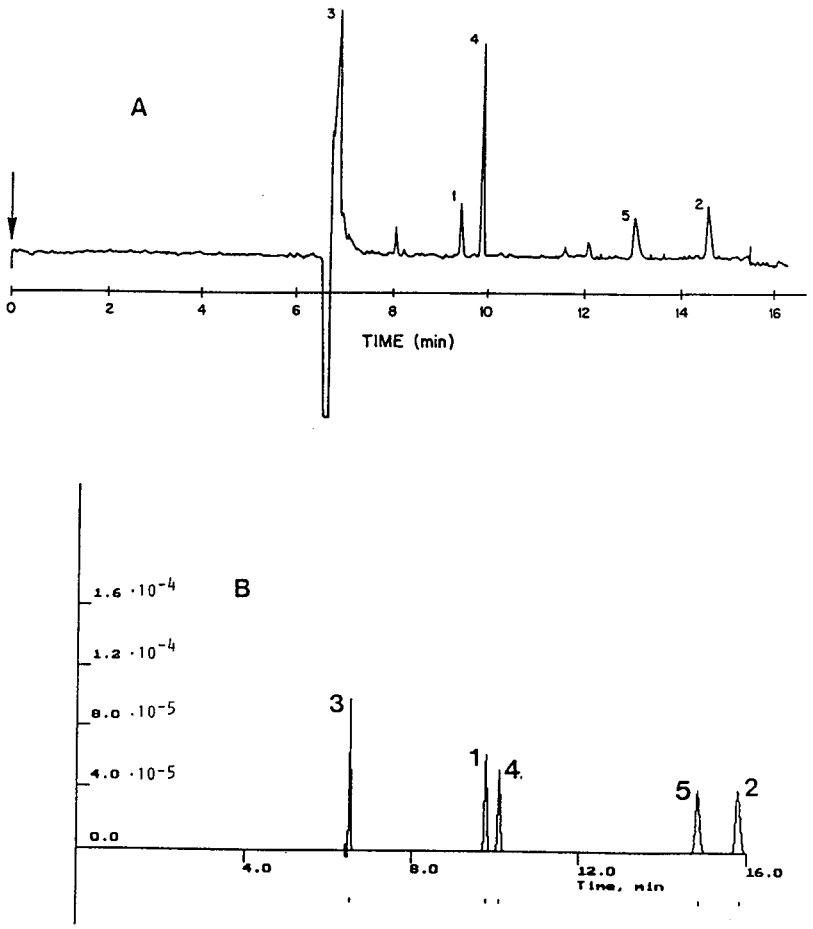

Fig. 7. Electropherograms of peptides from Table 5. (A) Conditions as in Fig. 4, except run voltage, 15 kV, buffer, 40 m*M* CAPS (pH 11.5) ($\mu_{eo} = 51.4 \cdot 10^{-9}$ m^2/s·V) and injection at 2000 V for 5 s. (B) Simulated electropherogram.

from the statistical tables an average F value of 1.64. Employing this F value no significant differences ($\sigma_i^2/\sigma_j^2 < 1.64$) were observed between the Grossman, Offord and Compton equations (this result is marked with minus signs Table 3). Therefore, the ability of these equations to predict mobility values can be considered to be similar. However, when the Eq. 5 was compared with the other models significant differences were found ($\sigma_i^2/\sigma_j^2 > 1.64$). This result was corroborated when the σ values were calculated for the 25 mobility values from our experiments. As can be seen in Table 2, the best result ($\sigma = 1.72$) was also obtained employing Eq. 5.

3.4. Rapid identification of peptides knowing their amino acid sequence

The utility of employing the described mobility Eq. 5 and the corrected pK_a values for predicting peptides separations from its amino acid sequence can be seen in the simulated separation of six different peptides at pH 2.5. The correct migration order of peptides and their peak shape in the simulation (Fig. 1B) agrees fairly well with the real electropherogram [8] (Fig. 1A). In this instance, and also for Fig. 12 and 9, it was impossible to obtain the electroosmotic flow values from the literature, so these were adjusted in order to obtain similar migration times. It should be noted, however, that this is the only parameter adjusted; all other necessary data were derived at this stage from the amino acid sequence of the peptides. This also holds in Section 5, 6 and 7.

The rapid identification of peptides can be shown using the CE separation of five peptides obtained by Nyberg et al. [38] (Fig. 2A). They mixed the sample from an enzymatic reaction with each standard peptide in order to identify the different peaks. Using the computer program and the amino acid sequence of each peptide, their identification is obtained immediately (Fig. 2B). Identical results were achieved employing other separations from the same work (Fig. 3A), showing again that with the present scheme the correct migration order is predicted (Fig. 3B).

3.5. Choosing the best buffer and pH for peptide analysis in order to improve the separation efficiency and resolution

The application was carried out by simulating the separation of five short peptides with very similar size and pK values (Table 4) and five larger peptides (Table 5) ranging from a highly basic (e.g., peptide 3) to a highly acidic (e.g., peptide 2) with about 30 different running buffers with different pH values (data not shown). As the necessary time for each simulation is only a few seconds, the best buffers in terms of resolution and speed can be found quickly. The results (Figs. 4A, 5A, 6A and 7A) show that the experimentally obtained electropherograms agree fairly well with those predicted theoretically (Figs. 4B, 5B, 6B and 7B, respectively).

We also tested for these simulations the pK_a values given in Ref. [6] instead the pK_a values that we had obtained (given in Tables 4 and 5). Employing those pK values and for the simulation at pH 11.5 an incorrect migration order appeared (data not shown) between peaks 1 and 4. In order to obtain good agreement it was necessary to shift the pK value of peptide 1 from

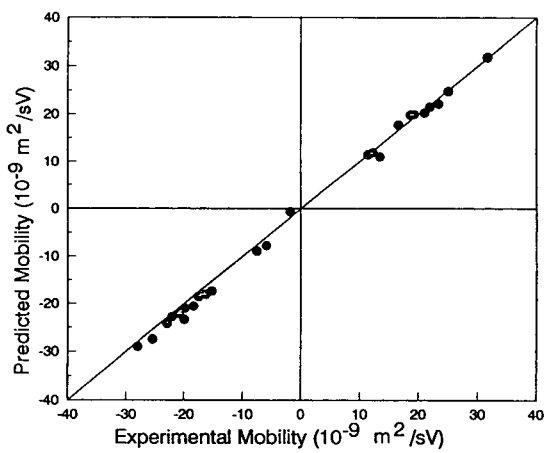

Fig. 8. Correlation between predicted and experimental mobility for the five peptides in Table 4 (at pH 1.9 and 10.4) and the five peptides in Table 5 (at pH 1.9, 8.1 and 11.5). The slope is 1.04 with a correlation coefficient of 0.9993 determined by linear regression.

10.3 to 11.8. This effect is probably the result of electrostatic interactions within the molecule, because in this peptide the side-chain charge on the amino acid lysine (K) is very close to the terminal charge on leucine (L). However, the program that we have developed considers this effect and such shifts of pK values were not necessary.

When the predicted mobility was plotted against the experimental mobility (Fig. 8) for those peptides we obtained good agreement, although five different buffer systems were used. The slope was 1.04 with a correlation factor of 0.9993 determined by linear regression.

The computer program also permits us to study the separation conditions in terms of sample capacity. Thus, buffer containing 0.1 M Tricine permitted injections ten times larger than that shown in Fig. 6A without a noticeable decrease in efficiency. This possibility should be useful in the future for micropreparative applications of CE.

3.6. Checking impurities assigned to peaks

As an example of this application we can consider the separation obtained by Nielsen and

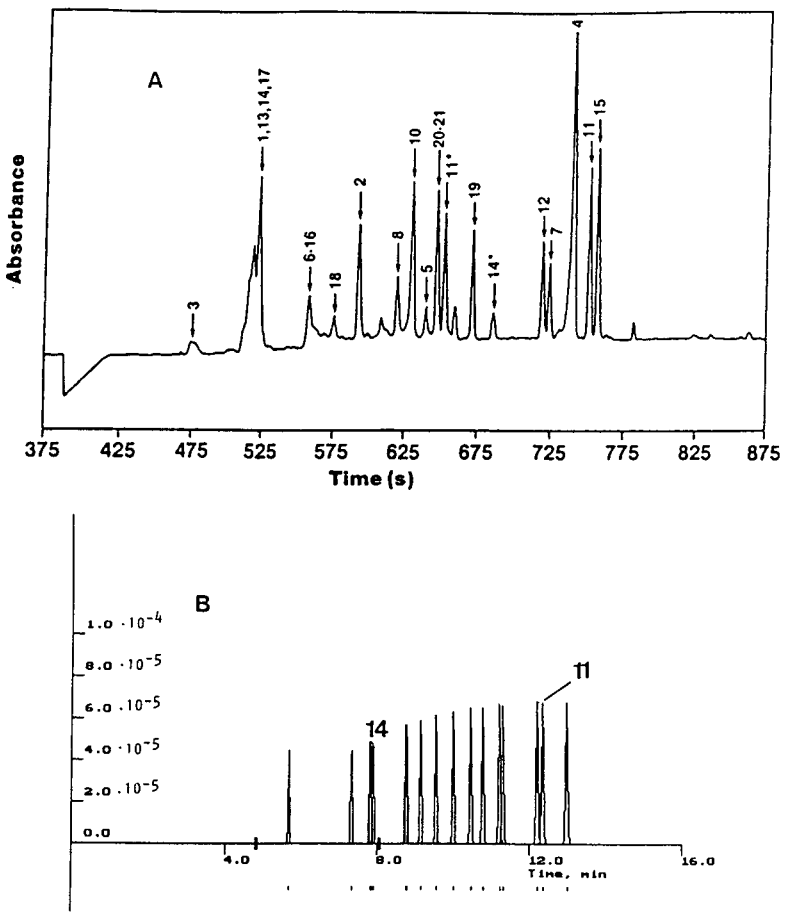

Fig. 9. Electropherogram of hGH digest. Sample concentration, 90 μM for each peptide. (A) Capillary, 100 cm (80 cm to detector) × 50 μm I.D. × 360 μm O.D.; separation voltage, 30 kV; buffer, 0.1 M Tricine–20 mM morpholine (pH 8.1); UV detection at 200 nm. Redrawn from Ref. [9]. (B) Simulated electropherogram: Injection length, 3 mm; electroosmotic flow considered to be $\mu_{eo} = 55 \cdot 10^{-9}$ m^2/s·V.

Rickard [9] (Fig. 9A). They isolated the peptides by RP-HPLC or anion-exchange chromatography, and their sequence was confirmed by spiking individual fragments for RP-HPLC or amino acid analysis. However, they had difficulty in distinguishing impurities 14* and 11* from the peptides 14 and 11, respectively; they showed [5] an initial error in the peak assignment [2] between peaks 14 and 14* because of their very similar composition. Comparing the predicted separation (Fig. 9B) with the real one (Fig. 9A), these peptides could be easily distinguished from their respective impurities taking into account the very different migration times for the proper peptides and their impurities.

Nevertheless, several problems appeared in the simulation of this separation. First, we could not include the peptides with double chain (numbers 6–16 and 20–21) in the simulated electropherogram because the computer program cannot predict the corrected pK_a values for these structures. Second, several peptides showed strange behaviour in the simulation when it was compared with the real electropherogram; a summary of these inconsistencies is given in Fig. 10. Namely, peptides 4, 5, 10, 15 and 17 show an incorrect order in the simulated electropherogram. This effect is probably due to the charge variation that several amino acids suffer around the separation pH employed (8.1), where sufficiently accurate predictions are much more difficult to carry out than at extreme values. In order to achieve a better simulation, in addition to the electrostatic effect [39,40] other effects that can influence the peptide mobility should also be considered, e.g., hydrophobic effects [7] and the influence of the different orientation of the side-chains [7] that can appear in long peptides. The determination of detailed long peptide surface charge distributions directly from the sequence is an unsolved problem [6,27,39,40].

3.7. Understanding the electrophoretic behaviour of various peptides

We employed the separation of six peptides at pH 11 obtained by Grossman et al. [8] (Fig. 11A). In their work they explained that "the poor peak shape seen in peak 3 is probably due to a perturbation of the electrical field caused by an increased conductivity in the sample band relative to the buffer". Looking at the simulated electropherogram (Fig. 11B) we can see that this explanation seems correct for peak 3. Nevertheless, they did not give any explanation about the poor shape of peak 5; if we compare the theoretically obtained peak 5 with that in the real electropherogram, we can see that, in this in-

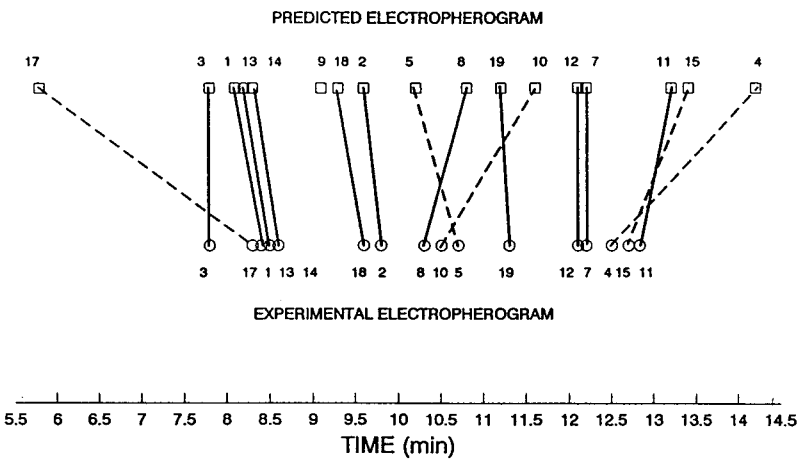

Fig. 10. Summary of the inconsistencies (dashed lines) observed in Fig. 9 between the real and predicted electropherogram.

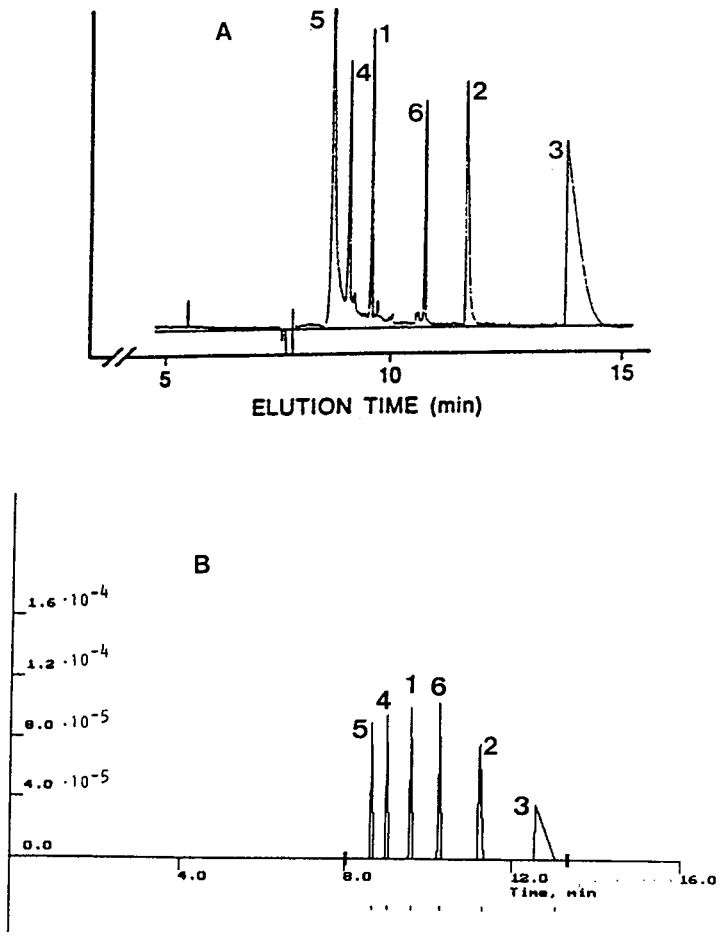

Fig. 11. Electropherogram of the six model peptides in Fig. 1A. (A) Capillary, 120 cm (100 cm to detector) × 50 μm I.D. × 320 μm O.D.; electric field, 250 V/cm ($\mu_{eo} = 83 \cdot 10^{-9}$ $m^2/s \cdot V$, calculated from the figure); buffer, 20 m*M* CAPS (pH 11); UV detection at 200 nm. Redrawn from Ref. [8]. (B) Simulated electropherogram: injection length, 4 mm; sample concentration, $1.2 \cdot 10^{-4}$–$1.8 \cdot 10^{-4}$ *M*.

stance, the explanation cannot be the conductivity difference. In our opinion the peak broadening more likely to be due to solute–capillary wall interactions, because of the strongly basic character of this peptide. A similar effect can be observed when comparing the peak shape obtained experimentally for peptide 3 at pH 8.1 (Fig. 6A) with the peak shape for the same peptide in the simulated electropherogram (Fig. 6B). Actually, the computer program can predict peak shapes, fronts or tailings, due to conductivity effects, injection and axial diffusion, fairly well but it cannot predict analyte–capillary wall adsorption effects. On the other hand, comparing the theoretical (Fig. 12A) and experimental (Fig. 12B) electropherograms at pH 4, we observed that two more peaks appear after 60 min of analysis.

Acknowledgements

We thank Hans Boelens and Raivo Kilg for assistance with the statistical calculations and data optimization. This work was supported by the Commission of the European Communities

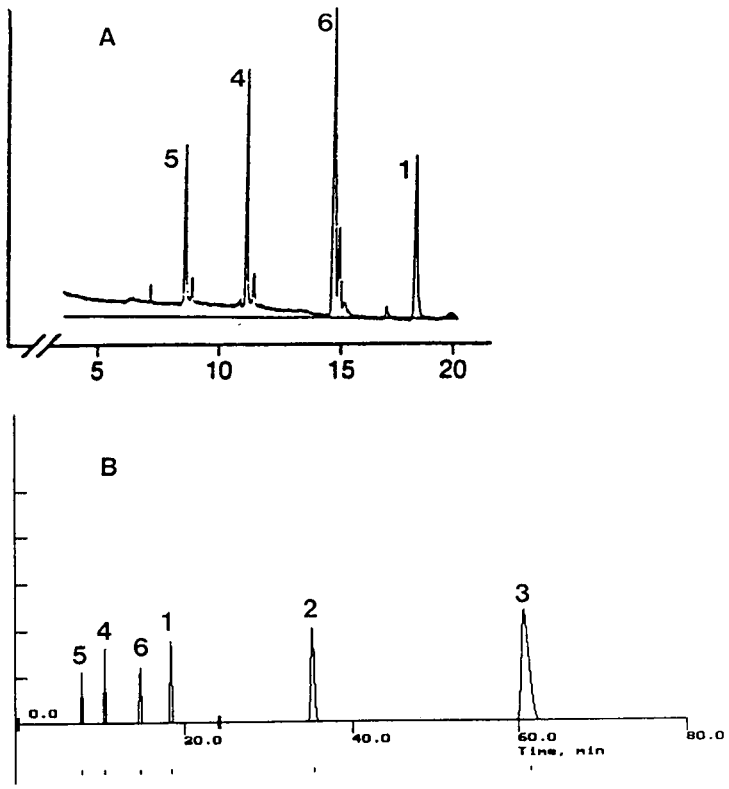

Fig. 12. (A) Conditions as in Fig. 1A except buffer pH, 4. Redrawn from Ref. [8]. Electropherogram simulated (B): injection length, 2 mm; sample concentration, $1.2 \cdot 10^{-4}$–$1.8 \cdot 10^{-4}$ M; electroosmotic flow, considered to be $\mu_{eo} = 11 \cdot 10^{-9}$ $m^2/s \cdot V$.

(Human Capital and Mobility Programme, bursary No. ERB4001GT920989).

References

[1] M. Novotny, K.A. Cobb and J. Liu, *Electrophoresis*, 11 (1990) 735.
[2] P.D. Grossman, J.C. Colburn, H.H. Lauer, R.G. Nielsen, R.M. Riggin, G.S. Sittampalam and E.C. Rickard, *Anal. Chem.*, 61 (1989) 1186.
[3] K.A. Cobb and M. Novotny, *Anal. Chem.*, 61 (1989) 2226.
[4] W.G. Kuhr and C.A. Monning, *Anal. Chem.*, 64 (1992) 389R.
[5] R.G. Nielsen, R.M. Riggin and E.C. Rickard, *J. Chromatogr.*, 480 (1989) 393.
[6] E.C. Rickard, M.M. Strohl and R.G. Nielsen, *Anal. Biochem.*, 197 (1991) 197.
[7] H.J. Gaus, A.G. Beck-Sickinger and E. Bayer, *Anal. Chem.*, 65 (1993) 1399.
[8] P.D. Grossman, K.J. Wilson, G. Petrie and H.H. Lauer, *Anal. Biochem.*, 173 (1988) 265.
[9] R.G. Nielsen and E.C. Rickard, *J. Chromatogr.*, 516 (1990) 99.
[10] H. Poppe, *Anal. Chem.*, 64 (1992) 1908.
[11] S.C. Smith and M.G. Khaledi, *Anal. Chem.*, 65 (1993) 193.
[12] T.A.A.M. van de Goor, P.S.L. Janssen, J.W. van Nispen, M.J.M. van Zeeland and F.M. Everaerts, *J. Chromatogr.*, 545 (1991) 379.
[13] J.C. Reijenga and E. Kenndler, *J. Chromatogr. A*, 659 (1994) 403.
[14] J.C. Reijenga and E. Kenndler, *J. Chromatogr. A*, 659 (1994) 417.
[15] E.V. Dose and G.A. Guiochon, *Anal. Chem.*, 63 (1991) 1063.
[16] R.A. Mosher, P. Gebauer and W. Thormann, *J. Chromatogr.*, 638 (1993) 155.
[17] J. Pospichal, P. Gebauer and P. Bocek, *Chem. Rev.*, 89 (1989) 419.
[18] T. Hirokawa, M. Nishino and Y. Kiso, *J. Chromatogr.*, 252 (1982) 49.

[19] J. Pospichal, M. Deml and P. Bocek, *J. Chromatogr.*, 390 (1987) 23.
[20] B. Skoog and A. Wichman, *Trends Anal. Chem.*, 5 (1986) 82. .
[21] A. Sillero and J.M. Ribeiro, *Anal Biochem.*, 179 (1989) 319.
[22] E.Q. Adams, *J. Am. Chem. Soc.*, 38 (1916) 1503.
[23] N. Bjerrum, *Z. Phys. Chem.*, 106 (1923) 219.
[24] A.E. Martell and R.M. Smith, *Critical Stability Constants: Amino Acids*, Vol. 1, Plenum Press, London, 1974.
[25] D.D. Perrin, *Dissociation Constants of Organic Bases in Aqueous Solution*, Butterworth, London, 1972.
[26] E.P. Serjeant and B. Dempsey, *Ionization Constants of Organic Acids in Aqueous Solution (IUPAC Chemical Data Series*, No. 23), Pergamon Press, Oxford, 1979.
[27] P.D. Grossman, J.C. Colburn and H.H. Lauer, *Anal. Biochem.*, 179 (1989) 28.
[28] J. Bongers, T. Lambros, A.M. Felix and E.P. Heimer, *J. Liq. Chromatogr.*, 15 (1992) 1115.
[29] R.E. Offord, *Nature*, 211 (1966) 591.
[30] H.J. Issaq, G.M. Janini, I.Z. Atamna, G.M. Muschik and J. Lukszo, *J. Liq. Chromatogr.*, 15 (1992) 1129.
[31] J. Frenz, S.L. Wu and W.S. Hancock, *J. Chromatogr.*, 480 (1989) 379.
[32] Z. Deyl, V. Rohlicek and M. Adam, *J. Chromatogr.*, 480 (189) 371.
[33] B.J. Compton, *J. Chromatogr.*, 559 (1991) 357.
[34] B.J. Compton and E.A. O'Grady, *Anal. Chem.*, 63 (1991) 2597.
[35] N. Chen, L. Wang and Y.K. Zhang, *Chromatographia*, 37 (1993) 429.
[36] V.J. Hilser, G.D. Worosila and S.E. Rudnick, *J. Chromatogr.*, 630 (1993) 329.
[37] T. Hirokawa, Y. Kiso, B. Gas, I. Zuskova and J. Vacik, *J. Chromatogr.*, 628 (1993) 283.
[38] F. Nyberg, M.D. Zhu, J.L. Liao and S. Hjerten, in C. Schafer-Nielsen (Editor), *Electrophoresis '88*, VCH, Weinheim, 1988, pp. 141–150.
[39] C. Tanford and J.G. Kirkwood, *J. Am. Chem. Soc.*, 79 (1957) 5333.
[40] J.B. Matthew, *Annu. Rev. Biophys. Biophys. Chem.*, 14 (1985) 387.

ELSEVIER

Journal of Chromatography A, 680 (1994) 341–351

JOURNAL OF CHROMATOGRAPHY A

Multiple-buffer-additive strategies for enhanced capillary electrophoretic separation of peptides

Robert P. Oda[a], Benjamin J. Madden[a], John C. Morris[b], Thomas C. Spelsberg[a], James P. Landers[a,*]

[a]*Department of Biochemistry and Molecular Biology, Mayo Clinic/Foundation, Rochester, MN 55905, USA*
[b]*Endocrine Research Unit, Mayo Clinic/Foundation, Rochester, MN 55905, USA*

Abstract

A dodeca-peptide from the β-subunit of thyroid stimulating hormone (TSH) was used as a model system for developing "multiple-buffer-additive" strategies to effect the separation of structurally-similar peptides. A series of synthetic peptides included six peptides with identical amino acid composition and two with multiple alanine substitutions at selected positions. Those with identical amino acid composition included the native and reverse sequences of residues 101–112 of the β-TSH and four "computer-shuffled" amino acid sequences. Buffer additives such as acetonitrile (ACN), hexane sulfonic acid (HSA), and hexamethonium bromide (HxMBr), were shown to alter selectivity dramatically. HSA, an ion-pairing agent, and ACN, known to alter the hydrophobic environment of the solute, and HxMBr, which is thought to negate solute–wall interactions, are shown to independently effect only partial resolution of the mixture. It is shown that only with the proper combination of HSA and ACN are all mixture components resolved. These results re-affirm that CE selectivity may be altered by changes in buffer ionic strength or with the addition of HSA, but also show that further changes in selectivity can be achieved through alteration of buffer hydrophobicity. The observed changes in selectivity accompanying the addition of HSA and ACN may be due to differing electrophoretic mobilities resulting from nearest-neighbor effects or subtle differences in peptide secondary structure or solvation. This emphasizes the importance of employing multiple-buffer-additive strategies for effecting the resolution of peptide mixtures that are difficult to separate.

1. Introduction

High-performance capillary electrophoresis (HPCE) is an analytical technique applicable to both small (drug-like) and large (macromolecular) components of biological interest. The capability of attaining separation selectivities complementary to those with high-performance liquids chromatography (HPLC) in a rapid, automated and reproducible manner has set the stage for HPCE to become a premier method for the separation of molecules of a diverse size and nature in complex matrices [1–4]. The use of polyimide-coated fused-silica capillaries allows for the efficient dissipation of Joule heat and, hence, for electrophoretic separations to be carried out in free-solution under high fields (up to 30 000 V).

* Corresponding author.

SSDI 0021-9673(94)00532-E

The identification of conditions for the separation of synthetic dipeptides was one of the first successes for HPCE [5,6]. In the time since these initial reports, the high separation efficiencies inherent with HPCE have been shown to be useful for the analysis of peptides which have undergone subtle structural changes including deamidation [1], single amino acid substitution [7,8], geometrical isomers which vary only in the surface of the peptide exposed to the matrix [9] and oxidation [10] as well as glycosylation, sulfonation, phosphorylation or covalent bond formation (e.g. disulfide) [11]. Key to achieving high-efficiency separations is the use of low-pH buffer systems which leads to maximal protonation of silanol groups on the inner capillary wall (i.e. reduction of the negative character) and the peptides (making them highly positively charged). Under these conditions, high separation efficiencies are attainable as a result of minimal peptide–wall interactions).

The tremendous selectivity of CE is clearly defined through the ability to resolve peptides with the small structural differences described above. The selectivity is further emphasized in a study by Frenz et al. [7] who used strategically located histidine and arginine residues in "shuffled" peptide sequences (same total composition, shuffled amino acid order) to evaluate the parameters governing selectivity. These peptides, all theoretically possessing the same charge-to-mass (q/m) ratio were shown to have different mobilities upon modification of the pH. This demonstrated that separation was not simply based on a simple mass-to-charge ratio, but that other parameters, such as the variable nature of the surface presented to the matrix or "nearest-neighbor" effects, may play a role.

With the series of experiments described in this study, we demonstrate the utility of various buffer additives to effect the separation of structurally similar peptides. The remarkable separations obtained by appropriate combinations of additives demonstrates the sensitivity of CE to subtle differences in the charge-to-mass ratio, peptide secondary structure, and "nearest-neighbor" effects.

2. Experimental

2.1. Materials

Sodium hydroxide, phosphoric acid (85%), hydrochloric acid and acetonitrile (ACN; HPLC–UV spectral grade) were purchased from Fisher Scientific. All chemicals for peptide synthesis were purchased from Applied Biosystems (Foster City, CA, USA). Borax (sodium tetraborate), boric acid, hexamethonium bromide (HxMBr), hexamethonium chloride (HxMCl), decamethonium bromide (DcMBr), and hexanesulfonic acid (HSA) were purchased from Sigma (St. Louis, MO, USA). Trifluoroacetic acid (TFA) was from Pierce (Rockford, IL, USA).

2.2. Peptide synthesis

The thyroid-stimulating hormone (TSH) peptide corresponding to the native sequence (residues 101–112) and its analogues were synthesized by 9-fluorenylmethoxycarbonyl (FMOC) amino acid strategy on an ABI 431A peptide synthesizer (Applied Biosystems) using the protocols and reagents provided by the manufacturer. Each peptide was purified by RP-HPLC using a Vydac C_{18} column (25×2.2 cm) using a trifluoroacetic acid (TFA)–acetonitrile buffer system. Peptide integrity was monitored by either amino acid analysis or plasma desorption mass spectrometry.

2.3. Buffer and sample preparation

Phosphate buffer was made by diluting a 1.0 *M* stock solution and adjusting the pH with NaOH. All buffers were made with Milli-Q (Millipore) water, and filtered through an 0.2-μm filter (Gelman) before use. Additives were made as 1 *M* stock solutions, and added to the appropriately pH'ed buffer to the final concentration. Stock solutions of peptides were solubilized in Milli-Q purified water at a final concentration of 1 mg/ml. The mixture of peptides was made by taking an equal volume of each

peptide resulting in a concentration of 125 μg/ml for each peptide. Samples were frozen until used. Peptide solutions were filtered (0.2 μm, Millipore) before use. Confirmation of peptide peak identity was made by double injection of the mixture and a solution containing a single peptide.

2.4. High-performance liquid chromatography

HPLC separation was carried out on an ABI 130A separation system (Applied Biosystems) using an ABI Aquapore OD-300 (C_{18}) (100 × 2.1 mm) column. Running conditions included a flow-rate of 0.2 ml/min with a gradient of 0 to 25% B over the course of 30 min starting at 6 min (buffer A: 25 m*M* sodium phosphate, pH 2.5; buffer B: acetonitrile–water (40:60) with 25 m*M* sodium phosphate, pH 2.5). Detection was at 215 nm.

2.5. CE Instrumentation

HPCE separation was carried out on a Beckman P/ACE System 2050 or 2100 interfaced with an IBM 55SX computer utilizing System Gold software (V. 7.1) for instrument control and data collection. All peak information (migration time) was obtained through the System Gold software.

2.6. CE separation conditions

Separations were carried out in a phosphate running buffer, ranging in concentration from 50 to 150 m*M*, pH 2.0 with or without additives, such as HSA, ACN and HxMBr. The standard method used was as follows: a three-column volume rinse with running buffer, 5 s pressure injection (0.5 p.s.i.; 1 p.s.i. = 6894.76 Pa) of peptide mixture (125 μg/ml of each peptide), separation at constant voltage (with the inlet as the anode and the outlet as the cathode), a five-column volume wash with 0.1 *M* NaOH followed by a five-column volume rinse with running buffer. Capillaries were polyimide-coated fused silica, 57 cm (50 cm to the detector) × 50 μm I.D. Capillary temperature was maintained at 28°C. Detection was by absorbance at 200 nm.

3. Results and discussion

One of the clear advantages of CE over other complimentary techniques is the ease with which the selectivity can be changed. This can be achieved through a number of approaches including the use of buffer additives which add a chromatographic component to the separation (e.g. micelles with detergents) or those which dynamically coat the inner surface of the capillary (alkylamines).

The vast literature on peptide analysis by CE clearly defines the utility of this technique for resolving peptides (see [11] and references cited therein). Among these are numerous examples describing the usefulness of single-component, low-pH buffer for resolving peptides with struc-

Table 1
Amino acid sequence of the peptide containing residues 101 to 112 from the β-subunit of TSH and its analogues used in this study

Peptide	Description	Amino acid sequence
1	Native	Lys–Thr–Asn–Tyr–Cys–Thr–Lys–Pro–Gln–Lys–Ser–Tyr
2	Ala_8-Substituted	Lys–Ala–Ala–Ala–Cys–Ala–Lys–Ala–Ala–Lys–Ala–Ala
3	Ala_7-Substituted	Lys–Ala–Ala–Tyr–Cys–Ala–Lys–Ala–Ala–Lys–Ala–Ala
4	Reverse	Tyr–Ser–Lys–Gln–Pro–Lys–Thr–Cys–Tyr–Asn–Thr–Lys
5	Shuffle 1	Lys–Pro–Asn–Lys–Ser–Tyr–Cys–Tyr–Thr–Gln–Thr–Lys
6	Shuffle 2	Gln–Pro–Ser–Lys–Lys–Thr–Tyr–Cys–Lys–Thr–Tyr–Asn
7	Shuffle 3	Lys–Pro–Thr–Gln–Tyr–Asn–Lys–Ser–Thr–Tyr–Lys–Cys
8	Shuffle 4	Lys–Lys–Asn–Lys–Pro–Tyr–Cys–Thr–Gln–Thr–Ser–Tyr

tural differences as minimal as a single amino acid change. For the purpose of defining subtle selectivity changes in low pH buffer systems as a function of "multiple-buffer additives", a series of peptides were used where the peptides involved differed only in amino acid sequence. Using a dodeca-peptide (residues 101–112) from the β-subunit of TSH as a model peptide, a series of synthetic dodeca-peptides containing variations on the "native" primary sequence (Table 1) was synthesized. The synthetic peptides included the "native" and "reverse" sequences, as well as four peptides with "shuffled" amino acid sequences of the native TSH peptide. Two additional peptides containing multiple alanine substitutions at selected (neutral) positions in the sequence were also synthesized. These eight peptides provide an excellent model mixture for evaluation of buffer additives for enhancing selectivity for the CE separation of structurally similar peptides.

The RP-HPLC separation of the peptide mixture is given in Fig. 1. Four peptides are completely resolved, while the remaining four are only partially resolved. The fact that the native (peptide 1) and reverse (peptide 4) sequences are well resolved highlights the importance of nearest-neighbor effects or slight differences in secondary structure resulting from the reversed N- and C-terminal amino acids.

Fig. 2 shows the separation of the model peptides in a phosphate buffer, pH 2.05, where the concentration of phosphate is varied from 50 to 150 m*M*. As the phosphate concentration is increased the expected increase in migration time for all peaks as a result of decreased electroosmotic flow (EOF) is observed. The resolution of the structurally similar peptides, 1, 4, 5 and 6, is enhanced slightly at higher phosphate concentrations, despite the increase in system current accompanying these higher concentration buffers (37, 52 and 75 μA for 50, 100 and 150 m*M*, respectively). The fact that peptide 6 is only barely resolved as a shoulder in 50 m*M*, lost into the peak containing peptides 1 and 4 (as a back shoulder) in 100 m*M*, and optimally

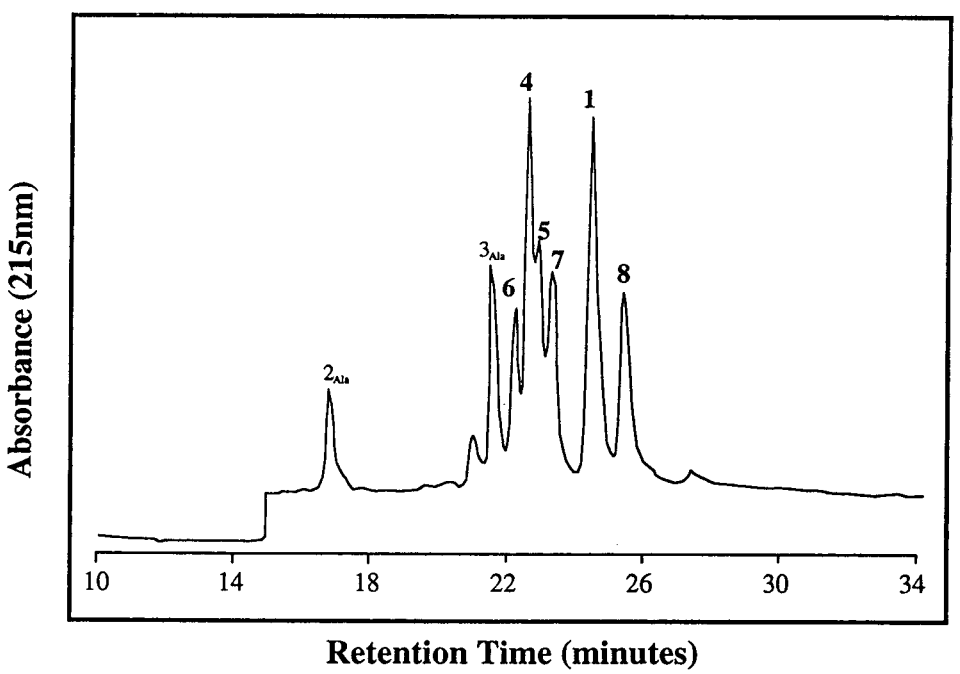

Fig. 1. HPLC separation of the components of the peptide mixture. An ABI Aquapore OD-300 (100 × 2.1 mm) column was equilibrated with buffer A (25 m*M* sodium phosphate, pH 2.5) and a gradient of 0 to 25% B [buffer B: acetonitrile–water (40:60) with 25 m*M* sodium phosphate, pH 2.5] applied over the course of 30 min starting at 6 min.

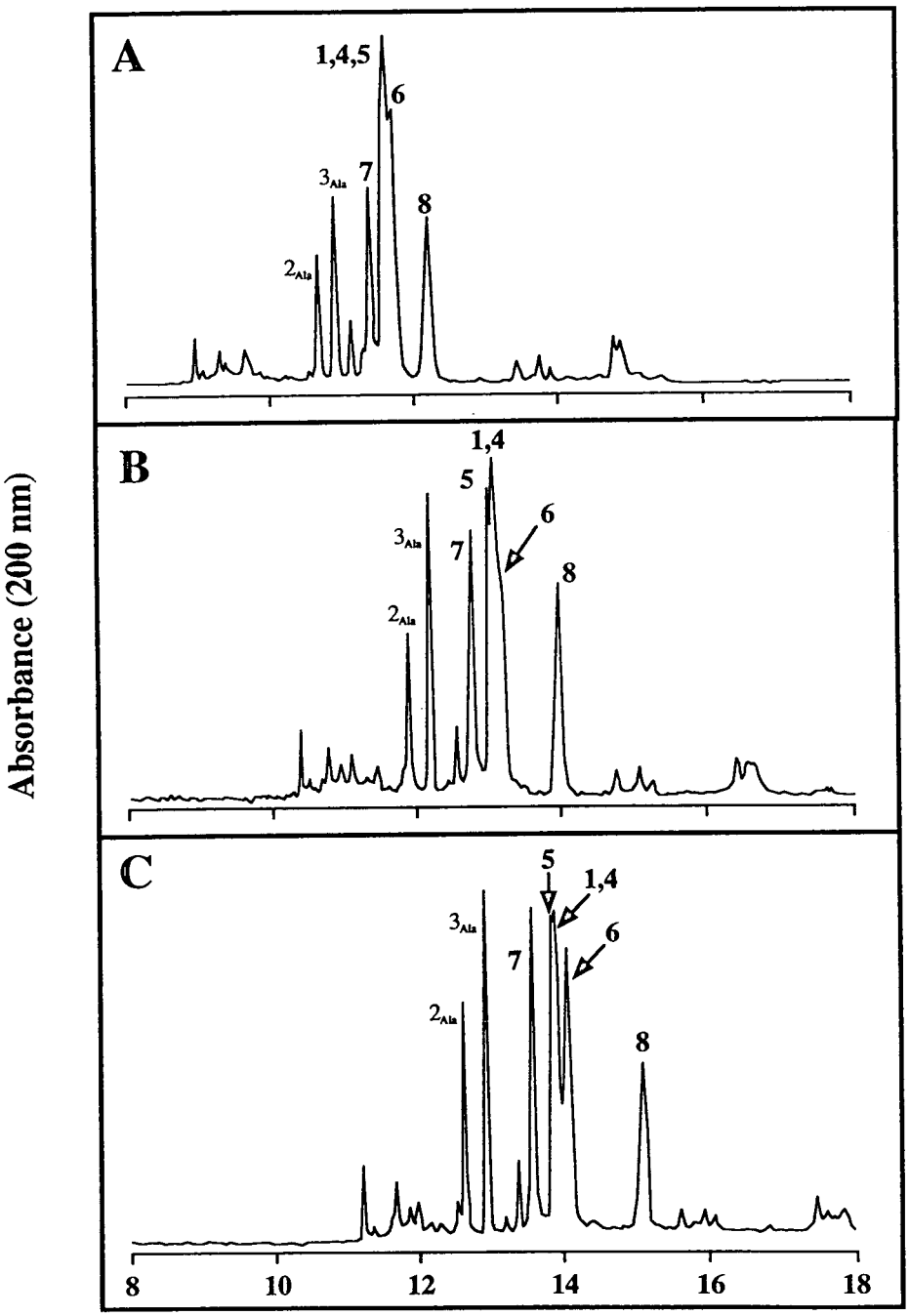

Fig. 2. Separation of the shuffled peptides in varied concentrations of phosphoric acid, pH 2.0. (A) 50 m*M* phosphoric acid, (B) 100 m*M* phosphoric acid, (C) 150 m*M* phosphoric acid. Bare fused-silica capillary, 57 cm (50 cm to the detector) × 50 μm I.D. Separation conditions: 15 kV, 28°C.

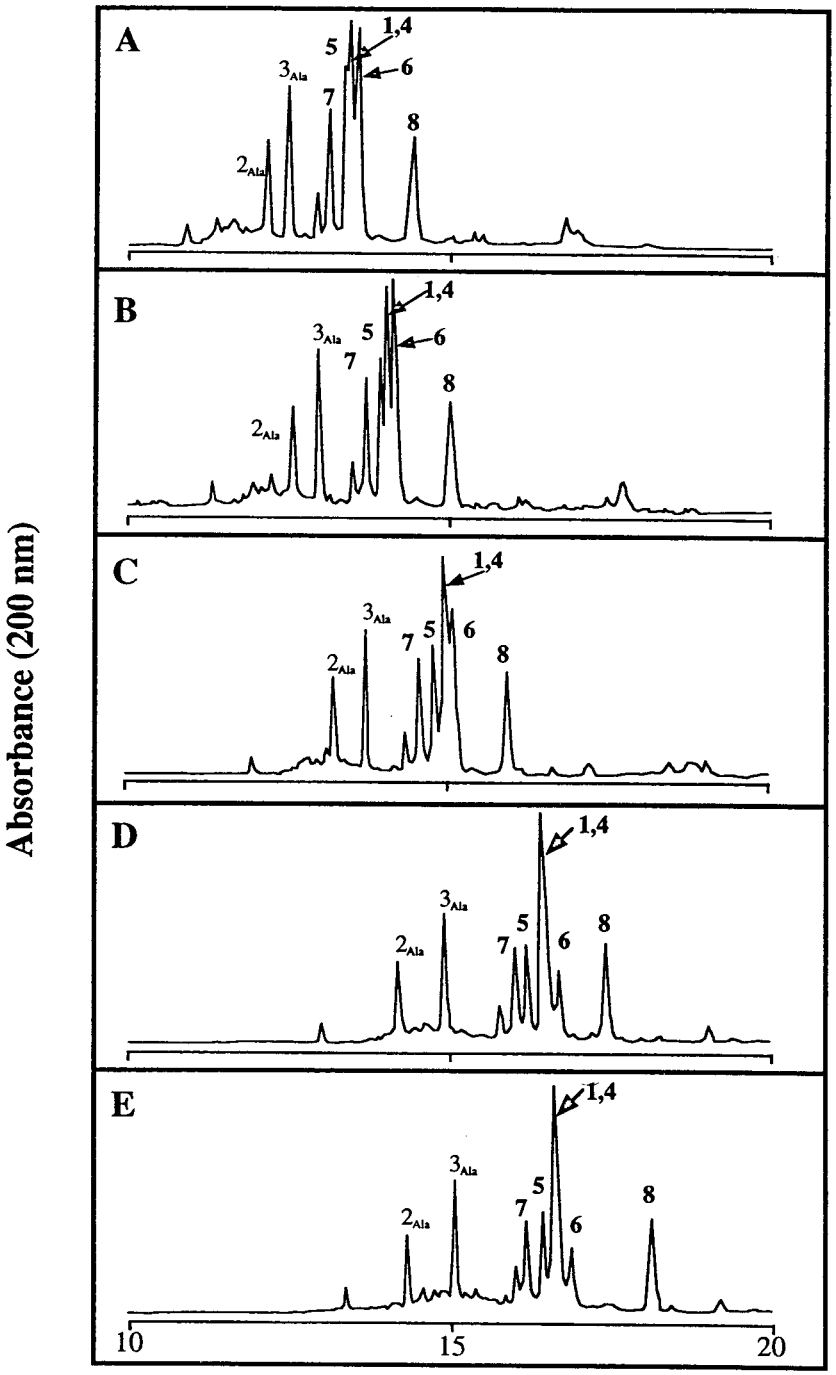

Fig. 3. Dependence of the separation of the peptides on the concentration of hexanesulfonic acid. The separation buffer contained: (A) 50 m*M* phosphoric acid, pH 2.0, 10 m*M* HSA; (B) 50 m*M* phosphoric acid, pH 2.0, 25 m*M* HSA; (C) 50 m*M* phosphoric acid, pH 2.0, 50 m*M* HSA; (D) 50 m*M* phosphoric acid, pH 2.0, 100 m*M* HSA; (E) 100 m*M* HSA, in distilled water, titrated to pH 2.0 with sulfuric acid. Bare fused-silica capillary, 57 cm (50 cm to the detector) × 50 μm I.D. Separation conditions: 15 kV, 28°C.

resolved in 150 m*M* phosphate indicates that slight changes in selectivity are occurring with the increases in ionic strength and decreases in EOF.

The addition of HSA to the separation buffer has been shown to be useful for the separation of peptides [12]. Its effect on the separation of the model peptide mixture as a result of the addition of HSA to 50 m*M* phosphate buffer (pH 2.05) is given in Fig. 3. The most obvious effect resulting from the presence of HSA is the increased migration time for all peaks as a result of the increased ionic strength and subsequent decrease in EOF. When HSA is present at concentrations below the critical micellar concentration (Fig. 3A; HSA = 10 m*M*), the resolution of peptide 6 is very similar to that observed with no HSA and 150 m*M* phosphate (Fig. 2C). The resolution is significantly improved with the addition of HSA at the critical micellar concentration (CMC = 460 m*M*) where peptide 6 is clearly resolved and peptide 5 begins to resolve from the peak containing peptides 1 and 4 (Fig. 3B). Further increase in the HSA concentration led to better resolution of peptide 5 from the peak containing peptides 1 and 4 and appeared to be optimal at 100 m*M* (Fig. 3C and D). Analysis of the same sample mixture in 100 m*M* HSA without 50 m*M* phosphate (pH 2.05 attained by titration with sulfuric acid) showed that the observed resolution was not dependent on the presence of phosphate in the separation buffer (Fig. 3E).

Acetonitrile has been shown to be a useful additive for peptide analysis by CE [13]. This additive has been postulated to enhance CE separation through either differential solvation of the peptides or solvent-induced differences in the ionization of the peptide termini and/or charged amino acid side chains. The effect of acetonitrile (in 50 m*M* phosphoric acid, pH 2.0) on the resolution of the model peptides is given in Fig. 4. The presence of this organic additive at a concentration of 10% (v/v) led to the separation of peptides 4 and 5 from 1 and 6. Doubling the acetonitrile concentration resulted in better separation of peptide 6 from peptide 1 which was now a shoulder on the peak containing peptides 1, 4 and 5.

When none of the individual components (described in the previous figures) allowed for resolution of all eight peptides, combinations of these additives were tested. The separation conditions that proved to be optimal for separation of these peptides, including the partial resolution of the native (1) and reverse (4) peptides, was a buffer containing 50 m*M* phosphate (pH 2.05), 100 m*M* HSA and 10% ACN. Fig. 5 shows a comparison of the separation obtained with phosphate alone (A), phosphate and HSA (B) and phosphate, HSA and ACN (C and D). Resolution of the native and reverse peptides appears to be optimal in the presence of 10% ACN. This separation was observed under no other conditions. Increasing the ACN concentration to 20%, changes the selectivity to a significant extent leading to the single peak resolution of peptide 4, but the loss of resolution between peptides 1 and 6.

A buffer additive shown to be useful for resolving glycoproteins with small structural differences [14] was also tested (Fig. 6). The separation of the peptide mixture in the presence of hexamethonium bromide, a bis-quaternary ammonium compound, in the presence and absence of acetonitrile was tested. The addition of HxMBr (final concentration, 5 m*M*) to 50 m*M* phosphate buffer, pH 2.05, resulted in a slight increase in migration time, but not near the magnitude observed at more neutral pH values [14]. The general migration order of the peaks was similar to that observed in phosphate buffer alone, i.e. peak 2, peak 3, peak 7, peaks 1, 4, 5, 6 and peak 8. Partial resolution of peptides 4 and 5 from the peak containing 1 and 6 was observed and could be selectively changed by the addition of 10% acetonitrile. Under these conditions, peptides 1, 4, 5 and 6 are not resolved as single entities but instead as two peaks, one containing peptides 4 and 5 the other containing peptides 1 and 6.

4. Conclusions

The results of this study demonstrate that the presence of multiple additives in the separation

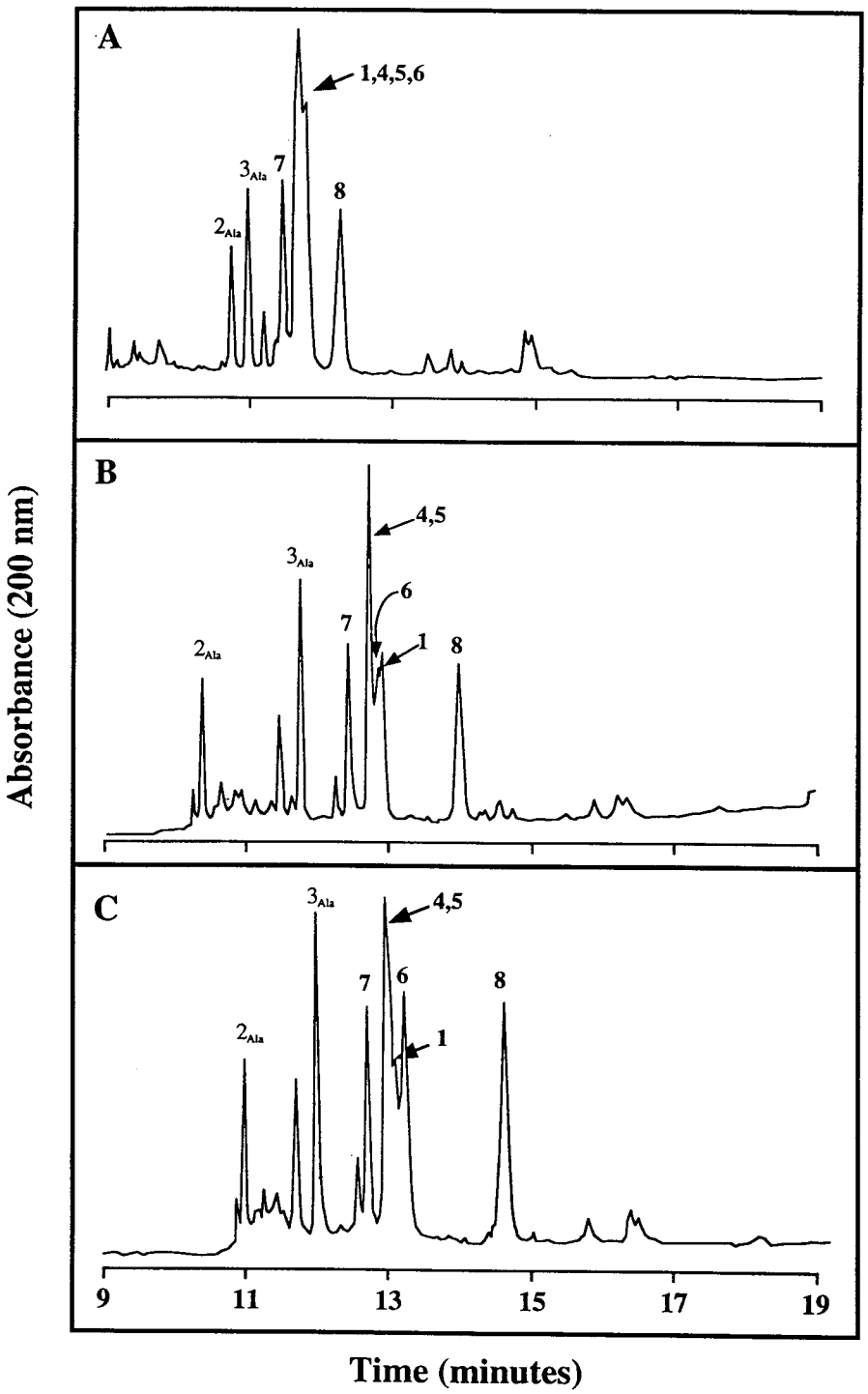

Fig. 4. The effect of acetonitrile on resolution of the peptides in 50 m*M* phosphoric acid, pH 2.0. The separation buffer contained: (A) 50 m*M* phosphoric acid, pH 2.0, no additive; (B) 50 m*M* phosphoric acid, pH 2.0, 10% (v/v) acetonitrile; (C) 50 m*M* phosphoric acid, pH 2.0, 20% (v/v) acetonitrile. Bare fused-silica capillary, 57 cm (50 cm to the detector) × 50 μm I.D. Separation conditions: 15 kV, 28°C.

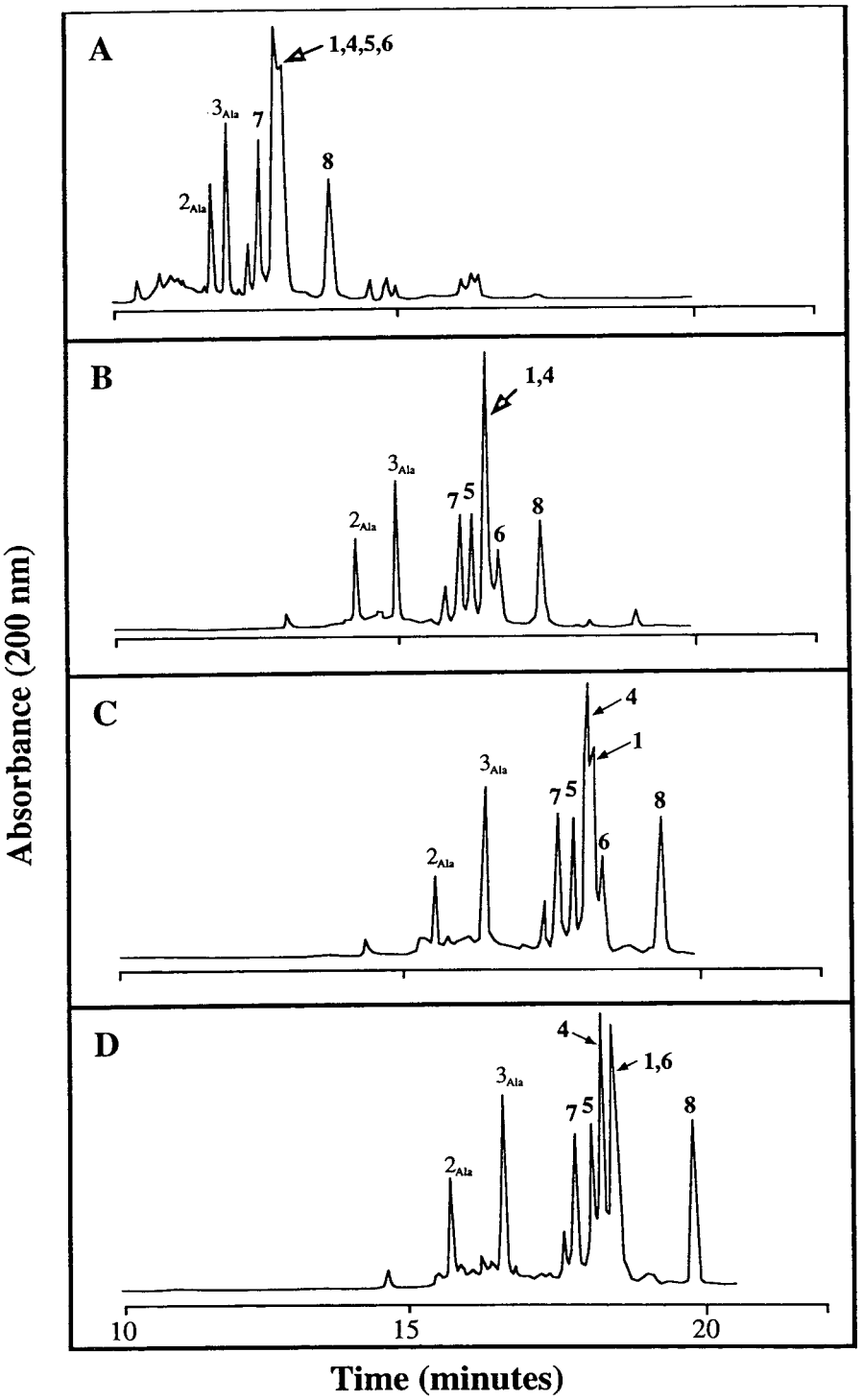

Fig. 5. The combined effect of acetonitrile and hexanesulfonic acid on the separation of the peptides in 50 m*M* phosphoric acid, pH 2.0. The separation buffers contained: (A) 50 m*M* phosphoric acid, pH 2.0; (B) 50 m*M* phosphoric acid, pH 2.0, 100 m*M* HSA, 0% (v/v) acetonitrile; (C) 50 m*M* phosphoric acid, pH 2.0, 100 m*M* HSA, 10% (v/v) acetonitrile; (D) 50 m*M* phosphoric acid, pH 2.0, 100 m*M* HSA, 20% acetonitrile. Bare fused-silica capillary, 57 cm (50 cm to the detector) × 50 μm I.D. Separation conditions: 15 kV, 28°C.

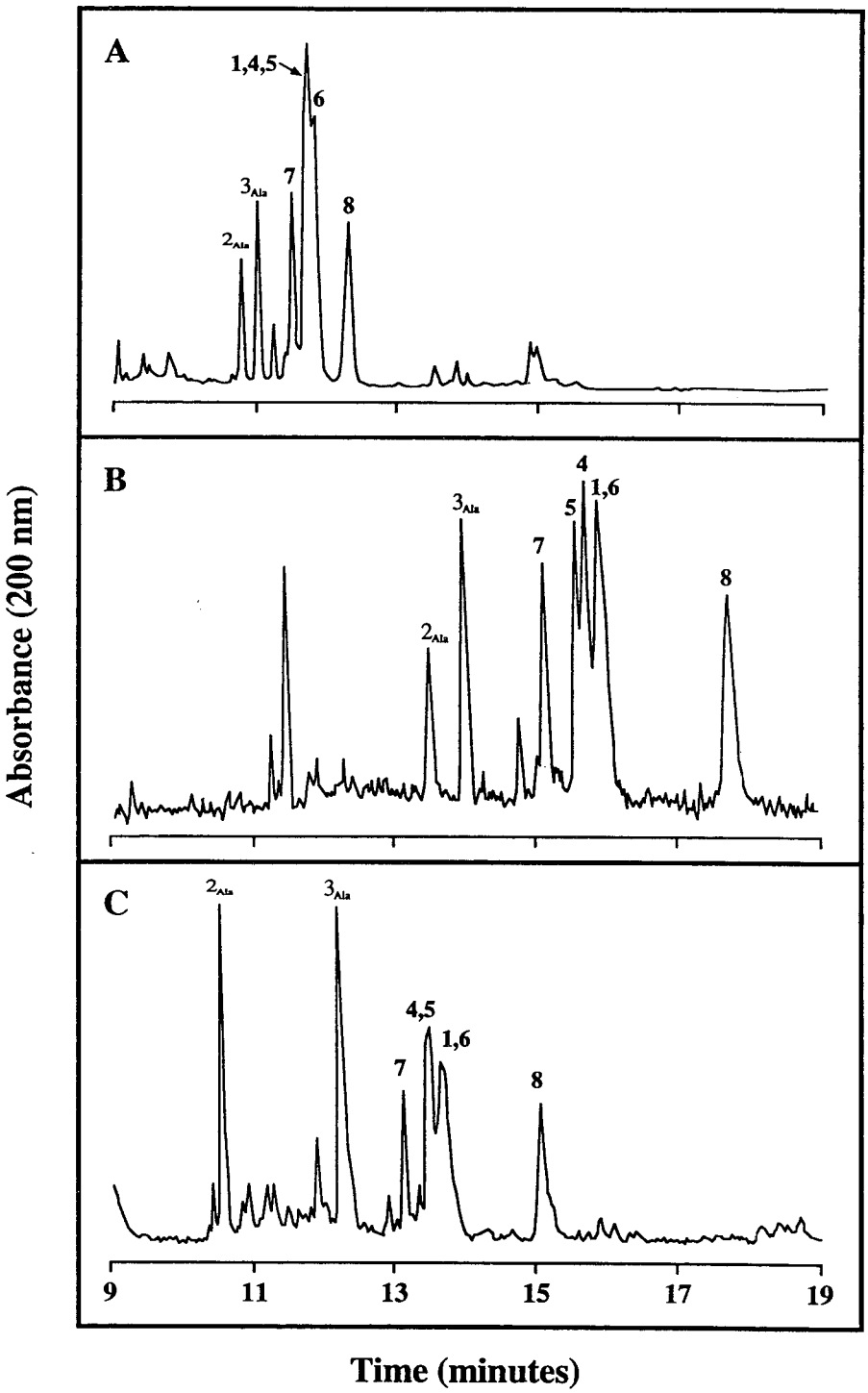

Fig. 6. The separation of the peptides in the presence of hexamethonium bromide and acetonitrile. The separation buffer contained: (A) 50 m*M* phosphoric acid, pH 2.0; (B) 50 m*M* phosphoric acid, pH 2.0, 5 m*M* hexamethonium bromide; (C) 50 m*M* phosphoric acid, pH 2.0, 5 m*M* hexamethonium bromide, 10% (v/v) acetonitrile. Bare fused-silica capillary, 57 cm (50 cm to the detector) × 50 μm I.D. Separation conditions: 15 kV, 28°C.

buffer can lead to subtle but important changes in CE selectivity. This has been shown through the successful separation of peptides with identical composition but different amino acid sequence. In free solution CE or CZE, charge and mass are thought to be the main parameters determining the electrophoretic mobility of analytes. The partial separation of the model peptides effected with simple changes in buffer ionic strength highlight the sensitivity of CE to subtle changes in mass-to-charge ratio, perhaps through nearest-neighbor effects on the pK_a value of the protonatable residues. The addition of the ion-pairing agent, HSA, at concentrations considerably less than the CMC has dramatic effects on the resolution of the peptides. There may be sequence-specific differences in the ability of the negatively-charged HSA to ion-pair with the positively-charged peptides, perhaps a result of subtle charge differences due to nearest-neighbor effects. The addition of ACN changes the hydrophobicity of the solvent and affects separation probably by changing the solvation state of the peptide and/or alterating the interaction of the peptides with HSA. None of the individual manipulations in buffer composition (ionic strength, ion pairing or hydrophobicity) resulted in resolution of all mixture components; it was only through modification of all of these parameters that resolution of the individual components was successful. This study indicates that by altering the ionic environment, the solvation state of the peptide and the hydrophobicity of the buffer, one may effect the separation of structurally-similar molecules. Multiple-buffer-additive strategies should therefore be explored to exploit the combinatorial selectivities when individual additives do not effect adequate separation.

Acknowledgements

The authors wish to thank Collen Allen for her expert clerical assistance and acknowledge the support of the Canadian Medical Research Council (J.P.L.) for financial support.

References

[1] P.D. Grossman, J.C. Colburn, H.H. Lauer, R.G. Nielsen, R.M. Riggin, G.S. Sittampalam and E.C. Rickard, *Anal. Biochem.*, 179 (1989) 28.
[2] M.J. Gordon, X. Huang, S.L. Pentoney, Jr. and R.N. Zare, *Science*, 242 (1988) 224.
[3] B.L. Karger, A.S. Cohen and A. Guttman, *J. Chromatogr.*, 585 (1989) 492.
[4] J.P. Landers, *Trends Biochem. Sci.*, 18 (1993) 409.
[5] J.W. Jorgenson and K.D. Lukacs, *Anal. Chem.*, 53 (1981) 1298.
[6] J.W. Jorgenson and K.D. Lukacs, *J. High Resolut. Chromatogr. Chromatogr. Commun.*, 4 (1981) 230.
[7] J. Frenz, R. Palmieri and W. Hancock, presented at the *2nd International Symposium on High Performance Capillary Electrophoresis, San Fransisco, CA, 1990.*
[8] M. Field, R. Keck and J. O'Connor, presented at the *200th American Chemical Society National Meeting, Washington, DC, August 1990.*
[9] H. Ludi and E. Gassman, *Anal. Chim. Acta*, 213 (1988) 215.
[10] J.P. Landers, R.P. Oda, J.A. Liebenow and T.C. Spelsberg, *J. Chromatogr. A*, 652 (1993) 109.
[11] R.M. McCormick, in J.P. Landers (Editor), *Handbook of Capillary Electrophoresis*, CRC Press, Boca Raton, FL, 1993, pp. 287–324.
[12] S.E. Moring and J.A. Nolan, presented at the *2nd International Symposium on High Performance Capillary Electrophoresis, San Francisco, CA, 1990.*
[13] A. Pessi, E. Bianchi, L. Chiappinella, A. Nardi and S. Fanali, *J. Chromatogr.*, 557 (1991) 307.
[14] R.P. Oda, B. Madden, T.C. Spelsberg and J.P. Landers, *J. Chromatogr. A*, 680 (1994) 85–92.

PUBLICATION SCHEDULE FOR THE 1994 SUBSCRIPTION

Journal of Chromatography A and *Journal of Chromatography B: Biomedical Applications*

MONTH	1993	J–J	J	A	S	O	
Journal of Chromatography A	652–657	Vols. 658–672	673/1 673/2 674/1 + 2 675/1 + 2 676/1	676/2 677/1 677/2 678/1	678/2 679/1 679/2 680/1	680/2	The publication schedule for further issues will be published later.
Bibliography Section		Vol. 681			682/1		
Journal of Chromatography B: Biomedical Applications		Vols. 652–656	657/1 657/2	658/1 658/2	659	660/1 660/2	

INFORMATION FOR AUTHORS

(Detailed *Instructions to Authors* were published in *J. Chromatogr. A*, Vol. 657, pp. 463–469. A free reprint can be obtained by application to the publisher, Elsevier Science B.V., P.O. Box 330, 1000 AH Amsterdam, Netherlands.)

Types of Contributions. The following types of papers are published: Regular research papers (full-length papers), Review articles, Short Communications and Discussions. Short Communications are usually descriptions of short investigations, or they can report minor technical improvements of previously published procedures; they reflect the same quality of research as full-length papers, but should preferably not exceed five printed pages. Discussions (one or two pages) should explain, amplify, correct or otherwise comment substantively upon an article recently published in the journal. For Review articles, see inside front cover under Submission of Papers.

Submission. Every paper must be accompanied by a letter from the senior author, stating that he/she is submitting the paper for publication in the *Journal of Chromatography A* or *B*.

Manuscripts. Manuscripts should be typed in **double spacing** on consecutively numbered pages of uniform size. The manuscript should be preceded by a sheet of manuscript paper carrying the title of the paper and the name and full postal address of the person to whom the proofs are to be sent. As a rule, papers should be divided into sections, headed by a caption (*e.g.*, Abstract, Introduction, Experimental, Results, Discussion, etc.). All illustrations, photographs, tables, etc., should be on separate sheets.

Abstract. All articles should have an abstract of 50–100 words which clearly and briefly indicates what is new, different and significant. No references should be given.

Introduction. Every paper must have a concise introduction mentioning what has been done before on the topic described, and stating clearly what is new in the paper now submitted.

Experimental conditions should preferably be given on a *separate* sheet, headed "Conditions". These conditions will, if appropriate, be printed in a block, directly following the heading "Experimental".

Illustrations. The figures should be submitted in a form suitable for reproduction, drawn in Indian ink on drawing or tracing paper. Each illustration should have a caption, all the *captions* being typed (with double spacing) together on a *separate sheet*. If structures are given in the text, the original drawings should be provided. Coloured illustrations are reproduced at the author's expense, the cost being determined by the number of pages and by the number of colours needed. The written permission of the author and publisher must be obtained for the use of any figure already published. Its source must be indicated in the legend.

References. References should be numbered in the order in which they are cited in the text, and listed in numerical sequence on a separate sheet at the end of the article. Please check a recent issue for the layout of the reference list. Abbreviations for the titles of journals should follow the system used by *Chemical Abstracts*. Articles not yet published should be given as "in press" (journal should be specified), "submitted for publication" (journal should be specified), "in preparation" or "personal communication".

Vols. 1–651 of the *Journal of Chromatography*; *Journal of Chromatography, Biomedical Applications* and *Journal of Chromatography, Symposium Volumes* should be cited as *J. Chromatogr.* From Vol. 652 on, *Journal of Chromatography A* (incl. Symposium Volumes) should be cited as *J. Chromatogr. A* and *Journal of Chromatography B: Biomedical Applications* as *J. Chromatogr. B.*

Dispatch. Before sending the manuscript to the Editor please check that the envelope contains four copies of the paper complete with references, captions and figures. One of the sets of figures must be the originals suitable for direct reproduction. Please also ensure that permission to publish has been obtained from your institute.

Proofs. One set of proofs will be sent to the author to be carefully checked for printer's errors. Corrections must be restricted to instances in which the proof is at variance with the manuscript.

Reprints. Fifty reprints will be supplied free of charge. Additional reprints can be ordered by the authors. An order form containing price quotations will be sent to the authors together with the proofs of their article.

Chiral HPLC Column

Application Guide for Chiral HPLC Column Selection

SECOND EDITION!

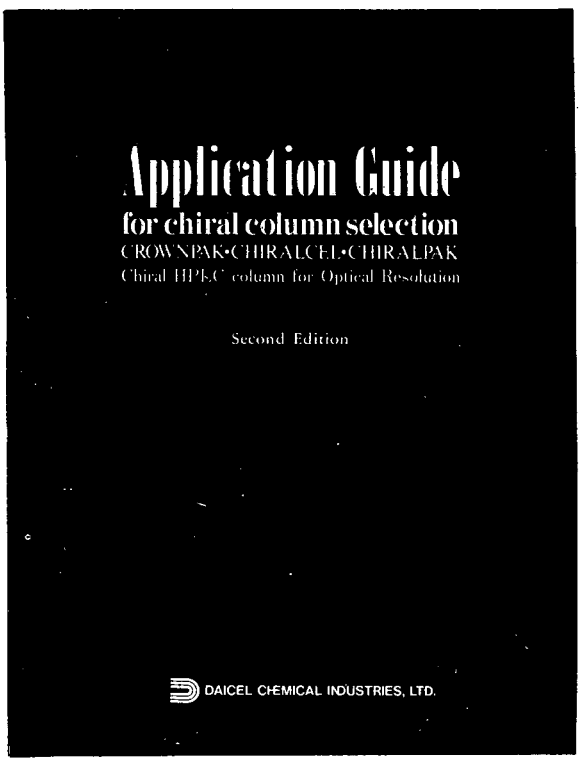

GREEN BOOK

The 112-page green book contains chromatographic resolutions of over 350 chiral separations, cross-indexed by chemical compound class, structure, and the type of chiral column respectively. This book also lists chromatographic data together with analytical conditions and structural information. A quick reference guide for column selection from a wide range of DAICEL chiral HPLC columns is included.

To request this book, please let us know by fax or mail.

DAICEL CHEMICAL INDUSTRIES, LTD.

AMERICA

CHIRAL TECHNOLOGIES, INC.

730 Springdale Drive, P.O. Box 564, Exton, PA 19341
Phone: +1-215-594-2100
Facsimile: +1-215-594-2325

EUROPE

DAICEL (EUROPA) GmbH

Oststr. 22
D-40211 Düsseldorf, Germany
Phone: +49-211-369848
Facsimile: +49-211-364429

ASIA/OCEANIA

DAICEL CHEMICAL INDUSTRIES, LTD.
CHIRAL CHEMICALS NDD
8-1, Kasumigaseki 3-chome,
Chiyoda-ku, Tokyo 100, JAPAN
Phone: +81-3-3507-3151
Facsimile: +81-3-3507-3193